

TN  
1  
A5  
Vol. 110  
N/C

# TRANSACTIONS/

OF THE

## AMERICAN INSTITUTE OF MINING AND METALLURGICAL ENGINEERS

(INCORPORATED)

Vol. 110

*American Institute of Mining, Metallurgical  
and Petroleum Engineers,*

## GEOPHYSICAL PROSPECTING 1934

---

PAPERS AND DISCUSSIONS PRESENTED AT MEETINGS OF THE INSTITUTE HELD  
AT NEW YORK, FEB. 15-18, 1932, FEB. 20-23, 1933 AND FEB. 19-22, 1934.

---

NEW YORK, N. Y.

PUBLISHED BY THE INSTITUTE

AT THE OFFICE OF THE SECRETARY

29 WEST 39TH STREET

U. OF I.  
LIBRARY

## NOTICE

This volume is the third of a series devoted to papers and discussions on Geophysical Prospecting. The three volumes are as follows:

1929, Geophysical Prospecting—TRANSACTIONS A.I.M.E., Volume 81

1932, TRANSACTIONS A.I.M.E., Volume 97

1934, TRANSACTIONS A.I.M.E., Volume 110

This volume contains papers and discussions presented at the New York Meetings in February, 1932, 1933 and 1934.

Volume 74 of the TRANSACTIONS contains one paper on electrical prospecting.

COPYRIGHT, 1934, BY THE

AMERICAN INSTITUTE OF MINING AND METALLURGICAL ENGINEERS

(INCORPORATED)

PRINTED IN THE UNITED STATES OF AMERICA

THE MAPLE PRESS COMPANY, YORK, PA.

## CONTENTS

	PAGE
FOREWORD. . . . .	5
INSTITUTE OFFICERS AND DIRECTORS . . . . .	7
COMMITTEE ON GEOPHYSICAL METHODS OF PROSPECTING. . . . .	7

### PAPERS

#### Electrical Methods

Results of Earth-resistivity Survey on Various Geologic Structures in Illinois. By M. KING HUBBERT. (With discussion). . . . .	9
Location of Faults in Hardin County, Illinois, by the Earth-resistivity Method. By M. KING HUBBERT AND J. MARVIN WELLER. (With discussion). . . . .	40
Some Practical Applications of Resistivity Measurements to Highway Problems. By KARL S. KURTENACKER. . . . .	49
Location and Study of Pipe-line Corrosion by Surface Electrical Measurements (Abstract). By C. AND M. SCHLUMBERGER AND E. G. LEONARDON . . . . .	60
Electrical Methods in Prospecting for Gold. By FOLKE H. KIHLESTEDT. (With discussion). . . . .	62
Discovering Gold-quartz Veins Electrically (Abstract). By S. F. KELLY, THEODOR ZUSCHLAG AND BELA LOW . . . . .	75
Application of Resistivity Methods to Northern Ontario Lignite Deposits. By R. H. HAWKINS. (With discussion). . . . .	76
Geophysical Studies in Placer and Water-supply Problems (Abstract). By J. J. JAKOSKY AND C. H. WILSON . . . . .	121
Electrical Exploration of Water-covered Areas. By C. AND M. SCHLUMBERGER AND E. G. LEONARDON. (With discussion). . . . .	122
Interpretation of Resistivity Measurements. By G. F. TAGG. (With dis- cussion) . . . . .	135
Interpretation of Three-layer Resistivity Curves. By SYLVAIN J. PIRSON . . . . .	148
Some Observations Concerning Electrical Measurements in Anisotropic Media, and Their Interpretation. By C. AND M. SCHLUMBERGER AND E. G. LEONARDON. (With discussion). . . . .	159
Some Interpretations of Earth-resistivity Data. By IRWIN ROMAN. (With discussion). . . . .	183
A Contribution to the Theory of the Interpretation of Resistivity Measure- ments Obtained from Surface Potential Observations. By R. J. WATSON. (With discussion). . . . .	201
Electrical Coring; a Method of Determining Bottom-hole Data by Electrical Measurements. By C. AND M. SCHLUMBERGER AND E. G. LEONARDON . . . . .	237
A New Contribution to Subsurface Studies by Means of Electrical Measurements in Drill Holes. By C. AND M. SCHLUMBERGER AND E. G. LEONARDON. (With discussion). . . . .	273

#### Magnetic Methods

Use of Magnetic Data on Michigan Iron Ranges. By C. O. SWANSON. (With discussion). . . . .	290
Magnetic Measurements on Auriferous Veins in Brazil. By MARK C. MAL- AMPHY. . . . .	313



	PAGE
An Accurate Simplified Magnetometer Field Method. By HUBERT O. DE BECK . . . . .	326
Theory and Experiments Concerning a New Compensated Magnetometer System. By C. A. HEILAND AND W. E. PUGH . . . . .	334
A Magnetic Gradiometer. By IRWIN ROMAN AND THOMAS C. SERMON. (With discussion). . . . .	373

### Seismic Methods

Reflection Methods in Seismic Prospecting. By H. M. RUTHERFORD . . . . .	391
Certain Instrument Problems in Reflection Seismology. By C. A. HEILAND. . . . .	411
Certain Field Problems in Reflection Seismology. By W. E. PUGH. (With discussion). . . . .	455
Seismic Refraction Methods as Applied to Shallow Overburdens. By F. L. PARTLO AND JERRY H. SERVICE. (With discussion). . . . .	473
Analysis of Seismic Profiles. By IRWIN ROMAN. . . . .	493

### General

Recent Geothermal Measurements in the Michigan Copper District. By JAMES FISHER, L. R. INGERSOLL AND HARRY VIVIAN. (With discussion). . . . .	528
Geophysics in the Nonmetallic Field. By C. A. HEILAND. (With discussion). . . . .	546
INDEX. . . . .	579



## FOREWORD

WITH the present volume, the third in series, the Committee on Geophysical Methods of Prospecting transmits the principal papers accepted by the Institute since early in the year 1932. Most of the papers have to do with the electrical method. Most of them are presentations of physical data and interpretations. Most of them bear on the problems of prospecting in the mining rather than the petroleum industry. The volume contains no papers on the gravimetric methods.

In the present state of their development, the geophysical methods begin to stand revealed as delicate geologic tools for securing structural information not as readily procurable by other means. Notable exceptions to this generalization are the use of electrical methods in the direct location of sulfide orebodies at shallow depths, the use of magnetic methods in iron prospecting, the use of electrical coring in oil prospecting and, perhaps, various direct but minor uses for the electrical methods in engineering problems such as the location of bedrock at dam sites, the location of water tables, etc.

In the mining industries, at the present time, only the electrical and magnetic methods are in substantial use, the chief efforts being structural investigations for gold prospecting and the search for quartz veins in gold-bearing districts.

In the petroleum industry, geophysical prospecting has increased to a new peak. Structural investigations by the seismic method (reflection) are being conducted in Venezuela, Mexico and Canada and in California, Colorado, Wyoming, Montana, New Mexico, Texas, Oklahoma, Louisiana, Arkansas, Mississippi, Florida, New York and Pennsylvania. As many as one hundred reflection crews are known to be working at the present time, Texas being the chief center of activity. Gravimetric surveying, chiefly by the torsion balance method and to some extent by the pendulum method, continues at an unabated rate. Magnetic surveys are used slightly and electrical surveys very little or not at all. One notable advance has been the demonstration of usefulness and general acceptance of electrical coring both in field development and wildcat drilling on the Gulf Coast.

A notable series of geophysical papers of high quality having to do with oil prospecting has been published during the current year in volume

one of the Proceedings of the World Petroleum Congress, which was held in London in 1933.

The chairman takes this opportunity to present his thanks to the members of his committee and in particular to its vice chairman, Mr. Sherwin F. Kelly, without whose work the present volume would not have been possible.

E. DEGOLYER, *Chairman,*  
Committee on Geophysical  
Methods of Prospecting.

## A. I. M. E. OFFICERS AND DIRECTORS

For the year ending February, 1935

President and Director, HOWARD N. EAVENSON, Pittsburgh, Pa.  
 Past President and Director, SCOTT TURNER, Washington, D. C.  
 Past President and Director, FREDERICK M. BECKETT, New York, N. Y.  
 Vice President, Treasurer and Director, KARL EILERS, New York, N. Y.

### VICE PRESIDENTS AND DIRECTORS

EUGENE MCAULIFFE, Omaha, Neb.      HENRY KRUMB, Salt Lake City, Utah  
 PAUL D. MERICA, New York, N. Y.      EDGAR RICKARD, New York, N. Y.  
 LOUIS S. CATES, New York, N. Y.

### DIRECTORS

ERLE V. DAVELER, New York, N. Y.      MILNOR ROBERTS, Seattle, Wash.  
 HARVEY S. MUDD, Los Angeles, Calif.      FRANK L. SIZER, San Francisco, Calif.  
 J. V. W. REYNERS, New York, N. Y.      H. A. BUEHLER, Rolla, Mo.  
 J. B. UMPLEBY, Norman, Okla.      CHARLES B. MURRAY, Cleveland, Ohio  
 CHARLES C. WHITTIER, Chicago, Ill.      BRENT N. RICKARD, El Paso, Texas  
 ELI T. CONNER, Scranton, Pa.      GEORGE B. WATERHOUSE, Cambridge,  
 JOHN M. LOVEJOY, New York, N. Y.      Mass.  
 HUGH PARK, Cobalt, Ont.      WILLIAM WRAITH, New York, N. Y.

Secretary, A. B. PARSONS, New York, N. Y.

Assistant Secretary, EDWARD H. ROBBIE, New York, N. Y.  
 Assistant to the Secretary, JOHN T. BREUNICH, New York, N. Y.  
 Assistant to the Secretary, E. J. KENNEDY, JR., New York, N. Y.  
 Assistant Treasurer, H. A. MALONEY, New York, N. Y.

## GEOPHYSICAL METHODS OF PROSPECTING

EVERETTE DeGOLYER, Chairman

SHERWIN F. KELLY, Vice-chairman	FREDERICK W. LEE, Secretary
DONALD C. BARTON	E. EUGENE ROSAIRE
HENRY A. BUEHLER	W. G. SAVILLE
IRVING B. CROSBY	L. A. SCHOLL, JR.
ADAM M. C. DRATH	L. B. SLICHTER
F. LEROY FOSTER	NOEL H. STEARN
C. A. HEILAND	C. E. VAN ORSTRAND
W. O. HOTCHKISS	PAUL WEAVER
J. J. JAKOSKY	ALBERT G. WOLF
E. LANCASTER-JONES	FRED E. WRIGHT
J. C. KARCHER	THEODOR ZUSCHLAG
E. G. LEONARDON	
HANS LUNDBERG	
MARK C. MALAMPHY	
D. H. McLAUGHLIN	
L. MINTROP	
E. E. MUESER	
D. MUSHKETOV	
O. S. PETTY	
WALLACE E. PRATT	
LEOPOLD REINECKE	





# Results of Earth-resistivity Survey on Various Geologic Structures in Illinois\*

BY M. KING HUBBERT,† NEW YORK, N. Y.

(New York Meeting, February, 1932)

DURING the past summer the writer was asked by the Illinois State Geological Survey to make a study of some of its economic geological problems with regard to the applicability of geophysical methods of prospecting to their solution. The following four problems were suggested for investigation: (1) the fluorspar area of Southern Illinois, (2) oil structures in the south central part of the state, (3) the lead and zinc-bearing area of northwestern Illinois, and (4) the water supply and gravel deposits of the glacial drift. The prime requirements were to find a means of obtaining a maximum of useful information with a fairly modest outlay of expenditure for technical staff and equipment.

The method of procedure adopted was that of making a preliminary study of each of the problems named by means of available office data and published reports with supplementary field reconnaissance where necessary.

## PRELIMINARY STUDIES

*Fluorspar.*—The fluorspar deposits of southern Illinois as shown by Weller,<sup>1</sup> Bastin<sup>2</sup> and others are of two main types: (1) vein deposits along steeply dipping normal fault planes, and (2) "blanket" deposits occurring practically horizontally along a certain sedimentary horizon. The vein deposits are composed mostly of calcite and fluorspar in sheetlike veins of thicknesses, where mined, ranging from about 2 to 12 ft. The surrounding topography is in a mature state of development with a relief of about 100 ft. or more.

Any geophysical prospecting for this ore would have to depend either upon the physical properties of the ore and associated minerals or upon the properties of the geologic structure containing them. Fluorspar has a density of 3.18, which is somewhat greater than 2.7, that of calcite. Its

\* Published with permission of M. M. Leighton, Chief, Illinois State Geological Survey.

† Instructor in Geophysics, Columbia University; Associate Geologist, Illinois State Geological Survey.

<sup>1</sup> S. Weller: The Geology of Hardin County, Illinois State Geol. Survey *Bull.* 41 (1920).

<sup>2</sup> E. S. Bastin: The Fluorspar Deposits of Hardin and Pope Counties, Illinois. Illinois State Geol. Survey *Bull.* 58 (1931).



specific electrical resistivity is of the order of that of calcite and crystalline limestone. Its magnetic permeability is about that of calcite and the less magnetic sedimentary rocks and hence negligible.

The only physical property that might be used for the direct detection of fluorspar is that of density. The deposits, however, are so small that it is extremely doubtful that they would ever be detected by gravitational means and differentiated from the local topographic disturbances.

Detection of associated structures, on the other hand, seemed to offer more promise. Since the vein deposits occur as mineralization along fault planes, the location of unknown faults would afford a step toward the location of deposits of fluorspar. For this purpose either earth resistivity or seismic means might be applicable. Because of its greater simplicity and less expensiveness trial by the former was recommended.

*Oil Structures.*—The petroleum of Illinois is obtained mostly from anticlinal structures in the southern half of the state. This area is covered with glacial drift so that there are few outcrops of bedrock. The structural details of a very large part of this area are little known, though it seems probable that there may be many hidden oil-bearing structures underneath this drift cover. The question of whether such structures, if they did exist, could be discovered by geophysical measurements of the surface was asked.

Field work for two seasons with an Askania magnetometer had previously been done in Illinois in an attempt to correlate magnetic anomalies with structures of oil-bearing type, and it was found that no consistent correlation could be established.

One of the oil companies that had done torsion balance work in the area provided the information that the largest known oil structure there gave a barely perceptible gravitational anomaly. Again, earth resistivity and seismic methods seemed the most likely, so it was decided to try the former first.

*Lead and Zinc.*—The preliminary study of this problem made it seem improbable that there are many major deposits remaining in the known productive area, so further investigation of it has been postponed, at least for the present.

*Water Supply and Gravel Deposits.*—A large part of the state is underlain by a coal basin which is covered with glacial drift. The deep water is contaminated by the coal, so that water supply for domestic uses has to be obtained largely from glacial drift. While it is true that below the water table the glacial drift is saturated with water at all places, the availability of this water depends upon the rate at which it can be withdrawn. This, in turn, is a direct function of the size of the particles of the water-bearing material. A shale or clay, for instance, may be saturated with water and have as high as 30 to 40 per cent water and still yield, for all practical purposes, a dry well. Any large sand and gravel deposit below the water



table, on the other hand, not only affords a reservoir of water but usually has large enough particles to allow sufficient flowage into a well when a pressure differential is produced by pumping the well. The problem of water supply, therefore, resolved itself into that of finding gravel deposits hidden in the glacial drift. L. E. Workman, of the Survey, provided the information that gravel deposits were commonly found along buried river channels.

This information afforded two possible methods of attack, (1) that of finding gravel directly, and (2) that of finding buried river channels in the bedrock. For each of these, earth resistivity seemed the most likely means of investigation.

#### APPARATUS AND FIELD TECHNIQUE

The apparatus used was the Megger Ground Tester, manufactured by Evershed and Vignoles, London, England. The essential elements of this instrument are a hand-cranked direct-current generator, a double commutator system and an ohmmeter. There are four outside electrodes, two current electrodes  $C_1$  and  $C_2$ , and two potential electrodes  $P_1$  and  $P_2$ . If leads are run from the electric terminals  $C_1$  and  $C_2$ , to two parts of any conductor and the generator crank turned, an alternating current is sent through the conductor. This current alternates at 50 cycles and the potential difference set up on open circuit is 50 volts. If two other leads are run from the potential terminals  $P_1$  and  $P_2$ , and are connected to different parts of the same conducting body to which the current leads are attached, an alternating potential difference  $E$  will be led off.

The double commutator system is so arranged that the direct current generated is led through the current coil of the ohmmeter and is then alternated by one-half of the commutator. A part of this is picked up by the potential electrodes, taken through the other half of the commutator where it is rectified, and then passes through the potential coil of the ohmmeter as direct current. As a result, the ohmmeter reads directly in ohms the result

$$R = \frac{E}{I},$$

where  $R$  is the resistance in ohms of the block between the two equipotential surfaces through the points of attachment of the two potential electrodes,  $E$  the potential difference between these points and  $I$  the total current flowing through the conductor.

The instrument thus lends itself to the determination of the specific resistivity of a semi-infinite homogeneously conducting medium by the method worked out by Wenner.<sup>3</sup> Wenner showed that if on the surface

<sup>3</sup> F. Wenner: A Method of Measuring Earth Resistivity. U. S. Bur. Stds. Bull. 258 (1916).

of a homogeneously conducting medium having a plane surface and infinite extent on one side of that plane four electrodes in the same straight line and having an equal spacing  $a$  are placed then  $\rho = 2\pi a \frac{E}{I}$  where  $\rho$  is the specific resistivity of the median,  $E$  the potential difference between the two inner electrodes, and  $I$  the current between the two outer electrodes. Gish and Rooney<sup>4</sup> developed the technique of resistivity prospecting for inhomogeneous media by considering  $\rho$  of Wenner's formula to be merely the apparent specific resistivity and letting the value of  $\rho$  serve as an index of the variation of resistivity as a function of the electrode interval  $a$  and the position and azimuth of the lines of the electrodes.

The point midway between the two potential electrodes is herein taken as the position of the station.

In actual field technique there are only three independent variables: (1) the position of the station, (2) the electrode separation  $a$ , and (3) the azimuth  $\alpha$  of the line of the electrodes.

The apparent specific resistivity  $\rho$  is measured as an empirical function of any or all of these variables. If  $\rho$  is measured as a function of position of station while both  $a$  and  $\alpha$  are kept constant, the resulting curve indicates the approximate position of the bodies having marked differences in conductivity. If at any particular station there is approximate horizontal homogeneity of resistivity, a curve of  $\rho$  measured as a function of electrode separation  $a$  gives variations due to a change of resistivity with depth.

The determination of  $\rho$  as a function of the azimuth  $\alpha$  while keeping the position and the electrode separation  $a$  constant will indicate both the presence of major horizontal inhomogeneities and to a great extent the orientation of the body exhibiting it.

The essential problem of prospecting by this method is to determine by means of combinations of the above mentioned function of three variables the horizontal position, depth, and, as nearly as possible, nature of bodies near the earth's surface differing markedly with respect to specific resistivity from that of their surroundings.

In field practice the author has accordingly differentiated the following techniques:

1. A *traverse profile* is a series of observations taken along a line of traverse while both  $a$  and  $\alpha$  are kept constant.
2. A *longitudinal traverse profile* is a traverse profile wherein the line of electrodes is parallel to the line of traverse.
3. A *transverse traverse profile* is a traverse profile taken with the line of electrodes perpendicular to the line of traverse.

---

<sup>4</sup> O. H. Gish and W. J. Rooney: Measurement of Resistivity of Large Masses of Undisturbed Earth. *Terr. Mag. and Atm. Elec.* (1925) **30**, 161-188.

4. A circular "profile" is obtained by rotating the line of electrodes about a given station and reading  $\rho$  at equal angular intervals. The results of a circular profile may be represented graphically by plotting from a point representing the station vectors whose directions correspond to the azimuths of the line of electrodes and whose lengths are proportional to the corresponding values of  $\rho$ .

5. A "depth profile" is obtained by measuring  $\rho$  for successive increased values of  $a$  while keeping the position and azimuth constant.

## EARTH-RESISTIVITY FIELD STUDIES

### *Fault Investigation*

Fig. 1 shows a longitudinal traverse profile across a known fault. The fault is a normal steeply dipping one of which the vertical component

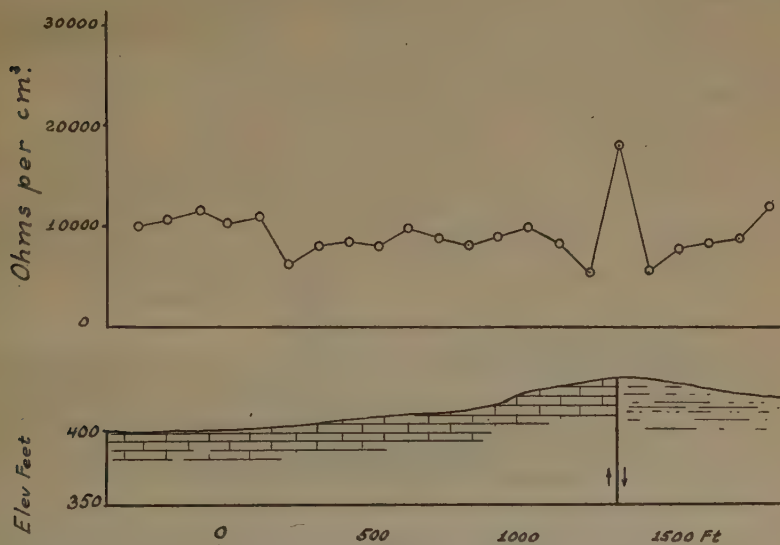


FIG. 1.—LONGITUDINAL TRAVERSE PROFILE ACROSS A NORMAL FAULT.

of movement is about 1200 ft. To the west of the fault plane the surface formation is a limestone; to the east, a sandy shale. The outcrop of the fault plane itself is visible in the road cut along the line of traverse. The traverse was taken with the electrode separation  $a$  equal to 100 ft. and with stations spaced 100 ft. apart.

The essential characteristics of the anomaly obtained are that when the fault plane was located between one of the potential electrodes and one of the current electrodes the apparent resistivity  $\rho$  is relatively lower than the surrounding normal values. When the fault plane is between



the two potential electrodes, however,  $\rho$  is relatively very high. This produces in the curve a sort of  $W$  with an unusually high middle.

It was suspected that this peculiar anomaly may have been due to fault gouge and water along the fault plane which made it a better conductor than the rocks on either side. To check this, the line of electrodes was rotated until essentially parallel to the fault trace. The value then obtained was lower than any of the other three and suggested a high conductivity parallel to the fault plane.

As a further check, the experimental profile shown in Fig. 2 was taken. In this a piece of sheet metal was immersed in water as shown and stations were taken 6 in. apart with  $a$  equal to 6 in. The same kind of  $W$  was

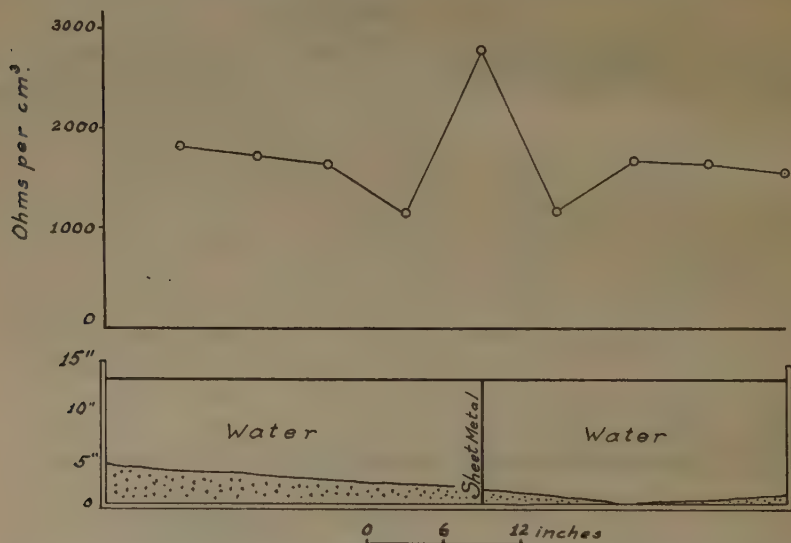


FIG. 2.—EXPERIMENTAL TRAVERSE<sup>5</sup> PROFILE ACROSS A PIECE OF SHEET METAL IMMERSSED IN WATER.

Note resemblance of anomaly produced by sheet metal to that produced by the fault, in Fig. 1.

obtained with respect to the sheet metal as had previously been obtained with respect to the fault plane. These results apparently do not accord with those reported by Low, Kelly and Creagmile.<sup>5</sup> In the experiments recorded by these authors a distinct drop was observed in the resistivity profiles when a conductive body was interposed between the potential electrodes. It should be noted, however, that the conductive body in their experiments occupied a considerable portion of the volume between those electrodes, whereas in the present case the conductive sheet was extremely thin. In a personal communication, Theodor Zuschlag stated

<sup>5</sup> B. Low, S. F. Kelly and W. B. Creagmile: Applying the Megger Ground Tester in Electrical Exploration. *Trans. A. I. M. E.* (1932) 97, 114.

that he had obtained results which checked with the foregoing. He found that a thick conductive sheet between the potential electrodes produced a drop in the resistivity curve, which became less pronounced as the sheet was made progressively thinner, and finally passed over into a peak. A theoretical explanation of these phenomena would be extremely interesting.

A circular profile also was taken, having its center above the sheet metal. This gave the very interesting result shown in Fig. 3. It will be noted that one axis of symmetry of the resulting curve is parallel to the disturbing body while the other is perpendicular to it.

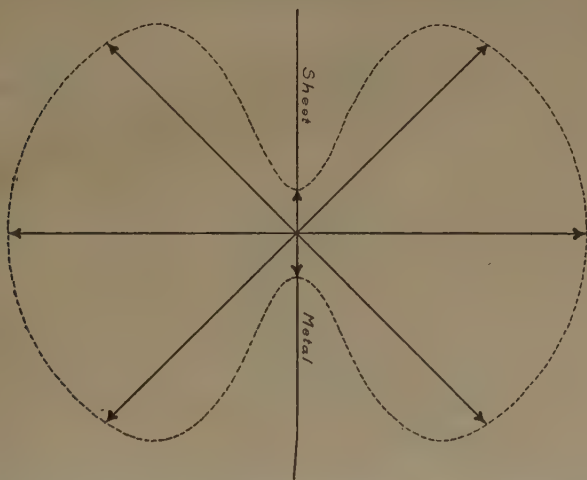


FIG. 3.—CIRCULAR "PROFILE" OVER THE SHEET METAL SHOWN IN FIG. 2.

Note relation between axes of symmetry of resistivity figure and direction of strike of metal sheet.

These two cases indicate that not only is it possible to locate at least some faults by this method but that it is also possible by a proper combination of the two variables, azimuth and position, to determine its strike as well.

Fig. 4 is another geologic section and two resistance profiles. The stations, as before, are 100 ft. apart and the electrode interval  $a$  equal to 100 ft. The solid line curve was obtained by a longitudinal traverse profile; the broken line curve from a transverse profile.

From west to east the visible geology along the line of traverse consists of the limestone outcrops, the fault separating limestone from sandstone, another limestone outcrop and finally sandstone with a much shattered zone in the hilltop near the eastern end of the profile. The two intermediate faults bordering the central limestone member were not seen, though from outcrop pattern alone their existence would be inferred.

The earth-resistivity profile follows the known geology faithfully. High resistivity corresponds to the limestone with an abrupt drop upon crossing a fault into the sandstone area. The sandstone shattered zone to the east produced a small *W* in the curve.

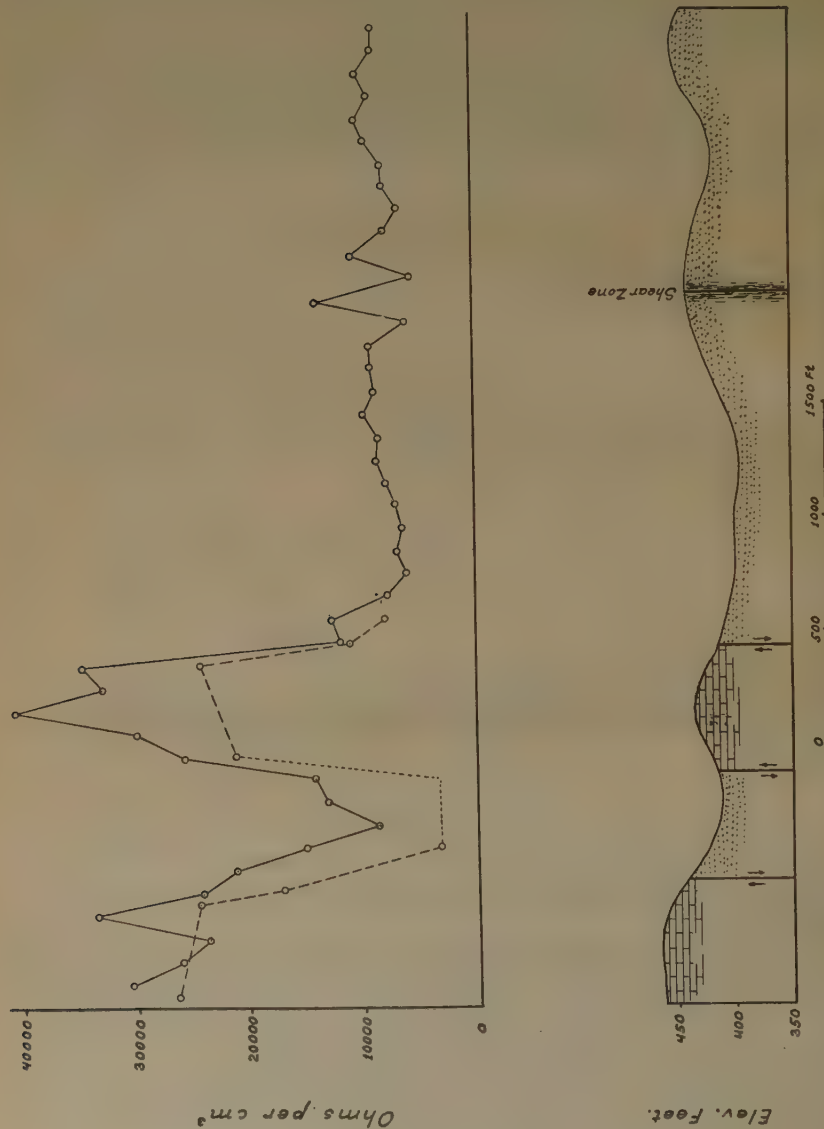


FIG. 4.—TRAVERSE PROFILES ACROSS LIMESTONE AND SANDSTONE FAULTS. Solid line curve is a longitudinal traverse profile. Broken line is of a transverse traverse profile.

Because of thick underbrush, only a few transverse stations were taken. The curve so obtained is in all essentials similar to the first, though apparently slightly more nearly rectangular.



*Monoclinal Strata*

One profile was run perpendicular to the strike and over the truncated edges of a series of monoclinical strata dipping about  $10^{\circ}$  to  $12^{\circ}$ . There are two main parts to the profile; the first is from Devonian limestone across the hard, black, slatelike Chattanooga shale and then over a chert, the second is across an alternating series of sandstone and shaly limestones.

The geologic section and corresponding profiles are shown in Fig. 5.  $a$  is 100 ft. and the stations are 100 ft. apart. It is interesting to note that to the Chattanooga shale outcrop there corresponds an extremely

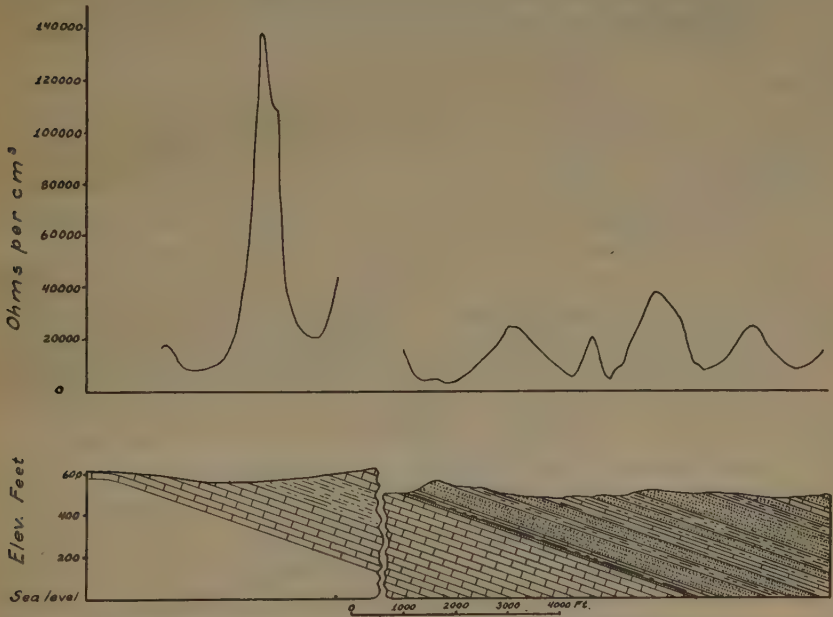


FIG. 5.—TRAVERSE PROFILE ACROSS TRUNCATED EDGES OF MONOCLINAL STRATA.

high value for  $\rho$ . There was some doubt as to the validity of this, so another profile was taken across this part of the section with a short offset along the strike. Similar results were obtained. Across the alternating sandstones and shaly limestones the profile shows a crest for the sandstone outcrop and a trough for the shaly limestone. The last crest is due to a hard, crystalline limestone.

This profile was taken in dry weather over a very hard and sun-baked ground, consequently a number of the ground contacts were very poor. No correction for this was applied in the computations, so that the minor variations in the curve are probably due to this cause.

## Gravel Deposits

Fig. 6 is a subsurface contour map of the top of bedrock and the bottom of the glacial drift made by L. E. Workman. The topography in the

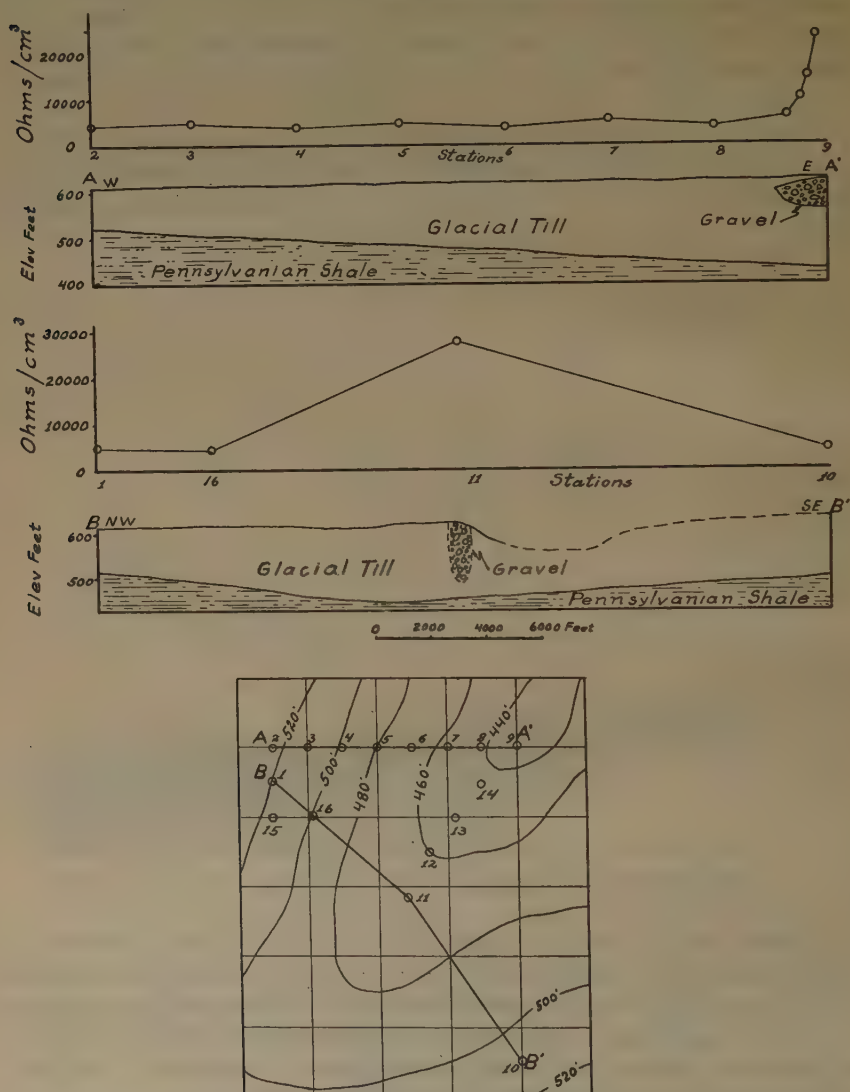


FIG. 6.—MAP AND PROFILES IN GLACIAL DRIFT-COVERED AREA.

Contour lines represent bedrock surface under glacial drift. Anomalies in curves are interpreted to be due to gravel deposits in glacial drift.

area is essentially flat, so it was decided to use this area as a check in an attempt to determine depth to bedrock and thereby locate the trough shown on the map.

Accordingly a series of depth stations at half-mile intervals along the line  $AA'$  were taken and also along the line  $BB'$  and the other few stations not included in these lines. The bedrock in this area is Pennsylvanian shale and the depth curves showed only very slight decline in  $\rho$  as a function of  $a$ , for  $a$  considerably greater than the depth to bedrock. This indicated that the shale was only slightly better as a conductor than the drift, so that no reliable results on depth to bedrock were obtained.

A totally unexpected feature was observed in connection with stations 9 and 11. Whereas all the other stations showed values for  $\rho$  ranging around 4000 to 6000 ohms per cu. cm., these two stations gave values between 20,000 and 30,000 ohms per cu. cm. Depth determinations in these two cases indicated that the highly resistant material was encountered at very shallow depths and is confined to the glacial drift. From station 9 a traverse profile was run westward using  $a$  equal to 100 ft. and stations 100 ft. apart. The value of  $\rho$  rapidly declined and within one-quarter mile quite normal glacial drift values were obtained.

For both stations 9 and 11 there was a very slight topographical elevation above the station, showing normal values. Stations 12, 13 and 14 were all normal.

The profiles in Fig. 6 are made from the values of  $\rho$  for  $a$  equal to 100 feet.

The electrical results give the information that within ordinary glacial till there exists a body of some material of relatively very high resistivity, which occurs only locally and is rather sharply bounded.

The problem is: What geologically possible bodies fulfill the above conditions and of these which is the most probable? From a knowledge of the geology of glacial deposits, the most likely deposit fulfilling such conditions seems to be gravel. If the anomaly is due to a gravel deposit the data suggest a linear deposit of gravel sharply bounded on the northwest and extending parallel to the axis of the subsurface trough.

Fig. 7 shows another subsurface map of a trough in the bedrock which is buried underneath glacial drift. This map, which was made by G. H. Cady, is based on coal test holes and well logs.

In this case a series of depth "profiles" with  $a$  taken at 20-ft. intervals from 20 to 300 ft. were taken in an east-west line at stations one-half mile apart. The profiles shown in Fig. 7 are made from the values of  $a$  equal to 100,  $a$  equal to 200, and  $a$  equal to 300 ft. The bedrock in this case is again highly conductive Pennsylvanian shale. The profile obtained shows two significant features. In all cases station 13 shows an abnormally high value of apparent specific resistivity and this value is highest for  $a$  equal to 100 ft. and declines for greater values of  $a$ . This can only indicate that there is a shallow, highly resistant body underlain by a relatively better conductor. Hence, as the electrodes are spread more widely apart, a greater proportion of the current cross-section falls within



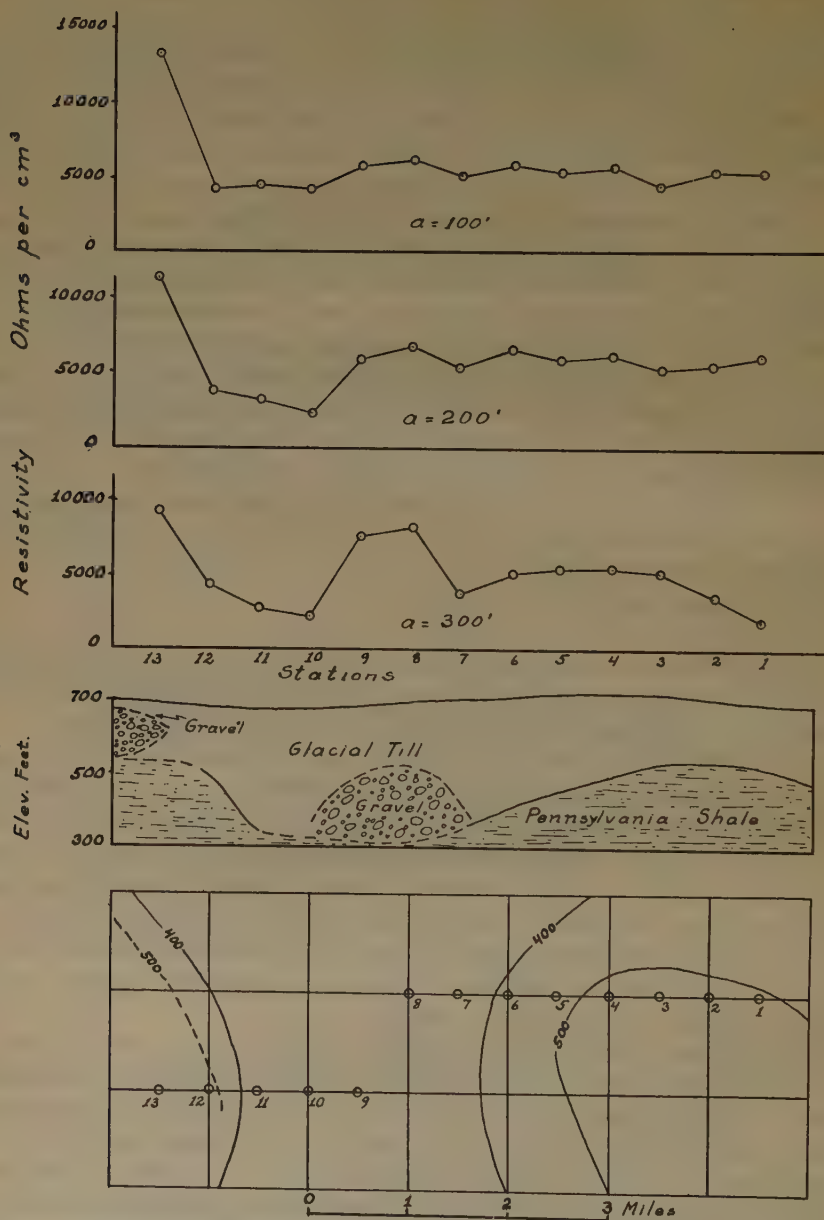


FIG. 7.—MAP, GEOLOGIC CROSS-SECTION AND RESISTIVITY PROFILES ACROSS BURIED RIVER CHANNEL.

Anomaly at station 13 is interpreted as due to shallow gravel deposit. Those at stations 8 and 9 supposedly are due to a more deep-seated deposit.

the deeper, more conductive medium, and the smaller is the consequent apparent resistivity.

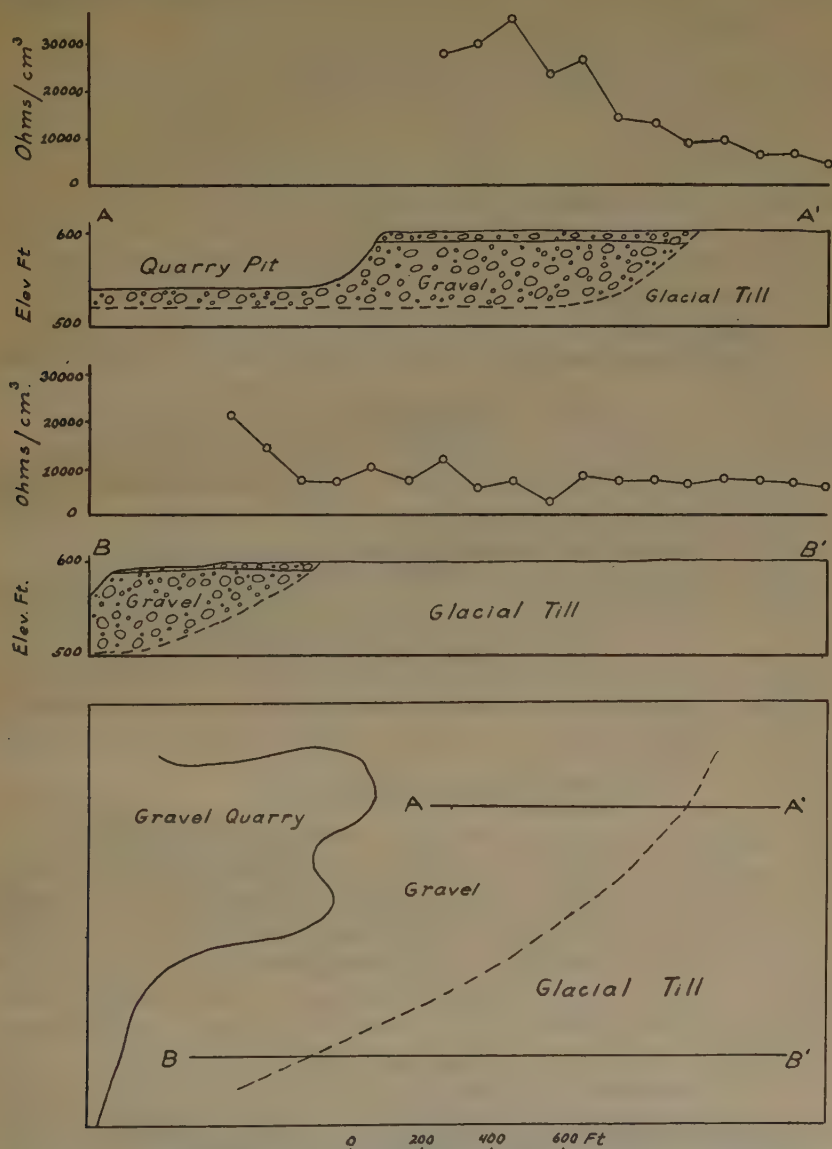


FIG. 8.—MAP, CROSS-SECTIONS AND RESISTIVITY PROFILES ACROSS A GRAVEL QUARRY. Broken line representing boundary between gravel and till is in agreement with both test-pit and earth-resistivity data.

The second significant feature shown by the profiles occurs at stations 8 and 9. For  $a$  equal to 100 ft., it will be noted that with exception of station 13 the profile is essentially flat. For  $a$  equal to 200 ft. a peak is

beginning to be noticeable at stations 8 and 9. For  $a$  equal to 300 ft. the peak at these two stations has become very pronounced. This tells

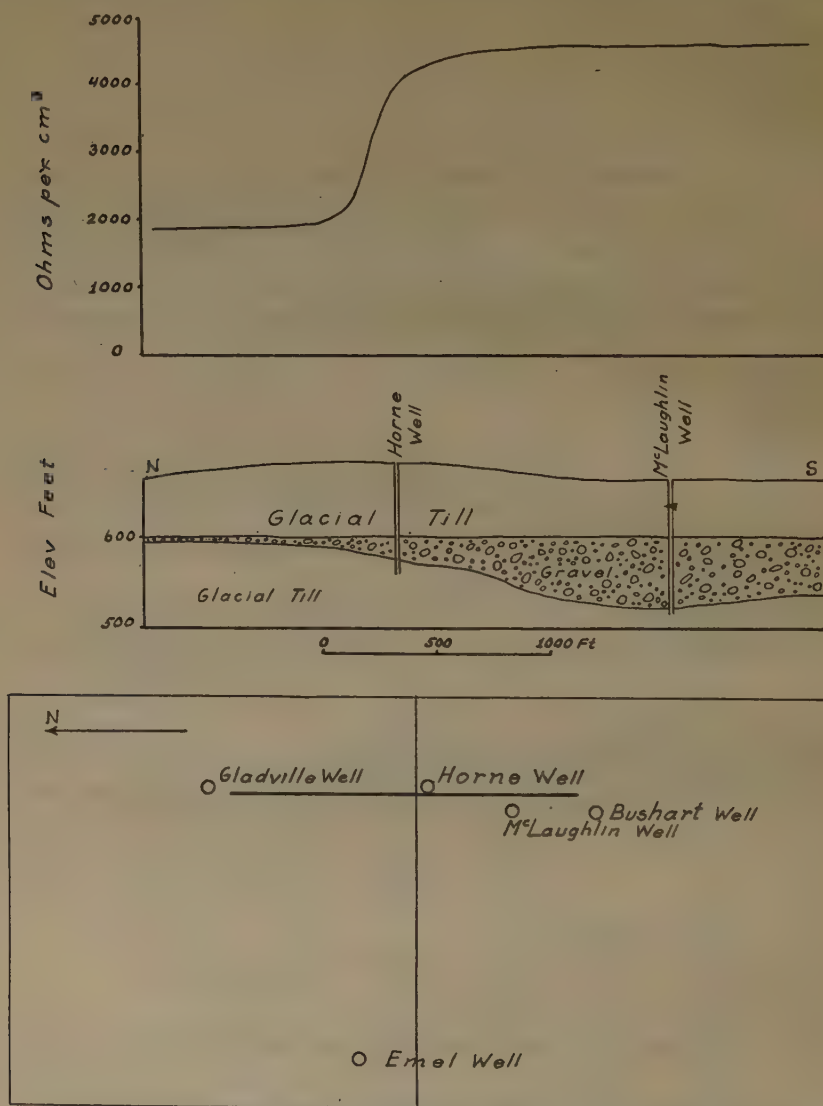


FIG. 9.—MAP, CROSS-SECTION AND PROFILE OVER BURIED WATER-FILLED GRAVEL DEPOSIT.

Note increase in apparent specific resistivity with increase in thickness of gravel deposit.

that there is a local resistant body that is deep enough to be imperceptible for small values of  $a$  but that is well within the region of influence for  $a$  equal to 200 ft. and more.

The hypothesis of gravel deposits as the most probable causes of these anomalies still seemed reasonable, so as a check upon the hypothesis a known gravel deposit was sought. The quarry used is shown in Fig. 8. Here gravel was being quarried from a 60-ft. wall of a delta deposit. Test pits of the quarry company showed that the deposit ended in the vicinity of the broken line in the diagram. A well to bedrock 700 ft. north of A' shows no gravel.

Two traverse profiles were taken, using  $a$  equal to 100 ft. and stations 100 ft. apart. The results are plotted in the upper part of the figure. In both profiles values of  $\rho$  ranging from 10,000 to over 30,000 ohms per cu. cm. are obtained over the gravel, while over the glacial till which contained no gravel normal values about 5000 ohms per cu. cm. are obtained. The points of separation between these high values and the normal values coincide almost exactly with the gravel boundary as determined by test holes.

The upper 60 ft. of gravel in the quarry was drained of water, and it was desired to have a test on a gravel bed known to be water-bearing. Such a bed is shown in Fig. 9. Here well records show about 8 ft. of gravel at a depth of 60 ft. over a large area. This gravel thickens downward rather abruptly to the southward. The profile shown is that of a longitudinal traverse having stations 100 ft. apart and  $a$  equal to 100 ft. The profile shows a uniformly low resistivity over the thin gravel and a high value over the thick part of the gravel.

Sherwin F. Kelly, in a personal communication to the author, reports mistaking a deeply buried gravel deposit for bedrock in a dam-site investigation, because of the high resistivity of the former.

### *Buried Anticlines*

In order to ascertain whether anticlines covered by glacial drift might be located by this method, the profile shown in Fig. 10 was taken. The geological cross-section was constructed from an unpublished subsurface map by A. H. Bell, of the Illinois State Geological Survey. The structure is an anticline with its central outcrop of massive Devonian limestone flanked on both sides by younger Mississippian and Pennsylvanian shales and sandstones. Over this is spread a very flat cover of glacial drift which, according to available well records, is of the order of 60 ft. thick over the limestone and 120 ft. over the shales and sandstones.

The electrical profile, which is about five miles long, was made, using  $a$  equal to 200 ft. and with stations 200 ft. apart. The profile was run in ignorance of the exact location of the anticlinal axis. The corresponding geologic cross-section was made from totally independent well record data. The exact coincidence between the peak of the curve and the limestone outcrop band is remarkable. While this constitutes only a first preliminary test in problems of this sort, it seems probable that



much valuable information concerning otherwise unknown anticlines beneath the glacial drift may be obtained in this manner.

### *Depth to Bedrock Determinations*

As was mentioned above, various attempts were made to determine the thickness above bedrock of the mantle of glacial drift. The method of measurement was that of taking depth profiles whereby at a given station  $\rho$  was determined as a function of  $a$  for values of  $a$  taken usually at increasing intervals of 20 ft. from 20 to 300 ft. It was found that for stations having Pennsylvanian shale as bedrock the value of  $\rho$  usually

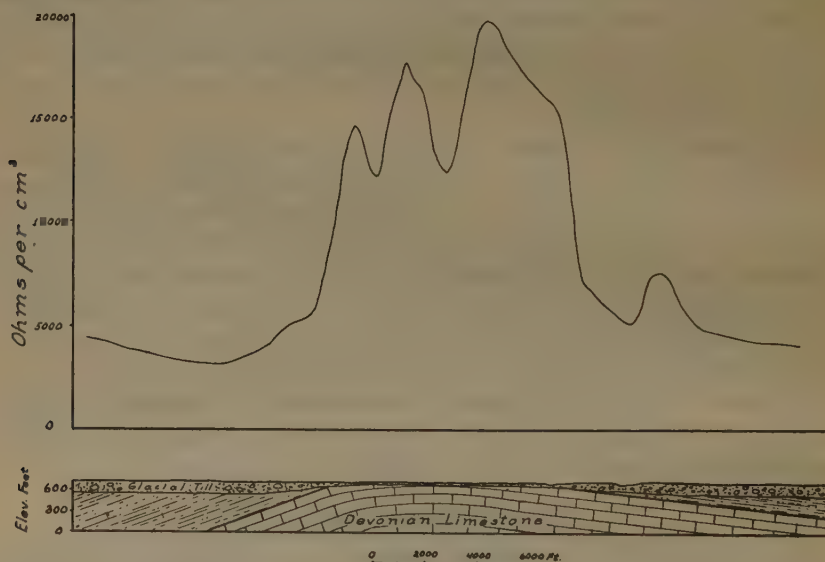


FIG. 10.—TRAVERSE PROFILE ACROSS BURIED ANTICLINE, TAKEN WITH ELECTRODE SPACING  $a$  EQUAL TO 200 FT. CAUSES OF SMALLER VARIATIONS ARE UNKNOWN.

went through a maximum and then declined somewhat for the greater values of  $a$ . This indicated that the shale was a slightly better conductor than the drift. For the few stations taken above limestone,  $\rho$  increased almost linearly with  $a$ .

Nothing revealed by a direct study of the depth curves could be correlated with the depth to bedrock as determined from well logs. What seems to be a more likely method for this purpose is that given by Tagg<sup>6</sup> which is based upon an earlier theoretical study by E. Lancaster-Jones.<sup>7</sup> The essence of Tagg's method is as follows:

<sup>6</sup> G. F. Tagg: The Earth-Resistivity Method of Geophysical Prospecting. *Min. Mag.* (1930).

<sup>7</sup> E. Lancaster-Jones: The Earth-Resistivity Method of Electrical Prospecting. *Min. Mag.* (1930).

Consider two horizontal uniformly conducting strata of different specific resistivities and separated by a plane horizontal interface.

Let  $\rho_a$  be the observed apparent specific resistivity,

$\rho_1$  specific resistivity of the upper stratum,

$\rho_2$  specific resistivity of the lower stratum;

$h$  thickness of the upper stratum;

$a$  the electrode spacing;

$$k \text{ the ratio } \frac{\rho_2 - \rho_1}{\rho_2 + \rho_1} = \frac{1 - \frac{\rho_1}{\rho_2}}{1 + \frac{\rho_1}{\rho_2}}$$

If  $a$  is taken small compared with  $h$ , the value of  $\rho_a$  so obtained is very nearly equal to that of  $\rho_1$ . It is possible, therefore, by this method to determine directly  $\rho_1$ . Hence, of the quantities enumerated above  $\rho_a$ ,  $\rho_1$  and  $a$  are directly determinable while  $\rho_2$  and  $h$  are the unknowns sought.  $k$ , being a function of  $\rho_1$  and  $\rho_2$ , is not a primary unknown.

Suppose such an arrangement as that described above wherein  $a$  and  $k$  are constant and  $h$  is allowed to vary. Then suppose that the ratio  $\rho_a/\rho_1$  is measured and plotted in a graph as a function of  $h$ . The curve so obtained will vary between the limits  $\rho_2/\rho_1$  for  $h = 0$  and  $\rho_1/\rho_1$  for very large values of  $h$ . If a similar curve is obtained for different values of  $k$  between its limits of  $+1$  and  $-1$ , a whole family of  $\rho_a/\rho_1$ ,  $h$  and  $k$  curves will be obtained for each value of  $a$ .

Suppose that such families of curves have been obtained for two or more values of  $a$ . Now for each of these values of  $a$  one can obtain

TABLE 1.—*Field Data for Determinations of Table 2*

Station 1		Station 2		Station 3		Station 4	
$a$ , Ft.	Ohms per Cu. Cm.	$a$ , Ft.	Ohms per Cu. Cm.	$a$ , Ft.	Ohms per Cu. Cm.	$a$ , Ft.	Ohms per Cu. Cm.
20	3,906	20	3,100	10	2,300	20	2,600
30	4,481	40	4,200	20	3,000	40	4,100
40	5,362	60	5,200	30	3,400	60	4,300
50	6,128	80	6,100	40	3,900	80	5,200
60	6,664	100	6,900	50	4,100	100	5,500
70	7,507	120	7,500	60	4,200	120	5,000
80	8,120	140	8,000	70	4,300	140	4,600
90	8,790	160	8,900	80	4,300	160	4,300
100	9,384	180	9,500	90	4,500	180	4,500
120	10,801	200	10,000	100	4,400	200	3,800
180	13,788	220	10,500	120	4,100	220	3,800
		240	11,500	140	4,300	240	3,700
		260	12,000	160	4,300	260	3,200
		280	12,600	180	4,100	280	3,200
		300	13,200	200	3,800	300	2,900

experimentally the corresponding value of  $\rho_a/\rho_1$ . When this value is supplied to the corresponding family of curves, the value of  $k$  as a function of  $h$  can be read off directly and plotted as a separate graph. If this operation is repeated for each of the two or more values of  $a$  for which curves have been constructed, the resulting  $h$ - $k$  graphs must when plotted together intersect at a point whose coordinates are the values of  $h$  and  $k$  sought.

Tagg has computed the families of curves for the values of  $a$  equal to 50, 100 and 150 ft. with all values of  $k$  at intervals of 0.1.

Tagg's method was applied to two stations having a limestone bedrock and to two having shale bedrock. In each case the depth to bedrock was obtained from near-by well logs. Tables 1 and 2 give the observational field data upon which the determinations are based. The limestone stations 1 and 2 (Fig. 11)<sup>8</sup> give very good intersections of the three curves but the errors of the results obtained for  $h$  as compared with the well-log depths are respectively 50 and 54 per cent. The shale stations 3 and 4 gave much more erratic results. For No. 3 the curves do not intersect at all and for No. 4 the triangle of error is large. The estimated error of station 4 is about 70 per cent.

TABLE 2.—*Determinations According to Tagg's Method*

Stations	Bedrock	Well Log Depth to Bedrock, Ft.	Calculated Depth to Bedrock, Ft.	Percentage of Error
1	Limestone	60	30	50
2	Limestone	100	46	54
3	Shale	90		
4	Shale	160	50	70 $\pm$ 15

Assuming that the computed families of curves are correct, there is no question that the method otherwise is theoretically sound. The discrepancies seem therefore to be due to the fact that the geological cases used are not close enough approximations to the conditions assumed in the theory. It is hoped that additional field work may yet produce results that will show a more satisfactory agreement.

#### *Performance of Instrument*

The Megger Ground Tester used in these investigations is light, compact, durable, and very simple and convenient to operate. Its chief limitations are its scale ranges. The scale reads  $R = \frac{E}{I}$  directly in ohms and there are four ranges 0 to 3, 0 to 30, 0 to 300 and 0 to 3000 ohms.

In Paleozoic sediments, values of apparent specific resistivity rarely fell outside the ranges of 5000 to 50,000 ohms per cu. cm. In glacial till,

<sup>8</sup> The writer is indebted to Mr. A. N. Labounsky for computing these curves and for the drafting of all of the illustrations used in this paper.



the range of values lay between 3000 and 6000 ohms per cu. cm. Hence it is rare that any work requires the use of any but the 0 to 3 ohms range and by far the greater part falls within 0 and 0.3 ohms.

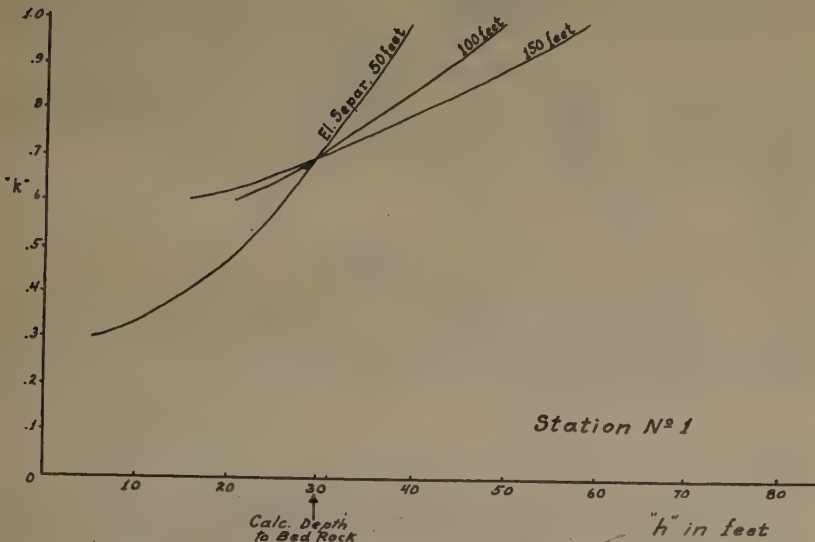
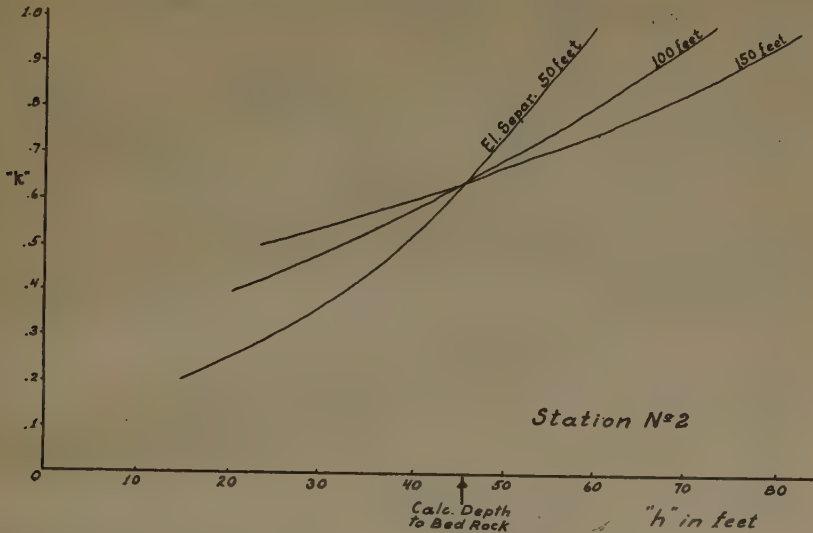


FIG. 11.—CURVES FOR DETERMINATION OF DEPTH TO BEDROCK OF LIMESTONE BY TAGG'S METHOD.  
Point of intersection of curves gives computed values of  $h$  and  $k$ .

It is evident that this rigorously limits the maximum electrode separation  $a$  that can be used on any particular problem. It is extremely unsafe to use the instrument for readings less than the first scale division. Therefore if we take the mean apparent specific resistivity of glacial

drift to be 5000 ohms per cu. cm. the electrode spacing  $a$  for a reading of one scale division, or 0.1 ohm, will be

$$A_{\max} = \frac{\rho}{2\pi R} = \frac{5000}{2\pi \times 0.1} = 79.6 \text{ m. or } 262 \text{ ft.}$$

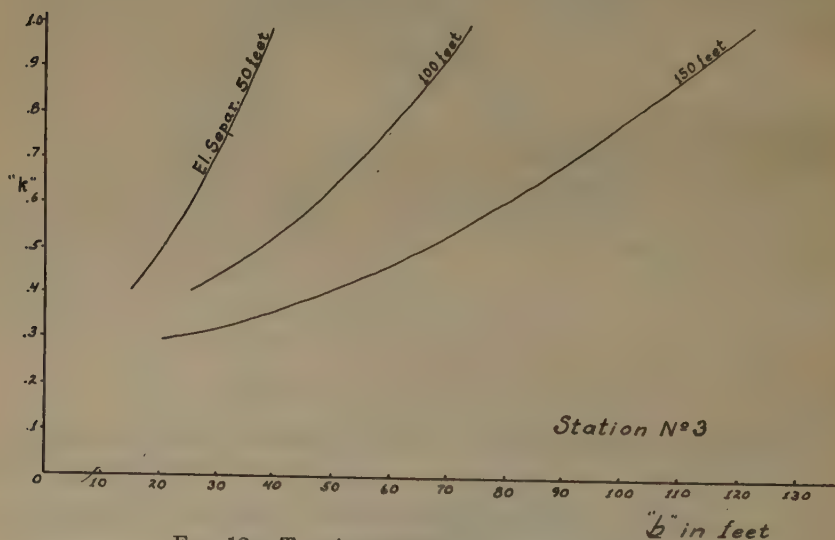
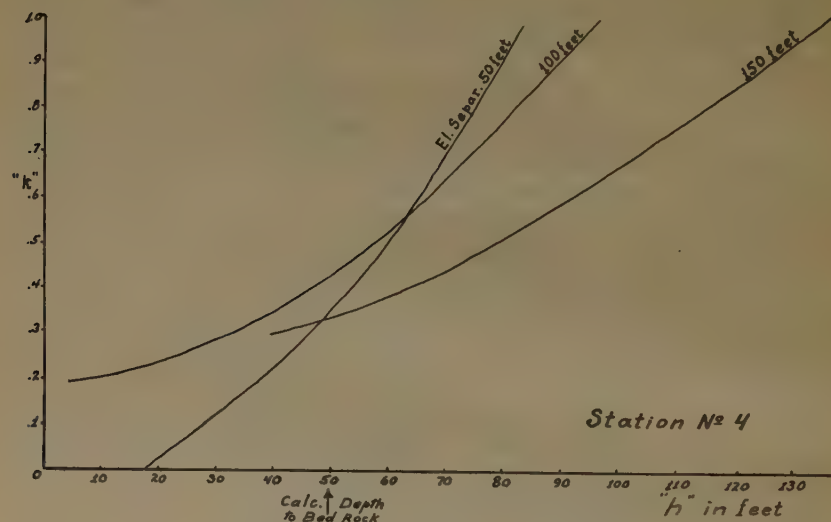


FIG. 12.—TAGG'S METHOD FOR SHALE STATIONS.

For Paleozoic sediments taking  $\rho$  equal to 25,000 ohms per cu. cm. and  $R$  equal to 0.1 ohm,

$$A_{\max} = \frac{\rho}{2\pi R} = \frac{25,000}{2\pi \times 0.1} = 398 \text{ m. or } 1310 \text{ ft.}$$

In the actual work done in Illinois a maximum value of  $a$  equal to 300 ft. was found to be about the practicable limit for most of the work. At present, if greater ranges are desired it is practically necessary to supplement this instrument with some form of Gish-Rooney apparatus.

### SUMMARY AND CONCLUSION

Three types of problems were investigated by the earth-resistivity method of Wenner and that of Gish and Rooney; namely, (1) faults in Paleozoic sediments, (2) gravel deposits and ground-water supply in glacial drift, and (3) anticlines buried beneath glacial drift.

It was found that faults could be discovered especially if the outcrops on the opposite sides were different, or if there were a considerable shear zone associated with the fault plane. Some minor faults shown on the geological map that had the same formation outcropping on both sides were not detected.

It was found that major gravel deposits having fairly sharp boundaries, even if full of water and buried under considerable till cover, could be detected readily because of their relatively higher specific resistivity. It was found also that the one buried anticline tested gave a pronounced anomaly which coincided with the anticlinal axis as independently determined from well-log data. Attempts at precise depth determinations have not as yet been successful.

It seems, therefore, that for problems of this nature this method of investigation has, in spite of its limitations, fairly demonstrated itself to be a highly useful and economical means of at least doing reconnaissance work and is capable of supplanting a great deal of more expensive means of investigation.

### DISCUSSION

*(Donald H. McLaughlin presiding)*

J. H. SWARTZ,\* Washington, D. C.—Referring to your experiment with the thin conductive sheet in the tank of water, did you measure the resistivity of the water with no metallic conductor in it?

M. K. HUBBERT.—No.

J. H. SWARTZ.—We performed some experiments of much the same character, and measured the water resistivity. We discovered that the resistivity of the water was the same as the peak obtained when the sheet was between the potential electrodes. In other words, the sheet of metal, being very thin and occupying exactly the position of the median equipotential surface, does not disturb the distribution of current. We also used the Lee partitioning method, and found the two halves of the field decidedly asymmetrical when the plate was not in the center. If the sheet is not at the midpoint between the two potential electrodes, the Wenner calculations are not applicable because the sheet distorts the field.

---

\* U. S. Bureau of Mines.



MEMBER.—I am surprised at the peaks of resistivity being obtained in the field over water-bearing gravel.

J. H. SWARTZ.—That is undoubtedly due to the purity of the water in the gravel.

E. G. LEONARDON,\* Paris, France.—It is quite normal. We have found that water-bearing gravel has a high resistance as a rule.

T. ZUSCHLAG,† New York, N. Y.—I have carried out a number of experiments with different thicknesses of conductive and resistant vertical sheets, placing them between the potential electrodes. With a thick sheet, there is a pronounced sag in the curve, which gradually becomes less as the thickness is decreased. After a certain point, the sag passes through a flat stage, to turn into a peak. Substituting a resistant sheet for the conductive one, the peak continues to rise in height as the thickness of the sheet is increased.

H. N. JOHNSON,‡ Los Angeles, Calif.—I am not a geophysicist, but as a geologist I have had some experience in attempting to interpret geophysical data. Mr. Hubbert's

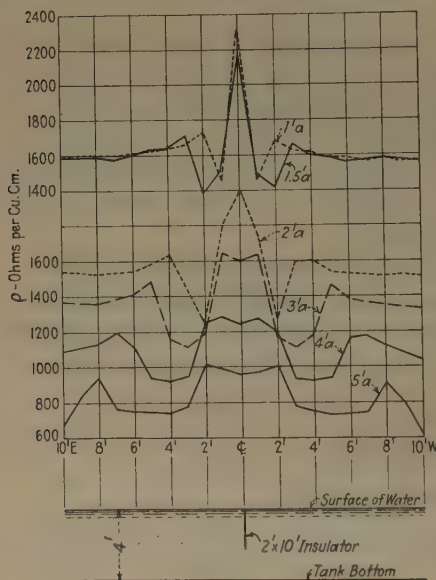


FIG. 13.

humps and depressions, which have been thus interpreted, belong in reality to this class.

Vertical bodies are not the only ones that cause erratic anomalies. A small horizontal insulator beneath and between a current electrode and the adjoining potential electrode raises the value of  $\rho$  above normal, and when located between the potential electrodes lowers the value of  $\rho$ . A small horizontal conductor has the same effect, though to a lesser degree.

Figs. 1 and 2 introduce a subject which has not, I believe, received the attention it deserves; that is, the effects of small inhomogeneities near the surface along the line of an electrical traverse. These figures show that the presence of a narrow vertical conductor between either current electrode and the adjoining potential electrode lowers the value of  $\rho$ , and when between the potential electrodes it increases the value of  $\rho$ .

Identical results would have been obtained had the vertical conductor been replaced by a similar insulator, as the accompanying profiles (Fig. 13) over such an insulator clearly show. In either case, the curves for the individual stations showing the values of  $\rho$  plotted against the corresponding  $a$  spreads would be misleading if interpreted as indicating the relative resistivity of the volume beneath the station location to depths corresponding to the lengths of  $a$ . I have suspected that some of the published curves with

\* Société de Prospection Électrique.

† Research Engineer.

‡ Geologist.

We have a complicated problem when attempting to make geological interpretations of resistivity data which not only represent variations of resistivity with depth but which are influenced also by the shape, size, and the relative location of finite bodies near our traverse lines.

W. B. CREAGMILE,\* Philadelphia, Pa. (written discussion).—Results reported by Low, Kelly and Creagmile, as referred to by Mr. Hubbert (footnote 5) were obtained with conducting and nonconducting sheets placed horizontally under water at various depths, and with the electrodes at various spacings. Where a conducting body was placed between the two potential electrodes, it was of considerable thickness and volume, and so gave a lowered value of  $\rho$  as expected.

Mr. Hubbert's tests to determine depth to bedrock are of particular interest. If  $a$  (spacing in feet of the electrodes) and  $\rho$  (ohms per centimeter cube) as given in Table 1 are plotted in the form of curves, we see that the curves for stations 1 and 2 are of one general form; and the curves for stations 3 and 4 are of a different general form. For stations 1 and 2, the data show that as  $a$  is increased there is a decided change in  $\rho$ , always in the same direction. This is also true (if surface effects are neglected) for the tests reported by Tagg.<sup>9</sup> In one of Tagg's tests  $\rho$  decreases as  $a$  is increased; in his other test and in Hubbert's tests at stations 1 and 2,  $\rho$  increases as  $a$  is increased. However, the change is very definite in all four cases. When results are worked out by Tagg's method for these four tests, curves plotted between  $k$  and  $h$  meet in an approximately common point. Why the calculated depths to bedrock in Hubbert's tests at stations 1 and 2 do not agree closely with the known depths, I cannot say, but believe it may have to do with the value of  $\rho_1$  selected for the upper stratum.

For stations 2 and 3, the data show that as  $a$  is increased  $\rho$  first increases and then decreases, although the change is slight. Under this condition the value to be chosen for  $\rho_1$  is very indefinite. It seems to me the form of the curves may indicate the presence of more than two strata, or a considerable lack of uniformity electrically in one or both strata if only two are present. Either effect might account for the curves between  $k$  and  $h$  plotted according to Tagg, failing to meet near a common point.

Tagg's method of calculation seems sound. I agree with Mr. Hubbert that what we need is additional field work and experience in selecting the correct value for surface resistivity  $\rho_1$ . This will surely enable us to apply the method with a much greater degree of certainty.

It is encouraging to note that an outfit so easy to use as the Megger Ground Tester, and of such small size and light weight, has demonstrated itself to be highly useful and economical in the survey. I believe it is not too much to expect that the instrument, the method of application and the interpretation of results obtained may all be subject to improvement in the near future, so that the Megger will be much used in geophysical surveys by the resistance method.

K. SUNDBERG,† Stockholm, Sweden.—Could not the discrepancies between the predicted and the actual depth to bedrock be accounted for by irregularities in the bedrock, or changes in the overlying glacial drift?

M. K. HUBBERT.—I cannot answer that question entirely, as the only data we have to go by are the neighboring well logs and the subsurface maps made up from them. These show that we are over a solid, homogeneous limestone. Variations may occur,

\* James G. Biddle Co.

<sup>9</sup> G. F. Tagg: Interpretation of Resistivity Measurements. See page 135, this volume.

† Chief Engineer, A. B. Elektrisk Malmletuing.

however, in the overburden. I did not have a chance to test these questions out in the field with Tagg's formulas, because his paper did not come to my attention until after the field season was over.

F. W. LEE,\* Washington, D. C.—When carrying out resistivity work, it should be kept in mind that several factors have to be left out in connection with the simplifying assumptions necessary to the interpretation. All such formulas as these assume the resistivity to be constant, whereas it actually varies in different directions.

E. DE GOLYER,† New York, N. Y.—Can you depend upon the geological interpretations of the geophysical readings? For example, it seems to me that the curves obtained over anticlines and faults are somewhat similar, and that you might interpret a fault under that big W on the graph of resistivity for your anticline.

M. K. HUBBERT.—The W obtained over a fault is complete in three stations, whereas the big W over the anticline was spread out over several stations 200 ft. apart. Whether or not given high readings are due to buried strips of gravel can be determined by spreading the electrode separation to see if the strip is underlain by conductive material. In this region, the gravel is followed in depth by more conductive material. Thus, it behooves the geophysical prospector to determine the conditions that obtain in a given region, by cut and try methods, if necessary.

E. G. LEONARDON.—Dr. Lee said that the resistivity of a formation may change according to the direction in which it is measured; that is, there is a resistivity trans-

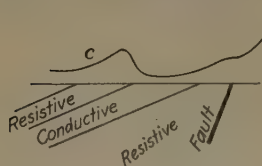


FIG. 14.

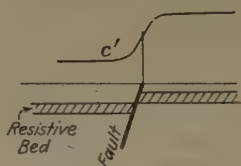


FIG. 15.

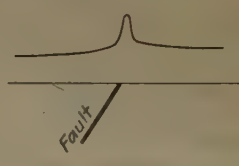


FIG. 16.

verse to the bedding, and another along it. Therefore, if a survey deals with a region underlain by tilted strata, measurements of the resistivity in two directions are not comparable.

There is a question of nomenclature introduced by Mr. Hubbert's paper. I should like to suggest that when the resistivity measurements are being taken by moving the same length of line across country, we call this a "horizontal exploration." If an expanding electrode separation is being used for the purpose of determining the resistivities at increasing depth, we could call it a "vertical exploration" or a "vertical electrical drilling."

In the matter of detecting faults and inclined beds at the same time, it should be remembered that a fault and a series of tilted beds constitute two different disturbing factors, which cannot be easily separated.

For instance, if we have to deal with a series of inclined beds alternatively resistive and conductive, the resistivity profile across the formations will be a curve like C in Fig. 14.

Things will be different, however, if we consider the case of horizontal or approximately horizontal formations. In such case, each of the two compartments will show regular resistivity figures and the appearance of the resistivity profile will be somewhat similar to the one shown on Fig. 15.

\* U. S. Bureau of Mines.

† Petroleum Geologist.



E. DE GOLYER.—What is the effect of an inclined fault plane, say dipping 45°?

E. G. LEONARDON.—It will depend on the character of the two compartments of the fault. Should the two compartments be distinctly differentiated, the phenomenon will *electrically* appear as shown on Fig. 15; if not, the fault may simply show a resistance of passage to the current (Fig. 16).

H. N. JOHNSON.—We made some small-scale tests of the effect of the displacement of resistors by submerging in water two 6 by 12-ft. horizontal insulators 3 ft. and 2 ft. deep respectively, with the 12-ft. edges on either side of a line, and running an electrical traverse across them. The profiles for the various  $\alpha$  spreads of this traverse indicated the presence of each insulator by increased values of  $\rho$  and the zone of displacement by lower values of  $\rho$ .

E. DE GOLYER.—In all this work it should be kept in mind that the task of the geophysicist is to collect a certain type of information. When this is done, he specifies what conditions must be fulfilled by the underground formations to produce these phenomena. It is the business of the geologist to guess the geological conditions that fulfill the terms thus imposed, and which is most likely to occur. So far, the most successful work has been in the seismic exploration for salt domes in the Gulf Coast fields.

G. F. TAGG,\* London, England (written discussion).—I am particularly interested in Mr. Hubbert's efforts to determine the depth to bedrock, using the method I suggested, based on the theory for a single horizontal stratum. By the application of my theoretical curves, Mr. Hubbert has obtained what would be considered very accurate agreement in the final curves of Fig. 11, and it is extremely unfortunate that the results so obtained should be only one-half of the value as given by a near-by well log. The three curves deduced from the theoretical curves intersect in a point for both stations 1 and 2. This is in fact a much better intersection than that given in Figs. 5 and 7 of my paper.<sup>10</sup> A small triangle of error is usually to be expected.

I have carefully checked the theory and the computed curves on which the method of interpretation is based. These are quite correct. If some other form of geological structure, such as a vertical body or even a sloping stratum, were producing the results given in Table 1, the point of intersection given in Fig. 11 would not have been obtained, and a result somewhat similar to that given in Fig. 12 for station 3 would be expected. The mere fact that the three curves intersect in a point is a fairly good proof that the stratum in question is a single horizontal one. The error is practically the same for both stations, and it therefore appears that in some way a factor of two has been overlooked in the results.

On the other hand, it would be interesting to know how near the well logs were to the stations, although if the depths given by these well logs are correct, and the values given by the theory are also correct, the well logs would have to be a considerable distance from the stations for the stratum to behave as if it were perfectly horizontal.

I trust that some further depth determinations will be made using this method, as I feel that only methods based on theory can be satisfactorily employed for this purpose.

M. K. HUBBERT (written discussion).—The computations using Tagg's method for stations 1 and 2 have since been rechecked independently to see if, as Mr. Tagg suggests, a factor of two could have been overlooked. No such error has been found. Other solutions have been tried using various values for the surface resistivity. These have not helped appreciably.

---

\* Evershed & Vignoles Ltd.

<sup>10</sup> See pages 142 and 144.

The stations were in each case less than 200 to 300 ft. from the well of which the log was used. The data from other well logs in the region indicate that the bedrock surface undulates but gently. Inspection of the resistivity data makes it appear that the trouble lies in not having a two-layer case to work with.

J. M. PEARSON,\* Philadelphia, Pa. (written discussion).—Mr. Hubbert has used the only reasonable approach to the rather complex field of interpretation of electrogeophysical phenomena. He has determined what independent variables control the readings of his instrument, and then has found experimentally the effect of each variable, and its usefulness in making geological interpretations. As is usual, he finds that theoretical predictions, based upon simplifying assumptions, are fulfilled at best only in order of magnitude.

I should like to suggest a fourth variable,  $T$ , the period of reversal of the commutating system. A simple consideration of dimensions shows that if:  $E$  = potential difference between the potential stakes;  $\rho$  = resistivity in ohm-centimeters;  $A = 3a$  = spacing of current stakes;  $\mu$  = permeability of ground; and  $t$  = time in seconds needed for  $E$  to settle to within a given fraction of its steady state value after the current circuit is closed;

$$t = k \frac{\mu A^2}{\rho}$$

where  $k$  = constant (dimensionless)

$\mu \cong 1$  for most rock.

From Conrad and Marcel Schlumberger's work in resistivities at great depths  $k = 2.32 \times 10^{-6}$  approximately when  $t$  is the time it takes the difference  $E - E_{\text{steady}}$  to reduce to  $E - E_{\text{steady}} = \frac{1}{e}(E_{\text{max.}} - E_{\text{steady}})$ .

From this it would seem that, for the electrode spacing used by Mr. Hubbert the order of magnitude of the time of duration of the transitory state is so small as to make this time insignificant compared to  $T$ . However, as this type of measurement is made on an increasing scale, the variable  $T$  rapidly makes itself felt. We can see, therefore, that any investigations of very deep structures by means of a rapidly commutated direct current will have to be regarded from an electromagnetic point of view rather than from the point of view of steady direct current. This means the introduction of the variables  $T$ , period of reversal, and  $\phi$ , phase relationship of commutators, etc., into the hitherto comparatively simple picture.

L. G. HOWELL,† Houston, Tex. (written discussion).—In the paper under discussion, Hubbert has employed the Gish-Rooney method in obtaining electrical resistivity results, some of which, it seems, should be considered in further detail; in particular, the results that he obtained in the laboratory and used for explaining the data obtained in making surveys in the field. In the Gish-Rooney<sup>10</sup> method of geophysical exploration four electrodes are placed in the surface of the ground along a straight line in such a manner that the three segments between successive electrodes are equal. A measured direct current (which may be reversed rather rapidly) is passed through the two extreme electrodes with the ground as the conducting medium and the difference of potential set-up between the two inner electrodes is measured.

Then

$$\rho_a = 2\pi a \frac{V}{I} \quad [1]$$

\* Sun Pipe Line Co.

† Geophysics Research Dept., Humble Oil & Refining Co.

<sup>10</sup> O. H. Gish and W. J. Rooney: *Terrestrial Magnetism and Atmospheric Electricity* (1925) **30**, 161-188.

where  $\rho_a$  is the so-called "apparent resistivity" of the ground,  $a$  is the length of the segment between successive electrodes,  $V$  is the difference of potential between the two potential electrodes and  $I$  is the current flowing through the two current electrodes. For a homogeneous ground of resistivity  $\rho_0$ , eq. 1 reduces to the Wenner<sup>11</sup> equation and

$$\rho_a = \rho_0$$

Hubbert carried out some measurements on a small scale ( $a = 6$  in.) with water as a medium instead of the ground. He found that when a metal sheet was placed midway between the potential electrodes at right angles to the line of the electrodes  $\rho_a$  was greater than the normal resistivity; when the electrodes were moved so that the sheet was between a potential and a current electrode the resistivity was less than the normal resistivity; and, finally, as the electrodes were moved away from the sheet  $\rho_a$  approached the normal value.

Since the result that the value of  $\rho_a$  was increased when the sheet was placed between the potential electrodes is unexpected, let us consider the theory of such measurements.

### THEORETICAL RESULTS

As is well known, the solutions of current flow are analogous to the solutions of electrostatic fields.<sup>12</sup> Let the perfectly conducting sheet of thickness very small in comparison to  $a$  and of infinite extent in the other two dimensions be situated between the potential electrodes  $P_1$  and  $P_2$  at a distance  $x$  from the origin  $O$  as shown in Fig. 17.

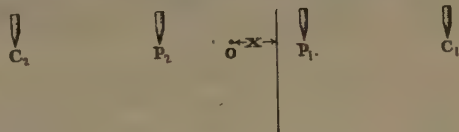


FIG. 17.

If  $I$  is the current and  $\rho_0$  is the resistivity of the medium, then the potential  $U_1$  at  $P_1$  is due to the pole  $\frac{I\rho_0}{2\pi}$  at  $C_1$  and in addition to its image  $-\frac{I\rho_0}{2\pi}$  at the mirrored distance  $\frac{3}{2}a - x$  to the left of the sheet. Thus,

$$U_1 = \frac{I\rho_0}{2\pi} \cdot \frac{1}{a} - \frac{I\rho_0}{2\pi} \cdot \frac{1}{(2a - 2x)}$$

The potential  $U_2$  at  $P_2$  is due to the pole  $-\frac{I\rho_0}{2\pi}$  at  $C_2$  and its image  $\frac{I\rho_0}{2\pi}$  at the mirrored distance  $\frac{3}{2}a + x$  to the right of the sheet.

$$U_2 = -\frac{I\rho_0}{2\pi} \cdot \frac{1}{a} + \frac{I\rho_0}{2\pi} \cdot \frac{1}{(2a + 2x)}$$

$$V = U_1 - U_2 = \frac{I\rho_0}{2\pi a} \left[ \frac{a^2 - 2x^2}{a^2 - x^2} \right]$$

From equation 1,

$$\frac{\rho_a}{\rho_0} = \frac{a^2 - 2x^2}{a^2 - x^2} = 1 - \frac{x^2}{a^2 - x^2} \quad 0 \leq x \leq \frac{a}{2} \quad [2]$$

By similar calculations the value of  $\rho_c/\rho_0$  can be obtained for the case of the sheet between  $P_1$  and  $C_1$ ,

$$\frac{\rho_a}{\rho_0} = \frac{1}{2} \left[ 1 + \frac{a^2}{(a + 2x)(a + x)} \right] \quad \frac{a}{2} \leq x \leq \frac{3}{2}a \quad [3]$$

<sup>11</sup> F. Wenner: U. S. Bur. Stds. *Bull.* 258 (1916).

<sup>12</sup> A. B. Broughton Edge and T. H. Laby: *Geophysical Prospecting*, 250. Cambridge, 1931. University Press.

and for the case of the sheet beyond  $C_1$ ,

$$\frac{\rho_a}{\rho_0} = 1 - \frac{3a^2x}{(4x^2 - a^2)(x^2 - a^2)} \quad x \geq \frac{3}{2}a \quad [4]$$

In equations 2, 3 and 4  $x$  is always taken positive and may be measured either to the right or to the left of  $O$ , since we have symmetry about that point.

It might also be interesting to consider the results obtained by substituting a thin perfectly insulating sheet for the conductor. With the conductor the tangential

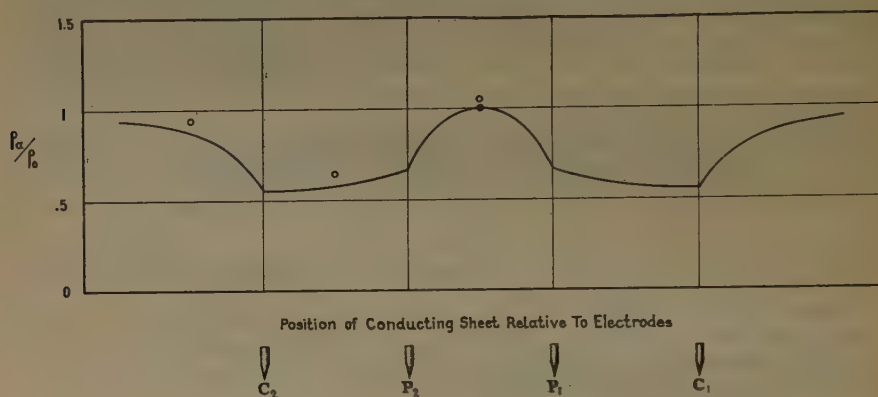


FIG. 18.

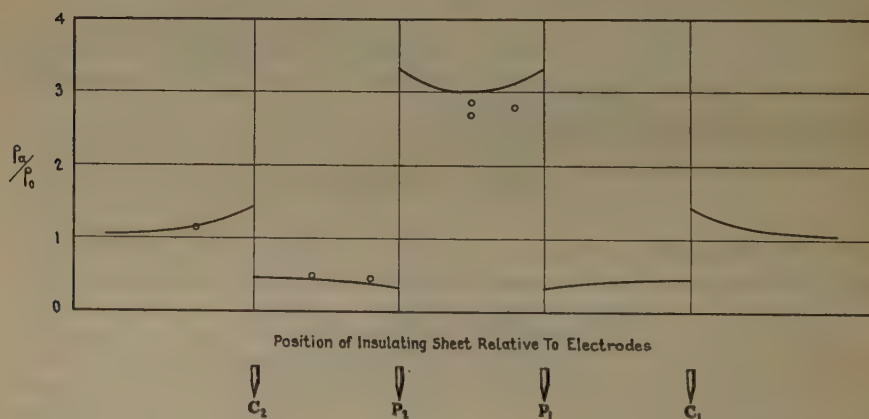


FIG. 19.

component of the current flow at the surface of the conductor is zero while for an insulator the normal component at its surface is zero. Thus the image of a pole obtained with the insulating sheet has the same algebraic sign as well as the same strength as the pole. We now obtain for the insulating sheet of small thickness and of large dimensions in the other two directions in comparison to  $a$ , assuming that charges do not collect on the insulator and that a pole does not influence the potential in the medium on the other side of the sheet



$$\frac{\rho_a}{\rho_0} = 3 + \frac{x^2}{a^2 - x^2} \quad 0 \leq x < \frac{a}{2} \quad [5]$$

$$\frac{\rho_a}{\rho_0} = \frac{1}{2} \left[ 1 - \frac{a^2}{(a + 2x)(a + x)} \right] \quad \frac{a}{2} < x < \frac{3}{2}a \quad [6]$$

$$\frac{\rho_a}{\rho_0} = 1 + \frac{3a^2x}{(4x^2 - a^2)(x^2 - a^2)} \quad x > \frac{3}{2}a \quad [7]$$

Again as before  $x$  is taken as positive in either direction. Figs. 18 and 19 show the theoretical curves obtained for a perfectly conducting sheet and a perfectly insulating sheet, respectively. In the ordinate direction the ratio  $\rho_a/\rho_0$  of the apparent resistivity to the resistivity of the medium is plotted while in the abscissa direction the position of the sheet relative to the electrodes, which are placed as shown, is plotted.

### EXPERIMENTAL RESULTS

Measurements were made in order to confirm the theoretical curves. Tap water about one foot in depth in a wooden tub approximately one yard in diameter was used as the medium of which the resistivity was to be measured. Four pointed copper electrodes were used with a spacing of 5 in. The current was measured with a milliammeter and the difference of potential determined with a potentiometer. Readings were taken with the current flowing in one direction and then with the current reversed.

The circles shown on Fig. 18 represent experimental points taken using a copper sheet  $\frac{1}{64}$  in. thick. Also, experimental points are shown in Fig. 19 for a bakelite sheet  $\frac{1}{32}$  in. thick. Although the experimental accuracy was not of a high degree, the points in the main lie fairly close to the theoretical curve. Therefore we can conclude that under perfect experimental conditions the experimental points would lie on the theoretical curve.

It is very likely that the surface of the metal sheet that Hubbert used was not sufficiently clean, and thus he obtained a value of  $\rho_a$  greater than  $\rho_0$  for a position of the sheet midway between the potential electrodes because his sheet was not perfectly conducting. It seemed that the copper sheet that we used acted more nearly as a perfect conductor when it was cleaned with acid. The value of  $\rho_a/\rho_0$  obtained with an aluminum sheet placed midway between the current electrodes was 2.2. After the sheet was washed with alcohol and a solution of potassium hydroxide, the value of  $\rho_a/\rho_0$  dropped to 1.3. It must be remembered that a very thin film of grease forms a good insulating surface. Also, galvanic effects might become disturbing, if there are impurities on the surface of the plate in the presence of an electrolyte. Again, polarization at the electrodes may influence the results.

In conclusion, it may be stated that Figs. 18 and 19 seem to represent the true picture of resistivity measurements obtained under ideal conditions with a perfectly conducting and a perfectly insulating sheet when each is moved with its plane kept at right angles to the line of the electrodes to various positions with respect to the electrodes. The condition of the surface of the sheet plays an important role in such measurements; for example, a very thin film of grease can form a highly insulating surface on a material which itself is highly conducting. Also, the measurements may be influenced when the lines of current flow are disturbed by the collecting of charges on the surface of the plate or by the setting up of electromotive forces between the impurities on the sheet and the electrolyte of the medium. Still another disturbing effect is polarization at the electrodes.

The writer wishes to acknowledge his indebtedness to Dr. L. W. Blau for suggestions in the experimental work.

M. K. HUBBERT (written discussion).—I am extremely appreciative of Mr. Howell's settling of the problem that I raised regarding the resistivity of a thin metal sheet in a tank of water.

Subsequent theoretical analysis both by myself and others has yielded the same results as those presented by Mr. Howell. Thanks are due him even more for indicating what almost certainly is the real cause; namely, the grease film on the metal plate. The plate used was one picked up around a mine. It was not specially cleaned and in all probability was covered by a grease film sufficient to account for the observed resistivity peak.

S. F. KELLY,\* New York, N. Y.—It seems to me that in discussing the discrepancy between Hubbert's depth determinations and the depth to the limestone stratum as *assumed* from well-log data, we are straining at a gnat and swallowing a camel. Previous speakers have mentioned the possibility that the assumed depth may not be accurate. I would stress this point. Where the *assumed* depth departs

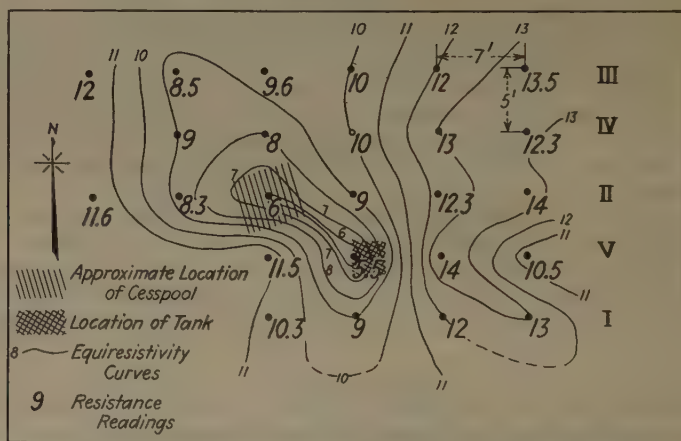


FIG. 20.—LOCATING BURIED TANK BY RESISTANCE READINGS WITH A MEGGER GROUND TESTER.

The lines of equal resistance, based on the readings taken, are shown on the map.

so radically from an electrical depth determination that has all the signs of being a good one, I should be inclined to credit the electrical data. It should be remembered that we are dealing with a limestone area, and if the top of this formation represents an old erosion surface, hills and valleys in that surface may easily bring about a difference in elevation sufficient to account for the discrepancy. Furthermore, if the old surface were of a typically karst topography, abrupt differences in elevation would be quite in order. Glacial erosion may have played its part in scouring out irregularities in the soft limestone, too. However, before finally blaming either the electrical measurements or the limestone for the difficulty, we need more information on the subsurface topography, and on the distance of the well from the site of the electrical determination.

Although not directly related to Mr. Hubbert's paper, the following incident is interesting because it illustrates the use of the Megger Ground Tester. Mr. Bela Low has a country place at Katonah, Westchester County, N. Y., in the grounds of which he buried a septic tank some years ago. In the summer of 1931 it became advisable to locate the tank, but the stake that had been erected to mark its location had dis-

\* Geologist and Geophysicist, Low & Kelly.

appeared, therefore we made some resistivity measurements with a Megger. The tank is of steel, about 4 ft. on an edge. An area approximately 20 by 40 ft., within which it was known to lie, was marked off with three lines 5 ft. apart, and stake intervals set out along these lines at 7-ft. separations. Resistance measurements were then made in the usual manner, with the results shown in the diagram (Fig. 20). A low value of 6 ohms was observed at a point on line II. (Since the stake interval was constant, the resistance readings have not been converted from ohms to resistivities in meter-ohms). A steel rod was thrust into the ground there, and broke through the rotted top of an old cesspool, now filled with mud. Evidently the wet mud had given the low resistance at that point. Intermediate lines IV and V were then run between lines II and III, and between I and II; a new set of resistances was then read. A still lower value than before, 5.5 ohms, was this time observed on line V. A few minutes' work with a shovel at this point revealed the top of the steel tank at a depth of about one foot.

# Location of Faults in Hardin County, Illinois, by the Earth-resistivity Method\*

BY M. KING HUBBERT,† NEW YORK, N. Y. AND J. MARVIN WELLER,‡ URBANA, ILL.

(New York Meeting, February, 1934)

PRELIMINARY investigations were undertaken with a Megger Ground Tester in 1931 by Hubbert to determine whether the faults in Hardin County, Illinois, could be located by earth-resistivity surveys. The results of these investigations, which were in part presented before this Institute in 1932,<sup>1</sup> were sufficiently promising to warrant a more extensive field program in the same general area the following summer.

During the second season an apparatus of the Gish-Rooney type was employed because of its greater sensitivity and to avoid the troublesome correction for resistance of potential electrodes necessitated by the use of a Megger instrument.

The discussion of earth-resistivity traverses which constitute the main part of this paper is based entirely upon the results of the second season's work. All of the traverses were made with a constant electrode spacing of  $a$  equal to 100 ft., and the four-electrode technique was employed. Successive stations in these traverses were spaced at intervals of 100 ft. and the line of electrodes was carried parallel to the line of traverse.

The graphs of resistivity profiles presented here (Figs. 1 to 3) are plotted with resistivities in ohm-centimeters as ordinates and with distance divided into stations at 100-ft. intervals as abscissas.

After the traverses were run by Hubbert the results were computed, the profiles plotted, and tentative interpretations were made by him. These curves and interpretations were then taken into the field by Weller, who made a careful geological examination along the lines of traverse for the purpose of checking and supplementing Hubbert's interpretations. Weller then constructed a geologic cross-section extending along the line of each traverse. The accompanying diagrams graphically illustrate the correlation that can be made between earth resistivity and geology in this area.

---

Manuscript received at the office of the Institute May 22, 1934.

\* Published by permission of the Chief, Illinois State Geological Survey.

† Instructor in Geophysics, Columbia University; Associate Geologist, Illinois State Geological Survey.

‡ Geologist and Head, Stratigraphy and Paleontology Section, Illinois State Geological Survey.

<sup>1</sup> M. K. Hubbert: See page 9, this volume.



## GEOLOGY OF HARDIN COUNTY

The geological formations throughout most of Hardin County consist of a series of alternating sandstone and limestone-shale units, most of which vary from 50 to 200 ft. in thickness. These rocks are cut by an intricate system of nearly vertical faults and the more important known fluorspar deposits, which make this area one of the world's leading sources of fluorspar, occur as veins that follow a few of these faults near Rosiclare.

Because of the known association of the fluorspar veins with faults, an accurate knowledge of the fault pattern is essential to future efficient prospecting. The bedrock of this region, however, is generally mantled by considerable thicknesses of residual material, loess and alluvium, so that in many parts outcrops are rare. Furthermore, the limestones, sandstones and shales that are exposed do not possess physical characters that make it easy to distinguish and correlate them. Consequently the geological mapping of the faults in this area is difficult and requires much careful observation and an intimate acquaintance with the stratigraphic section. Even so the accuracy of the map depends largely upon the distribution and nature of the outcrops.

A geological survey of Hardin County was made by Stuart Weller and a report and geologic map were published in 1919.<sup>2</sup> This map shows the distribution of the known faults. Most of the larger faults are probably shown but undoubtedly there are many minor faults that have not yet been discovered, and as there is no relation between the magnitude of displacement and the size of the associated fluorspar vein, some of these undiscovered faults may be of great potential economic value. Also, because of inadequate outcrops, the location of many of the major faults is known only approximately. Consequently any means that gives promise of discovering unknown faults or more accurately locating those that have already been mapped is worthy of careful consideration because it may furnish information of the greatest value for further prospecting.

## ELECTRICAL RESISTIVITY OF ROCKS

The resistivity offered by the earth to the passage of an electric current depends to a large extent upon the amount of water present. As the ground-water table is much nearer the surface beneath valleys than it is beneath hills, a resistivity curve should conform to some extent to the topography. Different types of rock, however, vary greatly in their ability to absorb and retain water. Although shales possess little obvious porosity, they are generally able to hold a considerable amount of adsorbed water rich in electrolytes, which does not drain out readily, and as a result shales commonly exhibit relatively low resistivity. Most lime-

<sup>2</sup> S. Weller: The Geology of Hardin County. Illinois State Geol. Survey Bull. 41 (1919).

stones possess very little primary porosity and unless altered should be highly resistive. As a matter of fact, however, all limestones near the surface have been attacked more or less by solution and if the solution cavities are abundant, as they are in some parts of Hardin County, resistivity will be low where they are filled with water or abnormally high if they are dry. Coarse or porous sandstones may hold much water but the water drains from them fairly easily, and consequently their resistivity will vary considerably in accordance with the height of the ground-water table. There are, of course, all gradations between these three main types of rock, and as sandstones or limestones become more argillaceous their resistivities rapidly approach that of shale. In addition to the bedrock, earth resistivity is also influenced by the overburden of unconsolidated material. As this is commonly clayey or silty, its influence approaches that of shale, but as the surficial material varies much in thickness from place to place it may mask to a greater or less extent the resistivity of the underlying bedrock.

If the rocks of Hardin County consisted of thick formations of homogeneous and distinct lithologic types, which might be expected to possess different electrical resistivities, it should be easy to locate faults. Actual conditions, however, are not so simple. The sandstones are fine grained and locally argillaceous, shales and limestones are intimately associated as alternating thin beds in several of the formations, and such thick limestones as do occur are commonly more or less cavernous. Many of the formations are not thick enough to warrant the interpretation that the resistivity readings reflect the influence of a single formation. Moreover, the topographic relief in the area studied is about 200 ft. and the surficial materials vary greatly in thickness from place to place. All of these complications must be carefully considered in connection with the interpretation of earth-resistivity measurements.

#### EARTH-RESISTIVITY TRAVERSES

##### *Traverse No. 1<sup>3</sup>*

This 5-mile traverse illustrates fairly well the varying degrees in which faulting is reflected by earth resistivity. The peak in the resistivity curve recorded between stations 267 and 245 is one of the most spectacular anomalies obtained in the entire region. In order to make certain that it is not the result of error or accident this part of the traverse was rerun a few yards to one side of the original traverse. Except for minor details the second measurements are practically identical with those made on the original traverse.

---

<sup>3</sup> This and the following traverses constitute part of a study that will be described in a future publication of the Illinois State Geological Survey.

The traverse here crosses a wide sandstone area in which the beds dip gently to the left. Judging by the identification of a limestone-shale formation overlying the sandstone to the left and another limestone-shale formation underlying the sandstone to the right, there must be a fault bringing one sandstone formation in contact with another. Because lithology does not permit the identification of these sandstone formations, this fault cannot be located by outcrop observations. The sharp rise in the profile between stations 267 and 263 runs counter to the topographic slope, and there can be little doubt, therefore, as to the location of this fault, No. 1, which formerly had been mapped about 600 ft. farther to the left.

Fault No. 2 is somewhat doubtful. It is drawn on the basis of a sheared zone in sandstone. It has not affected the resistivity profile appreciably and probably is of very small displacement.

The fall in the profile over the next quarter mile to the right corresponds mainly to topography but it is very steep and a fault may be present here also. A tentative fault was drawn at about this position on the preliminary geological map of Hardin County but was not included on the published map. A re-study of near-by exposures suggests that the dip of the strata is not sufficient to carry the beds that outcrop on the right side of the valley (at station 236 or 237) below those underlying the hillside to the left, therefore a small fault, No. 3, has been indicated in the cross-section. The location of this fault, if present, is somewhat doubtful. It cannot be accurately located by outcrops. The resistivity profile suggests that it occurs several hundred feet farther to

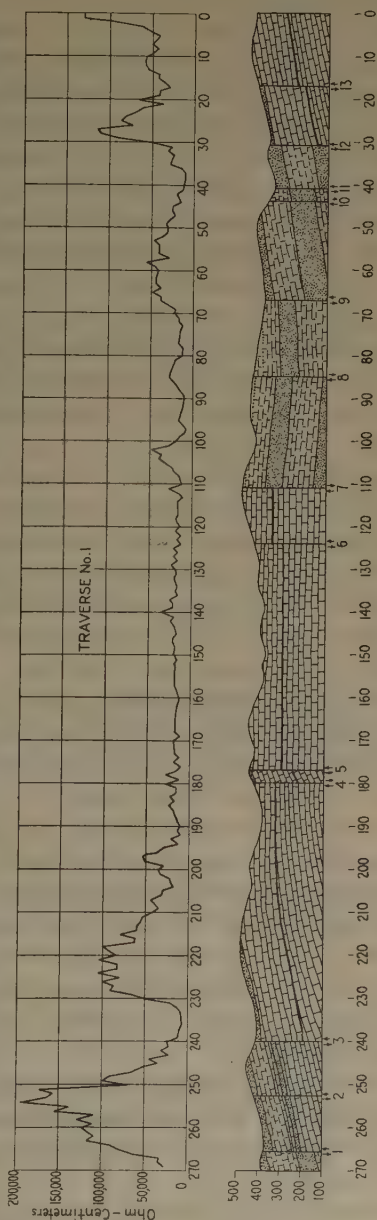


Fig. 1.



the left but it has been located in the cross-section on the basis of topography.

This traverse for over a mile to the right of fault No. 3 passes over a wide limestone area mantled in part by thin sandstone. The rise between stations 233 and 228 is sharp but corresponds to topography, and no indication of a fault here was recognized. The irregularities in the profile east of station 228 are rather characteristic of a limestone region. The curve suggests faulting near stations 206, 201 and 195 but outcrops are lacking here and, even if present, faults could probably not be recognized in this limestone unless they were actually exposed. It is equally possible that these irregularities result from sink holes.

Faults 4 and 5 bound a much sheared block of sandstone. They correspond to two small peaks in the profile but their existence could not be determined except by outcrop observations.

To the right for  $1\frac{1}{4}$  miles the traverse passed over continuous limestone. The resistivity is unusually regular and low for such a limestone area. A small fault, No. 6, occurs at about station 120 but it is not even suggested in the profile. Its existence is known from the workings of a small mine but neither the amount of displacement nor the relations of upthrow and downthrow sides are apparent.

The position of fault No. 7 is shown accurately in outcrop. This is a fault of large displacement and its very slight reflection in the resistivity profile is noteworthy but probably results from the abnormally low resistivity of the limestone to the left.

The fluctuations of the resistivity profile between stations 110 and 88 are unexplained. They do not correspond to topography and although a fault is suggested at about station 100, outcrops seem to show that there is no interruption of the strata.

The existence of fault No. 8 is somewhat doubtful and the difference in elevation of a sandstone bed on the opposite sides of the hill may be the result of slight folding rather than faulting. The small high between stations 89 and 80 does not conform to topography but is unusually wide to be produced by a fault of small displacement.

Fault No. 9 is clearly shown by outcrops and is well represented in the resistivity curve as the rise east of station 69 does not conform to topography.

Fault No. 10 is indicated by the repetition of about 10 ft. of beds in a small gully. It is unimportant and has not appreciably affected the profile, which roughly corresponds to the topography between stations 50 and 35.

Fault No. 11, known from outcrops, possesses nearly twice the displacement of fault No. 9, but is not conspicuously reflected in the resistivity profile.



Fault No. 12 is accurately located by outcrops and is reflected in a conspicuous rise in the profile. This is the type of anomaly that might be expected to occur at the contact between solid limestone and shaly beds. Fault No. 12 is second in importance in this traverse only to fault No. 7 but the latter is by no means clearly recorded in the profile.

The fluctuations in the profile to the right of fault No. 12 seem to be rather characteristic of an upland limestone area with numerous sink holes. Fault No. 13 corresponds to the low point in this part of the curve. Its location is known from outcrops, and several small mines and prospect pits mark its course. Without such evidence, however, it would be impossible to interpret this part of the profile.

### Traverse No. 2

This traverse, which is nearly  $3\frac{1}{2}$  miles long, appears to be one of the most satisfactory that was run in this district. Fault No. 1 has not been

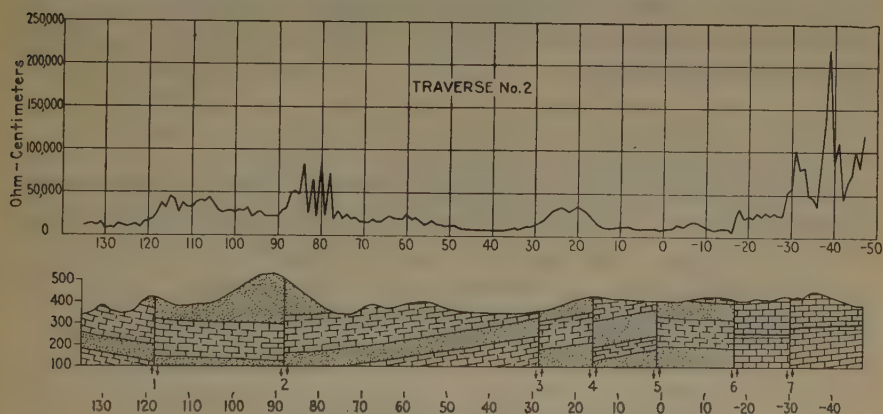


FIG. 2.

located by outcrop observations. The sharp rise in the profile between stations 122 and 117, however, does not accord with the topography, and a fault is believed to be indicated here.

The next sharp rise, to the right of station 90, likewise does not correspond to the topography and a fault is tentatively drawn at this position, but outcrops are unsatisfactory for checking the interpretation. Steeply dipping sandstone beds occur here but they may represent cross bedding. The very irregular profile between stations 85 and 77 is unexplained unless it is the result of unsatisfactory ground connections on a steep sandstone hillside.

Fault No. 3 is somewhat doubtful because only alluvium is present for a considerable distance on the left-hand side. It is possible that the rise in the resistivity profile to the right of station 30 is a reflection of topography but it seems to be much too steep to result from this cause

alone. It is believed that this same fault is indicated in the profile of another parallel traverse  $1\frac{1}{2}$  miles away. It is interesting to note that a fault was shown at about this position on a preliminary copy of the Hardin County geological map although it does not appear on the published map.

Fault No. 4 has not previously been recognized. Its presence is indicated in the rapid decline in resistivity between stations 20 and 14. Evidence substantiating the existence of this fault was found in the exposure of different formations in an outcrop and a near-by test pit.

Fault No. 5 is known from outcrop observations but is not reflected in the profile.

No. 6 is an important fault that has long been known. Its position is accurately indicated by the short but sharp rise between stations 16 and 18.

Fault No. 7 is somewhat doubtful and the great irregularity of the profile to the right of station 28 may be entirely the result of sink-hole topography. However, the alignment of steep dips in this curve with those recorded in two near-by parallel traverses strongly suggests the presence of a small fault.

### Traverse No. 3

The resistivity profile of the third traverse is of considerable interest because there are few outcrops in this vicinity and consequently the

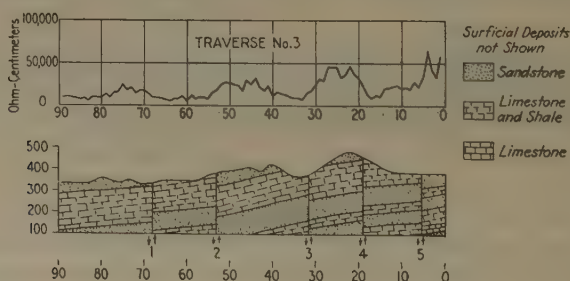


FIG. 3.

previous geological mapping is rather uncertain. Faults probably occur at about the positions of Nos. 1 and 2, because the dip of the strata is not great enough to allow the sandstone that underlies the hill to the right of fault No. 2 to pass beneath the sandstone that caps the fault block to the left of Fault No. 1.

The location of fault No. 1 is not accurately indicated in the profile. It is projected across this traverse from another parallel traverse some distance away, where its presence seems to be more clearly shown.

Fault No. 2 is fairly accurately located by the rise in the profile between stations 55 and 51. This fault also is well shown in a parallel traverse.

A parallel traverse indicates the presence of a fault which, if projected, would pass down the valley between stations 36 and 31. The sharp rise in the profile between stations 33 and 29 is good evidence that this fault, No. 3, occurs near the right side of this alluvium-filled valley.

The sharp drop in the profile between stations 22 and 17 does not conform to topography and makes it seem probable that a fault, No. 4, occurs here. There is no other evidence of its presence.

Fault No. 5 has been located by prospectors near this traverse. Its position is accurately shown by the sharp rise in resistivity between stations 6 and 4.

### CONCLUSIONS

Electrical resistivity surveys in Hardin County have proved of considerable value as an aid in locating faults where outcrops are scattered and inadequate. Although some of the important and well-known faults of this district are not indicated by notable variations in the resistivity profiles, others appear to have been located more accurately than by outcrop observations alone and several new faults are thought to have been discovered.

Many faults are indicated by rapidly increasing or decreasing resistivity measured at several successive stations. Therefore some of them have not been located within several hundred feet by these traverses in which the electrodes were uniformly spaced at 100 ft. It is probable that retraversing these critical sections with decreased electrode intervals would result in more accurate location. It is also possible that retraverses with different electrode spacing would serve to locate known faults that are not reflected in the resistivity measurements already made. By running additional parallel traverses the existence of doubtful faults that cannot be located by outcrop observations could probably be substantiated or disproved. A detailed survey of an area would involve checks of these and possibly other types.

Electrical resistivity surveys intended to explore faulted districts attain their greatest usefulness when subordinated to detailed geologic field mapping and when so planned that they supplement the information obtained from outcrop observations. It should be emphasized that a thorough knowledge of the stratigraphic section and local structural relations are essential for an adequate and satisfactory interpretation of the resistivity anomalies, because fluctuations suggestive of faults may be produced in the resistivity profiles by other geologic or topographic conditions. As the profiles show simply the relative conductivity in the surficial materials and upper portion of the bedrock, the amplitudes of their fluctuations are not measures of the amounts of displacement that may have occurred along the faults encountered and the upthrow and downthrow sides of the faults cannot be determined from them except indirectly.

## DISCUSSION

(*Sherwin F. Kelly presiding*)

W. M. WEIGEL,\* St. Louis, Mo.—As I understand, this profile was made by taking the resistivity at definite, fixed, points, and just one reading. Would it have been possible to clear up some of those anomalies if you had taken them at different spacings and gotten a resistance farther down? I mean a combination of the two, another method by which you have different spacings.

M. K. HUBBERT.—Mr. Kihlstedt showed a profile of the sort you ask about which I think would give results better than ours, but we did not have that kind of apparatus. These profiles were run in a manner similar to an eight-wheel wagon, or something of the sort, crossing a railroad track—that is, every time a set of wheels went across, there was a jolt. When we went across the fault, it took three stations, and we got oscillations as we went across. A part of those slightly objectionable features is due to the fact that the apparatus is not, perhaps, the best that has been developed for the purpose. On the other hand, if we changed the electrode spacing we would probably cause trouble because it would spread the stations farther apart. Also, we would get into more layers of different kinds of bedrock by taking in more depth, so it is better to take the shortest spacing possible.

S. H. DOLBEAR,† New York, N. Y.—To what extent are the results portrayed here regarded as justifying the use of similar methods in other places?

M. K. HUBBERT.—It depends entirely upon how important it is to obtain information. In a region where it is very important to locate one or a few faults in a relatively small area, one can afford to detail to almost any extent necessary, but if the area is large and it is not necessary to know the minute details, any method of this kind, which necessarily involves a fairly detailed working, would, I think, not be desirable because of its costliness.

S. F. KELLY,‡ New York, N. Y.—It is hardly necessary to point out the extrapolation that can be made from Mr. Hubbert's paper; namely, a technique of this kind can be advantageously used wherever the fault system has a direct bearing on the occurrence of the mineral body, whether that mineral is nonmetallic or metallic in nature and where the rocks involved show a sufficient difference in electrical characteristics to make the faults apparent.

---

\* Mineral Technologist, Missouri Pacific R. R. Co.

† Consulting Mining Engineer.

‡ Geologist and Geophysicist, Combined Geophysical Methods, Inc.



# Some Practical Applications of Resistivity Measurements to Highway Problems

BY KARL S. KURTENACKER,\* MADISON, WIS.

(New York Meeting, February, 1934)

IN attempting to find a rapid and economical means for solving many of the subsurface problems that confront the highway engineer, the author for the past two years has utilized a Megger Ground Tester on resistivity surveys in conjunction with highway construction. Electrical surveys in connection with highway work are largely shallow depth surveys, thus differing from most other types of resistivity work. Consequently, the readings are affected by a great many qualifying factors such as the density and moisture content of the media under observation and the amount of weathering and leaching. In most cases the surface layer is decidedly heterogeneous in character, and, because of the great number of side hill cuts, the second layer, which in most cases is rock overlain by some sort of surface soil, silt, or debris, seldom lies in a horizontal position.

Shallow strata, lacking homogeneity and not lying in a horizontal position, do not lend themselves readily to accurate theoretical interpretations, therefore the author has used empirical rules to a large extent in interpreting depth soundings. The following empirical rules of interpretation are surprisingly adequate for highway work, since much of the work is in the nature of reconnaissance surveying and the results are construed to be approximations. The writer is careful not to risk interpretation on some special feature of the curve, since such features are usually due to random errors or lack of homogeneity among the subsurface strata.

## EFFECT OF SURFACE MEDIUM

A resistivity depth sounding taken to a depth of 200 or 300 ft. is not much affected by superficial conditions, but these conditions have a great effect in depth soundings to 25 or 30 ft. In shallow soundings the character of the surface medium has a very marked effect on the entire resistivity graph. Fig. 1 illustrates a very striking example. Graphs *A* and *B* are depth soundings taken in approximately the same place. The surface stratum is a clay loam but at the place where graph *B* was taken

---

Manuscript received at the office of the Institute Feb. 5, 1934.

\* Junior Geologist, Wisconsin Highway Commission.

the surface is stripped of sod. Consequently, the medium in which the electrodes were inserted was more moist and more dense at *B* than at *A*. At *A* the roots of the grasses caused the soil to be more porous, thus allowing the sun to evaporate the moisture to a greater depth. Graph *A* is a sharply falling curve to the top of the rock at a depth of 8 ft., while graph *B* shows no marked changes in resistivity value.

The geologist must carefully note the conditions of the surface medium. Changes in resistivity are not always representative of corresponding geological changes, hence it is possible to have one geological stratum represented by one or more strata of resistance.

### ELECTRICAL SURVEYS IN QUARRY INVESTIGATIONS

Electrical surveys have been used very successfully in investigations in limestone quarries. The operation of quarries in the limestone-capped

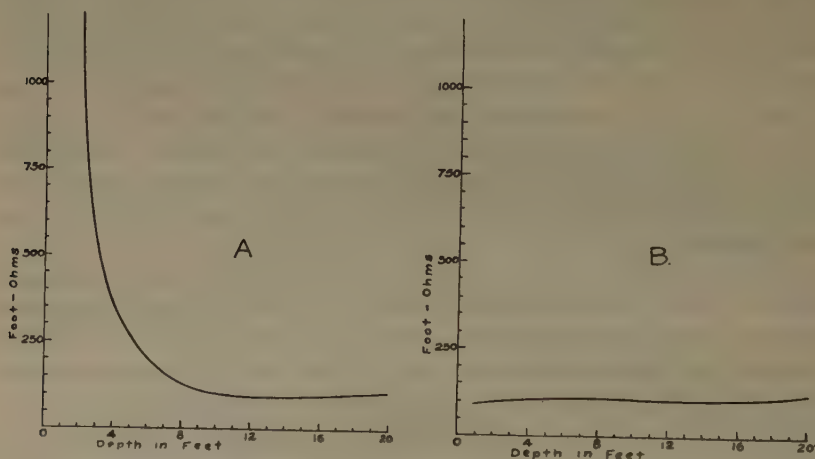


FIG. 1.—ANOMALOUS RESISTIVITY DEPTH PROFILES OBTAINED AT APPROXIMATELY THE SAME LOCATION IN THE SAME MEDIUM.

ridges of western Wisconsin has long been a source of trouble. A contractor never knows when a clay-filled sink hole will be encountered. Often these sinks are 20 to 30 ft. deep and in width embrace upwards of 50 per cent of the working face. By taking resistivity depth profiles every 50 ft. in both an east-west and north-south direction across the surface of the proposed quarry, not only can the depth of stripping be determined, but clay-filled sinks that are large enough to hinder operations can be detected.

Fig. 2 is a schematic cross-section through a limestone ridge. The three resistivity depth curves show that the stripping, which appeared negligible at the old quarry face, increases to serious depths toward point *C*. The same story is told by the equiresistivity traverses, which show a decrease in resistance as point *C* is approached.

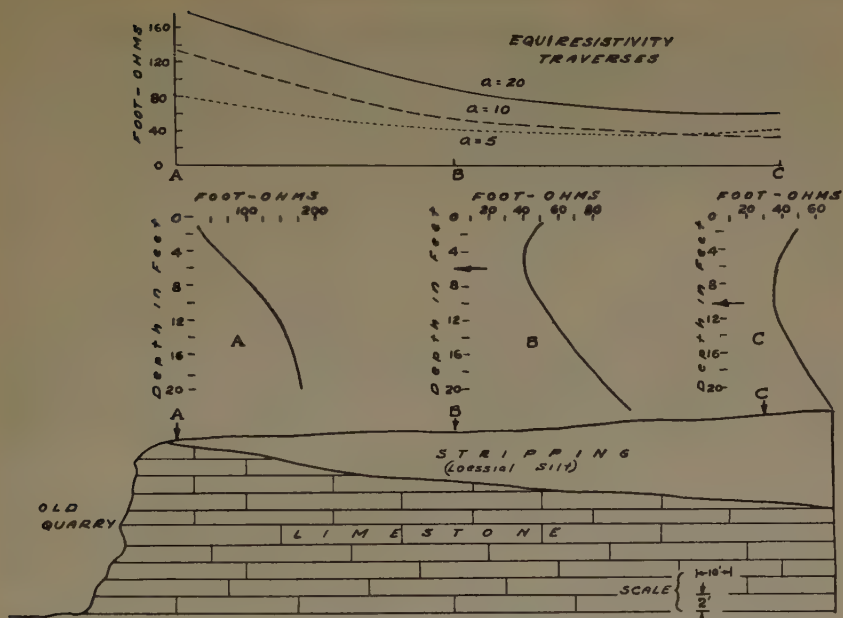


FIG. 2.—DEPTH CURVES AND EQUIRESISTIVITY TRAVERSES, SHOWING THICKNESS OF STRIPPING ON PROPOSED QUARRY.

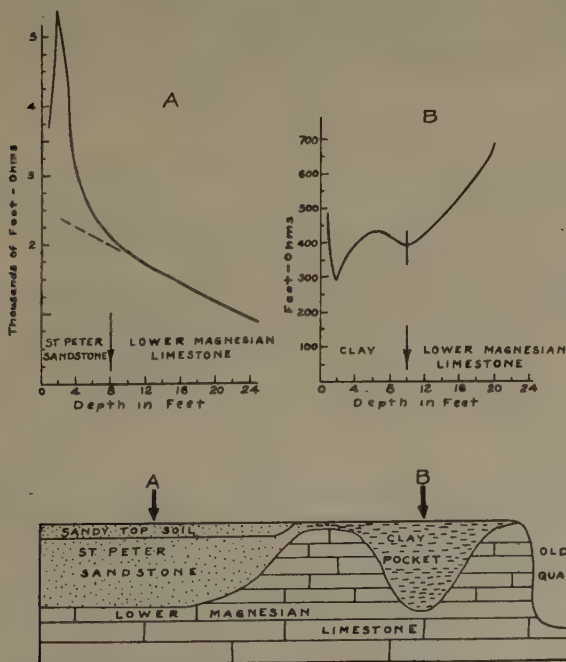


FIG. (3).—(A) DEPTH PROFILE REVEALING SANDSTONE OVER QUARRY BEDS; (B) DEPTH PROFILE SHOWING CLAY POCKET IN QUARRY BEDS.

Fig. 3 represents a cross-section through a limestone spur of which only the old quarry was exposed. To all outward appearances the excellent face of massive limestone, with almost no stripping, carried back through the spur. However, because the top surface of the Lower Magnesian was badly dissected before the St. Peter sandstone was deposited, it is always wise to conduct some sort of an investigation prior to quarrying. This is especially true if the proposed quarry is to be opened in the upper beds of the Lower Magnesian.

It was necessary to take only two resistivity depth profiles to see what sort of difficulties would be encountered in the quarry illustrated by Fig. 3. Depth profile *A*, 150 ft. back along the ridge from the quarry face, revealed 9 ft. of St. Peter sandstone resting above the Lower Magnesian. The same comparable 9 ft. at the quarry face exposed good limestone. Depth profile *B*, taken between *A* and the quarry face, revealed a clay-filled sink hole 10 ft. deep.

Simple reconnaissance such as this saves money. This quarry surely would have been abandoned after the set-up was made and a small amount of stone removed. The equipment would then have to be moved to some other location to obtain the necessary amount of material.

Notice that in depth profile *A* both the sandstone and the limestone are represented by resistivity values that decrease with depth. This is due to the very highly resistant, unconsolidated, dry sand just beneath the thin sod cover. Although the resistance of the sandstone is high, it is not as high as the dry sand, hence the falling values.

### CUT CLASSIFICATION

The interpretation of electrical quarry data is comparatively simple because conditions are fairly uniform. Most of the quarries are opened in the driftless area, where gravel is scarce and where the limestone uplands are usually overlain with silt or clay.

Cut-classification work is much more complicated because the many types of soils overlying the great variety of rocks result in curves that vary greatly in shape and behavior. Much more anomalous data are obtained because of the many subsurface combinations.

Table 1 is a list of the various types of overburden and bedrock native to Wisconsin.

The classification of various materials into the two groups helps in referring to the electrical character of a formation. Materials that are highly resistant and, inversely, weakly conductive, are classified as "resistant"; materials that are highly conductive and, inversely, weakly resistant are called "conductive." It is impossible to establish limits in resistivity values for any one type of material because the amount of moisture is such a dominating influence. However, it can be said that in normal seasons the materials in the "resistant" group exhibit a greater



TABLE 1.—*Overburden and Bedrock Native to Wisconsin*

	RESISTANT	CONDUCTIVE
<i>Earth</i>	Glacial tills of Wisconsin age	Glacial tills of pre-Wisconsin ages
	Glacial sands and gravels of all ages	Glacial flood silts of all ages
	Residual sandstone soils	River clays and silts
		Marls, mucks and (wet) peat
		Residual limestone and shale soils
		Loessial silts
<i>Rock</i>	Limestones	
	Sandstones	Shales
	Granites, basalts, syenites, etc.	
	Quartzites, marbles, etc.	

resistivity than any of the materials in the "conductive" group. Materials are "resistant" either because of lack of pore space or lack of soluble salts. The "conductive" materials are all porous to various degrees and in all there is an abundance of soluble salts.

Interpretable resistivity data cannot always be obtained in regions where a "resistant" earth covers a "resistant" bedrock, or where a "conductive" earth covers a "conductive" rock. Similarly, it is usually difficult and sometimes impossible by electrical methods to differentiate between two "resistant" earths, two "resistant" rocks, or two "conductive" earths. That is, glacial sand and gravel cannot be distinguished nor can granite be differentiated from quartzite or sandstone.

Whenever any member of the resistant column overlies any member of the conductive column, or vice versa, resistivity data that are easily interpreted are nearly always obtained.

When the contact between two resistant or two conductive materials appears on a resistivity graph, the corresponding discontinuity will be small, as in curve *C*, Fig. 4. In this figure, curves *A* and *B* are resistivity depth soundings revealing conductive loessial silt overlying resistant limestone. Curve *A* shows the contact perfectly, but in curve *B* the contact is not clearly shown. This is a very common type of curve for these conditions, especially when the limestone is 15 ft. or more beneath the surface. Considerable care must be taken in their interpretation.

Curves *A*, *B* and *C* in Fig. 5 are typical depth soundings obtained on a classification survey. Curves *A* and *B* reveal the contact between glacial outwash gravels and the Franconia silty greensand, curve *A* being interpreted empirically. In curve *B* there exist two logical discontinuities, one at point *X* and another at point *Z*. Consequently, Tagg's theoretical method of interpretation was applied and was found to be but one-third of a foot in error. Curve *C* shows the contact between the Franconia silty greensand and the Dresbach sandstone. Notice that the resistance of the Franconia is very low. Although this stratum is a solid rock formation containing 50 per cent or more quartz grains,<sup>1</sup> the calcareous

<sup>1</sup> Quartz, in itself, is a highly resistant material, pure quartz sandstones being almost devoid of soluble salts.

silts and the glauconite present in the greensand are extremely conductive. What we have here, then, is a "conductive" sandstone.

Fig. 6 is an equiresistivity traverse across a small ridge in the glaciated area. Topographically it is impossible to determine whether or not

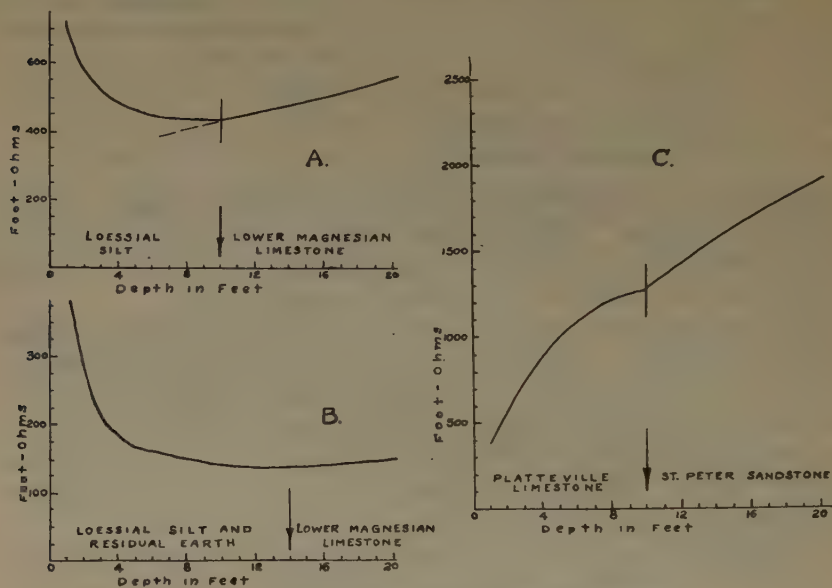


FIG. 4.—TYPICAL RESISTIVITY DEPTH CURVES.

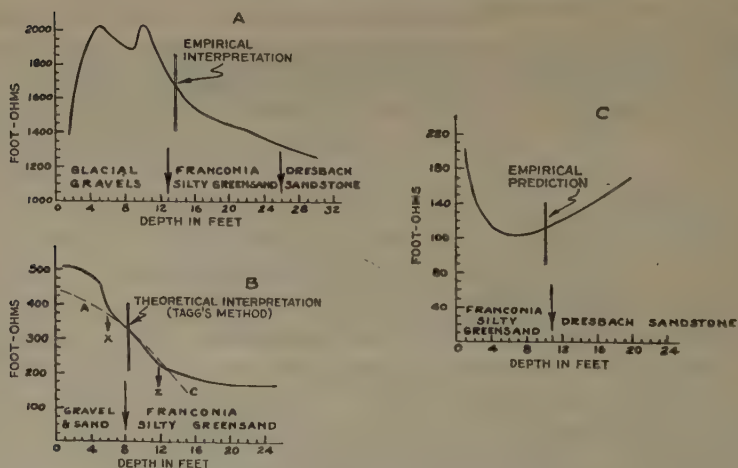


FIG. 5.—TYPICAL DEPTH CURVES OBTAINED ON CLASSIFICATION SURVEY.

these prominences of drumloidal shape are rock-controlled. Because of the great number of erratics in the drift, mechanical soundings cannot be obtained at small expense. An equiresistivity traverse across the ridge

will indicate the presence of a rock core and outline its boundaries very accurately.

The cross-section in Fig. 6 shows the backslope of the finished cut. The dashed line is the actual outline of the rock core; the solid line is the outline predicted by the resistivity traverse. Although the two lines are not in perfect agreement, yardage computed from either of the enclosed areas would not differ materially.

Even though the electrical data may outline the top of the rock accurately in a given cut, it may be that the final classification of the

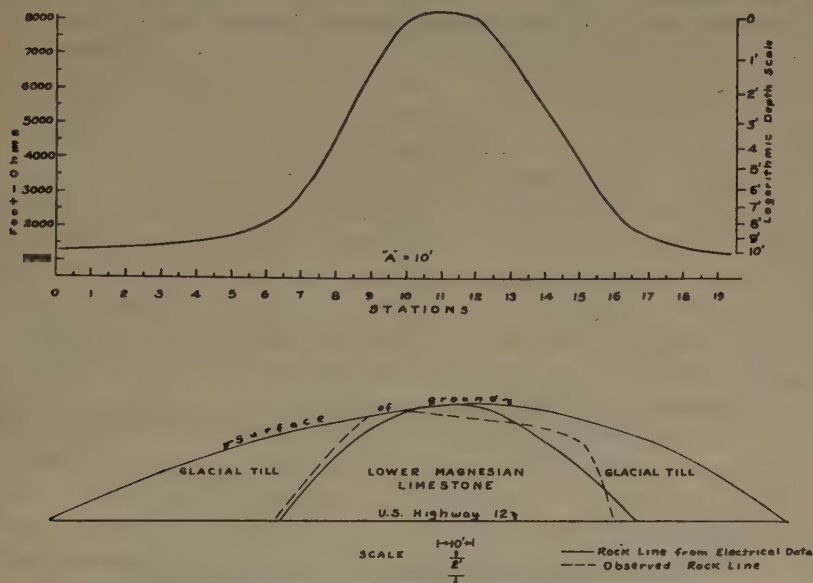


FIG. 6.—PROFILE OF RESISTIVITY TRAVERSE SHOWING ROCK CORE IN GLACIAL HILL.

project will show discrepancies when compared to the estimate. This is usually due to the human element involved in determining just what material moved by the contractor is solid rock, loose rock, and earth. In some cuts the boundaries are clear and sharply defined, while in others there is a thick transitional zone of fractured, fragmentary loose rock. Some of the material in this zone is classified as "solid rock" but does not reveal itself as such on the resistivity graphs.

The writer has found that in areas where there is a thick zone of loose rock between the residuum and the solid ledge, the estimates derived from resistivity soundings tend to underclassify the amount of solid rock. This is because the lower part of the fractured zone, while not fresh, unweathered, solid rock in the geological sense, is solid rock from the standpoint of cost of excavating.

## SWAMP PROBLEMS AND HIGHWAY GRADE SETTLEMENT

Resistivity surveys have a valuable application to highway swamp problems. It is possible to determine the depth to hard, stable material at the bottom of the swamp. Electrical soundings on a newly constructed fill will determine whether or not the fill is properly settled on a firm foundation, and, if a fill is not settled, will indicate the thickness of peat and muck that lies between the fill and the hardpan at the bottom of the swamp.

The latter information is valuable in estimating the cost of settling long-existent fills. In many states, highways across swamps have been

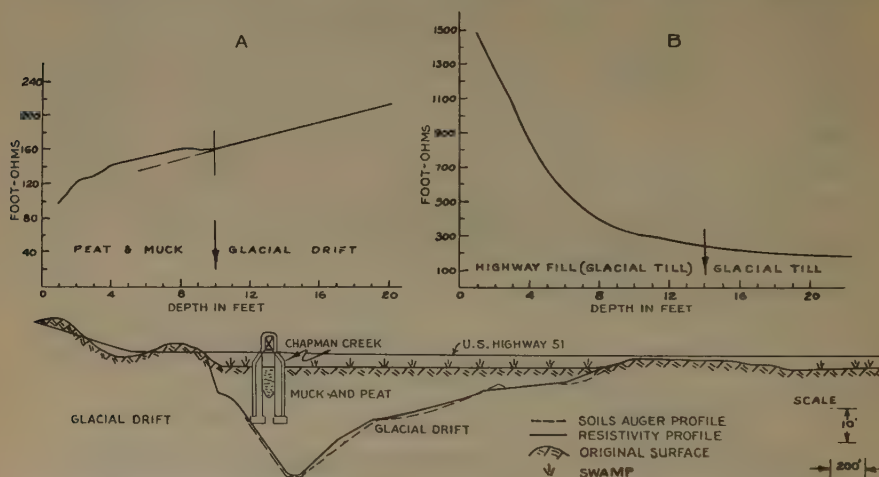


FIG. 7.—RESISTIVITY DEPTH CURVE IN SWAMP (A) AND ON SETTLED HIGHWAY FILL (B), WITH CROSS-SECTION THROUGH PORTION OF SWAMP.

left unpaved because of the habitually unstable condition of the fill. In the future these gaps are going to be paved, and to insure a smooth riding pavement, removal of the muck will be necessary.

Experience has shown that resistivity depth readings taken in marshes and swamps result in depth curves that reveal the bottom of the swamp with an exceptionally high degree of accuracy. This is because the strata are so thoroughly saturated with water that the observed resistivities are not affected by zones of variable moisture content. Nor are there rocks or fragments of alien material on or near the surface to locally affect the conductivity of the medium under observation.

Curve A, Fig. 7, is a resistivity depth profile obtained in Packwaukee Swamp, a rather shallow but very large swamp. Curve A was taken at the location of a boring, the log of which is as follows: 0 to 10 ft., peat and muck with sand lenses; 10 ft. to bottom, stony glacial till. The graph revealed a pronounced discontinuity at 10 ft., it being an uneven curve



from 0 to 10 ft. and a rising tangent from 10 to 25 ft. The uneven curve conforms to the heterogeneous character of the swamp materials, and the straight line to the glacial till.

The difference in resistance between the marsh materials and the hardpan is not compatible with the difference in chemical or physical characteristics of the two strata, because the media under observation are so thoroughly saturated with water, which tends to equalize the resistances. The cross-section in Fig. 7 shows the bottom of a portion of the swamp as determined by borings compared to the determination by resistivity methods.

In a shallow swamp where the depth to solid bottom is from 5 to 15 ft., resistivity soundings are, if anything, a little slower than soils-auger soundings, but in a swamp deeper than 15 ft. such a length of sounding rod becomes unwieldy.

Many swamps are known to have occasional beds of sand or gravel interspersed in the muck and peat. These beds vary in thickness from a few inches to 3 or 4 ft. Cases are on record where soils-auger soundings have encountered one of these sand beds and the survey party, failing to bore through the sand, assumed the layer to be solid bottom. Resistivity readings easily eliminate this error.

Resistivity depth profiles were obtained on the shoulder of the existing highway that crosses the Packwaukee marsh, the object being to ascertain whether or not the fill was properly settled on solid bottom. The material used for the fill was borrowed from the low hills forming the south margin of the swamp. This material is the same type of glacial till that bottoms the swamp. Settlement was made by blasting.

If a fill is properly settled, the depth profile should be a regular falling curve because the fill material and the underlying till are identical, and because, though dry at the surface, the fill becomes very moist with increasing depth, owing to capillary action. Curve *B*, Fig. 7, is an excellent example of a depth profile on a well settled fill. Irregular graphs indicate a floating fill, anomalies in the electrical data being caused by the muck and peat upon which the fill is floating. The thickness of the fill can be ascertained by electrically sounding through the fill, while the solid bottom can be determined by electrically sounding at the toe of the fill, using the swamp as a surface medium. Thus the thickness of the swamp material between the fill and the solid bottom can be ascertained.

#### OTHER HIGHWAY PROBLEMS

A small amount of work has been done by the writer in connection with bridge surveys. Electrical depth profiles were obtained at proposed bridge sites to determine the depth to a material of sufficient bearing strength to support piling.

Because most of the river valleys have been filled with considerable amounts of silt, clay and glacial debris, depth profiles for bridge estimates must, in general, be carried to greater depths than soundings for other types of highway work.

Good results can be obtained in silt and clay-filled valleys because of the great difference in resistivity between the silts and the underlying

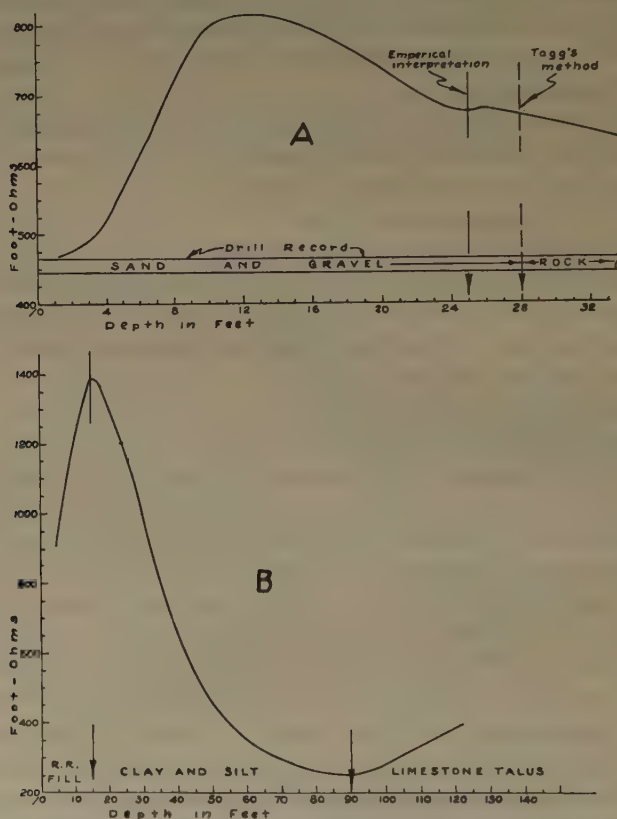


FIG. 8.—DEPTH CURVES AT (A) INDIANFORD BRIDGE, ROCK RIVER, AND (B) CHARME BRIDGE, JUNCTION DU CHARME CREEK AND MISSISSIPPI RIVER.

rock. Some valleys are filled with sand that is in turn overlain by silt and clay. It is difficult to ascertain the contact between the rock and the sand, but the sand can be differentiated from the clay very easily. For smaller structures, sand has sufficient bearing strength to hold piling in place.

Fig. 8 shows two depth profiles in river valleys, curve A obtained at the location of a boring in the sand and gravel-filled valley of the Rock River, and curve B in the silt-filled valley of the Mississippi. There was no control for curve B, but the Chicago, Burlington & Quincy R. R. Co.

reported a depth of 80 ft. to solid bottom beneath one of its bridges, 60 ft. away from the point where curve *B* was obtained.

It is easy enough to obtain data in the bottom lands, but taking resistivity soundings for a pier to be constructed in the water is a different story. It is impossible to work from boats or rafts, but the data might be collected in the winter. Even then, work would be slow, because holes would have to be chopped in the ice for every reading.

In other states, resistivity surveys have been used to locate and outline gravel deposits that are buried in river clays and glacial ground moraines. None of this work has been done by the writer because Wisconsin is plentifully endowed with excellent gravel deposits that are topographically prominent. The writer did attempt to locate areas of gravel in a sandy outwash plain, but neither by depth soundings nor traversing could the gravel be distinguished from the sand.

### CONCLUSIONS

Resistivity measurements are not infallible. The method is not an ideal one from the standpoint of accuracy. The results of some of the observations with the Megger Ground Tester have shown geological discontinuities as clearly and correctly as could be desired. Most of the data are slightly erroneous but not enough so to be serious, and every so often curves are obtained that are quite uninterpretable.

Fortunately, good, interpretable results can readily be obtained by resistivity measurements in the areas of bouldery glacial drift, cherty overburden, and similar ground, where it is most difficult to obtain accurate mechanical soundings. One of the paramount advantages of resistivity equipment is that it can be taken into country that is inaccessible to many drilling outfits.

Field technique is simple; interpretation of the data is difficult. Whenever a resistivity party goes into unfamiliar country, control should be established. The interpretation of electrical data without control, or without previous experience with similar conditions, is little better than a guess. For shallow data, control can be supplied by geological maps, well records, outcrops, and occasional borings.

# Location and Study of Pipe-line Corrosion by Surface Electrical Measurements

By C. AND M. SCHLUMBERGER\* AND E. G. LEONARDON,\* PARIS, FRANCE

(New York Meeting, February, 1932)

## ABSTRACT†

THE authors give a definition of the various types of corrosion that may affect a metallic conductor buried in the ground, namely:

1. The metallic conductor may be attacked by the surrounding soil. This phenomenon is purely local and is called by them soil corrosiveness.

2. The metallic conductor may connect two regions of the ground when the electrolytes have a different composition. An electrical current will then be generated and certain zones of the conductor will be oxidized. This is autogalvanic corrosion.

3. Stray current may flow in the ground and enter the conductor in certain sections and leave it in others, thus causing oxidization in certain zones; this is electrolytic corrosion.

The soil corrosiveness has been studied extensively by the United States Bureau of Standards and the authors give a summary of the work carried out and results obtained along this line.

In autogalvanic corrosion it has been shown, by the investigation of buried pipes, that the zones of corrosion are associated with the zones of egress of the electric current (anodic zones). The location of these zones can be determined by measuring at the surface of the ground the difference of potential that exists along the path of the pipe. This work is performed easily and quickly with the apparatus invented by the authors for the exploration of conductive orebodies.

The problem of electrolytic corrosion is a difficult one because it is a question of stray current which may vary in direction and intensity at every instant. Therefore the components of the electrical field must be known at a given station and compared with the components of the electrical field at another station, at the same moment. This is achieved by a recording apparatus that will register the variations of the intensity of the electric current along two rectangular directions, during several minutes.

---

\* Compagnie Générale de Géophysique, Paris, and Schlumberger Electrical Prospecting Methods, New York.

† The paper was published as A.I.M.E. *Tech. Pub.* 476 (1932).



In addition the zones of ingress or egress of the current flowing through the pipe must be determined in spite of the fact that stray currents of larger magnitude may be flowing through the surrounding ground. The authors dispose of this delicate problem by the use of a "differential measuring arrangement" which comprises three electrodes, located a few feet apart, and a potentiometer.

Several examples of field work are discussed and a comprehensive description of the apparatus employed is given.

# Electrical Methods in Prospecting for Gold

BY FOLKE H. KIHLESTEDT,\* NEW YORK, N. Y.

(New York Meeting, February, 1934)

GEOPHYSICAL prospecting for ore has been more or less at a standstill during the present crisis owing to the lack of interest in base-metal exploration. A notable exception is the increased use of electrical and magnetic methods in prospecting for gold, the former in Canada, United States, Sumatra, Africa and Western Australia, and the latter on the Rand. This application to gold prospecting marks a forward step in ore prospecting because it is based upon mapping the geology instead of a direct location of the ore in question, as the amount of gold in an average gold ore is far too small to have any influence upon the physical properties of the rock in which it occurs. The development has thus gone in the same direction as geophysical prospecting for oil; that is, to find geological conditions that are genetically connected with the gold ore as exemplified by known occurrences. Naturally the success of this indirect prospecting depends upon two things: (1) the soundness of the geological conclusions upon which is based the hope of discovering new deposits, because a great many geological "set-ups" are barren, and (2) the ability of geophysical methods to help the geologist to collect the pertinent geological data within reasonable cost, after which favorable structures may be drilled or trenced.

The first point is one to be considered by the mining geologist. In the vicinity of producing mines or promising prospects, the chances of finding ore in quartz veins and shear zones are great, and a survey giving the location of these features will materially guide both surface and underground exploration. Even in outside exploration the chances are sometimes favorable. As an example may be taken the Northeastern Ontario-Western Quebec gold zone. Large areas are here covered with glacial and post-glacial deposits and a simple study of available maps reveals the fact that less than 30 per cent of the area can ever be even preliminarily prospected by commonly used prospecting methods, of which the pick and shovel are the main tools. Considering the number of deposits found, it is evident that many deposits remain hidden below the overburden. The knowledge of gold geology gives a starting point

---

Manuscript received at the office of the Institute Jan. 13, 1934.

\* Swedish American Prospecting Corporation.

for an intelligent search for new deposits in many areas, where sufficient data are on hand to suggest their presence.

Our first consideration will be to study geological data of gold deposits, to find the features that are amenable to electrical prospecting. Gold occurs in base-metal ores, in placer deposits, in certain conglomerates, and in zones mostly connected with quartz of hydrothermal origin. The last type is of greatest interest in Canada and the United States and the following discussion is limited to that type of deposit.

### GEOLOGICAL CONDITIONS

Comparatively few gold mines are true fissure veins without any alteration of the wall rock, or without some fracturing or shearing extending into it. As a rule, shearing or fracturing is necessary to form the channels along which the gold-bearing solutions could ascend. These solutions carried many other constituents than gold, and at some time during the deposition they usually replaced part of the wall rock, forming new minerals that characterize the zone of alteration surrounding the quartz veins. The width of this zone of alteration varies from district to district and from place to place within a mine, but it is always present in some form or another.

Typical features of gold deposits are therefore the vein quartz and the zone of alteration and, as will be shown later, these rocks have electrical characteristics, which as a rule are quite different from those of the rock in which they occur.

The alteration usually consists of a softening of the wall rock by shearing and by the development of a number of minerals, such as chlorite, sericite, carbonates, etc., and pyrite. In deposits formed close to the surface, as at Goldfield, Nev., kaolin and alunite are present. This alteration usually produces a rock of higher porosity than the unaltered rock. The porosity of a rock is one of the factors determining its ability to conduct the electric current,<sup>1</sup> and the altered rock, because of its higher porosity, will show a lower resistivity to a current passing through it.

As the information on pore volume in the literature is rather meager, the following figures are not restricted to auriferous veins but include other veins where the chemical action has been of a similar nature.

	PORE VOLUME
Willow Creek, Idaho: <sup>2</sup>	
Fresh granitic rock.....	0.3
Altered granite along auriferous veins.....	1.0

<sup>1</sup> K. Sundberg: Effect of Impregnating Waters on Electrical Conductivity of Soils and Rocks. *Trans. A. I. M. E.* (1932) **97**, 367.

<sup>2</sup> Data from Lindgren: Mineral Deposits. New York, 1919. McGraw-Hill Book Co.

	PORE VOLUME
Bonanza district, Colo: <sup>3</sup>	
Fresh, black augite-mica andesite.....	1.0
Fresh, gray quartz-latite.....	1.5
Altered andesite: red jasper type.....	4.5
black jasper type.....	5.0
red type with pyrite.....	3.5
Silicified andesite.....	2.5
Rock with sericite and kaolin.....	8.0
Copper Gulch, Utah: <sup>4</sup>	
Fresh quartz-monzonite.....	2.5
Altered quartz-monzonite, adjacent to quartz-tourmaline vein.....	12.0
O.K. Mine, Utah: <sup>4</sup>	
Fresh quartz-monzonite.....	5.0
Altered quartz-monzonite adjacent to quartz-copper vein.....	19.2
Goldfield, Nev.: <sup>5</sup>	
Unaltered lava.....	1.0
Quartz-kaolin-alunite-pyrite rock (altered lava).....	9.9

The increased pore volume due to the alteration varies in these cases between 2 and 10 times that of the unaltered rock, which would produce differences in resistivity at least of the same order. Larger differences usually are found in actual resistivity tests on fresh and altered and sheared rocks.

	OHMS PER METER CUBE
Porcupine district, Ontario: <sup>6</sup>	
Fresh dacite-andesite.....	about 10,000
Slightly altered andesite.....	3,460
Completely altered rock, consisting of chlorite, sericite, carbonates..	95-760
Serpentine gabbro.....	about 10,000
Serpentine.....	2,140-5,300
Sheared serpentine.....	610
Slightly altered syenite (showing some carbonate).....	2,440-3,690
Slightly altered minette.....	1,030
Altered and sheared minette.....	190
Mineralized, slightly silicified schist.....	670-1,200
Silicified schist, with some vein quartz.....	11,300
Massive vein quartz.....	above 20,000

<sup>3</sup> Data from Burbank: *Geology and Ore Deposits of the Bonanza Mining District, Colorado*. U. S. Geol. Survey *Prof. Paper* 169 (1932).

<sup>4</sup> Based on data of specific gravity and mineral composition in *The Ore Deposits of Utah*, by Butler, Loughlin, Heikes and others. U. S. Geol. Survey *Prof. Paper* 111 (1920).

<sup>5</sup> Ransome: *Geology and Ore Deposits of Goldfield, Nevada*. U. S. Geol. Survey *Prof. Paper* 66 (1909).

<sup>6</sup> Tests made on diamond-drill cores soaked in subsurface waters from the area. Samples were put in a vise with plastic metallic contacts carefully wetted with salt water. The resistivity was determined with direct current, reversing poles, and with alternating current about 200 cycles. Schistosity, where present, cut across sample at an angle.



## Buchans, Newfoundland:

OHMS PER METER CUBE

Fresh sediments (tuffs and arkose).....	average	8,000
Sheared and altered.....	average	412
Fresh lavas, varying between rhyolite and andesite.....	average	3,200-6,640
Schisted and altered lavas.....	average	166
Quartz and feldspar porphyry, fresh.....	average	3,900
Slightly altered quartz porphyry (of yellow color).....	average	350
Intensely altered quartz porphyry.....	average	60
Silicified tuff with mineralization.....	up to	11,600

The difference in resistivity between unaltered and altered or sheared rock thus appears to be much greater than the pore volume indicates. The presence of pyrite or other sulfides, as well as some schistosity, making better connection between the pores, presumably accounts for this difference. An extreme example of these two factors is found in the Homestake mine, South Dakota, where the ore is a schisted rock carrying sulfides, some of which are oriented along the bedding planes or the schistosity. Tests of the resistivity along the schistosity show:

OHMS PER METER CUBE

Ellison quartzite, average.....	25,800
Ellison phyllite.....	528
Homestake formation, ore.....	4.6
Homestake formation, not mineralized.....	2,045
De Smet, biotite-garnet schist.....	505

The resistivity of vein quartz is extremely high, often approaching or even exceeding 100,000 ohms per meter cube. An example from Woman Lake, Ontario, gives:

OHMS PER METER CUBE

Fresh greenstone.....	5,000-8,000
Massive vein quartz.....	150,000

Sometimes all of this high resistivity is not realized in a survey, because the quartz may occur as a great number of stringers in the schist, as at Alaska Juneau and frequently at Porcupine, Ont. The current will pass more freely at places, thus reducing somewhat the resistivity of the quartz zone as a whole.

The width of the altered zone may vary between a few inches and several hundred feet, and the width of the quartz veins between a few inches and several tens of feet.

The geologic-electrical circumstances at an idealized quartz-gold deposit are thus a series of rapid changes of resistivity. From fresh rock we pass through an altered zone, vein quartz, altered zone and back into the fresh wall rock. The accompanying resistivity ratios are of the order of up to 50:1 between fresh rock and altered rock and often several hundred to one between quartz and altered rock.

Another feature to be noted is that the zones attain great depth, often extending down for several thousand feet, an important feature, as will be explained later.

### GEOPHYSICAL CONSIDERATIONS

It is apparent that the electrical property of altered or sheared rock and of vein quartz is generally such that with a proper electric method one can trace out the system of fracturing and the veins of an area covered by overburden. In the beginning the matter was not so easily solved. The electrical characteristics are not so pronounced as in the case of sulfide ores. Some of the important rocks are nonconductors instead of conductors. There is, therefore, required a method of great utility range, of great sensitivity but also a method that is free from outside influences, as these are apt to be much more disturbing with relatively small resistivity anomalies than with sulfide ores, where the anomalies due to the ore are much more pronounced.

A suitable potential instrument, the Racom, was developed by Zuschlag<sup>7</sup> in 1930. This instrument has undergone extensive tests and development in many parts of the world during recent years and its quality as an accurate all-round instrument has been well proved.

The theoretical principles of potential methods applied to general geological problems have been comprehensively studied by Hedstrom,<sup>8</sup> who, referring to this application as "electric trenching," has studied the cases of contacts and of vertical sheets of a conductivity differing from that of the homogeneous material in which they are embedded.

In their practical application potential methods suffer from the same disturbing factors as all other geophysical methods; namely, the influence of anomalies arising from the surface. In this case the anomalies are due to irregular thickness and composition of the overburden. As the overburden usually has a resistivity different from the bedrock, these irregularities will greatly affect the surface potential distribution, many times to such an extent as to overshadow completely the anomalies sought in the bedrock. In order to utilize fully the sensitivity of the Racom and the possibilities offered by potential methods in general, it became necessary to find a way to eliminate the surface influence, and after many laboratory tests, theoretical considerations and field tests this has been accomplished.

The elimination is done by the help of a property of the potential field, heretofore overlooked, which is *a function of the depth extent of the anomaly*, so that one limited to the surface will not give any indication

---

<sup>7</sup> H. Lundberg and T. Zuschlag: A New Development in Electrical Prospecting. *Trans. A.I.M.E.* (1932) 97, 47.

<sup>8</sup> H. Hedstrom: Electrical Prospecting for Auriferous Quartz Veins and Reefs. *Min. Mag.* (April, 1932).

whereas one extending to depth will be clearly indicated in spite of irregularities that may occur in the overburden. The method will be briefly explained by presenting two cases of potential distribution, expressed in the potential drop ratio between two subsequent potential drops, properly reduced for normal ratio. The arrangement of power electrodes and Racom instrument with rods is shown on Fig. 1.

The first case, a laboratory case (Fig. 1), is a rectangular body with lower resistivity than the surrounding material. The depth extent  $a$  of this body is varied, all other factors remaining the same. In this way a

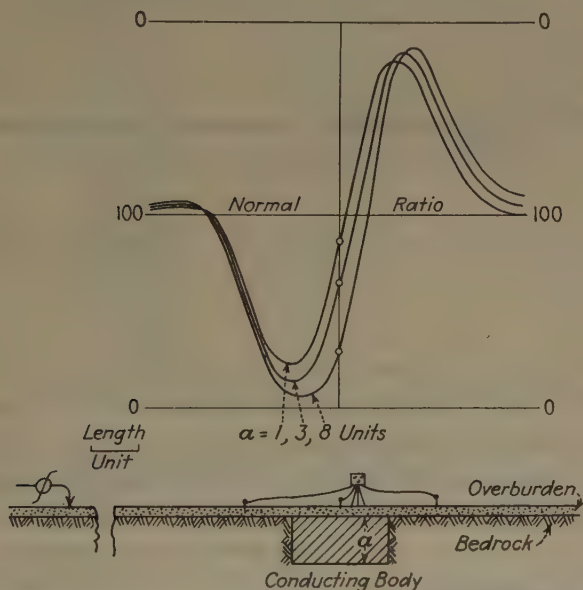


FIG. 1.—POTENTIAL-DROP RATIO CURVES OVER A CONDUCTING BODY, FOR DIFFERENT DEPTH EXTENTS OF THE BODY.

curve series is obtained, showing the influence of  $a$  upon the potential drop ratio. Three of these curves are shown in Fig. 1, for  $a = 1, 3$  and  $8$ .

It may first be observed that the strength of the indication increases only slowly when  $a$  increases, showing that the indication is caused mainly by the surface portion of the conductive body. When  $a$  increases, the indication moves slowly to the right, away from power electrode, so that it becomes more and more unsymmetrically located with regard to the center of the conductive body. The lack of symmetry may be best observed by measuring on Fig. 1 the distance between the normal ratio and the intersection point between the ratio curve and the vertical line through the center of the body.

If the power source is moved to the other side the same ratio curves are obtained, but rotated  $180^\circ$  around the vertical axis, as in Fig. 2, where the cases of  $a = 1$  and  $a = 8$  are plotted. A symmetry line

following points at equal distance between the curves clearly shows the lack of symmetry of the original curves in the sense explained above. The impression upon the symmetry line further emphasizes the lack of

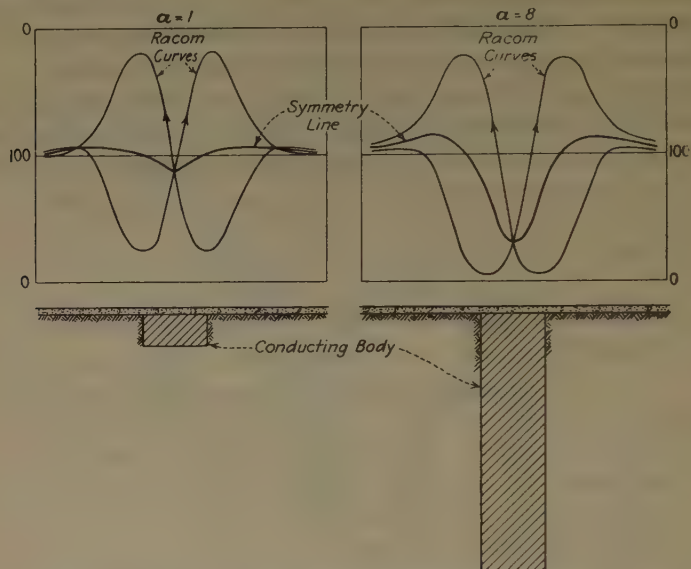


FIG. 2.—COMPLETE RACOM CURVES AND SYMMETRY LINE FOR TWO CASES OF FIG. 1.

symmetry as a function of the depth extent of the body. The symmetry line will, in fact, show no indication at all when the corresponding anomaly is limited to the surface (overburden). The case  $a = 8$  would correspond in the field to a depth of 200 to 600 ft., a depth that generally is exceeded by vein deposits.

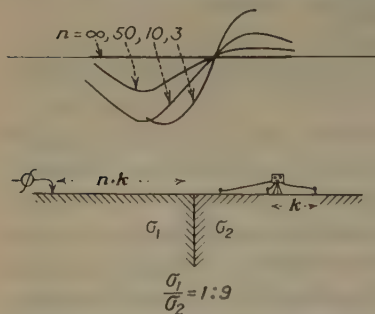


FIG. 3.—SYMMETRY LINE OF RACOM SURVEY OVER A CONTACT FOR DIFFERENT DISTANCES BETWEEN THE CONTACT AND THE POWER ELECTRODE.

line indication. In Fig. 3 the symmetry line for the distances  $d = 3, 10, 50$  and  $\infty$  are plotted, the original ratio determinations being left out. The indication is slowly decreasing in size when  $d$  increases, until for  $d = \infty$  it has disappeared. From this we may assume that the cause of

The second case, Fig. 3, is a vertical contact between two materials extending infinitely downward, a condition that gives a ratio picture as on Fig. 4. It has been calculated by using Maxwell's theory of images. Here the distance from the contact to the power electrode is varied, all other factors remaining the same. Another curve series is obtained, showing the influence of this distance upon the symmetry-



the phenomenon of unsymmetry is the inhomogeneity of the electric field in the vicinity of the power electrode, where the equipotential surfaces are spheres, as compared with vertical planes, when the power electrode is far removed.

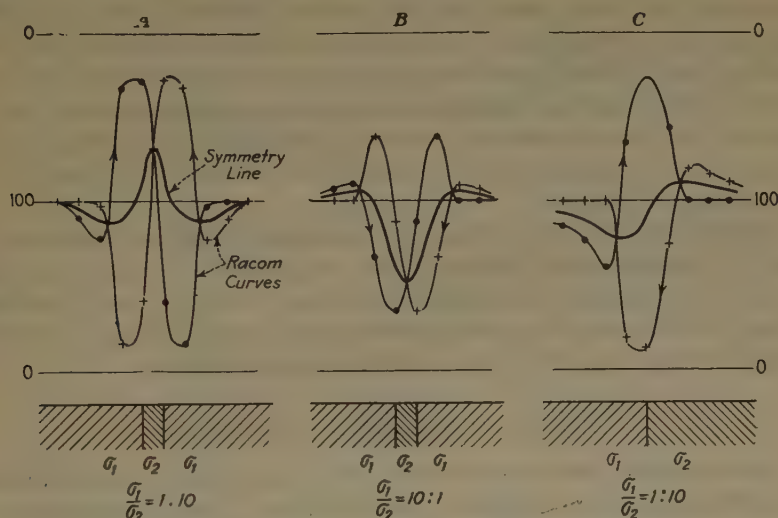


FIG. 4.—TYPICAL RACOM INDICATIONS OVER A SHEET OF POOR CONDUCTIVITY (A), ONE OF GOOD CONDUCTIVITY (B), AND A CONTACT (C).

In Fig. 4 are plotted three calculated cases of a sheet of poor conductivity, one of good conductivity and a contact. The resistivity ratio 1:10 between the different rocks has been chosen so as to represent actual

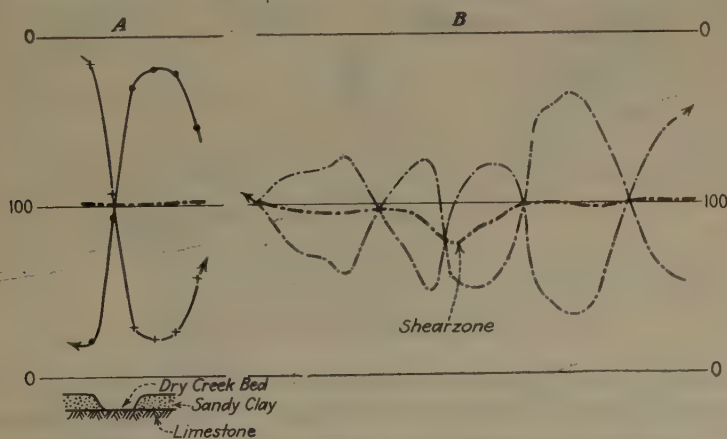


FIG. 5.—EXAMPLES OF ELIMINATION OF SURFACE ANOMALIES.

cases in nature, which, however, often may be expected to surpass this figure; for example, in the case of a quartz vein and a shear zone. The width of the sheet is assumed to be 10 ft. and the electrode spacing 20 ft.

The considerable indications obtained testify to the sensitivity of the method. As the thickness of the overburden increases, the indications naturally become weaker. This is also the case when the resistivity of the overburden is small compared with that of the bedrock. Experiments and field tests show that the method is still reliable for rather extreme cases of this kind. For example, surveys in Western Australia recently have disclosed shear zones with enclosed auriferous quartz veins below an overburden containing layers saturated with salt water. In the following will also be shown a survey in Ontario, where details in the bedrock were determined and interpreted despite a cover of glacial drift of depths up to 300 feet.

The elimination of overburden anomalies is further illustrated in Fig. 5. The right-hand drawing is part of a profile at Porcupine, which is typical for glaciated pre-Cambrian areas. Among the sometimes violent disturbances, there is one indicating a known shear zone, whereas all the others disappear as being due to surface effects.

#### SURVEY AT SHILLINGTON, ONTARIO

An interesting survey was carried out during 1932-33 at Shillington, about 23 miles east of Timmins, Ont. (Fig. 6). It was thought that, in

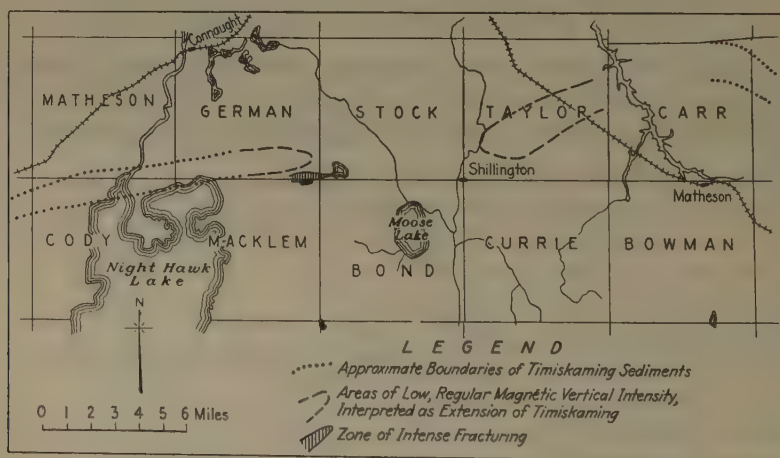


FIG. 6.—THE SHILLINGTON AREA, ONTARIO.

this general vicinity, the same structural conditions that control the deposition of gold at Porcupine would recur. The area is covered by glacial and post-glacial deposits to a depth of 60 to over 300 ft., and there are no outcrops within a radius of some 5 miles. The rocks occurring outside of this basin belong to the formations common in this part of Ontario; Keewatin lavas, Temiskaming sediments, intrusive dikes of Algonian age, usually granitic, diabase dikes and some quartz veins.

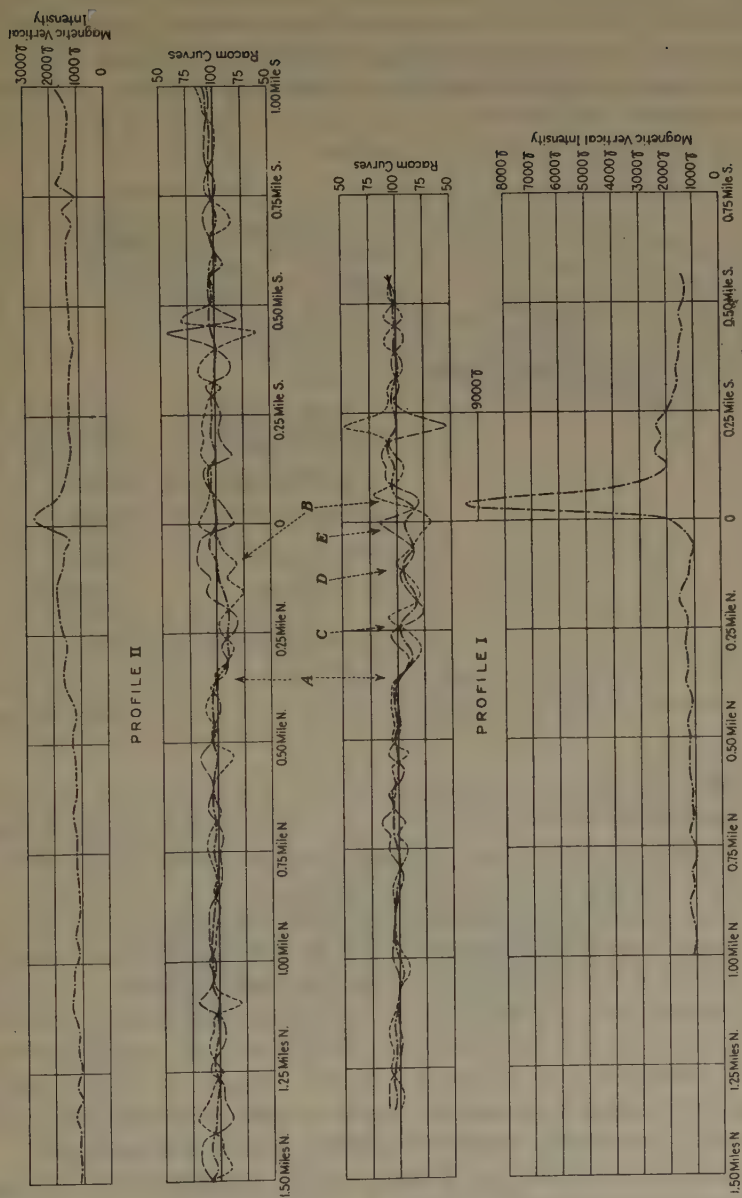


FIG. 7.—PROFILE I AND II, SHILLINGTON AREA, ONTARIO.

Resistivities of rocks found in the subsequent drilling are shown earlier in this paper.

The survey began with a magnetic reconnaissance to ascertain the location of the Temiskaming sedimentary formation, which was found to be interrupted in Stock Township, as indicated on Fig. 6. This fact is of importance because some of the structural control at Porcupine is definitely linked with a similar occurrence.

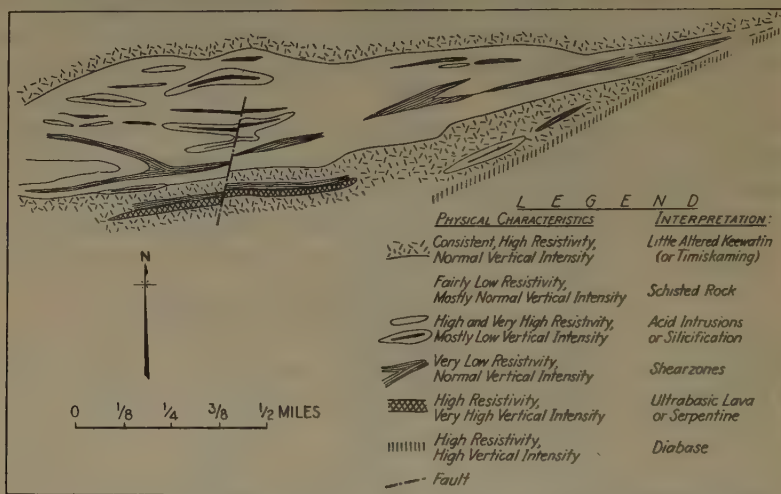


FIG. 8.—INTERPRETATION OF ELECTRIC AND MAGNETIC SURVEY, SHILLINGTON AREA, ONTARIO.

An extensive Racom reconnaissance survey revealed a wide zone of better conductivity within the area. This zone was surveyed in detail with profiles 330 ft. apart over a distance of about 2 miles and in addition some magnetic detail work was carried out.

Examples of electrical and magnetic results are shown in Fig. 7. The zone of lower resistivity is between A and B. Within this zone there are a number of indications of higher as well as lower resistivity. A study of the electrical and magnetic data permitted the detailed interpretation of Fig. 8, where the physical properties determined are "translated" into probable geological formations and rocks. Based upon this map a drilling plan was made mainly to test the zones of higher resistivity, interpreted as being due to acid intrusions or highly silicified rock.

In Fig. 9 is shown a drilled profile together with the geo-physical results of the same profile. A comparison of these data reveals the following:

1. The main zone, interpreted as a zone of fracturing, schisting or shearing of the lava, is composed of strongly fractured and altered rocks of Keewatin origin.



2. The zones of higher resistivity, which were interpreted as acid intrusions or possible silicified rock, corresponded to intrusive dikes of granite and syenite, partly with porphyritic texture.

3. An electric and magnetic indication south of the main zone was interpreted as a body of serpentine or possibly a mass containing pyrrho-

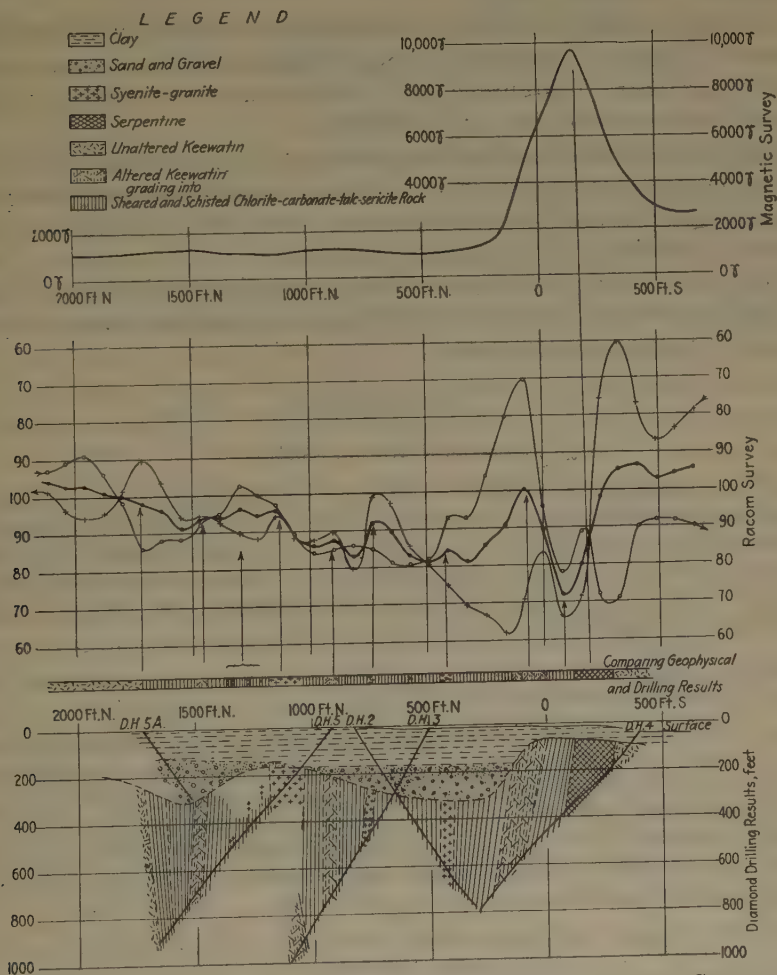


FIG. 9.—COMPARISON OF DRILLING RESULTS AND GEOPHYSICAL RESULTS, SHILLINGTON AREA, ONTARIO.

tite. The fact that the Racom survey showed this body to occupy a ridge in the bedrock surface argued against the latter possibility, and drilling revealed a body of serpentine, the northern contact of which was intensely sheared.

4. The neutral rock north and south of the main zone, interpreted as unaltered Keewatin or Temiskaming, was normal, unaltered Keewatin.

5. A number of smaller indications could be interpreted as quartz, narrow acid intrusions or less altered sections of lava flows. As it was apparent that the overburden was very heavy, these indications were considered too uncertain to warrant any detailed interpretation. The drilling revealed, however, that even these reflected definite geological features in the drilled section.

The geophysical conclusions and predictions were thus closely confirmed by drilling in spite of the unfavorable conditions, such as the exceedingly heavy overburden and the total absence of any outcrops within several miles of the area prospected.

As vein quartz is practically absent and as, in addition, the acid intrusions are granite and syenite rather than quartz porphyry, the conditions are not of such nature as to constitute definitely favorable factors for finding a gold deposit in this area.

The survey does show, however, how geophysical methods can be used for solving geological problems in drift-covered areas, problems which are abundant in prospecting for gold.

## DISCUSSION

*(Sherwin F. Kelly presiding)*

A. H. ROGERS,\* New York, N. Y.—I think Mr. Kihlstedt treated the Western Australian work a little too cavalierly. It really has developed into a very important orebody. The work was done for a company in which Gold Fields and some other Western Australian operators have cooperated. The work consisted, of course, in looking for the shear zones that are known to go through that country, and was conducted over a part of the country covered by drift.

M. K. HUBBERT,† New York, N. Y.—How far do you run the test profiles away from the current electrode, and what is the spacing between test probes?

F. H. KIHLESTEDT.—It depends entirely upon the conditions in the area of the survey. For instance, if there is heavy overburden, it is always better to increase the spacing. By increasing the spacing, you can go a little further out. If the overburden is shallower, or the feature being sought is merely a small detail, the spacing must be decreased and you must stay closer to the power electrode. The limit we have used so far is about 1500 ft. distance from the power electrode. In some cases we have stayed within 400 or 500 feet.

M. K. HUBBERT.—What current do you use on power electrodes, and what frequency?

F. H. KIHLESTEDT.—Alternating current, a simple burner run by a portable 6-volt battery. The frequency usually is about 250 cycles.

---

\* Rogers, Mayer and Ball.

† Instructor in Geophysics, Columbia University.

## Discovering Gold-quartz Veins Electrically

By SHERWIN F. KELLY,\* THEODOR ZUSCHLAG,\* AND BELA LOW,\* NEW YORK, N. Y.

(New York Meeting, February, 1934)

### ABSTRACT†

GOLD has been mined in the State of Georgia for over 100 years, and although the total production is nearly \$18,000,000, the output has declined to an insignificant figure in recent times. The increase in price of gold has brought about a revival of interest in this district, with the result that an electrical survey was undertaken in the McDuffie County gold belt to see whether new quartz veins could be discovered. The problem of locating quartz veins electrically has only rarely been attempted by geophysicists, because of technical difficulties. New improvements in apparatus and field procedures, the most recent of which is the designing of the Ground Comparator, now make possible the differentiation of quartz veins and enclosing rock. This instrument is designed to eliminate the effect of ground contact resistances, and measures the ratio of potential drops between successive stations. These are transformed into resistivity ratios, the highly resistant quartz veins manifesting themselves by sharp breaks in the resistivity-ratio curves. Surface variations of resistance are eliminated by a special technique.

Electrical surveys were made on two properties about 40 miles west of Augusta, Georgia. A reconnaissance of the Woodall and detail work on the Hamilton required about 13,000 ft. of electrical profile. Typical profiles from each are given, with the results of trenching certain of the electrical indications. Comparisons are made between the reactions due to veins several feet wide and those from small quartz stringers. Instances are cited where the electrical profiles were used to trace extensions of known veins, or to establish their nonextension. The discovery of several veins is described, most of which were barren, but of which at least two showed gold in encouraging amounts.

The field of application of the Comparator to the prospecting for metallic and nonmetallic minerals, and to the study of various geological problems, is discussed at the close of the paper.

\* Combined Geophysical Methods, Inc.

† The paper was published in *Mining and Metallurgy*, June, 1934.

# Application of Resistivity Methods to Northern Ontario Lignite Deposits

By R. H. HAWKINS,\* TORONTO, CANADA

(New York Meeting, February, 1933)

AN investigation of the applicability of geophysical methods to northern Ontario lignite deposits was undertaken early in 1930 by the Ontario Research Foundation at the request of the Ontario Department of Mines

TABLE 1.—*Formations Associated with Moose River Basin*

System	Formation	Lithology	Maximum Observed Thickness, Ft.	Correlation
Pleistocene.....		Marine clays Glacial till Interglacial clay and peat Glacial till	150 (Minimum 30)	
Lower Cretaceous or Upper Jurassic.	Mattagami	Fireclay, sand and lignite	138	Kootenay (?)
Devonian (Upper)....	Long Rapids	Petroliferous, black and gray shale	50	Portage and Genesee
	William's Island	Limestone and calcareous shale	87	Tully (?)
Devonian (Middle)....	Abitibi River	Gray fossiliferous limestone	65	Onondaga
Devonian (Lower) ?..	Moose River	Limestone and gypsum	50	
Devonian (Lower)....	Sextant	Arkose, clay, etc.	50	

Pre-Cambrian. . . . Syenite, granite gneiss, etc.

Igneous intrusives.. Lamprophyre dikes cut the Abitibi River and lower formations.  
(Permission of Ontario Dept. of Mines)

and was financed in part from a research grant made by the latter organization. The work to date has included gravitational, magnetic and electrical resistivity studies. The gravitational and magnetic measure-

\* Research Fellow in Physics, Ontario Research Foundation.



ments will be described elsewhere by A. H. Miller, of the Dominion Observatory, Ottawa, Canada.

The main object of the resistivity studies was to determine whether resistivity methods could be used to find new lignite deposits; to delineate the Onakawana deposit between the exploratory drill holes already made at 1000 to 2000-ft. intervals; or to assist in working out the geologic structure of the lignite area. A secondary object was to compare observed resistivity effects with those theoretically calculated from known underground conditions.

#### *Geology of Area*

As shown in the key map (Fig. 1) the Onakawana lignite deposit occurs in the Moose River basin, 125 miles north of Cochrane on the Temiskaming and Northern Ontario Railway. For detailed information regarding the geology of this area and its development up to May, 1930, the reader is referred to the reports of W. S. Dyer.<sup>1</sup> Table 1 and Fig. 2 show the features of most interest in connection with this paper. Table 1, reproduced from Dyer's 1928 report (p. 15), gives the series of formations associated with the Moose River Basin. The known lignite deposit occurs in the overlying formation near the central region of an extensive synclinal fold in the pre-Cambrian shield. A deep drill hole designated A (Fig. 2), believed to be near the center of this

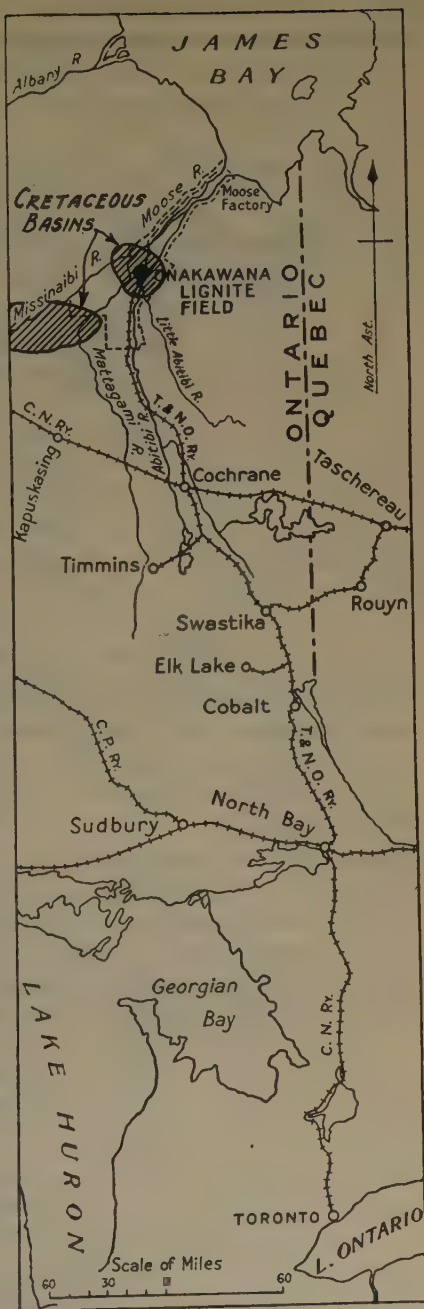


FIG. 1.—LOCATION OF ONAKAWANA LIGNITE DEPOSIT. (PERMISSION OF ONTARIO DEPARTMENT OF MINES.)

<sup>1</sup> W. S. Dyer: Ontario Dept. of Mines (1929) **37**, Pt. 6; *Ibid.* (1931) **39**, Pt. 6; *Trans. Royal Soc.* [3] (1931) **25**, 85.

basin, encountered the basal pre-Cambrian rock at a depth of 1030 ft. The Cretaceous series with which the lignite is associated is overlain with

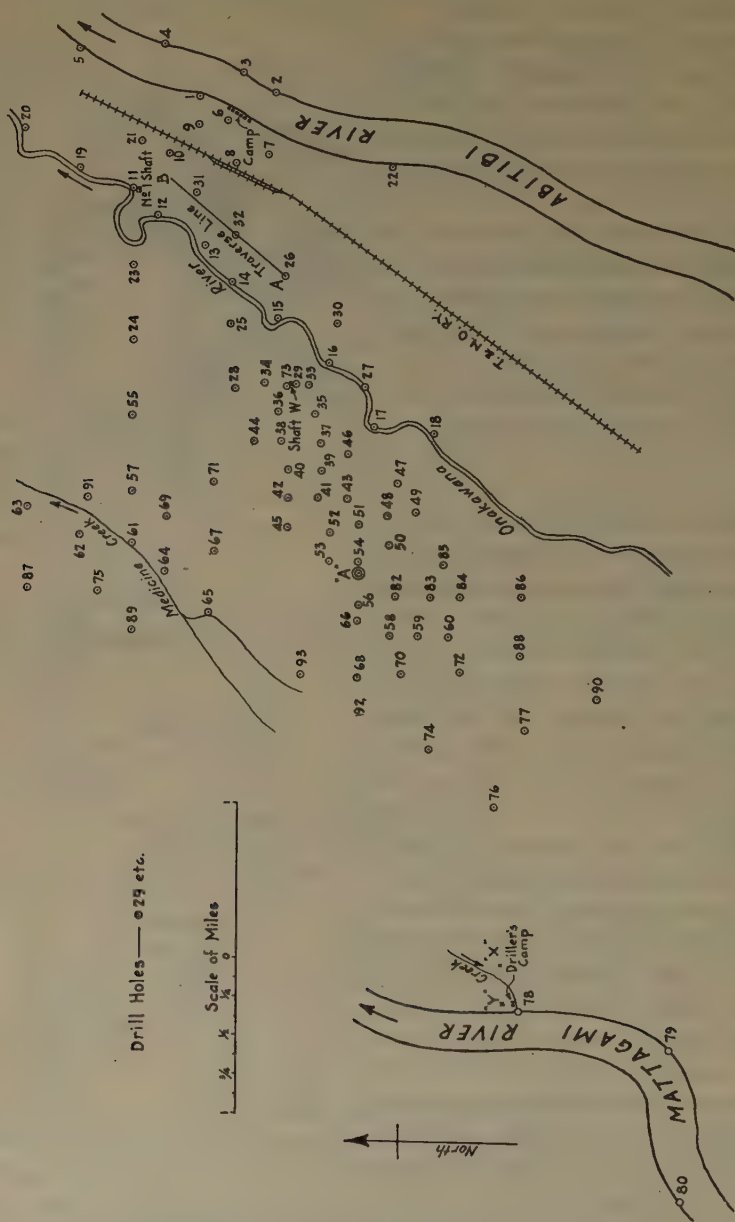


FIG. 2.—LOCATION OF DRILL HOLES, ONAKAWANA LIGNITE FIELD.

glacial drift, varying degrees of glacial erosion and replacement having taken place. Except where cut by water courses, the surface of the ground is quite flat. Irregularities in the glacial drift surface have been

smoothed by more recent marine clay deposits, exposed by retreat of the sea, and covered in turn by muskeg of 4-ft. average thickness. Swampy, water-soaked conditions exist generally, except near the drainage courses, where spruce, poplar, and other soft woods occur in varying vigor and density.

### *Scope of This Report*

Unless otherwise specified, the resistivity studies will be described in the sequence in which the measurements were conducted, under the following main divisions:

1. Laboratory Examination of Samples.
2. Preliminary Field Tests, August, 1930.
3. Field Survey, September, 1930.
4. Winter Measurements.
5. Laboratory Preparations.
6. Birch Cliff Tests.
7. Field Work, Onakawana, 1931.

A general summary will be given, and an appendix describing the instruments and apparatus.

### *Methods: Nomenclature and Description*

In all resistivity methods, current is supplied to the earth by input electrodes and the resulting potential distribution at the surface is determined by means of selected configurations of pick-up electrodes. Four arrangements for depth investigations were used in the present work, hereafter designated as follows:

*Central Electrode Method.*<sup>2</sup>—A single current electrode is placed at the site selected for study with four symmetrically placed outer current electrodes (theoretically a continuous circle), each distant at least twice the depth of the structure under investigation. The potential fall is measured over successive intervals suitably chosen about the central electrode and in any azimuths desired. The theoretical expression for a homogeneous medium is

$$\rho = 2\pi R \cdot \frac{ab}{b - a}$$

where  $a$  = distance from central electrode to inner potential electrode, centimeters.

$b$  = corresponding distance to outer potential electrode.

$R$  = observed interbowl resistance in ohms.

$\rho$  = resistivity of the homogeneous medium (ohms per cm. cube).

---

<sup>2</sup> L. Gilchrist: Geol. Survey, Dept. of Mines, Canada, *Mem.* 165 (1931) 167.

*Single Distant Probe Method.*<sup>3</sup>—This method is identical with the central electrode scheme except that the circle of outer current electrodes is replaced by a single electrode distant four or five times the depth to be investigated. For practical purposes this distance is generally adequate, although the above formula is strictly applicable only with the distant electrode at infinity.

*Wenner's Method.*<sup>4</sup>—Four electrodes are spaced in line at equal intervals. The two most distant are current electrodes, and the two inner are potential pick-ups. For depth investigations, readings are taken

TABLE 2.—*Resistivities of Specimens of Materials from Onakawana Lignite Fields*

Specimen	Approx. Resistivity, Ohms per Cm. Cube
1. Water shaken with a portion of clay.....	4,440
2. Muskeg saturated with water.....	8,950
3. Boulder clay from shaft No. 1 (typical of clay in contact with lignite).....	11,000
4. Wet lignite.....	900
5. Lignite dried to the crumbling point.....	3,800
6. Samples from shaft No. 1.	
Silt from 2 ft. below surface of ground.....	1,880
Silt from 4 ft. below surface of ground.....	7,620
Boulder clay from upper levels.....	2,500
Marine clay.....	2,500
Fireclay.....	1,880

with a series of electrode intervals. The expression for calculations in a homogeneous medium is:—

$\rho = 2\pi aR$  where  $\rho$  and  $R$  are as before, and

$a$  = potential electrode interval, =  $\frac{1}{3}$  current electrode interval.

*Lee's Partitioning Method.*<sup>5</sup>—This is but a slight modification of Wenner's method; a third potential pick-up is placed at the central site (mid-point of line of Wenner system) to study the two halves of the potential interval separately. The expression corresponding to each half is:

$$\rho = 4\pi aR$$

where the symbols have the same meaning as in Wenner's method, above.

<sup>3</sup> A. S. Eve and D. A. Keys: Applied Geophysics, 107–111. Cambridge Univ. Press, 1929.

<sup>4</sup> F. Wenner: U. S. Bur. Stds. *Bull.* 12 (1916) 469.

<sup>5</sup> J. H. Swartz: U. S. Bur. Mines *Inf. Circ.* 6445 (1931).



*Limitations of Simple Expressions*

Although the above formulas are inadequate when the resistivity of the earth material is not uniform throughout, many observers have used the apparent resistivities calculated from these expressions to predict the presence of and depth to concealed structural changes. Of the earlier workers, Gish and Rooney,<sup>6</sup> using Wenner's method over a filled-in ravine, found empirically that an abrupt change of slope of the resistivity graph, calculated from the simple expression, occurred at a potential electrode interval corresponding closely to the depth of the fill. They were able thus to outline the former ravine quite satisfactorily. The rule suggested by these tests has been found to fit the facts well in some cases; in others, there has been disagreement. Hummel<sup>7</sup> and others by precise theoretical calculations have shown that even for the simple case of a uniform upper layer overlying an infinite homogeneous medium of different resistivity, the presence of the lower medium influences the shape of the resistivity curve for intervals much less than the depth to the lower medium, and that no abrupt indications of such a change can be expected. The theoretical treatment of the ideal two-layer case is discussed later in this paper (p. 95).

## LABORATORY EXAMINATION OF SAMPLES

*Measurements and Findings*

Before field tests were undertaken, the resistivities of specimens of formations from a shaft put down the previous winter were measured with Wheatstone bridge equipment in the laboratory. Current was passed through shaped bars of the materials, or through cylindrical blocks packed in sections of glass tubing, pools of mercury which covered the entire cross-section providing a fairly uniform current density. The potential drops were observed over intermediate portions of the shaped bars by means of small probes driven into the specimens; the total resistance between the end contacts of the clays packed in glass tubing alone was determined. As the two methods gave accordant values in comparative tests on selected samples, the contact resistance in the latter method appeared to have a negligible effect. Repeated measurements on the same materials gave consistent values, the averages of which are shown in Table 2. Here, and throughout this paper, all resistivities are expressed in ohms per centimeter cube.

Of the samples studied, the wet lignite was the best conductor, showing a ratio of 12:1 with the most resistant clay, though more generally

<sup>6</sup> O. H. Gish and W. J. Rooney: *Terrestrial Magnetism* (1925) **30**, 161-188 and *Phys. Rev.* (1925) **25**, 254.

<sup>7</sup> J. N. Hummel: *Trans. A. I. M. E.* (1932) **97**, 392.

a ratio of about 3:1. As this ratio depended on the moisture content, it was fortunate that the samples had been kept in sealed containers, although they had not been secured for resistivity studies. Because of the small ratios observed, the meagerness of the data and the lack of information from the samples of clay distribution with depth, the utility of resistivity methods could not be reasonably predicted. However, as the level topography and extensive horizontal lignite beds were favorable factors, a brief field test was undertaken.

#### PRELIMINARY FIELD TESTS, AUGUST, 1930

Investigations directed by Dr. L. Gilchrist of the Department of Physics, University of Toronto, were conducted for eight days at the lignite deposit. The full report of this work, prepared by Dr. Gilchrist, will appear in a Memoir of the Geological Survey, Department of Mines, Canada. A summary of the tests follows:

##### *Purpose and Measurements of Preliminary Field Tests*

The objects of the preliminary investigations were to determine whether resistivity methods would differentiate between barren areas and those where lignite existed; whether the observations could be correlated to the drilling records and to the laboratory measurements; and to establish the procedure essential to more extensive investigations. Resistivities were studied by both the central electrode method and the single distant probe method at three sites; *viz.*, drill holes 10, 23 and 29, located on the map, Fig. 2. At two unproved sites 400 and 800 ft. west of drill hole 10, the single distant probe method was used alone. The readings were taken with a Megger (appendix A), and because of the dangers of insulation leakage due to rainy weather, and of the limitations of the Megger on very small readings, the measurements were checked at times by potentiometer, milliammeter and commutator equipment (appendix B) in a manner similar to the scheme used by Rooney<sup>8</sup> and others.<sup>9</sup>

##### *Findings and Conclusions, Preliminary Field Tests*

The drill-hole records, included in Fig. 6, reveal lignite seams 58 ft. thick with overburden of 74 ft., and lignite 36 ft. thick with overburden of 61 ft., at drill holes 29 and 10 respectively. At these points, and at the two unproved sites, there was a rapid decrease in resistivity at depths corresponding closely to the overburden thickness; in fact, the rate of decrease approached abruptness.

<sup>8</sup> W. J. Rooney: *Terrestrial Magnetism and Atmospheric Electricity* (1927) **32**, 100-102.

<sup>9</sup> A. B. Broughton Edge and T. H. Laby: *Principles and Practice of Geophysical Prospecting*, 25-26. Cambridge Univ. Press, 1931.

*Ibid.*, 31-42.

*Ibid.*, 248-250.

At drill hole 23, where lignite was absent, the results were pronouncedly different. Although Cretaceous clay bearing lignite fragments occurred below a depth of 105 ft., the resistivity values remained at about 10,000 ohms per cm. cube to a depth of 150 ft., followed by gradual decrease to 7000 ohms per cm. cube, a value twice as large as the minimum at depth found at the other points.

For potential intervals out to 300 ft. from the center, adequate for the depths involved, the single distant probe method, with the current electrodes 800 ft. apart, gave practically the same values as the central electrode method with the outer electrodes at any distance greater than 500 ft. For further studies, the application of the single distant probe method, with a current electrode interval of 800 ft., appeared justifiable.

These preliminary findings warranted a number of tentative conclusions:

1. Fairly abrupt decreases in resistivity values at potential electrode intervals corresponding closely to the overburden thickness might be correlated with the better conductivity of lignite compared with the associated clays. No such marked decrease was observed where the lignite was absent.

2. The overburden thickness could be fairly accurately estimated by accepting the above correlation at the points investigated.

3. As the abrupt changes in the resistivities observed were not to be expected from the theoretical investigations of Hummel (ref. 7) and others, it appeared that conditions in the earth, other than those existing in simple continuous conductors, gave rise to marked distortions of the normal potential distribution.

Although the tests definitely supported the tentative conclusion that resistivity methods were applicable to the existing problems, further work was essential to establish the degree of generality of these findings.

#### FIELD SURVEY, SEPTEMBER, 1930

The writer and three assistants were detailed for a further month's survey to determine whether the difference between resistivity conditions found at good and barren sites existed generally, and whether the Megger with the other portable equipment required for the single distant probe method could help the geologists in selecting sites for drilling.

#### *Preliminary Tests at Drill Hole*

A fairly extensive series of measurements at drill hole 7 was undertaken to determine the most satisfactory procedure for an extended survey. Readings were taken with a Megger and checked by a potentiometer (appendix C); with the latter, average readings with direct current in reversed directions were necessary, as a commutator was not available. Copper stakes 3 ft. long and  $\frac{1}{2}$  in. in diameter were used as

TABLE 3.—*Resistivity Data Obtained in 4 Azimuths at 90° Intervals about Drill Hole 48 as Center, by the Single Distant Electrode Method*

Interval (Feet from Drill Hole)	North Line			East Line			South Line			West Line		
	$R_{P_1-P_2}$	Bowl $R$	$\rho_{P_1-P_2}$	$R_{P_1-P_2}$	Bowl $R$	$\rho_{P_1-P_2}$	$R_{P_1-P_2}$	Bowl $R$	$\rho_{P_1-P_2}$	$R_{P_1-P_2}$	Bowl $R$	$\rho_{P_1-P_2}$
5-10	330	2.39	6510	320	2.65	6660	310	2.78	6990	330	2.31	5810
10-20	310	1.075	4520	265	1.14	4790	245	1.07	4500	239	1.18	4960
20-30	270	0.44	5200	178	0.47	5560	283	0.48	5680	165	0.475	5620
30-40	217	0.27	6190	204	0.255	5850	278	0.265	6070	148	0.275	6310
40-50	186	0.17	6490	280	0.16	6110	283	0.16	6110	195	0.16	6110
50-60	213	0.125	7160	300	0.13	7450	310	0.125	7160	196	0.12	6880
60-70	350	0.085	6820	210	0.08	6420	330	0.08	6420	214	0.08	6420
70-80	375	0.06	6420	192	0.055	5880	335	0.06	6420	205	0.06	6420
80-100	340	0.085	6490	260	0.085	6490	320	0.075	5730	198	0.08	6110
100-120	206	0.045	5160	300	0.05	5730	275	0.045	5160	184	0.05	5730
120-150	234	0.045	5160	350	0.045	5160	325	0.04	4580	300	0.045	5160
150-200	241	0.035	4010	268	0.04	4580	350	0.04	4580	220	0.04	4580
200-300	265	0.03	3440	150	0.025	2870	300	0.025	2870	187	0.03	3440

Resistance values in ohms; resistivity values in ohms per cm. cube.

 $R$  $\rho$  $P_1-I_1$  = potential electrode resistance.  $P_1-P_2$  = resistivity of interbowl material.



electrodes, instead of porous pots; they were easier to place, had much lower contact resistance, and required little care. Their use with direct current is generally not feasible, but for resistances greater than 0.5 ohm they proved satisfactory; for smaller resistances, polarization effects prevented their use.

As the available range of the potentiometer without shunts was 100 mv., natural earth potentials of greater magnitude over some intervals rendered the instrument rather inadequate for rapid work. These natural potentials were random surface effects due to the electrolytic character of the water-saturated muskeg, and were quite unrelated to underlying formations.

#### *Extent of Further Tests*

After the work at drill hole 7 was completed, measurements were made by the single distant probe method at 14 other drill holes. These sites were selected because a ready comparison of resistivities with local structure could be obtained, and because they included a range of underground conditions fairly representative of the known deposit. At each drill hole, the current electrodes were placed 800 ft. apart and Megger readings were taken of interbowl resistances out to 300 ft. from the drill hole and generally in four azimuths at 90° intervals. Time and facilities did not permit checking with the potentiometer.

#### *Typical Record and Graphic Presentation of Data*

In Table 3 the field data obtained at one of the sites, drill hole 48, are shown, with resistivities calculated from the expression given on

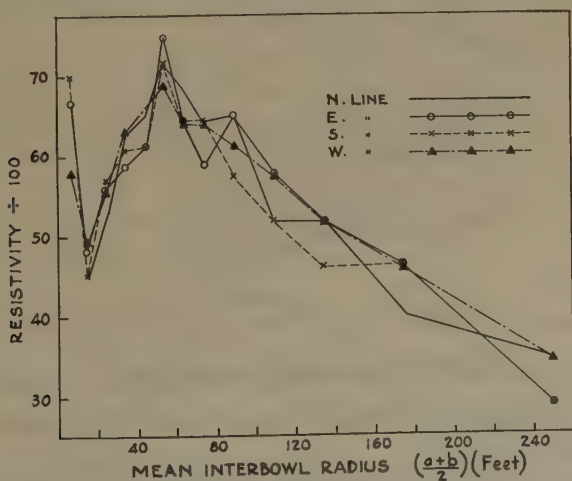


FIG. 3.—SYMMETRY OF RESISTIVITY DISTRIBUTION, CENTER AT DRILL HOLE 48.

page 4, and corrected for electrode penetration as described in appendix G. Besides the interbowl resistances for each interval, the electrode

contact resistances are recorded (appendix A). In Fig. 3, the resistivities of Table 3 are plotted as ordinates with the corresponding average inter-bowl radii  $\left(\frac{a+b}{2}\right)$  as abscissas. The corresponding resistivities in all four directions were nearly identical. Since practically equal symmetry

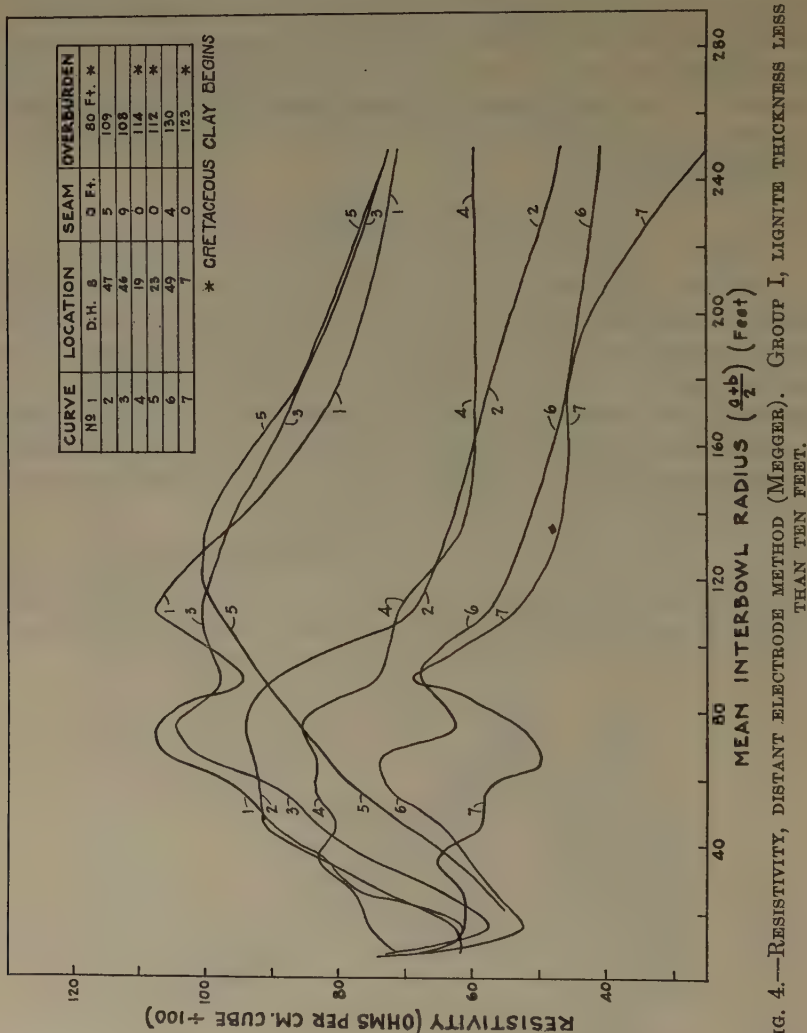


Fig. 4.—RESISTIVITY, DISTANT ELECTRODE METHOD (MEGGER). GROUP I, LIGNITE THICKNESS LESS THAN TEN FEET.

was found at all test sites, only the average values from the four azimuths are presented hereafter.

On account of the amount of data obtained, the average resistivity values at each site have been shown graphically only in Figs. 4 and 5, following the scheme of Fig. 3. The curves have been divided, for convenience, into two groups, depending on whether the lignite thickness

was less or greater than 10 ft. The graphs of the tests previously made at drill holes 10, 23 and 29 are included, and for handy reference the over-

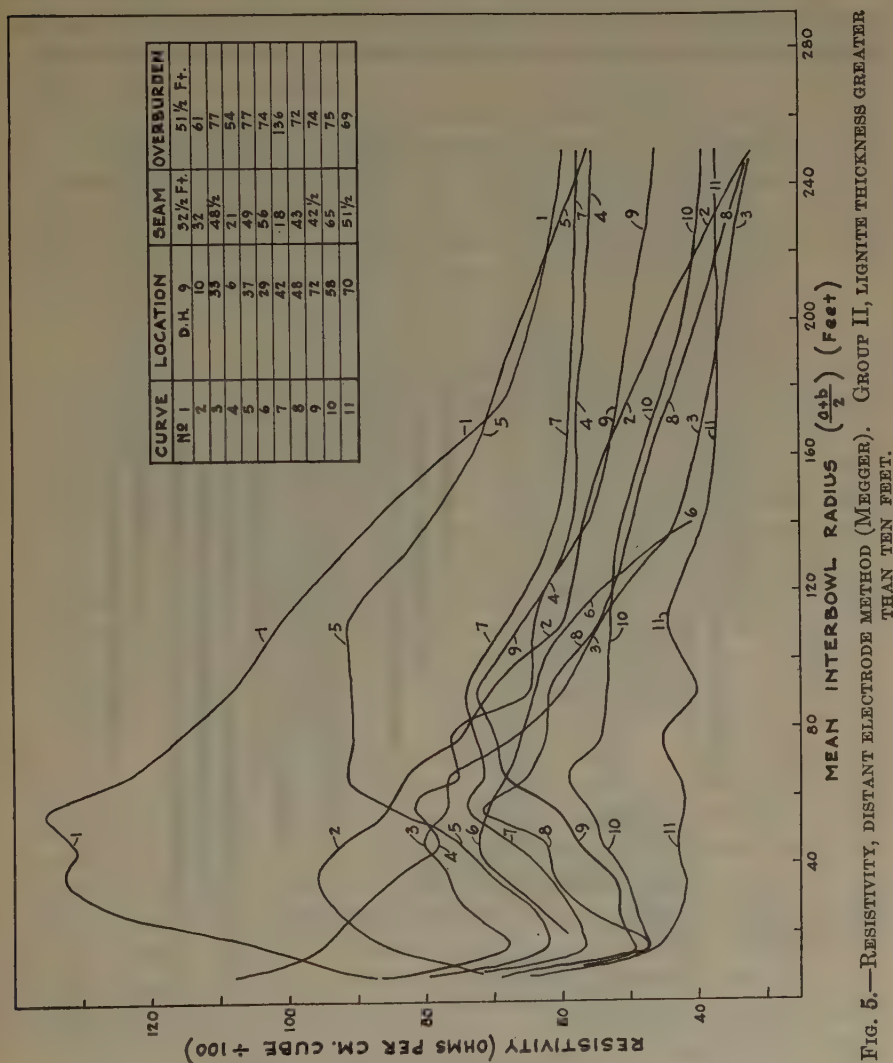


FIG. 5.—RESISTIVITY, DISTANT ELECTRODE METHOD (MEGGER). GROUP II, LIGNITE THICKNESS GREATER THAN TEN FEET.

burden and seam thickness for each location are shown. In Fig. 6 the drill-hole records for all the sites are shown schematically.

### *Methods of Interpreting Resistivity Curves*

Essentially, three methods of interpretation existed, viz:

1. The strictly empirical method—in which possible characteristic differences in the resistivity curves from favorable areas compared to

those from barren ones were used as a basis for predicting conditions at undrilled locations.

2. The semi-empirical method—in which the observed trend of the resistivity curve formed the basis of interpretation, the values having been calculated from the expressions for potential distribution in homo-

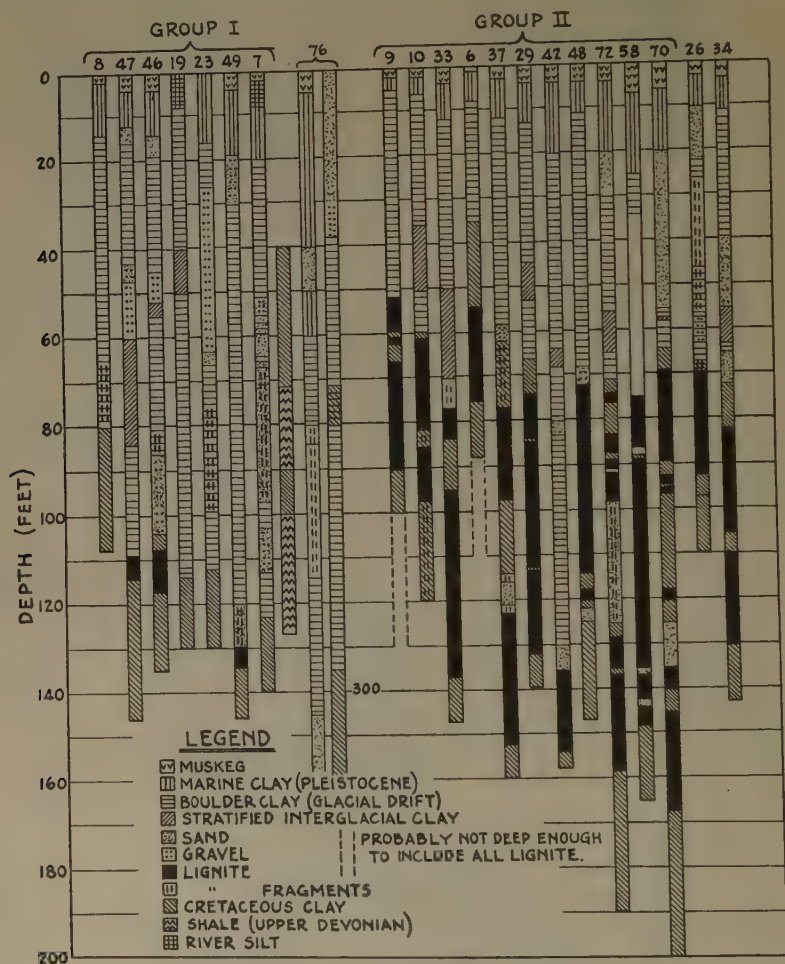


FIG. 6.—DRILL-HOLE RECORDS, GROUPS I AND II.

geneous media. An abrupt change of slope of the graph was taken to indicate a marked change in resistivity of the underground at a depth corresponding roughly to the mean radius of the interbowl section concerned. Where the correspondence was inexact, drill-hole records might permit a factor to be deduced for estimating depths at unproved locations. In the papers of other workers,<sup>10</sup> various factors had been suggested.

<sup>10</sup> A. S. Eve and D. A. Keys: Geol. Survey, Dept. of Mines, Canada, *Mem.* 165 (1931) 111.



3. The theoretical method—in which the observed data were compared with those calculated from the theoretical potential distribution in non-homogeneous media. With certain fundamental assumptions, such workers as Hummel,<sup>11</sup> Weaver,<sup>12</sup> Peters and Bardeen,<sup>13</sup> Roman,<sup>14</sup> Ehrenburg and Watson,<sup>15</sup> and others had calculated the theoretical surface potential distribution about point current sources for various simple conditions of the underground, and particularly for the case of homogeneous horizontal strata of different resistivities. For cases of more than two layers the numerical calculations became very involved, and to avoid complex functions, simplifying approximations had to be used. The inverse problem of fitting a theoretical solution to observed resistivity values rarely could be solved uniquely.

### *Adequacy of Drilling Records*

It might be argued that drill-hole records should not be used to check the conclusions from resistivity measurements, because a drill hole might not give a true picture of the entire volume of earth defining the potential distribution. In the locality of drill hole 29, mining operations showed that the lignite seams were quite flat, continuous, and uniformly thick, but similar conditions were not known to apply to the clay formations. On the contrary, study of the records of adjacent drill holes and findings from resistivity and gravitational investigations along a traverse indicated that decided changes in the character of the overburden might occur in short distances. This consideration limited the extent to which resistivity curves and drilling records could be correlated fully.

### *Discussion of Resistivity Curves*

The two groups of graphs, Figs. 4 and 5, revealed no characteristic difference between the vertical resistivity distributions at barren and good areas upon which a successful empirical interpretation might be based. Although a general inspection suggested that except for the curves of drill holes 7, 9, 37, 47 and 49, the resistivities at depth tended to lower values at good holes than at barren ones, yet from later evidence it would appear that any delineation of lignite from the associated clay by this means was a chance coincidence for the sites chosen, and not due to consistent resistivity ratios throughout. Although the resistivities at all the points were of the same order of magnitude, considerable variations occurred within the range for the overburden. These irregularities

---

<sup>11</sup> Reference of footnote 7.

<sup>12</sup> W. Weaver: *Trans. A. I. M. E.* (1929) **81**, 68–83; *Amer. Math. Monthly* (1930) **37**, 165–181.

<sup>13</sup> L. J. Peters and J. Bardeen: *Univ. of Wisconsin Bull. Ser.* **71** (1930).

<sup>14</sup> I. Roman: *U. S. Bur. Mines Tech. Paper* 502 (1931).

<sup>15</sup> D. O. Ehrenburg and R. J. Watson: *Trans. A. I. M. E.* (1932) **97**, 423–438.

rendered empirical analysis untrustworthy in view of the small ratios of resistivities of lignite and clay. As the information was inadequate for accurate theoretical solutions for each point, the only basis of analysis possible was a semi-empirical interpretation guided by all available geological evidence and past experience.

When the average interbowl radius for which the resistivities began to show a persistent decrease was adopted as the probable depth to a better conductor, the overburden thickness for the sites of group II was determined to within 10 ft. at drill holes 6, 9, 29, 33, 48, 58, 70 and 72; whereas the estimate was in error by more than 10 ft. for drill holes 10,

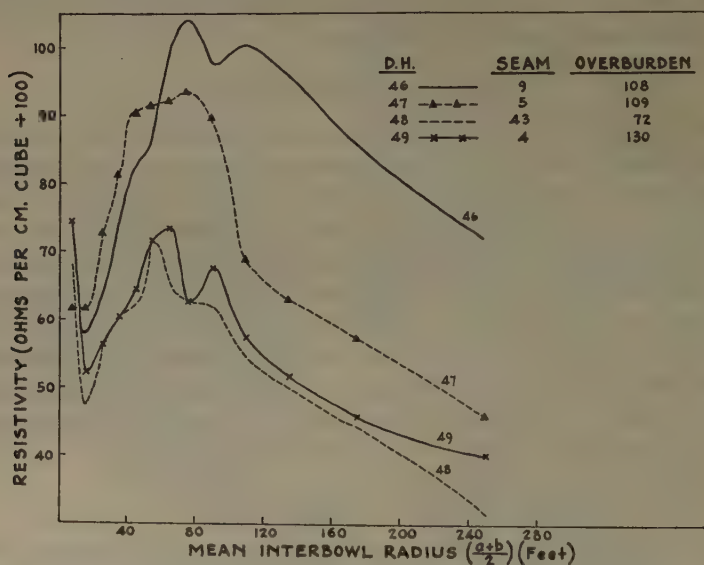


FIG. 7.—COMPARISON OF RESISTIVITIES AT ONE LOCALITY (SINGLE DISTANT ELECTRODE WITH MEGGER).

37 and 42. This consideration would be useful only if the presence or absence of lignite could be reliably predicted. There was no significant feature in any of the data to estimate the thickness of the lignite, or to reveal the presence of clay partings where these existed.

Although the area was extremely flat, the surface layers were drained better at drill holes 6, 7, 8, 19, 23, 29 and 33 than at the other points. No apparent relation existed between these conditions and the observed resistivities, although the almost uniform values found at drill holes 42, 58 and 70 suggested an averaging effect due to stagnant waters saturating the formations. It was improbable that the resistivities at any site were altered by drilling operations. A change could result only through the transfer of considerable water between the drill hole and adjacent clays, but no such effect was observed during the drilling at any point.

### *Data of Conflicting Character*

In Fig. 7 the resistivities were compared at four sites in one locality of the area with similar drainage conditions. The decided difference between the graphs of drill holes 46, 47 and 49, all practically barren sites, showed that successful correlation of the resistivity curves with the drilling records could not be made. The semi-empirical analysis of the curves of drill hole 47 suggested an extensive better conductor at a depth of about 80 ft., whereas only 5 ft. of lignite was found at 109 ft. Further, a close similarity in resistivity conditions was indicated at drill holes 48 and 49, despite the marked differences in the drill records.

### *Check on Observations*

Measurements were repeated during this survey along one line at drill hole 10, formerly used for resistance determinations, to find out

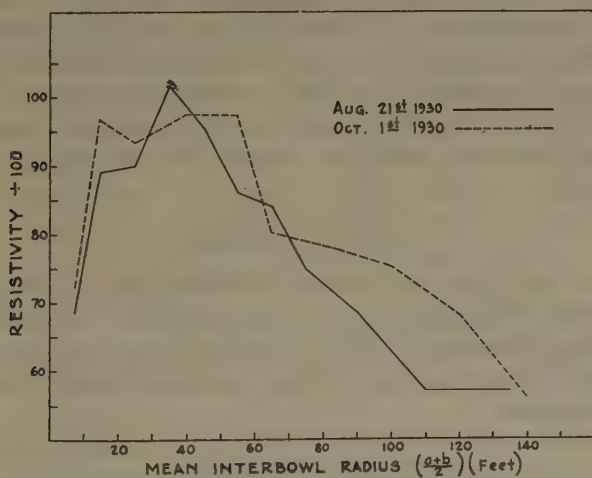


FIG. 8.—RESISTIVITIES FROM NORTH LINE, DRILL HOLE 10, ON SUCCESSIVE SURVEYS WITH SAME MEGGER.

whether any differences existed due to errors of instruments or technique. In Fig. 8 the agreement of results for the two dates was satisfactory, when allowance was made for differences due to new potential electrode positions, and for normal errors of observation.

### *General Conclusions from Field Survey*

1. This survey showed emphatically that extensive field work was necessary to determine the applicability of resistivity methods to a widespread area. Although at some locations the resistivity curves empirically gave the overburden thickness quite accurately, the single distant probe method failed to reveal the lignite distribution consistently. The interpre-

tation of measurements on new ground presented formidable difficulties.

2. The investigations confirmed the complex overburden structure revealed by drilling, although the data could not be correlated with these variations in every case.

3. Where resistivity magnitudes and ratios were so small, equipment to check Megger readings was essential.

4. Further tests in the area were needed to determine whether other resistivity methods with equipment capable of more precision would give better results. It was desirable to establish whether the variations in overburden and in underground saline waters caused the inconsistent values, and whether the theory of the methods, as applied to simple conditions, was adequate to deal with the structures existing.

5. Other geophysical methods should receive a field test.

### WINTER MEASUREMENTS

The writer and members of the geological staff at the deposit made further field measurements in November and December, 1930, to determine the actual resistivities of various formations *in situ*, by small-scale studies during the sinking of a shaft; to study the effect of the winter freeze-up on surface resistivity values, and to obtain the density of the clays and of lignite in order to estimate the feasibility of gravitational methods.

#### *Shaft Measurements*

The data from shaft studies are presented later (p. 106) along with the data obtained subsequently in the mine drifts. The density values obtained during this period and later have been recorded by A. H. Miller, of the Dominion Observatory, Ottawa, with the findings from gravitational investigations.

#### *Surface Measurements*

*Effect of Freeze-up.*—The resistance values over a series of surface intervals were observed before the winter freeze-up and after several days of severe weather had frozen the electrodes in the ground. No appreciable change occurred except for unimportant effects on intervals within 20 ft. of the center. Freezing increased the contact resistances by about 50 ohms per electrode. Other workers<sup>16</sup> have shown that rainfall does not affect resistivity conditions at depth. This study has shown that satisfactory measurements can be made on frozen ground if other conditions permit.

*Previous Sites Restudied.*—When the foregoing had been established, Megger readings were repeated at drill holes 9 and 42 along the same

<sup>16</sup> A. S. Eve and D. A. Keys: Geol. Survey, Dept. of Mines, Canada, *Mem.* 165 (1931) 110.



azimuths studied in the September survey. Confidence in the relative accuracy of all the earlier measurements was established by good agreement with the previous values.

*Observations at New Sites.*—Readings were taken (in two azimuths only) at three sites of special interest, using the single distant probe method and a Megger. At drill hole 76, deep boulder clay (Fig. 6) was believed to mark the course of a pre-glacial river. Stations X and Y were selected west of drill hole 76 (Fig. 2) in a region where drilling had not yet been done. Station X was about 1800 ft. from the Mattagami

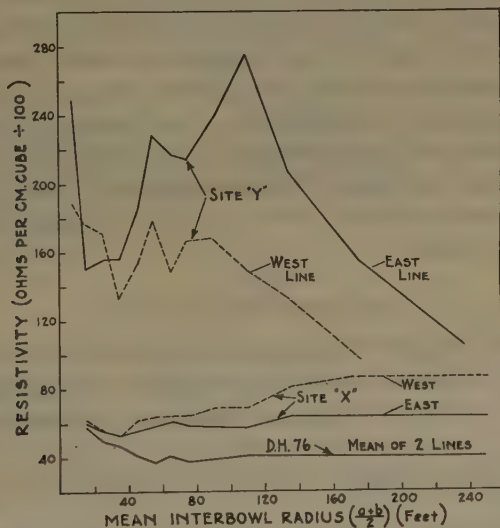


FIG. 9.—RESISTIVITY AT SITES X AND Y AND DRILL HOLE 76 (SINGLE DISTANT ELECTRODE AT 800 FT., MEGGER ONLY, IN WINTER).

River, in a well timbered, swampy area; station Y was 250 ft. from the river, on an old flood plain about 20 ft. lower than station X, but 30 ft. above present river level. From the graphs of Fig. 9 it was concluded that:

1. Since the resistivities at drill hole 76 were quite uniform with depth, and of small value not characteristic of boulder clay, the structural conditions were probably masked by saturating water.

2. At station Y, good drainage conditions and erosion of the better conducting marine clay caused the highest resistivities observed at the deposit.

3. At station X, resistivity increased slightly with depth and tended toward the same limit as that at station Y. Although at the latter point the decreasing resistivities at depth might have been attributed to lignite, a greater concentration of conducting water was believed to be responsible. The results from the two sites taken together warranted the

prediction of a barren area. Subsequent drilling at drill hole 78 confirmed this conclusion.

### *Conclusions from Winter Work*

The effect of the winter freeze-up on surface resistivity observations in depth investigations was shown to be negligible; the accuracy of previous measurements was established; and additional data served to emphasize the complexity of resistivity conditions.

### LABORATORY PREPARATIONS

During the winter of 1931, preparations were made for more adequate investigations. The utility of any geophysical measurement is restricted by the limited precision of the observations, but more seriously by the difficulties of correlation of the data to actual subsurface conditions. To increase precision, the improvement of existing instruments and the design of verifying equipment was undertaken. For a more powerful method of analysis of data, a further study of the basic theory of resistivity methods was begun.

### *Instruments and Apparatus*

*Megger Earth Tester.*—Because of the portability and convenience of the Megger, modifications of the instrument to insure accuracy over the range 0.01 to 0.5 ohm were very desirable. In appendix A the findings from tests of the behavior of a Megger under defined conditions have been given, and precautions to be observed in using the instrument have been mentioned.

*Deflection Potentiometer.*—The component parts of a potentiometer-milliammeter circuit with a commutator to provide alternating current have been described in appendix D. This instrument was named a "deflection potentiometer." It possessed a working range up to 2 volts, required no standard cell or periodic standardization, and its use was not restricted to temperatures above freezing.

*Behavior of Deflection Potentiometer.*—With both steady and commutated current, series of voltage/current ratios for various applied potentials were obtained in the laboratory with non-inductive resistances of the range of values found in field practice. With commutated current the true resistances were about 92 per cent of the observed ratios, within the limits of instrumental error. This effect was to be expected, as the millivoltmeter measured the peak voltage, whereas the milliammeter measured the time average of the current, which was less than the value of the steady current because of the gaps in the commutator. With steady current, the readings of the deflection potentiometer agreed well with those obtained by the Cambridge potentiometer (appendix C) over its range.

*Theoretical Considerations*

The theoretical distribution of potential in a number of uniform homogeneous horizontal strata of different conductivities, and the resultant resistivity values obtained by surface measurements, have been dealt with by Weaver, Hummel, Roman, Peters and Bardeen, Ehrenburg and Watson,<sup>17</sup> and others. With the conditions governing potential distribution about point sources at the surface of semi-infinite conductors, for the case of a uniform upper layer underlain by an infinite lower medium, the apparent resistivity  $\rho_a$  observed by Wenner's method is related to the resistivity  $\rho_1$  of the upper stratum by the relation

$$\rho_a/\rho_1 = 1 + 4F.$$

$$\text{where } F = \sum_{n=1}^{\infty} \left\{ \frac{K^n}{\sqrt{1 + \left(2n\frac{h}{a}\right)^2}} - \frac{K^n}{\sqrt{4 + \left(2n\frac{h}{a}\right)^2}} \right\}$$

and  $K$  has the value

$$\frac{\rho_2 - \rho_1}{\rho_2 + \rho_1}$$

$\rho_2$  = resistivity of the lower medium.

$h$  = thickness of the upper stratum.

$a$  = Wenner potential electrode interval.

The value of  $\rho_1$  may be experimentally observed by using small intervals.

$K$  may take any value between  $+1$  and  $-1$ ; for negative  $K$ 's, the values of  $\rho_a/\rho_1$  all lie between 0 and 1; similarly, for positive values (*i. e.*, a poorer conductor at depth), the same limits exist for the ratios  $\frac{\sigma_a}{\sigma_1}$  (where  $\sigma$  signifies conductivity). For convenient application to observed data it is most useful to plot a series of curves for different  $K$  values, with the calculated ratios of  $\rho_a/\rho_1$  for negative  $K$ 's and of  $\sigma_a/\sigma_1$  for positive  $K$ 's as ordinates, and the corresponding  $h/a$  ratios as abscissas.

The series for  $F$  is rapidly convergent for all  $K$  values between  $\pm 0.1$  and  $\pm 0.9$ , a range that includes almost all conditions usually met in practice. The writer has prepared graphs for all values of  $K$  in this range differing by multiples of 0.1, for  $h/a$  values from 0.2 to 2.0 with intervals of 0.2. For values of  $K$  not an integral multiple of 0.1, the corresponding  $\rho_a/\rho_1$  (or  $\sigma_a/\sigma_1$ ) ratio may be obtained with sufficient accuracy by linear interpolation from the graphs.

A more extended treatment of these considerations has been presented by G. F. Tagg.<sup>18</sup> Their use in determining the depth to a discontinuity

<sup>17</sup> References of footnotes 12, 7, 14, 13, 15 respectively.

<sup>18</sup> G. F. Tagg: *Min. Mag.* (June, July, Sept., 1930).

at two locations has been described by the same worker.<sup>19</sup> Although the results agreed with geological conditions, confirmatory drilling records were not available for verifying the reliability of the analysis.

Even though the resistivity data from the lignite deposit suggested that the structure might approximate to a three-layer case at places, in general a considerable gradation of values probably existed. For cases of more than two layers the mathematical calculations of theoretical solutions became tedious and involved, and the difficulties in obtaining a unique solution were great.

### BIRCH CLIFF TESTS

Before further resistivity investigations were undertaken at the lignite deposit, some field tests were conducted at a site convenient to the laboratory, to establish the reliability of the deflection potentiometer in field service; to study data by Wenner's method where the structure approximated closely to an ideal two-layer type, to which the analysis proposed by Tagg might be applied; and to compare resistivity values obtained by the various methods (pp. 80 and 81) over the same ground.

#### Site Selected

A vacant lot of approximately 600 ft. frontage and 2000 ft. depth, located  $\frac{1}{2}$  mile from the shore of Lake Ontario at Birch Cliff, in the

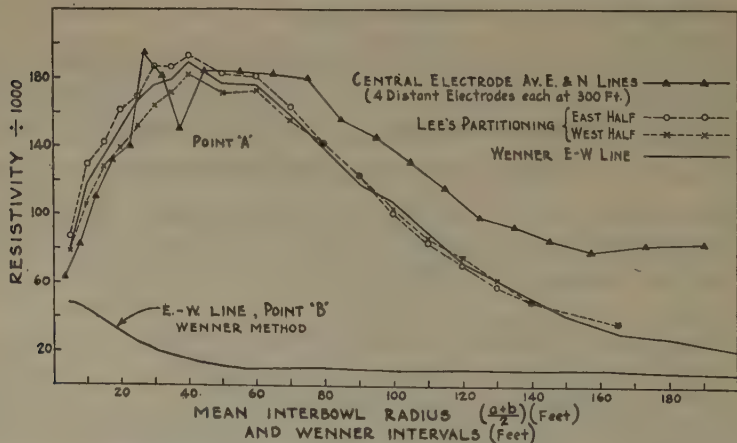


FIG. 10.—RESISTIVITY AT POINTS A AND B, BIRCH CLIFF (MEGGER ONLY).

eastern outskirts of Toronto, was selected. At the lake shore, opposite this lot, cliffs of sand underlain by sedimentary clays, known as Scarborough Bluffs, rise sharply to a height of about 100 ft. from the water level, and present a fairly homogeneous appearance. At a depth of about 30 ft. below water level, bedded shales dipping slightly toward the lake are

<sup>19</sup> G. F. Tagg: *Proc. Phys. Soc.* (1931) **43**, Pt. 3.



known to begin. It seemed probable that inland  $\frac{1}{2}$  mile similar structure would be found, although the only records available were confined to the shallow depths reached in laying water pipes on adjacent streets. For the resistivity studies it was hoped that the shale horizon was a boundary between uniform layers of different conductivity.

### *Test Measurements*

*Point A.*—To ascertain the general resistivity conditions, preliminary readings were taken with the Megger. The first site was selected centrally on a bed of gravel of undetermined thickness covered thinly with stony humus of almost level surface. This bed crossed the lot, extending northward from the southern boundary for about 700 ft. In Fig. 10 is shown a comparison of measurements made by the central electrode method, and Wenner's method supplemented by Lee's partitioning method. As the resistivity curves clearly indicated that simple two-layer structure did not exist here, a location with less complex conditions was sought.

TABLE 4.—*Data from Point B of Proving Grounds*

Electrode Interval, Ft.	Apparent Resistivity, Ohms per Cm. Cube, $\rho_a$	Apparent Resistivity
		Resistivity of 5 Ft. Interval
5	50,300	1.0
10	44,700	0.894
15	35,800	0.716
20	30,200	0.604
25	24,200	0.484
30	20,000	0.40
35	16,600	0.332
40	14,600	0.292
50	11,200	0.224
60	10,200	0.204
70	9,400	0.188

TABLE 5.—*Data from Theoretical Graphs to Deduce Depth of Upper Stratum*

$a$	10	15	20	25	30	$h$ , Ft. 35	40	50	60	70
$K$										
-0.1	4.7									
0.2	8.1	3.9								
0.3	10.0	7.4	5.5							
0.4	11.6	9.4	9.1	6.2						
0.5	12.7	11.0	11.2	10.1	8.2					
0.6	13.7	12.3	13.1	12.6	12.1	10.5	9.3			
0.7	14.6	13.4	14.4	14.2	14.5	14.4	14.3	12.7	13.1	
0.8	15.4	14.4	15.6	15.8	16.4	16.9	17.7	18.5	20.6	22.3
0.9	16.1	15.2	16.6	17.2	18.1	18.9	20.1	21.8	24.6	27.6

*Point B.*—At this site, 600 ft. north of point A, the surface was of sandy humus, free from stones, fairly level, and about 10 ft. lower than the surface of the gravel bed about point A. Included in Fig. 10 is the

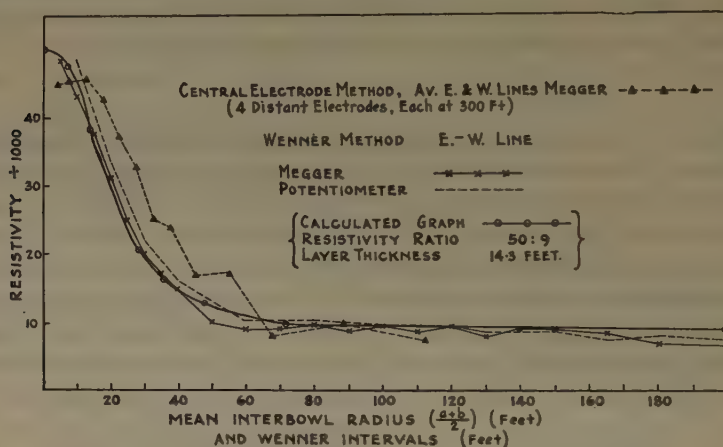


FIG. 11.—RESISTIVITY AT POINT B, BIRCH CLIFF.

curve of resistivities obtained by Wenner's method along one line about this point as center, with the Megger alone for the measurements. The latter graph is much simpler, suggesting a fairly uniform medium begin-

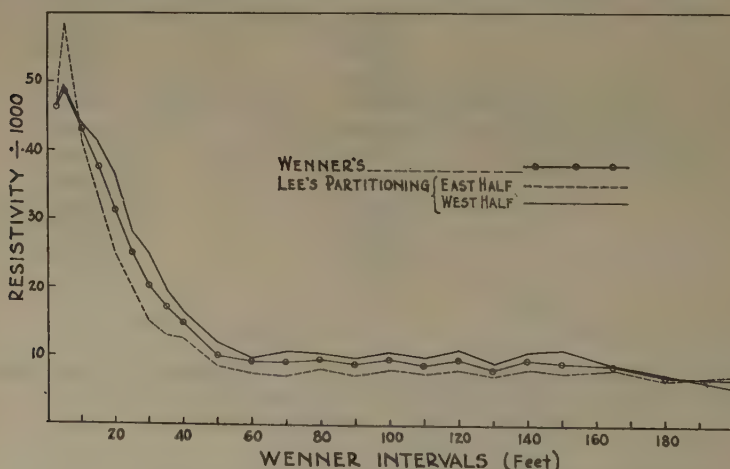


FIG. 12.—RESISTIVITY AT POINT B, BIRCH CLIFF (MEGGER ONLY).

ning at shallow depths. Although the resistivity of the surface layers was nearly the same at both sites, the underground conditions must have been quite different. In Fig. 11 a comparison is made between the resistivities at this site calculated from data of Wenner's method obtained in one case by a Megger and in the other by the deflection potentiometer. The resistivity conditions revealed by the central electrode method about

this same point, using a Megger alone, are also shown. In Fig. 12, the result of supplementing Wenner's method by Lee's partitioning is revealed.

*Theoretical Analysis at Point B.*—It was of interest to apply the analysis suggested by Tagg (ref. 19) for an ideal two-layer case, to estimate the depth to the better conductor. The values of  $\rho_2/\rho_1$  given in Table 4 were obtained, when the average value for the 5-ft. Wenner interval was

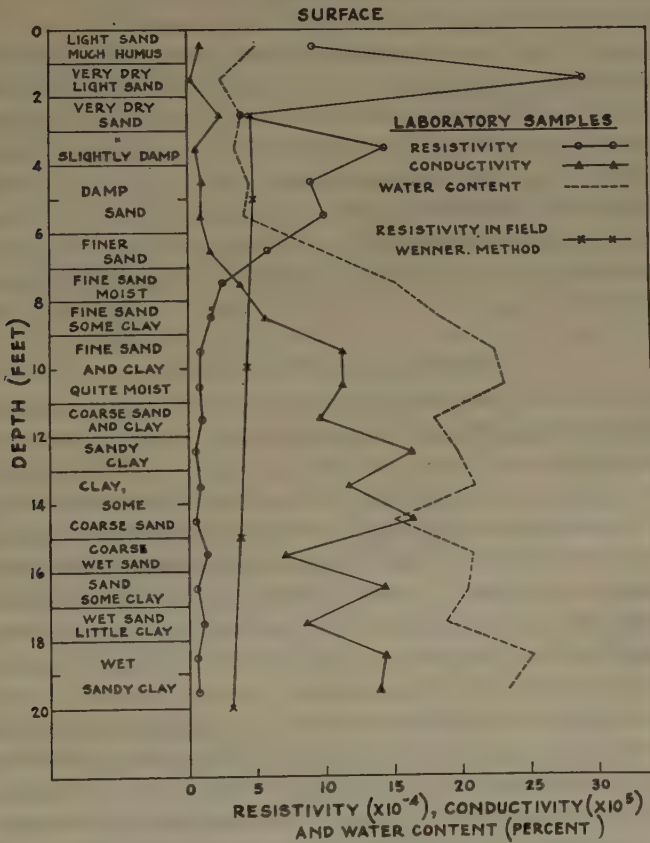


FIG. 13.—COMPARISON OF AUGER TEST-HOLE DATA AND WENNER DATA.

adopted as the resistivity of the upper layer. The data of Table 5 were read off the calculated graphs discussed on page 95. For  $K = -0.7$ , the deduced values of  $h$  are most nearly constant; *i. e.*, independent of the electrode interval. For the intervals 10 to 40 ft., the average value was 14.3 ft. The calculated value of  $\rho_2$  was approximately 9000 ohms per cm. cube, in accord with the average observed value for long intervals. In Fig. 11 the close agreement is revealed of the observed graph with the theoretically calculated ideal case for  $\rho_1 = 50,000$  ohms per cm. cube.  $\rho_2 = 9000$  ohms per cm. cube, and  $h = 14.3$  feet.

*Structure in Detail at Point B.*—As a change of resistivity at shallow depth alone was indicated, a detailed study was made of the upper layers to determine how closely the above deductions fitted the facts. A test hole was driven by means of a 5-in. scoop-type hand auger and representative samples of the soil from each foot of depth were immediately sealed in glass jars for laboratory study. At a depth of 20 ft. water coming into the hole precluded further sampling.

Fig. 13 presents a description of the soil composition, with the associated resistivity and water content of each foot, and the Wenner field data. Almost identical conditions were found at a second test hole 100 ft. distant. The resistivities of the individual soil samples were measured in a simple conductivity cell constructed for the purpose (appendix E). For the entire series the deflection potentiometer was employed, with a standard dry cell as current source. Repacked and duplicate samples of the same soil gave values agreeing to within 5 per cent. The current that leaked through the empty cell was negligible even when the surface was wet from repeated use.

#### *Discussion of Birch Cliff Tests*

*Point A.*—For intervals out to 60 ft. Wenner's method and the central electrode method gave resistivity values with quite similar trends; for further intervals out to 150 ft., the Wenner values appeared to be affected by better conductivity at depth. Beyond 150 ft. the data of the central electrode method were influenced by the nearness of the outer current electrodes, in this case only 300 ft. from the center; disregard of this in calculations gave too large observed resistivities. Although minor variations revealed by the central electrode method were largely averaged out in Wenner's method, readings from several azimuths by the former method, when reasonably comparable, gave smoother average values than those shown. If irregularities in the shorter intervals are interpretable as shallow structural changes, without masking more deep-seated effects, their detection is advantageous; in other cases, the greater averaging of shallow variations by Wenner's method appears desirable.

A general semi-empirical interpretation of the data suggested that surface soil of fair conductivity was underlain by a more resistant gravel bed, in turn succeeded by better conducting material. When the contribution of the upper layers became comparatively small over long intervals, the resistivity at depth tended to the corresponding values at point B. As it was not clear what average resistivity might be assigned to the upper layer, efforts to analyze the Wenner data as a two-layer case were not fruitful. The central electrode data revealed a definite resistivity decrease for an interbowl interval of about 75 ft., empirically suggesting a better conductor at about this depth. This estimate is not in disagreement with that obtainable from the Wenner data, when curves



calculated with the general conditions outlined are compared with the observed.

*Point B.*—(a) In Fig. 11 the comparison of data yielded by the Megger and the deflection potentiometer established the essential agreement of the two measuring devices. The graph from the deflection potentiometer readings was slightly smoother, suggesting greater relative precision than the Megger provided, though the gain was of no practical importance in this study.

(b) The semi-empirical interpretation of the single distant probe curves suggested a depth of between 15 and 20 ft. to a better conductor, as compared with an estimate of 14.3 ft. obtained by analyzing the Wenner data in the way defined by Tagg. These methods gave closely corresponding results. For the longer intervals the predominating effect of the lower medium made the two graphs practically coincide.

(c) From the individual values for the upper 5 ft. of soil given in Fig. 13, considerable variation in resistivity of the immediate surface layers was expected. A series of 15 contiguous 2.5-ft. Wenner intervals gave corrected values of resistances ranging from 45.2 ohms to 79.8 ohms, the average being 57.4 ohms, which corresponds to a resistivity of, roughly, 46,200 ohms per cm. cube; the resistivity of the 5-ft. Wenner interval used previously to calculate the layer depth was but little different from this.

(d) *Conductivity Cell Studies.*—The resistivities of samples taken from the auger hole between the depths of 5 and 10 ft. decreased almost uniformly with depth to about 10,000 ohms per cm. cube, a value that was characteristic of all samples from 10 to 20 ft. The surface measurements showed that this almost constant value for the lower medium persisted to the maximum depth studied. There was no evidence of a change at a shale horizon if such existed. Unfortunately, the dimensions of the lot prevented measurements over intervals greater than 200 ft., if the risk of disturbances by water pipes and other factors was to be avoided.

At the second test hole the uniform lower medium was found at between 8 and 9 ft.; the approximate depth was evidently about 10 ft. The analysis as a two-layer structure (p. 22) gave a depth indication of about 14 ft., and the empirical estimate from single distant electrode data was slightly more. It is not believed that variations in ground level and in depth to the uniform conductor were sufficient to account for even this small difference; however, the upper layer was too shallow to permit a fair, adequate test of Tagg's method of analysis, as surface variations were of undue significance compared to the usual problem.

The gradation of resistivities near the surface observed by the Wenner scheme agreed closely with those calculated for the simple case (Fig. 11). Referring to Table 5, values of  $h$  were nearly constant also for  $K = -0.5$ ,  $-0.6$  and  $-0.8$ , but these gave values of 16,700, 12,500, and 5,600 ohms

per cm. cube respectively, none of which fitted the experimental case nearly as well as the solution adopted. As other workers<sup>20</sup> have suggested, it is necessary to apply some empirical factor to the mean electrode interval, its value depending upon the particular conditions, in order to obtain an accurate depth estimate for any structures not extremely simple.

Since the test-hole data showed that the resistivities of all samples below 10 ft. depth were practically the same as the apparent resistivity by Wenner's method for potential electrode intervals beyond 50 ft., it was unlikely that a significant change in the resistivity of the underground occurred at about 50 ft. depth, to correspond to the greater curvature of the graph at the 50-ft. interval. In the light of these tests, correlation between such inflections and resistivity differences at a depth equal to the electrode interval, as proposed by Broughton Edge and Laby,<sup>21</sup> and by numerous other workers, must be questioned.

The close relation between the conductivity of the samples and their water content was of interest. The water content *in situ* of the five lowest samples was probably less than the values recorded. The water coming into the test holes from the 18-ft. level onward had a resistivity of about 2700 ohms per cm. cube.

(e) The study of such shallow layers was of interest because the findings were a guide to the interpretation of resistivity data associated with more deep-seated discontinuities. Extension would be applicable to cases where the dimensions of all features, including overburden irregularities, were proportionately magnified.

#### *Discussion of Lee's Partitioning Method*

With the relative symmetry existing about point *B*, the partitioning scheme advocated by Lee added little further information to that from other methods; with conditions less symmetrical, good judgment is required to interpret differences in the two parts of the field, because the simple formula for average resistivity may be quite inadequate. The method may be regarded as a rough guide only, to indicate lack of symmetry in complex cases. However, the partitioning provides a useful check on observed Wenner data, as the separate resistances of the two halves must add up to the total resistance of the Wenner interval. With the Megger, these sums would check and still be in error only if the instrument were yielding the same fraction of the true resistance for all parts of the scale, a behavior unlikely to occur for long without being detected.

Little can be stated from this work with regard to the empirical depth estimates by the Lee method obtained by Swartz (ref. 5) in small-scale measurements on artificial beds. Swartz found that the depth to a layer of different resistivity was equal to the Wenner interval for which an

<sup>20</sup> Reference of footnote 10.

<sup>21</sup> Reference of footnote 9.

abrupt change of slope of the resistivity graph occurred, measured beneath the current stake in the half of the field overlying the structure change. This rule was obtained empirically with Lee's method for cases where irregularities in the topography would make differences in the elevations of the electrodes being used. In Fig. 12, the data were not in disagreement with this rule, as the most abrupt change occurred between the 5 and 10-ft. intervals; more detailed intervals might have fixed this point more closely. On the other hand, the rather abrupt curvature change at about the 50-ft. interval (previously mentioned) could not be explained satisfactorily on this basis.

### *Conclusions from Birch Cliff Tests*

To sum up, the results of the Birch Cliff tests were:

1. The deflection potentiometer proved satisfactory in field service.
2. The data from point *A* showed that the structure there was rather complex and difficult to describe from resistivity measurements alone.
3. At point *B*, the data indicated a fairly simple two-layer structure which a calculated curve fitted very closely. A test hole yielded valuable detailed information, revealing irregular surface layer conditions over a fairly homogeneous lower medium. Tagg's method of analysis yielded only an approximate depth indication; the upper layer was too shallow for an adequate test.
4. The measurements by several electrode arrangements gave similar results. Empirical estimates of depth of structural changes from abrupt changes of slope of resistivity graphs could not be made reliably in all cases.

### FIELD WORK, ONAKAWANA, 1931

The ratios of densities of the various clays secured from a shaft at the Onakawana lignite deposit to that of lignite justified a test of gravitational methods to outline the lignite seams. The torsion balance investigation referred to in the introduction was undertaken in August, 1931. At the same time, the writer and a field assistant made a number of studies to determine the actual resistivities *in situ* in the mine workings, of the lignite and Cretaceous clay; to establish the characteristics of underground waters, and to compare different methods of surface measurements using the deflection potentiometer to check the Megger.

### *Shaft and Underground Drifts*

In addition to the results of studies in the mine workings, the data obtained from the small-scale resistivity measurements on the various clays *in situ* during the shaft sinking toward the end of 1930 have been included here (see p. 92).

*Technique.*—In the shaft, a freshly exposed clay surface at the working level was smoothed off. The excess water which gradually accumulated



drained into a small sump at one corner of the space, and  $\frac{3}{8}$ -in. round copper rods, driven in not more than 3 in., were used as electrodes. For the measurements, the Megger was carried down the shaft to the level concerned; under appendix A, comment has been made to subsequent erratic behavior of this Megger, probably caused by the exposure to excess moisture.

In the underground drifts, measurements were necessarily made on the exposed side walls, freshly smoothed off at the selected points. The underground electrodes were connected to a Megger at the surface by the heavily insulated conductor used for surface studies (appendix F), carried down the shaft and along the drifts as required.

TABLE 6.—*Comparison of Data by Two Methods in Small-scale Measurements at Shaft*

$a = 1$  Ft.;  $b = 2\frac{1}{2}$  Ft.

Line	Stake Resistance, Ohms	Interbowl Resistance, Ohms		Resistivity, Ohms per Cm. Cube.		Difference between C.E. and S.D.E. Per Cent
		C.E. <sup>a</sup>	S.D.E. <sup>b</sup>	C.E.	S.D.E.	
MARINE CLAY AT 4-FT. LEVEL						
North.....	490	11.3	10.9	3,600	3,470	3.8
East.....	510	12.1	11.25	3,850	3,580	7.5
South.....	500	12.3	11.5	3,920	3,660	7.1
West.....	500	11.7	11.0	3,720	3,500	6.3
Averages.....		11.85	11.16	3,770	3,550	6.2
BOULDER CLAY AT 17½-FT. LEVEL						
North.....	1,070	33.5	27.6	10,660	8,780	21.4
East.....	1,080	33	27.8	10,500	8,850	18.6
South.....	1,060	27.0	23.5	8,600	7,430	15.7
West.....	1,050	29.6	25.1	9,420	7,990	17.9
Averages.....		30.75	26.0	9,800	8,280	18.4

<sup>a</sup> Central electrode method.

<sup>b</sup> Single distant electrode method.

#### *Data from Shaft*

Readings were not obtained above the 17½-ft. level, as the shaft was down this distance with side walls lagged in, when the writer reached the field. In measurements, two methods to provide comparative checks were tried. Fig. 14 shows the arrangements. In one case, a distant single probe was located on the surface at a considerable distance from the shaft head, with potential electrode intervals 1 to 2½ ft. about the



near current electrode, which was placed in the center of the bottom of the shaft; in the other, the same potential intervals were used, but with an outer ring of 16 current electrodes arranged at  $22.5^\circ$  intervals about a circle of  $3\frac{1}{2}$ -ft. radius, which constituted the outer electrode of a modified central electrode method.

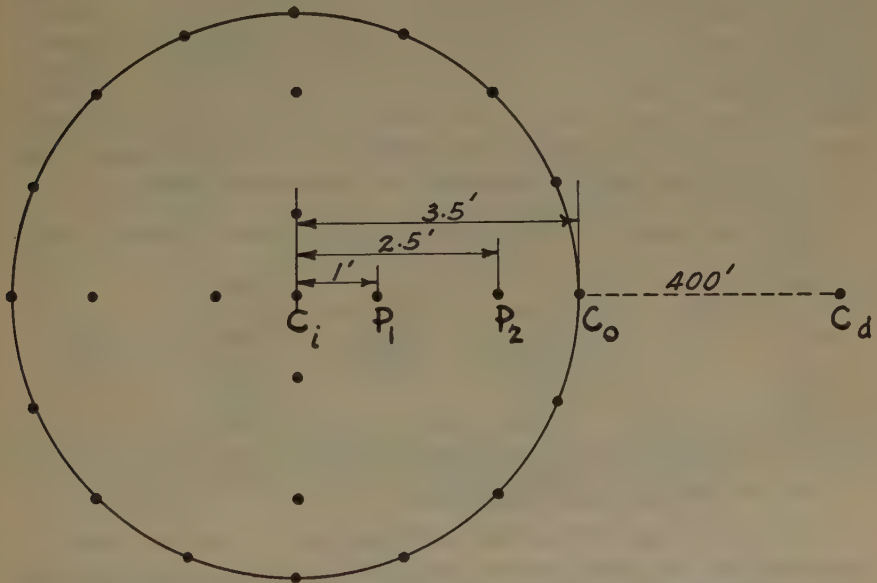


FIG. 14.—ELECTRODE ARRANGEMENTS USED IN RESISTIVITY MEASUREMENTS IN SHAFT.

Resistances were first measured on an area of marine clay which had been exposed near the shaft head. In Table 6 these data, and the corresponding data from the boulder clay at the  $17\frac{1}{2}$ -ft. level in the shaft, have been given. For the latter, the outer ring of current electrodes of the central electrode method were restricted by the shaft dimensions to a circle of 3-ft. radius. As the central electrode values were uncorrected for the nearness of the outer current electrodes, the agreement was satisfactory; when arranged on the smaller circle, the influence of the outer electrodes was greater by about the amount expected theoretically.

In Table 7 are given the average values obtained down to the 23-ft. level by the single distant probe method.

#### *Data from Drifts*

Resistivity measurements were made on the side walls of both upper and lower seams of lignite by the single distant probe method and Wenner's method. The woody material of the lower seam gave values almost identical with those of the earthy material of the upper seam. Table 8 shows a typical set of values from one point.

TABLE 7.—*Resistivity Values by Small-scale Measurements at Successive Levels in the Shaft*

Clay Type	Shaft Level, Ft.	Resistivity, Ohms per Cm. Cube
Marine clay.....	4	3,550
Boulder clay, side wall.....	14	9,980
Boulder clay, gray.....	17.5	8,280
Boulder clay, brown.....	20	7,720
Boulder clay, gray sandy.....	23	15,700

TABLE 8.—*Typical Resistivity Data Obtained on Lignite of Lower Seam by Small-scale Measurements in Underground Drifts*

Stake Resistance, Ohms		Interbowl Resistance, Ohms		Resistivity, Ohms per Cm. Cube	
S.D.E. <sup>a</sup>	W <sup>b</sup>	S.D.E.	W	S.D.E.	W
234	215	4.0	3.1	1273	1185
185	214	4.7	3.2	1497	1223
210		4.5		1433	
200		3.8		1210	

<sup>a</sup> Single distant electrode method; interval 1 to 2½ ft.<sup>b</sup> Wenner method; interval 2 ft.

Thirty-seven observations on the lignite gave a mean resistivity of 1370 ohms per cm. cube, and 6 determinations on the only accessible exposure of Cretaceous clay, in the parting between the upper and lower seams, gave an average of 1420 ohms per cm. cube. The greatest deviation of any individual reading from the quoted means was about 25 per cent.

Although much of the water entering the mine was draining from a sand seam at a depth of about 35 ft., yet considerable quantities flowed from cleavages randomly distributed in the lignite seams. The following resistivities on collected samples were observed:

ORIGIN OF WATER SAMPLE	RESISTIVITY OHMS PER CM. CUBE
Draining into shaft from 35-ft. level.....	650
Draining into drift from upper seam.....	300
Draining into drift from lower seam.....	225

Repeated tests on fresh fillings of the conductivity cell from the same source gave almost check values. The water draining into the lower drift showed on analysis a content of 1 gram of chlorine and of 2.85 gram total dissolved salts per liter.

#### *Discussion of Small-scale Data*

The utility of such detailed studies was evident as a guide to the actual resistivities existing in this locality, even though the data were incom-

plete. The lignite and Cretaceous clay appeared to have almost identical resistivities, which would preclude their differentiation in surface investigations; the other clays at the shaft site had resistivities ranging from

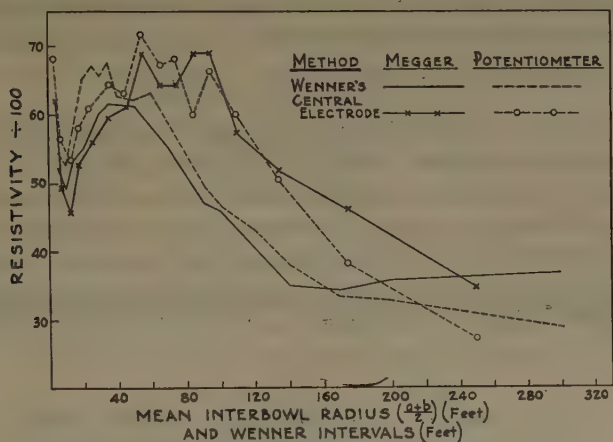


FIG. 15.—RESISTIVITY AT DRILL HOLE 34.

two to ten times that of the Cretaceous series. The range of values was in fair agreement with the data from laboratory studies (Table 2). The high saline content of the underground water sample, and the good con-

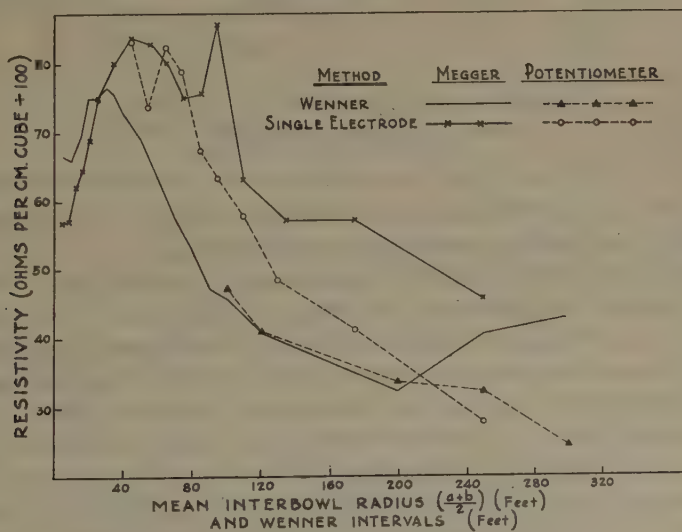


FIG. 16.—RESISTIVITY AT DRILL HOLE 26.

ducting properties of the water from the three levels, led to the conviction that these waters, existing in considerable amount, were largely responsible for the variation of the observed surface resistivity data, both in depth and in areal extent. Many workers have reported instances where

resistivity measurements to reveal structural changes have been of no avail, because of the predominating effects of saline waters. In particular, during their recent work in Australia, Broughton Edge and Laby (ref. 9) found that resistivity methods were not applicable in some localities because brackish waters had saturated the earth materials.

### *Further Surface Investigations*

1. A comparison of resistivities by Wenner's method and the central electrode method was made at drill hole 34, as its proximity to the shaft, with further evidence from drilling, assured reasonable continuity and uniformity of the lignite seam. However, as the distance was 1000 ft., electrical conditions would be undisturbed by the mine workings. At drill hole 26, data were obtained by Wenner's method and the single distant probe method. The Megger and deflection potentiometer were

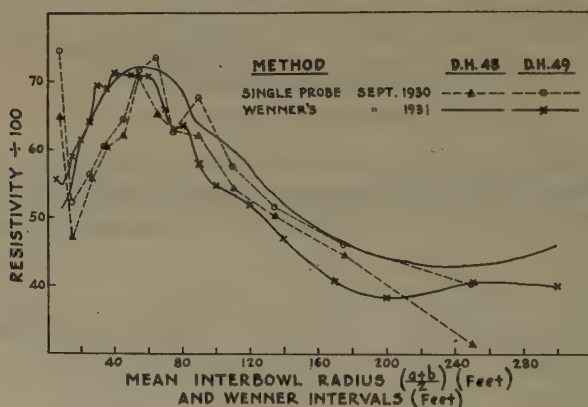


FIG. 17.—COMPARISON OF TWO METHODS AT TWO ADJACENT LOCATIONS.

employed as mutual checks at both locations. Figs. 15 and 16 embody the results; the drilling records are included in Fig. 6.

2. At drill holes 48 and 49, readings were obtained using Wenner's method with the Megger alone, checked by Lee's method of partitioning. In Fig. 17, the Wenner data from both sites are compared, along with the data of the previous year when the single distant probe method was used.

3. Resistivity conditions were determined for nearly 5000 ft. along a traverse line (*AB*, Fig. 2) which had been previously followed in torsion balance investigations. Measurements were made with the Megger alone using Wenner's method checked by Lee's partitioning. Readings were taken at 200-ft. intervals, with 35, 70, 120 and 200-ft. potential intervals at each site; the 200-ft. intervals were contiguous, with the shorter potential intervals about the mid-point at each site. In Fig. 18, the results are shown accompanied by the geological section obtained by linear interpolation from the records of drill holes 10, 11, 12 and 31, and by the direct use of the records of drill holes 26 and 32.



*Discussion of Surface Studies*

1. For all intervals beyond 80 ft. the data of Wenner's method from drill holes 34 and 26 were almost identical; for shorter distances overburden differences were evident. The resistivity at depth approached a common value at both places. It is of interest to note that the Cretaceous

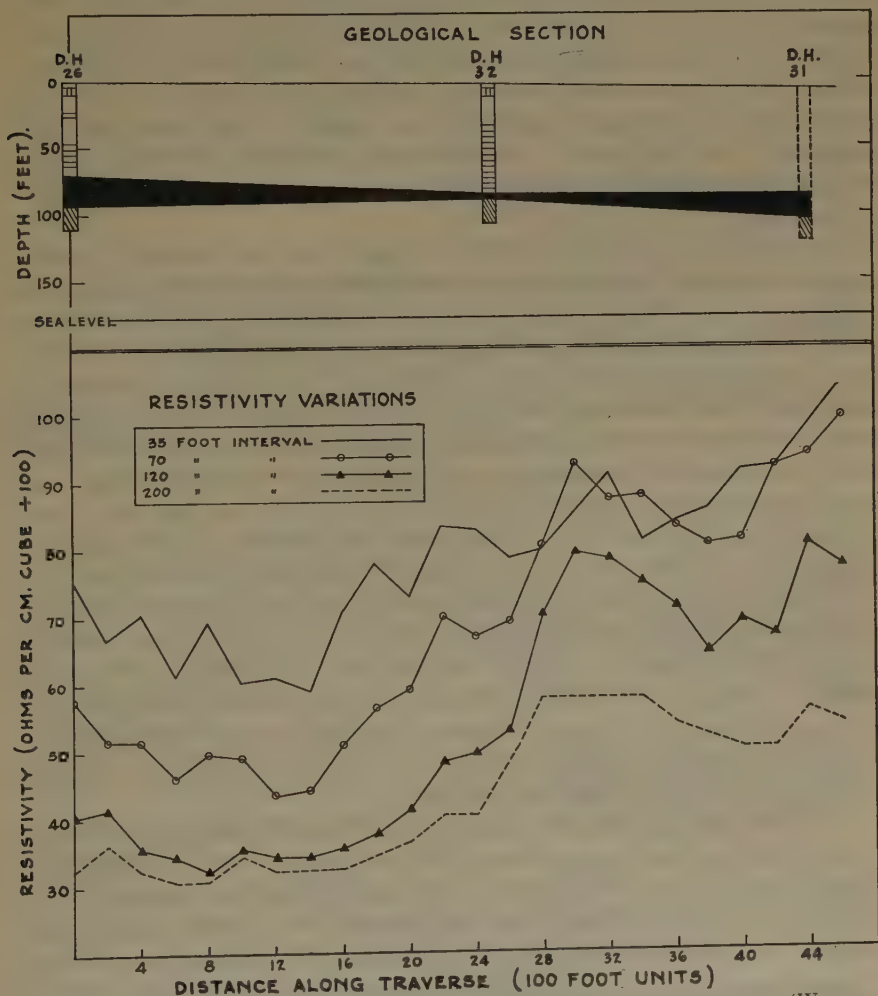


FIG. 18.—COMPARISON OF RESISTIVITY VARIATIONS ALONG A TRAVERSE (WENNER METHOD) AND GEOLOGICAL SECTION.

series began at almost the same depth. The central electrode method at drill hole 34, and the single distant probe method at drill hole 26 gave similar trends of values, revealing a definite decrease of resistivity beginning almost abruptly at the 80 to 100-ft. interval, which agreed fairly

well with overburden depth. There was no marked change of curvature of the Wenner graphs for this interval, to suggest any direct empirical depth correlation. Instead, the most abrupt change occurred for an interval of between 30 and 40 ft. These Wenner curves, as well as those of the Birch Cliff test sites, did not show any changes of slope more abrupt than those theoretically expected from measurements on complex inhomogeneous media; the small departures from smooth curves may be entirely accounted for by the irregularities in both horizontal and vertical extent. There was no experimental evidence that the fundamental assumptions defining the potential distribution in the underground which were adopted in the theoretical papers mentioned previously (p. 95) were not both necessary and sufficient. Undoubtedly subsurface structure often departs greatly from the simpler cases which alone permit of exact mathematical analysis.

The readings obtained with the Megger and the deflection potentiometer diverged appreciably for resistances of less than 0.1 ohm; the Megger gave the larger values. As there appeared to be a tendency to record too large Megger readings on these low resistances, it is believed that the other data were more accurate. The possible existence of induction effects dependent on the commutator speed, of sufficient magnitude to be significant in the low readings, was not adequately investigated with the deflection potentiometer. The work of Broughton Edge and Laby<sup>22</sup> did not come to the writer's attention until the field tests were suspended for the season. In any case, the accuracy of the measurements was sufficient to establish the major trend of the resistivities.

2. At drill holes 48 and 49, the Wenner results confirmed the similarity of resistivities previously observed (Fig. 17), but no further light was shed to reconcile this similarity with the underground differences revealed by drilling. The Cretaceous series began at 72 ft. at drill hole 48, but not until a depth of 120 ft. at drill hole 49. In this instance the resistivity values have failed to indicate that the overburden was of quite different depth and character at the two locations.

3. Along the traverse the resistivities for each interval showed variations of 50 per cent from the least value observed. Although the geological section (Fig. 18) was drawn from meager data, yet these variations were evidently due to changes in the character of the overburden, rather than to marked fluctuations in the thickness of overburden or of the Cretaceous series. An equi-resistivity contour map built up from a network of measurements could not be of much service in delineating lignite in this part of the area.

4. In Fig. 19 are shown the graphs of theoretical resistivities associated with ideal two-layer cases for overburden thicknesses of 65 ft. and of 115 ft., and for resistivity ratios of 9 to 3 and of 9 to 1. Although the

<sup>22</sup> Third reference of footnote 9.

extreme cases gave distinctly different trends,<sup>1</sup> yet, in practice, when marked irregularities superimpose their effects, the interpretation of data

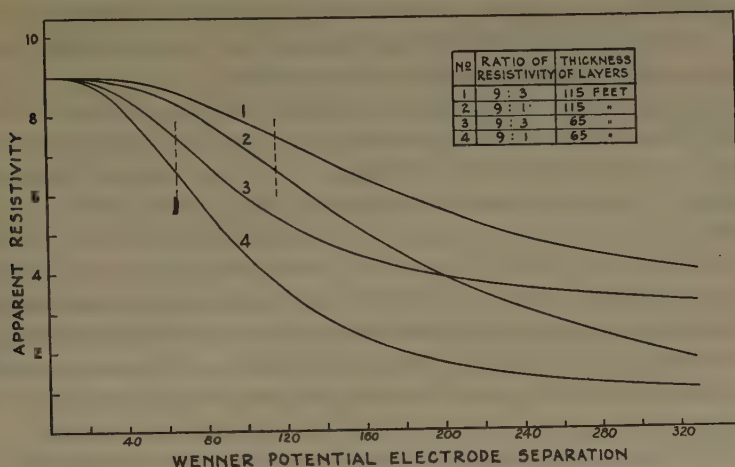


FIG. 19.—CALCULATED RESISTIVITY FOR HOMOGENEOUS HORIZONTAL UPPER LAYER ON A UNIFORM INFINITE LOWER MEDIUM (WENNER METHOD).

obtained by Wenner's method with the general resistivity conditions of this area would not be consistently reliable.

#### GENERAL SUMMARY

1. Laboratory examination of clay and lignite samples from Onakawana lignite deposit had shown a small range of resistivities, with lignite 12 times a better conductor than the most resistant clay. A short preliminary field test tentatively indicated that favorable and barren areas were differentiated by simple resistivity methods, and that the overburden thickness, but not the seam thickness, could be approximated empirically.

2. A further month's field work, with studies at sites having representative conditions, showed that the preliminary findings were not consistently sustained; no dependable general correlation of resistivity data with drilling records was obtained.

3. Winter measurements showed that resistivity values were not appreciably changed by the freeze-up; overburden resistivities were found to vary considerably at different points, further confirming the complex conditions revealed in the previous survey.

4. The limitations of a Megger in measuring resistances of less than 0.5 ohm were investigated in the laboratory. A "deflection potentiometer" was constructed for verifying field readings; its behavior under defined conditions was satisfactory.

5. The new equipment was tested in field service at Birch Cliff during a study of data obtained by several electrode arrangements. As the

structure approximated to a two-layer case, the mathematical analysis proposed by Tagg was applied to Wenner data; the deductions were compared with the findings from detailed study of samples from a test hole. Although the upper layer was too shallow for an adequate test of the analysis, the studies proved very instructive.

6. At Onakawana lignite deposit, subsequent measurements in underground drifts showed that lignite and Cretaceous clay were indistinguishable by resistivity methods, because of almost identical conducting properties. The formations were saturated with saline water, of which the conductivity depended on its source in the underground. No doubt the resistivity conditions at any point were determined largely by the local water content. Although various electrode arrangements were used for further surface studies, the correlation of data with drill records was not more consistent than was observed previously. Measurements along a traverse showed such variable overburden resistivities that equi-resistivity contour maps would be of little value in delineating lignite.

7. To sum up, the investigations showed that the resistivities of the clays associated with the lignite were too variable, and the ratios were too small, to consistently differentiate good and barren lignite areas in this part of the Moose River basin by any of the resistivity methods investigated. The value of similar measurements to reveal lignite in other parts of the region would depend on the conditions existing; better results could not be predicted with confidence.

#### ACKNOWLEDGMENTS

The writer wishes to acknowledge his great indebtedness to Dr. L. Gilchrist, of the Department of Physics, University of Toronto, for his interest and help in the beginnings of the investigation; to Mr. A. H. Miller, of the Dominion Observatory, Ottawa, for his cooperation; to those officers of the Ontario Department of Mines who were concerned with the problem, especially Dr. W. S. Dyer and Mr. A. R. Crozier, for furnishing geological information and assistance in the field; to Dr. A. E. R. Westman, of the Ontario Research Foundation; to the several field assistants who rendered invaluable service in obtaining the data; and to the Department of Physics, University of Toronto, and the Geological Survey, Department of Mines, Ottawa, for the loan of instruments and equipment during the initial surveys.

#### APPENDIX A.—MEGGER EARTH TESTER

This instrument, manufactured by Evershed and Vignoles, is described in their catalogues, as well as by such workers as Lee,<sup>23</sup> Lancaster Jones,<sup>24</sup>

<sup>23</sup> F. W. Lee: U. S. Bur. Mines *Tech. Paper* 440 (1928).

<sup>24</sup> E. Lancaster-Jones: *Min. Mag.* (June, July, Sept., 1930).



Broughton Edge and Laby,<sup>25</sup> who have further indicated its application in resistivity measurements.

The 3000-ohm, 4-range a.c. type instrument was used in these investigations. These ranges are generally adequate for determining the electrode contact resistances and the interbowl resistances found in practice. Where the former are greater than 3000 ohms, the values usually may be brought within measurable range by watering the electrodes or by using two or more in parallel. As others have emphasized, it is essential to correct the observed interbowl resistances for the effects of the corresponding contact resistances, because the instrument is not based on a null method.

At the lignite deposit the contact resistances were generally of the order of values allowed in calibration of the Megger. Many of the interbowl resistances were less than 0.1 ohm, for which the readings fall within the last division of the lowest range of the instrument. The percentage error in observation of these, apart from other possible sources, may be considerable.

A number of factors that have influenced the behavior of Meggers during their operation by the writer were:

1. *Level*.—The suspension of the moving system of one instrument used was not adequately adjusted for small inaccuracies of level. This condition has been noted by other workers. In measuring low resistances, slight tilting of the instrument vitiated the readings, the feeble forces then acting being insufficient to prevent the pointer from drifting seriously under the influence of gravity. As level, firm bases are often difficult to maintain in field work, the sensitivity to changes of level of all instruments should be checked before use.

2. *Current Electrode Resistance*.—A study was made in the laboratory of the behavior of a Megger, using fixed non-inductive resistances and various current electrode resistances. Provided the latter are not over 500 ohms, and allowing for the potential electrode resistance used in calibration, readings accurate to within 5 per cent may be obtained for the range 0.5 to 0.1 ohm. For current stake resistances over 1000 ohms, greater discrepancies may be expected. It would appear that the Megger readings for low resistances are independent of current electrode resistances only when the latter are within fairly low limits.

3. *Moisture*.—During the surface investigations under winter conditions in 1930, the instrument previously used in shaft studies began to read half-values of the lower resistances, and a smaller fraction of resistances over 1000 ohms. It was suggested, by those who later tested the instrument, that probably moisture had caused a phase change in the current relationships, as the instrument began to function normally after standing in a dry laboratory for a period. However, the cause was

---

<sup>25</sup> Reference of footnote 9.

not established, as the instrument later resumed its erratic behavior while in the same laboratory conditions. In any work, the Megger should be protected against dampness.

The writer has been advised that Evershed and Vignoles have a new type of Megger under construction for geophysical work with a full scale range of 0.3 ohm. If this can be produced successfully, it will represent a distinct advance in equipment for measuring these low resistances with facility. The present type was not designed for the precise measurement of such small resistances as were encountered at the lignite deposit.

#### APPENDIX B.—POTENTIOMETER, MILLIAMMETER AND COMMUTATOR EQUIPMENT

The equipment in this section was the property of the Department of Physics, University of Toronto:

*Potentiometer.*—Leeds & Northrup portable type, with two ranges; 0 to 16 and 0 to 80 mv. respectively. This instrument had good sensitivity but was of rather limited range.

*Current Measuring Equipment.*—This comprised a Rawson multimeter suitable for use over a wide range, and a number of Weston milliammeters of laboratory type with full scale values ranging from 10 to 250 milliamperes.

*Commutator.*—This unit had brass sectors mounted on ebonite blocks. The brushes were of "whisker" type supported in posts of ebonite, and were difficult to keep in adjustment. An electric motor operating from storage cells, and requiring at least 18 volts, was used to drive the commutator. This commutator was an old laboratory unit pressed into service because no other was then available, even though it was unsuitable for field work.

#### APPENDIX C.—POTENTIOMETER AND MILLIAMMETERS

For the measurements with direct current, during the survey of September, 1930, the following instruments were available:

1. A portable Cambridge potentiometer of two ranges, 0 to 20 and 0 to 100 mv., used generally for thermocouple work.
2. The Rawson multimeter, and a number of Weston milliammeters, which were mentioned in appendix B.

#### APPENDIX D.—DEFLECTION POTENTIOMETER SYSTEM

To provide the advantages of alternating current through the earth accompanied by determinations of direct voltages, a measuring system was prepared with component parts as follows:

1. *Potentiometer.*—A unit was constructed of simple parts based on a circuit attributed to Hildebrand. Fig. 20 shows (a) the essentials of the circuit, and (b) the layout of the unit built.

$B_1$  and  $B_2$  = unit flashlight cells, used to impress either  $1\frac{1}{2}$  volts or 3 volts on the circuit.

$R_1$  = radio resistor, potentiometer type, 200 ohms.

$R_2$  = radio resistor, 500 ohms.

$R_3$  = radio resistor, 10 ohms.

$R_4$  = radio resistor, 1000 ohms.

$R_2$  and  $R_3$  serve as finer adjustments for balancing on  $R_1$ ;  $R_4$  influences the sensitivity of the galvanometer  $G$ , and provides for critical damping.

$G$  = Type 440 Weston portable galvanometer, with sensitivity of 0.25 microamperes per scale division.

These parts, except for the galvanometer, were mounted on a panel of  $\frac{1}{4}$ -in. Bakelite, provided with three binding posts  $X_1$ ,  $X_2$ ,  $X_3$ . One lead of the galvanometer connected with  $X_3$ . The standardized leads of the millivoltmeter were connected to  $X_1$  and  $X_2$ .

$V$  = model 322 Weston millivoltmeter, four ranges; 0 to 2, 0 to 20, 0 to 200, and 0 to 2000 millivolts.

At the point of balance indicated by no current through the galvanometer, the reading of the millivoltmeter gives the potential fall between  $P_1$  and  $P_2$ .

2. *Milliammeter*.—To measure the current flow through the earth, a model 1, d.c. Weston milliammeter was obtained, with three ranges: 0 to 15, 0 to 150 and 0 to 1500 milliamperes.

3. *Switches*.—By means of a system of knife switches laid out on a Bakelite panel, either a Megger or the deflection potentiometer could be connected to the cables leading to the earth electrodes, to measure either the interbowl resistances or electrode contact resistances, as desired.

*Mounting for Transport*.—All the above component parts were fixed in a wooden tray, in turn cushioned by pads of  $\frac{1}{2}$ -in. felt in a strong outer case with hinged cover and removable wooden legs. This has proved adequate to protect all the instruments from injury during shipment for considerable distances by truck and express, and during field transport under severe conditions.

4. *Current Supply*.—A set of 4 B batteries, each of 45 volts, mounted in a suitable case, provided for any voltage across the current electrodes in the range of 22.5 to 180 volts, by steps of 22.5 volts.

5. *Double Commutator*.—In Fig. 21, the dimensions of the vital units of the commutator are shown. The commutating sectors were cut from  $\frac{3}{16}$ -in. seamless copper tubing of 2.5-in. diameter, and were mounted on machined, hand-fitted blocks of "electrical" Bakelite, which were flush with the copper bearing surface in the sector gaps. Projecting parts of Bakelite on each of the current and potential units were cut to dovetail together, to lock the units in proper orientation and to provide adequate insulation. A  $\frac{1}{2}$ -in. steel axle set in ball bearings mounted in suitable housings carried the units, which were carefully turned in a lathe in their

operating position to remove any eccentricity of the copper surfaces. A train of gears giving a step-up ratio of 25 to 1 provided a frequency of 40 cycles in normal operation by hand turning.

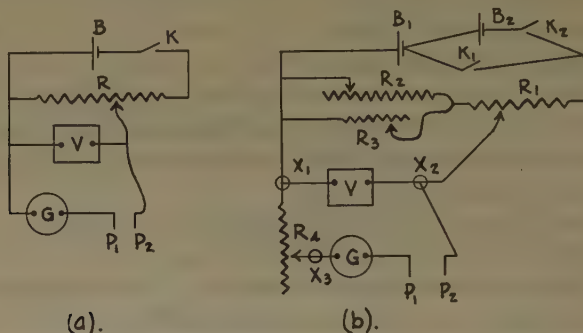


FIG. 20.—POTENTIOMETER CIRCUIT USING MULTIPLE RANGE MILLIVOLTMETER AND NOT REQUIRING A STANDARD CELL.

The input and pick-up brushes were a type used in vacuum cleaner motors; for the present purpose they were of copper carrying a small amount of graphite lubricant. They were about  $1\frac{1}{2}$  in. long and  $\frac{3}{8}$  by

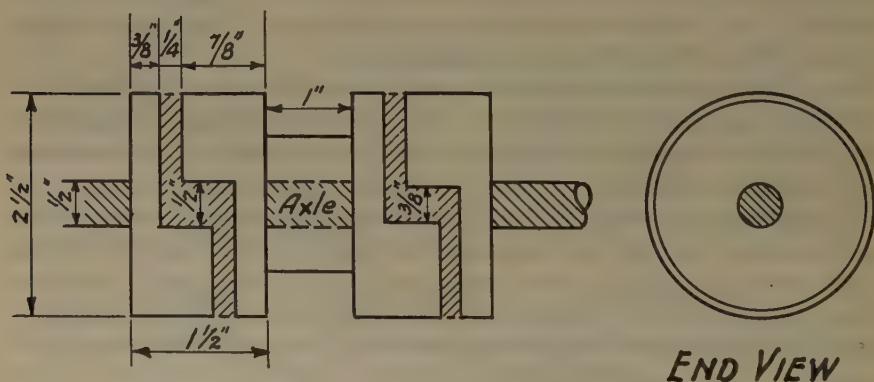


FIG. 21.—COMMUTATOR UNITS.

$\frac{1}{4}$  in. in cross-section; the faces were ground to fit the commutator surface when the brushes were mounted radially in their operating position. Each brush was backed by a coil spring of suitable strength, both held in a guiding sleeve. These holders for the four alternating current brushes were supported horizontally on opposite sides of the commutator in pairs, on posts of machined Bakelite of adjustable height; the holders of the four continuous contact brushes were set vertically in an ebonite plate in line beneath the axle. From each brush an insulated lead was brought to a binding post on a Bakelite panel. The set-up, in working position, was mounted on a plate of  $\frac{1}{4}$ -in. brass, to which the Bakelite panel was fixed vertically at one end. The complete assembly was



incased in a fitted wooden box from which it could be withdrawn readily. To operate the commutator, it was necessary only to let down a hinged side to expose the Bakelite panel, as a folding crank outside the box was used for turning.

*Criticism of Deflection Potentiometer.*—To obtain reasonable length of service from B batteries, the current drawn must not exceed about 200 ma. With this condition, the deflection potentiometer as built was not satisfactory for measuring resistances of less than about 0.03 ohm. Three factors combined to cause this limitation:

1. The most serious was that imposed by insufficient sensitivity of the galvanometer, which had an internal resistance of 150 ohms, compared to 6.7 ohms in the low range system of the millivoltmeter.

The galvanometer and the low range of the millivoltmeter were of almost equal sensitivity provided there was no contact resistance in the potential circuit. At the lignite deposit, the electrode resistances were usually of the order of twice the internal resistance of the galvanometer. This caused a corresponding decrease in the galvanometer sensitivity and in the precision of balance.

2. The setting of the variable resistors was restricted to a full turn of wire in each unit, rather than being continuously adjustable. On the low range of the millivoltmeter exact settings could not be readily made, but with the galvanometer used, this was not a significant factor. With a more sensitive galvanometer a continuous adjustment would be essential.

3. Owing to imperfect commutation, slight impulses of random nature reaching the galvanometer caused difficulty in balancing the circuit for low readings. Other workers have smoothed these out by using a small condenser in series with the potential electrodes. For the best commutation a very well built commutator is essential; the one used had been constructed as a preliminary effort.

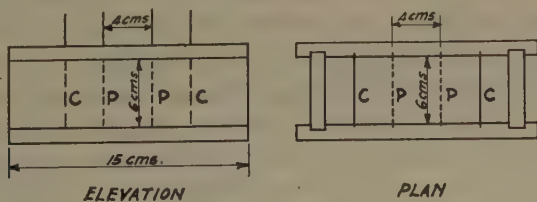


FIG. 22.—CONDUCTIVITY CELL.

For the measurement of low resistances only, a sufficiently sensitive portable potentiometer would be generally more satisfactory than the deflection potentiometer.

#### APPENDIX E.—CONDUCTIVITY CELL

Fig. 22 shows the plan and elevation (cover removed) of the conductivity cell. The material was of wood, thoroughly glued and shellacked.

The electrodes, to which leads were soldered, fitted snugly into shallow grooves in the cell walls and occupied the entire cross-section. The current electrodes were thin bronze plates, while the inner (potential) electrodes were galvanized wire gauze. The space between the electrodes was packed firmly with the samples by hand tamping. From Fig. 22, it will be seen that the potential electrodes defined the potential drop across a block of material 6 cm. square by 4 cm. long, whence for this particular cell the resistivity of the sample was nine times the observed resistance.

#### APPENDIX F.—INSULATED CONDUCTORS

Single conductor, multiple-strand, rough usage cable was used to connect the electrodes to the instruments. No. 14 gage wire was covered with a heavy insulation of 40 per cent pure rubber, making a cable  $\frac{3}{8}$  in. in diameter weighing 60 lb. per 1000 ft. Such heavy cable was necessary to provide ample insulation and to withstand the wear when it was dragged over rough, rocky ground; it was sufficiently strong and flexible for ease in reeling.

#### APPENDIX G.—CORRECTION FOR EFFECT OF ELECTRODES

Apart from experimental errors, the resistivities calculated from the simple formulas on pages 4 and 5 for point sources at the surface have three sources of error when the electrodes penetrate to some depth:

1. The properties of the ground do not correspond exactly to those of the conducting medium of mathematical theory. In particular, there will be variable contact resistance between the ground and the electrodes.
2. Unless the pick-up electrodes lie exactly and for their whole length in the initial equipotential surfaces, they will not leave the field unaffected.
3. The current will flow from a rod of finite length, not from one point on the surface. The last of these may be partly eliminated by theoretical considerations. For a more exact solution of the potential distribution about a current stake in an ideal medium, the stake may be identified with the lower half of a vertical thin ellipsoid of revolution. The equipotential surfaces and the density of current spreading into the medium correspond respectively to the equipotential surfaces and the surface density of charge of a complete ellipsoid of revolution isolated in space and carrying an electrostatic charge. The current density will, therefore, be high toward the lower end of the stake. We may conclude that upper and lower limits for the potential are given by taking the current to come from a point source (1) on the surface, and (2) at the lower end of the current stake. For the latter case, if  $x$  cm. be the electrode penetration, then following Wenner's derivation,<sup>26</sup> the expression for the central electrode method or the single distant probe method (neglecting the influence of the distant current electrode) becomes:

<sup>26</sup> Reference of footnote 4.

$$\rho = 2\pi R \frac{ab}{b-a} \left[ \frac{1}{0.5 + \frac{ab}{2(b-a)} \left\{ \frac{1}{\sqrt{4x^2 + a^2}} - \frac{1}{\sqrt{4x^2 + b^2}} \right\}} \right]$$

The surface point source expression is modified by the factor in square brackets. For Wenner's method, the similar expression becomes:

$$\rho = 2\pi aR \left[ \frac{1}{0.5 + \frac{a}{\sqrt{4x^2 + a^2}} - \frac{a}{2\sqrt{x^2 + a^2}}} \right]$$

The differences between cases 1 and 2 for points close to the test site are shown in Table 9 for two usual values of  $x$ . For intervals greater

TABLE 9.—*Correction Factor to Be Applied to Observed Resistances Obtained by the Wenner Method and the Central Electrode (or Distant Probe) Method to Provide for Depth of Electrode Penetration*

Wenner Method			Central Electrode Method		
Interval, Ft.	Factor		Interval, Ft.	Factor	
	$x = 2$ Ft.	$x = 2.5$ Ft.		$x = 2$ Ft.	$x = 2.5$ Ft.
2.5	1.564	1.684	2.5-5	1.564	1.684
5	1.224	1.316	5-10	1.224	1.316
10	1.066	1.100	10-15	1.080	1.120
15	1.030	1.047	10-20	1.066	1.100
20	1.017	1.027	10-30	1.054	1.082
25		1.017	15-20	1.038	1.061
30		1.012	20-25	1.024	1.037
			20-30	1.019	1.032
			25-30	1.016	1.025

than 30 ft., the correction becomes negligible. To depths for which electrode penetration is of consequence, information can be readily obtained by other means; *e. g.*, by auger holes. We may conclude that the true resistivities of the upper layers lie between the values calculated by using the factors of Table 9 and those obtained by applying no correction.

## DISCUSSION

(*Louis B. Slichter presiding*)

MEMBER.—Is the lignite wet or dry?

R. H. HAWKINS.—The lignite is saturated with water of a relatively high salt content.

E. G. LEONARDON,\* Paris, France.—What is the resistivity of the formations underlying the lignite, and could they be differentiated from the lignite? The figures would indicate that the underlying formations were not tested.

R. H. HAWKINS.—No sample could be obtained of the underlying formations because the shaft was not deep enough, so they were not tested.

H. LUNDBERG,† New York, N. Y.—The title of this paper is too broad. It indicates that all possible resistivity methods were applied, and the paper records their failure. As a matter of fact, other resistivity methods could be applied, which might be more successful.

L. GILCHRIST,‡ Toronto, Ont.—As I had something to do with this work, I may be able to contribute a few words about it, especially from the point of view of the place to be occupied by geophysics in mining exploration. The mining work was done wrong end first, as is so frequent in cases like this. Drill holes were put down and the blank ones were abandoned. Later geophysical examination was made in the neighborhood of the abandoned holes. The proper thing to do is not to neglect any hole; to test every one by the available geophysical methods at the time of drilling, in order to obtain the maximum information. In this work, the geophysicist should play an important role because of the types of data he is peculiarly equipped to obtain.

---

\* Société de Prospection Électrique.

† Manager, Swedish-American Prospecting Corporation.

‡ Professor of Physics, University of Toronto.



# Geophysical Studies in Placer and Water-supply Problems

By J. J. JAKOSKY\* AND C. H. WILSON,\* LOS ANGELES, CALIF.

(New York Meeting, February, 1934)

## ABSTRACT†

IN recent years geophysical prospecting methods have become well established as important steps in economically initiating new mining ventures in the field of base-metal exploration, placer mining and water-supply problems. The value of these methods as applied to these problems has been greatly increased by new and improved instruments, and a greater degree of skill in laboratory and interpretative technique.

Considerable success has been attained, with subsequent drilling checking the predicted depths within 1 to 5 per cent, on problems requiring information on thickness of fill material, depth to and contour of bedrock, extent and yardage of gravels to be mined, and location of hydrostatic water table. In these applications the geophysical work gives data comparable to drilling, and at a cost of about one-fiftieth that of drilling.

Discussion of several surveys with accompanying illustrations showing geophysical methods applicable to both simple and complicated placer problems are contained in the paper. The electrical instruments for measuring electromagnetic field strength and surface potentials are described, and their use, coupled with that of other geophysical instruments in modern field procedure, is noted.<sup>‡</sup>

---

\* International Geophysics, Inc.

† The paper was published as A.I.M.E. *Tech. Pub.* 515.

# Electrical Exploration of Water-covered Areas

BY C. AND M. SCHLUMBERGER\* AND E. G. LEONARDON\*

(New York Meeting, February, 1934)

THE object of this paper is to describe the adaptation of electrical resistivity measurements to the particular case of exploration in which the surface is an expanse of water (river, lake, sea). Water in itself does not constitute an obstacle to electrical exploration. It is merely an overburden, which is fluid instead of being solid, and as a consequence the routine of the measurements has to be modified. Also, in many instances, the liquid under consideration is highly conductive (salt water). This introduces an additional difficulty into exploration work, and has to be overcome by the geophysicist.

We do not propose to discuss here the basic principles of electrical resistivity measurements, which have been dealt with in various previous papers,<sup>1</sup> but will simply recall the two fundamental techniques which govern its field application:

1. *Horizontal exploration, or method of the resistivity map*, in which a series of electrical measurements are carried out at various stations, keeping the same electrode spacing. Thus, a horizontal layer of the subsoil, of a practically constant thickness, is explored.

2. *Vertical exploration, or "vertical sounding"*<sup>2</sup> *method*, in which a series of measurements is made with increasing electrode spacings at one or several stations. In this way, the apparent resistivity is determined at a given station for various increasing thicknesses of the ground.

---

Manuscript received at the office of the Institute Dec. 1, 1933.

\* Compagnie Générale de Géophysique, Paris, and Schlumberger Electrical Prospecting Methods, New York.

<sup>1</sup> In particular,

I. B. Crosby and E. G. Leonardon: *Electrical Prospecting Applied to Foundation Problems*. A. I. M. E. (1929) *Geophysical Prospecting*, 199.

J. N. Hummel: *Der scheinbare spezifische Widerstand*. *Ztsch. f. Geophysik* 5, 89; *Der spezifische Widerstand bei vier plan-parallel Schichten*. *Idem.*, 228.

S. Stefanescu and C. and M. Schlumberger: *Sur la distribution électrique potentielle autour d'une prise de terre ponctuelle dans un terrain homogène à couches horizontales homogènes et isotropes*. *Le Journal de Physique et le Radium* (1930) 1, 132.

<sup>2</sup> The term "vertical drilling" has been used by the authors in previous communications. The expression "vertical sounding" seems, however, more appropriate.

In other words, the constitution of the subsoil is investigated, along the vertical beneath the station.

These two techniques can evidently be applied over an expanse of water, provided that slight adaptations are made. This new procedure will be described, and several practical cases of its application discussed.

#### TECTONIC EXPLORATION IN FRENCH EQUATORIAL AFRICA

In the course of the years 1932 and 1933, the organization with which the authors are connected was entrusted with the exploration of a large



FIG. 1.—AREAS STUDIED GEOPHYSICALLY IN FRENCH EQUATORIAL AFRICA.  
1. Region of Pointe Noire. 3. Region of Kouilou River.  
2. Region of Rembo N'Komi.

territory in French Equatorial Africa, in the neighborhood of Pointe Noire and Fernand Vaz, for the purpose of locating structures favorable to oil occurrences (Fig. 1).

In the course of this exploration, several geophysical methods were applied simultaneously. Among the serious obstacles encountered was the difficulty of carrying out the observations in the thick jungle, which covers a large part of the territory under consideration. On the other hand, there are rivers and shallow bodies of water on which traveling by boat is an easy matter. This circumstance was of great importance in making possible a considerable improvement in the efficiency of the electrical system, which was easily and rapidly adapted to working conditions on water.

For horizontal exploration, a motor boat *M* in front carried one of the primary electrodes *A*, and towed a cable to which two canoes *C* were attached at convenient distances (Fig. 2). The first canoe was fitted up as a measuring station. It carried the potentiometer and its accessories, and was connected to the secondary electrodes *M* and *N*. The canoe at the end of the cable carried the primary electrode *B*. The whole outfit was towed along at a low speed by the motor boat. The rear canoe was carefully maintained in line with the two preceding boats.

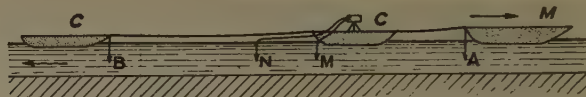


FIG. 2.—ARRANGEMENT OF CANOES.

The operator using the potentiometer at regular intervals of time observed the differences of potential between *M* and *N*, and the intensity of the current flowing in the line *AB*. Incidentally, the latter quantity is quite constant in a river, facilitating greatly the immediate interpretation of the differences of potential measured. The speed of the outfit was regulated according to the more or less rapid variations of the potential differences observed, so as always to study in detail the measurements in the zones particularly disturbed. In certain instances, it was possible to record an electrical profile 4 km. long in about one hour.

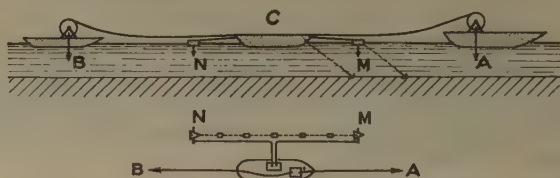


FIG. 3.—ARRANGEMENT OF CANOES FOR VERTICAL SOUNDINGS.

A third canoe accompanied the measuring outfit, in order to put down markers along the banks, or in the river, as often as was deemed necessary.

The carrying out of vertical soundings was equally simple (Fig. 3). A boat *C*, containing the measuring instruments, was firmly anchored in the neighborhood of the measuring point, so as to preserve a satisfactory stability. The secondary electrodes *M* and *N* were anchored in the neighborhood, and maintained on the surface of the water by a line of wooden floats. The primary electrodes *A* and *B* were carried by two canoes, which moved up and downstream of the line *MN*. These canoes also carried two reels of cable, so as to unwind the convenient lengths of



cable required for a given spacing of the electrodes. During the measurements, these canoes were maintained motionless in the water by means of anchors. All these maneuvers were regulated by means of whistle or telephone.



4



5

FIGS. 4 AND 5.—APPARATUS ON CANOE.

Figs. 4 and 5 illustrate this technique of exploration on water (view of the instruments installed on a boat, and laying down of a cable in the water).

STRATIGRAPHIC STUDY IN CASPIAN SEA, NEAR BIBI EIBAT<sup>3</sup>

As is well known, the oil field of Bibi Eibat is near Baku, on the shore of the Caspian Sea. The part of the anticline located on



land was first exploited. This is the zone of the "Old Exploitations" (Fig. 6). The outcrops of the Middle Apsheron limestones outline the form of this part of the structure. The later exploitations followed the prolongation of the anticlinal fold under the Caspian Sea, and for this purpose a large area was reclaimed from the sea. This constitutes the so-called "New Exploitations," marked on the map.

The problem put before electrical prospecting was to determine accurately the remainder of the structure underlying the Caspian Sea. This problem was solved quickly and satisfactorily by tracing the outcrop of the Apsheron limestones at the bottom of the sea.

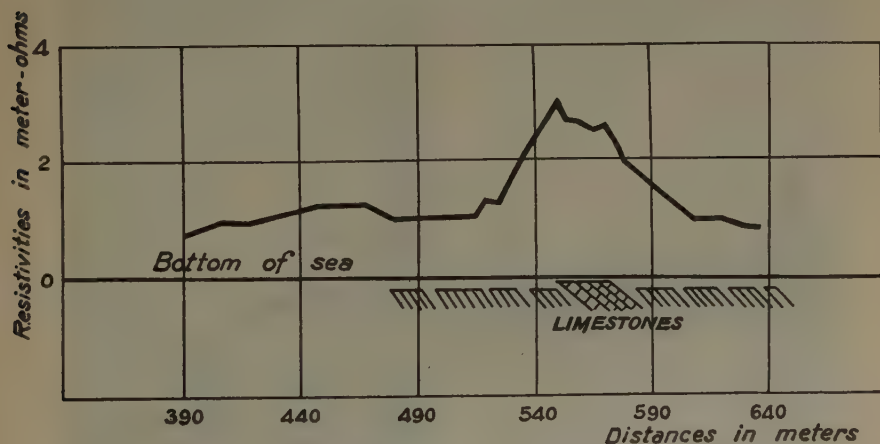


FIG. 7.—TYPICAL RESISTIVITY PROFILE ACROSS LIMESTONES.

In this region, the thickness of water and mud is in the order of 3 to 10 m. only. The resistivity measurements might have been performed according to the technique previously described. However, owing to the varying thickness of the thin, very conductive sheet of salt water, it was deemed preferable to utilize a measuring arrangement laid down at the bottom of the sea, so as to eliminate more readily the disturbances due to the variations in the thickness of this overburden. To this end, a triconductor cable (usually employed in electrical coring operations) was resorted to. A system of three electrodes *AMN* was prepared at the end of the cable, with *AM* = 45 m. and *MN* = 10 m. The second primary electrode *B* was located on land, at a long distance from *A*, *M* and *N*, and did not play any role in the differences of potential observed.

The cable, wound up on a winch located on shore, was drawn out and laid down in the sea by means of a motor boat. It was then wound up again slowly on the winch, and electrical readings taken every 15 m. apart, or even at shorter intervals in the interesting zones. Fig. 7 gives an example of the typical resistivity profiles obtained across the

limestones. These rocks, which are surrounded by shales, are clearly indicated by a characteristic hump on the resistivity diagrams.

On Fig. 6 the position of the various electrical profiles has been indicated, as well as the resistivity map deduced therefrom. The limestones of Bailov Cape extend  $2\frac{1}{2}$  km. towards the south, along two beds  $AB$  and  $A'B'$ . In the same way, in the southern part of the map, the limestones of Chikhov Cape extend along  $DD'$ , over a length of about 1200 m. The outcrop seems to be disturbed by at least two small faults. In the central zone, the resistive spots  $C$  and  $C'$  very likely



FIG. 8.—RECLAIMED ZONE AT BAKU.

correspond to the limestones, with the conclusion that this zone constitutes a *graben*, limited towards the north and south by two important faults.

Finally, the Brovtzina resistive zone is caused by the volcanic nature of the underlying formations.

New tectonic data obtained recently by electrical coring in the zone of the New Exploitations seems to be in complete accordance with the results of the surface exploration.

Fig. 8 shows a view of the reclaimed zone at Baku, with the Caspian Sea on the right, where the electrical exploration took place.

#### STUDY OF ROCK CONDITIONS IN ALGIERS HARBOR

The study in question was carried out in August and September, 1932, in connection with a program for altering and enlarging the harbor



of Algiers. The project (Fig. 9) included in particular the prolongation towards the sea of the northern breakwater. This prolongation was to be completed in two successive stages, first 400 m. being laid, and later another 450 m. The building of a new coal wharf was also contemplated, behind the eastern breakwater, and finally a passenger pier had to be constructed in order to supplement the one now in use, which is insufficient.

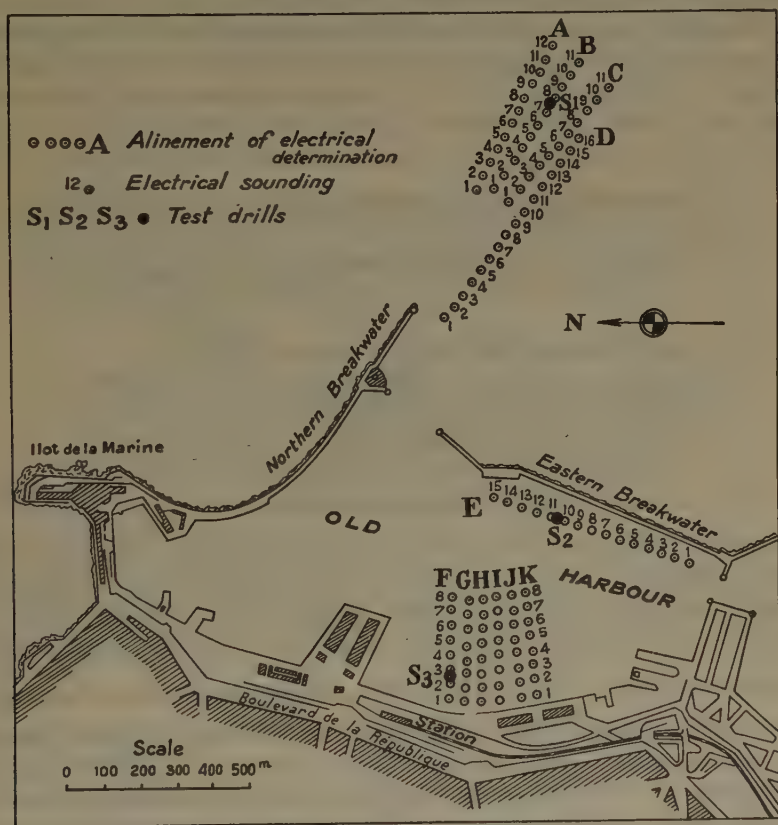


FIG. 9.—LOCATION OF PROJECT IN ALGIERS HARBOR.

For the systematic study of this new engineering project, it was necessary to know the elevation of the bedrock at the bottom of the sea. This bedrock is made up of old crystalline schists, which are found outcropping in numerous places around Algiers. They are overlain in the harbor by a variable and unknown thickness of muds and unconsolidated sediments. It was necessary to know the thickness of these sediments in order to determine more definitely the type of structures to be built.

In order to procure these data, a campaign of mechanical drilling might have been resorted to. However, the carrying out of such a

campaign at sea is relatively laborious and slow. Besides, the information gained is local, and it is not possible to obtain therefrom a general outline of the underlying topography, except by drilling a very large number of holes, with the consequence that the program of investigation would be very expensive. This explains why the harbor authorities, as well as the contractors themselves, agreed to apply simultaneously mechanical drilling and geophysical exploration.<sup>4</sup>

The problem put before electrical prospecting was a typical so-called "three-layer" problem, the particular conditions of which may be explained as follows (Fig. 10). The first layer is sea water, with a resistivity of 0.2 ohm, its thickness  $E$  being very accurately known. The second layer is made up of muds and unconsolidated sediments; the

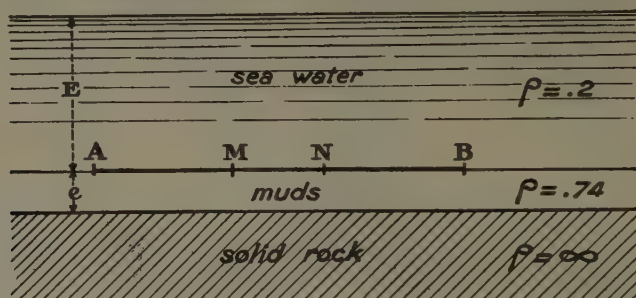


FIG. 10.—THREE-LAYER PROBLEM.

purpose of the exploration is to give an estimate of its unknown thickness. Preliminary experimentation showed that this unconsolidated material, saturated with salt water, possessed a remarkably constant resistivity of 0.74 ohm. This result, incidentally, proves that the muds contain a regular percentage in volume of  $\frac{0.2}{0.74}$ , i.e., about 27 per cent, of salt water. Finally, the underlying third layer is composed of crystalline schists, with a practically infinite resistivity in respect to the two previous layers. This layer, of course, is practically of indefinite extent. If a current is caused to flow in such a layered medium by means of a punctual electrode, it is evident that the state of the electric potentials will depend upon quantities of which all are known except the unknown thickness  $e$  of the intermediate layer. A relation, therefore, exists between the electric potentials and the thickness  $e$ , which makes it possible, at least from a mathematical point of view, to determine this latter quantity if the former is known.

In order to solve the problem, electrical vertical soundings might be carried out from the surface of the sea. The resistivity diagrams obtained would be utilized to determine the position of the different

<sup>4</sup> C. Schlumberger and P. J. M. Renaud: Étude Géophysique Sous-Marine Exécutée dans le Port d'Alger. *Ann. des Ponts et Chaussées* (1933) 2, No. 4.

underlying layers. However, there is a distinct advantage in placing the measuring arrangement as near as possible to the surface of contact, whose position has to be determined, so that this particular heterogeneity may cause the largest possible perturbation in the measurements. This is the reason that led to the decision to place the measuring arrangement at the bottom of the sea. This measuring arrangement comprised three electrodes  $AMN$ , so that  $AM = MN$ . These three electrodes were connected to three insulated conductors of a triconductor cable. The fourth electrode  $B$  was located on land, together with the measuring apparatus, as illustrated by Fig. 11.

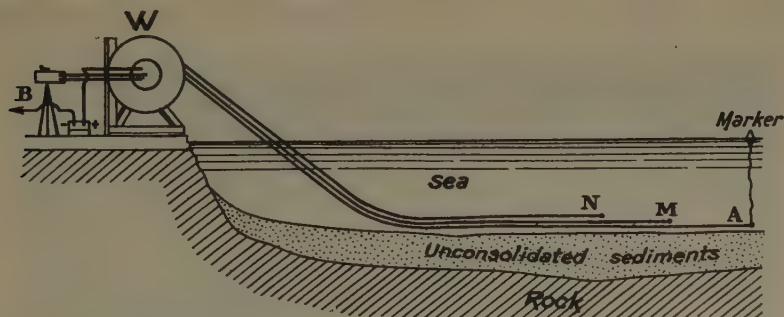


FIG. 11.—PROBLEM WITH ONE ELECTRODE ON LAND.

There is a decided advantage in locating the measuring apparatus on land instead of setting it up on a boat, since the lack of stability entails serious difficulties in the carrying out of the minute measurements to be made. This course was always possible, since the whole zone to be investigated was within a distance of 1000 m. or less from the shore.

The cable was wound up on a winch  $W$ , and could be laid in the sea along a given alignment by means of a motor boat. A buoy fastened to the end was used as a marker, and showed at any moment the position of the electrode  $A$ .

For the carrying out of the vertical soundings, the cable was first unwound along a given direction. Then a series of measurements with a given measuring arrangement  $AMN$  was performed. The successive positions of the electrode  $A$  were carefully noted. The electrode spacing was then modified on the cable, and a new series of measurements performed for the same positions of the electrode  $A$ . The same procedure was applied five or six times, with varying electrode spacings, so as to obtain for each position of  $A$  a complete series of resistivities at various depths, as is customary in the vertical sounding method.

### Interpretation

For each resistivity diagram the abscissas of the various values of  $\frac{AM}{E}$  were plotted. This means that the thickness of the sea at the point of

the station is taken for the unit of length. In the same way, the ratio of the apparent resistivity with respect to that of the salt water was plotted in ordinates. The experimental curves obtained are of the type shown by curve *C* (Fig. 12) which was measured at point  $S_3$ . On the other hand, the whole series of theoretical curves corresponding to different values

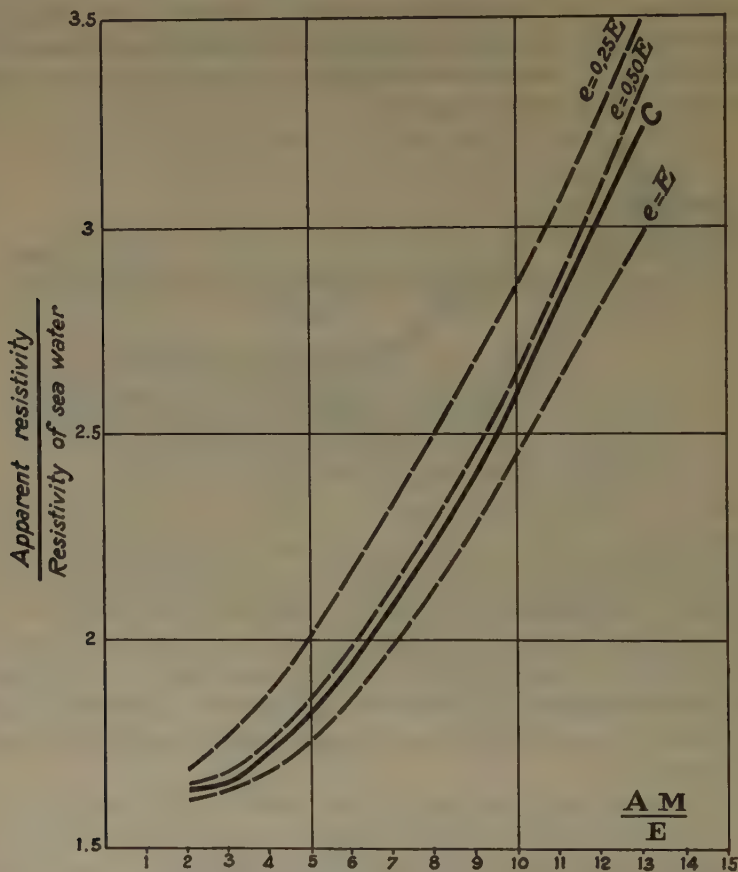


FIG. 12.—EXPERIMENTAL CURVE AT POINT  $S_3$ .

of the ratio  $\frac{e}{E}$  had been computed beforehand. On the figure are shown three of these theoretical curves ( $e = 0.25 E$ ,  $e = 0.5 E$ , and  $e = E$ ). From the position of the curve *C*, among the family of the theoretical curves, the thickness of the intermediate layer was deduced.

Among the difficulties encountered in the course of this exploration, we will mention the stray currents which were very important in the neighborhood of a large town like Algiers, and which rendered the accurate electrical readings very difficult to carry out. Another dif-



ficulty was due to the salt mist, which was quite detrimental to the good insulation of different parts of the equipment.

Fig. 13 shows a view of the operations in Algiers Harbor.

### Results

All of the measuring stations have been marked on the map (Fig. 9) and are arranged along eleven alignments, *A* to *K*. Alignments *A*, *B*, *C*, *D* indicated a thickness of the muds from 10 to 21 m. (depth of the sea water from 34 to 38 m.). A test drill was put down at  $S_1$  and gave a depth of 20.65 m., while the electrical prediction was 17.50 m. It is worth emphasizing that the information obtained from this drill hole



FIG. 13.—OPERATIONS IN ALGIERS HARBOR.

is neither precise nor certain, since the hole was difficult to drill, owing to weather conditions on the sea. On several occasions, the barge which carried the drilling equipment was taken away from its anchored position. No core samples were taken.

On alignment *E*, the thickness determined for the sediments was between 4.5 and 6.5 m., under a depth of water of 15 and 18 m. A drill hole put down at  $S_2$  found a thickness of the muds of 5 m., exactly as predicted by the electrical measurements.

On profiles *F*, *G* . . . *K*, the figures determined varied between 1.5 and 5 m., under a depth of 5 to 15 m. of water. The test drill  $S_3$  found 3.35 of loose formations, instead of 4 predicted by the electrical survey.

In short, the results of the electrical investigation checked satisfactorily with the drill-hole exploration. The process is particularly useful for the survey of an expanse of water where rough conditions exist, and constitute a serious hindrance to easy investigation by mechanical drilling. On the other hand, the economic advantage that results

from the possibility of obtaining a large number of depth determinations speedily and at low cost is worth emphasizing. Thus, very large areas can be studied, and general conclusions arrived at regarding underground conditions. Such information is of great value in orienting the civil engineer in his choice between the various and different types of structures that may be adopted for the engineering project under consideration.

## DISCUSSION

*(E. DeGolyer presiding)*

F. H. KIHLESTEDT,\* New York, N. Y.—Our company carried out some investigations at sea, in connection with the efforts to salvage the wreck of the "Egypt." The usual procedure of dragging a cable along the bottom had been followed, but although the cable was hung up a number of times, it seldom proved to be a ship that was responsible, and considerable time was wasted to find this out. We were then called in to make some tests to determine whether or not, in given cases, a conductive body was catching the cable. I do not recall the technical details of the survey, but I know that the work we did was of considerable help. In one case, I remember, we found that it was a conductor that was catching the cable, but unfortunately the divers that went down found that it was another ship, not the "Egypt."

F. W. LEE,† Washington, D. C.—Further applications could be made of the technique described; for example, in the study of foundation conditions in connection with such bridges as that over the Chesapeake Bay.

E. DEGOLYER,‡ New York, N. Y.—The part in which I found myself particularly interested is that showing the practical results obtainable in the oil fields. It must be remarked, however, that in some of our own sea-going oil fields, where the conditions are less simple, such work might run into greater difficulties.

---

\* Swedish-American Prospecting Corporation.

† U. S. Bureau of Mines.

‡ Petroleum Geologist.

# Interpretation of Resistivity Measurements

By G. F. TAGG,\* LONDON, ENGLAND

(New York Meeting, February, 1932)

EARTH-RESISTIVITY measurements are often of service in obtaining information regarding geological formations, particularly when applied to structural problems. In such problems the masses of the various bodies are large, and have a corresponding effect on the average resistivity of the soil. Much work has been done using such measurements, but in general the method of interpretation employed is empirical. Since certain simple cases can be investigated mathematically, it appears to be quite sound to endeavor to apply the mathematical solutions to the practical results, in order to deduce from the latter such unknown quantities as depth. This paper deals with such a method of interpretation for the simple case of a single horizontal stratum.

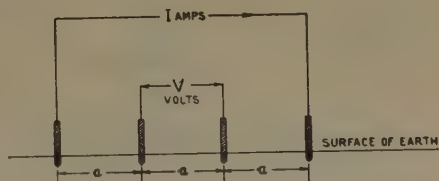


FIG. 1.—WENNER'S METHOD OF MEASURING EARTH RESISTIVITY.

In the method described by Wenner<sup>1</sup> for measuring earth resistivity, four stake electrodes are driven into the earth in a straight line as shown in Fig. 1. A current  $I$  amperes is passed between the two outer stakes and the potential difference  $V$  volts between the two inner stakes is measured. Then if  $a$  is the electrode separation, the specific resistance of the soil, which is assumed to be homogeneous, is given by the formula

$$\rho = 2\pi a \frac{V}{I} \quad [1]$$

or if  $\frac{V}{I}$  is called a resistance  $R$  ohms,

$$\rho = 2\pi a R \quad [2]$$

If  $a$  is in inches,  $\rho$  will be in ohms per inch cube, or ohm-inches, and if  $a$  is in centimeters,  $\rho$  will be in ohms per centimeter cube or ohm-centimeters.

As stated above, this formula is true only if the earth is homogeneous, and when this is not the case an application of one of these formulas

\* Evershed & Vignoles.

<sup>1</sup> F. Wenner: A Method of Measuring Earth Resistivity. U. S. Bur. Stds. *Sci. Paper* 258 (1915).

gives only an "average" resistivity. This "average" is not an average in the true sense of the word, since the soil nearest to the surface contributes most to the resistance, and so in this paper the resistivity obtained from an application of formula 1 or formula 2 when the earth is not homogeneous is termed an apparent resistivity. This apparent value will be affected by the extent of the nonhomogeneity and the electrode separation.

### SINGLE HORIZONTAL STRATUM

For a single underlying horizontal stratum, the value of this apparent resistivity will be affected by the electrode separation, the depth to the stratum, the specific resistance of the surface layer and the specific

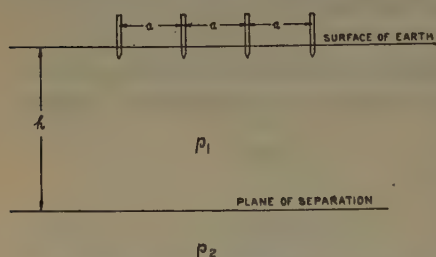


FIG. 2.—APPARENT RESISTIVITY IN RELATION TO ELECTRODE SEPARATION.

resistance of the stratum. By means of a mathematical investigation, a definite relation can be deduced between these various quantities and a method of interpretation can be based on it. If, as in Fig. 2, it is assumed that the depth of the stratum is  $h$  below the horizontal surface of the earth, that the specific resistance of the surface is  $\rho_1$ , and the specific resistance of the underlying stratum is  $\rho_2$ , it has been shown by Lancaster Jones<sup>2</sup> that the value of the apparent specific resistance  $\rho_a$  as obtained by an application of equation 2 to the resistance obtained by measurement is related to the various quantities involved by an expression of the form

$$\frac{\rho_a}{\rho_1} = 1 + 4F \quad [3]$$

$F$  is a function representing the sum of an infinite series and may be written

$$F = \sum_{n=1}^{n=\infty} \left\{ \frac{k^n}{\sqrt{1 + \left(2n\frac{h}{a}\right)^2}} - \frac{k^n}{\sqrt{4 + \left(2n\frac{h}{a}\right)^2}} \right\} \quad [4]$$

in which  $k$  has the value  $(\rho_2 - \rho_1)/(\rho_2 + \rho_1)$  [5]

In actual measurements  $\rho_a$  and  $a$  are definitely known, and  $\rho_1$  can be determined by very careful measurements at small electrode separations. Thus there are two unknown quantities  $k$  and  $h$ , which have to be determined. From equations 3, 4 and 5, it is possible to calculate the value

<sup>2</sup> E. Lancaster-Jones: *Min. Mag.* (1930) 3.



of the ratio  $\rho_a/\rho_1$  for definite values of  $k$ , and of the ratio  $h/a$ . The quantity  $k$ , equation 5, may be written in the form

$$(1 - \rho_1/\rho_2)/(1 + \rho_1/\rho_2).$$

and is therefore only dependent on the ratio  $\rho_1/\rho_2$ . Thus  $k$  may have any value between  $+1$  and  $-1$ . The values of  $\rho_1/\rho_2$  corresponding to various values of  $k$  are given in Table 1.

TABLE 1.—Corresponding Values<sup>a</sup> of  $\rho_1/\rho_2$  and  $k$

$k$	$\rho_1/\rho_2$	$k$	$\rho_1/\rho_2$
1.0	$1/\infty$	-1.0	$\infty$
0.9	$1/19$	-0.9	19
0.8	$1/9$	-0.8	9
0.7	$1/5.67$	-0.7	5.67
0.6	$1/4$	-0.6	4
0.5	$1/3$	-0.5	3
0.4	$1/2.33$	-0.4	2.33
0.3	$1/1.85$	-0.3	1.85
0.2	$1/1.5$	-0.2	1.5
0.1	$1/1.33$	-0.1	1.33
0.0	$1/1$	0.0	1

<sup>a</sup> Positive values of  $k$  correspond with the condition that the lower stratum has the higher resistivity, while negative values correspond with the condition that the surface layer has the higher resistivity.

A series of curves can be drawn showing the relationship between  $\rho_a/\rho_1$  and  $h/a$  for various values of  $k$ . When  $k$  has positive values, however, it is more convenient to express the relation in terms of conductivity by plotting the values  $\sigma_a/\sigma_1$  instead of  $\rho_a/\rho_1$ ,  $\sigma_a$  being the apparent conductivity as measured  $= 1/\rho_a$ , and  $\sigma_1$  the conductivity of the surface layer  $= 1/\rho_1$ . Sets of curves showing the relationship between  $\sigma_a/\sigma_1$  and  $h/a$ , when  $k$  is positive, and the relationship between  $\rho_a/\rho_1$ , and  $h/a$  when  $k$  is negative are given in Fig. 3. The sets of curves marked A correspond with the positive values of  $k$  and those marked B with the negative values of  $k$ .

#### METHOD OF INTERPRETATION

The author suggests that the curves in Fig. 3 can be used to determine the depth to horizontal stratum from the practical results obtained. The method would be as follows.

Resistivity measurements are first made with one or two small electrode intervals, the electrodes in each case being symmetrically dis-

posed along the traverse about the selected station. These will enable a fairly accurate determination of  $\rho_1$  to be made. Then further tests are

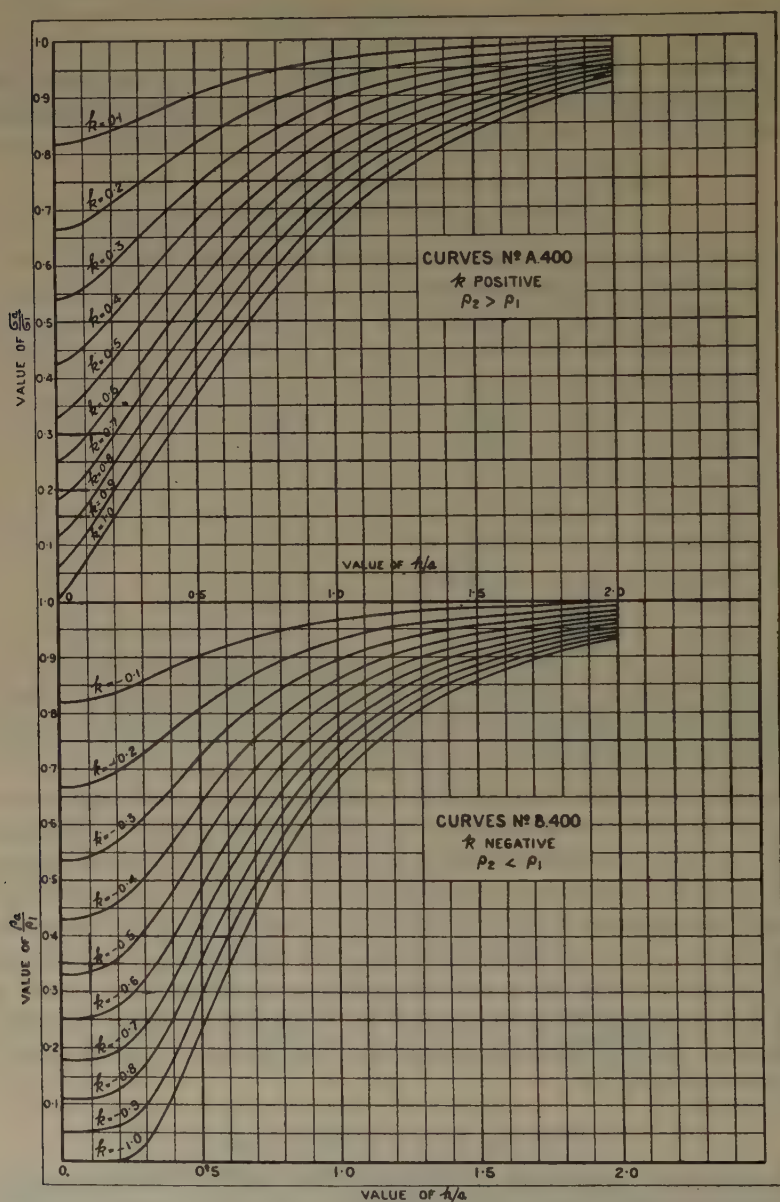


FIG. 3.—RELATION OF  $\sigma_a/\sigma_1$  AND  $\rho_a/\rho_1$  TO  $k$ .

carried out at larger electrode intervals, 150, 200, 250 ft., and so on. For each of these electrode intervals a value of  $\rho_a/\rho_1$  can thus be obtained.

If these ratios are less than unity, it is possible to read off from the curves in Fig. 3 a series of values of  $h/a$  and  $k$  corresponding to each value of  $\rho_a/\rho_1$ . Since the value of  $a$ , the electrode interval, is known, these can be converted into a series of values of  $h$  and  $k$ . Thus for each value of electrode separation, there will be a series of these corresponding values of  $h$  and  $k$ . If these series of values are then plotted as curves of  $k$  against  $h$ , they should intersect at a point corresponding to the value of  $h$  equal to the depth to the stratum. It can hardly be expected in practice that they will intersect in a point, but they should intersect in a fairly small area, and thus give a close indication of the value of  $h$  and incidentally of  $k$ . When the ratio  $\rho_a/\rho_1$  is greater than unity, its reciprocal  $\sigma_a/\sigma_1$  must be taken. Then on referring to the curves A in Fig. 3, a similar method can be used to deduce the value of  $h$ .

#### EXPERIMENTAL SURVEY

In order to test out this theory an experimental survey was carried out. To do this satisfactorily, it was necessary to obtain a site where the geological conditions conformed as closely as possible to those assumed in the mathematical investigation. The Director of the Geological Survey of Great Britain was asked to suggest a site where there was a single underlying stratum practically horizontal, and the surface was approximately level. A number of suitable sites were suggested, and the one finally chosen was on Cleeve Hill Common near Cheltenham, Gloucestershire. Permission to carry out tests was kindly given by the Board of Conservators of Cleeve Common. The surface material of this common is limestone overlain by about 6 in. of loam. The depth of this limestone varies from 50 to 266 ft., and underneath the limestone is either sand or clay. Sites were selected on the Common which were practically level, and large enough for the tests. Tests were carried out at two stations, which were termed A and B. The apparatus available for the tests consisted of a Megger Ground Tester and a potentiometer-milliammeter equipment with reversing commutators.

It is interesting to note in the experimental results that the agreement between these two sets of apparatus was within a very few per cent.

#### RESULTS AT STATION A

The electrodes were placed on a line running approximately north and south, and tests made at electrode intervals varying from 20 to 500 ft. The results of these tests are plotted in the form of curves of varying specific resistance against electrode interval in Fig. 4. These curves show an increase in the specific resistance with increasing electrode separation, which indicates that the resistance of the underlying stratum is higher than that of the surface material. It was first necessary to obtain a value for the average specific resistance of the surface limestone,

and to do this, the values obtained at electrode intervals up to 70 ft. were averaged. This average value is 6703 ohm-in. From the experi-

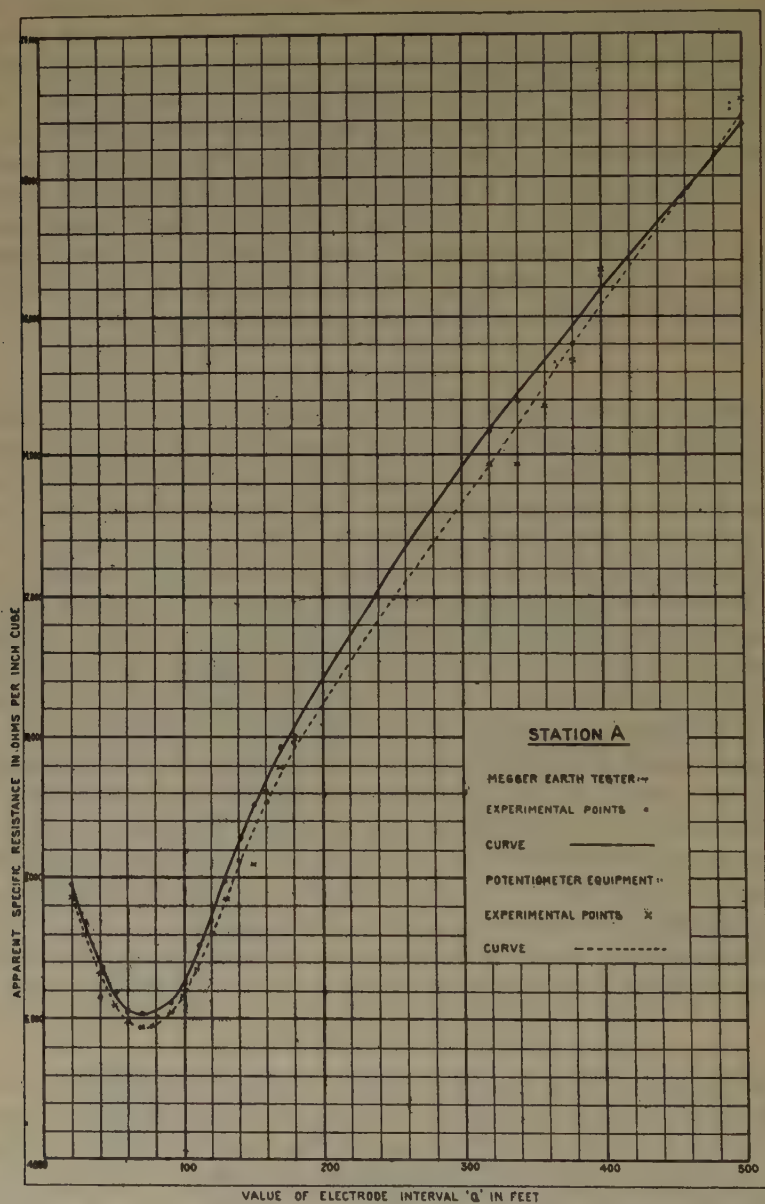


FIG. 4.—Specific resistance in relation to electrode interval, station A.

mental curve, a series of values of the apparent specific resistance and electrode interval were read off and the ratio  $\rho_a/\rho_1$  determined for each



interval. These ratios were greater than unity, and so the reciprocals corresponding to  $\sigma_a/\sigma_1$  were obtained (Table 2). The values of  $\sigma_a/\sigma_1$  were then referred to theoretical curves *A* in Fig. 3, and a series of corresponding values of  $h/a$  and  $k$  read off for each value of  $\sigma_a/\sigma_1$ . These values and the corresponding values of  $h$  are given in Table 3. This

TABLE 2.—*Resistivities at Station A*

Electrode Separation, Ft.	Apparent Specific Resistance, Ohm-in.	Ratio, $\rho_a/\rho_1$	Ratio, $\sigma_a/\sigma_1$
150	8,960	1.338	0.748
200	10,740	1.601	0.625
250	12,320	1.840	0.544
300	13,860	2.068	0.483
350	15,220	2.270	0.441
400	16,480	2.460	0.407

TABLE 3.—*Values of  $k$  at Station A*

Value of $k$	150 Ft.		200 Ft.		250 Ft.		300 Ft.		350 Ft.		400 Ft.	
	$\sigma_a/\sigma_1 = 0.748$		$\sigma_a/\sigma_1 = 0.625$		$\sigma_a/\sigma_1 = 0.544$		$\sigma_a/\sigma_1 = 0.483$		$\sigma_a/\sigma_1 = 0.441$		$\sigma_a/\sigma_1 = 0.407$	
	$h/a$	$h$	$h/a$	$h$	$h/a$	$h$	$h/a$	$h$	$h/a$	$h$	$h/a$	$h$
1.0	1.19	179	0.915	183	0.770	193	0.675	202	0.61	214	0.560	224
0.9	1.12	168	0.850	170	0.705	176	0.610	183	0.545	191	0.500	200
0.8	1.045	157	0.775	155	0.640	160	0.545	163	0.485	170	0.435	174
0.7	0.96	144	0.700	140	0.565	141	0.478	143	0.41	144	0.36	144
0.6	0.87	130.5	0.620	124	0.485	121	0.390	117	0.325	114	0.28	112
0.5	0.785	118	0.525	105	0.39	97.5	0.295	74	0.226	78	0.17	68
0.4	0.66	99	0.42	84	0.27	67.5	0.16	40	0.06	21		
0.3	0.525	79	0.26	52	0.03	7.5						
0.2	0.315	47										
0.1												

table shows that the values for  $k = 0.7$  agree very closely, but to obtain the exact values, the figures in Table 3 were plotted in the form of the curves given in Fig. 5. The six curves intersect in a small area, and the center of this area gives a value of  $h$  of 142, and the value of  $k$  of 0.702. This means that the thickness of limestone at this point is 142 ft., and so far as it was possible to judge from the geological map, this was approximately correct.

### RESULTS AT STATION B

At this station tests were carried out with the electrodes on both the north-south and east-west lines, but while the results obtained on the north-south line are for electrode separations varying from 20 to 400 ft.,

those on the east-west line were obtained only for electrode intervals varying from 20 to 240 ft. The results are all plotted in the form of curves of apparent specific resistance against electrode interval in Fig. 6. The average value of the specific resistance of the surface layer was found to be 45,700 ohm-in., on adopting the same procedure as at station A. This value is very much higher than that obtained at station A, although the material in both cases is limestone. The probable explanation of

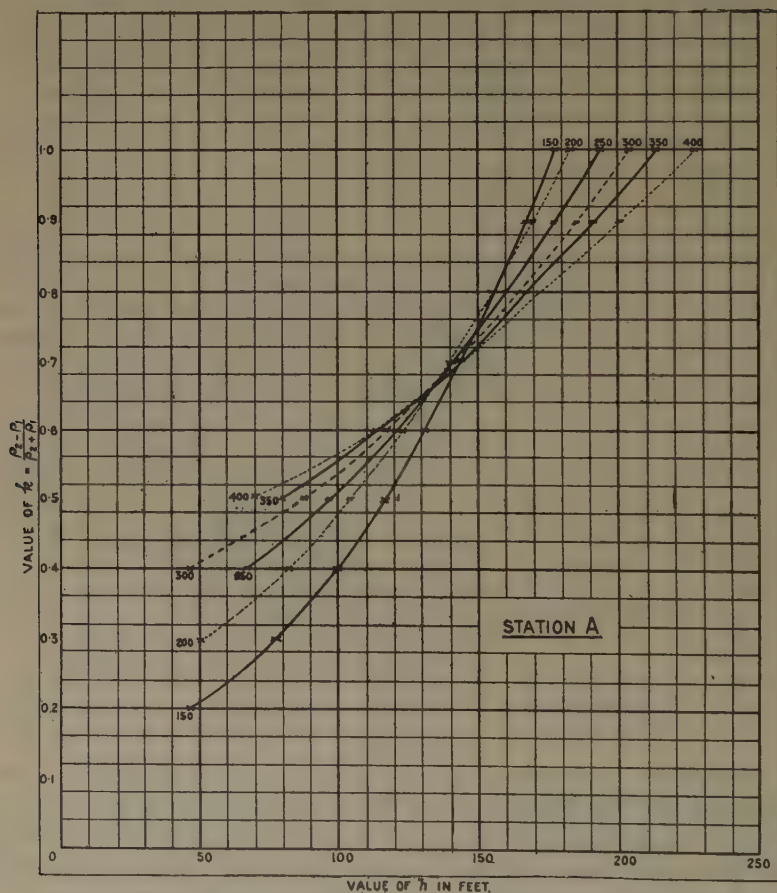


FIG. 5.—VALUES OF  $k$  IN RELATION TO DEPTH OF STRATUM, STATION A.

the difference is that at station A the stratum under the limestone was clay, which would keep the limestone waterlogged and thus of a low resistance, while at station B the stratum was sand, which would permit water to filter away, leaving the limestone comparatively dry and thus of a higher resistance. In this case the experimental curves show a decrease in the apparent specific resistance with increasing electrode interval, thus showing that the resistance of the underlying stratum is lower than

that of the surface material. Again, as at station A, a series of values of the apparent specific resistance were read off the curves for a number of electrode intervals, and the values of  $\rho_a/\rho_1$  calculated for each (Table 4).

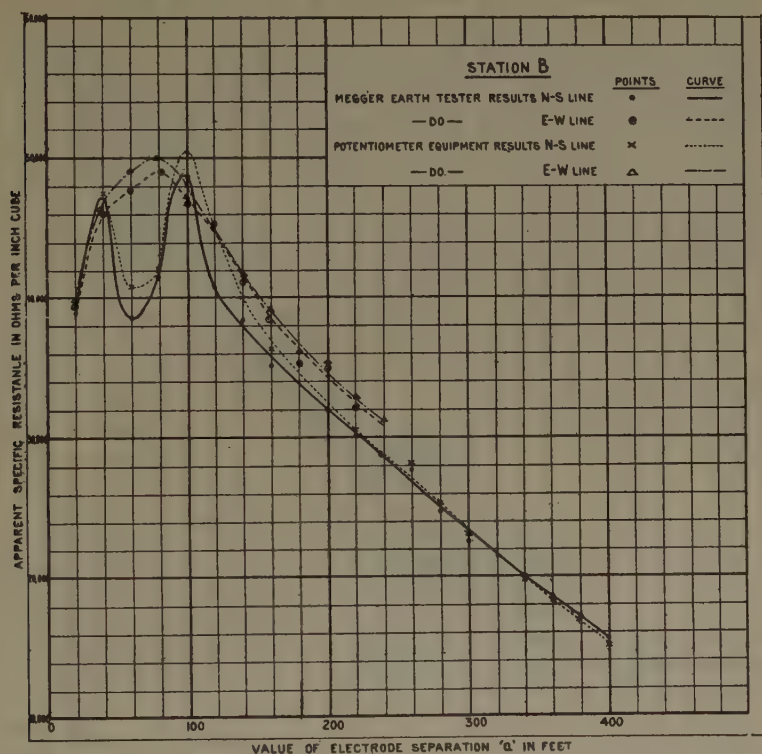


FIG. 6.—SPECIFIC RESISTANCE IN RELATION TO ELECTRODE INTERVAL, STATION B.

For each of the values of  $\rho_a/\rho_1$  in the last column, a series of values of  $h/a$  and  $k$  were read off curves *B* in Fig. 3, and from these, corresponding values of  $k$  and  $h$  were deduced. These figures are all given in Table 5.

TABLE 4.—Resistivities at Station B

Electrode Separation, Ft.	$\rho_a$	$\rho_a/\rho_1$
150	36,800	0.805
200	32,000	0.700
250	27,400	0.600
300	23,000	0.503
350	19,400	0.424
400	15,500	0.339

The values of  $h$  and  $k$  from this table were plotted in the form of curves, and are given in Fig. 7. The center of the area of intersection of the

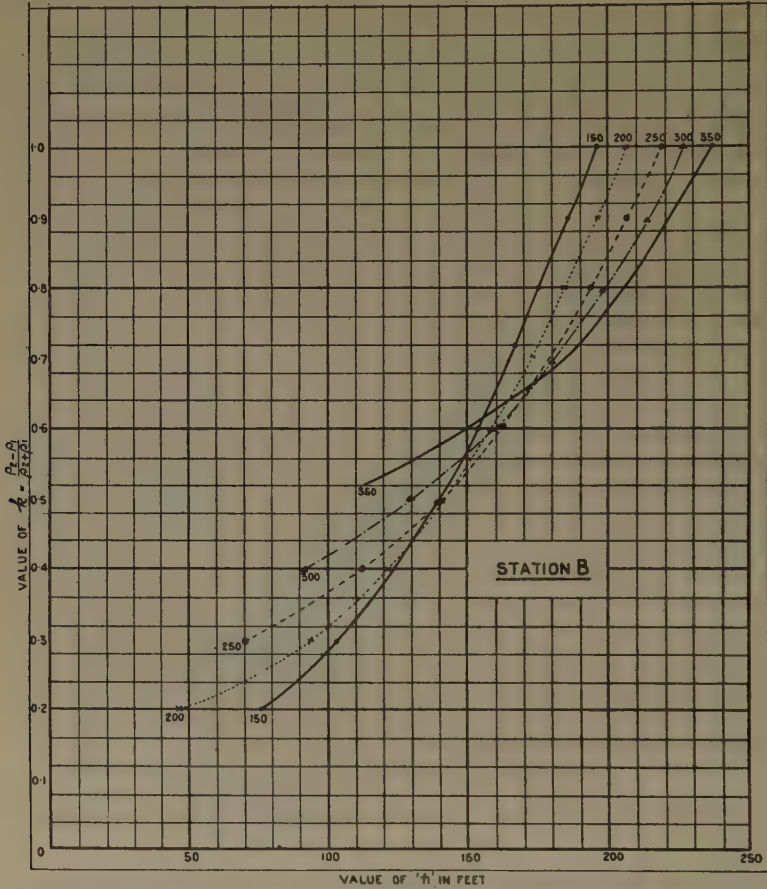


FIG. 7.—VALUES OF  $k$  IN RELATION TO DEPTH OF STRATUM, STATION B.

curves gives a value of 156 ft. for  $h$  and  $-0.6$  for  $k$ . This value of  $h$  against  $k$  agrees closely with that estimated on the geological map.

### CONCLUSION

From the experimental results it appears that the method of interpretation based on theoretical considerations given yields satisfactory results when the geological conditions conform to those assumed in the mathematical investigation. It is possible that similar theories and methods of interpretation can be worked out for other forms of geological structure.



TABLE 5.—*Values of  $k$  at Station B*

Value of $k$	150 Ft.		200 Ft.		250 Ft.		300 Ft.		350 Ft.	
	$\rho_a/\rho_1 = 0.805$		$\rho_a/\rho_1 = 0.700$		$\rho_a/\rho_1 = 0.600$		$\rho_a/\rho_1 = 0.503$		$\rho_a/\rho_1 = 0.424$	
	$h/a$	$h$	$h/a$	$h$	$h/a$	$h$	$h/a$	$h$	$h/a$	$h$
-1.0	1.29	194	1.025	205	0.870	217	0.760	228	0.680	238
-0.9	1.225	184	0.98	196	0.820	205	0.710	213	0.625	218.5
-0.8	1.16	174	0.92	184	0.775	194	0.646	194	0.570	199
-0.7	1.1	165	0.86	172	0.71	177	0.595	179	0.505	177
-0.6	1.015	152	0.79	158	0.64	160	0.520	156	0.425	149
-0.5	0.940	141	0.71	142	0.55	137.5	0.430	129	0.322	113
-0.4	0.825	124	0.60	120	0.45	112	0.295	88.5		
-0.3	0.695	104	0.47	94	0.28	70				
-0.2	0.5	75	0.22	44						
-0.1										

## DISCUSSION

(Donald H. McLaughlin presiding)

T. ZUSCHLAG,\* New York, N. Y.—My experience has been that attempts to base an interpretation upon rigid formulas of the type given generally end in disappointment because of the impossibility of determining accurately the value of the surface resistivity. The value of surface resistivity changes with the direction in which it is measured, and with the spacing of the electrodes, so good results may be obtained in some cases but not in others. Consequently, the method should be used with discretion.

K. SUNDBERG,† Stockholm, Sweden.—The Tagg method is applicable only in the two-layer problem. Generally, the field problems are more complicated than that because several layers are encountered. For these another method can be followed, which is effective but simple.

As shown by Hummel and others, the apparent resistivity  $\rho$  for a two-layer combination approaches a definite limit  $\rho_{\text{lim}}$  for infinite distance between the electrodes in potential measurements, using Wenner's or similar arrangements. The value of  $\rho_{\text{lim}}$  is obtained from the following:

$$\frac{h_2}{\rho_{\text{lim}}} = \frac{h_1}{\rho_1} + \frac{h_2 - h_1}{\rho_2} \quad [A]$$

where  $\rho_1$  = specific resistance of upper layer.

$h_1$  = thickness of upper layer.

$\rho_2$  = specific resistance of lower layer.

$h_2$  = total thickness of upper plus lower layer.

Hummel has shown that the potential distribution on the surface of the upper layer in points at a long distance from the power electrodes compared with the total thickness  $h_2$  is approximately identical with the potential distribution for a single

\* Research Engineer.

† Managing Director, A. B. Elektrisk Malmletning.

layer with thickness  $h_2$  and specific resistivity  $\rho_{lim}$ . If a third layer exists below the second, the potential distribution on the upper surface of the top layer in points at considerable distance from the power electrodes compared to the total thickness of the layers may be obtained by substituting similarly the three layers by one, and so on (substitution principle).

It is further generally recognized that the potential distribution close to a power electrode practically is determined only by the electrical properties at shallow depth

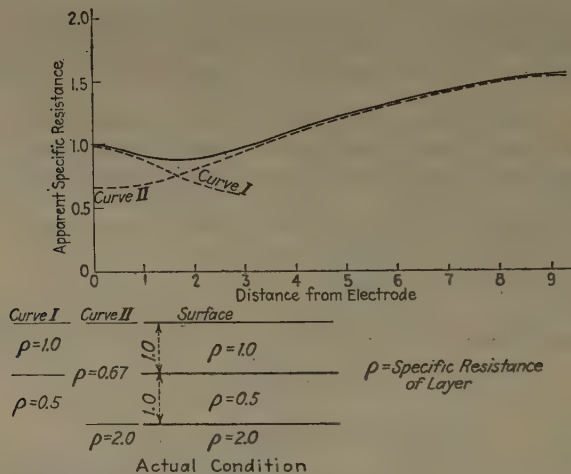


FIG. 8.—APPARENT RESISTANCE OF THREE LAYERS MAY BE APPROXIMATELY OBTAINED FROM TWO TWO-LAYER COMBINATIONS.

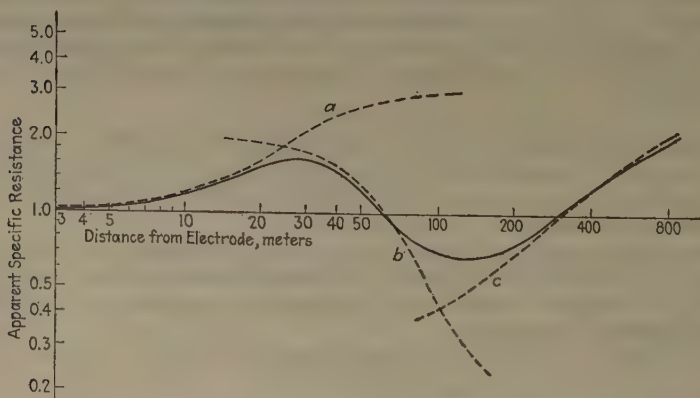


FIG. 9.—INTERPRETATION OF APPARENT RESISTANCE CURVE (SOLID) BY THREE TWO-LAYER CURVES (a, b, c).

and that with increasing distance from the electrode deeper and deeper strata have to be taken into consideration in calculating the potential distribution. The potential distribution for a two-layer combination, consisting of a top layer of certain thickness and a lower layer of infinite thickness, has been investigated by Hummel, Tagg, Hedström and others and diagrams have been constructed, giving for instance the apparent specific resistivity at different distances from the power electrode. Such diagrams may be referred to as "two-layer diagrams."

The method of interpretation I have referred to consists in making a series of two-layer interpretations, using "two-layer diagrams" in combination with the "substitution principle." To further illustrate this method of interpretation, I submit Figs. 8 and 9. Fig. 8 illustrates the theoretical correctness of the method and Fig. 9 shows an example of an actual interpretation. The solid curve in Fig. 8 represents the variation of the apparent resistivity according to theory for the three-layer conditions. Assuming the third layer to be absent and the second layer to extend to infinite depth, we obtain from the two-layer diagram the dashed apparent-resistivity curve I. Substituting one layer for the two top layers, we obtain as specific resistance for this layer, according to formula A, the value 0.67. The second two-layer combination consequently consists of a top layer of specific resistance 0.67 above a medium of specific resistance 2, for which combination we obtain the apparent-resistivity curve II.

The figure shows that the actual apparent-resistivity curve (solid) coincides well with curve I for small electrode distances and with curve II for large electrode distances. Consequently, the first mentioned curve may be divided into pieces, for which two-layer conditions approximately apply. These pieces, therefore, may be interpreted with the help of "two-layer diagrams." Fig. 9 shows an example of such interpretation. The solid curve represents the actual apparent resistivity according to measurements; the dashed curves *a*, *b* and *c* were obtained from a two-layer diagram, applying the substitution principle. The final solution in this case is found to be:

DEPTH METERS	SPECIFIC RESISTANCE	DEPTH METERS	SPECIFIC RESISTANCE
0-10	1	40-100	0.2
10-40	3	Over 100	3.1

J. FISHER,\* Houghton, Mich.—You spoke of two examples of interpretation, one where  $\rho_1$  was greater than  $\rho_2$ , and the depth to bedrock was predicted to be 142 ft. The other case was where  $\rho_2$  was the greater, and the predicted depth was 156 ft. How closely did these predictions check with the facts?

E. G. LEONARDON,† Paris, France.—I agree that the ideas expressed in Mr. Tagg's paper are essentially correct, but in field work it is never known beforehand whether the problem being approached is a two-layer, a three-layer, or a many-layer one. Hence the operator is under a considerable handicap in the interpretation unless he has prepared beforehand a series of diagrams showing the theoretical possibilities in numerous and various cases.

M. K. HUBBERT,‡ New York, N. Y.—In some of my field work I attempted to use Tagg's curves. The depth indicated by the Tagg curves proved to be as much as 50 per cent in error, however.\*

G. F. TAGG.—I am much interested in the development of the two-layer solution described by Mr. Sundberg, in order to make it applicable to multilayer problems. This appears to be a useful development.

It has been pointed out several times that all these methods depend on an accurate measurement of the surface resistivity, and I do think that this point has been somewhat overaccentuated. In one or two tests I have found that the specific resistance of the surface layer may be considerably in error without preventing a fairly accurate interpretation of the results by the method described.

Mr. Fisher asks how closely the predicted values of 142 and 156 ft. agreed with the actual values. The true depth of the limestone was between 145 and 150 feet.

Head, Department of Mathematics and Physics, Michigan College of Mining and Technology.

† Société de Prospection Electrique.

‡ Instructor in Geophysics, Columbia University.

# Interpretation of Three-layer Resistivity Curves

BY SYLVAIN J. PIRSON,\* GOLDEN, COLO.

(New York Meeting, February, 1934)

THE question of the interpretation of apparent resistivity curves is still a much disputed subject although the discussion has been going on for several years, mainly since Gish and Rooney<sup>1</sup> made their first measurements on the Tidal Basin at Washington, D. C. As a first approximation, they interpreted the depth to a horizontal discontinuity in terms of the electrode spacing at which a maximum or a minimum occurs in the resistivity curve. Later on, Lancaster-Jones<sup>2</sup> proposed a closer approximation of depth determination by evaluating the depth to a horizontal discontinuity as the two-thirds of the electrode spacing at which a point of inflection occurs in the resistivity curve. An accurate determination of the depth was recently proposed by Tagg<sup>3</sup> for a two-layer problem. It is a graphic solution of the problem by means of charts calculated from the formula of the apparent resistivity based on the theory of electrical images. Tagg's method is theoretically sound but the fact that the layers have been assumed to be homogeneous and isotropic must not be overlooked. Abusive use of the method has been made by geologists who have failed to recognize the fact that nature offers only few cases where the conductivity of the rocks may be assumed to be the same parallel and perpendicular to the bedding plane. Actually the ratio of the two resistivities in those directions may take values ranging from one (isotropic medium) to three for shales. In such conditions Tagg's method leads to disappointments.

A method recently advocated by Manhart<sup>4</sup> and Tattam<sup>5</sup> forces Tagg's method to give a solution where manifestly the case under

---

Manuscript received at the office of the Institute Jan. 22, 1934.

\* Instructor in Geophysics, Colorado School of Mines.

<sup>1</sup> O. H. Gish and W. J. Rooney: Measurement of Resistivity of Large Masses of Undisturbed Earth. *Terr. Magnetism and Atm. Elec.* (December, 1925) **30**, 261-88.

<sup>2</sup> E. Lancaster-Jones: The Earth Resistivity Method of Geophysical Prospecting. *Min. Mag.* (1930) **42**, 355-60 and **43**, 19-28.

<sup>3</sup> G. F. Tagg: Interpretation of Resistivity Measurements. See page 135, this volume.

<sup>4</sup> T. A. Manhart: Contributions to the Interpretation of Resistivity Curves. Master's Thesis, Colorado School of Mines, April, 1932.

<sup>5</sup> C. M. Tattam: Application of the Electrical Resistivity Method of Geophysical Prospecting to Problems of Underground Water. Doctor's Thesis, Colorado School of Mines, April, 1932.



investigation does not satisfy the requirements and simplifications that were necessary to establish the formula of apparent resistivity. The method may give a solution indifferently under isotropic or nonisotropic conditions. Although the method is of a certain value in isotropic ground, it would not be advisable to use it without ascertaining the ground conditions. In a nonisotropic ground, the error made may be as high as 50 per cent.

The author of the present article proposes the following "successive approximation method" for the interpretation of resistivity curves when Tagg's charts are applied to the solution of a three-layer case. The steps are as follows:

1. Average the resistivities of the surface formation for electrode spacings smaller than one-third of the estimated depth to the second layer. This will give an average value of the resistivity of the top layer  $\rho_1$ . Very careful measurements must be made in the field and precautions should be taken to prevent the depth of penetration of the electrode stakes from exceeding one-fifth of the electrode spacings. It is recommended that measurements be made for different values of the current, of the commutating frequency, and at different locations along the electrode spread. Since the value of the method depends largely on the accuracy with which the resistivity of the top layer is known, too much precaution cannot be taken in this determination.

2. The value of  $\rho_1$  is plotted to scale on the resistivity axis and a graphic approximation curve is drawn from  $\rho_1$  meeting tangentially the first part of the resistivity curve.

3. Resistivities are read for several electrode spacings on the curve just drawn and Tagg's method is applied to that first part of the curve. The process yields the resistivity of the second layer  $\rho_2$ , the thickness of the first layer  $h_1$ , and the resistivity factor  $k_1 = \frac{\rho_2 - \rho_1}{\rho_1 + \rho_2}$ .

4. The depth to the third layer is estimated by Lancaster-Jones' method. Thus  $h_1 + h_2 = \frac{2}{3}d$  where  $d$  is the spacing at which occurs the inflection point comprised between the two lower maximum curvature points.

5. The apparent or equivalent resistivity  $\rho_1'$  of the two layers of resistivities  $\rho_1$  and  $\rho_2$  in parallel is calculated by Kirchhoff's law:

$$\frac{h_1 + h_2}{\rho_1'} = \frac{h_1}{\rho_1} + \frac{h_2}{\rho_2}$$

6. Tagg's method is then applied to the lower part of the curve. A more accurate depth  $h_1 + h_2'$  than the one previously estimated is then obtained by tracing the curves of depth-resistivity factor. When they converge in a small area, the depth  $h_1 + h_2'$  and the resistivity factor  $k_2 = \frac{\rho_3 - \rho_2}{\rho_2 + \rho_3}$  are known with a fair degree of accuracy. From

this expression of  $k_2$ , the value of the resistivity  $\rho_3$  of the lower medium supposedly of infinite vertical extent can be calculated.

7. If the degree of accuracy with which  $h_1 + h_2'$  is obtained is not considered sufficient, the process may be repeated by using  $h_1 + h_2'$  instead of  $\frac{2}{3}d$  in the calculation of the equivalent resistivities of the two top layers. A value  $\rho_1''$  will be obtained for the equivalent

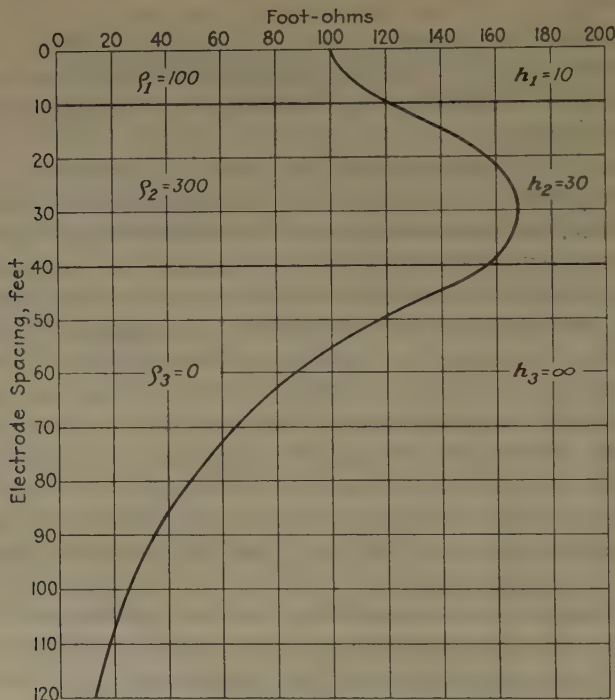


FIG. 1.—THEORETICAL CURVES FOR RESISTIVITY ELECTRODE SPACING.

resistivity of the two upper layers and a more accurate value of  $h_1 + h_2''$  will be found for the depth to the third layer. In other words, the mathematical process known as the “successive approximation method” is proposed.

As an example of the method, a theoretical case will be first investigated.

The theoretical resistivity curve (Fig. 1) calculated by Hummel<sup>6</sup> for the respective resistivities and thicknesses:

$$\begin{aligned}\rho_1:\rho_2:\rho_3 &= 1:3:0 \\ h_1:h_2:h_3 &= 1:3:\infty\end{aligned}$$

as given in Fig. 5 of the reference, will be used here. Suppose that the

<sup>6</sup> J. N. Hummel: Der scheinbare spezifische Widerstand bei vier planparallelen Schichten. *Ztsch. f. Geophysik* (1929) **B5**, 228-238 (Fig. 5).

spacing is in feet and the resistivity in foot-ohms. The resistivity of the surface formation is assumed to be 100 foot-ohms.

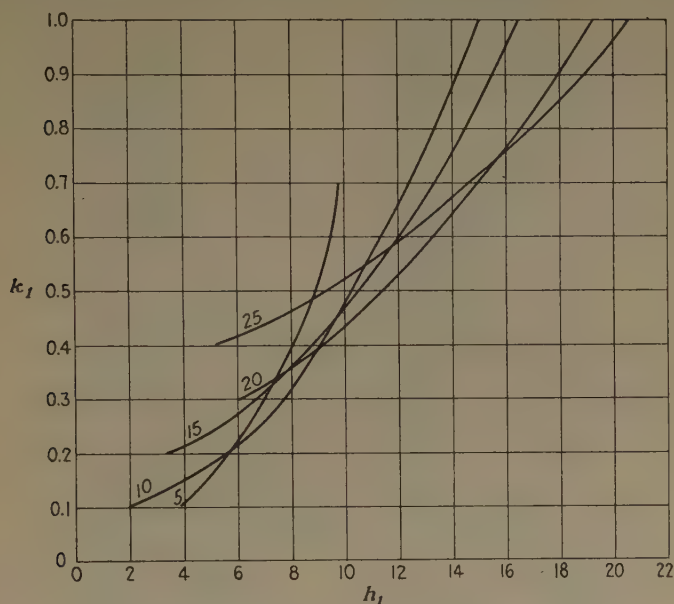


FIG. 2.—DEPTH-RESISTIVITY FACTOR, CURVES OF UPPER PART.

Since we deal here with a theoretical case, steps 1 and 2 can be overlooked and we proceed directly with step 3. The ratio  $\frac{\rho_1}{\rho_a}$  is computed for spacings 5, 10, 15, 20 and 25 ft. Table 1 is then obtained by using

TABLE 1

$\rho/\rho_a$	0.945		0.835		0.715		0.650		0.607	
$a$	5		10		15		20		25	
$k_1$	$\frac{h_1}{a}$	$h_1$	$\frac{h_1}{a}$	$h_1$	$\frac{h_1}{a}$	$h_1$	$\frac{h_1}{a}$	$h_1$	$\frac{h_1}{a}$	$h_1$
0.1	0.76	3.8	0.17	1.7						
0.2	1.13	5.65	0.55	5.5	0.21	3.16				
0.3	1.4	7.0	0.77	7.7	0.44	6.60	0.3	6.0		
0.4	1.6	8.0	0.9	9.0	0.58	8.62	0.45	9.0	0.21	5.25
0.5	1.77	8.9	1.01	10.1	0.70	10.5	0.56	11.2	0.37	9.25
0.6	1.88	9.4	1.13	11.3	0.79	11.85	0.66	13.3	0.47	11.9
0.7	1.98	9.8	1.23	12.3	0.88	13.20	0.75	15.0	0.58	14.6
0.8			1.33	13.3	0.96	14.40	0.82	16.4	0.66	16.5
0.9			1.42	14.2	1.02	15.40	0.89	17.8	0.74	18.5
1.0			1.51	15.1	1.10	16.60	0.96	19.3	0.81	20.6

TABLE 2

$\frac{\rho_a}{\rho_l'}$	0.83	0.64	0.54	0.42	0.32	0.24	0.17
$a$	30	40	50	60	70	80	90
$k_2$	$\frac{h_1 + h_2'}{a}$	$\frac{h_1 + h_2'}{a}$	$\frac{h_1 + h_2'}{a}$	$\frac{h_1 + h_2'}{a}$	$\frac{h_1 + h_2'}{a}$	$\frac{h_1 + h_2'}{a}$	$\frac{h_1 + h_2'}{a}$
	$h_1 + h_2'$	$h_1 + h_2'$	$h_1 + h_2'$	$h_1 + h_2'$	$h_1 + h_2'$	$h_1 + h_2'$	$h_1 + h_2'$
0.1	0.13	3.4					
0.2	0.56	16.9					
0.3	0.76	22.8	0.36				
0.4	0.90	27.0	0.50	14.4			
0.5	1.00	30.0	0.60	20.0	0.08		
0.6	1.10	33.0	0.70	24.2	0.36	18.0	
0.7	1.18	35.4	0.77	28.0	0.47	23.8	
0.8	1.25	37.6	0.82	30.8	0.56	28.0	
0.9	1.32	39.6	0.88	33.0	0.63	31.5	
1.0	1.38	41.4	0.93	35.2	0.69	34.5	
				37.2	0.74	37.0	
				40.0	0.80	40.2	
					0.67		
					0.56		
					0.62		
					0.47		
					0.31		
					0.41		
					0.39		
					0.31		
					0.45		
					0.51		
					0.45		
					0.39		
					0.31		
					0.45		
					0.51		
					0.45		
					0.39		
					0.31		
					0.45		
					0.51		
					0.45		
					0.39		
					0.31		
					0.45		
					0.51		
					0.45		
					0.39		
					0.31		
					0.45		
					0.51		
					0.45		
					0.39		
					0.31		
					0.45		
					0.51		
					0.45		
					0.39		
					0.31		
					0.45		
					0.51		
					0.45		
					0.39		
					0.31		
					0.45		
					0.51		
					0.45		
					0.39		
					0.31		
					0.45		
					0.51		
					0.45		
					0.39		
					0.31		
					0.45		
					0.51		
					0.45		
					0.39		
					0.31		
					0.45		
					0.51		
					0.45		
					0.39		
					0.31		
					0.45		
					0.51		
					0.45		
					0.39		
					0.31		
					0.45		
					0.51		
					0.45		
					0.39		
					0.31		
					0.45		
					0.51		
					0.45		
					0.39		
					0.31		
					0.45		
					0.51		
					0.45		
					0.39		
					0.31		
					0.45		
					0.51		
					0.45		
					0.39		
					0.31		
					0.45		
					0.51		
					0.45		
					0.39		
					0.31		
					0.45		
					0.51		
					0.45		
					0.39		
					0.31		
					0.45		
					0.51		
					0.45		
					0.39		
					0.31		
					0.45		
					0.51		
					0.45		
					0.39		
					0.31		
					0.45		
					0.51		
					0.45		
					0.39		
					0.31		
					0.45		
					0.51		
					0.45		
					0.39		
					0.31		
					0.45		
					0.51		
					0.45		
					0.39		
					0.31		
					0.45		
					0.51		
					0.45		
					0.39		
					0.31		
					0.45		
					0.51		
					0.45		
					0.39		
					0.31		
					0.45		
					0.51		
					0.45		
					0.39		
					0.31		
					0.45		
					0.51		
					0.45		
					0.39		
					0.31		
					0.45		
					0.51		
					0.45		
					0.39		
					0.31		
					0.45		
					0.51		
					0.45		
					0.39		
					0.31		
					0.45		
					0.51		
					0.45		
					0.39		
					0.31		
					0.45		
					0.51		
					0.45		
					0.39		
					0.31		
					0.45		
					0.51		
					0.45		
					0.39		
					0.31		
					0.45		
					0.51		
					0.45		
					0.39		
					0.31		
					0.45		
					0.51		
					0.45		
					0.39		
					0.31		
					0.45		
					0.51		
					0.45		
					0.39		
					0.31		
					0.45		
					0.51		
					0.45		
					0.39		
					0.31		
					0.45		
					0.51		
					0.45		
					0.39		
					0.31		
					0.45		
					0.51		
					0.45		
					0.39		
					0.31		
					0.45		
					0.51		
					0.45		
					0.39		
					0.31		
					0.45		
					0.51		
					0.45		
					0.39		
					0.31		
					0.45		
					0.51		
					0.45		
					0.39		
					0.31		
					0.45		
					0.51		
					0.45		
					0.39		
					0.31		
					0.45		
					0.51		
					0.45		
					0.39		
					0.31		
					0.45		
					0.51		
					0.45		
					0.39		
					0.31		
					0.45		
					0.51		
					0.45		
					0.39		
					0.31		
					0.45		
					0.51		
					0.45		
					0.39		
					0.31		
					0.45		
					0.51		
					0.45		
					0.39		
					0.31		
					0.45		
					0.51		
					0.45		
					0.39		
					0.31		
					0.45		
					0.51		
					0.45		
					0.39		
					0.31		
					0.45		
					0.51		
					0.45		
					0.39		



Tagg's charts.<sup>7</sup> From this table the depth-resistivity factor curves are traced (Fig. 2), which show that the convergence of the curves is not definite. This is due to the fact that, even for small electrode spacings on the ground, the influence of the lower medium is not negligible. However, the coordinates of the center of gravity of the converging

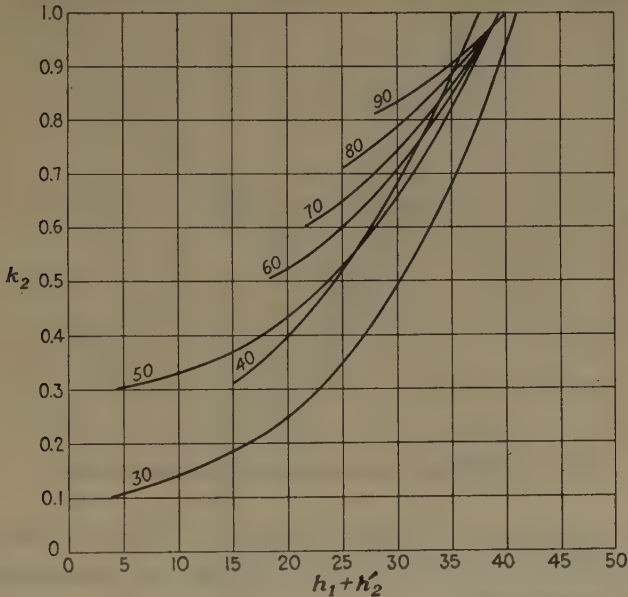


FIG. 3.—DEPTH-RESISTIVITY FACTOR, CURVES OF LOWER PART.

area are  $k_1 = 0.48$  and  $h_1 = 9.8$ , whereas the assumed value of  $h_1$  is 10 and of  $k_1$  is  $\frac{300 - 100}{300 + 100} = 0.5$ .

In step 4, we estimate the depth to the third layer as being  $h_1 + h_2 = 40$  ft. The equivalent resistivity  $\rho_1'$  of the upper two layers in parallel is given by:

$$\frac{40}{\rho_1'} = \frac{10}{100} + \frac{30}{300}$$

and  $\rho_1' = 200$  foot-ohms. By applying Tagg's method to the lower part of the resistivity curve, using  $\rho_1'$  as the resistivity of the surface formations, Table 2 is obtained.

The curves of depth-resistivity factor are plotted from Table 2 in Fig. 3. For electrode spacings of 50 to 90 ft., a very good convergence is obtained at the point where coordinates are  $h_1 + h_2' = 39$  ft. and  $k_2 = 0.96$ , which are practically the theoretical values assumed for the mathematical computation of the curve. For the electrode spacing 30 and

<sup>7</sup> Reference of footnote 3.

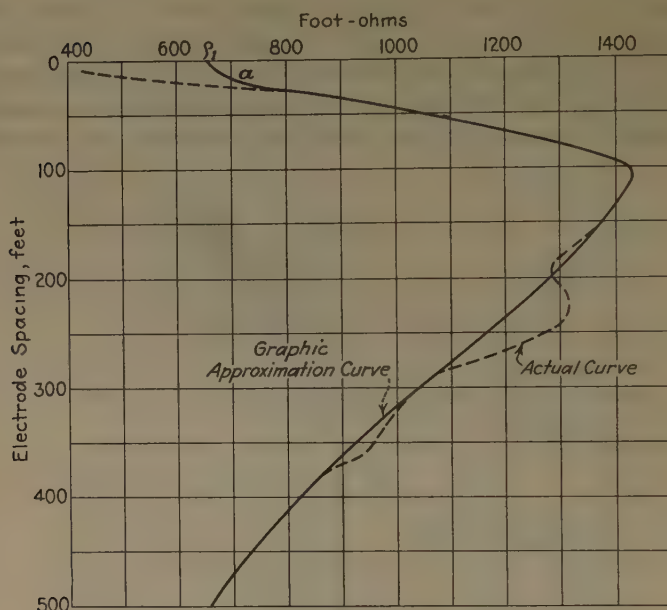


FIG. 4.—CURVE OF RESISTIVITY-ELECTRODE SPACING.

40, no convergence of the curves is obtained, which indicates that for such spacings the upper layers have an effect on the apparent resistivity that cannot be neglected.

A practical example worked from an actual resistivity curve follows: The problem is one of water-table determination, which was worked

TABLE 3

$\alpha$	10	20	40	60	80	100
$\rho_1/\rho_0$	0.982	0.920	0.718	0.582	0.505	0.463
$k_1$	$\frac{h_1}{a}$	$h_1$	$\frac{h_1}{a}$	$h_1$	$\frac{h_1}{a}$	$h_1$
0.1	0.576	15.2	0.228	9.5		
0.2	0.920	18.4	0.450	18.0	0.156	9.3
0.3	1.17	23.4	0.588	23.5	0.331	19.9
0.4	1.33	26.6	0.709	28.3	0.436	26.1
0.5	1.51	30.2	0.799	31.9	0.540	32.4
0.6	1.625	32.5	0.889	35.6	0.621	36.6
0.7	1.765	35.5	0.969	38.7	0.700	42.0
0.8	1.835	36.7	1.039	41.5	0.770	46.0
0.9	1.095	38.1	1.118	44.8	0.834	50.0
1.0	2.00	40.0				

by Tattam.<sup>8</sup> It is a typical three-layer curve (Fig. 4) with some irregularities of the order of the error of observations expected with the equipment in use. Therefore they are smoothed out before calculations are made. The observations were taken in an area underlain by valley fill at about two miles from two wells that encountered water at 271 ft. Consequently the cone of exhaustion was not expected to have an appreciable effect in the area where the measurements were taken.

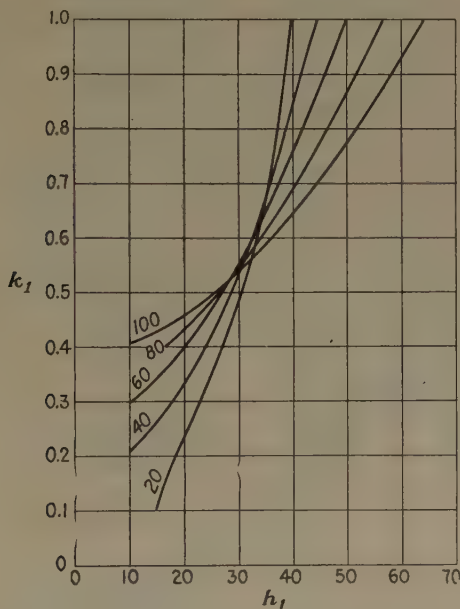


FIG. 5.—DEPTH-RESISTIVITY FACTOR, CURVES OF UPPER PART.

According to the method developed here, the three first values of the resistivities are averaged, which gives  $\frac{1}{3}(428 + 611 + 932) = \rho_1 = 657$  foot-ohms for the resistivity of the top layer. The graphic approximation curve *a* is then traced, meeting the original curve tangentially. This curve is used to determine the thickness of the upper layer by the application of Tagg's method, which gives the figures of Table 3. The curves of depth-resistivity factor plotted from Table 3 on Fig. 5 converge in a small area, consequently the depth determination to the second layer may be considered good.  $h_1 = 33$  ft. and  $k_1 = 0.6$ ; thus the value of the resistivity of the second layer is

$$\rho_2 = \rho_1 \frac{1 + k_1}{1 - k_1} = 2630 \text{ foot-ohms.}$$

<sup>8</sup> Reference of footnote 5, curve 26.





By making use of the inflection point on the lower part of the curve situated approximately at the electrode spacing 300 ft., the total thickness of the two top layers is estimated at

$$h_1 + h_2 = \frac{2}{3} 300 = 200 \text{ ft.}$$

Thus

$$h_2 = 200 - 33 = 167 \text{ ft.}$$

The equivalent resistivity of the two upper layers in parallel is then given by

$$\frac{200}{\rho_1'} = \frac{33}{657} + \frac{167}{2630}$$

and  $\rho_1' = 1755$  foot-ohms. By the application of Tagg's method to the lower part of the curve, Table 4 is obtained.

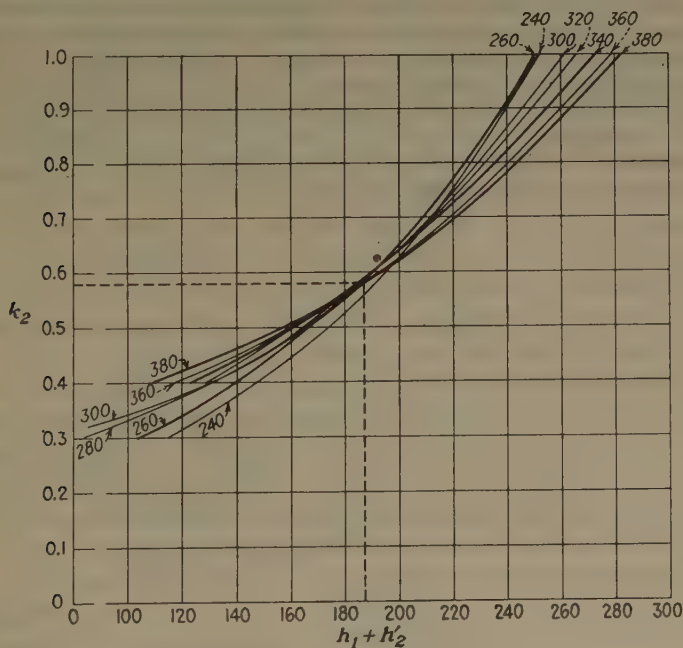


FIG. 6.—DEPTH-RESISTIVITY FACTOR, CURVES OF LOWER PART.

The curves of depth-resistivity factor computed from Table 4 give a good area of convergence (Fig. 6) for which the coordinates are  $h_1 + h_2' = 187$  ft. and  $k_2 = 0.58$ . The value of the resistivity of the lower medium is obtained by  $\rho_3 = 1755 \times \frac{0.42}{1.58} = 467$  foot-ohms. If a better approximation for the depth to the third layer is desired the process may be repeated using 187 ft. instead of 200 for the calculation

of the equivalent resistivity of the upper two layers. In general, however, one determination gives a close enough approximation.<sup>9</sup>

### CONCLUSIONS

The present method of interpretation offers a means of solving a three-layer resistivity curve, the thicknesses and resistivities of the individual layers being obtained. The isotropy or equal anisotropy of the individual layers is a necessary condition for the applicability of this method. An acceptable probable error of 5 to 10 per cent can be expected in isotropic conditions. Corrections must be made when the ground is anisotropic. In particular, evidences of non-equal anisotropy of the individual layers will be indicated by the absence of a satisfactory area of convergence of the curves of depth-resistivity factor.

---

<sup>9</sup> Since this writing, the author has studied the cases of equal and different anisotropies in the sedimentary formations. Theoretical resistivity-depth curves have been computed for varying anisotropy coefficients. By superposition with the curve of Fig. 4, the anisotropy coefficient was estimated to be 2. The theory shows that the method described here is still applicable in cases of equal anisotropy coefficients and that the depths obtained must be multiplied by the square root of the anisotropy coefficient. Consequently the depth to the water table, as given by the present method, is  $187 \times \sqrt{2} = 264$  ft. This theory will appear in the *Transactions* of the American Association of Petroleum Geophysicists.

# Some Observations Concerning Electrical Measurements in Anisotropic Media, and Their Interpretation

By C. AND M. SCHLUMBERGER AND E. G. LEONARDON\*

(New York Meeting, February, 1933)

IN the search for practical geological problems amenable to solution by the potential methods, the geophysicist is led to study mathematically various theoretical cases. In these idealistic discussions, the media under consideration are generally supposed to be homogeneous and isotropic. The geophysicist, of course, realizes perfectly that these conditions do not occur in their entirety in reality. However, the assumptions made are justified, because very often they are necessary in order to render possible an exhaustive study of a given problem, which otherwise would be too complicated, and would not lend itself to a complete mathematical analysis.

Of the above two assumptions, that concerning the homogeneity of a given geological formation is satisfactorily realized except in so far as isotropy is concerned, since this property is not often encountered in practice. As a consequence, it is very desirable for the geophysicist to have quite an extensive knowledge of the properties of anisotropic formations, and of the laws that govern the propagation of electric current therein. With such principles in mind, he will be able to decide whether the conclusions arrived at in simple, isotropic conditions are still correct in more complex cases, or in what way they must be modified or adapted in order to constitute a sound basis for the interpretation of the results obtained in anisotropic media.

On the other hand, the fact that in anisotropic formations the mobility of the ions is greater along the strike than perpendicular thereto can be utilized for determining the direction of the dip by induction measurements.

We therefore propose to study in three successive chapters the following points:

1. Propagation of the electric current in anisotropic media.
2. Some consequences of the anisotropy of geological formations with reference to the surface electrical measurements, and their interpretation.
3. Determination of the direction of the dip of anisotropic formations by surface induction measurements.

---

\* Compagnie Générale de Géophysique, Paris, and Schlumberger Electrical Prospecting Methods, New York.

## PROPAGATION OF ELECTRIC CURRENT IN ANISOTROPIC MEDIA

It is a well-known fact that in stratified rocks the strike offers a particularly favorable path for the propagation of electric current. The reason for this property is that a great number of mineral crystals possess a flat or elongated shape (mica, kaolin, etc.). At the time of their precipitation, they naturally took an orientation parallel to the sedimentation. The fissures in the rocks are, therefore, parallel to the strike, and it is along these fissures, which are saturated with imbibed water, that the electric current travels with the greatest facility.<sup>1</sup> Such rocks, therefore, do not possess the same conductivity in all directions. They are anisotropic.

*Coefficient of Anisotropy*

For a clearer comprehension of the phenomenon of the propagation of current in anisotropic media, we propose to discuss the simple and idealistic case of a terrain composed of two thin, homogeneous, isotropic layers 1 and 2, the respective thicknesses and resistivities of which are  $h_1$  and  $h_2$ , and  $r_1$  and  $r_2$ .

Along the strike, the resistivity  $r_t$  of this formation will be given by:<sup>2</sup>

$$\frac{h_1 + h_2}{r_t} = \frac{h_1}{r_1} + \frac{h_2}{r_2} \quad [1]$$

In the same way, the resistivity characterizing the propagation of current perpendicular to the direction of the beds  $r_i$ , will be given by the formula:<sup>3</sup>

$$r_i(h_1 + h_2) = r_1h_1 + r_2h_2 \quad [2]$$

The ratio  $\frac{r_t}{r_i}$  characterizes the fact that the medium conducts the current along the strike better than perpendicular to it. The coefficient:

$$\lambda = \sqrt{\frac{r_t}{r_i}}$$

which gives an idea of this property, is called the coefficient of anisotropy. If

$$\frac{h_1}{h_2} = e; \frac{r_1}{r_2} = m$$

<sup>1</sup> In certain instances, the direction of fissility is a consequence of mechanical stress due to tectonic movements which occurred a long time after deposition of the sediments, and is not coincident with the strike of the formations. This is especially the case with metamorphosed shales and slates.

<sup>2</sup> Application of Kirchhoff's law to conductors connected in parallel.

<sup>3</sup> Application of Kirchhoff's law to conductors connected in series.



the value of  $\frac{r_t}{r_l}$  can be drawn from equations 1 and 2, as follows:

$$\frac{r_t}{r_l} = \lambda^2 = \frac{1}{(1+e)^2} \frac{(e+m)(1+em)}{m} \quad [3]$$

It is interesting to remark that the value of  $\lambda$  is not modified when  $e$  is replaced by  $\frac{1}{e}$ . It is thus possible to interchange the thicknesses of the layers 1 and 2 without modifying the coefficient of anisotropy of the medium under consideration. This result has already been indicated by one of the authors.<sup>4</sup>

In the particular instance where  $h_1 = h_2$ , the following simple expression is obtained:

$$\lambda = \frac{1}{2} \frac{1+m}{\sqrt{m}} \quad [4]$$

This formula is evidently correct for a series of infinitely thin alternating layers, and makes it possible to get an idea of the order of magnitude of  $\lambda$  for various values of the ratio  $\frac{r_1}{r_2}$ . These values are shown in Table 1.

TABLE 1.—Values of Ratio  $r_1/r_2$

Values of $\frac{r_1}{r_2}$	$\lambda$	Observations
2	1.06	Low anisotropy.
4	1.25	Anisotropy frequently observed in common rocks.
10	1.74	High anisotropy, still frequently encountered.
20	2.35	Very high anisotropy; unusual.

#### *Average Resistivity*

In addition to the longitudinal and transversal resistivities, it is useful to consider the mean square root of their product, which is called the average resistivity of the anisotropic medium  $r_m$  as follows:

$$r_m = \sqrt{r_l r_t} \quad [5]$$

Between  $\lambda$ ,  $r_l$ ,  $r_t$  and  $r_m$ , there exist the following relations:

$$r_m = \lambda r_l = \frac{1}{\lambda} r_t \quad [6]$$

#### *Path of the Current in an Anisotropic Medium*

We now propose to study how the current travels in an anisotropic medium, and we will first discuss the simple case of a parallel current.

<sup>4</sup> C. Schlumberger: Étude sur la Prospection Électrique du Sous-sol. Gauthier-Villars, Paris, 1920. Reprinted in 1930.

Suppose that this current makes an angle  $\alpha_1$  with the direction of the beds in the medium 1, and that it is refracted in the medium 2, making an angle  $\alpha_2$  with the same direction (Fig. 1). As is known, between the angles  $\alpha_1$  and  $\alpha_2$ , there exists the relation:

$$\frac{\tan \alpha_1}{\tan \alpha_2} = \frac{r_1}{r_2} \quad [7]$$

If the layers become infinitely thin, maintaining, however, the ratio  $\frac{h_1}{h_2}$  between their thicknesses, the direction of the current will finally be  $AC$ , at an angle  $C$  to the strike. Between  $C$ ,  $\alpha_1$  and  $\alpha_2$  there is the relation:

$$\frac{h_1 + h_2}{\tan C} = \frac{h_1}{\tan \alpha_1} + \frac{h_2}{\tan \alpha_2} \quad [8]$$

In each medium, the equipotential surfaces are perpendicular to the direction of the lines of current. The surface passing through  $A$  is per-

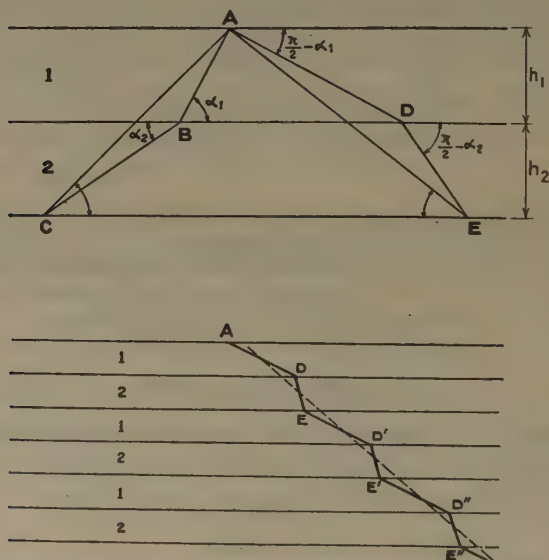


FIG. 1.—PROPAGATION OF A PARALLEL CURRENT IN A MEDIUM CONSTITUTED OF TWO LAYERS.

pendicular to  $AB$ . It is shown as  $AD$  in medium 1, and prolonged as  $DE$  in medium 2. The direction  $DE$  is perpendicular to  $BC$ . When the layers become infinitely thin, the equipotential surface finally makes an angle  $E$  with the strike, and between  $E$ ,  $\alpha_1$  and  $\alpha_2$  there is the relation:

$$\frac{h_1 + h_2}{\tan E} = h_1 \tan \alpha_1 + h_2 \tan \alpha_2 \quad [9]$$

From equations 8 and 9 we deduce:

$$\frac{1}{\tan C \tan E} = \frac{1}{(h_1 + h_2)^2} (h_1 \tan \alpha_1 + h_2 \tan \alpha_2) \left( \frac{h_1}{\tan \alpha_1} + \frac{h_2}{\tan \alpha_2} \right)$$
and, taking into consideration equation 7 we easily obtain:

$$\frac{1}{\tan C \tan E} = \frac{r_t}{r_i} = \lambda^2 \quad [10]$$

which may also be written:

$$\tan E - \frac{1}{\lambda^2} \times \frac{1}{\tan C} = 0 \quad [11]$$

Consequently, the equipotential surfaces are no longer perpendicular to the lines of current. Such a proposition would be true only if the condition of perpendicularity

$$1 + \tan C \tan (\pi - E) = 0 \quad [12]$$

were realized, a condition that necessitates  $\lambda = 1$  (isotropic medium).

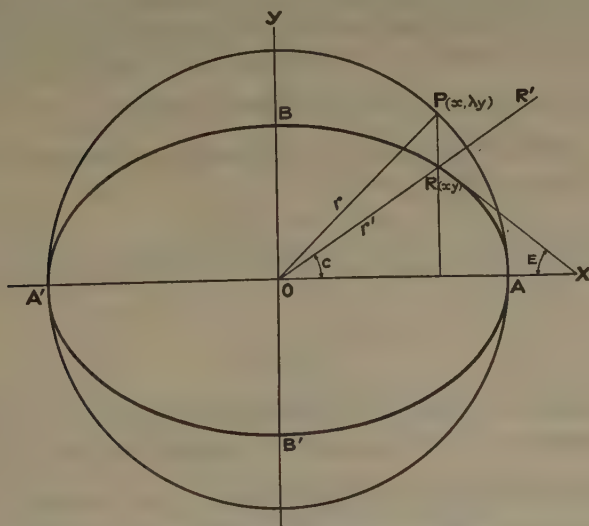


FIG. 2.—PROPAGATION OF AN ELECTRIC CURRENT SENT FROM A PUNCTUAL SOURCE INTO AN ANISOTROPIC MEDIUM.

In the case of a punctual source of current  $O$ , the lines of current are straight lines passing through  $O$  (Fig. 2). This proposition is evident, by reason of similitude. The picture of the electric field is necessarily independent of the scale. The direction of the current at two points  $R$  and  $R'$ , located on the same radius  $OR$ , is therefore the same, and must pass through  $O$ .

Also, by reason of symmetry, the equipotential surfaces are surfaces of revolution around an axis  $OY$  perpendicular to the strike.

This being admitted, let us take two axes of coordinates  $OX$  and  $OY$ , passing through the source of current and respectively parallel and per-

pendicular to the stratification, and let us determine the shape of an equipotential curve located in the plane of the figure. In this plane, we have:

$$\tan C = \frac{y}{x} \quad \tan E = -\frac{dy}{dx} \quad [13]$$

which necessitates for the equipotential curves located in the plane of the figure the differential relation:

$$\tan C \times \tan E = -\frac{ydy}{x dx} = \frac{1}{\lambda^2} \quad [14]$$

As is known, this relation, which may be written

$$d(x)^2 + d(\lambda y)^2 = 0$$

corresponds to a family of ellipses,

$$x^2 + \lambda^2 y^2 - M^2 = 0 \quad [15]$$

the greater axis of which is parallel to the strata. The equipotential surfaces are flattened ellipsoids of revolution around the axis  $OY$  perpendicular to the strike. If we make  $a = OA$  and  $b = OB$ , the great and the small semi-axes of such an ellipsoid, the ratio  $\frac{a}{b}$  is equal to  $\lambda$ .

If  $\lambda = 1$  (isotropic medium), the above ellipses become circles represented by the equation:

$$M = \sqrt{x^2 + y^2} \quad [16]$$

In such a case the equipotential curves in the plane of the figure are given by

$$V = \frac{K}{\sqrt{x^2 + y^2}} \quad [17]$$

$K$  being a constant factor and  $V$  the potential function in the medium under consideration. By comparing equations 16 and 17, we come to the assumption that  $M$  is of the form  $\frac{K}{V}$ . As a matter of fact, this coefficient is equal<sup>5</sup> to the product of the average resistivity  $r_m$ , by the emissivity  $Q$  of the source  $O$ . If  $I$  is the intensity of the current, this emissivity is equal to  $\frac{I}{4\pi}$  or  $\frac{I}{2\pi}$ , according to whether the source is situated in a limitless medium or at the surface of a medium limited by a plane.

<sup>5</sup> R. Maillet and H. G. Doll: Sur un théorème relatif aux milieux électriquement anisotropes, et ses applications à la prospection électrique en courant continu. *Ergänzungshefte für angewandte Geophysik* (1932) 3, 1. In this paper the reader will find very interesting and complete considerations on the propagation of the current in anisotropic media, based on tensorial calculus. In their discussion, these authors make use of a coefficient of anisotropy smaller than unity and which is the reciprocal value of the coefficient adopted by us.



The equipotential ellipses in the plane of Fig. 2 are thus finally represented by:

$$V = Qr_m \frac{1}{\sqrt{x^2 + \lambda^2 y^2}} \quad [18]$$

Let us consider the circle centered on  $O$ , and with a radius  $OA$ . If, on this circle, we take the point  $P$ , which possesses the same abscissa as  $R$ , and if we write  $OP = r$ , we see that the potential of point  $R$  can be expressed by:

$$v = Qr_m \frac{1}{r} \quad [19]$$

Thus, the potential of a given point  $R$  on the equipotential ellipsoid can be deduced by compression from the equipotential sphere, whose radius is  $OA$ , such sphere being supposedly located in an isotropic medium whose resistivity is  $r_m$ .

If we call  $\Delta_x$  and  $\Delta_y$  the components of the intensity at a given point, we know, since the axes of coordinates are parallel to the principal directions of the ellipsoid, that we can write:

$$\Delta_x = -\frac{1}{r_i} \times \frac{dV}{dx} = \frac{Qr_m}{r_i} \frac{x}{(x^2 + \lambda^2 y^2)^{3/2}} \quad [20]$$

$$\Delta_y = -\frac{1}{r_t} \times \frac{dV}{dy} = \frac{Qr_m}{r_t} \frac{\lambda^2 y}{(x^2 + \lambda^2 y^2)^{3/2}} \quad [21]$$

From which may be deduced the intensity of the current at a given point:

$$\Delta = (\Delta_x^2 + \Delta_y^2)^{1/2} = \frac{Qr_m}{(x^2 + \lambda^2 y^2)^{3/2}} \cdot \left( \frac{x^2}{r_i^2} + \frac{\lambda^4 y^2}{r_t^2} \right)^{1/2} \quad [22]$$

and remarking that:

$$\frac{r_t}{r_i} = \lambda^2; \text{ and } \frac{r_m}{r_i} = \frac{r_t}{r_m} = \lambda$$

we obtain:

$$\Delta = \lambda Q \frac{(x^2 + y^2)^{1/2}}{(x^2 + \lambda^2 y^2)^{3/2}} = Q \lambda \frac{r'}{r^3} \quad [23]$$

where  $r$  and  $r'$  are the lengths  $OP$  and  $OR$ .

### *Measurement of the Anisotropy of Rocks in the Laboratory*

It will often be useful to obtain an idea of the anisotropy of rocks by measurements performed in the laboratory. Such a determination will be easy if a sample of sound rock is available, and if it is possible to experiment upon it by utilizing faces approximately parallel and perpendicular to the direction of the beds. It is, of course, necessary that the sample should have kept its water of imbibition.

With two electrodes  $E$  and  $E'$ , good contacts may be made on two parallel faces. By means of a battery  $B$ , a current is sent through the

sample, as shown in Fig. 3. In order that the current flowing from  $E$  may be approximately parallel, a circular electrode  $GG'$  is arranged around  $E$ . The intensity  $I$  of the current passing through  $E$  is measured with an ammeter  $A$ . If  $V$  is the electromotive force of the battery  $B$ , and  $R$  the resistance of the circuit,

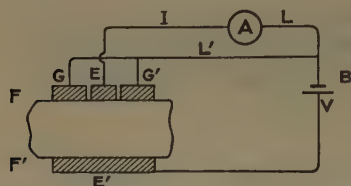


FIG. 3.—MEASUREMENT OF THE RESISTIVITY OF A ROCK SAMPLE.

$$R = \frac{V}{I}$$

The quantity  $R$  represents approximately the resistance of the rock, since the interior resistance of the battery, the resistance of the ammeter and connections are negligible in comparison with the resistance of the rock. Should this not be the case, there would be no special difficulty in measuring directly the difference of potential  $V'$  between  $E$  and  $E'$ , which would be substituted for  $V$  in the computation of  $R$ .

Let us call  $r$  the specific resistance of the rock,  $l$  the distance between the faces  $F$  and  $F'$ , and  $S$  the surface of the electrode  $E$ . Then

$$r = R \frac{S}{l}$$

Two measurements performed on the sample, with the current flowing successively parallel and perpendicular to the strike, will furnish approximate data, from which can be computed the anisotropy of the sample.

Another method of measuring the anisotropy of a sample consists in tracing, in a plane section perpendicular to the strike, a small equipotential ellipse around a punctual source of current. Thus, the ratio of the great to the small axis of the ellipse will be known, and, with it, the value of  $\lambda^2$ .

As already stated, the coefficients of anisotropy commonly encountered vary from 1 to 2.5, roughly. The figures near unity are given by unconsolidated rocks (sands in particular), or rocks made up of slightly differentiated, elementary layers. Compact rocks, or rocks that show either a good fissility or quite large variations in conductivity between their elementary layers (schists, for instance), give, on the other hand, fairly high figures.

### *Macroscopic Anisotropy*

The anisotropy previously studied characterizes finely stratified rocks with a homogeneous appearance to the naked eye, and, in fact, a real homogeneity of constitution in numerous cases. This anisotropy might be called "microscopic." In electrical prospecting, which takes in considerable volumes of ground, it is necessary to consider a second

kind of anisotropy, which we propose to call "macroscopic." This anisotropy is caused by the fact that the terrain is generally constituted of a succession of homogeneous, parallel layers, with distinct electrical characteristics. These layers are no longer infinitely thin, as in the case discussed before, but may possess important thicknesses.

If there are only two kinds of layers, with definite thicknesses and resistivities, alternating regularly, the considerations developed above will still be correct. There will exist a longitudinal and a transversal conductivity, as well as a coefficient of anisotropy.

If the current is sent into such a medium by means of a punctual earth, the equipotential surfaces, provided they possess a sufficient size in comparison with the thickness of the layers, will have an ellipsoidal shape. We are leaving out, of course, the question of the successive refractions occurring at the contacts of the alternating layers.

It is evident, however, that in practice cases differing widely from this ideal example will be encountered. Consider, for instance, a geological complex made up of horizontal, isotropic layers, alternately conductive and resistant. The profile representing the resistivities of several neighboring beds, in terms of their depth, will oscillate in a sawtooth manner. In such a medium, the equipotential surfaces will no longer be ellipsoids. They will, however, remain surfaces of revolution around an axis perpendicular to the stratification, but in certain instances their shape will be so different from that obtaining in ellipsoidal propagation that it will be well-nigh impossible to consider a coefficient of anisotropy, since the definitions previously given will be meaningless.

However, in order to give numerical expression to the fact that the current flows differently along the strike than at right angles thereto, it will be useful to continue utilizing the concept of the ellipsoidal propagation, in all cases where such a propagation will be approximately correct.

This pseudo-ellipsoidal propagation will be realized in a satisfactory way in alternating layers possessing thicknesses of the same order of magnitude, and resistivities fluctuating around an average figure. If  $L_1 \dots L_n$  represents these layers,  $h_1 \dots h_n$  their thicknesses and  $r_1 \dots r_n$  their resistivities, the transversal and longitudinal average resistivities will be given by the two following equations:

$$r_t(h_1 + \dots + h_n) = r_1 h_1 + \dots + r_n h_n \quad [24]$$

$$\frac{h_1 + \dots + h_n}{r_t} = \frac{h_1}{r_1} + \dots + \frac{h_n}{r_n} \quad [25]$$

from which the pseudo coefficient of macroscopic anisotropy will be obtained.

Electrical coring, which measures the resistivities of the various layers traversed in the uncased part of a drill hole, furnishes a good means

of estimating roughly the macroscopic anisotropy of a large thickness of stratified sediments.

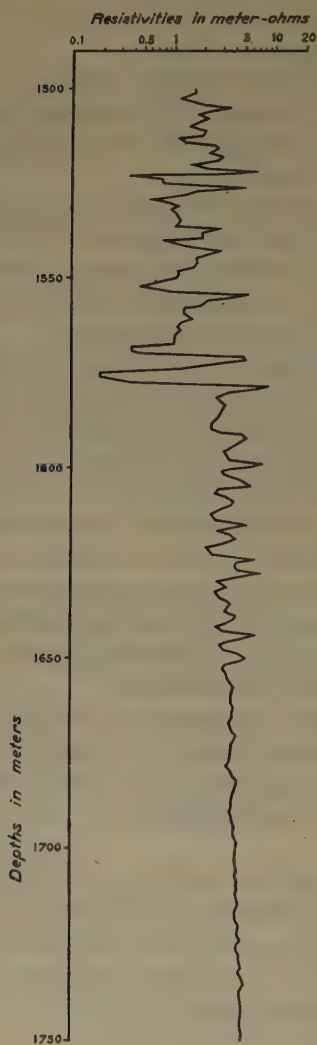


FIG. 4.—RESISTIVITY DIAGRAM TAKEN IN DRILL HOLE NO. 1803 OF THE STEAUA ROMANA, AT PODENI NOI, RUMANIA.

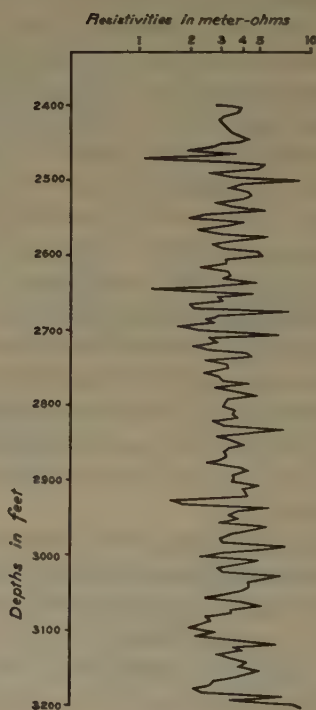


FIG. 5.—RESISTIVITY DIAGRAM TAKEN IN WELL MACKEY NO. 1, IN THE OKLAHOMA CITY POOL.

The resistivity figures measured in a drill hole are represented on diagrams, in which they are carried as abscissas against the depths in ordinates. If such a diagram is available, the detailed succession of



the beds constituting the geological column, together with their electrical resistivities, is known.

By means of formulas 24 and 25, it will be possible therefore to compute the longitudinal and transversal resistivity, as well as the anisotropy of the whole terrain.

Fig. 4 represents a part of the resistivity diagram obtained at Podeni Noi (Rumania), in hole 1803 of the Steaua Romana company. The average transversal and longitudinal resistivities between the depths 1580 and 1650 meters are 3.74 and 4.25 ohms respectively, which gives for the coefficient of macroscopic anisotropy:

$$\lambda_M = 1.07$$

Fig. 5 refers to Mackey No. 1 well of the Oklahoma City pool. Between the depths 2500 and 3000 ft., the longitudinal and transversal resistivity are respectively 3.75 and 3.17, showing that the Pennsylvanian formations under consideration possess a macroscopic anisotropy of 1.1.

### *Total Anisotropy*

We are now in a position to elucidate the following problem. Consider a succession of parallel, anisotropic layers possessing thicknesses equal to  $h_1 \dots h_n$ , average resistivities equal to  $r_1 \dots r_n$ , and coefficients of anisotropy  $\lambda_1 \dots \lambda_n$ . Does a coefficient of anisotropy exist for the whole terrain? Such an anisotropy, if it exists, might justly be called "total anisotropy."

Consider the simple case of two anisotropic layers<sup>6</sup> with thicknesses  $h_1$  and  $h_2$ , average resistivities  $r_1$  and  $r_2$ , and coefficient of anisotropy  $\lambda_1$  and  $\lambda_2$ . Parallel to the strata the longitudinal resistivity is defined by:

$$\frac{h_1 + h_2}{r_l} = \frac{h_1 \lambda_1}{r_1} + \frac{h_2 \lambda_2}{r_2} \quad [26]$$

Perpendicular to the strata the transversal resistivity furnishes the following equation:

$$(h_1 + h_2)r_t = h_1 r_1 \lambda_1 + h_2 r_2 \lambda_2 \quad [27]$$

Multiplying equations 26 and 27 gives:

$$\begin{aligned} (h_1 + h_2)^2 \frac{r_t}{r_l} &= \left( \frac{h_1 \lambda_1}{r_1} + \frac{h_2 \lambda_2}{r_2} \right) (h_1 r_1 \lambda_1 + h_2 r_2 \lambda_2) \\ &= \lambda_1^2 h_1^2 + \lambda_2^2 h_2^2 + \lambda_1 \lambda_2 h_1 h_2 \left( \frac{r_1}{r_2} + \frac{r_2}{r_1} \right) \end{aligned}$$

From this may be deduced the total anisotropy  $\Lambda$  of the medium under consideration:

<sup>6</sup> The following demonstration has been furnished by Mr. R. Maillet, General Manager of the Compagnie Générale de Géophysique. Paris.

$$\Lambda^2 = \frac{r_i}{r_l} = \lambda_1^2 \frac{h_1^2}{(h_1 + h_2)^2} + \lambda_2^2 \frac{h_2^2}{(h_1 + h_2)^2} + \lambda_1 \lambda_2 \frac{h_1 h_2}{(h_1 + h_2)^2} \left( \frac{r_2}{r_1} + \frac{r_1}{r_2} \right) \quad [28]$$

If  $\lambda_1 = \lambda_2$  this expression becomes simpler:

$$\Lambda^2 = \lambda_1^2 \left[ \frac{h_1^2 + h_2^2}{(h_1 + h_2)^2} + \frac{h_1 h_2}{(h_1 + h_2)^2} \left( \frac{r_1}{r_2} + \frac{r_2}{r_1} \right) \right] \quad [29]$$

Writing  $\frac{h_1}{h_2} = e$  and  $\frac{r_1}{r_2} = m$

gives

$$\Lambda^2 = \lambda_1^2 \frac{1}{(1 + e)^2} \times \frac{1}{m} (1 + m)(e + m) \quad [30]$$

In the expression following  $\lambda_1^2$ , we recognize the second member of equation 3, which gives the value of the coefficient of anisotropy of two layers in terms of the ratios of the thicknesses and of the resistivities. Therefore the total anisotropy is represented by

$$\Lambda = \lambda_1 \lambda_M \quad [31]$$

which shows that the total anisotropy is the product of the microscopic by the macroscopic anisotropy.

This proposition, however, is not true in the general case. All that can be said is that the total anisotropy is appreciably greater than the macroscopic anisotropy, owing to the individual anisotropy of the different layers. In many instances, to obtain an idea of the total anisotropy, it will be quite reasonable to multiply the macroscopic anisotropy by 1.2 or 1.3.

### *Measurement of Total Anisotropy of a Formation by Tracing Surface Equipotential Curves*

If a current is caused to flow into tilted, stratified ground at a point  $O$  at the surface, and if the second electrode is located at a great distance from  $O$ , the equipotential surfaces are flattened ellipsoids of revolution around an axis  $OR$  perpendicular to the stratification. Fig. 6 shows the cross-section of one of these ellipsoids, by a vertical plane perpendicular to the stratification and passing through  $O$ . The semi-axes of the ellipsoid are equal to  $OA$  and  $OR$ , and the coefficient of anisotropy is equal to  $\frac{OA}{OR}$ . Tracing at the surface an equipotential ellipse, its minor axis will be  $BB'$  and its major semi-axis perpendicular to the plane of the figure will be equal to  $OA$ . Let us call  $\alpha$  the dip of the formations, and  $OA = a$ ;  $OC = b$ , the semi-axes of the ellipsoid. If we consider the sphere with radius  $OA$  centered on  $O$ , we know that we pass from this sphere to the equipotential ellipsoid by compressing the ordinates, with reference to the plane parallel to the strike passing through  $O$ , in the ratio:

$$\frac{OC}{OD} = \frac{BH}{EH} = \frac{1}{\lambda}$$

On the other hand, if we call  $c$  the length  $OB$ , we have:

$$BH = c \sin \alpha$$

$$EH = \sqrt{OE^2 - OH^2} = \sqrt{a^2 - c^2 \cos^2 \alpha}$$

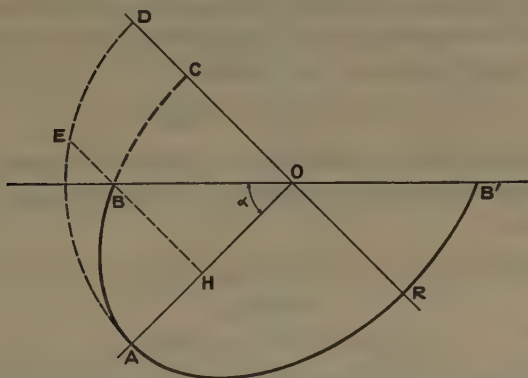


FIG. 6.—EQUIPOTENTIAL ELLIPSOID IN AN ANISOTROPIC, TILTED FORMATION.

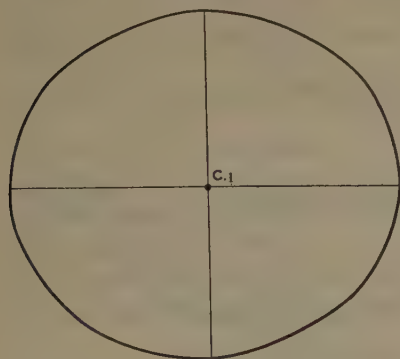


FIG. 7.—SURFACE EQUIPOTENTIAL CURVE TRACED ON THE MIDDLE LEVANTIN FORMATION AT CAMPINA, RUMANIA. ELLIPTICITY AT THE SURFACE, 1.12; DIP, 40°;  $\lambda = 1.25$ .

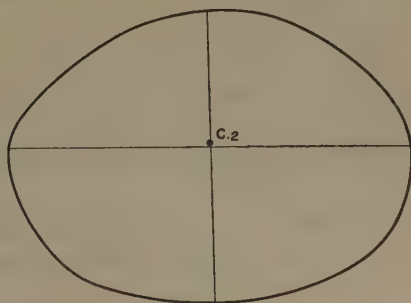


FIG. 8.—SURFACE EQUIPOTENTIAL CURVE TRACED ON THE MIDDLE DACIAN FORMATION AT CAMPINA, RUMANIA. ELLIPTICITY AT THE SURFACE, 1.35; DIP, 40°;  $\lambda = 1.65$ .

therefore:

$$\lambda = \frac{EH}{BH} = \frac{\sqrt{a^2 - c^2 \cos^2 \alpha}}{c \sin \alpha} \quad [32]$$

If  $\mu = \frac{a}{c}$ , the ellipticity of the surface equipotential curve:

$$\lambda = \frac{\sqrt{\mu^2 - \cos^2 \alpha}}{\sin \alpha} \quad [33]$$

The values of  $\lambda$  in terms of  $\mu$  and  $\alpha$  can be easily represented on a diagram, if so desired.

To illustrate the above method of determining the coefficient of anisotropy, Figs. 7, 8 and 9 show three determinations made in the neighborhood of Campina, Rumania, on three different Tertiary formations. The conclusions arrived at are summarized under the figures.

Formula 33 can also be used to get an idea of the ellipticity of the curves traced at the surface of an anisotropic formation tilted at a given angle. From equation 33 may be deduced:

$$\mu = \sqrt{\cos^2 \alpha + \lambda^2 \sin^2 \alpha} \quad [34]$$

if  $\lambda = 1.2$ , and  $\alpha = 20^\circ$ , we find  $\mu = 1.1$ . Such an ellipticity is already sufficiently great to be easily measured at the surface by tracing equipotential curves.

#### SOME CONSEQUENCES OF ELECTRICAL PROSPECTING BY POTENTIAL METHODS

##### *Paradox of the Anisotropy*

We will suppose that we are dealing with a stratified vertical formation. The equipotential curves (Fig. 10) around a punctual earth  $O$

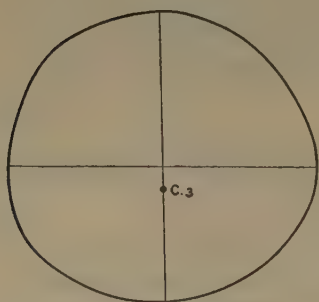


FIG. 9.

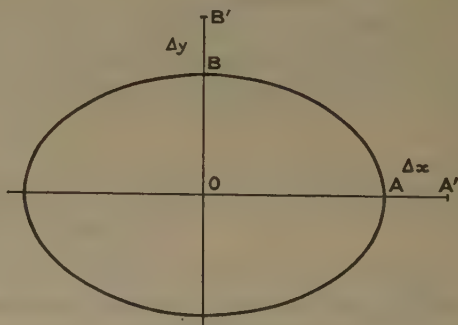


FIG. 10.

FIG. 9.—SURFACE EQUIPOTENTIAL CURVE TRACED ON THE UPPER PONTIAN FORMATION, CAMPINA, RUMANIA. ELLIPTICITY AT THE SURFACE, 1.05; DIP,  $45^\circ$ ;  $\lambda = 1.1$ .

FIG. 10.—EQUIPOTENTIAL ELLIPSE TRACED AT THE SURFACE OVER A VERTICAL, ANISOTROPIC FORMATION.

are ellipses whose semi-axes  $OA$  and  $OB$  are in the ratio

$$\frac{OA}{OB} = \lambda = \sqrt{\frac{r_t}{r_l}}$$

In the direction  $OA$  the difference of potential  $\Delta V$  between two points  $AA'$ , located at a distance  $\Delta x$  apart is:

$$\Delta V = -Qr_m \frac{x\Delta x}{x^3} = -Qr_m \frac{\Delta x}{x^2}$$



In an isotropic medium, under such conditions the apparent resistivity is computed by the formula:

$$r = \frac{1}{Q} \times \frac{\Delta V}{\Delta x} x^2$$

Therefore we obtain, in the direction of the strike, an apparent resistivity  $r_{at}$ , equal to the average resistivity  $r_m$ :

$$r_{at} = r_m = \lambda r_l$$

Along the axis  $OY$ , in the same way:

$$\Delta V = -Q r_m \times \frac{\lambda^2 y \Delta y}{\lambda^3 y^3} = -Q r_m \frac{\Delta y}{\lambda y^2}$$

But if the resistivities are computed by means of the formula for homogeneous isotropic media, we obtain a value of the resistivity  $r_{at}$ , equal to:

$$r_{at} = \frac{1}{Q} \times \frac{\Delta V}{\Delta y} y^2 = \frac{r_m}{\lambda} = r_l$$

Thus, the formula of the isotropic, homogeneous media, applied to anisotropic formations, gives resistivity figures that are incorrect. The "apparent" transversal resistivity is smaller than the "apparent" longitudinal resistivity, while the inverse proposition holds for the true resistivities. In addition, the ratios  $\frac{r_{at}}{r_{al}}$  and  $\frac{r_l}{r_t}$  are different, being equal respectively to  $\frac{1}{\lambda}$  and to  $\frac{1}{\lambda^2}$ . We will call this unexpected result the "paradox of the anisotropy." Such a proposition is worthy of emphasis, since the idea that would naturally come into one's mind is that the highest apparent resistivity figure should correspond to a direction perpendicular to the strike.

We will also note the remarkable result that the "apparent" transversal resistivity is equal to the true longitudinal resistivity.

### *Study of Horizontal Formations*

We will consider a horizontal, stratified medium, constituted of several parallel, homogeneous, isotropic layers, and cause a current to flow into it by means of an earth ground  $A$ , located at the surface. We know that it is possible to compute the value of the potential at the surface, provided that the thicknesses and the resistivities of the various formations under consideration are known.<sup>7</sup> The mathematical prin-

<sup>7</sup> S. Stefanescu and C. and M. Schlumberger: Sur la distribution électrique potentielle autour d'une prise de terre ponctuelle dans un terrain homogène à couches horizontales, homogènes et isotropes. *Le Journal de Physique et le Radium* (1930) **1**, 132.

J. N. Hummel: Der scheinbare spezifische Widerstand. *Ztsch. f. Geophysik*, **5**, 89; Der spezifische Widerstand bei vier plan-parallel Schichten. *Idem*, 228.

ciples underlying these computations were outlined for the first time by Maxwell.<sup>8</sup>

These computations are still correct when certain of the layers are no longer isotropic, but anisotropic. In this case, it is merely necessary to replace every isotropic layer whose average resistivity is  $r_m = \sqrt{r_1 r_2}$ , whose thickness is  $h$ , and whose coefficient of anisotropy is  $\lambda$ , by a homogeneous, anisotropic layer with the resistivity  $r_m$  and the thickness  $\lambda h$ . A very general demonstration has been given by R. Maillet and H. G. Doll<sup>9</sup> for a series of parallel alternating layers, which can be, at will, either anisotropic or isotropic.

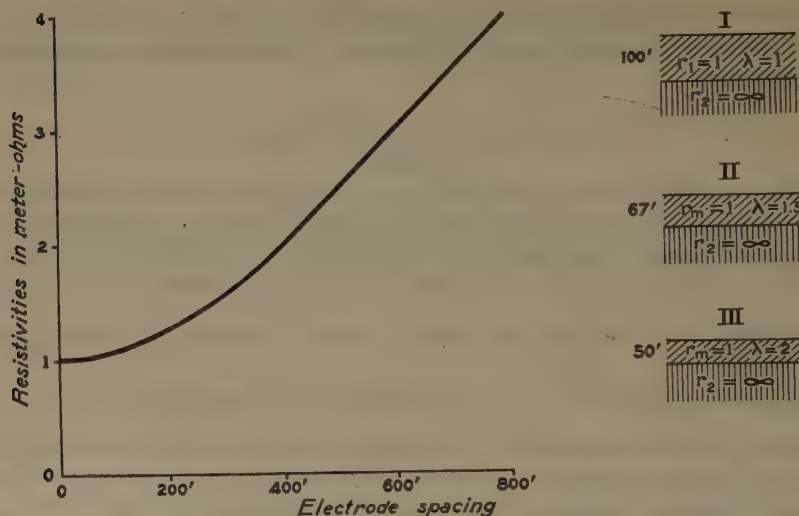


FIG. 11.—DIAGRAM OF RESISTIVITIES CORRESPONDING TO A TWO-LAYER PROBLEM WITH A BEDROCK OF INFINITE RESISTIVITY.

These facts modify somewhat the principles governing the exploration at depth of horizontal, isotropic formations, by resistivity measurements carried out at the surface with increasing electrode spacings. It will no longer be sufficient to know the resistivity diagram in terms of the spacing of the primary electrodes in order to interpret the electrical results accurately and surely, even in very simple cases. For instance, the diagram shown on Fig. 11 can correspond to thicknesses of overburden amounting to 100, 67 and 50 ft., according to the value of the coefficient of anisotropy, which will be successively equal to 1, 1.5 and 2. We suppose, of course, that in these different cases the average resistivity of the overburden remains unchanged.

<sup>8</sup> J. C. Maxwell: Electricity and Magnetism, 1.

<sup>9</sup> R. Maillet and H. G. Doll: Reference of footnote 5.

Fig. 12 represents in the same way an electrical diagram of the three-layer type. On the right hand of the figure, three different geological cases to which it might theoretically correspond have been indicated.

It is easy to see by these simple examples how important it is for the geophysicist to possess a wide experimental knowledge of the anisotropic properties of stratified formations, if the electrical results obtained in the study of horizontal or pseudo-horizontal formations (gently folded structures, etc.) are to be interpreted accurately.

### *Resistivity Measurements across an Anisotropic Syncline or Anticline*

The principle of compression, briefly indicated above, has a very general significance, and can be outlined as follows. Consider a space  $S$ , made up of one or several isotropic media, and suppose that a state of

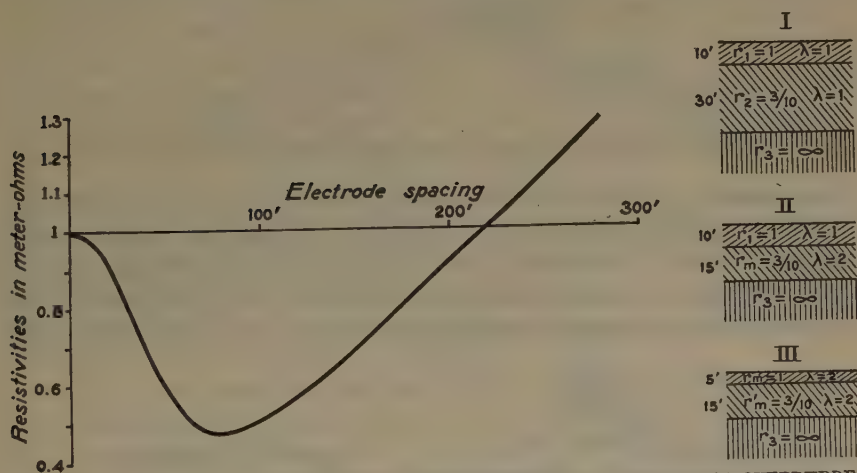


FIG. 12.—DIAGRAM OF RESISTIVITIES CORRESPONDING TO A TWO-LAYER OVERBURDEN UNDERLAIN BY A BEDROCK OF INFINITE RESISTIVITY.

electrical equilibrium is known to exist in it. Consider also an elementary volume  $dx \, dy \, dz$  of this space, limited by the coordinate surfaces. Keep  $dx$  and  $dy$  unchanged, and replace  $dz$  by  $\frac{dz}{\lambda}$ ,  $\lambda$  being a constant. We thus establish a correspondence between the space  $S$  and a new space  $S'$ . In this space, all the media are anisotropic, with the coefficient of anisotropy  $\lambda$ . The emissivities of the electrodes are unchanged, and the potential at two corresponding points also remains the same.<sup>10</sup>

An interesting illustration of these principles will be furnished by an anisotropic syncline with semicircular strata, which can be discussed in the following way (Fig. 13). We will consider a medium limited by a

<sup>10</sup> R. Maillat and H. G. Doll: Reference of footnote 5.

plane  $POP'$ , and constituted by semicircular, anisotropic layers centered on  $O$ , whose coefficient of anisotropy is  $\lambda$ . We will establish a correspondence between a given point  $R$  of this medium and a point  $R'$  of an isotropic medium, in such a way that  $O'R' = \lambda OR$ , and the angle  $POR = \lambda P_1O'R'$ .

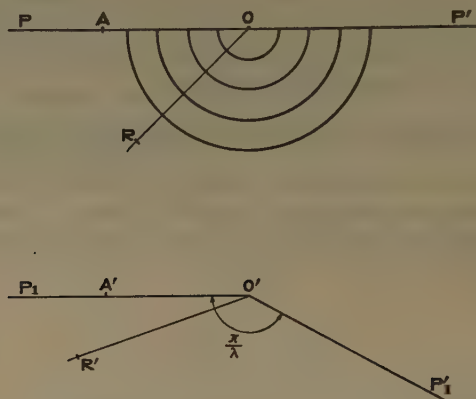


FIG. 13.—SKETCH ILLUSTRATING A SYNCLINE CONSTITUTED OF SEMICIRCULAR LAYERS.

In accordance with the above principles, it can be demonstrated that the potentials of the points  $R$  and  $R'$  are the same, if, from two corresponding electrodes  $A$  and  $A'$  currents of the same intensity are sent into the two respective media. In the practical case where  $\lambda = 2$ , the distribution of the potentials in the anisotropic syncline can be deduced from the study

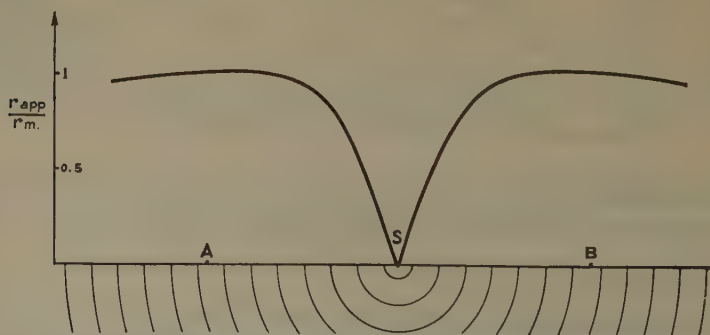


FIG. 14.—DIAGRAM OF RESISTIVITIES OBTAINED ACROSS AN ANISOTROPIC SYNCLINE CONSTITUTED OF SEMICIRCULAR LAYERS.

of the potentials in an isotropic medium limited by two rectangular planes. This latter problem is very easy to study.

At point  $O'$  of the isotropic medium, the intensity of the current is equal to zero. The same is true at  $O$  on the syncline. The apparent resistivity measured at the surface will not be constant, and a profile of resistivities across the syncline will have the shape represented on Fig. 14.



In connection with an anticline, the opposite conclusions will be arrived at, and a maximum of resistivities will be observed at the passage of the axis of the anticline.

These results are verified satisfactorily by experience. Of course, the experimental resistivity diagrams are not exactly similar to the theoretical curves, since in practice the geophysicist has not to deal with a homogeneous, anisotropic terrain, but with a succession of beds which sometimes possess appreciable thicknesses. Fig. 15 shows the results obtained on an anticline and a syncline in a coal basin of Central France, in the course of a tectonic exploration. On a part of the map, the property has already been exploited and explored. The anticlinal fold is known in great detail, and is in good accordance with the electrical results. As to the synclinal fold, it has not as yet been verified by exploration, but there is every reason to assume that the results are correct.

#### STUDY OF THE DIRECTION OF DIP IN ANISOTROPIC FORMATIONS BY INDUCTION METHODS

The fact that stratified sediments are usually anisotropic furnishes an interesting possibility of determining the direction of their dip, by means of induction measurements. The principle of the technique employed by the authors is the following:

Let us cause a current to flow into a homogeneous and *isotropic* terrain, by means of an electrode grounded at *A* on the surface. If the second electrode *B* is located at a great distance from *A*, the equipotential surfaces are spheres centered on *A*, and the current is regularly distributed around *A*; or more accurately, two cones with their summits at *A*, and possessing the same solid angle, contain the same fraction of the total current. It is easy to demonstrate that the magnetic field generated at the surface of the ground by all the diverging currents issuing from *A*



FIG. 15.—RESISTIVITY MEASUREMENTS OBTAINED ON AN ANTICLINAL AND SYNCLINAL FOLD IN A COAL BASIN IN CENTRAL FRANCE.

is the same as though all the current were concentrated along the vertical passing through  $A$ . At the surface, this magnetic field  $H$ , at a distance  $R$  from point  $A$ , is horizontal, and equal to  $\frac{I}{R}$ .

Consider now the case of two electrodes  $A$  and  $B$ . The vector magnetic field at point  $C$  on the prolongation of  $AB$  will be:

$$H = I \left( \frac{1}{R} - \frac{1}{R'} \right)$$

in which  $R$  and  $R'$  are the distances from  $C$  to  $A$  and  $B$ .

If point  $C$ , where the magnetic field is measured, is not on the line connecting  $A$  and  $B$ , the actions of the currents flowing into the ground at  $A$  and  $B$  must be added geometrically.

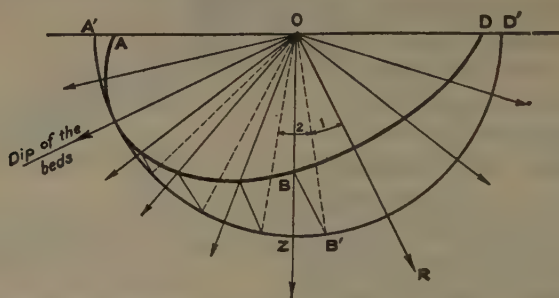


FIG. 16.—DISTRIBUTION OF CURRENT AROUND A PUNCTUAL SOURCE IN AN ANISOTROPIC GROUND.

In addition, since a current flows in the line  $AB$ , the action of this line must be taken into consideration,<sup>11</sup> in all the above cases.

Applying the same problem to an electrode grounded in a homogeneous and *anisotropic* ground, the lines of current remain straight lines. Their distribution, however, is derived from the distribution in an isotropic ground by compressing the equipotential spheres perpendicularly to the stratification, with a rate of compression equal to  $\frac{1}{\lambda}$  ( $\lambda$ , coefficient of anisotropy). Therefore, the lines of current present a maximum of density along the plane of stratification, and a minimum perpendicular to it (Fig. 16). Evidently the distribution is a phenomenon of revolution around the axis  $OR$  perpendicular to the strike.

As a consequence of this concentration of the currents in the direction of the dip, a larger ratio of the total intensity will flow into the rectangular

<sup>11</sup> For the complete study of the magnetic field created by a direct current flowing into an isotropic ground by means of two electrodes  $A$  and  $B$ , connected by a straight wire  $AB$ , see S. S. Stefanescu: *Études Théoriques sur la Prospection Électrique du Sous-sol*. 1. Rumanian Geol. Survey, 1929.

angle constituted by the planes  $AO$  and  $OZ$  than into the angle constituted by the planes  $OZ$  and  $OD$ . This results immediately from the consideration of formula 23, which demonstrates that in every direction the intensity of the current is proportional to the radius of the equipotential ellipsoid passing at this point.

Owing to this displacement of the current, it is easy to understand that if the current is being sent into the ground by means of two electrodes  $A$  and  $B$ , with  $AB$  parallel to the strike, and if a loop  $L$  is disposed horizontally on the ground on the line connecting  $A$  and  $B$ , there will exist a coefficient of mutual induction between loop  $L$  and the circuit constituted by the line  $AB$ , and the currents flowing into the ground at  $A$  and  $B$ .<sup>12</sup> To annul this mutual induction, it will be necessary to rotate the plane of the loop around a horizontal axis parallel to the strike, in order to bring it into position more or less perpendicular to the plane of stratification. This will furnish a means of determining the direction of the dip.

### *Principle of the Field Measurements*

A line  $AB$ , carrying the current, is laid down parallel to the strike. At its center  $O$ , a loop  $S$  is arranged symmetrically with reference to  $AB$  (Fig. 17). This loop will generally be a square, a side or diagonal of which is parallel to  $AB$ . Since the mean circuit in the soil and the horizontal loop  $S$  are not rectangular, owing to the dip of the formations, they possess a coefficient of mutual induction. By measuring this coefficient, and taking into account the direction of the induction current, the direction of the dip will be obtained.

Either one or the other of the two circuits may be utilized for the secondary circuit. As to the current sent into the primary circuit, two techniques are available, namely:

1. Use of an alternating current of audible frequency. The observations are made in the secondary circuit by means of a telephone and amplifier. This technique, which already uses high frequencies, does not appear to be very satisfactory, as explained further on, and is not applied by the authors.

2. A galvanometer is disposed in the secondary circuit, and a current of very low frequency is caused to flow in the primary circuit by means of a commutator. This apparatus commutates also the galvanometer

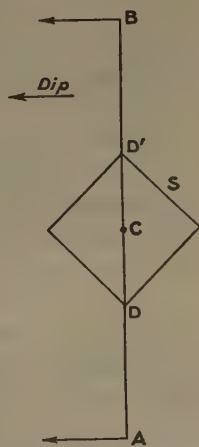


FIG. 17.—SKETCH OF THE LOOP TECHNIQUE.

<sup>12</sup> All of this part of the discussion is presented in an intuitive and physical, rather than in a strictly mathematical way.

in such a manner that this latter instrument always receives induction impulses of the same direction. This potentiometric process makes it possible to use a current of very low frequency, decreasing considerably the skin effect phenomena, which are so detrimental as far as the penetration of the current at depth is concerned.

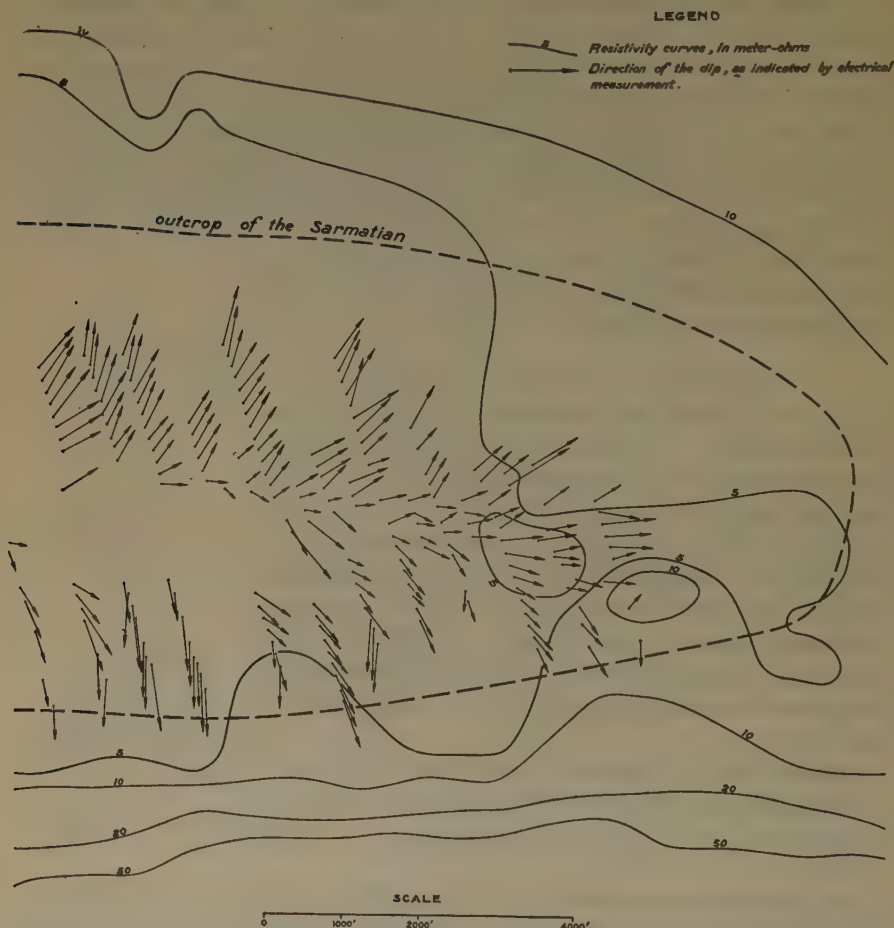


FIG. 18.—RESULTS OBTAINED BY THE LOOP METHOD ON THE GROZNY ANTICLINE.

The magnitude of the mutual induction phenomenon that takes place between the two circuits is represented by a vector, issuing from  $O$  and perpendicular to  $AB$ . In an anisotropic, homogeneous terrain, this vector gives a rough indication of the direction of the dip.

In all the above it has been supposed that the direction of the strike was known approximately, and that  $AB$  was disposed parallel thereto. Experience shows that when this datum is not available, satisfactory results can still be obtained by carrying out two observations at the same



station, with the line  $AB$  located in two successive rectangular positions. The corresponding vectors of mutual induction are determined and composed geometrically. Their resultant gives the direction of the dip.

*Practical Application of Method to Study of Grozny Anticline*

In order to illustrate by an example the use of the loop method, the results obtained on the Grozny anticline, North Caucasus, U.S.S.R. are shown<sup>13</sup> in Fig. 18. Numerous determinations of dip were made, especially along the edges of the structure. They are in good accordance with the geological data. In the center, the ridge of the anticline is determined with great precision.

### SUMMARY

In electrical prospecting, it frequently occurs that the formations to be studied are stratified and decidedly anisotropic, and that an exhaustive knowledge of the laws governing the propagation of the current in anisotropic media is necessary for a satisfactory comprehension and interpretation of the results.

The laws of such propagation have been discussed, with special reference to the propagation due to a punctual source of current.

In order to account both for the properties of the homogeneous anisotropic rocks and for the anisotropy of a series of alternating layers, definitions of a "microscopic," a "macroscopic," and a "total" anisotropy have been offered.

Some consequences of the electrical measurements in anisotropic terrains have been explained, and among them, the "paradox of the anisotropy," by which the apparent transversal resistivity is smaller than the corresponding longitudinal determination.

Finally, a technique has been described by means of which it is possible, by induction measurements, to determine the direction of the dip of tilted anisotropic formations.

### DISCUSSION

(Paul Weaver presiding)

L. B. SLICHTER, \* Cambridge, Mass.—I am especially enthusiastic over the study of anisotropy and its effect on depth determinations. This may prove to be a fruitful field of inquiry in the matter of depth investigations.

P. WEAVER, † Houston, Tex.—This may be of importance in small-scale prospecting. We have found trouble, for example, with the effect of the weathered surface soil on electrical measurements. Close to the electrodes is a layer from 10 to 50 ft.

<sup>13</sup> See A. Chaiderov: Results of Electrical Prospecting at the New Field of Grozny Azerbaijan Oil Ind., No. 9, Baku, 1930.

\* Associate Professor of Geophysics, Massachusetts Institute of Technology.

† Geologist, Gulf Production Co.

thick which, owing to vegetable matter, growth and decay of minerals in the soil, etc., manifests an anisotropic character which interferes with the interpretation of the readings.

E. G. LEONARDON.—If we liken the surface layer of the earth to a sheet of copper, the resistant material underlying the surface conductive layer can be represented by the air *under* the copper sheet. If the four-electrode set-up is used, with increasing separation between the electrodes, there will be a rising resistivity curve. But suppose there are bubbles of heterogeneous material at the surface of the copper sheet near some of the points at which electrode contacts are made. Such a bubble will act as resistant material and distort the equipotential surfaces near it. The potential drop, as measured there, will not follow the regular potential curve which should be observed, but will show a decided anomaly, which might be interpreted as a change in the underlying material. In this manner, the anisotropy of the surface material can complicate the interpretations of the readings as relating to subsurface structure.

F. W. LEE,\* Washington, D. C.—There is another point I should like to make concerning layers of different resistivities. Although theoretically two layers of differing resistivity should show the same ratio between voltage and current, no matter what the current is, as a matter of fact in the field the same ratios are not obtained when using different current strengths.

---

\* U. S. Bureau of Mines.

# Some Interpretations of Earth-resistivity Data

BY IRWIN ROMAN,\* HOUGHTON, MICH.

(New York Meeting, February, 1934)

IN a previous paper,<sup>1</sup> a method was suggested for determining the depth to a bed in the simple case of a uniform overlying layer of constant thickness. The main purpose of the present paper is to show how a slight modification of that method has been used to interpret specific data obtained in the upper peninsula of Michigan by the staff of the Depart-

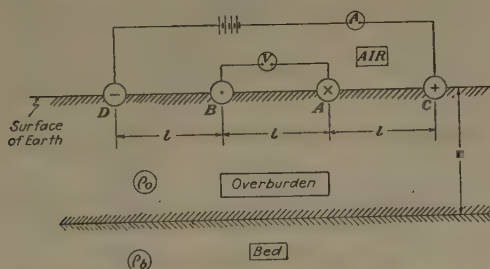


FIG. 1.—THE TECTONIC CONFIGURATION.

ment of Mathematics and Physics of the Michigan College of Mining and Technology. The method of Tagg<sup>2</sup> has also been used on the same data, thus furnishing a comparison of the two methods, as well as a method of using the two methods jointly.

The method of measuring the apparent resistivity is that suggested by Wenner,<sup>3</sup> and illustrated in Fig. 1. A current  $I$  enters the earth at the positive pole  $C$  and leaves it at the negative pole  $D$ . The potential  $V$  of the high electrode  $A$ , with respect to the low electrode  $B$  is measured by suitable means. The separation of the collinear points in the order shown,  $DBAC$ , is  $l$ , the same for each interval.

If the resistivity of the overburden is  $\rho_0$ , and that of the bed is  $\rho_b$ , the apparent resistivity is given by

Manuscript received at the office of the Institute Nov. 20, 1933.

\* Assistant Professor of Mathematics and Physics, Michigan College of Mining and Technology.

<sup>1</sup> I. Roman: How to Compute Tables for Determining Electrical Resistivity of Underlying Beds and their Application to Geophysical Problems. U.S. Bur. Mines Tech. Paper 502 (1931) 22.

<sup>2</sup> G. F. Tagg: Interpretation of Resistivity Measurements. Page 135, this volume

<sup>3</sup> F. C. Wenner: A Method of Measuring Earth Resistivity. U.S. Bur. Stds. Sci. Paper 258 (1915) 469-478.

$$\rho_a = 2\pi l \frac{V}{I}, \quad [1]$$

and the disturbing factor is:

$$M = \frac{\rho_a}{\rho_0} = 1 + \frac{2l}{c}(W' - W'') \quad [2]$$

where:  $W' = W\left(Q, \frac{l}{2c}\right)$  [3]

and  $W'' = W\left(Q, \frac{l}{c}\right)$  [4]

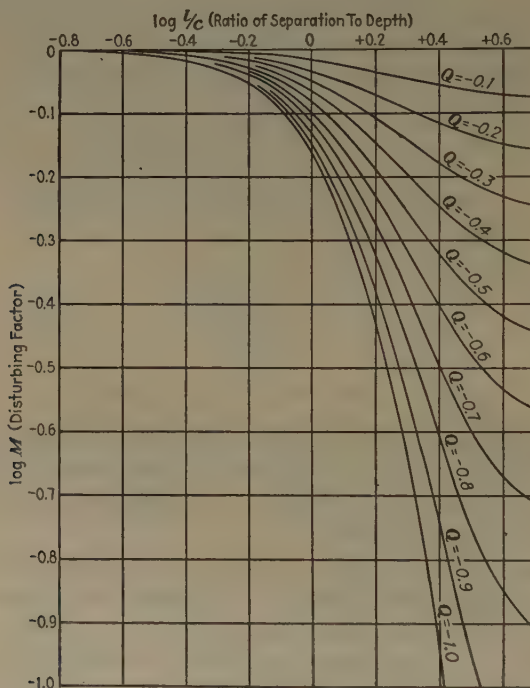


FIG. 2a.—LOGARITHMS OF THEORETICAL DISTURBING FACTORS FOR CONDUCTING BEDS. are the values of the  $W$  function<sup>4</sup> taken from the table for the proper value of the reflecting factor:

$$Q = \frac{\rho_b - \rho_0}{\rho_b + \rho_0} \quad [5]$$

and the value of the argument  $a$  as shown by the second component in the parenthesis, the thickness of overburden being  $c$ .

The value of  $M$  may be calculated as a function of  $Q$  and  $\frac{l}{c}$  so that for

<sup>4</sup> Reference of footnote 1.



each value of  $Q$ , a curve may be plotted with the ordinate  $M$  and the abscissa  $\frac{l}{c}$ . Actually, it is more convenient to plot  $\log M$  as ordinate and

$\log \frac{l}{c}$  as abscissa, as shown in Fig. 2, each curve corresponding to a selected value of the reflection factor  $Q$ .

By equation 2, we have

$$\log \rho_a = \log \rho_0 + \log M \quad [6]$$

If we plot the observed values of  $\log \rho_a$  against  $\log l$  in the same scales as

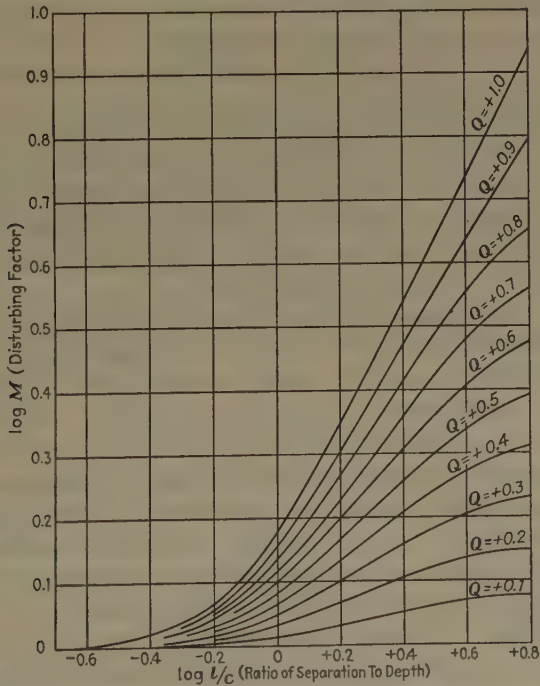


FIG. 2b.—LOGARITHMS OF THEORETICAL DISTURBING FACTORS FOR INSULATING BEDS.

used in the theoretical curves, we may superpose the two graphs since

$$\log \frac{\rho_a}{\rho_0} = \log \rho_a - \log \rho_0$$

$$\log \frac{l}{c} = \log l - \log c$$

and since both  $\log \rho_0$  and  $\log c$  are constant. If the observed curve can be made to fit one of the theoretical curves, four quantities may be determined as follows:

1. The value of the reflecting factor  $Q$  is given by the theoretical curve which fits the data.

2. For  $\log M = 0$ ,  $\log \rho_a = \log \rho_0$ , so that the value on the observed ordinate ( $\log \rho_a$ ) scale corresponding to zero on the theoretical ordinate ( $\log M$ ) scale is the value of  $\log \rho_0$ , from which the overburden resistivity is available.

3. For  $\log \frac{l}{c} = 0$ ,  $l = c$ , so that the value on the observed abscissa ( $\log l$ ) scale corresponding to zero on the theoretical abscissa ( $\log \frac{l}{c}$ ) scale is  $\log c$ , from which the depth  $c$  is available.

4. Knowing the values of  $\rho_0$  and  $Q$ , the resistivity of the bed is obtainable from:

$$\rho_b = \frac{1 + Q}{1 - Q} \rho_0 \quad [7]$$

The application of the method is direct and simple. The theoretical curves are plotted in the selected scales, on thin coordinate paper. The observed curves are plotted on heavy coordinate paper in the same scales. Then the two graphs are superposed, preferably over a light table, and the data taken directly from the curves. The reduction of the data is mainly a matter of finding antilogarithms.

In some of the cases in which the method was tried, the fitting was quick and definite, different observers finding essentially the same results, independently, and the same observer checking his own results after an interval of several days or even months. In other cases, the results are more ambiguous and there is choice in the fitting. In still other cases, the observed curves are obviously not due to a single layer. In some cases, parts of a curve may correspond to a single layer and the rest not so correspond. It is to be hoped that a similar method eventually will be available for multiple layers, but the theoretical curves have not been prepared for these cases, at the present writing.

In the method of Tagg,<sup>5</sup> the value of the overburden resistivity  $\rho_0$  is obtained by taking observations with small spreads. Using this value for  $\rho_0$ , the value of the disturbing factor  $M = \frac{\rho_a}{\rho_0}$  is calculated for each observation at the longer spreads. From theoretical curves, or from tables such as those shown in this paper, the value of  $\frac{l}{c}$  corresponding to the disturbing factor  $M$  may be found for each value of the reflection factor  $Q$ . Since the separation is known, we may thus find the depth  $c$ , which will cause the observed disturbing factor for each value of the reflection factor. If the value of  $Q$  is plotted as a function of  $c$ , there will be one curve for each observed disturbing factor, or for each of the larger

<sup>5</sup> Reference of footnote 2.

separations. If the interpretation is unique, the various lines will meet in a point. In practice, this point is often spread out into a network, whose center must be found visually, and in some cases, the point is not determinable.

To eliminate the errors involved in taking the disturbing factors from the curves, a table has been prepared directly from the  $W$  tables by the use of equation 2. The results are shown in Tables 1 and 2. The figures at the heads of the columns are the values of the reflection factor  $Q$ , while the figures at the left of the lines are the values of the ratio of  $l$  to  $c$ . The tables are sufficiently reliable for second order interpolation, but ordinary linear interpolation is usually ample for the accuracy obtainable in the observations. In interpolating, the final figure may be incorrect. These tables apply only to the Wenner configuration of current poles and potential electrodes. However, when the potential of  $A$  is found with respect to the midpoint of  $A$  and  $B$  (see Fig. 1), the same formulas, curves and tables apply, if the observed potentials are multiplied by the factor 2. The method of superposition can be applied to other configurations of electrodes, but the disturbing factors would need to be calculated directly from the  $W$  tables and the interpretation would usually not be so simple. The Wenner system simplifies the problem by always keeping the ratio of the potential electrode distance to the current pole distance constant, thus eliminating one variable.

#### ANALYSIS OF OBSERVATIONS

The application of the method of superposition may be illustrated by considering specific data. The data have been selected from the files of the Department of Mathematics and Physics of the Michigan College of Mining and Technology and represent a part of the research work of the department during about five summers. No attempt has been made to examine the observations statistically, but numerous surveys have been examined and the examples selected may be considered as typical. Each example has been selected to illustrate a specific aspect of the analysis. In each case, the actual observed apparent resistivities are represented by small circles on the graphs and the tabulation of the data is omitted, since the values may be read from the graph with sufficient accuracy.

Unfortunately, no drilling records are available for the portions of the diamond-drill holes above ledge, the drillers' interests being below this level. The depths in the interpretations are shallower than ledge and hence no accurate geological correlations are possible. The depths may represent water tables or soil contacts. The interpretations should be checked by some other method, but the agreements between the theoretical and observed curves are such as to make the analysis significant.

TABLE 1.—*Disturbing Factors, Wenner System, Conducting Bed*

$l/c \backslash Q$	-0.1	-0.2	-0.3	-0.4	-0.5	-0.6	-0.7	-0.8	-0.9	-1.0
0.1	0.9999	0.9999	0.9998	0.9997	0.9996	0.9995	0.9995	0.9995	0.9994	0.9993
0.2	0.9994	0.9989	0.9983	0.9978	0.9973	0.9968	0.9963	0.9958	0.9953	0.9948
0.3	0.9982	0.9964	0.9946	0.9929	0.9912	0.9896	0.9880	0.9864	0.9848	0.9833
0.4	0.9959	0.9919	0.9880	0.9842	0.9804	0.9768	0.9732	0.9697	0.9662	0.9629
0.5	0.9925	0.9853	0.9782	0.9713	0.9646	0.9580	0.9515	0.9452	0.9390	0.9330
0.6	0.9881	0.9767	0.9654	0.9545	0.9439	0.9335	0.9233	0.9134	0.9037	0.8942
0.7	0.9828	0.9662	0.9500	0.9343	0.9190	0.9041	0.8896	0.8754	0.8615	0.8479
0.8	0.9768	0.9543	0.9326	0.9114	0.8909	0.8710	0.8516	0.8326	0.8141	0.7960
0.9	0.9702	0.9414	0.9137	0.8867	0.8606	0.8353	0.8107	0.7867	0.7633	0.7405
1.0	0.9633	0.9279	0.8938	0.8609	0.8290	0.7981	0.7682	0.7391	0.7108	0.6833
1.1	0.9562	0.9141	0.8736	0.8346	0.7969	0.7605	0.7253	0.6911	0.6580	0.6259
1.2	0.9490	0.9002	0.8534	0.8084	0.7650	0.7233	0.6829	0.6439	0.6061	0.5696
1.3	0.9419	0.8865	0.8335	0.7827	0.7339	0.6870	0.6418	0.5982	0.5561	0.5154
1.4	0.9350	0.8732	0.8142	0.7579	0.7039	0.6522	0.6024	0.5546	0.5085	0.4640
1.5	0.9284	0.8604	0.7958	0.7342	0.6754	0.6192	0.5652	0.5135	0.4638	0.4159
1.6	0.9220	0.8482	0.7783	0.7118	0.6485	0.5881	0.5304	0.4751	0.4222	0.3714
1.7	0.9159	0.8366	0.7617	0.6908	0.6233	0.5592	0.4980	0.4396	0.3839	0.3305
1.8	0.9101	0.8257	0.7462	0.6711	0.5999	0.5324	0.4682	0.4071	0.3488	0.2932
1.9	0.9047	0.8155	0.7317	0.6528	0.5782	0.5077	0.4408	0.3773	0.3169	0.2594
2.0	0.8996	0.8059	0.7182	0.6358	0.5582	0.4850	0.4157	0.3502	0.2880	0.2289
2.1	0.8949	0.7970	0.7056	0.6201	0.5398	0.4642	0.3929	0.3257	0.2620	0.2016
2.2	0.8904	0.7887	0.6940	0.6056	0.5229	0.4452	0.3723	0.3036	0.2387	0.1773
2.3	0.8862	0.7810	0.6833	0.5923	0.5075	0.4280	0.3536	0.2836	0.2178	0.1556
2.4	0.8823	0.7738	0.6734	0.5801	0.4934	0.4124	0.3367	0.2657	0.1991	0.1364
2.5	0.8787	0.7672	0.6642	0.5689	0.4806	0.3982	0.3215	0.2497	0.1825	0.1194
2.6	0.8753	0.7610	0.6558	0.5587	0.4689	0.3854	0.3078	0.2354	0.1677	0.1044
2.7	0.8721	0.7553	0.6480	0.5494	0.4582	0.3738	0.2955	0.2226	0.1546	0.0911
2.8	0.8691	0.7500	0.6409	0.5408	0.4485	0.3633	0.2844	0.2111	0.1430	0.0795
2.9	0.8664	0.7451	0.6344	0.5329	0.4397	0.3538	0.2744	0.2009	0.1327	0.0693
3.0	0.8639	0.7406	0.6283	0.5256	0.4316	0.3452	0.2655	0.1918	0.1236	0.0604
3.1	0.8615	0.7364	0.6227	0.5190	0.4243	0.3374	0.2575	0.1838	0.1156	0.0526
3.2	0.8593	0.7324	0.6175	0.5130	0.4176	0.3304	0.2503	0.1766	0.1085	0.0457
3.3	0.8573	0.7288	0.6128	0.5075	0.4116	0.3241	0.2438	0.1702	0.1023	0.0397
3.4	0.8554	0.7255	0.6084	0.5024	0.4061	0.3183	0.2380	0.1645	0.0968	0.0345
3.5	0.8536	0.7224	0.6043	0.4977	0.4011	0.3130	0.2328	0.1594	0.0919	0.0299
3.6	0.8519	0.7195	0.6005	0.4934	0.3965	0.3083	0.2282	0.1548	0.0876	0.0259
3.7	0.8503	0.7168	0.5970	0.4895	0.3923	0.3041	0.2240	0.1507	0.0839	0.0225
3.8	0.8488	0.7143	0.5939	0.4859	0.3884	0.3003	0.2202	0.1471	0.0806	0.0195
3.9	0.8474	0.7119	0.5910	0.4825	0.3849	0.2968	0.2167	0.1440	0.0777	0.0169
4.0	0.8461	0.7097	0.5882	0.4794	0.3817	0.2935	0.2136	0.1412	0.0751	0.0146
4.1	0.8449	0.7076	0.5856	0.4765	0.3788	0.2905	0.2108	0.1386	0.0728	0.0126
4.2	0.8437	0.7057	0.5832	0.4739	0.3761	0.2879	0.2083	0.1362	0.0708	0.0109
4.3	0.8426	0.7039	0.5810	0.4715	0.3736	0.2855	0.2061	0.1341	0.0690	0.0095
4.4	0.8416	0.7022	0.5790	0.4693	0.3712	0.2833	0.2041	0.1323	0.0674	0.0082
4.5	0.8406	0.7007	0.5771	0.4672	0.3690	0.2813	0.2022	0.1307	0.0660	0.0070
4.6	0.8397	0.6992	0.5753	0.4652	0.3671	0.2794	0.2004	0.1292	0.0648	0.0061
4.7	0.8389	0.6978	0.5736	0.4634	0.3654	0.2777	0.1988	0.1278	0.0637	0.0053
4.8	0.8380	0.6965	0.5720	0.4618	0.3637	0.2761	0.1974	0.1266	0.0627	0.0046
4.9	0.8372	0.6953	0.5705	0.4603	0.3621	0.2746	0.1962	0.1255	0.0618	0.0039
5.0	0.8366	0.6941	0.5691	0.4587	0.3607	0.2733	0.1950	0.1245	0.0610	0.0034



TABLE 2.—*Disturbing Factors, Wenner System, Insulating Bed*

$l/c \backslash Q$	0.1	0.2	0.3	0.4	0.5	0.6	0.7	0.8	0.9	1.0
0.1	1.0001	1.0002	1.0002	1.0003	1.0004	1.0005	1.0006	1.0007	1.0008	1.0009
0.2	1.0006	1.0012	1.0018	1.0024	1.0031	1.0038	1.0045	1.0053	1.0061	1.0070
0.3	1.0019	1.0038	1.0058	1.0079	1.0101	1.0123	1.0146	1.0171	1.0198	1.0227
0.4	1.0042	1.0085	1.0131	1.0177	1.0226	1.0276	1.0329	1.0385	1.0445	1.0512
0.5	1.0076	1.0156	1.0238	1.0323	1.0412	1.0504	1.0602	1.0705	1.0816	1.0939
0.6	1.0122	1.0249	1.0380	1.0516	1.0658	1.0807	1.0964	1.1131	1.1311	1.1513
0.7	1.0178	1.0361	1.0552	1.0751	1.0959	1.1178	1.1409	1.1656	1.1924	1.2225
0.8	1.0241	1.0490	1.0750	1.1022	1.1307	1.1607	1.1926	1.2268	1.2640	1.3062
0.9	1.0310	1.0632	1.0968	1.1320	1.1691	1.2084	1.2502	1.2952	1.3445	1.4008
1.0	1.0383	1.0782	1.1200	1.1639	1.2104	1.2596	1.3123	1.3694	1.4322	1.5045
1.1	1.0458	1.0937	1.1441	1.1972	1.2535	1.3134	1.3779	1.4480	1.5257	1.6157
1.2	1.0534	1.1095	1.1686	1.2312	1.2977	1.3689	1.4458	1.5298	1.6235	1.7329
1.3	1.0610	1.1253	1.1932	1.2654	1.3424	1.4253	1.5151	1.6138	1.7245	1.8550
1.4	1.0685	1.1408	1.2176	1.2995	1.3872	1.4819	1.5851	1.6991	1.8278	1.9810
1.5	1.0758	1.1560	1.2415	1.3331	1.4316	1.5383	1.6553	1.7851	1.9327	2.1099
1.6	1.0828	1.1708	1.2649	1.3660	1.4753	1.5942	1.7251	1.8713	2.0385	2.2410
1.7	1.0895	1.1851	1.2876	1.3981	1.5180	1.6492	1.7942	1.9572	2.1448	2.3740
1.8	1.0959	1.1987	1.3094	1.4292	1.5597	1.7031	1.8624	2.0424	2.2510	2.5083
1.9	1.1020	1.2118	1.3304	1.4593	1.6002	1.7558	1.9295	2.1268	2.3571	2.6438
2.0	1.1078	1.2243	1.3505	1.4883	1.6395	1.8072	1.9954	2.2103	2.4627	2.7799
2.1	1.1134	1.2362	1.3698	1.5162	1.6776	1.8573	2.0599	2.2926	2.5678	2.9167
2.2	1.1186	1.2475	1.3882	1.5429	1.7143	1.9059	2.1230	2.3737	2.6721	3.0540
2.3	1.1235	1.2582	1.4058	1.5686	1.7497	1.9531	2.1847	2.4535	2.7756	3.1916
2.4	1.1281	1.2683	1.4255	1.5932	1.7838	1.9989	2.2450	2.5321	2.8782	3.3294
2.5	1.1325	1.2780	1.4384	1.6168	1.8168	2.0434	2.3039	2.6093	2.9800	3.4675
2.6	1.1367	1.2871	1.4536	1.6395	1.8486	2.0865	2.3613	2.6852	3.0808	3.6057
2.7	1.1406	1.2957	1.4681	1.6612	1.8792	2.1283	2.4173	2.7598	3.1806	3.7439
2.8	1.1442	1.3039	1.4820	1.6820	1.9087	2.1688	2.4719	2.8330	3.2795	3.8823
2.9	1.1476	1.3117	1.4952	1.7019	1.9372	2.2081	2.5252	2.9050	3.3774	4.0208
3.0	1.1508	1.3190	1.5077	1.7210	1.9646	2.2462	2.5772	2.9757	3.4743	4.1593
3.1	1.1538	1.3259	1.5196	1.7392	1.9910	2.2831	2.6280	3.0451	3.5703	4.2978
3.2	1.1567	1.3325	1.5309	1.7567	2.0164	2.3189	2.6776	3.1133	3.6653	4.4364
3.3	1.1595	1.3388	1.5417	1.7735	2.0409	2.3536	2.7259	3.1804	3.7593	4.5750
3.4	1.1621	1.3448	1.5521	1.7896	2.0646	2.3873	2.7730	3.2463	3.8525	4.7135
3.5	1.1645	1.3504	1.5620	1.8051	2.0875	2.4200	2.8191	3.3109	3.9447	4.8522
3.6	1.1668	1.3558	1.5715	1.8200	2.1096	2.4518	2.8640	3.3746	4.0360	4.9907
3.7	1.1690	1.3609	1.5806	1.8343	2.1309	2.4825	2.9079	3.4371	4.1263	5.1294
3.8	1.1711	1.3657	1.5892	1.8479	2.1514	2.5124	2.9508	3.4986	4.2159	5.2679
3.9	1.1730	1.3703	1.5974	1.8610	2.1712	2.5415	2.9928	3.5590	4.3045	5.4065
4.0	1.1748	1.3747	1.6053	1.8737	2.1905	2.5698	3.0338	3.6184	4.3922	5.5452
4.1	1.1765	1.3789	1.6128	1.8859	2.2092	2.5973	3.0738	3.6767	4.4791	5.6838
4.2	1.1781	1.3829	1.6200	1.8977	2.2271	2.6240	3.1129	3.7343	4.5651	5.8224
4.3	1.1797	1.3867	1.6269	1.9090	2.2444	2.6499	3.1512	3.7908	4.6504	5.9610
4.4	1.1813	1.3903	1.6336	1.9199	2.2613	2.6751	3.1886	3.8464	4.7348	6.0997
4.5	1.1827	1.3938	1.6400	1.9304	2.2776	2.6996	3.2251	3.9010	4.8183	6.2384
4.6	1.1840	1.3972	1.6461	1.9405	2.2933	2.7235	3.2609	3.9548	4.9012	6.3769
4.7	1.1853	1.4004	1.6519	1.9502	2.3086	2.7469	3.2959	4.0076	4.9832	6.5155
4.8	1.1865	1.4034	1.6575	1.9596	2.3234	2.7696	3.3302	4.0597	5.0646	6.6542
4.9	1.1877	1.4062	1.6630	1.9687	2.3377	2.7915	3.3637	4.1110	5.1451	6.7928
5.0	1.1888	1.4091	1.6683	1.9775	2.3517	2.8130	3.3965	4.1614	5.2250	6.9315

## INDIANA DIAMOND-DRILL HOLE No. 2

By direct superposition of the observations on the reference curves, the reflection factor for this survey is found to be between  $Q = 0.7$  and  $Q = 0.8$ . The fittings for each case lead to the values shown in the table accompanying Fig. 3. Using these determined values, the full curves of Fig. 3 are computed directly from Table 2, the bed being more insulating

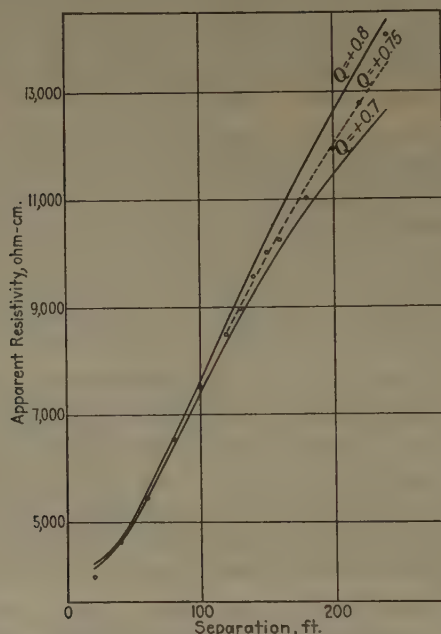


FIG. 3.—APPARENT RESISTIVITIES, INDIANA D.D.H. 2 SURVEY. (CIRCLES REPRESENT OBSERVED VALUES.)

Curve	Upper	Lower	Broken
Reflection factor $Q$ .....	0.8	0.7	0.75
Overburden resistivity, ohm-cm.....	4,160	4,030	4,100
Bed resistivity, ohm-cm.....	37,440	22,820	28,700
Overburden thickness $c$ , ft.....	64.5	56.3	60

than the overburden. Since the circles representing the observations seem to lie about midway between the full curves, the approximate averages of the respective values are used to compute the broken curve. Except for the two end points, the fit is satisfactory. The end point for the small separation may be due to local surface anomalies while the end point for the large separation may be influenced by a deeper formation.

In making the calculations for  $Q = 0.75$ , interpolation is needed in both of the arguments  $a$  and  $Q$ . This may be made in three steps, each

consisting of a single, linear interpolation in one of the variables. This method is to be preferred for persons not familiar with tables of two arguments. It is also possible to make the double linear interpolation directly, the degree of approximation being about the same as in the previous method. Let a value of the disturbing factor  $M$  be sought for the arguments

$$\begin{aligned}a_x &= a_0 + x(a_1 - a_0) \\ Q_y &= Q_0 + y(Q_1 - Q_0)\end{aligned}$$

For definiteness, let  $a_0$  be the tabulated value of  $a$  nearest to  $a_x$  and let  $a_1$  be the adjacent value of  $a$  such that  $a_x$  lies in the tabular step between  $a_0$  and  $a_1$ . Similarly, let  $Q_y$  lie in the tabular step between  $Q_0$  and  $Q_1$ , the nearer entry being  $Q_0$ . Let  $M_{hk}$  be the value of  $M$  for the arguments  $a = a_h$  and  $Q = Q_k$ . With sufficient accuracy for most purposes, a convenient formula for the direct double interpolation is:

$$M_{xy} = M_{00} + x(M_{10} - M_{00}) + y(M_{01} - M_{00})$$

for interpolation without a computing machine and

$$M_{xy} = (1 - x - y)M_{00} + xM_{10} + yM_{01}$$

for interpolation with a computing machine. For the notation selected, the phases  $x$  and  $y$  lie between minus one-half and plus one-half. If more accurate results are needed, higher order interpolation must be used, in which case it may be preferable to compute directly from the  $W$  tables instead of from the  $M$  tables given in this paper.

In making the determinations, the logarithmic curves are plotted in the same scales used in the reference curves. The constants are read by superposition and these constants are used as the data in a direct calculation from the tables. The final theoretical curves shown in Fig. 3 are apparent resistivities against separations, not the logarithms. The logarithmic curves have been omitted from this paper because a direct superposition is not feasible. Any reader interested in checking the

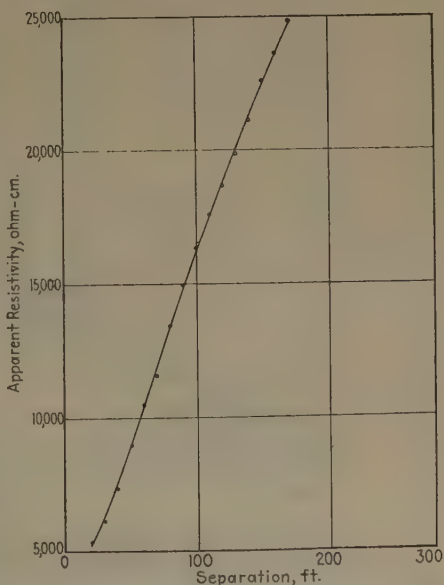


FIG. 4. APPARENT RESISTIVITIES, INDIANA D.D.H. 11 SURVEY.

Reflection factor, 0.9; overburden resistivity, 4730 ohm-cm.; bed resistivity, 90,000 ohm-cm.; overburden thickness, 33.9 feet.

superposition may plot both reference curves and observation curves without difficulty. The reference curves may be plotted from Figs. 2a and 2b, or directly from the tables. The observations may be read from Fig. 3.

### INDIANA DIAMOND-DRILL HOLE No. 11

In this survey, superposition leads to the values given in the table accompanying Fig. 4. Using these values and calculating directly from Table 2, the curve of Fig. 4 is obtained. The agreement between theory and observation is unusually good.

Using an overburden resistivity of 5327 ohm-cm., as determined from the short spreads, the same survey leads to the curves of Fig. 5, for

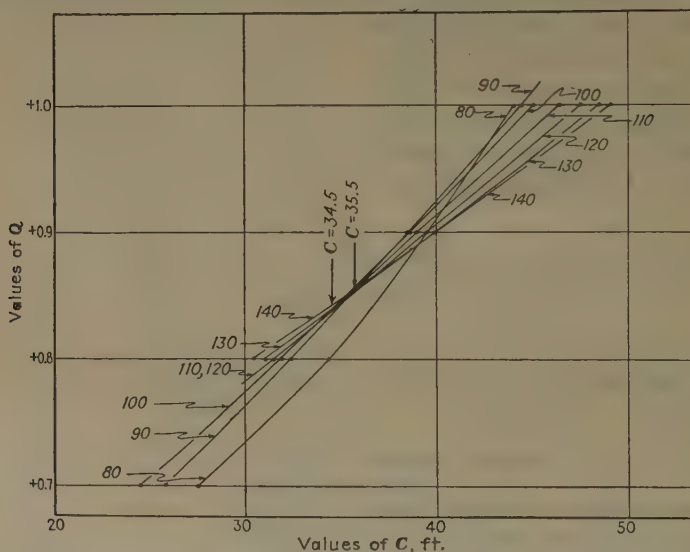


FIG. 5.—INDIANA D.D.H. 11 SURVEY. TAGG METHOD CURVES.

Overburden resistivity, 5327 ohm-cm.; each curve identified by the separation (feet).

Tagg's method. The intersections of the curves leaves a choice of 34.5 or 35.5 ft. for the thickness of the overburden with only a pair of lines crossing at 33.7. The value obtained by superposition is 33.9. The reflection factor is 0.85 by Tagg's method as compared with 0.9 by superposition.

### TAGG'S STATION A

For the data given by Tagg as station A, Fig. 6 shows the theoretical apparent resistivities on the basis of the constants determined by superposition and listed in the table accompanying the figure. The corresponding data tabulated under "Tagg" are taken directly from his paper. It may be noted that the agreement between the two methods is remarkably close.



## TAGG'S STATION B

For the data given by Tagg as station B, Fig. 7 shows the theoretical apparent resistivities on the two assumptions shown in the table accom-

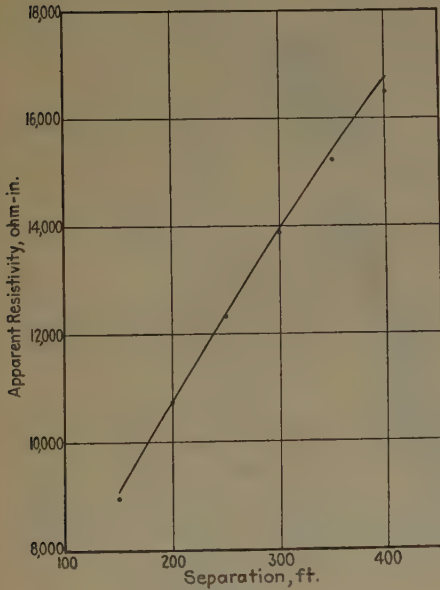


FIG. 6.

FIG. 6.—APPARENT RESISTIVITIES, TAGG'S STATION A.

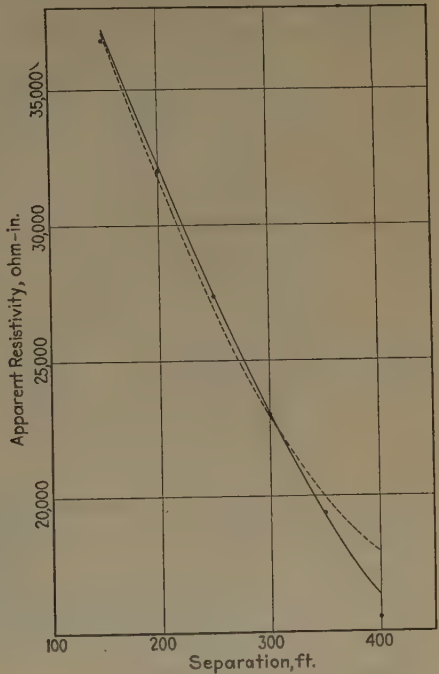


FIG. 7.

Constant	Superposition	Tagg
Reflection factor $Q$ .....	0.7	0.702
Overburden resistivity, ohm-in.....	6,720	6,703
Bed resistivity, ohm-in.....	38,080	38,280
Overburden thickness $c$ , ft.....	141	142

FIG. 7.—APPARENT RESISTIVITIES, TAGG'S STATION B.

Determination	Superposition	Tagg
Curve.....	Full	Broken
Reflection factor $Q$ .....	-0.85	-0.6
Overburden resistivity, ohm-in.....	42,700	45,700
Bed resistivity, ohm-in.....	3,460	11,400
Overburden thickness $c$ , ft.....	200	156

panying the figure. It may be noted that the observations agree very well with the full curve, obtained by the method of superposition, while

the agreement with the broken curve, obtained by Tagg's method is not as good. Fig. 8 shows the Tagg method curves on the assumption that the overburden resistivity is 42,700 ohm-in. as determined by superposition. The depth is determined as 200 ft. while the reflection factor

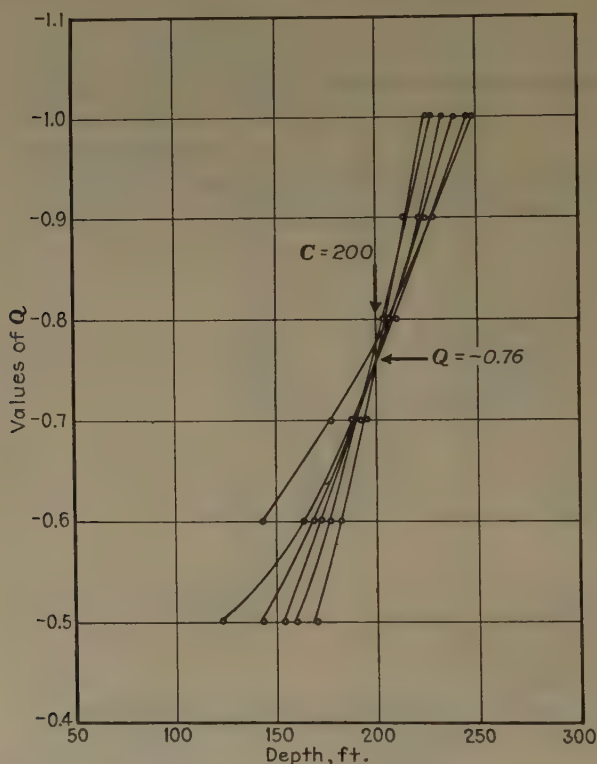


FIG. 8.—TAGG'S STATION B. TAGG METHOD CURVES.  
Overburden resistivity, 42,700 ohm-in.

is  $Q = -0.76$ . The intersection for the curves of the Tagg method on this revised interpretation is more clearly defined than on Tagg's original curves and the depth agrees well with that deduced by superposition. The 400-ft. curve is omitted from Tagg's graph, but is included in Fig. 8.

#### ORWELL

There are many surveys in which the observations indicate a more complex structure than has been assumed in this paper. In such cases, the method of superposition shows at a glance that the assumed structure is not correct. From numerous such surveys, one is shown in Fig. 9. The interpretation of such a survey must be qualitative until further theoretical studies are available.

## CONCLUSIONS

In the present paper, a method of superposing the observed apparent earth resistivities on a set of standard reference curves has been explained and illustrated by actual resistivity survey results. Tagg's method has also been applied to the same data. Either method is a serviceable tool

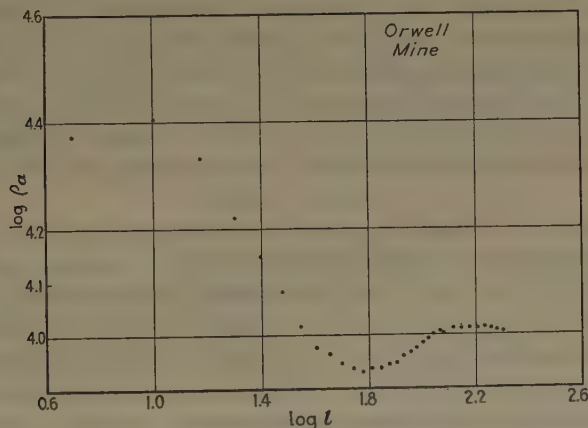


FIG. 9.—LOGARITHMS OF APPARENT RESISTIVITIES, ORWELL SURVEY.

in the interpretation of earth-resistivity data in cases where the observations justify the assumption of a single homogeneous overburden of uniform thickness overlying an infinite homogeneous bed. In this sense, the term "homogeneous" applies to the region as a whole and not to small-scale sections. In particular, the average resistivity may not be the actual resistivity at any point of the region and therefore cannot be determined by sampling. Thus, a mixture of sand, glacial drift, boulders and humus may be considered as homogeneous, if the mixture is uniform for the purposes of the survey.

Tables have been included to make possible a rapid determination of the apparent resistivity for a specified set of conditions when the measuring configuration is that of the Wenner four-electrode system and the geologic formations permit the assumption of the simple case.

Experience has shown that the method of Tagg and that of superposition are valuable partners. Used together, each serves as a check on the other. The two methods will be considered in various aspects.

*Speed.*—The method of superposition seems to have a slight advantage in the matter of speed of application. A single observation curve is sufficient for a specific survey. In Tagg's method, one curve is required for each size of separation. In each case, the reference curves, or the underlying tables are needed. The observation curve must also be made in Tagg's method, to show that a fit is possible. In either case, the conclusions should be checked by starting with the determined

constants and calculating the theoretical values for the apparent resistivity from the tables or the formulas. Without this check, the method of Tagg may lead to an interpretation without much foundation. The method of superposition is more likely to eliminate poor interpretations.

*Overburden Resistivity.*—Tagg's method assumes a value for the overburden resistivity and the conclusions are dependent on the value assumed. His method uses the short separations to determine this value. As explained above, the overburden resistivity may be an averaged resistivity and may not be the resistivity of a sample of the region. In the superposition method, the overburden resistivity is determined directly from the entire curve. Hence this resistivity as determined by superposition may be a good starting point for the method of Tagg.

*Uniqueness.*—In Tagg's method, the depth and the reflection factor are determined by the common intersection of several curves. Frequently, this intersection is not well defined, the common point being much spread out, as into a large triangle. A different value for the overburden resistivity may lead to a much better intersection, but this alone is not a valuable criterion. In the method of superposition, there is often much choice in the fitting of the curves. In such a case, a unique solution requires further knowledge. Apparently, the method of Tagg determines the reflection factor and the thickness of overburden as accurately as the graph can be read. However, this accuracy is only apparent, as a slight change in the assumed overburden resistivity may shift the intersection of the Tagg curves as much as the apparent indefiniteness of the superposition.

*Checking and Revaluation.*—The ultimate check on the interpretation lies in the agreement between the observed data and the theoretical apparent resistivity. Whatever values are decided for the constants, these values should be used to predict the observations as a check. If the theoretical and observed curve do not agree, it frequently is possible to use the lack of agreement as a means of revising the interpretation. This applies equally to both methods.

*Reliability.*—If the two methods can be made to furnish the same conclusions, it is likely that these conclusions will be useful, as a geophysical interpretation. However, it must be remembered that both methods are indirect, as are most geophysical methods, and that the conclusions should be checked against any other known facts about the region of the survey. It is always conceivable that an entirely different set of conditions may produce as good a fit as the ones accepted. In general, the method of superposition will eliminate impossible cases better than that of Tagg, but in both methods the results should be considered as an indicator rather than a fact. This is not a criticism of the resistivity method, as it applies also to other methods of subsurface



analysis. Even a drill record must be interpreted with this reservation, as the actual drilling may not properly represent the region.

### ACKNOWLEDGMENTS

In closing, the writer wishes to express his thanks to Prof. James Fisher, head of the Department of Mathematics and Physics of the Michigan College of Mining and Technology, for the use of the data and for permission to publish the results. He also wishes to express his thanks to Mr. Carlton M. Marquardt, student assistant in the same department, for his calculations, tabulation of the data, and the making of the plates.

### DISCUSSION

(E. DeGolyer presiding)

L. B. SLICHTER,\* Cambridge, Mass.—In connection with the curve of Fig. 9, and others, I would like to ask whether the potentials were measured in several azimuths, to establish the degree of symmetry, or lack of it, in the problem. This, it seems to me, is always a fundamental consideration. For if *symmetry* about a vertical axis exists, we are sure that the problem can be perfectly interpreted, theoretically, for any type of response curve. If symmetry with respect to a vertical plane occurs, one may be led to proceed with interpretations on the basis of *sloping* structures. If the symmetry is poor, the interpretations must be expected to be poor. In a word, the situation as to symmetry is always well worth special attention.

J. FISHER,† Houghton, Mich.—The curve was taken on the Mesabi Range, in a swampy area, so that all the electrodes were in muskeg. Beneath the swamp there is a layer of hardpan underlain by a paint rock, below which comes the iron formation. The conditions were known to be complicated, but it was hoped there would be sufficient homogeneity to permit a correlation to be made.

L. B. SLICHTER.—The curve was taken only once, then?

J. FISHER.—No. It is the result of three sets of observations, two at right angles, the third at 45°. Bedrock was 80 ft. down, and the slight dip of its surface resulted in showing no differences in the curves made for the various azimuths.

L. B. SLICHTER.—I am glad you brought this out. In so many commercial applications it is necessary to work near rivers, etc., where the symmetry is not ideal, and it should be studied by profiles in several azimuths.

J. FISHER.—We try to pick areas where enough is known of the subsoil conditions, from drill-hole data, to permit us to establish type curves.

F. W. LEE,‡ Washington, D. C.—How did you get the  $\rho_0$  value of the resistivity curves?

J. FISHER.—We find that it is not necessary to assume a zero value for the resistivity, as this can be obtained directly from the superposition. No matter how small

---

\* Associate Professor of Geophysics, Massachusetts Institute of Technology.

† Head, Department of Mathematics and Physics, Michigan College of Mining and Technology.

‡ U. S. Bureau of Mines.

the separation, bedrock enters into the figures from the very beginning, therefore the theoretical curves show no turning points.

F. W. LEE.—In connection with these efforts of depth determination by the resistivity method, I would like to mention the work reported in a paper recently published abroad, in which the induction method was used for the same purpose. Coils with progressively larger diameters were employed to determine the impedance of the ground. The experimenters found that they often secured better results than with the resistivity method.

J. FISHER.—One more phase of our work I should like to mention. We found, as a result of three or four years experimenting, that in practice it is not true that variation of electrode contact resistance merely affects the sensitivity of the instrument, when using a potentiometer method. This follows from the fact that the contact resistance may be many times that of the rock or soil. Consequently we always balance the electrode resistances, whether using metal stakes or porous pots.

F. H. KIHLESTEDT,\* Stockholm, Sweden (written discussion†).—The paper by Mr. Watson and that by Mr. Roman on interpretation of resistivity surveys are valuable contributions to the solution of electrical depth determinations. One advancement made is the negative one of showing that empirical rules, based on sharp turning points of the resistivity curve, are of little use for absolute depth determinations. It is highly improbable that there ever occur any sharp turning points caused by horizontal layers if the field survey is carried out properly.

There is at first the question of obtaining the resistivity curve. In potential surveys, there are two kinds of anomalies that affect the readings; namely, lateral variations, utilized in general prospecting work, and vertical variations used in depth determinations. Hedstrom has referred to the two principal methods of survey as "electrical trenching" and "electrical drilling."

In electrical trenching, influences from vertical variations of resistivity are avoided by using sufficiently large spacing (in the Wenner scheme) or by starting far enough from the current electrode (in the single current electrode system).

In electrical drilling, there is no such easy way to avoid lateral anomalies. The only way out is to survey the resistivity curve in several directions from the same starting point. An average curve, fairly free from lateral effects, is thus obtained, and if the electric-geological conditions are not too complicated, this curve corresponds to *only one combination of horizontal layers*. But the interpretation must be based on a curve free from lateral or surface effects, a matter that was stressed by Dr. Slichter and Professor Fisher at the meeting.

The problem of interpretation has been studied by many authors. I want to add a short description of the method used by the Swedish American Prospecting Corporation, which was developed by the engineers of that organization, notably Karl Sundberg and Helmer Hedstrom.

In solving the two-layer case, the Tagg method gives fairly good results, but, as the depth is determined by curve intersection, if more than two layers are present, an intersection point is usually not found and thus not even an approximate depth may be obtained. The Roman method is, in that respect, preferable, as it seems to permit a determination of the first interface even if a third layer is present at some greater depth. Hummel has shown that two layers with different resistivity may be considered as one layer, when the distance to the current electrode is far in

---

\* Mining Engineer and Geologist.

† This discussion refers also to the paper by Mr. Watson, which begins on page 201.

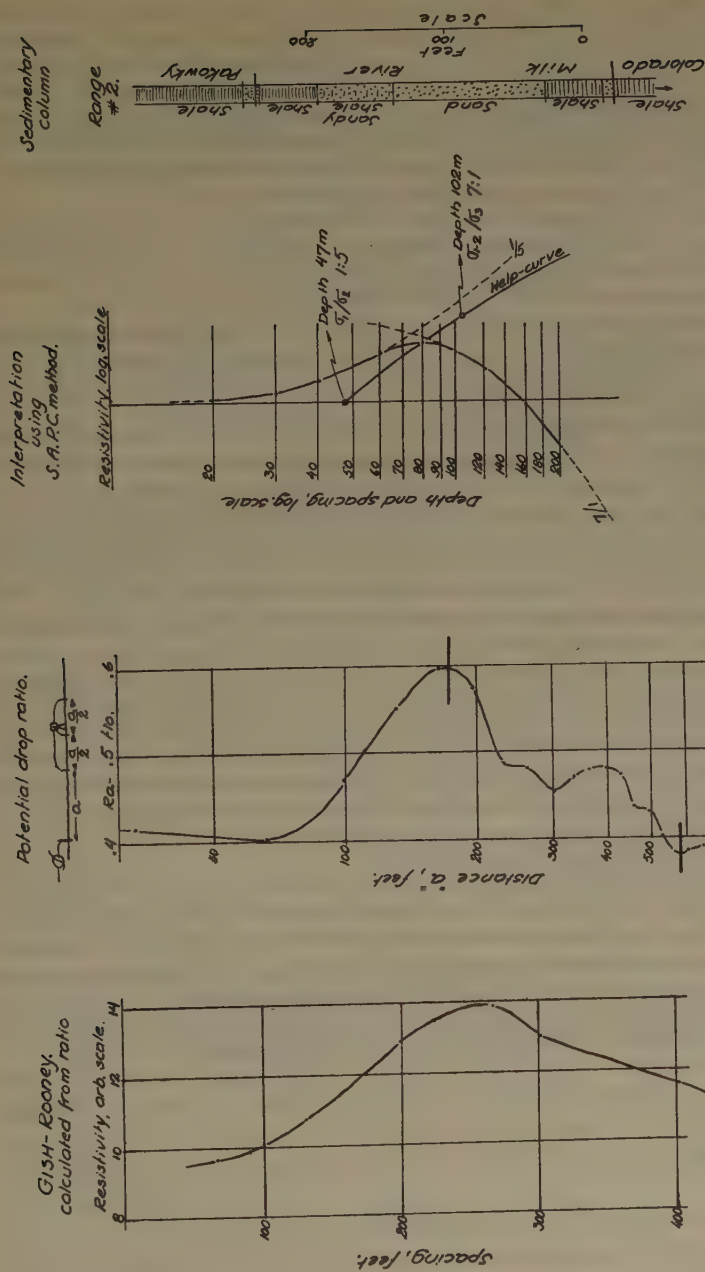


FIG. 27.—DETAIL OF DEPTH DETERMINATION IN SOUTHERN ALBERTA.

excess of the combined thickness of the two layers. The resistivity of this combined layer may be calculated according to Kirchhoff's law of parallel connected resistances.

This observation by Hummel may be used for reducing a multilayer problem to a series of two-layer problems and is used in the Swedish American method. Another feature of this method is that the two-layer base diagram is plotted in a double logarithmic scale, so that the interpretation is independent both of the actual value of the resistivity and the actual depth to the interface. The Racom may therefore be used for rapid and accurate surveying of the resistivity curve.

Presumably the first part of this curve is influenced only by the first interface. Thus the first part may be matched with one of the two-layer curves, which gives the depth to the interface, by observing the position of a point of origin of the base diagram with regard to the spacing of the resistivity curve, and the resistivity ratio.

Hummel's principle then provides a new position of the  $x$  axis for interpretation of the next part of the resistivity curve on the base diagram which corresponds to the third layer. In this way, any number of layers can be determined as long as they are sufficiently prominent to be clearly reflected in the resistivity curve.

One example of this method is shown in Fig. 27, from a survey in southern Alberta. At the time of the survey (several years ago) an empiric rule was used, based upon the potential-drop ratio curve, although we were aware of the fact that such depth determinations were only relative and could be used for structure work only if the electrical characteristics of the beds remained substantially constant. This curve was later interpreted by the method described above. In addition is shown the Gish Rooney resistivity curve calculated in arbitrary units from the ratio curve. The accompanying log is from a well some distance away and shows how the sedimentary column is fairly simple electrically.

In interpretation, two tendencies of the results obtained may be worth mentioning. One is that when the resistivity difference between two layers is very small, the depth determination naturally is not sharp, as a variation in depth is nearly equivalent to a variation of resistivity ratio, and great accuracy, both in the field survey and in the calculation of the base diagram, is required. Another tendency is observed if two interfaces are close together. They have in that case a tendency to spread, giving somewhat shallower depth to the upper and somewhat greater depth to the lower interface as compared with the actual depths.

Mr. Watson's systematic calculation of a set of conditions is very valuable for checking this and other schematic interpretation systems. The conditions he has chosen are also very common in nature; i. e., a poorly conducting layer in the surface, dry soil, etc., then a much better conductor, soil saturated with water, and finally a nonconductor, corresponding to a poorly conducting bedrock. It is feasible to introduce a correction factor for the second source of error mentioned above by systematically interpreting such data as Mr. Watson has presented.



# A Contribution to the Theory of the Interpretation of Resistivity Measurements Obtained from Surface Potential Observations

By R. J. WATSON,\* BOULDER, COLO.

(New York Meeting, February, 1934)

IN an earlier paper, Ehrenburg and Watson<sup>1</sup> published the development for a potential function by which it is possible to obtain the electric potential at points on the surface of the ground when a current  $I$  passes between two electrodes and the subsoil is composed of parallel, homogeneous layers. In view of the continued interest in the resistivity method of electrical prospecting, the author has considered it desirable to publish the results of a number of theoretical studies making use of this potential function, and also the results of a considerable number of tests with models designed to show the soundness of the mathematical theory. It is hoped that these results will prove how erroneous the various empirical rules for depth determination may be.

It has always seemed puzzling to the author that one can find, in papers published comparatively recently, statements upholding empirical rules for depth determination, and attributing most of the irregularities of resistivity curves to vertical discontinuities in resistivity in the subsoil. It would indeed be fortunate for the geophysical investigator if such a simple rule held. However, numerous investigators have proved both theoretically and by the success of their field work that such a rule does not hold, even by a "rough approximation" in many cases. On the other hand, as is shown in the development to follow, if the underground conditions are favorable it is possible for such empirical rules to give a satisfactory depth determination.

Authors should be more careful about making such sweeping statements about the accuracy of these empirical rules because the relative simplicity of the field work places the method in the hands of any interested experimenter, and he is likely to become completely disgusted with the method after he has made several obviously wrong interpretations by empirical rules.

There are simple and rapid methods for finding out whether the ground beneath the electrodes is sufficiently similar to the conditions

---

Manuscript received at the office of the Institute Oct. 16, 1933.

\* Department of Geology, University of Colorado.

<sup>1</sup> D. O. Ehrenburg and R. J. Watson: Mathematical Theory of Electrical Flow in Stratified Media, etc. *Trans. A.I.M.E.* (1932) **97**, 423.

postulated in the mathematical treatment to warrant a depth determination by scientific methods. If these conditions do not prevail, the interpretation must be considered as purely qualitative, and the interpreter should clearly say so and not be led into guessing. Such guessing in many cases has brought no great fame to electrical methods of prospecting.

The scientific methods of interpretation developed to date are of two types, the first being the method of Tagg, which can be used on two-layer problems and special types of problems involving more than two layers, and the second being the method of comparison in which field resistivity curves are compared with curves computed for ideal cases.

For problems involving two layers, Tagg's method<sup>2</sup> and the method of comparison with computed curves prove satisfactory when underground conditions justify a quantitative depth determination. The three-layer problems present more difficulties. However, a special type of three-layer problem in which each succeeding layer is several times thicker than the layer above can be treated as an extension of a two-layer problem after the fashion of Tagg's method, by breaking it into two parts. The first part is the determination of the thickness of the top layer and the ratio of resistivity between the top and the middle layer. The second part, which is the determination of the depth of the middle layer, can then be accomplished by making use of the idea of combined resistivity shown by Hummel.<sup>3</sup> The two top layers are combined following Hummel's method to give a single layer of resistivity determined from the resistivities and relative thicknesses of these two top layers. By a proper choice of this combined resistivity, the problem can be solved like one of two layers. Of course the kernel of this method lies in the assumption that the third layer is so deep that for small electrode spacings its effect will be negligible. With more than three layers the method becomes very cumbersome. Poldini<sup>4</sup> has shown how three-layer problems of this special type may also be interpreted by curve matching.

When the three-layer curve is not of this special type, the method of curve matching is then perhaps the most reliable. Of course for this purpose a great number of computed curves must be used, but this method of interpretation is not unusual in geophysical work. When the preliminary tests convince the investigator that the electrical character of the ground is sufficiently similar to that assumed in the mathematical development, he is justified in making the necessary mathematical

---

<sup>2</sup> G. F. Tagg: Interpretation of Resistivity Measurements. Page 135, this volume.

<sup>3</sup> J. N. Hummel: Theoretical Study of Apparent Resistivity. *Trans. A.I.M.E.* (1932) 97, 392.

<sup>4</sup> E. M. Poldini: Les sondages électrique (Electrical Drilling). *Bull. Technique de la Suisse Romande* (Lausanne) 7.

calculations as in torsion balance investigations. There exist already a number of computed data for torsion balance interpretations, and it seems to the author that it is time a nucleus of electrical data should be established. Tagg has made a fine beginning in his method for the two-layer problem and it is hoped that the small nucleus of computed curves offered in this paper will be added to by other investigators.

In this paper the mathematical theory is considered for several configurations of electrodes when the underground is either homogeneous or composed of parallel, homogeneous, isotropic layers. Following this, the method of calculating theoretical apparent resistivity curves, using the potential function of Ehrenburg and Watson, is briefly reviewed. The results of these calculations for 49 cases are given in the form of resistivity curves. Forty-one of these curves are for three-layer problems, and the remaining eight are for four-layer problems. The three-layer curves cover sufficiently varied conditions to make them useful for general interpretation purposes for cases where the bottom layer can be considered a perfect resistor. The four-layer curves are published chiefly to show the possibilities for error when an empirical rule is used for depth determination.

The results of 14 model experiments are given to serve as a check on the mathematical development. These comprise models for two, three and four layers, in all of which the lowest layer is a perfect resistor. These results confirm the mathematical theory.

#### MATHEMATICAL THEORY FOR ELECTRIC FLOW IN HOMOGENEOUS MEDIA

The electric potential at a point on the surface of homogeneous ground due to a point-source placed at the surface as given in the paper of Ehrenburg and Watson<sup>5</sup> is:

$$v = \frac{\rho I}{2\pi R} \quad [1]$$

where  $R$  is the distance from the point to the source of strength  $I$ , and  $\rho$  is the resistivity of the earth. Making use of this simple equation, expressions for the resistivity of the ground may be derived when two or more current electrodes are used and differences in potential between points on the surface are measured. This is exactly the procedure of resistivity prospecting. In the discussion to follow, expressions for the resistivity of the earth will be derived when the configuration of electrodes follows the plan of Wenner,<sup>6</sup> Lee,<sup>7</sup> and a method called by Ehrenburg and Watson

<sup>5</sup> Reference of footnote 1.

<sup>6</sup> Wenner, F.: A Method of Determining Earth Resistivity. U. S. Bur. Stds. *Sci. Paper* 258 (1915) 469-478.

<sup>7</sup> F. W. Lee, J. W. Joyce and P. Boyer: Some Earth Resistivity Measurements. U. S. Bur. Mines *Inf. Circ.* 6171 (1929).

the "one-electrode system" but which is identical with what Eve and Keys<sup>8</sup> call the "single-probe method."

In all these methods it must be remembered that the current penetrates more deeply as the current electrodes are placed farther apart. It can be shown, without much difficulty, that approximately 30 per cent of the current penetrates below a depth equal to one-third of the distance between the current electrodes. Weaver<sup>9</sup> and Bardeen and Peters<sup>10</sup> have discussed this in their papers.

*Derivation of Value of Resistivity of Earth Using Wenner Configuration of Electrodes*

The configuration is shown in Fig. 1.  $C_1$  and  $C_2$  are the current electrodes,  $P_1$  and  $P_2$  are the potential electrodes. They are placed in a line at a distance  $a$  apart. Taking advantage of this symmetrical configuration, the derivation of the value of the resistivity may be easily obtained.

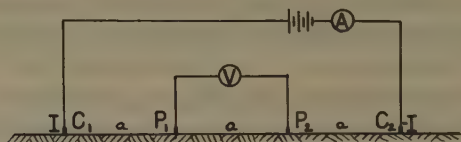


FIG. 1.—WENNER CONFIGURATION OF ELECTRODES.

Using equation 1,

$$v_1 = \frac{\rho I}{2\pi} \left( \frac{1}{a} - \frac{1}{2a} \right) = \frac{\rho I}{4\pi a} \quad (v \text{ at } P_1)$$

$$v_2 = \frac{\rho I}{2\pi} \left( \frac{1}{2a} - \frac{1}{a} \right) = \frac{-\rho I}{4\pi a} \quad (v \text{ at } P_2)$$

The difference in potential that may be measured with a potentiometer is  $(v_1 - v_2)$ . Thus,

$$v_1 - v_2 = \Delta v = \frac{\rho I}{2\pi a}$$

Transposing, the resistivity may be written

$$\rho = 2\pi a \frac{\Delta v}{I} \quad [2]$$

In connection with the Wenner configuration, it can be shown that it does not matter whether the current electrodes are inside or outside of the potential electrodes. At first thought this may seem rather odd

<sup>8</sup> A. S. Eve and D. A. Keys: Applied Geophysics, 107. Macmillan.

<sup>9</sup> W. Weaver: Certain Applications of the Surface Potential Method. *Trans. A.I.M.E.* (1929) 81, 68.

<sup>10</sup> J. Bardeen and L. J. Peters: The Solution of Some Theoretical Problems which Arise in the Electrical Method of Geophysical Exploration. Univ. Wisconsin Eng. Expt. Station *Bull.* 70 (1930).



because the current paths must be quite different in the two cases, the penetration being much greater in the latter case. The derivation is simple and is as follows:

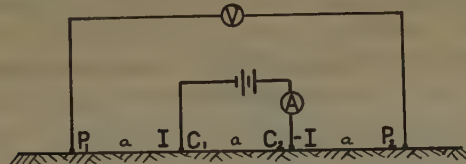


FIG. 2.—ALTERNATE WENNER CONFIGURATION.

$$v_1 = \frac{\rho I}{2\pi} \left( \frac{1}{a} - \frac{1}{2a} \right) = \frac{\rho I}{4\pi a} \quad (v \text{ at } P_1)$$

$$v_2 = \frac{\rho I}{2\pi} \left( \frac{1}{2a} - \frac{1}{a} \right) = \frac{-\rho I}{4\pi a} \quad (v \text{ at } P_2)$$

$$\Delta v = \frac{\rho I}{2\pi a}$$

and

$$\rho = 2\pi a \frac{\Delta v}{I} \quad [3]^*$$

#### *Derivation of Value of Resistivity of Earth Using Lee Configuration of Electrodes*

In Fig. 3 a plan of the Lee configuration of electrodes is shown.  $C_1$  and  $C_2$  are the current electrodes,  $P_1$ ,  $P_2$  and  $P_3$  are the three potential electrodes. They are all placed in a line and the configuration differs

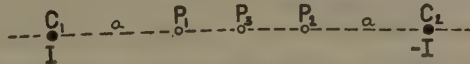


FIG. 3.—LEE CONFIGURATION OF ELECTRODES.

from the Wenner only in that a third potential electrode  $P_2$  is placed midway between the current electrodes and serves to partition the electrodes. For homogeneous ground this third electrode would constitute a "neutral tap."

In practice two values of  $\Delta v$  are measured, one between  $P_1$  and  $P_3$  and the other between  $P_2$  and  $P_3$ . In this derivation the strength of the sources is assumed equal to  $I$  and  $-I$ , and so the potential at  $P_3$  will be zero. The potential at  $P_1$  and  $P_2$  will be the same as in the Wenner system. Then the value for the resistivity taken from either side will be:

$$\rho = 4\pi a \frac{\Delta v}{I} \quad [4]$$

but the value of  $\Delta v$  will be only one-half of its value in the Wenner method.

Obviously, the chief advantage of this method over the Wenner is that the field operator obtains an idea of the uniformity of the resistivity of the ground, but as to depth determination, it has no advantage

\* See author's reply to discussion, page 235.

theoretically. If the measured resistivity of the two sides is very different, the interpreter is not justified in assuming that the resistivity of the subsoil is approximately uniform laterally, and an exact depth determination should not be attempted.

*Derivation of Value of Resistivity of Earth Using One-electrode Configuration of Electrodes*

A plan view of this configuration of electrodes is shown in Fig. 4. By placing  $C_2$  at a sufficient distance from  $C_1$ , the potential distribution around  $C_1$  can be assumed as due to  $C_1$  only. To make this most effective, the field practice is to measure the potential at points along the circumference of a circle with center at  $C_2$  and radius equal to the distance between  $C_1$  and  $C_2$ . However, for distances away from  $C_1$  small compared to the distance between  $C_1$  and  $C_2$ , the potential line may be taken at right angles to  $C_1C_2$  as shown in the figure. Then at points along the

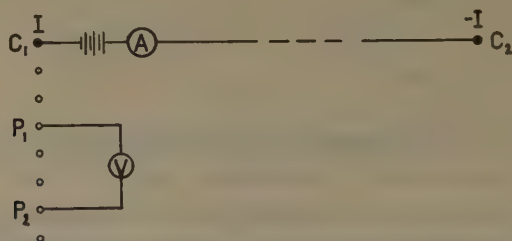


FIG. 4.—ONE-ELECTRODE CONFIGURATION OF ELECTRODES.

potential line, the potential due to  $C_2$  is very nearly equal and can be neglected because it will drop out in making the expression  $\Delta v$ .

The points at which the potential is measured are usually equally spaced for convenience in computing, and it is customary to place the two potential electrodes so that  $P_2$  is twice as far from  $C_1$  as  $P_1$ . The distance from  $C_1$  to  $P_1$  may be considered as  $a$ , and the distance to  $P_2$  as  $2a$ . Then,

$$v_1 = \frac{\rho I}{2\pi a} \quad (v \text{ at } P_1)$$

$$v_2 = \frac{\rho I}{4\pi a} \quad (v \text{ at } P_2)$$

$$\Delta v = \frac{\rho I}{4\pi a}$$

hence

$$\rho = 4\pi a \frac{\Delta v}{I} \quad [5]$$

This is the same expression as in the Lee method and is similar to the Wenner, differing only by the factor 2. Thus although the current flows

in an entirely different manner through the subsoil, because the two current electrodes are now very far apart, the expression for the resistivity is the same. It is also to be noted that in this method only the potential electrodes are moved, but that with increasing values of  $a$  the effects of the lower parts of the subsoil become more apparent. The extent of this effect will be made more clear when the subsoil is considered as composed of homogeneous parallel layers of different resistivities.

Now, the expressions derived for these three cases apply only to homogeneous ground. What can be said about this matter when the ground is not homogeneous in resistivity? As will be shown in the derivations to follow in the next section, the value of the resistivity obtained by any of these three configurations of electrodes will be the same when the subsoil is composed of homogeneous parallel layers. When the subsoil is not homogeneous in resistivity or is not composed of homogeneous parallel layers, the values of resistivity determined by the three methods may not be the same; in fact, they are practically always different. This can be easily imagined if one considers the possible distortions of the normal electric flow due to lateral variations in the resistivity of the subsoil.

When the ground is not homogeneous in resistivity, the value of resistivity determined has been called the "apparent resistivity" and cannot be considered to be the resistivity of a definite depth of earth but rather a weighted average of the layers of different resistivities, the weighing being constantly changed with the electrode spacing.

#### MATHEMATICAL THEORY OF ELECTRIC FLOW APPLIED TO DEPTH DETERMINATION OF DISTURBING MASSES HAVING RESISTIVITIES DIFFERENT FROM THOSE OF THE SURROUNDING MATERIAL

##### *Scope of Problem*

The problem of finite bodies of differing resistivity has been attacked with some success by Hummel.<sup>11</sup> A moment's consideration of the possible apparent resistivity curves that could be obtained when such conditions prevail convinces one that only with a considerable theoretical knowledge can one hope to distinguish the effects of lateral and vertical discontinuities in resistivity in the subsoil. Also, the more geological information the interpreter has at hand the better will he be able to ascribe the results obtained to their proper causes. In general, however, it is not safe to assume that changes in lithologic character are always accompanied by changes in resistivity. When one fully realizes the complexity of conditions that are possible with finite bodies, one is quickly led to the conclusion that the determination of the depth as well as the areal extent of such bodies is, even for the most favorable conditions, a most difficult problem. Resistivity problems thus can be divided

---

<sup>11</sup> J. N. Hummel: Reference of footnote 3, 397.

logically into two main groups, the one being the areal extent of finite bodies and the other the depth to layers of differing resistivity that are assumed to extend laterally to a great distance.

Since the problem of the areal extent of finite bodies is largely qualitative in its interpretation, this particular field of resistivity prospecting will be dismissed with this brief mention. The problem of depth determination, on the contrary, is largely quantitative in its interpretation, and thus it becomes imperative to have data prepared so that these interpretations may be made as directly as possible.

Obviously, the more closely the field conditions approach those assumed in the mathematical theory, the more exact will be the depth determination. If these ideal conditions are not closely realized in the field, the depth determination is likely to be in great error, because, not knowing the character of the departure from the ideal conditions, there is no way of compensating for it. When the possible departures from the ideal case of parallel homogeneous beds are considered, one can easily understand how much more abrupt changes in resistivity values with electrode spacing may be obtained than are allowed for in the ideal cases. That these abrupt changes are not always of diagnostic value in depth determination is only too true. When an empirical rule does give correct results, the rules are held up as sufficiently correct for general interpretation, but when they give wildly erroneous results, as they frequently do, some very interesting assumptions are put forward to explain away the trouble. The author's field experience has convinced him that there are many times when the only conclusion to be reached from the field data is that conditions are too complex to make a depth determination and that the results can be used only qualitatively, if at all.

The object of this paper is twofold: first, to show that the only safe method of interpretation is the one in which the physical principles demonstrated by mathematical computation and checked by model experimentation are used as a basis, and second, to present a first nucleus of computed data to be used in the interpretation of three-layer problems.

*Use of Ehrenburg-Watson Potential Function in Calculating Potential at Points on Surface When Subsoil Is Composed of Homogeneous Parallel Beds*

Only the application of this potential function to resistivity problems will be considered in this section, but this same function can be applied to any surface potential method when the subsoil may be considered as being made up of a series of parallel homogeneous layers. Naturally, this potential function is similar to those developed by other authors using the image theory, but it is believed that it possesses some points of superiority, which will be commented upon shortly. A detailed account



of the derivation of this function may be found in the paper by Ehrenburg and Watson.<sup>12</sup> The function will be assumed derived.

Ehrenburg and Watson found that in the case of a point electrode of strength  $I$  at the surface, the potential at any point  $P$ , also on the surface, at a distance  $R$  from this electrode could be expressed as follows

$$v = \frac{\rho_1 I}{2\pi} \left[ \frac{1}{R} + \frac{2Q_1}{\sqrt{R^2 + m^2}} + \frac{2Q_2}{\sqrt{R^2 + (2m)^2}} + \frac{2Q_3}{\sqrt{R^2 + (3m)^2}} + \cdots \right] \quad [6]$$

where  $\rho_1$  is the resistivity of the top layer,  $R$  is the distance along the surface from  $P$  to the current electrode  $I$ ,  $m$  is the distance from  $P$  to the first image,  $2m$  the distance to the second image, etc., and  $Q_1, Q_2$ , etc., are the coefficients of the strengths of the images. Thus, the first term within the bracket is due to the source and the following terms are due to the images. If the ground were homogeneous  $Q$  would vanish and the expression for potential would reduce to that given by equation 1. A clearer idea of how this potential expression is built up may be given by means of Fig. 5.

In setting up an ideal problem such as is shown in Fig. 5, all the beds are arbitrarily made  $m/2$  or some multiple of  $m/2$  in thickness. This makes all the images lie at distances of  $m$  apart, and herein lies the particular advantage of this potential function. The positions of all the images are always known, and the only difficulty becomes the determination of their strengths. In Fig. 5 a three-layer problem has been selected. Here, the top layer is  $m/2$  thick, the second layer,  $6m/2$ , and the lowest layer is assumed to extend infinitely downward. Of course all three layers are assumed to extend to an infinite distance laterally but for practical purposes all that is necessary is that the lateral extent be large compared to the depth of the two top layers.

As in every other case, the images will lie at  $m, 2m, 3m$ , etc., out to infinity. The factor 2 occurring with the  $Q$ 's in equation 6 takes into account the fact that the air-earth boundary acts as a perfect mirror and for every image underground there will be a corresponding one of equal strength in the air.

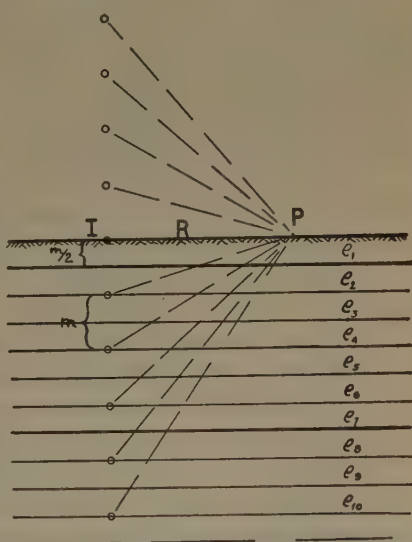


FIG. 5.—POSITIONS OF THE SOURCE, IMAGES AND ELECTRODES IN THE CASE OF PARALLEL, HOMOGENEOUS BEDS.

<sup>12</sup> Reference of footnote 1.

The formulas for  $Q$  were derived in the paper of Ehrenburg and Watson up to  $Q_4$  in terms of  $A$ , which has been called the "reflection coefficient." The general expression for  $A_n$  given in the earlier paper is

$$A_n = \frac{\rho_{n+1} - \rho_n}{\rho_{n+1} + \rho_n} \quad [7]$$

where  $\rho_n$  and  $\rho_{n+1}$  are the resistivities of the  $n$  and  $n+1$  layers, each of thickness  $m/2$ .

In the table for  $Q$  given below, the values of  $Q$  up to  $Q_6$  are given. For three-layer and four-layer problems all the remaining values of  $Q$  needed can be obtained easily by symmetry from those given here.

*Table of Values for  $Q$*

$$\begin{aligned} Q_1 &= A_1 \\ Q_2 &= (1 - A_1^2)A_2 + A_1Q_1 \\ Q_3 &= (1 - A_1^2)(1 - A_2^2)A_3 + (A_1 - A_1A_2)Q_2 + A_2Q_1 \\ Q_4 &= (1 - A_1^2) \cdot \cdot \cdot (1 - A_3^2)A_4 + (A_1 - A_1A_2 - A_2A_3)Q_3 \\ &\quad + (A_2 - A_1A_3 + A_1A_2A_3)Q_2 + A_3Q_1 \\ Q_5 &= (1 - A_1^2) \cdot \cdot \cdot (1 - A_4^2)A_5 + (A_1 - A_1A_2 - A_2A_3 - A_3A_4)Q_4 \\ &\quad + (A_2 - A_1A_3 - A_2A_4 + A_1A_2A_3 + A_1A_3A_4 - A_1A_2A_3A_4)Q_3 \\ &\quad + (A_3 - A_1A_4 + A_1A_2A_4 + A_2A_3A_4)Q_2 + A_4Q_1 \\ Q_6 &= (1 - A_1^2) \cdot \cdot \cdot (1 - A_5^2)A_6 \\ &\quad + (A_1 - A_1A_2 - A_2A_3 - A_3A_4 - A_4A_5)Q_5 \\ &\quad + (A_2 - A_1A_3 - A_2A_4 - A_3A_5 + A_1A_2A_3 + A_1A_3A_4 + A_1A_4A_5 \\ &\quad - A_1A_2A_3A_4 - A_1A_2A_4A_5 - A_1A_3A_4A_5)Q_4 \\ &\quad + (A_3 - A_1A_4 - A_2A_5 + A_1A_2A_4 + A_2A_3A_4 + A_1A_3A_5 \\ &\quad + A_2A_4A_5 - A_1A_2A_3A_5 - A_1A_3A_4A_5)Q_3 \\ &\quad + (A_4 - A_1A_5 + A_1A_2A_5 + A_2A_3A_5 + A_3A_4A_5)Q_2 + A_5Q_1 \end{aligned}$$

The ideal curves in this paper were computed with a potential electrode spacing interval of  $m/4$ . That is, if the thinnest bed in the vertical section has a thickness of  $m/2$ , the electrode spacing ( $a$  in the Wenner method) is increased by intervals of  $m/4$ . Obviously, the scale is purely arbitrary. For instance, if  $m/2$  is set equal to 20 ft., the electrode spacing will increase by intervals of 10 feet.

Now, since the positions of the images are the same for all the problems, it is convenient to make a set of tables of the distances from the point  $P$  on the surface to the various images. Fig. 6 shows how this is done.

Letting the value of the electrode spacing interval  $m/4$  be equal to unity, the depth of the images will be 4, 8, 12, 16, etc. Then in equation 6, the values of the radicals in the denominators will be as follows for  $v_1$ :

$$\begin{aligned} \sqrt{R^2 + m^2} &= \sqrt{1 + 16} \\ \sqrt{R^2 + (2m)^2} &= \sqrt{1 + 64} \\ \sqrt{R^2 + (3m)^2} &= \sqrt{1 + 144} \text{ and so forth,} \end{aligned}$$

and for  $v_2$ :

$$\begin{aligned}\sqrt{R^2 + m^2} &= \sqrt{4 + 16} \\ \sqrt{R^2 + (2m)^2} &= \sqrt{4 + 64} \\ \sqrt{R^2 + (3m)^2} &= \sqrt{4 + 144} \text{ and so forth,}\end{aligned}$$

and similarly for all other values of  $v$ .

For the purpose of computing, tables have been constructed giving the value of the reciprocal of the square roots. As many as *forty* terms of the series have been used in calculating the potential at a single point. Of course the points farther from the current electrodes require more terms for their calculation because the distances to the images do not increase as rapidly as for those close to the electrode. These tables may be used in any problem requiring the potential at points on the surface when the underground is composed of parallel homogeneous layers. The construction of these tables requires considerable time, but they are well worth the trouble when one considers the tremendous amount of labor they save in the routine calculation of resistivity curves.

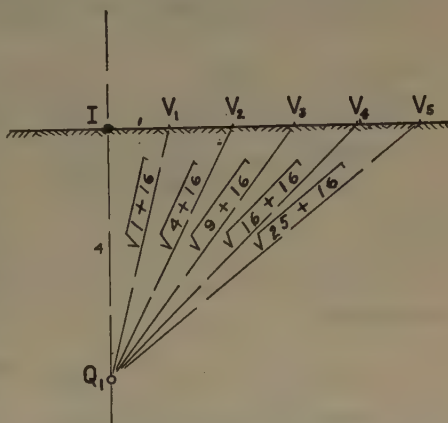


FIG. 6.—IMAGE DISTANCES TO POINTS ON THE SURFACE.

It is realized that the weakness of this solution and all other solutions that make use of the summation of image effects lies in the slow convergence of the infinite series. Several papers<sup>13</sup> published since that by Ehrenburg and Watson contain solutions in which more rapidly converging series are used, but an extensive knowledge of advanced mathematics is necessary to obtain numerical results.

#### *Derivation of Value of Resistivity of Earth as Measured on Surface When Subsoil is Composed of Parallel, Homogeneous Layers*

In this section formulas will be derived for the three configurations of electrodes used before; the Wenner, the Lee, and the One-electrode.

*Wenner Configuration of Electrodes.*—The derivation is identical with that on page 6 except that instead of using the simple potential function given by equation 1, equation 6 must now be used. Then,

<sup>13</sup> L. V. King: On the Flow of Electric Current in Semi-infinite Stratified Media. *Proc. Royal Soc. London* (1933) **139**, 237-277.

M. Muskat: Potential Distribution About an Electrode on the Surface of the Earth. *Physics* (1933) **4**, 129-147.

$$\begin{aligned}
 v_1 &= \frac{\rho_1 I}{2\pi} \left[ \frac{1}{a} + \frac{2Q_1}{\sqrt{a^2 + m^2}} + \frac{2Q_2}{\sqrt{a^2 + (2m)^2}} + \frac{2Q_3}{\sqrt{a^2 + (3m)^2}} + \dots \right. \\
 &\quad \left. - \frac{\rho_1 I}{2\pi} \left[ \frac{1}{2a} + \frac{2Q_1}{\sqrt{(2a)^2 + m^2}} + \frac{2Q_2}{\sqrt{(2a)^2 + (2m)^2}} + \frac{2Q_3}{\sqrt{(2a)^2 + (3m)^2}} + \dots \right] \right. \\
 &= \frac{\rho_1 I}{2\pi} \left[ \frac{1}{2a} + 2Q_1 \left\{ \frac{1}{\sqrt{a^2 + m^2}} - \frac{1}{\sqrt{(2a)^2 + m^2}} \right\} + \dots \right. \\
 v_2 &= \frac{\rho_1 I}{2\pi} \left[ \frac{1}{2a} + \frac{2Q_1}{\sqrt{(2a)^2 + m^2}} + \frac{2Q_2}{\sqrt{(2a)^2 + (2m)^2}} + \frac{2Q_3}{\sqrt{(2a)^2 + (3m)^2}} + \dots \right. \\
 &\quad \left. - \frac{\rho_1 I}{2\pi} \left[ \frac{1}{a} + \frac{2Q_1}{\sqrt{a^2 + m^2}} + \frac{2Q_2}{\sqrt{a^2 + (2m)^2}} + \frac{2Q_3}{\sqrt{a^2 + (3m)^2}} + \dots \right] \right. \\
 &= -\frac{\rho_1 I}{2\pi} \left[ \frac{1}{2a} + 2Q_1 \left\{ \frac{1}{\sqrt{a^2 + m^2}} - \frac{1}{\sqrt{(2a)^2 + m^2}} \right\} + \dots \right]
 \end{aligned}$$

Then

$$\Delta v = \frac{\rho_1 I}{2\pi} \left[ \frac{1}{a} + 4Q_1 \left\{ \frac{1}{\sqrt{a^2 + m^2}} - \frac{1}{\sqrt{(2a)^2 + m^2}} \right\} + \dots \right]$$

Now since

$$\rho_a = 2\pi a \frac{\Delta v}{I}$$

$$\rho_a = \frac{2\pi a}{I} \cdot \frac{\rho_1 I}{2\pi} \left[ \frac{1}{a} + 4Q_1 \left\{ \frac{1}{\sqrt{a^2 + m^2}} - \frac{1}{\sqrt{(2a)^2 + m^2}} \right\} + \dots \right]$$

or

$$\rho_a = \rho_1 [1 + 4a \{ Q_1 P_{a_1} + Q_2 P_{a_2} + Q_3 P_{a_3} + \dots \}] \quad [8]$$

where the  $P$ 's are the values of the brackets in the previous equation and remain the same for all the problems in which the two potential electrodes are placed so that one is always twice as far away from the current electrode as the other. Equation 8 may be written in more compact form,

$$\rho_a = \rho_1 \left[ 1 + 4a \sum_{n=1}^{n=\infty} Q_n P_{a_n} \right] = \rho_1 (1 + B_a) \quad [9]$$

*Lee Configuration of Electrodes.*—On substituting the potential function 6, results identical with the Wenner configuration are obtained.

*One-electrode Configuration of Electrodes.*—This method also gives identical results with the Wenner method.

#### *Computation of Typical Problem Using Ehrenburg-Watson Potential Functions*

One of the three-layer problems computed in this paper is shown in Fig. 7. The first operation is the calculation of the values of  $Q$  according to the formulas given above. For this problem the values are:



$n$	$Q_n$	$n$	$Q_n$	$n$	$Q_n$	$n$	$Q_n$
1	-0.960	8	0.916	15	-0.888	22	0.954
2	0.922	9	-0.886	16	0.946	23	-0.985
3	-0.885	10	0.934	17	-0.981	24	1.000
4	0.928	11	-0.971	18	1.000	25	-0.936
5	-0.966	12	1.000	19	-0.940	26	0.907
6	1.000	13	-0.947	20	0.907	27	-0.896
7	-0.954	14	0.911	21	-0.892	28	0.962

The set of tables giving the values of the distances of the images designated by  $P$  are assumed already prepared. For this work the values

of  $P_a$  for a particular value of  $a$  were mimeographed on a sheet that was used for computing. Each sheet contained the necessary values for computing *one* point on a resistivity curve. The values of  $Q$  given above could be used for all the points on the curve for a single problem. A sample sheet of the computation for potential electrode spacing No. 13, that is, for  $a = 13$ , is

shown below. If the first layer in Fig. 7 were 20 ft. thick, the sheet would give the calculations for  $a = 130$  ft.; if the thickness of the top layer were 50 ft., the calculations would be for  $a = 325$  feet.

Since the infinite series does not converge rapidly, it would be convenient to estimate the error caused by dropping terms. Only in cases where the series is alternating in sign and with each succeeding term of smaller absolute value than the preceding term can this error be conveniently determined. In all other cases in this paper the series has been continued until the last term included is not more than one per cent of the first term. This is the procedure followed in the four-layer curves. In the three-layer curves an independent check was used because the lowest layer in all these problems was considered to be a perfect insulator. In all problems of this type, given on Figs. 9 to 15, the value of resistivity approaches asymptotically a straight line through the origin. This fact was noted by Hummel.<sup>14</sup> The slope of this line can be calculated rather easily by making use of another fact brought out by Hummel. For values of  $a$  much greater than the depth of the several beds lying on the layer of infinite thickness, a combined resistivity can be used for the overlying beds which is obtained from the simple formula:

$$\frac{h_c}{\rho_c} = \frac{h_1}{\rho_1} + \frac{h_2}{\rho_2} + \frac{h_3}{\rho_3} + \dots + \frac{h_n}{\rho_n} \quad [10]$$

<sup>14</sup> J. N. Hummel: Reference of footnote 3, 406.

where  $\rho_c$  is the "combined resistivity,"  $h_c$  is the combined depth, and  $h_1, h_2, h_3$ , etc. are the thicknesses of the various beds of resistivities  $\rho_1, \rho_2, \rho_3$ , etcetera.

For example, in the problem of Fig. 7, for values of  $a$  much greater than the depth to the perfect insulator, the resistivities of the top layers may be lumped to give a combined resistivity as follows:

$$\frac{4}{\rho_c} = \frac{1}{1} + \frac{3}{1/49} = 148, \text{ or } \rho_c = \frac{4}{148} = 0.027$$

Thus, for calculating that part of the curve for which the potential electrode spacing is well in excess of the depth to the perfect resistor, the

n	Q <sub>n</sub>	P <sub>2n</sub>	Positive Product	Negative Product
1	- 0.960	0.0355		0.0341
2	0.922	0.0287	0.0265	
3	- 0.885	0.0216		0.0191
4	0.928	0.0158	0.0146	
5	- 0.966	0.0114		0.01105
6	1.000	0.00838	0.00838	
7	- 0.954	0.00622		0.00593
8	0.916	0.00470	0.00430	
9	- 0.886	0.00361		0.00311
10	0.934	0.00281	0.00262	
11	- 0.971	0.00223		0.00216
12	1.000	0.00189	0.00189	
13	- 0.947	0.00146		0.00138
14	0.911	0.00120	0.00109	
15	- 0.888	0.000995		0.000884
16	0.946	0.000836	0.000790	
17	- 0.981	0.000708		0.000695
18	1.000	0.000631	0.000631	
19	- 0.940	0.000519		0.000488
20	0.907	0.000450	0.000408	
21	- 0.892	0.000392		0.000350
22	0.954	0.000343	0.000327	
23	- 0.985	0.000302		0.000298
24	1.000	0.000268	0.000268	
			0.061804	0.079545
Positive Total		0.0618		
Negative Total		0.0795		
Difference		- 0.0177	$\times (4 \times 13) = - 0.922$	

$$e_{13} = 0.078$$

FIG. 8.—SAMPLE OF CALCULATION SHEET.

problem can be treated as one of two layers, the resistivity of the top layer being now 0.027 and of the lower layer infinity. In this way the straight line could be obtained more easily. This same method may be employed to calculate the portion of resistivity curves for which the potential electrode spacing is greatly in excess of the total depth to the layer of infinite thickness.

There is a still easier way to use Hummel's results in cases where the lowest layer is a perfect resistor. For any point on the curve the value of the resistivity is obtained by means of formula 9,

$$\rho_a = \rho_1(1 + B_a)$$

where  $B_a$  is four times the value of the infinite series multiplied by  $a$ . Since for these curves  $\rho_1$  has been selected arbitrarily as equal to unity, the value of resistivity is simply

$$\rho_a = 1 + B_a$$

The straight line given by Hummel for the case when the top layer has a resistivity of unity and the lower layer infinity has a slope equal to

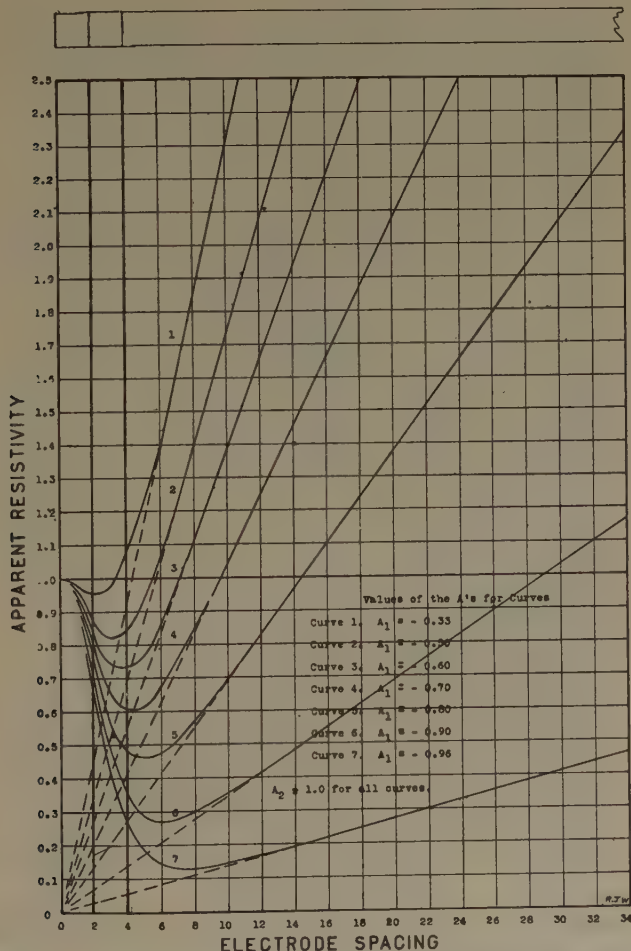


FIG. 9.—THREE-LAYER PROBLEM, SHOWING EFFECT OF VARYING RESISTIVITY OF MIDDLE LAYER.

1.3863 when the electrode spacing in units equal to the depth of the upper layer is plotted against the resistivity. Fig. 16 shows the situation clearly. To make use of this curve, the total thickness of the top layers above the perfect resistor in the three-layer problem is taken as one

unit of electrode spacing on Fig. 16. For the problem being considered, eight units of electrode spacing equal one unit on the abscissa of Fig. 16.

Referring to expression 9, it will be seen that the value of  $\rho_a$  will change with the value of  $\rho_1$ . Thus in Fig. 16, there may be drawn a series of straight lines of different slopes depending on the value of  $\rho_1$ . In the problem under consideration  $\rho_1$  is not unity but 0.027. For the electrode

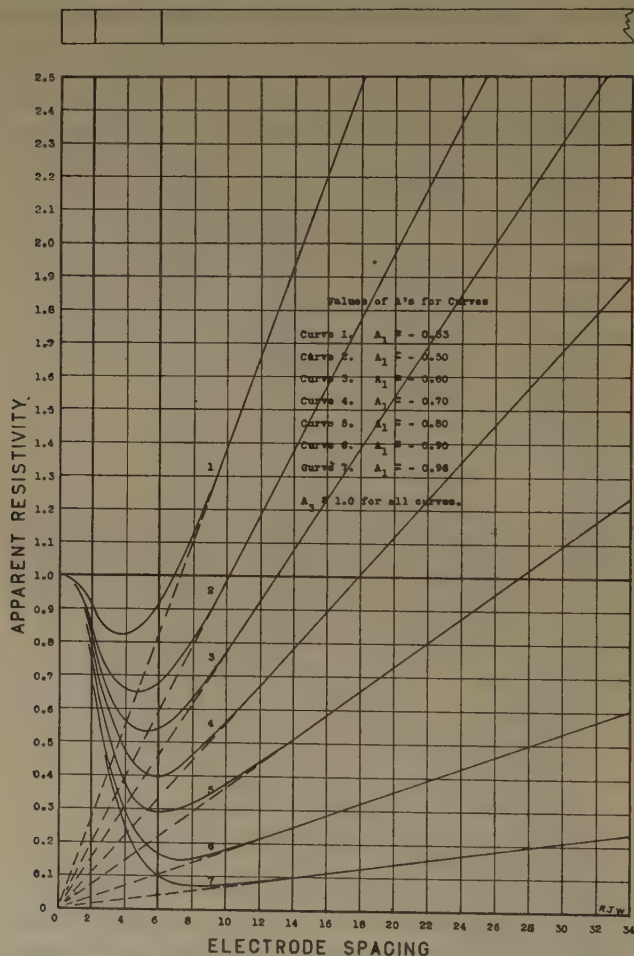


FIG. 10.—THREE-LAYER PROBLEM, SHOWING EFFECT OF VARYING RESISTIVITY OF MIDDLE LAYER.

spacing equal to the depth of the bed and with  $\rho_1 = 1$ , the value of the resistivity is given by a straight line with slope 1.386, then the value of  $1 + B_a$  for  $a = 1$  will be 1.386. Referring to the problem in question, for electrode spacing equal to eight units, the value of resistivity for the straight line will be  $0.027 \times 1.386$ . Thus the slope of the asymptotic line may be easily obtained.



Now the values of resistivity as computed from the infinite series gradually approach this line, and if a sufficient number of terms are used, the resistivity curve will gradually merge with it. However, for electrode spacings past 20 units, the number of terms that must be included in the series becomes cumbersome and any short cut is most

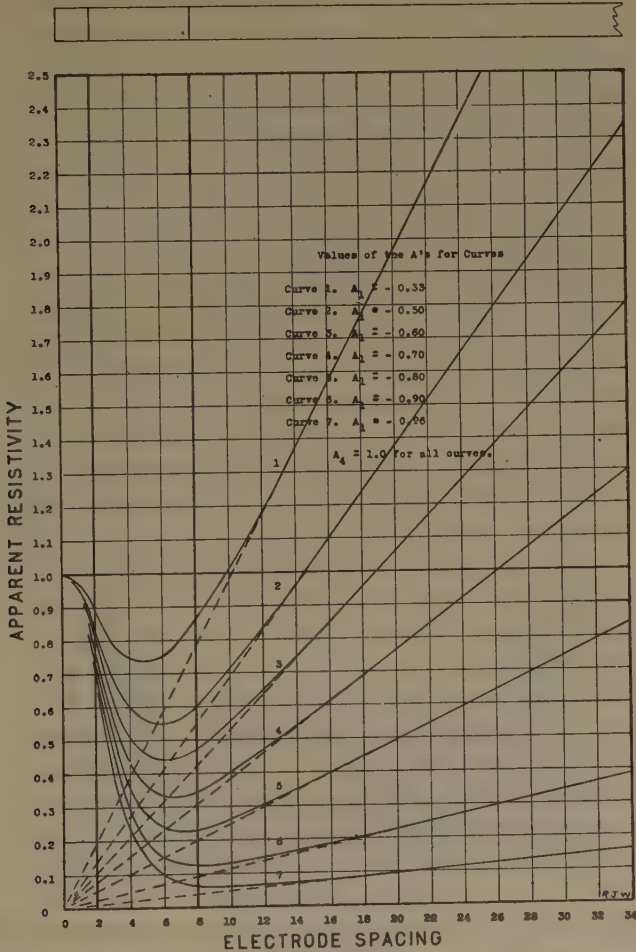


FIG. 11.—THREE-LAYER PROBLEM, SHOWING EFFECT OF VARYING RESISTIVITY OF MIDDLE LAYER.

welcome. In the three-layer problems computed, the resistivity curves approached the asymptotic line very closely before 20 units of electrode spacing was reached, and so the author was spared the great labor of computing these more distant points. In the four-layer problems, no perfect resistor was assumed below, hence the points on the resistivity curve beyond 20 units of electrode spacing had to be obtained by persist-

ent labor. Naturally, the accuracy of these points will not be as great as in the three-layer problems, but the general shape of the curve, the maxima, the minima and points of inflection will occur at the correct electrode spacing.

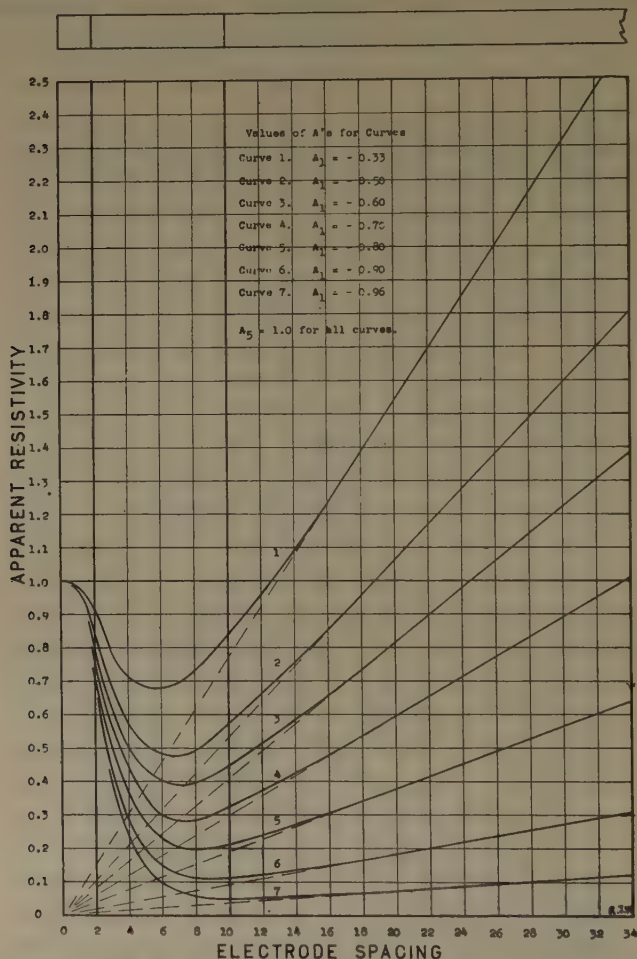


FIG. 12.—THREE-LAYER PROBLEM, SHOWING EFFECT OF VARYING RESISTIVITY OF MIDDLE LAYER.

#### DISCUSSION OF COMPUTED RESISTIVITY CURVES

Forty-nine theoretical curves are presented in this paper. Of these, 41 are for three-layer problems and 8 are for four-layer problems. The first 35, on Figs. 9 to 13, show the effect of thickening the intermediate layer for seven ratios of resistivity. It is believed that these ratios will cover most practical cases. The ratios of resistivity corresponding to the values of  $A_1$  indicated on the graphs are:

$A_1 = -0.33,$	$\rho_2 = \frac{1}{2}\rho_1$	$A_1 = -0.80,$	$\rho_2 = \frac{1}{9}\rho_1$
$A_1 = -0.50,$	$\rho_2 = \frac{1}{3}\rho_1$	$A_1 = -0.90,$	$\rho_2 = \frac{1}{19}\rho_1$
$A_1 = -0.60,$	$\rho_2 = \frac{1}{4}\rho_1$	$A_1 = -0.96,$	$\rho_2 = \frac{1}{49}\rho_1$
$A_1 = -0.70,$	$\rho_2 = \frac{1}{5.67}\rho_1$		

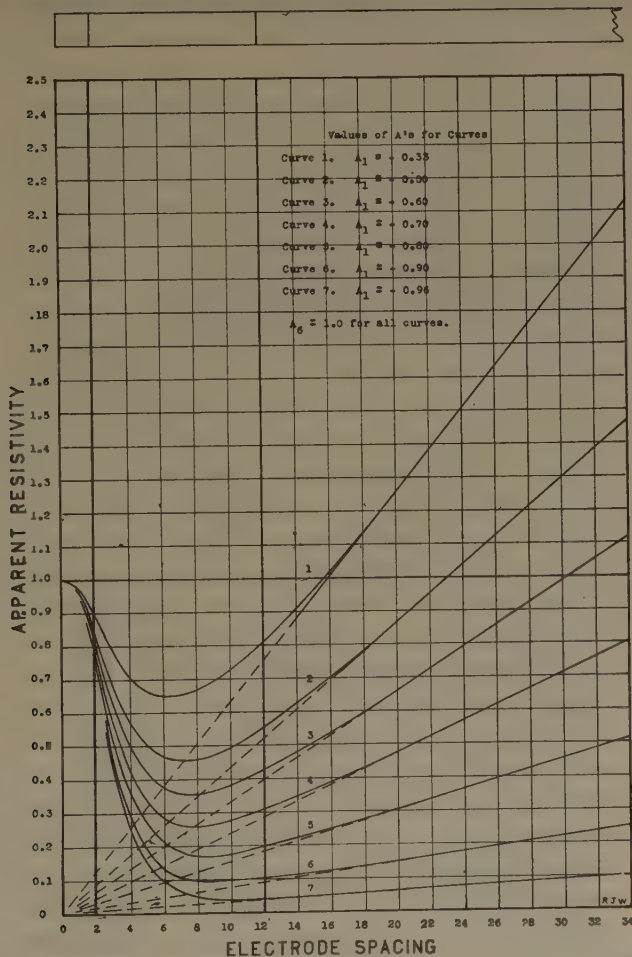


FIG. 13.—THREE-LAYER PROBLEM, SHOWING EFFECT OF VARYING RESISTIVITY OF MIDDLE LAYER.

On Figs. 14 and 15 are shown the effect of increasing the thickness of the top layer and keeping the middle one constant, for three values of  $A$ . This same effect was noticeable in the curves obtained from the model experiments.

In all these three-layer problems, the lowest layer is assumed to extend indefinitely downward and to have infinite resistivity. Thus the reflection coefficient for the lowest boundary will be unity in all the problems. For this reason all the curves approach asymptotes, which appear to

radiate from zero. Of course, if the resistivity of the lowest layer were only 50 times as great as the middle layer, the effect would be almost as great because of the "saturation effect." The idea of saturation effect is easily obtained by noting that the reflection coefficient  $A$  is determined by the ratio of resistivity of the beds on either side of the boundary and is

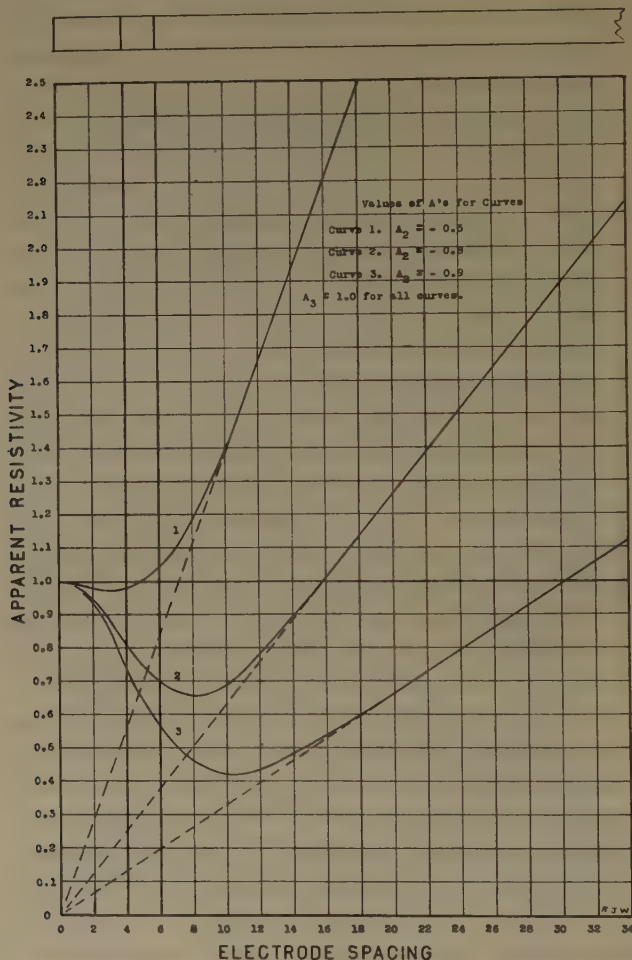


FIG. 14.—THREE-LAYER PROBLEM, SHOWING EFFECT OF VARYING RESISTIVITY OF MIDDLE LAYER.

given by equation 7. For a ratio of resistivity of 49:1, the value of  $A$  is 0.96, and for a ratio of 99:1 the value of  $A$  has increased only to 0.98. Thus a bed 100 times as resistive as the overlying beds acts almost as a perfect resistor. Such conditions are relatively common in practice, such as bedrock underlying glacial or alluvial material.

There is an important feature to be noted in these three-layer curves. Comparison of curves for various stratigraphic sections and ratios of



resistivity shows that, by properly adjusting the ratio of resistivity, the minimum may be made to coincide with the electrode spacing equal to the depth of the top of the resistor. This would seem to explain why it frequently happens that the Gish-Rooney empirical rule works so well under some conditions. That the rule has no theoretical basis is shown

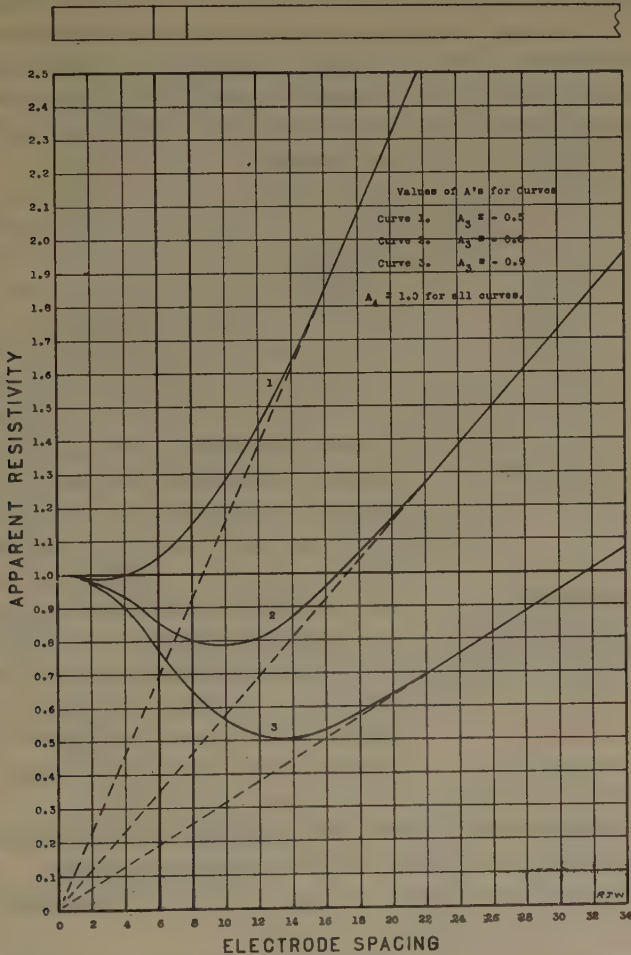


FIG. 15.—THREE-LAYER PROBLEM, SHOWING EFFECT OF VARYING RESISTIVITY OF MIDDLE LAYER.

by the fact that the minima may also lie on either side of the particular electrode spacing equivalent to the depth to the resistor. Obviously, no other similar empirical rule has any basis either.

One disturbing feature about these computed curves is the danger of a completely erroneous interpretation when the ratio of resistivity of the top to the middle layer is not known. There is a great similarity between curves belonging to one set of stratigraphic and ratio conditions

and other curves belonging to an entirely different set of stratigraphic and ratio conditions. While definite differences are noticeable on these computed curves, it is to be doubted whether field curves would be sufficiently accurate to make this difference detectable in some instances. To mention a specific case, curve 5 of Fig. 10 and curve 4 of Fig. 11 might be cited as being similar in features that are used for interpretation. If the field work was begun at a borehole where the depths to various layers are definitely known, it might be possible to deduce the ratios of resistivity from the character of the field curve; then, with this knowledge, the depth could be determined at points away from this first calibrating station.

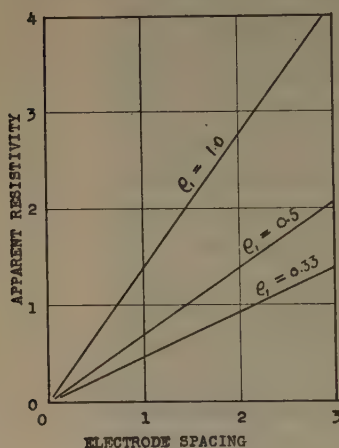


FIG. 16.—SLOPES OF ASYMPTOTIC LINES FOR RESISTIVITY CURVE WHEN A PERFECT RESISTOR IS LOWER LAYER IN A TWO-LAYER PROBLEM.

Turning to the four-layer problems given on Figs. 17 and 18, the effect of a comparatively thin layer of conducting or resisting material within a larger bed may be seen. In all cases presented, the conductor has a relatively greater effect than the resistor. This fact has been pointed out as a theoretical result by Weaver and also by Hummel. Also, unless the resistivity of the disturbing bed is sufficiently higher or lower than the surrounding medium, the existence of the bed is likely to pass unnoticed. Curve 1 on Figs. 17 and 18, where the disturbing bed is only three times as resistive or conductive as the surrounding medium, might be interpreted simply as a two-layer case. Note also curve 3 of these two plates. A Gish-Rooney interpretation for the top of the lowest bed would be quite incorrect.

From these computed curves, one can easily see the dangers of interpretation when more than three layers are present, especially when relatively thin conductors or resistors are embedded in relatively thick formations.

## DISCUSSION OF CURVES OBTAINED FROM MODEL EXPERIMENTS

### *Description of Model Technique*

The work with the models was done chiefly to confirm the correctness of the theoretical studies. An additional objective was to show that models could be constructed that would give results comparable with ideal cases. It has been the author's fortunate experience to realize both of these objectives.

The experiments were made in a box 10 by 15 ft. On the bottom was placed a rubber sheet. The significance of this sheet in all the experiments is that the lowest layer must be considered a perfect resistor of infinite depth because no current could flow below the rubber sheet. The material used for making the model strata was a sandy shale from the Pierre formation that outcrops at Boulder. This material was prepared

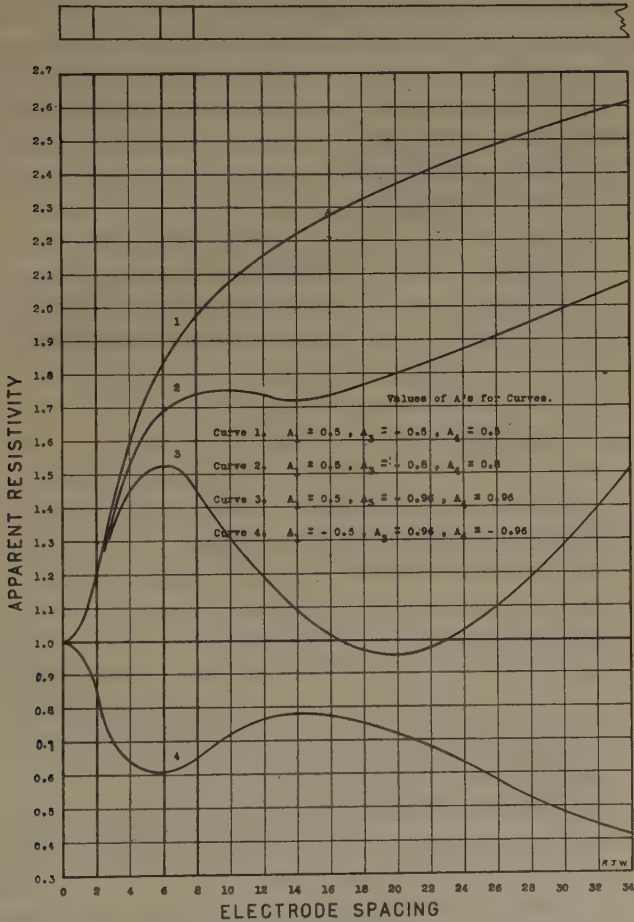


FIG. 17.—FOUR-LAYER PROBLEM, SHOWING EFFECT OF THIN LAYER OF CONDUCTING OR RESISTING MATERIAL.

by careful screening and mixing. The moisture content was altered to change the resistivity. Tests of the resistivity were made by placing a sample in a cylindrical tube the sides of which were of insulating material. A definite system of packing was employed to obtain approximately the same packing for the various samples. Contacts were made over the whole area of the two ends with clean copper plates. The voltage drop

across the length of the cylinder for a given current was measured and the resistivity calculated from the simple form of Ohm's law:

$$\rho = \frac{A}{L} \cdot \frac{\Delta V}{I}$$

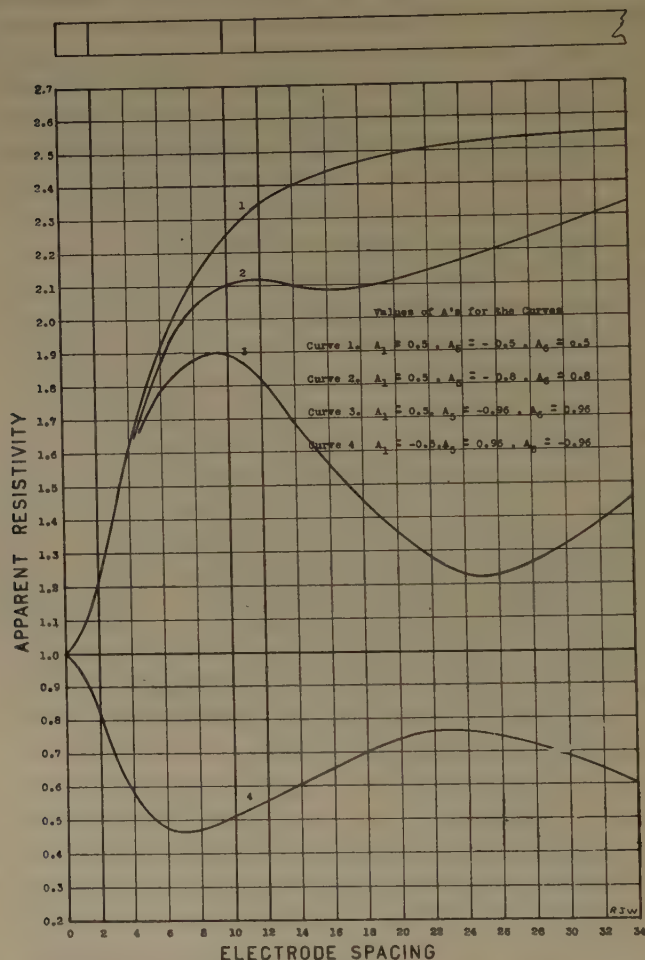


FIG. 18.—FOUR-LAYER PROBLEM, SHOWING EFFECT OF THIN LAYER OF CONDUCTING OR RESISTING MATERIAL.

where  $A$  is the area of each end,  $L$  is the length of the cylinder,  $\Delta V$  is the voltage drop, and  $I$  is the current passing through the clay. Of course it is only the ratio of resistivity that controls the shape of the curve, and not the absolute resistivity. Hence in many cases only the ratio of resistivity is given.

Masses of earth of different resistivity were placed in the box and rolled to form beds. A canvas sheet placed over the material to be rolled



made it possible to roll the material more efficiently with less sticking of the material to the roller. The roller was made by filling with concrete a piece of 14-in. stovepipe 30 in. long. After some preliminary work it was found that layers could be rolled with surprising uniformity of thickness and resistivity. The results to be given in the following pages will bear this out. The few curves presented here are only a small part of the results obtained from almost one hundred models.

As would be expected, the values of resistivity obtained from the cylindrical test box and those obtained from the measurements with electrodes on the model are not exactly the same. The packing done by the roller is different from that done by hand in the test box. However, since it is the *ratio* of resistivity that is important, it has been assumed that the ratio determined by the test box is the same as that which existed

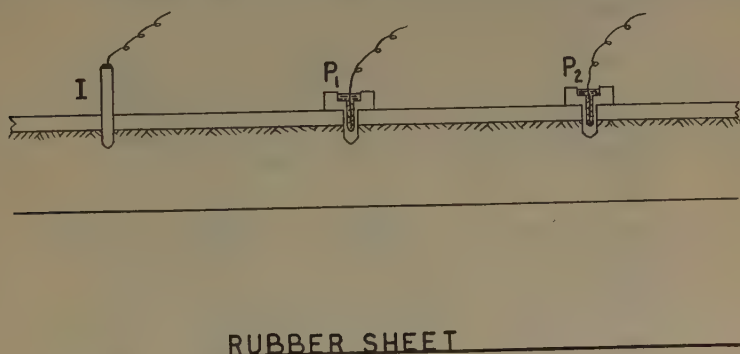


FIG. 19.—CROSS-SECTION OF MODEL.

in the model. It is freely admitted that this is an assumption, but the results obtained from the model work indicate that the assumption is sufficiently correct.

For current electrodes small monel metal nails slightly less than one-eighth inch in diameter were used. The nonpolarizing potential electrodes were miniature porous pots containing copper sulfate solution. These were of porous porcelain and were less than  $\frac{1}{8}$  in. in diameter where they entered the earth model. Fig. 19 is a cross-section of the model showing the beds, the electrodes and the template used to keep the electrodes accurately spaced and in place. This template was a thin piece of composition board about the size of a yardstick. Holes were bored at the proper intervals to accommodate the current and potential electrodes. In the figure the method being used is the one-electrode, hence only the one current electrode appears. The other one is some 7 ft. away. The unit of electrode spacing was the inch, and the unit of resistivity the ohm-inch.

Either the Wenner, or the one-electrode method was used in all the experiments. As shown before in the theoretical discussion for the case

of parallel homogeneous beds, it does not matter whether the Wenner, the Lee, or the one-electrode method is used, because the results are identical. If the parallel beds are not entirely homogeneous and lateral variations exist, the results obtained by the three methods may not be the same.

Problems involving two, three and four layers were attempted. The two-layer problems served to indicate that approximately homo-

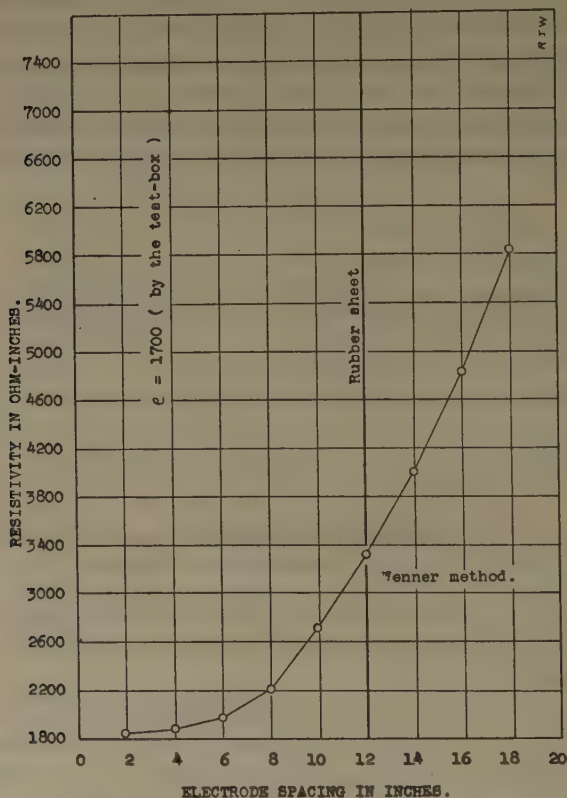


FIG. 20.—TWO-LAYER MODEL EXPERIMENT.

geneous layers could be laid over the rubber sheet, and also that the Wenner and the one-electrode methods yield substantially the same results. The three-layer problems show the effect of the thickness of the top layer, the thickness of the middle layer, and the ratio of resistivity between the top and middle layers. One interesting experiment performed with a three-layer case shows what has been proved mathematically before; namely, that with the Wenner method it does not matter whether the current electrodes are outside or inside of the potential electrodes. The four-layer problems attempted show that unless the ratio of resistivity is sufficiently high, such problems might be mistaken

for two-layer problems in the field. All the experiments bear out the truth of the mathematical development surprisingly well and prove conclusively that any rule of thumb method of interpretation is, to say the least, liable to great error.

### *Discussion of Results of Two-layer Problems*

A resistivity curve obtained from a two-layer problem is shown on Fig. 20. For the sake of brevity only the results of one such problem

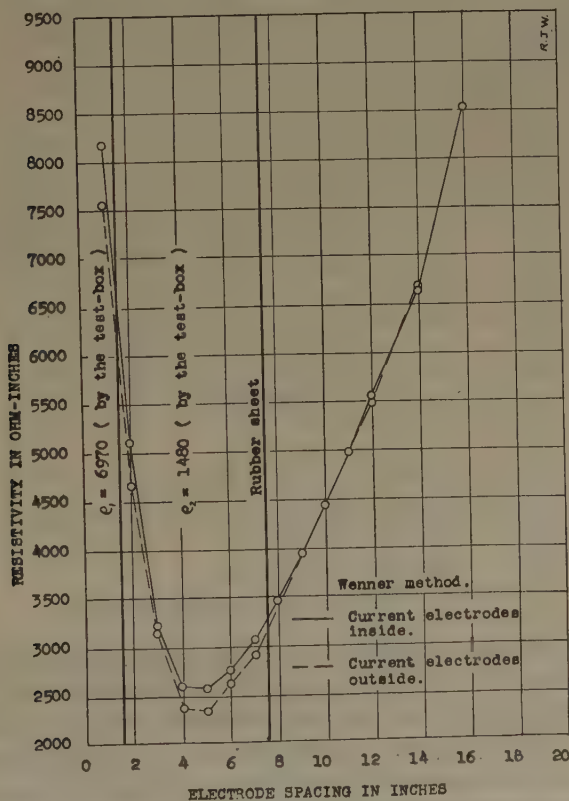


FIG. 21.—THREE-LAYER MODEL EXPERIMENTS FOR TWO WENNER CONFIGURATIONS OF ELECTRODES.

are shown, but the results of many other problems in which different thicknesses of material and different resistivities were used are equally convincing. The curve is of the type to be expected from the mathematical analysis and shows no abrupt change of resistivity in crossing the electrode spacing equivalent to the depth of the bed.

### *Discussion of Results of Three-layer Problems*

One of the most interesting three-layer problems performed was a check on the mathematical derivation for the Wenner method when the

current electrodes are placed *inside* instead of outside of the potential electrodes. Fig. 21 shows the results of this experiment. Considering the fact that changing the position of the current electrodes changes the current paths markedly, one must admit that these results prove that the layers were approximately homogeneous both laterally and vertically, and that the mathematical analysis is amply justified.\*

In Figs. 22, 23 and 24 are shown the results of three-layer problems in which the middle layer is 22.5 in. thick. In Fig. 24 the ratio of resis-

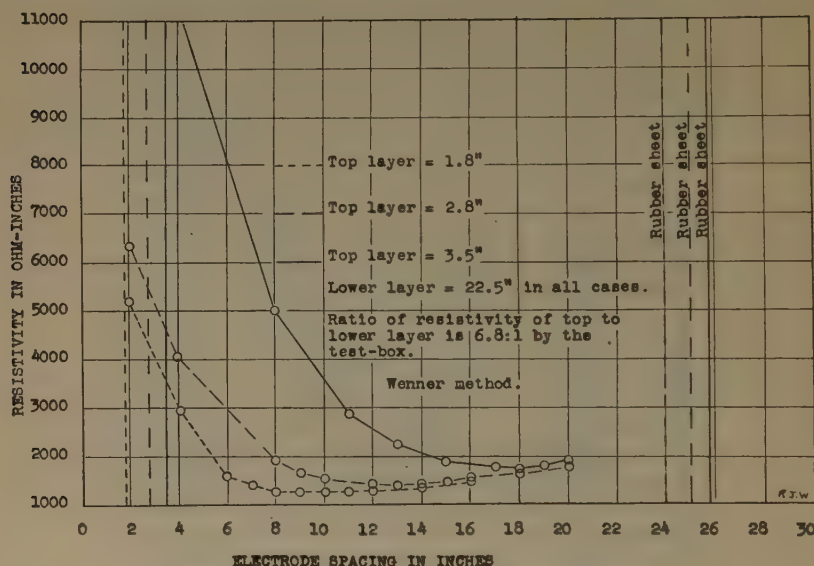


FIG. 22.—THREE-LAYER MODEL EXPERIMENTS.

tivity of the top to the middle layer is 1.6:1, in Fig. 23 the ratio is 4:1 and in Fig. 22 it is 6.8:1. All these ratios were determined by the test box. For each of these cases three experiments were performed with different thicknesses of the top layer. In all three figures an increase in the thickness of the top layer moves the electrode spacing of the minimum to a larger value and also increases the value of resistivity for the minimum. This is precisely what occurred for the same conditions given in the computed curves.

Ideal curves have been computed for conditions similar to the thickest layer curves in Figs. 22 and 23. In both these model curves the thickness of the middle layer is nearly five times that of the top layer. These conditions can be duplicated almost exactly on Fig. 13, both as to thickness and ratio of resistivity. If the model and computed curves are compared carefully, it will be found that the position of the minima in both the model curves occurs at electrode spacings equivalent to the electrode spacings in the computed curves. As noted before, the scale of

\* See author's reply to discussion, page 235.



the computed curves is purely arbitrary. For instance, in Fig. 24 the depth of the top layer is 5 in. for the deepest case. The ratio of resistivity

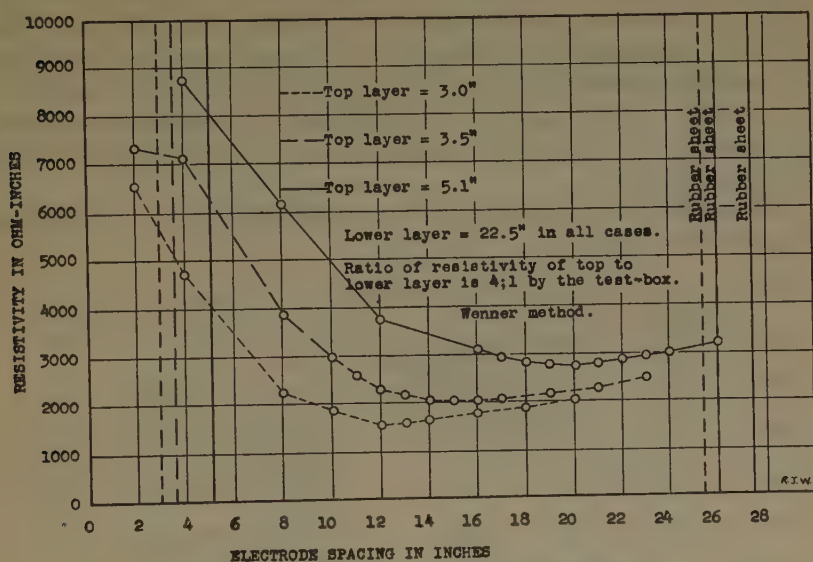


FIG. 23.—THREE-LAYER MODEL EXPERIMENTS.

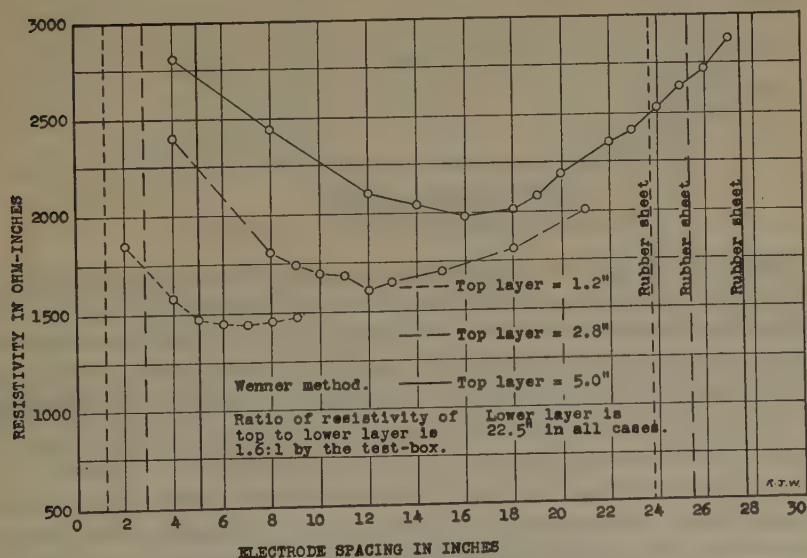


FIG. 24.—THREE-LAYER MODEL EXPERIMENTS.

is 1.6:1, which is close to 2:1. Now, on Fig. 13 for the ratio of resistivity 2:1, which makes  $A_1 = -0.33$ , the minimum occurs at 6.5, and the ratio of the electrode spacing of the minimum to the depth of the top layer is

6.5:2 or 3.25:1. In the model curve the same ratio is 16:5 or 3.2:1. This is a remarkably good check.

Another case is the curve corresponding to the thickest top layer of Fig. 23. Here the greatest depth of the top layer is again nearly one-fifth that of the second layer, so again Fig. 13 may be used for comparison. The ratio of resistivity for this model curve is 4:1 which means that  $A_1 = -0.6$ . In the computed curve the ratio of the electrode spacing of the minimum to the depth of the top layer is 8:2 or 4:1, and for the model the ratio is 4:1.

For the other curves of Figs. 22, 23 and 24 there are no corresponding computed curves given.

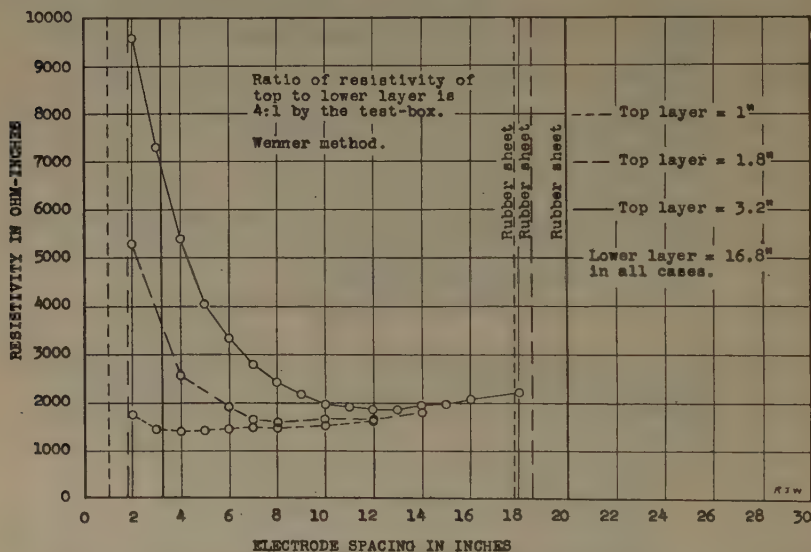


FIG. 25.—THREE-LAYER MODEL EXPERIMENTS.

Model curves for which the middle layer is 16.8 in. and the ratio of resistivity of the top to the middle layer is 4:1 are shown on Fig. 25. Several thicknesses of the top layer were used. The curve for which the thickest top layer was used may be matched with curve 3 of Fig. 13. In this computed curve the ratio of electrode spacing of the minimum to the depth of the top bed is 8:2 or 4:1. In the model curve the minimum is at 12.5 in. when the top bed is 3.2 in., which gives a ratio of 3.9:1.

In all these three-layer cases the smoothness of the model curves is remarkable. When one considers some of the irregular curves actually obtained from field work where one does not know about the stratigraphical conditions, let alone the electrical ones, it seems strange that investigators should put much trust in them as far as accurate depth determinations are concerned. Clearly, curves of this sort are not due to vertical discontinuities alone. This is easily proved either by comparing

the two sets of measurements obtained from the two sides of the Lee method, or by extending the line of potential measurements on both sides of the main current electrode when using the one-electrode system. Yet, one is confronted by statements in the literature such as that by Swartz:<sup>15</sup>

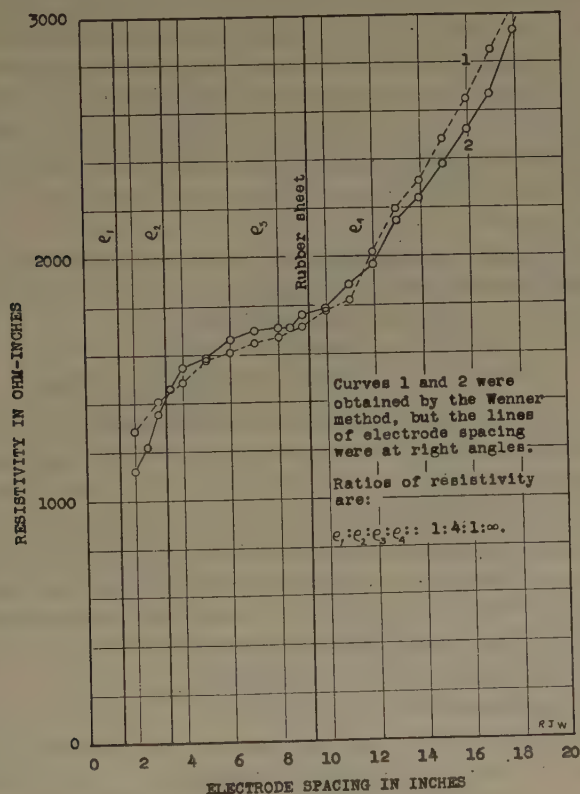


FIG. 26.—FOUR-LAYER MODEL EXPERIMENTS.

Various investigators have shown that there should be no break in the resistivity curve on passing from a bed of one resistivity to one of different resistivity. The resistivity curve should be smooth, not jagged. Such curves would be very difficult to interpret. It may be worth while to emphasize again that is fortunately not the case. The curves are actually jagged, broken and irregular, anything but smooth. The major breaks and peaks, at least, correspond to and locate real variations in resistivity, recording definite stratigraphic changes in beds.

Such a statement the author finds very difficult to reconcile with the mathematical treatment, the model work just presented and a great number of field results. Of course, when there are many beds of quite different resistivities, the resistivity curve even for ideal conditions will

<sup>15</sup> J. H. Swartz: Oil Prospecting in Kentucky by Resistivity Methods. U. S. Bur. Mines Tech. Paper 521 (1932) 17.

contain many highs and lows, and these will give evidence of the existence of the beds. However, the actual determination of the depths to the various beds is a much more difficult matter. Certainly if there are conditions in the field much more complicated than those assumed in ideal cases, and if the operator does not know these conditions, as is almost always the case, it seems that it is only by the merest coincidence that the erratic highs and lows of a resistivity curve should be due entirely to definite changes of resistivity in the vertical section of the underlying earth. Lateral changes in lithologic character are by no means uncommon, and a corresponding change in electrical character is certainly not improbable. As stated before, it is the author's firm belief that until the operator has assured himself by such tests as have been suggested in this paper or other similar ones that the major changes of resistivity in the resistivity curve are due to vertical changes, it is very unwise to make a depth determination from resistivity data.

### *Discussion of Results of Four-layer Problems*

In Fig. 26, the results of one of the four-layer problems attempted are shown. The two curves are for two sets of Wenner spacings taken at right angles to show just how homogeneous the layers were. The two curves are remarkably alike and clearly show that their shape is due to vertical changes in resistivity and not lateral changes. A Gish-Rooney interpretation on the depth to the thick better-conducting layer would be considerably in error while a similar interpretation for the top of the lowest resisting bed would be fairly accurate in this particular case. Such an interpretation cannot be relied upon.

Summarizing the results of the model work, it can be said that models of earth can be constructed which have a great similarity to the ideal cases assumed in the mathematical development. The results of resistivity tests on these models amply justify the mathematical development.

## DISCUSSION

*(E. DeGolyer presiding)*

L. GILCHRIST,\* Toronto, Ont. (written discussion).—Mr. Watson's paper is a successful extension and application of the results developed in a previous paper, by Ehrenburg and Watson, on the problem of stratified horizontal homogeneous conducting layers of different resistivities.<sup>16</sup> It is emphasized again that there is no abrupt change in the average resistivities with depth. It should also be emphasized that for this case no abrupt change in the potential gradient will be found on the uppermost surface when measured either in the application of the Wenner method or the "one-electrode" method. Ordinarily such measured results would defy interpretation or correlation with the depths of the underlying layers. Mr. Watson has developed a

---

\* Professor of Physics, Toronto University.

<sup>16</sup> D. O. Ehrenburg and R. J. Watson: *Trans. A.I.M.E.* (1932) **97**, 423.



method of interpretation that in skilful hands may be very useful in locating the underlying horizontal layers. This is a distinct advance. It would be well to compare the results of this method with a somewhat different method developed by G. F. Tagg<sup>17</sup> when applied to Mr. Watson's measured results. Attention should again be called to the fact that abrupt or rapid changes in the potential gradient on the surface are found commonly in the field and it is usually in these cases that investigators attempt interpretations seeking to delineate the location of underlying structures of different resistivities. In such cases it would seem to be imperatively necessary after the first indications are obtained (1) to devise a layout system that provides for the simplest possible boundary conditions on the surface; (2) to obtain a considerable body of suitably measured results, in order to determine the surface boundary conditions; (3) to make use of a solution of a modified Laplace equation, which should include scattered current flows and polarization potentials at interfaces along the lines of current flow.

J. H. SWARTZ,\* Washington, D. C. (written discussion).—I have read Mr. Watson's paper with much interest, an interest not lessened by the fact that, as he points out, we do not see quite eye to eye on the subject of the value and validity of empirical rules in the interpretation of resistivity observations. After expressing surprise that anyone should still place any faith in empirical rules, Mr. Watson implies that it is only by the merest coincidence that breaks in the resistivity curve should correspond to vertical changes in the stratigraphic sequence of underground beds. Fortunately, the possibility of coincidence can be determined mathematically from data concerning a Kentucky well given in the paper from which Mr. Watson quotes. This well, which, because of its complexity, affords a crucial test, was drilled  $\frac{3}{4}$  mile from the nearest neighboring well, in an area where well logs were unobtainable and where the detailed stratigraphy was unknown. With nothing to go on but the resistivity data, the writer predicted, before the well was drilled and on empirical grounds alone, the presence of and depths to eight horizons later encountered in drilling the well. The predicted depths of these eight horizons were correct within an error less than that to be expected from the depth interval employed in making the resistivity measurements. One horizon was salt water, the other seven were gas or oil. Since the total number of intervals measured was 40, it follows that the possibility that it was coincidence that the breaks in the resistivity curve should correspond to these eight horizons is

$$\frac{1}{40} \times \frac{7}{|39 - 32|}$$

or but one chance in approximately 195,000,000. The idea of coincidence cannot be supported.

In the discussion as a whole it seems to me that Mr. Watson has put the cart before the horse. He says that it is his purpose to prove by theoretical studies "how erroneous the various empirical rules for depth determination may be." The essence of an empirical rule is that it is the result of observation, founded on the facts of observation. To attempt to refute a rule based on observation by an appeal to theory is to reverse the process by which all modern scientific advancement has been made. I hold no particular brief for empirical rules. I certainly should not care to claim them perfect, or infallible, nor to imply that they may not need correction or amplification. But there is only one way in which their validity may be tested or such correction or amplification made; that is, by more and more extensive and complete field observations.

<sup>17</sup> See page 135, this volume.

\* U. S. Bureau of Mines.

To appeal to theory in the present case is particularly unfortunate since theory is in an unhappy position in treating this question. In the first place conditions in general are too complex to permit mathematical treatment. Hence the problem must be so simplified geologically before it can be attacked mathematically that its solutions can apply to only a limited number of geologically special cases. This fact, it may be noted in passing, means that theoretical solutions can be of use only in very simple geological cases. The vast majority of geological problems are complex and hence at present can be solved only by the application of empirical rules, however good or bad such rules may be. In the second place the assumption of ohmic conduction, on which all such mathematical studies are based, cannot be regarded as proved. In fact there is a very considerable body of evidence indicating that we are often dealing with an electrochemical rather than ohmic conduction.

To be sure, Mr. Watson gives the results of a series of model experiments to support his conclusions. But his models are constructed so as to fulfill the particular assumptions made in his calculations, even down to the rubber sheet at the base to form a bottom bed of infinite resistivity. As a geologist, I feel sure that no geologist would be willing to accept such an arrangement as having real geological significance, particularly in the absence of the soil and rock solutions found under natural conditions. The most that Mr. Watson can be said to have proved by his model studies is that his mathematical work is correct.

I do not wish to imply by these statements that theoretical mathematical studies are without value. Quite the contrary. Such studies have two very definite and important functions in geophysics. In the first place, in cases involving sufficiently simple geological conditions they may afford a valuable aid to geophysical interpretation, as shown by Dr. Fisher in his presentation of Dr. Roman's paper a few moments ago. In the second place a still more important function of such theoretical mathematical studies, to my mind, is their use to point out where theory fails to fit the facts. Scientific advance has always been more a function of failure than of success. The failure of theory to fit all the facts has indicated new lines of attack which eventually have opened up entirely new fields of knowledge. I have no doubt that equally great advances await us in geophysics when we have sufficiently tested our theories by facts.

L. B. SLICHTER,\* Cambridge, Mass.—As is well recognized, the computations in multiple-layer problems such as these are extremely tedious, unless mechanical means, such as the Differential Analyzer, are used; then they are relatively simple. In any work, one naturally welcomes opportunity for simple checks on accuracy. Such a check is afforded by the following fact.

As the electrode spacing becomes greater and greater, more and more distant from the power electrode, the surface material becomes thinner and thinner with respect to the total volume included in the measurements. Therefore the curves should become asymptotic to the value of the bottom layer's resistivity. Thus in both Fig. 17 and Fig. 18, the first three curves should ultimately become horizontal at the value 3, and the fourth at the value  $\frac{1}{3}$ . Clearly much greater electrode spacings than are given in these figures are required before this check can be attained. This illustrates how large the electrode spacing must be before the resistivity of the deep material can be ascertained. For example, in curve 3, Fig. 17, the error is still 100 per cent at an electrode spacing of  $4\frac{1}{4}$  times the depth to the lower region.

The reciprocity theorem applies in the case of three-dimensional flow also. Wenner in 1912 mentions<sup>1</sup> Helmholtz's treatment in 1853 of the reciprocity theorem in isotropic solids; also proofs of Rosen, Heaviside and Bromwich, for the nonisotropic case. In connection with resistivity work it is interesting to note that as early as

\* Associate Professor of Geophysics, Massachusetts Institute of Technology.

<sup>1</sup> U. S. Bur. Stds. *Bull.* (1912) 8, No. 3.

1884 F. Neumann proposed determining the resistivity of the earth by a four-electrode method nearly like our present technique, and carefully developed the mathematical theory of the method.

R. J. WATSON (written discussion).—The author could produce a great number of resistivity curves where the use of the empirical rule would give a wrong interpretation for practically every vertical discontinuity in the stratigraphic section. The fact seems well established by careful investigators that the empirical rule is not a safe one because it does not always work. The author has suggested reasons why it does not work for conditions which can be studied because of their relative simplicity. These simple conditions are not as rare in actual field practice as one might suppose.

If in addition to simple ohmic conduction, we add electromotive forces due to electrolytic action the complexity of the problem is only increased with factors that are scarcely determinate. To take one of the simplest problems of this type, assume that electromotive forces are generated at the interfaces of layers, and that these forces add to the electric potential at the surface. If these added potentials are really great enough they may influence the normal drop of potential away from the surface sources and give rise to sharp breaks in the resistivity curve. Granted that this may be true, there is certainly no known basis for the supposition that there will exist a simple linear relationship between the electrode spacing and the depth to the interfaces for such a condition.

M. K. HUBBERT,\* New York, N. Y. (written discussion).—On pages 204 and 205 Watson shows that in homogeneous media it makes no difference for a given electrode setting, using the Wenner electrode configuration, whether the current electrodes are the outer pair and the potential electrodes the inner, or vice versa, since the results in the two cases are identical. Later, in discussing the experimental verification, he shows (Fig. 21) that in a three-layer case the results obtained experimentally with the current electrodes inside are the same, within the limits of experimental accuracy, as those obtained with the current electrodes outside. He then remarks (p. 228): "Considering the fact that changing the position of the current electrodes changes the current paths markedly, one must admit that these results prove that the layers were approximately homogeneous both laterally and vertically, and that the mathematical analysis is amply justified."

Apparently Watson failed to take into account an important theorem of electric currents of which the results cited are only a special case. Let any four electrodes  $A$ ,  $B$ ,  $C$  and  $D$  be attached in any arbitrary configuration to any conducting medium, such as the ground. Let a current  $I$  be made to flow through the medium between any pair of these electrodes, say  $A$  and  $C$ . Let  $E$  be the difference of potential between the other pair,  $B$  and  $D$ . Next, exchange the connections so that the same current  $I$  flows between  $B$  and  $D$ . Then  $E$ , the potential difference between  $A$  and  $C$ , will be the same as that formerly observed between  $B$  and  $D$ .

This theorem, to which Dr. Theodor Zuschlag directed the writer's attention, is a very old electrical theorem, known as the Reciprocity Theorem. It is true for circuit networks and for continuous media. It is independent of the relative configuration of the electrodes, and of the inhomogeneity of the medium.

In the light of this, Watson's conclusion that the agreement between his two results proves vertical and lateral homogeneity does not appear to be valid. The same results would have been obtained under any circumstance.

R. J. WATSON (written discussion).—The result on page 205 would be anticipated if the Reciprocity Theorem were considered. Concerning Mr. Hubbert's criticism of

---

\* Instructor in Geophysics, Columbia University.

the statement on page 228, the text of lines 2 to 6 should be changed to read: "Fig. 21 shows the result of these experiments. According to the Reciprocity Theorem the results should be identical regardless of the inhomogeneities of the model. Thus interchanging current and potential electrodes in field work gives no new information. The actual discrepancies shown in the two curves of Fig. 21 are probably due to the fact that the electrodes were not interchanged for each electrode spacing but two separate experiments were performed over the same part of the model."



# Electrical Coring; a Method of Determining Bottom-hole Data by Electrical Measurements

BY C. AND M. SCHLUMBERGER\* AND E. G. LEONARDON,\* PARIS, FRANCE

(New York Meeting, February, 1932)

SINCE the beginning of the year 1928 the senior authors and their associates have applied a series of procedures which makes possible the detailed study *in situ* of the formations traversed by a drill hole before the casing has been landed. They have given the name "electrical coring" to the ensemble of these processes, which now replace in a large measure the mechanical coring performed by the drillers, and permit the gathering of bottom-hole data hitherto unobtainable.

Three years have elapsed since the technique and interpretation of these measurements emerged from the experimental stage and entered the field of industrial application on a large scale. The total length of drill holes so far surveyed by the authors and their associates, all over the world, amounts to several millions of feet. Practical and strongly built equipment has been evolved, which permits the examination in a short time of an open hole several thousand feet long.

No comprehensive paper has yet been published discussing the essential principles of the processes applied and bringing into evidence their economic interest. This is the object of the present paper.<sup>1</sup> Numerous examples of field work performed under varied geological conditions are given, constituting a concrete illustration of the services rendered by the new methods.

The study *in situ* of the formations penetrated by a drill hole is based on the measurement of a given physical factor or parameter associated with these formations. Generally the measurements are made systematically along the whole length of the open hole. The physical factors or parameters which are now utilized by us to this end are: (1) the resistivities of the rocks; (2) their porosity; (3) their electrical anisotropy; (4) their temperature; (5) the resistivity of the muds. In order to

---

\* Société de Prospection Electrique, Procédés Schlumberger, Paris, and Schlumberger Electrical Prospecting Methods, New York.

<sup>1</sup> The only previous publication on the subject discusses solely the measurement of the resistivity in drill holes, *i. e.*, C. and M. Schlumberger: Communication sur le carottage électrique. Deuxième Congrès International de Forages, Paris, Septembre, 1929. A résumé of that paper was given in the November, 1929, issue of *Mining and Metallurgy*.

establish correct geological cross-sections, and to determine accurately the depths to the formations, we have been led to evolve a practical teleclinometer, the principles of which will also be described. The paper will therefore discuss:

A. Resistivity of the rocks; its measurement in open holes. Applications.

B. Porosity of the rocks; its measurement. Applications. Study of the rock pressure.

C. Electrical anisotropy of the rocks. Determination of the direction of the dip.

D. Temperature measurements.

E. Resistivity of the muds. Location of water flows.

F. The electromagnetic teleclinometer. Survey of crooked holes.

G. Conclusions.

#### A.—ELECTRICAL RESISTIVITY OF THE ROCKS; ITS MEASUREMENT IN OPEN HOLES AND APPLICATIONS

##### *Resistivity of the Rocks*

Among the parameters which can be utilized for differentiating geological formations, the electrical resistivity of rocks is one of the most efficient, since it varies within considerable limits from one formation to another. Furthermore, it can be measured easily at depth.

We will recall here that rocks are capable of transmitting the electric current only by means of the absorbed water which they contain. Were they entirely dry, they would be completely nonconductive. This absorbed water always contains dissolved salts, and thus constitutes the electrolyte necessary for the conduction of the current. The more electrolyte contained in a rock, and the richer this electrolyte is in dissolved salts, the greater is the conductivity of the rock. In practice, we do not measure the conductivity of the rocks, but its reciprocal, their electrical resistivity. This is the electrical resistance of a cylinder of rock having for height the unit of length and for section the unit of surface. We express the resistivity of rocks in ohms per meter square-meter, or ohm-meters, which is a suitable unit for practical purposes, giving figures comprised between one and several thousands of units.

If a rock is very compact, it is evident that the quantity of moisture it contains is exceedingly small, and that, consequently, its resistivity is high. This is true for dense and massive, hard rocks like granite, quartzite, gneiss and marble. Among the softer rocks, gypsum, rock salt and coal are also very resistant on account of their minute water content.

As to the unconsolidated rocks, they are generally rich in water, and normally possess good electrical conductivity. It is necessary, however, to establish a definite distinction between the pervious and the impervious

rocks. In a more or less impervious rock, like the clays, marls, and the more or less argillaceous shales, etc., the absorbed water is, so to speak, stationary in the rock. It will therefore contain in solution the maximum of soluble elements present in the rock, and its chemical composition will be uniform. Under such circumstances, the resistivity will generally be a reliable characteristic of the rock itself. Things are different, however, with porous formations. In sands, for instance, water may circulate quickly, and therefore may not everywhere maintain the same composition. The electrical resistivity will be high if the water is pure, and will be low if the water is appreciably mineralized. The electrical parameter, then, will characterize the liquid enclosed in the rock rather than the rock itself.

It is important to mention here the case in which the fluid contained in the rock is not a conductive electrolyte but an insulating liquid. This occurs when porous formations are saturated with oil or natural gas. These formations are very resistant, and this fact is of great moment in their detection, as will be seen later.

We will also mention briefly the influence of temperature. An increase of temperature decreases the resistivity of the rocks for two reasons: (1) the resistivity of an electrolyte of a given concentration decreases with the temperature; (2) the percentage of dissolved salts increases with the temperature. Roughly speaking, the specific resistance decreases by one-half for an increase of  $50^{\circ}\text{C}$ . This fact has an appreciable influence on the resistivity measurements taken in drill holes, since temperature differences of  $50^{\circ}\text{C}$ . between the surface and the bottom of a hole, may be encountered. For this reason, the electrical resistivity will have a tendency to become smaller with increasing depths.

If temperature thus plays an appreciable role in the variations of the resistivity, pressure, on the other hand, does not seem to have any marked influence, in spite of the fact that it reaches high figures at the bottoms of the holes.

### *Technique of Resistivity Measurements in a Drill Hole*

The measuring device usually employed is shown in Fig. 1. It comprises three insulated cables 1, 2 and 3, which are lowered into the drill hole. Three electrodes  $A$ ,  $M$  and  $N$  are attached to the lower ends of these cables and dip into the water or mud filling the hole. The distances  $AM = r$  and  $AN = r'$  are supposed to be large in comparison with the diameter of the hole; they are, for instance, 10 to 20 times greater. The electrode  $A$  is used to send the current into the ground and electrodes  $M$  and  $N$  to measure the difference of potential caused between these two points by the passage of the current through the ground.





the potentiometer), the average resistivity of the ground  $R$ , in the region of the measuring arrangement  $AMN$ , can be calculated.

The computation of this resistivity results from the following considerations. The current  $i$ , which flows from  $A$  into the ground, gives rise, by ohmic effect, to a series of equipotential surfaces surrounding  $A$ . These surfaces in the region of the electrodes  $M$  and  $N$ , by reason of symmetry, are spheres approximately centered on  $A$ , being given the dimensions chosen for  $r$  and  $r'$ . They intersect the column of water in the drill hole without undergoing any appreciable disturbance. The measurement of potential between the electrodes  $M$  and  $N$ , therefore, is equivalent to a measurement made inside the ground at the same distances  $r$  and  $r'$  from the electrode  $A$ . The application of Ohm's law between the spheres  $S$  and  $S'$ , of radii  $r$  and  $r'$ , leads to the following formula:

$$R = 4\pi \cdot \frac{\Delta V}{i} \cdot \frac{rr'}{r' - r} \quad [1]$$

which gives the required resistivity.

Contrary to what might be expected, the presence of water or mud in the hole constitutes an advantage and not a drawback. In an empty hole it would be necessary to establish reliable and stable contacts with the wall of the hole, a problem which meets with considerable practical difficulty. On the other hand, the disturbance caused by the presence of water is entirely negligible, provided a measuring arrangement of a sufficient length is adopted.<sup>2</sup>

In practice, the equipment is set up as shown in the sketch given at the right in Fig. 1. The three insulated wires are woven together into a single cable that has great tensile strength. This is wound up on a winch  $w$ , and at the casinghead passes over a standardized pulley provided with a measuring device, which indicates at any given time the length of cable lowered into the hole. From the winch, cable 1 is connected to a battery  $E$ , then to the earth  $B$ . Cables 2 and 3 are connected to the terminals of a potentiometer  $P$ . Since it is necessary to

<sup>2</sup> At a sufficient distance from electrode  $A$ , the volume of the hole is unimportant compared to that of the surrounding formations; the mud, therefore, has a negligible influence upon the value of the resistivity measured. To illustrate this point, we will consider the case in which resistivity of the mud is 2 ohms; resistivity of the surrounding rocks is infinite; diameter of the hole is 30 cm.; (section: 0.071 sq. m.);  $AM = 5$  m.;  $AN = 6$  m.; intensity of the current: 1 amp. All of the current will be transmitted by the mud; one-half will flow towards the top, the other half towards the bottom of the hole. The drop of potential between  $M$  and  $N$  will be (application of Ohm's law):

$$\Delta V = 0.5 \text{ amp.} \times 2 \text{ ohms} \times \frac{1}{0.071} = 14 \text{ volts.}$$

Therefore the resistivity computed by means of formula 1 will be 5300 ohms; in other words, a figure 2650 times greater than the resistivity of the mud.

carry out the measurements rapidly in order not to keep the drill hole idle for a long time, a registering apparatus has been combined with the potentiometer, thanks to which the electrical observer needs only to maintain a needle between two graduations. The resistivities are registered automatically on coordinate paper, which unwinds at a speed proportional to that of the cable. Thus a continuous diagram of the resistivities of the formations is obtained, showing the resistivities as abscissas and the depths as ordinates. The time required to install the equipment at the drill hole does not exceed  $\frac{1}{2}$  hr., except when the access to the hole or the setting up of the equipment presents some particular



FIG. 2.—DEPTH RECORDER AND REGISTERING APPARATUS.

difficulty. As to the run itself, about 1000 ft. can be examined in 1 hr. As a matter of fact, it is unusual for a regular run to keep the drill hole idle for more than 4 or 5 hr. altogether.

Fig. 2 gives a view of the apparatus set up at the hole and ready for operation. There are three types of winches. One is mounted on a truck and driven by the motor of the truck (Fig. 3); another is provided with independent electrical motors (Fig. 4). The third type is equipped with a gasoline engine, and is particularly useful in wildcatting.

To carry out the measurements, it is necessary to lower the measuring arrangement in the heavy mud-laden fluid which usually fills the drill hole. This hole is more or less vertical, its walls are far from being regular, and sometimes the depth is very great. In practice, this is one of the main difficulties with which the electrical engineer is confronted upon his arrival in a field. Plummets weighing 100 to 300 lb. are hung

on the end of the electrical cable to weight it. These plummets sometimes do not go down satisfactorily; they may be stopped in a crooked hole, or by a cave-in or a lump of clay left in the hole by the drillers while pulling out the drilling pipes. These difficulties, however, are quickly



FIG. 3.—SPECIAL TRUCK COMPLETELY EQUIPPED FOR ELECTRICAL SURVEYS IN DRILL HOLE.

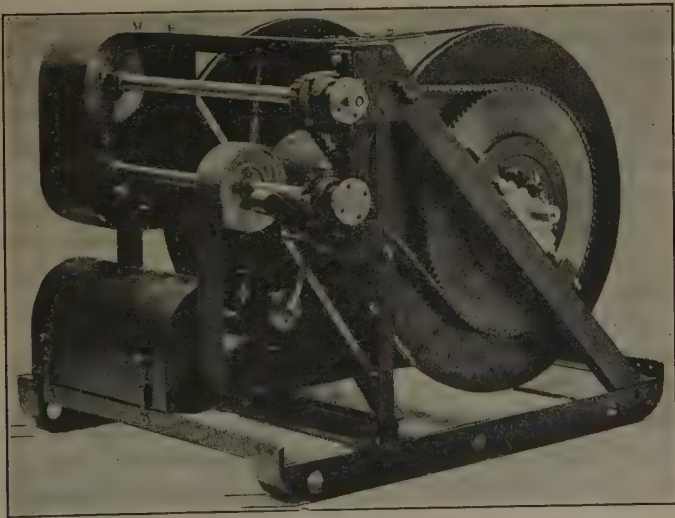


FIG. 4.—WINCH EQUIPPED WITH ELECTRIC MOTORS.

overcome, thanks to the cooperation of the drillers, who condition the hole by rotating the drill pipes for a short time, with a low pressure on the bit at the bottom of the hole. This conditioning, which is generally accompanied by a circulation and thinning of the mud, does not require more than a few hours, and has never once caused any trouble in several thousand holes which have thus far been surveyed. It is indispensable in those holes which are deep or crooked.



The preceding explanations show that only the uncased part of the drill hole can be surveyed by the new process, as the casing constitutes a screen which completely masks the physical properties of the surrounding formations. Inside the casing, the resistivities are equal to zero. This fact may be utilized to check exactly the depth of the lower part of the casing, or to locate a lost pipe in the hole.

### *Use of the Resistivity Diagram*

*Geological Correlations.*—We have seen that the resistivity parameter makes it possible to differentiate between various formations, since it generally varies widely from one layer to another, and is relatively constant for a given layer. On the other hand, the mere numerical value of the resistivity is not necessarily a distinguishing characteristic of a given formation, except under particular circumstances, since two formations of a very different age, or even of different lithological facies, may show the same resistivities.

A single resistivity figure thus does not yield accurate information. On the other hand, if we consider a large and regular sedimentary complex, and study its resistivity diagram, the characterization becomes perfect. It may be possible, of course, to discover several places in a geological column where two beds, respectively 1 and 2 m. thick, show resistivities of 20 and 10 ohms. There is, however, only a single region in the geological column where, for instance, 10 successive layers will show, at the same time, the same relative thickness, the same resistivities, and the same arrangement.

Thus, the comparison of two resistivity profiles obtained on the same series of sedimentary formations will give, in a reliable manner, the relative depths to the various strata. Therefore, to obtain numerous and reliable correlations between several holes in a given area, it is no longer necessary to core all of them mechanically. It will suffice to perform the operation for the first hole drilled, and, subsequently, to take advantage of the electrical resistivity diagrams to deduce the geological columns in the new holes and to establish stratigraphical correlations in the whole district. Such cross-sections can be determined all along the open hole and are as reliable as the geological column obtained by mechanical coring. They give decidedly more detailed information than discontinuous coring. The new procedure far exceeds continuous coring in drilling speed, and is much cheaper than the most discontinuous drilling process.

An important point is whether or not it will be possible to discover numerous and reliable electrical horizon markers. In this connection, it must be pointed out that any given geological horizon characterized by a precise lithological change, for instance the passage from a sandstone or a limestone to a marl, will constitute also a good electrical marker.



The number of electrical horizon markers, therefore, will be nearly proportional to the number of definite lithological alternations. Fig. 5, which represents a series of diagrams measured in the Pechelbronn oil field, Alsace,<sup>3</sup> in the region of Kutzenhausen, demonstrates this point well. On the left of the figure, the cross-section of hole S.2955 is repre-

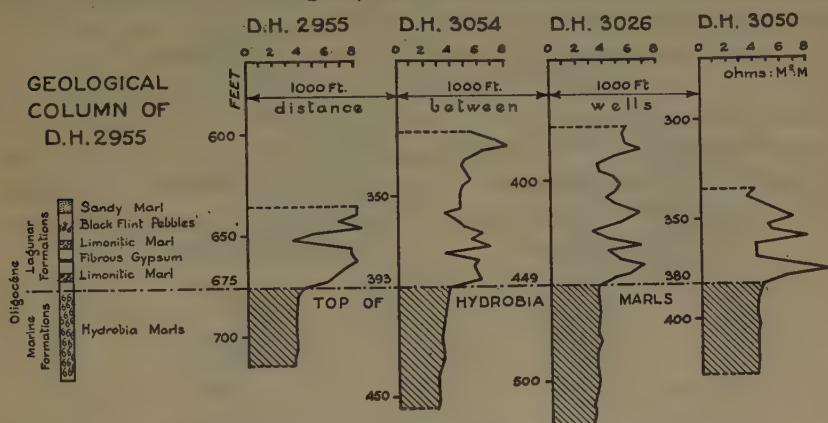


FIG. 5.—DETERMINATION OF A CONTACT BETWEEN TWO FORMATIONS, PECHELBRONN 1928.

sented. It is easy to ascertain that the variations of the resistivities follow closely the succession of the formations encountered. Even thin layers like a bed of black flint pebbles, or of limonitic marl, or a small

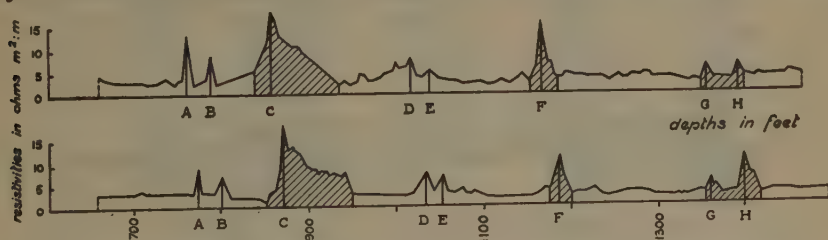


FIG. 6.—ELECTRICAL CORRELATIONS BETWEEN TWO WELLS, SUMATRA, 1930.

streak of fibrous gypsum, show up clearly in the diagram. At the 675-ft. level, an important drop is apparent on the graph (drop from 8 to 3 ohm-meters in a few ft.) which indicates the transition from lagoon sediments to a deep sea formation. This horizon marker is easily found throughout the Pechelbronn district, over an area of 40 square miles. It is clearly visible on holes S.3054, S.3026 and S.3050, although the latter are separated from hole S.2955 by an important fault.

Generally, electrical markers are not lacking, and the resistivity graphs have a saw-tooth silhouette showing numerous characteristic

<sup>3</sup> For a brief description of the Pechelbronn oil field, see G. S. Rice and J. A. Davis: Mining Petroleum in France and Germany. Petroleum Development and Technology for 1925, A.I.M.E., 278-314.

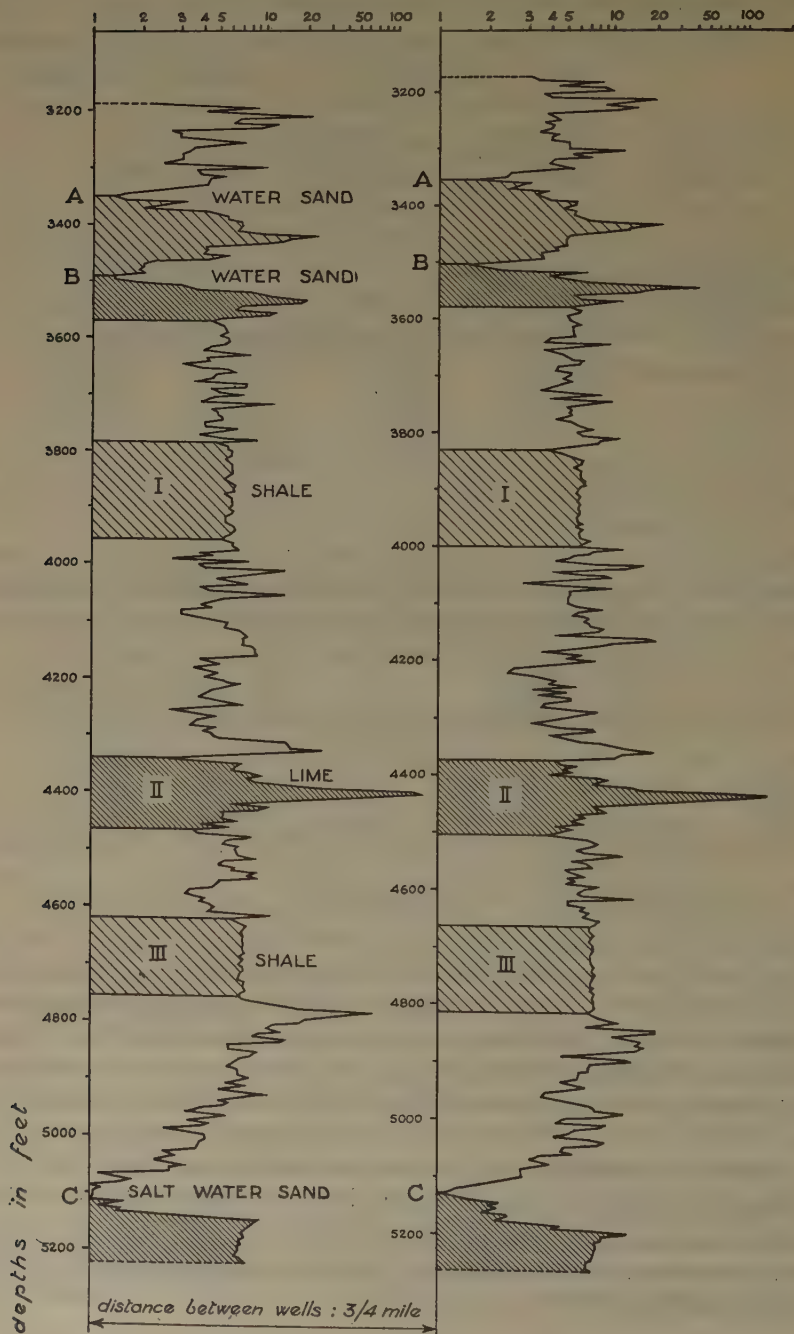
ELECTRICAL CORRELATIONS BETWEEN TWO WELLS  
OKLAHOMA CITY 1929.*Resistivities in ohms m<sup>2</sup>:m - Logarithmic scale.*

FIG. 7.—ELECTRICAL CORRELATIONS BETWEEN TWO WELLS, OKLAHOMA CITY, 1929.

beds. This point is illustrated in Fig. 6, where two electrical graphs taken in a Sumatra oil field are shown, and also in Fig. 7.

Fig. 7 refers, from left to right, to Waters No. 3 and Mackey No. 1 wells located three-quarters of a mile apart in the Oklahoma City pool, and shows nicely the results that may be expected in the case of a regular sedimentation. Due to the wide range of variation in the resistivities (variations from 1 to 100) they are shown on a logarithmic scale. The rocks studied are of Pennsylvanian age. The beds with a saw-tooth profile are limestones or sandy shales. The two zones with a fairly regular resistivity I and III correspond to two characteristic layers of homogeneous shales; the resistive region II corresponds to the Tonkawa limestones, and the depressions A, B and C indicate three water sands.

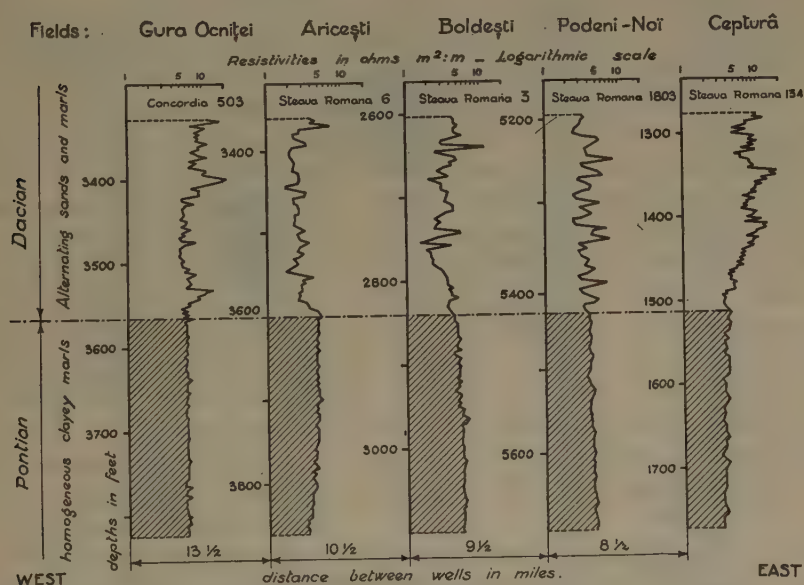


FIG. 8.—ELECTRICAL HORIZON MARKER EXTENDING OVER 45 MILES, RUMANIA, 1931.

Sand C, of which the resistivity is very low, is a very salty one. From now on, this determination of a water sand must be borne in mind. This is a particular feature of the electrical measurements with which we will deal in greater detail further on.

The reliability of the electrical markers depends on the regularity of the formations. In numerous cases, the sediments maintain their lithological facies over large areas. The consequence of this is that the diagrams possess remarkably similar silhouettes. Fig. 8 shows the characteristic resistivity profiles measured in five Rumanian fields. The Dacian is composed of alternating sands and marls, and gives wavy profiles which are in complete contrast with the very flat profiles given

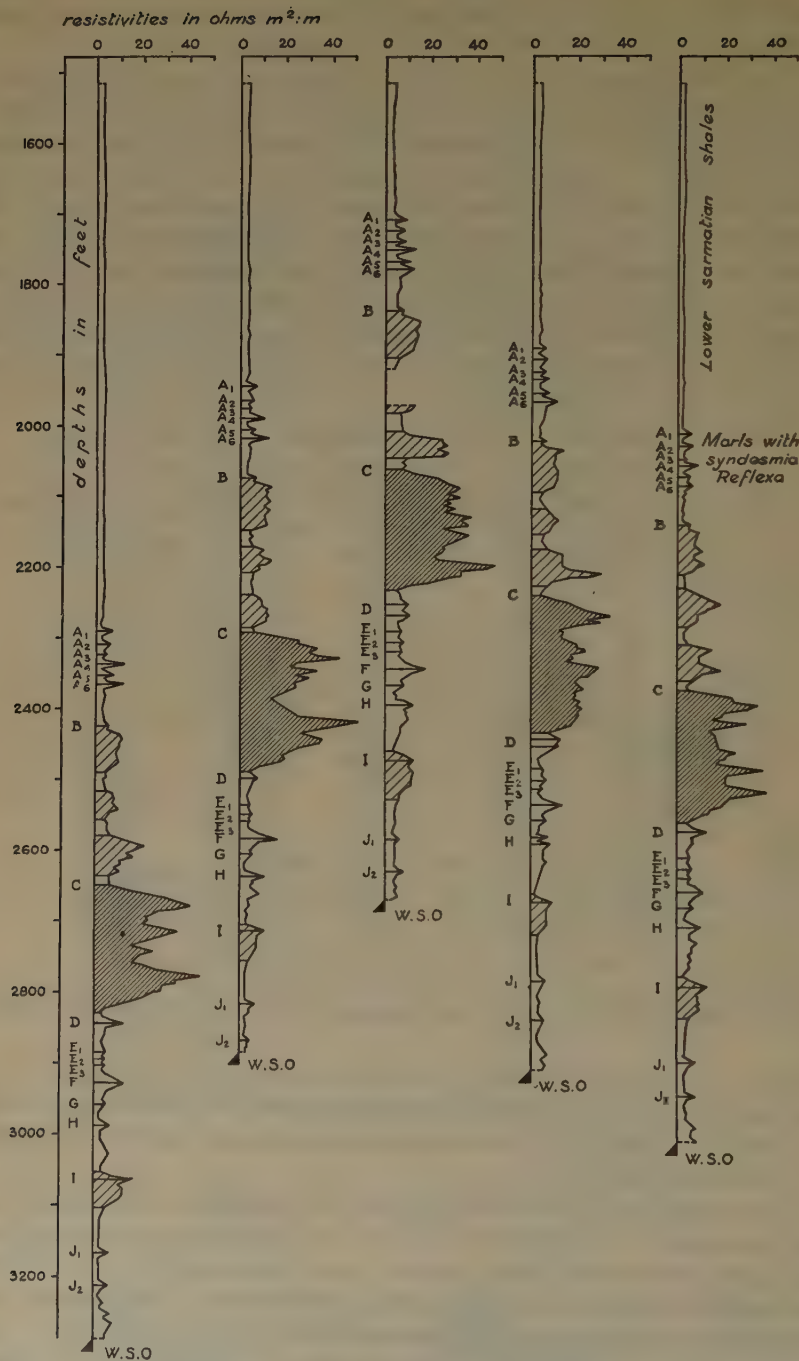


FIG. 9.—NUMEROUS CORRELATIONS BETWEEN WELLS. LETTERS SHOW PRINCIPAL HORIZON MARKERS ABOVE W. S. O.



by the Pontian, made up of argillaceous marls. The fact is worth noting that the most widely separated fields are 45 miles apart.

Naturally, on occasion certain geological horizons which are characterized by their appearance, or by the fossils which they contain, can not be differentiated electrically, since electrical differentiation is concerned with an entirely different parameter of the rocks. On the other hand, it will often happen that very satisfactory electrical markers will be discovered in a geological complex completely lacking in leading horizons. The stratigraphy will be lithologically obscure but electrically distinct. This case is very general in recent unconsolidated formations, and is well illustrated by Fig. 9, which will be commented upon further on.

*Some Examples of the Economic Services of Electrical Surveys.*—Fig. 9 represents the structural study of part of the Grozny oil field, U.S.S.R., by electrical correlations. The diagrams begin in the clays of the Lower Sarmatian, which, as is usual for clays, are very homogeneous in composition. The underlying horizon, that of the *Syndesmia Reflexa* marls, constitutes a leading horizon of very characteristic form and of remarkable uniformity. Below comes a series of alternating sands and clays, where the sandy layers are generally water-bearing, and show up by maximums of resistivities. An oil zone containing oil in nonexploitable quantities appears at *CD*. This is a thick formation, which, on account of the oil it contains, possesses a resistivity distinctly greater than that of the surrounding terrains. Below this oil zone, markers *I* and *J* should receive particular mention, since, although very unimpressive electrically, they are exceedingly reliable. They are apparent on drill holes located more than six miles apart, and are of great practical interest for determining the depth of the water shut-off. Previous to the regular use of the electrical surveys in this field, the only geological marker employed in practice to guide the drilling work was the zone of the *Syndesmia Reflexa* marls.

Fig. 10 shows a series of electrical measurements carried out in a field of the Maracaibo district, Venezuela. Outside of very satisfactory stratigraphic correlations, we will mention the first oil horizon (tar sands), which marks the top of the oil series, and the two underlying oil zones, which are good productive sands. Before the use of the electrical graph in this field, there existed a great uncertainty as to the level at which the water shut-offs had to be made. For instance, the two first diagrams on the left show water shut-offs which were thus placed incorrectly at too great a depth. Later on, the water shut-offs were located with accuracy in a clayey formation, thanks to the electrical measurements.

Without further emphasis on this point, the reader will readily realize the detail and precision with which the underground structures can be studied at different levels with such data in hand. Should a fault occur



between two holes, it would immediately be located with great accuracy, and its exact throw ascertained. Fig. 11 represents a fault which was thus discovered in a field of the Maracaibo district, Venezuela.

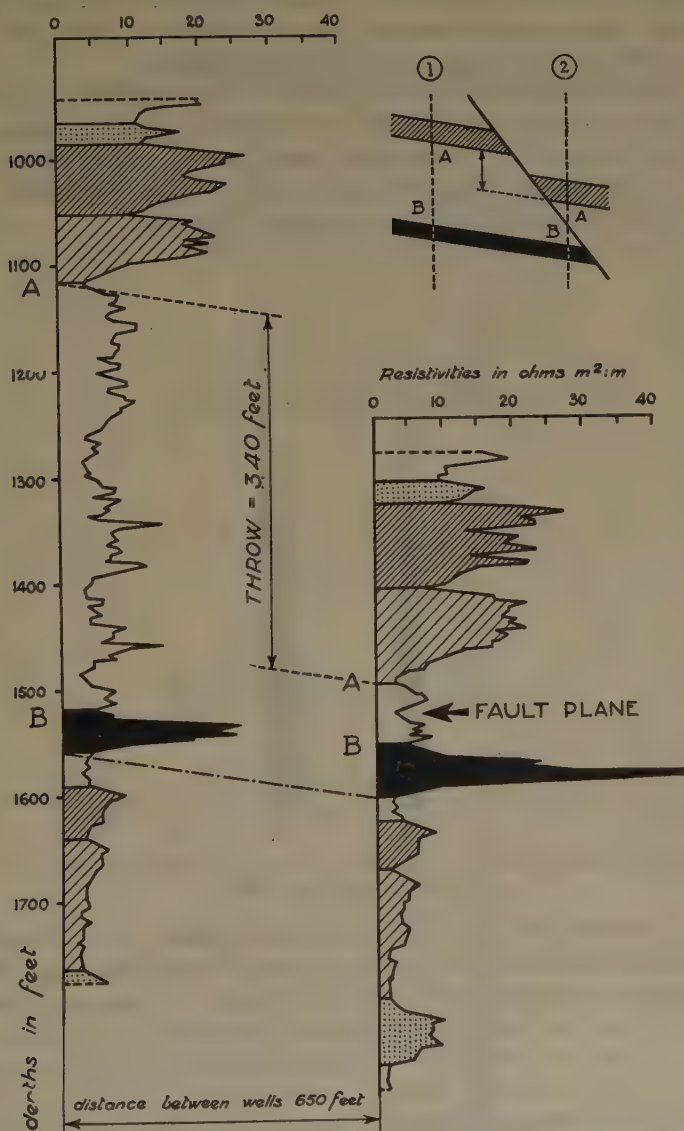


FIG. 11.—DETECTION OF A FAULT AND DETERMINATION OF ITS THROW, VENEZUELA, 1930.

*Location of Oil Sands and Coal Beds.*—At the beginning of the section on geological correlations, we pointed out that the numerical value of the resistivity does not ordinarily permit the sure determination of the

nature of the rock itself. Fortunately, however, in a few instances, which in practice are of paramount importance, the electrical diagrams permit the discovery of the only economically important layers penetrated by drill holes. Not only does the expense incurred with the electrical process not compare at all with the cost of continuous mechanical coring, but its accuracy and reliability probably are greater.

In describing the use of the process in establishing stratigraphic correlations, we mentioned incidentally the fact that the oil-saturated rocks were insulating. This point needs to be discussed in greater detail, on account of the considerable interest which it presents in connection with a more rational exploitation of oil fields.

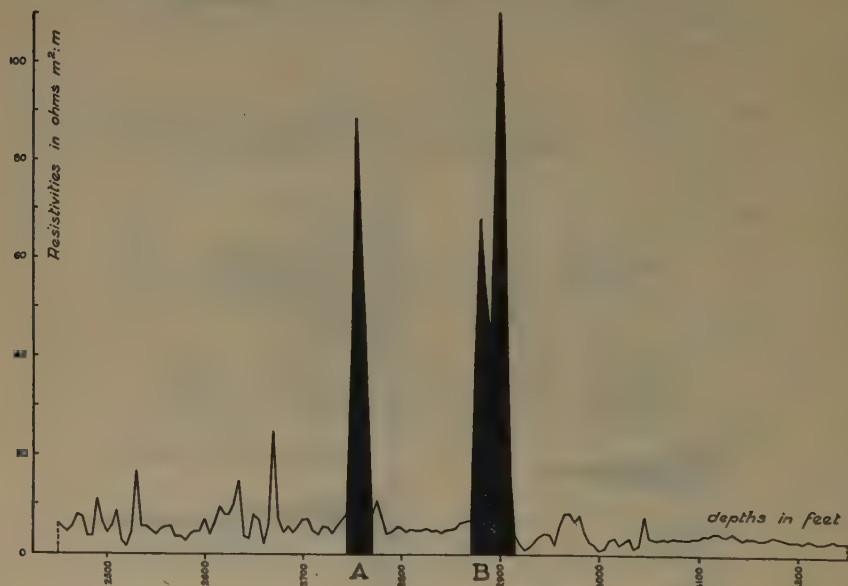


FIG. 12.—HIGH RESISTIVITY OF TWO PRODUCING SANDS, WEWOKA FIELD, SEMINOLE AREA, OKLAHOMA, 1929.

It is a well-known fact that mechanical drilling is confronted with real difficulties in determining with accuracy the position, the thickness and the productivity of a petroliferous horizon. It frequently happens that the recovery of cores is very limited. Sometimes, for this reason, a horizon is not even detected. As to the possibility of being able to determine with the naked eye the productivity of an oil sand, everyone knows that such an examination is very often fallacious, since a sand with a good appearance may well correspond to a lean bed with a small rock pressure.

The resistivity graph will perform a first service in locating with accuracy the resistant layers encountered by a drill hole. If there is any reason to suppose that one of them is an oil bed, it will at least be



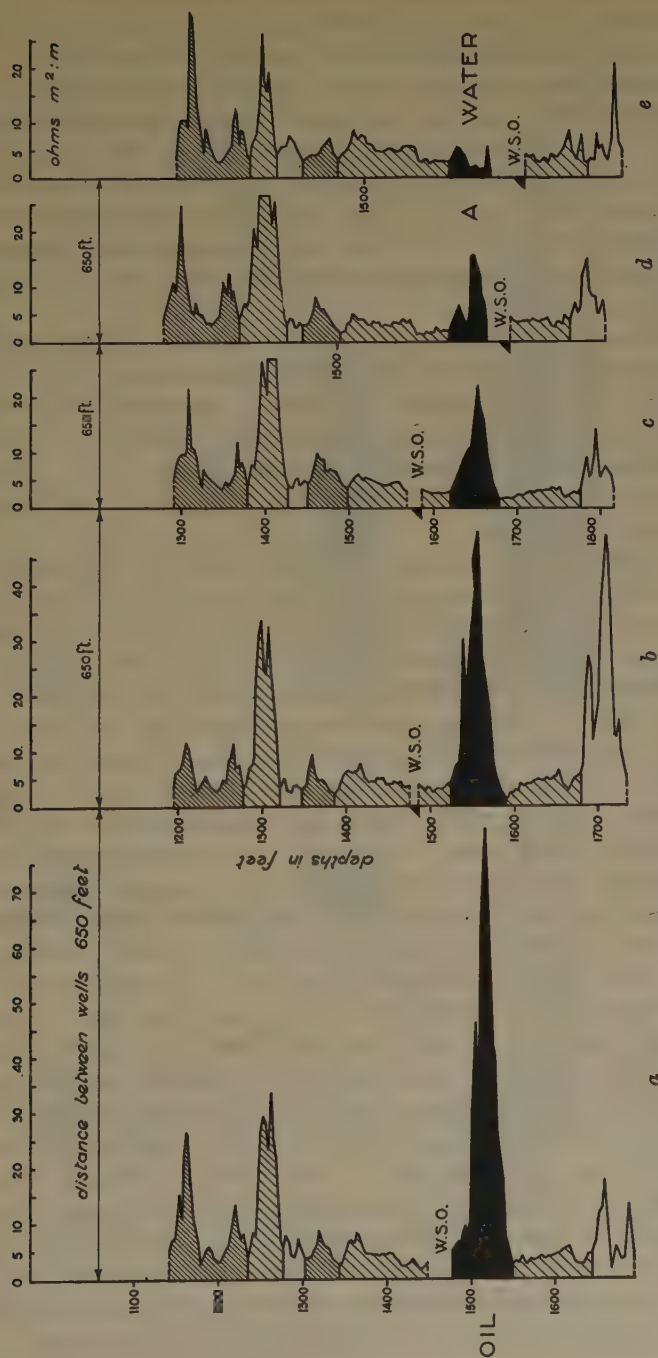


Fig. 13.—GRADUAL TRANSFORMATION OF A GOOD PRODUCING SAND INTO A WATER SAND, VENEZUELA, 1930-1931.

possible to make a production test under good conditions. It may be objected that an oil-bearing horizon might be mistaken for a compact resistant bed (limestone, dolomite or gypsum in particular). Such an error, however, is not likely to occur, as will be seen later on, provided that the resistivity and the porosity diagrams are registered simultaneously. Fig. 12 gives a good example of two heavy, oil-saturated sands (Cromwell sands) in the Wewoka pool, Seminole area, Oklahoma, (Peney Reed No. 1 well). Their resistivities show figures of about 100 ohm-meters, while the more resistant of the sterile beds does not reach 25 ohm-meters, and the average resistivities of the formations are close to 5 or 6 ohm-meters.

In numerous cases, there will exist a definite relation between the productivity of a sand and the order of magnitude of its electrical resistivity. Fig. 13 represents a series of electrical diagrams taken in a field in Maracaibo district, Venezuela. Sand *A* is a high producer in 13*a*, and is entirely saturated with water in 13*e*. From *a* to *e* the production decreases in a manner comparable to the decrease of the electrical resistivities.

An equally striking example is furnished by Fig. 14, which results from the surveys carried out in the Grozny field. Level *H* is an oil sand which gave rise to an eruption in well 1. It turns to a water sand with oil showings in well 2. In well 3 it is dry. The thin sand horizon *I* is sterile in wells 1 and 2, and petroliferous in 3. As to zone *J*, it gave in wells 1 and 3 eruptions which were respectively 400 and 14 tons daily. We may mention incidentally that 6 tons of water were obtained daily with the oil in well 3. This fact is to be noted in conjunction with the electrical diagram, which shows several minima of very low resistivity, which would seem to indicate a nonhomogeneous formation, the productive thickness of which must be somewhat limited. Level *K* is a further petroliferous sand, which is sterile in 1 and saturated in 3.

That such information may be used in practice to orient advantageously the drilling operations is evident. We will merely cite in this connection the profile shown on Fig. 15, which was taken in the Tintea field, Rumania, in well 52 of the Unirea Co. In this part of the pool, the lower sand from 4380 to 5300 ft. is exploited, and the lean sand from 4020 to 4230 ft. is neglected. From the appearance of the profile, the electrical observer strongly insisted upon a production test being made at first on the upper sand. This, however, was not the opinion of the petroleum engineers, and exploitation of the lower sands was decided upon, it being agreed that should this horizon prove to be a poor producer, the upper sands would be tested. For more than one month, the lower sands were maintained in production, and their average daily yield was only about 30 tons (210 bbl.) with a low pressure.<sup>4</sup> It was

---

<sup>4</sup> The total amount of oil recovered from these sands was only 900 tons.

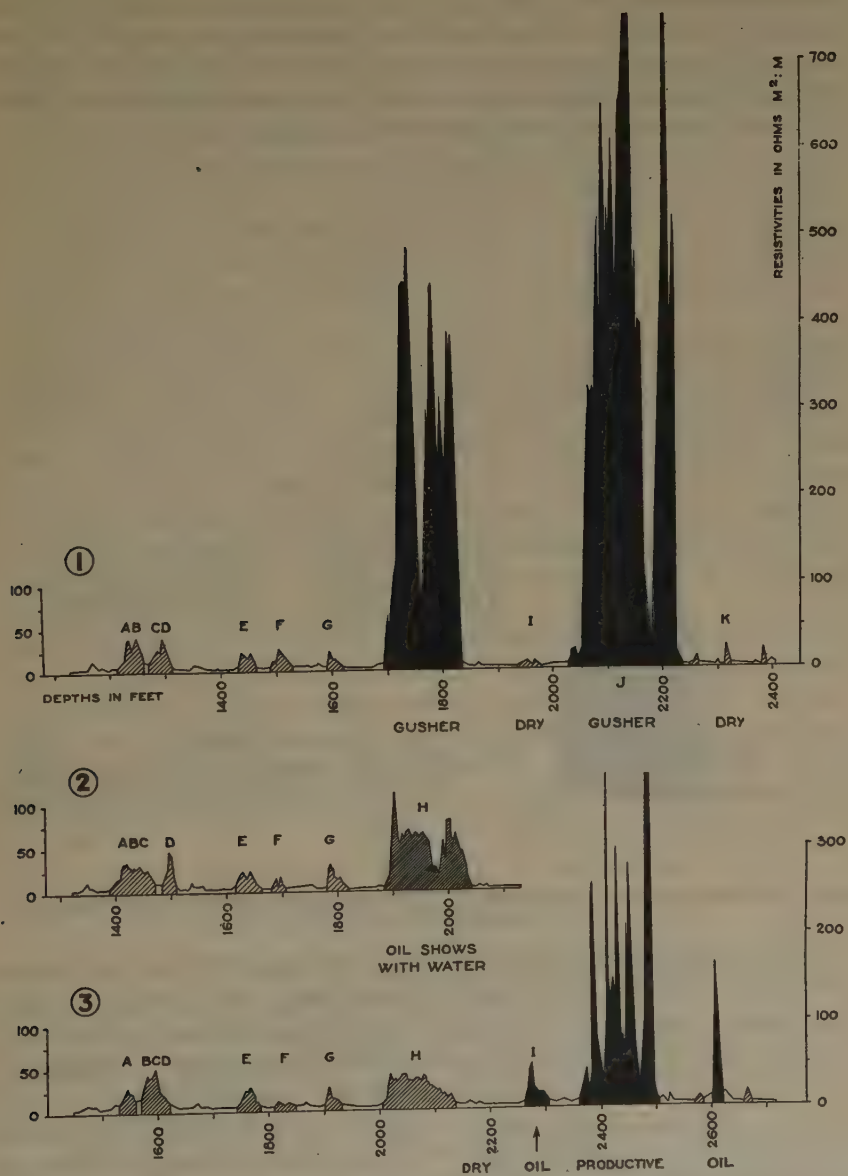


FIG. 14.—RELATION BETWEEN RESISTIVITY OF AN OIL SAND AND ITS PRODUCTIVITY  
GOSZNY, 1931.

then decided to cement the lower layer and to test the upper one. During the first 25 days the latter gave a production of about 2000 tons, and its daily production after a period of three months was still 60 tons (420 bbl.), with a pressure of 40 kg. According to all probabilities, this drill hole, which otherwise would have resulted in a small profit, will constitute instead a very profitable operation.

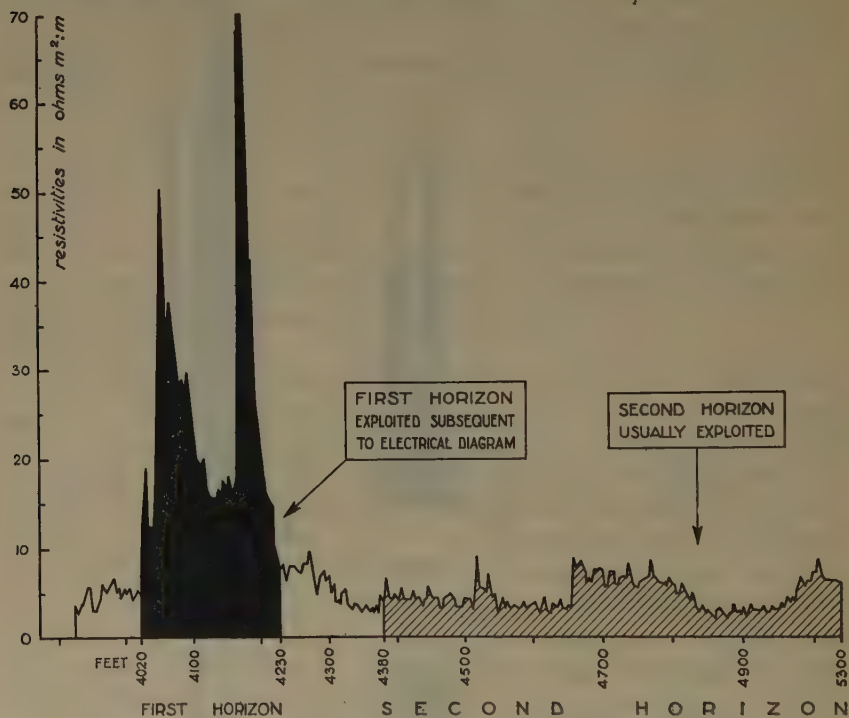


FIG. 15.—DISCOVERY OF A PAY SAND BY ELECTRICAL MEASUREMENTS, TINTEA FIELD, UNIREA 52, RUMANIA, 1931.

The precision of the electrical diagnosis concerning the productivity of oil horizons is very satisfactory in most fields. It may be poor, however, under certain circumstances. So far, we have encountered only one case of a field where oil is not electrically detectable. In Sumatra, light oil zones do not cause any important increase in the resistivity figures. This may be explained by the fact that the sands are very porous and possess a low rock pressure. They are invaded locally by the mud of the hole, which repulses the oil. Therefore, in the immediate vicinity of the hole there is practically no oil left. The use of special gelatinous muds (silicated fluids, for instance) will probably overcome this difficulty.

The preceding examples show that in many instances the resistivity figures permit a fairly correct estimate of the probable productivity of an oil sand. This information is of considerable value for the production



department. It has been, thus far, impossible to deduce it from the drilling data. Examples may be cited of oil zones which *a priori* were discarded by the geologists for a production test, merely on account of the poor appearance of the water-soaked core samples recovered from the hole, but which, as a result of the electrical measurements, were put into production and have yielded millions of barrels of oil.

It must be emphasized that the resistivity figures obtained on an oil horizon which is tested electrically for the first time will not permit, as a rule, the estimate of its future production. On the other hand, the comparison of the resistivity figures which refer to the same oil zone in a series of wells generally furnishes very satisfactory and accurate information.

A similar problem, which is economically less important than the discovery of oil zones but not negligible, is encountered in drilling for coal. In this case, also, it is difficult to obtain a satisfactory recovery, since the interesting beds are very brittle. Even with the use of continuous coring, it frequently happens that coal beds will be detected quite inaccurately, or will not be detected at all. It is necessary to follow the progress of the drilling with constant attention, and to use a very low drilling speed. The cost of the hole per foot is accordingly very high.

Electrically, on the contrary, the problem is easy. Coal is, by far, the most resistant rock found in a carboniferous formation. Furthermore, the other resistant rocks are very hard to drill, so that the mere inspection of the drilling speed records will suffice to dissipate any uncertainty concerning the interpretation of the electrical profile. A high peak of resistivity in a soft formation corresponds undoubtedly to a coal bed.

## B.—POROSITY OF THE ROCKS; ITS MEASUREMENT AND APPLICATIONS

The detection of porous strata such as sands, sandstones or fissured limestones is of paramount importance in the exploration of oil fields, since gas, oil and water are invariably stored in such porous horizons. This factor, likewise, may present a real economic interest in any kind of drilling exploration, in order to locate the water-bearing horizons correctly.

Up to the present time, the porosity of rocks has been studied by examining the cores recovered from drill holes. The process is expensive, and is all the more inefficient because porous formations are generally more or less unconsolidated. The new method, which will be described below, permits the determination of the porosity of the strata encountered without the necessity of bringing to the surface any samples or cores of the rocks under consideration.

*Principles of Electrofiltration Measurements*

When an electrolyte is caused to flow through a sheet made of a pervious, solid dielectric, an electromotive force occurs between the two sides of the sheet. This electromotive force is proportional to the pressure, to the electrical resistivity of the liquid, and inversely proportional to its viscosity. It is independent of the thickness of the filtering sheet, and of the radii and number of pores of the pervious medium. It may be expressed by the following formula:

$$E = m \times \frac{R}{V} P \quad [2]$$

in which

$E$  is the electromotive force of filtration,

$P$  the pressure of the liquid,

$R$  the electrical resistivity of the liquid,

$V$  the viscosity of the liquid,

$m$  a constant factor which depends on the porous medium.

It is interesting to compare this law with those discovered by Poiseuille for gases and by Slichter for liquids, which provide that the quantity of fluid flowing through a capillary tube is proportional to the difference of pressure and inversely proportional to the viscosity.<sup>5</sup> With the notations employed above, we have,

$$Q = m' \frac{P}{V} \quad [3]$$

$Q$  being the quantity of liquid which flows through the capillary tube and  $m'$  a constant factor.

Through the combination of formulas 2 and 3, we obtain the expression

$$\frac{E}{Q} = \frac{m}{m'} R$$

which shows that the electromotive force of filtration is, for a given electrolyte, proportional to the amount of liquid that filters through, and to its electrical resistivity. This force, as can be seen, is thus in close connection with the porosity of the filtering medium.

In most cases, the sign of this electromotive force is such that the electric current which it causes to flow possesses the same direction as the liquid in movement. In the case of a pervious sheet, then, it is the wall of ingress of the liquid which is negative with respect to the wall of egress.

<sup>5</sup> Poiseuille: C.R.A.S. (1842) 18, 1167.

C. S. Slichter: Theoretical Investigation of the Motion of Ground Waters. U. S. Geol. Survey 19th Annual Report (1897-98) pt. 2, 301.

In most drill holes, the well is filled with water in sufficient quantities to exert a pressure on the walls distinctly superior to the hydrostatic head which exists in the rocks. This is particularly true in the numerous cases where the muds filling the holes are purposely made heavier to avoid as much as possible the caving in of the hole and blow-outs of gas or oil. Under these circumstances, the water of the muds penetrates into the pervious layers traversed by the hole, repelling the liquid which they contain (water and oil) as shown on Fig. 16. It is this filtration which generates the phenomenon of electrofiltration. Since the potential is increasing in the direction of flow of the liquid, a minimum of the potential must be observed in practice at the face of any pervious layer encountered, as indicated at the right in Fig. 16. It is not a question of a minor electric phenomenon, and potential differences of 100 or 200 mv. usually are observed over a length of a few meters.

### *The Measuring Apparatus*

How can one measure the differences of potential thus existing inside the drill holes? The problem

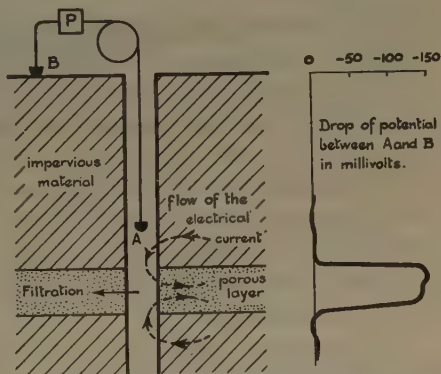


FIG. 16.—ELECTROMOTIVE FORCE OF FILTRATION GENERATED IN DRILL HOLE BY POROUS LAYER.

can be very simply solved with the apparatus previously described in connection with the resistivity measurements. An impolarizable electrode *A* is fixed to one of the insulated conductors of the tricable, and is lowered into the hole to various depths by means of a winch (Fig. 16). The upper end of the conductor is connected to one of the terminals of a potentiometer *P*, of which the other terminal is connected by an insulated wire to a second impolarizable electrode *B*, grounded to a fixed point at the surface. The potential of the latter electrode is arbitrarily assumed to be equal to zero. For each position of the movable electrode within the drill hole, the potentiometer will therefore give the value of the potential at this particular point. In practice, the recording apparatus used for registering the resistivity diagrams is employed, and a continuous graph of the potentials inside the drill hole is obtained. The smallest variations of this quantity can be observed. It goes without saying that the measurements can be performed only in the uncased part of the hole.

It has been stated previously that the electrodes must be of the "impolarizable" type. This is necessary so as to eliminate the errors caused by the chemical electromotive forces arising from the contacts between the metal and the water of the boring, or the wet soil at the surface. These electrodes are generally formed of a metallic electrode



surrounded by a porous cup filled with a concentrated solution of a salt of the same metal.

### *Use of the Porosity Diagram*

The porosity diagram permits one to study, conveniently and cheaply, the permeability of the rocks in the drill hole itself, and the direction of the flow of the fluids between the said rocks and the borehole. It is easy to understand the great importance of this information, which leads to the diagnosis of the petroliferous zones and water-bearing levels.

The most comprehensive results will be obtained by registering and studying simultaneously the resistivity and porosity profiles. Thanks to them, it becomes easy to decide whether a resistive bed is a compact rock such as gypsum, dolomite or limestone, or a porous sand saturated with oil. Fig. 17a represents a differentiation of this kind obtained in the Pechelbronn oil field, Alsace. The resistivity profile indicates, from a depth of 730 to 845 ft., a series of resistant beds. The porosity profile shows immediately that these beds do not possess any porosity. The beds, then, are made up of compact material. As a matter of fact, they are gypsiferous.

On the other hand, an oil stratum that is both resistant and porous will be clearly brought into evidence by the comparison of the two graphs. Such an example is presented in Fig. 17b, which shows the results obtained in a well of the Grozny oil field.

The same method will make it possible, in numerous cases, to decide whether or not a layer with a low resistivity is a clay or a more or less salty, porous sand. Fig. 17c shows a resistivity profile entirely flat, which merely indicates that the layer is not oil-bearing. An important electrofiltration phenomenon shows, however, that the rocks are very porous between 1872 and 1922 ft. The bed is a salt-water sand possessing approximately the same resistivity as the surrounding clays. The example comes from an oil field of the Maracaibo district, Venezuela.

Finally, Fig. 17d shows the detailed study of a pervious bed characterized by two peaks of the porosity profile. The comparison with the resistivity profile leads to the conclusion that the upper part of the bed is resistant and petroliferous while the lower part is conductive and salt water-bearing.

Naturally, it will be possible with the use of the porosity graph to detect the water-bearing diaclasses and faults.

It must also be pointed out, in order to complete the subject, that aside from the large anomalies caused by the very porous layers, numerous minor potential disturbances are registered on the porosity profile. They can be ascribed either to a slight porosity of the neighboring strata, involving appreciable phenomena of electrofiltration owing to the high



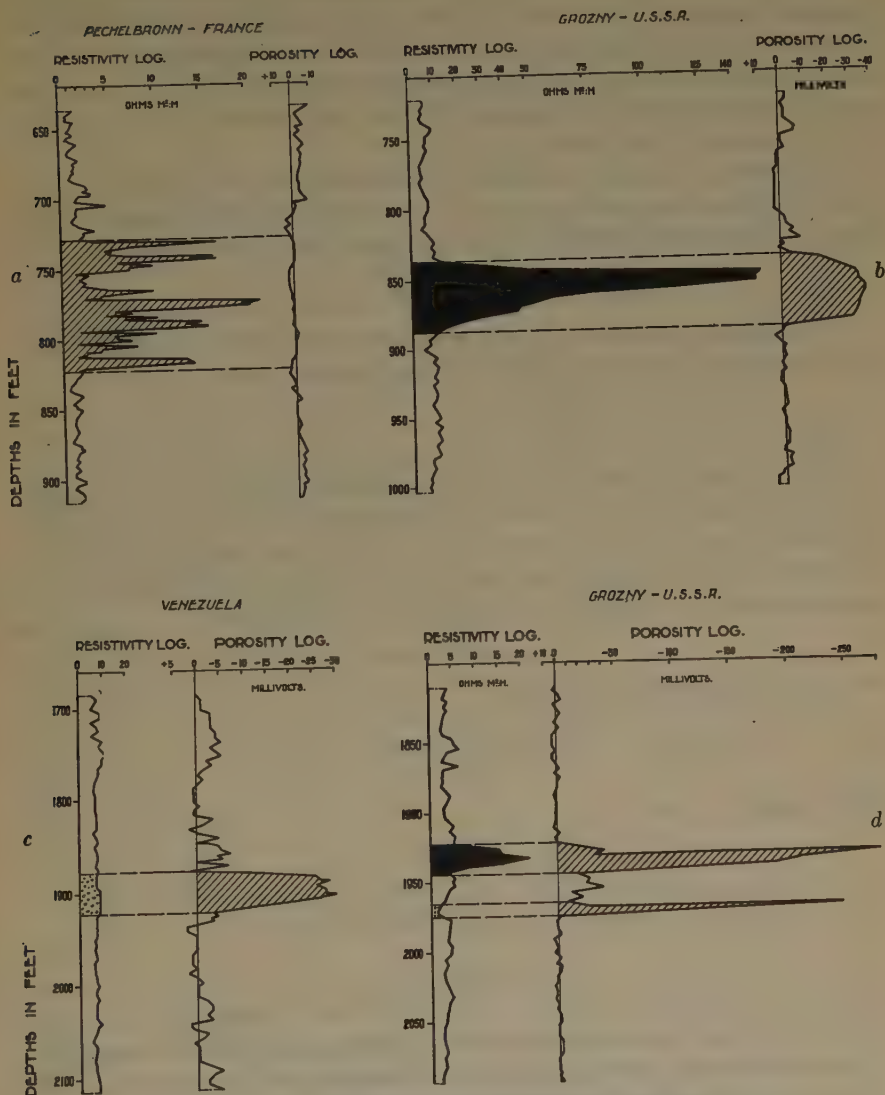


FIG. 17.—RESISTIVITY AND POROSITY DIAGRAMS.

- a. Impervious and resistant formation, gypsum. Pechelbronn.  
 b. Pervious and resistant formation, oil sand. Grozny.  
 c. Pervious and conductive formation, water sand. Venezuela.  
 d. Pervious formation resistant at top—oil. Conductive at bottom—salt water. Grozny.

pressure existing in the borings, or to other causes, such as electrochemical reactions between rocks of different compositions. These electrochemical reactions generally give rise in oil wells to electrical perturbations which are much smaller than those caused by the filtration phenomena. It is easy to distinguish experimentally between the two kinds of phenomena, since those caused by the porosity are the only ones to vary according to the pressure of the muds in the hole.

It must be borne in mind that these phenomena are normally found again on the corresponding layers in the neighboring drill holes, so that they complete advantageously the correlations by resistivities.

### *Measurement of the Rock Pressures*

If we again consider formula 2, let us call  $H$  the pressure of the water head and  $p$  the pressure of the fluids in the porous layer. Then

$$E = m \times \frac{R}{V} \times (H - p) = K(H - p) \quad [4]$$

$K$  being a constant factor for the layer under consideration. Let us now modify the water head, by lowering, for instance, the level of the water in the drill hole. If  $H'$  is the new value of the water head in the hole, at the depth of the porous layer, and if we call  $E'$  the new value of the electrofiltration potential which is observed, we will have

$$E' = K(H' - p) \quad [5]$$

Dividing [5] by [4] we obtain

$$\frac{E'}{E} = \frac{H' - p}{H - p} \quad [6]$$

If we write

$$\frac{H'}{H} = s, \text{ and } \frac{E'}{E} = t$$

we can deduce the value of  $p$  from [6]. This value is

$$p = H \frac{s - t}{1 - t}$$

Thus we see that the electrofiltration phenomena offer a possibility of measuring the pressures of the fluids inside the porous layer itself, without allowing the fluid to flow into the hole. To achieve this, it will suffice to modify the pressure of the muds in the drill hole, either by lowering the water level, by modifying the density of the muds, or by increasing the pressure by means of the mud pumps. Knowing the height of the column of mud and its density, the pressure  $H$  will then be known. It will therefore be easy to evaluate  $p$ .

As an example, Fig. 18 represents two porosity diagrams obtained with a water sand in the Pechelbronn oil field by varying the head. The

first diagram shows that with a column of mud of 309 m. an electrofiltration phenomenon of 60 mv. was obtained. On the second diagram, the corresponding figures are respectively 208 m. and 25 mv. The density of the muds being 1.2, we deduce immediately the pressure in the water sand,  $p = 16.6$  kg. It has been possible to verify the correctness of this pressure, by letting the level of the water reach its position of equilibrium in the drill hole.

We believe that the results to be expected from such pressure determinations are very important, since the determination of the rock pressure has, so to speak, thus far entirely escaped investigation. There is no doubt that the systematic study of factor  $p$ , for the various productive horizons of an oil field, would permit conducting the exploitation in a much more rational manner than has been possible heretofore.

These pressure measurements constitute an interesting new line of investigation. They are often considered as very delicate by the drillers, who are as yet reluctant to try them. The tests, therefore, were performed mostly on water flows, and have not received the confirmation of a large field practice. The authors hope that, in the near future, it will be possible to judge more completely the practical interest of this new technique, which, in their opinion, possesses far-reaching possibilities.

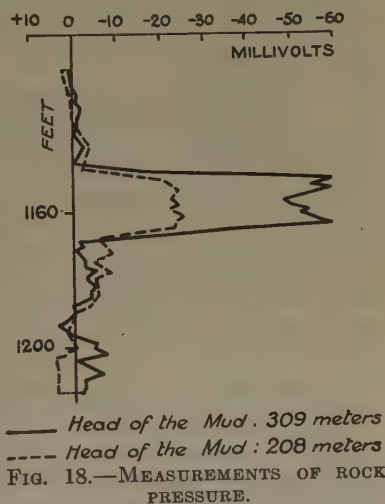


FIG. 18.—MEASUREMENTS OF ROCK PRESSURE.

#### C.—ELECTRICAL ANISOTROPY OF ROCKS; DETERMINATION OF DIRECTION OF DIP

It is well known that the conductivity of stratified rocks is not the same in all directions; it is a maximum in the direction of the stratification, and a minimum perpendicular thereto. In this connection, the electrical properties of the sedimentary formations are comparable to the optical properties of crystallized media. If an electric current is caused to flow from a grounded point-source into a stratified rock, the surfaces of propagation (equipotential surfaces) are not spheres, but flattened ellipsoids, the axis of revolution of which is perpendicular to the plane of stratification.

It is possible to take advantage of this property to determine the direction of dip of formations traversed by drill holes. On Fig. 19, a cross-section of the formations perpendicular to the plane of stratification

$SS'$  has been represented along the axis of the drill hole. If a current is sent into the ground by means of two grounds  $A$  and  $B$ , which are connected by an insulated cable one to a battery  $E$ , the equipotential surfaces in the neighborhood of  $A$  are flattened ellipsoids which have the line  $AZ$  for their axis of revolution. We have represented the section of one of these ellipsoids in the plane of the figure. This is an ellipse elongated along the axis  $SS'$ .

We will now lower into the hole two secondary electrodes  $M$  and  $N$  attached to a horizontal rod at a given distance apart. These two electrodes are connected by means of two insulated cables, 2 and 3, to a potentiometer  $P$ , at the surface. It is easy to see that if the line  $MN$  is oriented perpendicularly to the plane of the figure, electrodes  $M$  and  $N$  will be located on an equipotential surface, and no difference of potential will be observed with the potentiometer. On the other hand, if  $M$  and  $N$  are in the plane of the figure, the difference of potential will be at a maximum.

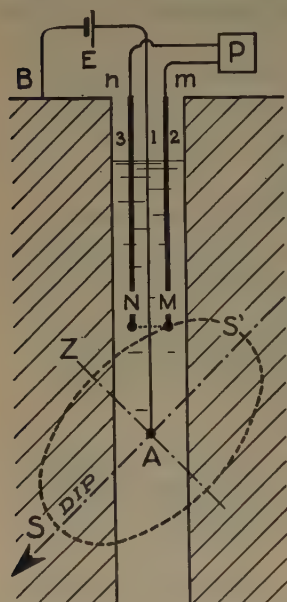


FIG. 19.—ELECTRICAL DETERMINATION OF DIRECTION OF DIP.

Suppose now that the rod  $MN$  is attached to the lower part of a pipe which extends to the mouth of the hole, and which may be rotated at the will of the observer. This pipe may be, for instance, the drill pipe itself. It will be of steel, except for its lower part, where necessarily it will be made of an insulating material, in order not to disturb the propagation of the current around  $A$ . The pipe is provided at its upper part with two marks  $m$  and  $n$ , which are located exactly on the vertical lines passing through  $M$  and  $N$ . The observer at the surface knows, then, accurately, the orientation of the rod  $MN$  by looking up the position of the marks  $m$  and  $n$ . It is evident that, under these conditions, it will be easy for him, by turning the pipe, to determine the position at which the electrodes  $M$  and  $N$  will be at the same potential while the current is passing through the ground. This first experiment will give the direction of the strike.

As to the direction of the dip, it will suffice to rotate the pipe at an angle of  $90^\circ$  from the first position, and observe the sign of the difference of potential between  $M$  and  $N$ .

Naturally, in practice it would be very inconvenient and very slow to determine the position of the line  $MN$  by means of a steel pipe. A simple way to achieve this is to make the determination with reference to the direction of the terrestrial magnetic field by means of an induction



compass, as will be explained later on, in the description of the electromagnetic teleclinometer.

A measuring apparatus has been built according to these principles. It has, like the teleclinometer, the form of a long, metallic, cylindrical case. It is lowered into the drill hole by means of the tricable which is employed for the resistivity and porosity measurements. Two of the insulated cables are connected to the electrodes *M* and *N*, and the third one is connected to the induction compass and to the ground *A*. The apparatus has given reliable results, but has not yet been employed extensively. It will be necessary to test it further, as to its strength, practicability and accuracy before putting it definitely in use on a commercial scale.

#### D.—TEMPERATURE MEASUREMENTS IN DRILL HOLES

With the same equipment shown in Fig. 1, it is easy to make an arrangement which permits an accurate determination of the temperature inside drill holes.

It will suffice to connect two of the insulated cables to a resistant spool formed of a metallic wire perfectly insulated and possessing a high temperature coefficient, and to lower this spool inside the hole. Considerable research work has been necessary in order to achieve a small time factor (metallic wire which will quickly assume the temperature of the surrounding medium) combined with a good electric insulation.

The resistance of the circuit is measured at the surface by the well-known method of the Wheatstone bridge. Since this resistance depends upon the temperature of the apparatus, it is possible to determine the temperature inside drill holes with great accuracy, rapidity, and in the form of a continuous graph. In practice, the potentiometer and the registering apparatus previously described are utilized. The temperature is automatically registered on a sheet of coordinate paper. It is plotted as abscissas, while the depths are shown as ordinates. The precision of the apparatus reaches the twentieth of a degree Centigrade, and can be easily increased. The measurements can be carried out in the course of a few hours. This apparatus thus seems to constitute a great technical advance, compared with those which have been thus far realized.

What is the information that can be derived from temperature measurements? Our practical experience is still too limited for us to formulate a definite opinion on the subject. There exist abundant literature and documentation regarding temperature measurements carried out in drill holes; in particular, *Bulletin* 205 of the American Petroleum Institute, on Earth Temperature in Oil Fields, is entirely devoted to such measurements performed in oil fields, with articles by

K. C. Heald, C. E. Van Orstrand, J. A. McCutchin, E. M. Hawtoff and A. J. Carlson.

Practically all of these measurements have been made with the mercury maximum thermometer method, but Van Orstrand mentions that experiments have been carried out by him with an electrical resistance thermometer. We will quote the following paragraph from his article:

On account of the initial expense of the necessary equipment, and the difficulty of constructing leads that will remain intact after being immersed in a mixture of crude oil and salt water, the electrical method has not been given the careful consideration that it deserves. Once these obstacles are overcome, however, the advantages of the electrical resistance thermometer method over the mercury maximum thermometer method are so great that the former method will undoubtedly come into general use.

We believe with Van Orstrand that the study of detailed temperature diagrams registered along the whole length of the open hole, by means of an electrical resistance thermometer, will furnish very interesting information. Such information will be useful not only for the working out of the general geological conditions, but also for the study of particular problems such as the location of gas horizons, water levels or oil-bearing strata which flow into the holes.

A party of observers equipped to perform resistivity and porosity measurements will have already at their disposal all the expensive equipment necessary to carry out temperature measurements. The additional expense required to add a reliable electrical thermometer to this equipment was not very high, and was therefore justified. We hope that, thanks to the low cost which they now entail, geothermic studies in drill holes will receive the attention which they justly deserve.

#### E.—RESISTIVITY OF THE MUDS; LOCATION OF WATER FLOWS

We have seen previously that the potential measurements made between electrodes *M* and *N* (Fig. 1) characterize the resistivity of the formations in the region of the three electrodes *A*, *M* and *N*. We were careful, however, to point out that this was true only if the length of the measuring arrangement *AMN* was sufficiently great in comparison with the diameter of the hole (10 to 20 times larger).

If, on the other hand, a measuring arrangement is adopted which is small in comparison with the diameter of the hole, it is no longer the resistivity of the formations that will be measured, but that of the mud surrounding the electrodes *A*, *M* and *N*. A practical apparatus has been built for the carrying out of such measurements—the resistivimeter. This apparatus is hung at the lower end of the tricable by connecting each of its three electrodes to one of the insulated conductors. The measurements are performed with the equipment and the same technique already described in connection with the resistivity measurements

They are likewise automatically registered on coordinate paper by means of the recording apparatus.

### Location of Water Flows

The interest of the resistivity measurements lies in the facility and accuracy with which they permit the location of water flows. We will describe the technique which is generally employed to this end, and illustrate it with an example drawn from the Pechelbronn field in Alsace (drill hole 3346). Before carrying out the measurements, the well was conditioned by washing with nonsalted mud. Immediately after this operation, the first run was effected. At that time the composition of the mud was approximately homogeneous along the whole length of the hole, and the diagram obtained (solid line on Fig. 20), showed a practically uniform resistivity. The level of the mud was then lowered by about 300 ft. so as to allow the water-bearing levels to flow into the hole, and a second run was made. A distinct perturbation appeared upon the new resistivity graph at a depth of 1160 ft. (broken line on Fig. 20). The explanation of this perturbation is evident. It was caused by the water flowing from a porous layer at a depth of 1160 ft. This water, as a result of the bailing of the mud, filled the drill hole from 1160 to 1080 ft. The graph shows that it is usually unnecessary to realize such a large flow of the porous layers into the drill hole. In the present case the amount of mud bailed out was exceedingly large, and a much smaller decrease of the water head would have been sufficient. This point is important, since it shows that the new process can be safely applied in drill holes where blow-outs are to be feared.

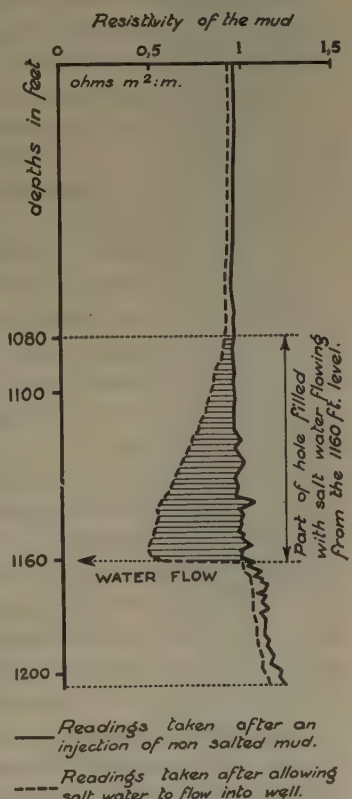


FIG. 20.—LOCATION OF A WATER FLOW.

These diagrams of the resistivities of the muds frequently make it possible to determine the levels where slight gas occurrences are to be found in drill holes, the gas bubbles generally carrying with them a distinct increase of the resistivity of the mud.

Another particular application of the apparatus consists in determining the respective levels of oil and water in a pumping well from which the pumping equipment has been removed.



Another apparatus called "water witch" has been in use for some time in oil fields for the location of water flows. This apparatus, at first sight, would appear to be similar to the resistivimeter described above. As a matter of fact, the two devices are based on entirely different principles. The water witch device measures the quantity of an electrical current flowing between two primary electrodes, while the resistivimeter measures the resistivity of the mud by means of two additional secondary electrodes.

#### F.—ELECTROMAGNETIC TELECLINOMETER; SURVEY OF CROOKED HOLES

The systematic use of geophysical measurements inside all the borings of a district permits the establishing of geological cross-sections of great accuracy. Water shut-offs, location of oil zones, etc., are obtained in practice, to an accuracy of one foot. In order to take advantage of this precision, however, it was necessary to eliminate the great uncertainty which results from the obliquity of the axis of the hole. When the depths are great, in particular, this obliquity may be the cause of considerable errors.

On the other hand, the determinations of dip obtained with the use of our "dipmeter" cannot be relied upon if the axis of the hole is not vertical or its position not well known. It is necessary, therefore, to know the inclination and the direction of the axis of the drill hole itself. We were consequently led to construct a teleclinometer, which makes it possible to obtain the exact picture of the path actually followed by the axis of the drill hole.

A full description of the practical realization of this apparatus is not necessary here. Its principles only will be indicated. It is composed essentially of an induction compass, a rotating spool composed of several loops of insulated wire, the ends of which are connected to a collector, also rotating, and with which brushes come in contact, and has an iron pendulum which can be magnetized at will from the surface by means of a current sent into the insulated solenoid. This magnetized pendulum is mobile around a double knuckle joint, and keeps permanently vertical. It is placed in the vicinity of the compass, and creates a magnetic field which is superposed on the terrestrial magnetic field. Each of these two magnetic fields (field of pendulum and terrestrial magnetic field) generates in the induction compass electromotive forces which are measured at the surface. To this effect, the measuring apparatus is connected to the brushes and to the induction compass, by means of two insulated cables. The measurement of these electromotive forces makes it possible to compute separately the values of the two magnetic fields, as well as their orientation with respect to the position of the brushes of the compass. From this the angle of inclination of the hole, and the orientation of this inclination, are obtained.



The apparatus has the form shown in Fig. 21. It is long enough so that it may be considered to remain parallel to the axis of the hole. It is attached to and lowered into the hole by means of insulated cables, which, as already mentioned, are connected to the magnetic compass and to the solenoid that regulates the magnetization of the magnetic pendulum. The general equipment utilized for the measurements is always that shown in Fig. 1; only the apparatus attached to the end of the tricable and lowered into the hole is different. At the surface, the registering apparatus, naturally, is not employed, and the measurements are made with the potentiometer alone. The inclination is correct to within  $0.5^\circ$ , and the drift of the hole from the vertical can be determined with a precision of about one per cent of the depth at which the measurement is effected.

There are already on the market several methods for the survey of crooked holes, the simplest being the use of an acid bottle. The principal advantage of the apparatus described here consists in the fact that numerous determinations at various depths can be effected in a very short time (about 2 hr.). It is therefore economical. The equipment utilized is the same as that employed for the registering of the resistivity and porosity diagrams, therefore if the resistivity or porosity survey of a hole has been decided upon, the study of its inclination and direction will not necessitate any special interruption of the drilling.

The principle of the apparatus, which is based on the use of an induction compass, does not offer the possibility of carrying out measurements inside the casing. They have to be made in the open hole, a fact which presents an advantage, since the survey is performed at a time when it is still possible for the drillers to rectify a crooked hole. In practice, the impossibility of carrying out measurements in the casing causes no serious inconvenience. When an electrical party is operating in a field, the observers have to survey all the holes being drilled, from the surface to the bottom. It is, therefore, easy for them to study from time to time, in the course of the drilling, the verticality along the whole length of the hole.

On the other hand, the use of the induction compass, which can be very strongly built, made it possible

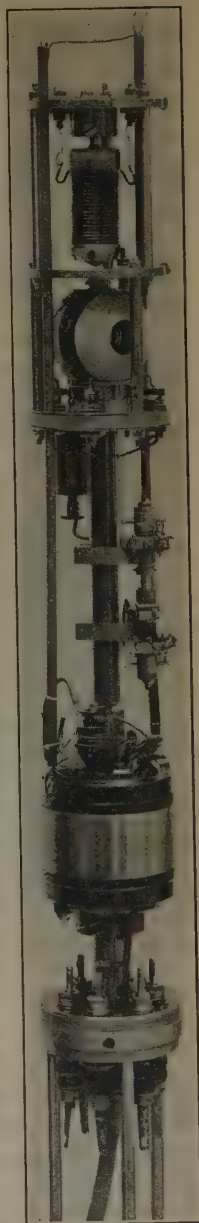


FIG. 21.—SCHLUMBERGER ELECTROMAGNETIC TELECLINOMETER, WITHOUT ITS METALLIC PROTECTING JACKET.

to construct an apparatus which is not affected by shocks. Such a result would not have been so easily feasible with a gyroscopic device.

### SUMMARY

The authors have described a series of methods and apparatus which permits the study of the formations penetrated by drill holes. They gave to the ensemble of these processes the name of "Electrical Coring," from analogy with mechanical coring, which has been thus far the only tool at the disposal of the geologist and production engineer to secure subsurface data in drilling exploration.

The process comprises a series of measurements carried out *in situ* by lowering the measuring apparatus into the drill hole. Thus, numerous bottom-hole data are obtained; namely, the electrical resistivity, the porosity, the temperature of the rocks, the direction of the dip of the formations, the resistivity of the muds, and the inclination and direction of the hole.

In the examination and identification of formations, the use of two physical parameters has been introduced: the electrical resistivity and the porosity. These parameters, measured inside the hole itself, make it possible to obtain numerous and reliable stratigraphical correlations. These correlations advantageously replace, in most cases, those obtained with the expensive and slow procedure of mechanical coring.

Strata saturated with oil or natural gas show up very distinctly on the resistivity diagrams, on account of their great electrical resistivity, and on the porosity diagrams on account of their great permeability. Their identification, therefore, is particularly clear. Furthermore, the numerical value of the resistivity itself, measured in a given oil-bearing stratum, generally gives a satisfactory idea of its future production. Finally, it is possible, with the use of quite a simple procedure, to determine the rock pressure itself inside a porous stratum.

### CONCLUSIONS

The fact that it now becomes possible actually to examine at depth the properties of the rocks, instead of bringing expensive core samples, lacking their initial absorbed fluids, to the surface for examination, is of paramount importance. It decidedly increases, in a large measure, the amount of useful information available for the technical man. Water-bearing formations can be located and studied in detail. Temperature measurements of the rocks, and measurements of the resistivities of the muds, will in numerous cases still further complete the amount of bottom-hole data at hand. Finally, measurement of the direction of the dip of the formations, and determinations of the inclination and direction of the hole, will make it possible to give to the different measure-

ments discussed above a geometric accuracy unknown up to the present time.

However, the greatest advantage of electrical coring is certainly the fact that the exploitation may be conducted more rationally, since, on the whole, more subsurface and bottom-hole data are gathered than with mechanical coring. As a matter of fact, as far as oil exploration is concerned, it is mainly the increase in the total amount of oil recovered

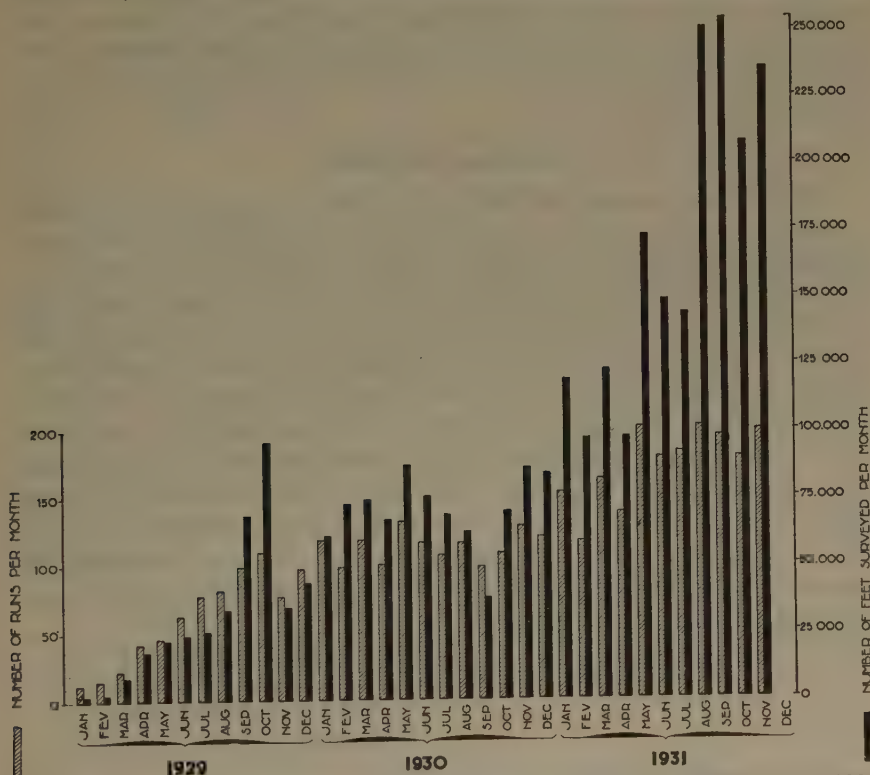


FIG. 22.—NUMBER OF RUNS AND LENGTHS IN FEET SURVEYED PER MONTH FROM 1929 TO 1931 INCLUSIVE.

per well that has been the deciding factor in the success of the new process. The saving in the cost, although considerable, in this instance is only of secondary importance.

Our experience now covers extensive field work in a number of districts, where electrical coring has practically replaced mechanical coring, with substantial advantages as to drilling speed and increase of production. We were, naturally, called in to these districts because the drillers experienced great difficulty in finding reliable horizon markers, as is generally the case with unconsolidated marl or clay formations drilled with the rotary process. Such cases are, of course, favorable to electrical coring. Among less favorable cases, we may cite those where cable-

tool drilling is utilized, or where a very evident lithological marker is found just in the neighborhood of the top of a producing horizon.

In spite of the commercial crisis, these new geophysical methods have been developing steadily during the past three years. Their application was commenced industrially on a small scale in 1928. In January, 1929, the number of resistivity runs made during the month was 12, representing a length of 2050 ft. In December of the same year, the corresponding figures were 98 runs and 43,972 ft. Since then, these figures have constantly increased, to 84,200 ft. (121 runs) monthly in December, 1930, and 236,000 ft. (200 runs) in November, 1931. Fig. 22 shows the monthly progress of this work.

#### ACKNOWLEDGMENTS

For the experimental data made public in this paper, we are greatly indebted to the following companies or organizations: N. V. de Bataafsche Petroleum Matschappij, The Hague, Holland; The Caribbean Petroleum Co., Maracaibo, Venezuela; The Gypsy Oil Co., Tulsa, Okla.; The Indian Territory Illuminating Oil Co., Bartlesville, Okla.; Pechelbronn Société Anonyme d'Exploitations Minières, Strasbourg, France; Concordia, Bucharest, Rumania; Steaua Romana, Bucharest, Rumania; Unirea, Ploesti, Rumania. We wish to express our appreciation of their spirit of coöperation, and of the interest which they have shown in the preparation of this paper. Also, a very extensive use of our process has been made during the past two years by the Government of the U. S. S. R. in its oil fields. Thanks to the very active and close cooperation realized by the Soviet geologists and engineers, considerable progress has been achieved in the course of this work.



# A New Contribution to Subsurface Studies by Means of Electrical Measurements in Drill Holes

BY C. AND M. SCHLUMBERGER\* AND E. G. LEONARDON,\* PARIS, FRANCE

(New York Meeting, February, 1933)

LAST year the authors presented a paper that discussed the various electrical measurements they perform in drill holes, which they name "electrical coring."<sup>1</sup> The object of the present paper is to give a brief account of the points of scientific interest that have been elucidated by further field work and laboratory research, as well as the economic results that have been attained recently.

The practical examples given in this paper are drawn, for the most part, from the field work performed in Russian oil fields during the years 1931 and 1932. This is due to the fact that, thanks to the comprehensive cooperation of the Russian geologists and scientists, the authors are allowed to make public a large amount of recent information. In other countries in which the authors are engaged in similar work, the competition between private companies makes it imperative, for a considerable lapse of time, to avoid publication of the results obtained.

The following points will be discussed successively, under separate headings:

1. Electrochemical phenomena in drill holes.
2. Stratigraphic correlations and tectonic studies.
3. Relations between the productivity of oil horizons and their electrical resistivity.
4. Location of coal seams.
5. Summary and conclusions.

## ELECTROCHEMICAL PHENOMENA IN DRILL HOLES

*Technical Publication 462*<sup>1</sup> described the author's discovery concerning the existence of important differences of potential spontaneously gener-

---

\* Société de Prospection Electrique, Procédés Schlumberger, Paris, and Schlumberger Electrical Prospecting Methods, New York.

<sup>1</sup> C. and M. Schlumberger and E. G. Leonardon: *Electrical Coring: a Method of Determining Bottom-hole Data*. See page 237, this volume.

The term "electrical coring" is probably not the best expression that might have been chosen. "Electrical logging," for instance, would be more appropriate. However, "electrical coring" is now more or less in common use in technical literature, therefore the expression is retained.

ated in open holes, where intersecting porous strata, without the introduction of any artificial current into the holes, and presented a scientific explanation of the phenomenon, the differences of potential observed therein being ascribed to two causes:

1. A phenomenon of electrofiltration, by which the fluids filtering through the porous media develop electromotive forces.

2. Electrochemical phenomena, resulting from the variable composition of the strata and from the percentage of dissolved salts contained therein.

The authors had considered this second cause of secondary importance, but more extensive experiments and field work have showed that, under certain circumstances, it could play a capital role. The whole subject will be discussed again, in the light of the experimental information newly acquired.

### *Electrofiltration*

To begin with, it must first be clearly stated that, in certain oil fields, electrofiltration appears really to constitute the essential cause of the differences of potential registered. The relationship that exists, in this case, between the difference of potential and the pressures in the hole and inside the porous layer can be verified with a satisfactory degree of accuracy. By lowering the pressure by means of bailing or increasing it by use of the mud pumps, it is thus possible to compute the pressure in any given porous layer; the figures obtained for the rock pressure are in accordance with those that could be obtained in some other manner.

Fig. 1 shows an example drawn from the Grozny oil field, North Caucasus, U.S.S.R., which illustrates this point. It represents the porosity diagrams registered in the same hole for two different positions of the mud level, at 0 and 80 meters below the derrick floor. The resistivity diagram also is given, at the left-hand side of the figure. Several porous horizons, numbered IV-VII, X, XI, XII and XIII, are known to exist in this part of the geological column. They are shown on the resistivity log, where they are marked by as many resistivity peaks. On the porosity diagrams the same porous layers show up by positive or negative centers of potential. A positive center corresponds to a layer discharging fluid into the hole, and its magnitude decreases with an increase of the head of the muds; these conditions are encountered at layer IV-VII. A negative center characterizes the opposite conditions; the mud penetrates the porous formations, and the greater the pressure, the stronger the negative potential. This is true for layers X, XI, XII and XIII.

Knowing the differences of potential measured, and the level of the mud in each experiment, the rock pressures in the above mentioned porous layers can be computed. This computation has been made, and

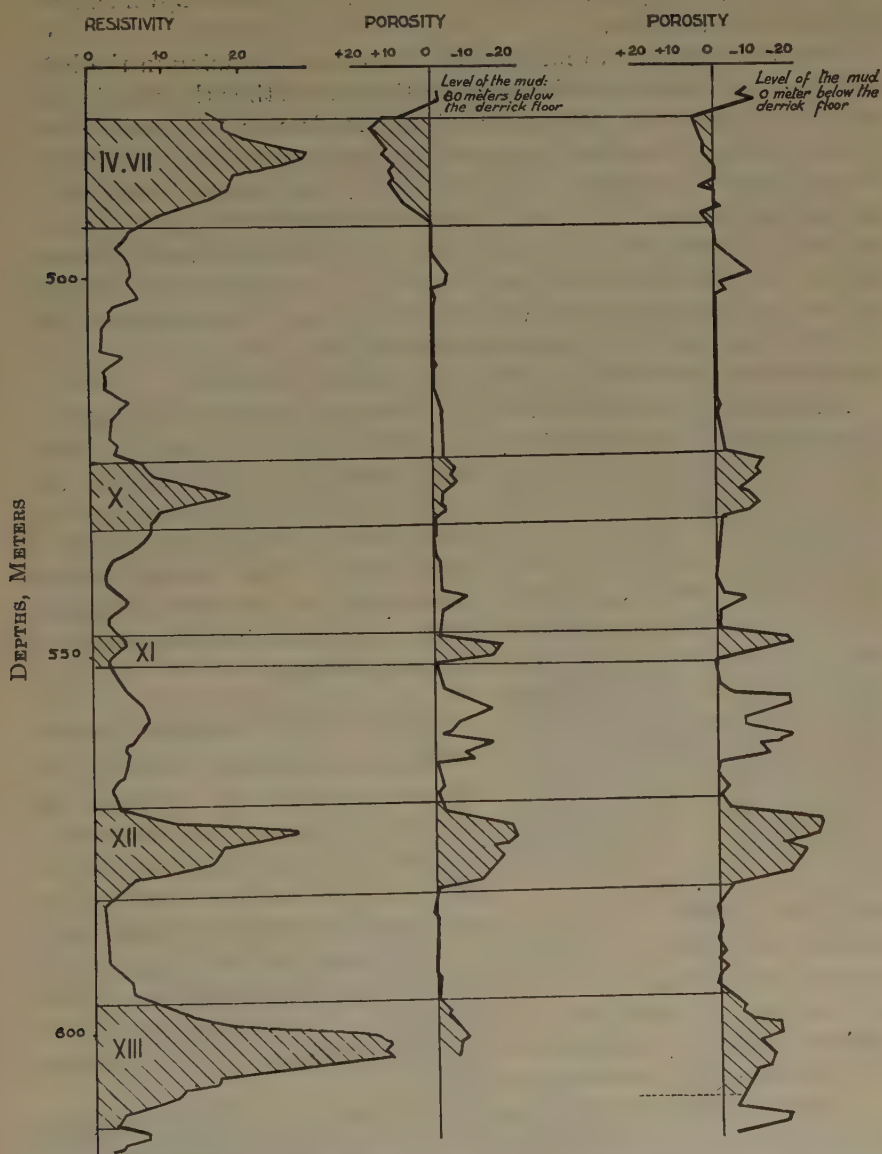


FIG. 1.—INFLUENCE OF PRESSURE OF MUDS ON MAGNITUDE OF ELECTROFILTRATION PHENOMENA. GROZNY, U. S. S. R., 1932.

Resistivities in meter-ohms; scales of porosity logs in millivolts.

the figures obtained are reasonable, according to the petroleum engineers at Grozny, with the possible exception of the IV-VII horizon, which gives a figure rather too high.

It is now advisable to mention the conditions obtaining in the hole, and in the porous layers under consideration, at the time the experiments were performed. The resistivity of the muds was 2.9 meter-ohms; in other words, it contained (supposing that its temperature was 18° C.) about 2 grams of sodium chloride per liter. The waters themselves in the porous horizons carry only limited quantities of dissolved salts; less than 3 grams per liter, in general, and even less for the thirteenth horizon. Under these conditions, it is but normal that no appreciable electrochemical phenomenon takes place between the muds and the porous formations, since the waters contained in the latter show approximately the same percentage of dissolved salts as the muds.

It must also be pointed out that the Grozny sandstones are made up

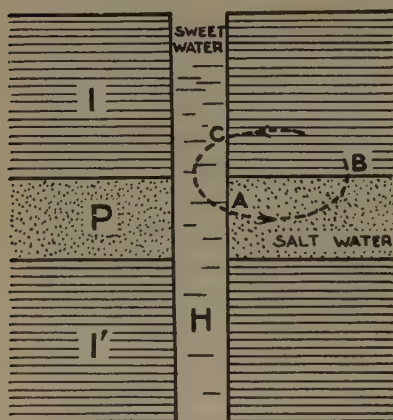


FIG. 2.—ELECTROCHEMICAL FORCE GENERATED IN A DRILL HOLE BY A SALTY, POROUS LAYER.

of comparatively coarse particles, which would seem to account for the fact that the porous horizons are not sealed off easily and quickly by the mud fluid. The electrofiltration phenomena are therefore probably much more stable in Grozny than in many other fields.

#### *Principles of Electrochemical Forces*

Similar conditions, however, are not maintained to the same extent in every oil field. For this reason, as soon as the authors' measurements became more widely utilized, they gradually discovered another cause of electrical differences of potentials, whose existence they theoretically surmised, but the importance of which had been underestimated. These are the electrochemical phenomena caused by the variable content in dissolved salts of the muds and waters in the porous horizons. This new phenomenon can be described as follows.

Consider a drill hole *H*, filled with sweet water. This hole encounters a porous sand layer *P*, containing salt water, and comprised between two impervious argillaceous layers *I* and *I'* (Fig. 2). Experience shows that, even in the absence of a difference between the rock pressure and the head of the water filling the hole, a negative potential is observed in the diagram of the electrical potentials along the drill hole, at the intersection with the porous layer. An electromotive force is set up, caused by the difference in concentrations of the electrolytes coming into contact in



the region of the layer *P*. The water in this layer, rich in dissolved salts, is positive in comparison to the sweet water in the hole, and the electric current that is caused to flow into the porous layer and the surrounding rocks follows the path shown in Fig. 2. In other words, there is a "concentration element," and the differences of potential registered correspond to the ohmic drop caused by the flow of electric current in the water filling the hole.

If, in addition, there exists an electromotive force of filtration caused by a difference of pressure between the mud in the hole and the fluid in the layer, the two phenomena are superposed, and only the resulting effect will be observed. In this case, it is no longer possible to compute the pressure inside the porous layer by allowing the head of the mud in the drill hole to vary. Such a computation is correct only where the electrochemical forces are negligible. Since drilling is usually performed with relatively sweet muds, this condition will be realized in the regions where the rocks (including porous formations) are only slightly saline. As noted above, this seems to be the case at Grozny.

To find the order of magnitude of the potential differences that will be observed in practice, follow the path of a line of current *ABCA* (Fig. 2) from the point where it leaves the hole until it reenters it again. In the neighborhood of *A*, there is a contact between sweet and salt water, in a medium where the pores have large dimensions, and where the mobility of the ions is not appreciably hindered by the presence of the porous material. Experience shows that the electromotive force is the same as though the contact took place directly between the two fluids alone. The value of this electromotive force of contact at 20° C. is given by the formula:

$$E = \frac{RT}{nF} \times \frac{v - u}{u + v} \times L \frac{C_1}{C_2} \quad [1]$$

where the letters have the following meanings:

*E*, electromotive force in volts,

*T*, the absolute temperature,

*n*, the valency of dissolved salt,

*R*, the constant of the perfect gases,

*F*, the Faraday (or 96,600 coulombs),

*u* and *v*, the mobilities of the cation and anion,

*L*, the Napierian logarithm,

*C*<sub>1</sub> and *C*<sub>2</sub>, the concentrations of the two solutions.

Applying the preceding formula to sodium chloride solutions, for which

$$n = 1; \quad \frac{u}{u + v} = 0.4; \quad \frac{v}{u + v} = 0.6,$$

the electromotive force is given, in millivolts, by

$$E = 11.6 \log_{10} \frac{C_1}{C_2} \quad [2]$$

and if  $C_1 = 10C_2$ ,  $E = 11.6$  millivolts.

The ratio  $\frac{C_1}{C_2}$  is equal to the ratio  $\frac{r_2}{r_1}$  of the specific resistances of the electrolytes. A ratio of 10 will correspond, for instance, to a resistivity of 0.5 meter-ohms for the waters included in the porous medium, and of 5 meter-ohms for the muds; this kind of mud is a rather usual type.

At points  $B$  and  $C$ , there are two contacts between the impervious medium and the electrolytes that fill respectively the porous layer and the hole. The authors do not know of any exhaustive research work regarding the electromotive forces created at such contacts. Laboratory experiments carried out by the authors in order to study this point have shown that the electromotive forces at the contacts  $B$  and  $C$  generate a current which flows also in the direction  $ABCA$ , and consequently increase the difference of potential observed in the hole at the porous layer. The total electromotive force  $E_t$ , of the circuit  $ABCA$ , can be represented by the formula:

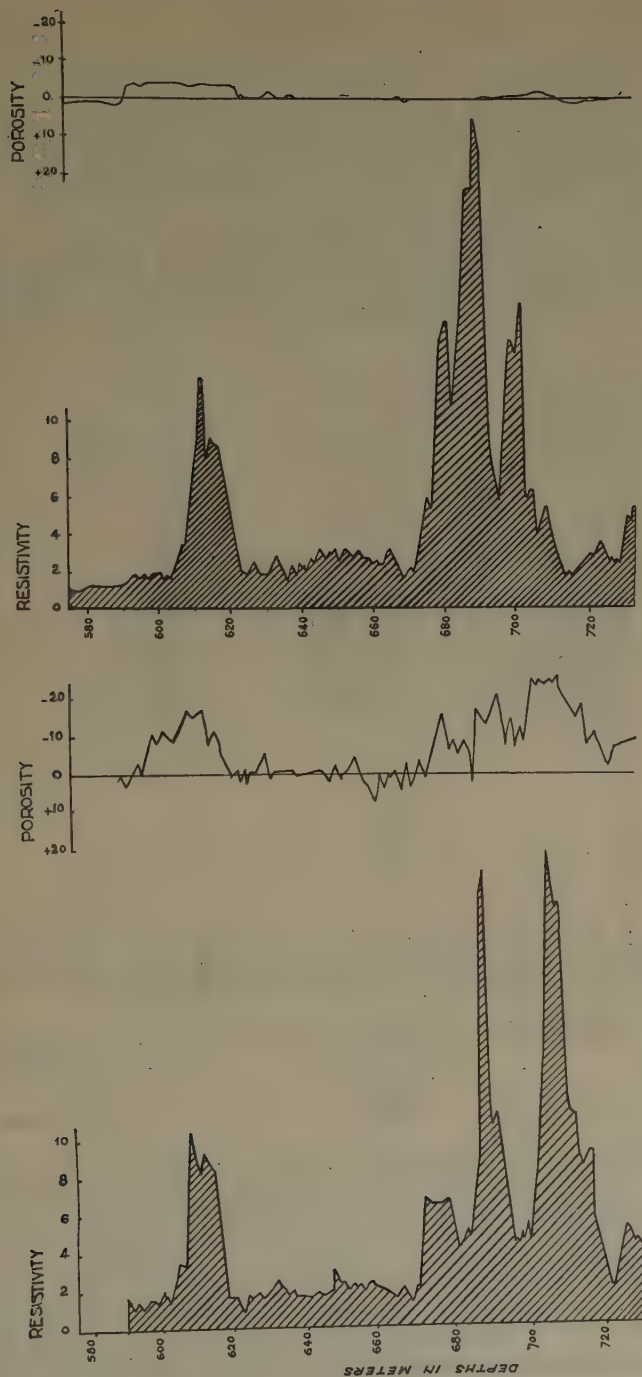
$$E_t = K \log_{10} \frac{r_2}{r_1} \quad [3]$$

where  $r_1$  is the resistivity of the salt water contained in the layer;  $r_2$ , that of the mud; and  $K$  a constant factor, which depends on the constitution of the impervious rock and the chemical compositions of the fluids in contact.

For a plastic gray clay, and a porous medium composed of coarse siliceous sand, saturated with a solution of sodium chloride, the value found for  $K$  is approximately 17 ( $E_t$  being expressed in millivolts). Table 1 shows a comparison between a series of laboratory measurements, and the corresponding electromotive forces computed from formula 3. The resistivity of the sweet water  $r_1$  was equal to 24 meter-ohms, while the resistivity of the salt water  $r_2$  varied from 17 to 0.04 meter-ohms.

TABLE 1.—*Electromotive Force, Measured and Computed*

$r_2$ , meter-ohms	$E_t$ (measured), Mv.	$E_t$ (computed), Mv.
17	4	2.5
10	6	6.5
3.5	15	14
1.08	23	23
0.25	27	34
0.067	45	43
0.04	45	46



Resistivity of the mud, 0.14 meter-ohms

Resistivity of the mud, 0.66 meter-ohms

Average resistivity of the water in the porous layers, 0.008 meter-ohms.

Fig. 3.—INFLUENCE OF VARIATIONS IN SALINITY OF MUDS ON ELECTROCHEMICAL FORCES DEVELOPED IN POROUS LAYERS. SURAKHANY, U. S. S. R., 1932.

Resistivities in meter-ohms; scales of porosity diagrams in millivolts.

*Results from Field Work*

These considerations are completed below by some practical results obtained in drill holes. Such results are very interesting, since they are useful in analyzing the causes of the electrochemical phenomena observed, and in sizing up their importance and significance for a more complete study of the formations in drill holes.

A first example, which illustrates the variations of the electromotive forces with the salinity of the muds, is given in Fig. 3. This figure represents, in the zone of the fourth horizon, the resistivity and porosity

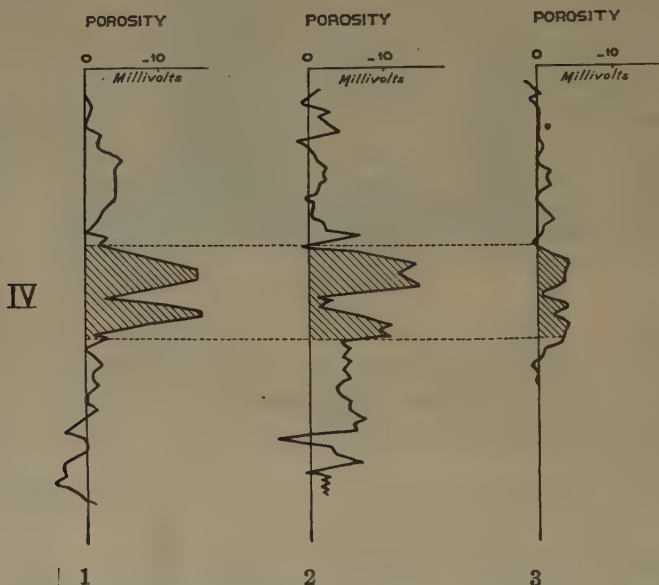


FIG. 4.—VARIATION OF ELECTROCHEMICAL FORCE IN GIVEN LAYER, WITH MUDS OF DIFFERENT SALINITY. BIBI-ELBAT, U. S. S. R., 1932.

*Average Resistivity of Water in Porous Layers, about 0.1 Meter-ohm*

No. of Hole	Resistivity of Muds, Meter-ohm	Differences of Potential, Mv.
1	0.61	15
2	0.44	14
3	0.18	4

diagrams obtained in two neighboring wells of the Surakhany oil field, Azerbaidjan, U.S.S.R. In this field, the average resistivity of the waters contained in the rocks at the depth under consideration is about 0.08 meter-ohms (corresponding to a density of about 10° Bé).

In drill hole No. 1, the mud filling the hole showed a resistivity of 0.66 meter-ohm. As a result of the great excess in salinity of the water contained in the porous horizons compared to that in the hole, important differences of potential were recorded at the porous layers. These layers also contain oil, which accounts for their high resistivity.



In drill hole 2, the resistivity of the muds was lowered to 0.14 ohm. With such a concentration, which does not differ much from that of the water contained in the porous layers, the electrochemical phenomenon is scarcely perceptible, and the diagram is practically flat. Thus, the magnitude of the potential differences varies according to the difference in the percentage of dissolved salts between the waters filling the hole and the porous layers.

Fig. 4 represents the electrochemical differences of potential observed at the passage of the fourth horizon in three different holes of the Bibi-Eibat field, Baku, U.S.S.R. As in the previous example, the measurements were performed in muds with increasing salinity.

It must be borne in mind that in the two cases mentioned the formations examined are the same (region of the fourth productive horizon), but at Bibi-Eibat the waters contained in these formations are less salty (resistivity about 0.1 meter-ohm, against 0.08 meter-ohm). This accounts for the fact that the electrochemical phenomena are less intense at Bibi-Eibat than at Surakhany.

Finally, observations were made in the Leninsky Rayon field, Baku district, U.S.S.R., on the deep formations of the Kirmaku series. The average salinity of this terrane is much less than in the two examples cited above (about 2° or 3° Bé, corresponding to an average resistivity of 0.25 meter-ohm), with the result that, in some instances, the muds show a salinity greater than that of the surrounding formations. In this case, positive, instead of negative, peaks of potentials are observed at the porous layers.

#### STRATIGRAPHIC CORRELATIONS AND TECTONIC STUDIES

The utility of the numerous correlations, furnished by the resistivity and porosity diagrams, for the detailed and accurate study of subsurface geology, has already been discussed and emphasized by the authors. It is interesting, however, to show some of the results that can be obtained by systematic and persevering application of the electrical technique.

Fig. 5 represents the subsurface map of Surakhany field, as it was known in October, 1930, previous to the use of electrical coring in this field.<sup>2</sup> Fig. 6 represents the same map in January, 1932.<sup>3</sup> It reveals the existence of eight new faults, hitherto unknown. The discovery of this system of faults makes it possible to explain satisfactorily the geological conditions of the Surakhany field, which formerly appeared so perplexing to the geologists. The lack of regularity that had been

---

<sup>2</sup> Published in *Azerbaijan Oil Industry* (August, 1931).

<sup>3</sup> D. Jabrev and K. Emilianov: Results of the Application of Electrical Coring in the Ordjonikidze (Surakhany) Oil Field. *Azerbaijan Oil Industry* (January, 1932).

observed in the productive horizons, which had been attributed to lateral changes in their lithological characters, is, in fact, a consequence of this system of fractures.

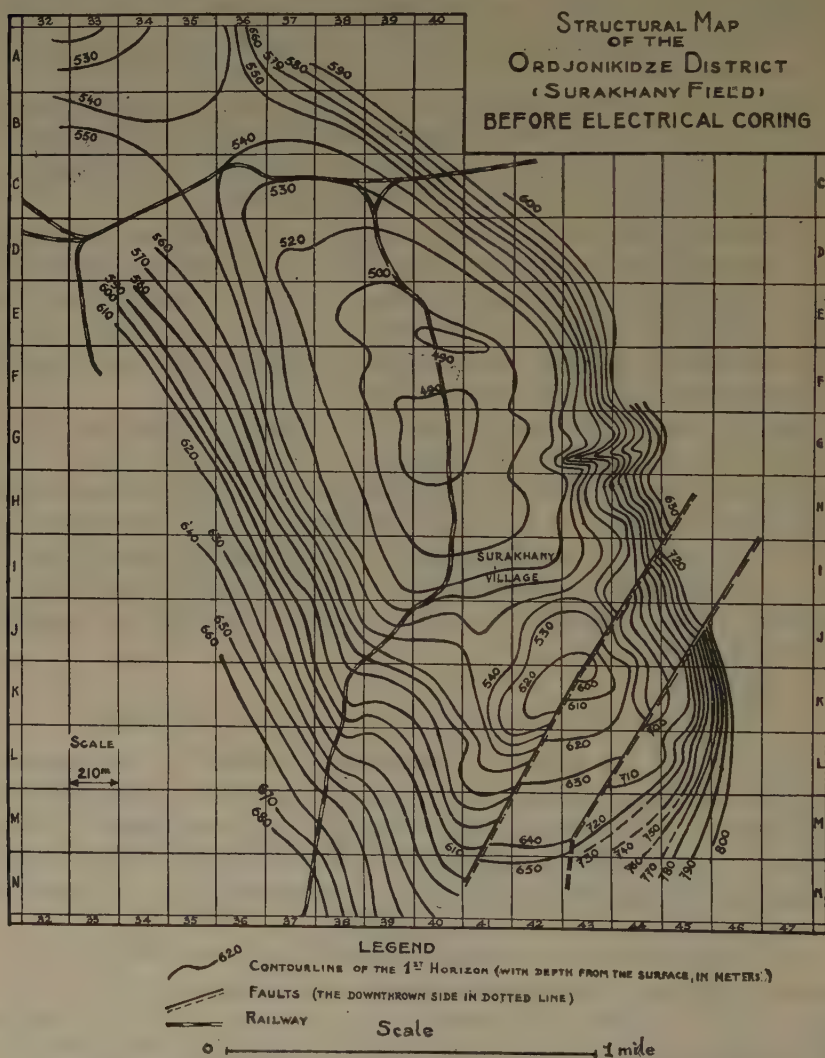


FIG. 5.—STRUCTURAL MAP OF SURAKHANY OIL FIELD AS KNOWN IN AUGUST, 1931.

During the course of the year 1932, additional electrical work made it possible to study in still greater detail the structural geology of this field. It is to be hoped that a new map, summarizing all the information regarding the Surakhany field available up to the present time, will shortly be made public by the Soviet Government.

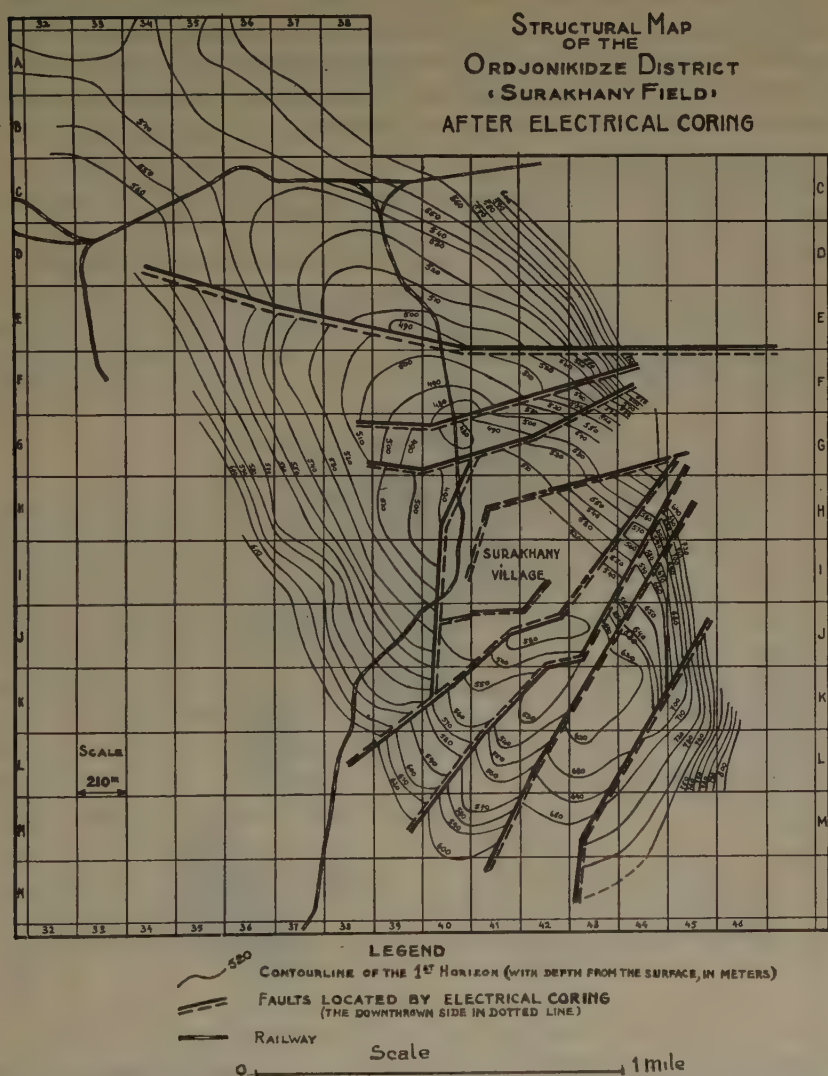


FIG. 6.—STRUCTURAL MAP OF SURAKHANY OIL FIELD AS KNOWN IN JANUARY, 1932

### RELATION BETWEEN RESISTIVITY OF OIL HORIZONS AND THEIR PRODUCTIVITY

Attention has already been drawn to the fact that a definite relation often seems to exist between the productivity of an oil horizon and the order of magnitude of its electrical resistivity. It goes without saying that it would not be safe to generalize this law too much, and that the comparison of oil horizons possessing entirely different constitution,

texture, pressure, salinity, etc., would lead to incorrect conclusions. On the other hand, the mere comparison of the resistivity figures obtained in different wells of an oil field for a given horizon will furnish useful information as to its degree of saturation, and thus will make it possible to orient its exploitation in a rational manner.

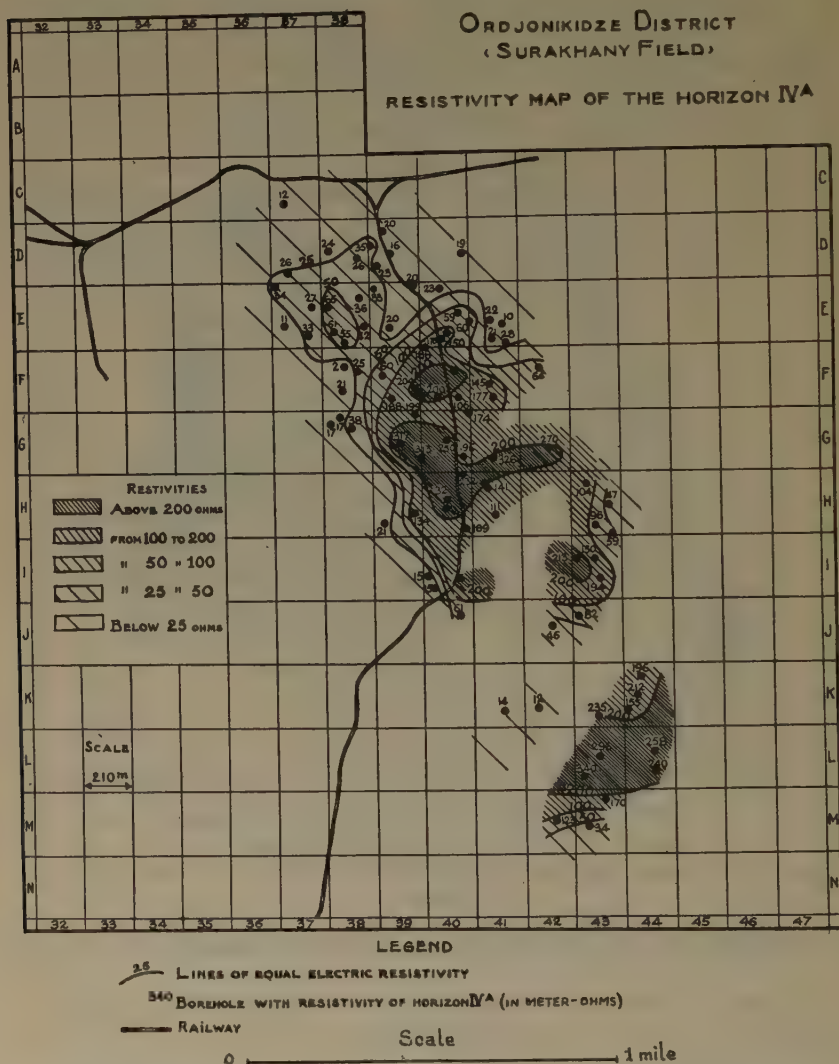


FIG. 7.—RESISTIVITY MAP OF 4a HORIZON IN SURAKHANY OIL FIELD.

Fig. 7 shows the resistivity figures measured on the fourth horizon in the Surakhany field. The high-resistivity zones are also the most productive. It is worth noting, by comparing this resistivity map with the structural map shown on Fig. 6, that these resistive zones are



located precisely on the different highs of the structure. One part of the field deserves special mention; the low-resistivity zone with coordinates 41K and 42K, where resistivity figures as low as 12 and 14 meter-ohms were recorded. Actually, these measurements are located in a compartment where the fourth horizon is sterile.

Usually, as already pointed out, it is well-nigh impossible to obtain permission to make public the structural maps and electrical results in an oil field in the process of discovery or exploitation. Such publication could easily be detrimental to the oil companies, which are in keen competition in the territory under consideration. For this reason, the authors believe that the example of accurate subsurface geology determination achieved in Surakhany field will be of particular interest to petroleum engineers.

#### LOCATION OF COAL SEAMS

A striking example of the difficulty of locating coal horizons is illustrated by the hole drilled near Estevelles, in 1931, by the Compagnie des Mines de Courrières (France). It was an exploration hole, drilled down to a total depth of 1238 m. (4060 ft.). In spite of continuous mechanical coring, no coal horizon was located. When drilling was discontinued, and the casing removed, it was decided to have recourse to electrical coring in order to check the negative information furnished by mechanical coring.

On the sandstone horizons, high resistivity figures, between 500 and 1000 meter-ohms, were obtained. The shales, on the other hand, furnished flat diagrams, with figures in the order of 100 to 200 meter-ohms. In two parts of the schists, however, sharp peaks, corresponding to two resistive seams, respectively 1 and 3 m. thick, were recorded. The resistivities obtained were as high as 1000 and 450 meter-ohms. On Figs. 8 and 9 are represented the two parts of the resistivity diagram where the peaks in question were discovered. In addition, the geological column, as furnished by the drillers, has been shown beside the electrical resistivity curves.<sup>4</sup>

At the two depths thus located by electrical measurements, the drillers had noticed only a few coal streaks without importance. The conclusion drawn from electrical coring, however, was that the two resistive peaks corresponded to two coal beds, owing to their high resistivity and to the fact that they were located within a layer of soft material. In order to check the deeper coal horizon, it was decided to deviate the drill hole so as to core it again mechanically. Although the position of the bed was known accurately at this time, it was again impossible to bring to the surface a single sample of coal. However, by carefully receiving on a

---

<sup>4</sup> The actual depths at which the observations were made have not been indicated on the diagrams. The diagram of Fig. 8 corresponds to the shallower coal bed.

sieve the water circulated in the hole, an amount of coal cuttings representing a coal seam 3 m. thick was recovered.

This operation demonstrates the efficacious help of electrical coring in the exploration by drilling of a substance as brittle as coal. The existence of the shallow seam was not checked by a new deviation of the hole, since the accuracy of the electrical conclusions was admitted by the company at the time.

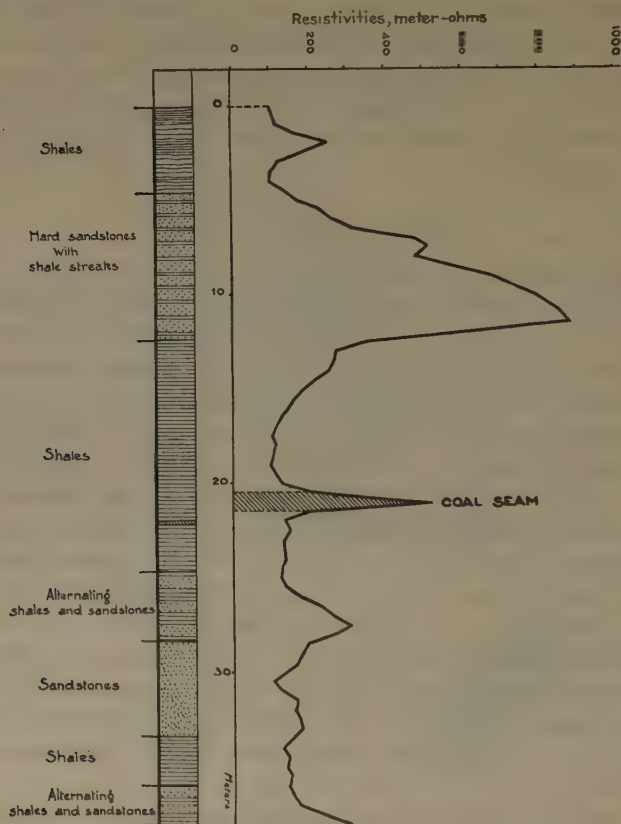


FIG. 8.—PART OF RESISTIVITY DIAGRAM REGISTERED IN A DRILL HOLE AT ESTEVELLES (FRANCE), SHOWING LOCATION OF SHALLOWER COAL SEAM.

A much broader application of the electrical coring method is now in progress in the Donetz coal basin, U.S.S.R., where the thin and brittle coal seams are frequently missed by the drillers. The work is satisfactory in every respect, and constitutes a great help in carrying out the exploration program in force at the present time.

#### SUMMARY AND CONCLUSIONS

Two aspects of the electrical coring process, one of scientific and the other of economic and statistical interest, are worth being emphasized.

As previously stated, the differences of potential spontaneously generated in drill holes are caused either by filtration of fluids through the porous layers or by osmotic electromotive forces generated at the contact of liquids that do not contain the same percentage of dissolved salts. According to the circumstances, one or the other of these phenomena takes a predominant place. When the electromotive forces of filtration distinctly play the capital role, it is possible to determine approximately

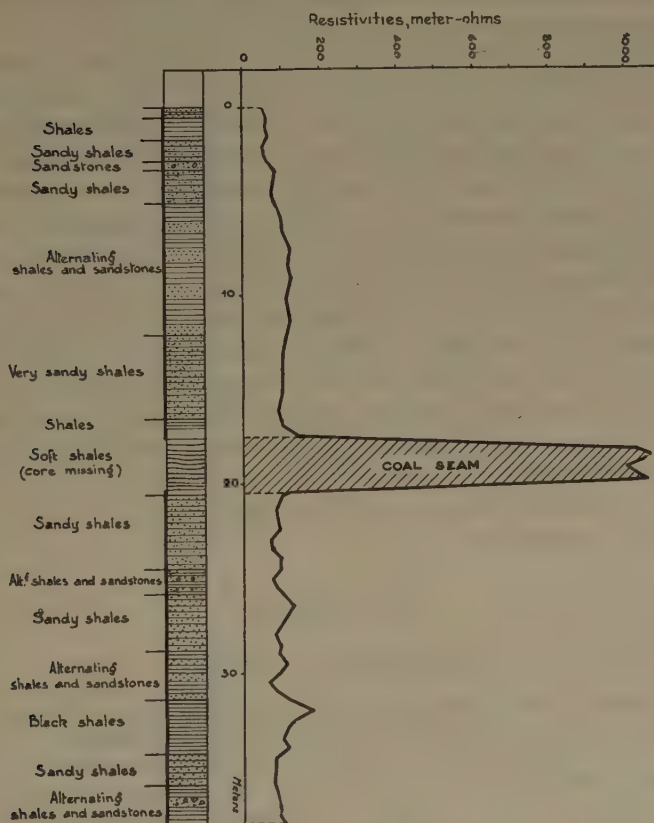


FIG. 9.—PART OF RESISTIVITY DIAGRAM REGISTERED IN A DRILL HOLE AT ESTEVELLES (FRANCE), SHOWING LOCATION OF DEEPER COAL SEAM.

the rock pressure inside the porous layers. On the other hand, when the osmotic forces constitute the essential basis of the phenomenon, it is the salinity of the water that can be measured. In the intermediate cases, the complexity of the phenomena makes it possible to give only a rough qualitative estimate of the pressure and the salinity. Whatever the conditions, however, the expression "porosity log," which has been given to the diagram of the differences of potential spontaneously generated in drill holes, is entirely justified, since this diagram puts into evidence, with

great accuracy, all the porous layers traversed by the drill hole. Its practical utility for supplementing the information given by the resistivity diagram is evident. It plays an essential role in the detailed study of the oil and water zones, and is also very useful for the mere purpose of establishing geological correlations between the various formations, since very often the disturbances registered on the porosity log possess a characteristic silhouette.

As to the economic and statistical point of view, electrical coring can render valuable services for the exploitation of oil fields, where geological correlations are often very difficult to establish. The examples given, drawn from the work performed by the Soviet oil trusts, constitute very striking illustrations of this fact. The extensive drilling activity of these trusts, and the fact that they are supervised by a central management, has made it possible for them to develop this new technique in a remarkably rapid manner. In the fields of Surakhany (Baku), Bibi-Eibat (Baku) and the New Field of Grozny, of which the total production represents 66 per cent of the U.S.S.R. production, mechanical coring has been replaced almost entirely by electrical coring, which is much cheaper and quicker. In the fields of Leninsky Rayon (Baku), Maikop, and the Old Field of Grozny, although electrical coring has not entirely eliminated mechanical coring, yet it plays a capital role there. The latter fields represent 24 per cent of the Soviet production. From these figures it is evident that electrical coring has either eliminated or considerably reduced mechanical coring for 90 per cent of the oil production of the Soviet Government.

## DISCUSSION

*(Louis B. Slichter presiding)*

H. LUNDBERG,\* New York, N. Y.—Is the electrofiltration phenomenon to be expected only in drill holes, or does it occur in undisturbed strata? I have in mind one locality where argillaceous quartzite forms a hill that is cut through, near the top, by a vertical aplite dike. There is absolutely no metallic mineralization visible, but we found there a negative center of over a volt, nearly twice as high as the theoretical maximum to be expected on sulfides. Under the topographic circumstances, water must be in fairly continuous flow down the contact, or near it, and I wonder if this could by any possibility account for the potential observed.

E. G. LEONARDON.—I cannot answer that question definitely, but I can say that water flowing in the sand of a sea beach will set up spontaneous potentials due to electrofiltration. Water rising by capillarity in a formation is also a cause of potential differences, but in a case such as that cited if capillarity would bring the water up to hilltops and peaks, it would produce a center of positive potentials, opposite in sign to that noted. Was there any graphite observable in the rocks? That often causes strong potential differences.

---

\* Manager, Swedish-American Prospecting Corporation.



H. LUNDBERG.—There was no graphite present, no metallic minerals, nothing but the siliceous minerals of the country rocks. The potentials were stronger than would be obtained on sulfides, anyway.

S. F. KELLY,\* New York, N. Y.—I have noted potentials of about 0.9 volt on sulfide outcrops.

L. B. SLICHTER,† Cambridge, Mass.—And I have found over a volt on graphite.

E. G. LEONARDON.—The difficult thing in Mr. Lundberg's case is merely to account for the magnitude of the phenomenon, if it is only due to electrofiltration.

---

\* Geologist and Geophysicist, Low, Kelly & Zuschlag.

† Associate Professor of Geophysics, Massachusetts Institute of Technology.

## Use of Magnetic Data in Michigan Iron Ranges

By C. O. SWANSON,\* HOUGHTON, MICH.

(New York Meeting, February, 1934)

IN the iron ranges of northern Michigan, magnetic data have been used as an aid in geologic field work since the time of the earliest surveys. The presence of complex structures containing magnetic formations, and the general scarcity of exposures, guided the early work into this line of attack, and later field studies tended to place more and more emphasis upon this geophysical relationship, until, at present, the collection of magnetic data is a matter of routine in any areal survey. At first, horizontal deflections of the compass needle were the only data collected. In subsequent surveys, greater dependence was placed on dip-needle readings, which record variations in the intensity and inclination of the earth's magnetic field. Recently the trend has been toward adjusting the instrument so as to reduce the influence of changes in inclination, and using a more sensitive modification, called the Superdip,<sup>1</sup> in weakly magnetic areas. To a minor extent, the magnetometer has also been employed.

The object of this paper is to present the writer's experience with magnetic data in this region. The conclusions are based on work covering a period of 10 years, and spread over nearly all of the iron ranges and a large part of the intervening areas. The viewpoints expressed are purely geological ones. In other words, any opinion as to the usefulness of a certain relationship is based upon the writer's experience with it as a guide in interpreting the structures of this region, and not upon its soundness theoretically, nor its usefulness under other conditions.

A very brief summary of the conclusions is as follows. The most important step is that of collecting the magnetic data. This requires a suitable adjustment of the dip needle, and sufficient readings to accurately portray the variations in the magnetic field, which are apt to be irregular. Once the readings are taken and plotted in some clear fashion, the interpretation of them is usually merely a matter of observing their relation-

---

Manuscript received at the office of the Institute April 19, 1933.

\* Professor of Geology, Michigan College of Mining and Technology.

<sup>1</sup> N. H. Stearn: Hotchkiss Superdip: a New Magnetometer. *Bull. Amer. Assn. Petr. Geol.* (1929) 13; Practical Geomagnetic Exploration with the Hotchkiss Superdip. *Trans. A.I.M.E.* (1932) 97, 169.

ship to the geologic data. In other words, one uses empirical relationships established separately for each area. The paper is divided into three sections: (1) outline of the general practice, (2) comments on the practice, (3) examples of the practice.

### OUTLINE OF THE GENERAL PRACTICE

The purpose of this outline is to acquaint outside readers with the field conditions of the region and the survey methods used in it.

#### *Field Conditions and General Geology*

The region has a generally low relief. A large part is covered by glacial and fluvioglacial deposits, which form flat, rolling, or hummocky surfaces. Although some townships are lacking in outcrops, most of them contain scattered exposures and small areas of abundant outcrops, which have quite rugged relief on a small scale. The vegetation usually is thick enough to make the discovery of small exposures a matter of careful search.

In very general terms, the oldest rocks form a basement complex of granite and metamorphosed volcanics. Overlying this is the Huronian series, which is dominantly of sedimentary origin, although it also contains volcanic members. It has been folded and faulted in intricate fashion, and intruded by basic and acid igneous rocks. The Huronian rocks are therefore generally metamorphic, and the bedding is usually steeply inclined. The Keweenaw series overlies the Huronian in the northwest part of the region. It consists of sedimentary, volcanic, and intrusive rocks, and is generally less metamorphosed than the Huronian. Structurally, the Keweenaw forms the south limb of the Lake Superior syncline.

#### *Traverse Methods*

Locations are determined by compass and pacing surveys. Because of the magnetic attractions, the sun-dial type of compass is commonly used. The fundamental reference points are the section corners and quarter-posts, but of course use is made of any other established locations that may be present.

The traverse lines mostly follow north-south or east-west directions. Naturally, one chooses the direction that is more nearly transverse to the geologic structure. In places the lines may be run in both directions where the structure is very complex, or diagonally across the sections where a fairly regular linear structure prevails and strikes obliquely with reference to the section lines. In many surveys the distance between traverse lines is  $\frac{1}{4}$  mile, and magnetic readings are taken every 50 paces, or  $\frac{1}{40}$  mile. These are very general statements, given to indicate the type of traverse found most satisfactory under average conditions of

visibility of outcrops, lack of pattern in topography, complexity in geologic structure, etc. Naturally, where outcrops of magnetic rocks are found, observations are taken more closely together to determine the details of the distribution of the magnetite and its relation to geologic structures. Or, where a sudden variation is found, closely spaced readings are taken to learn whether the abnormal reading is a freak due to some local interference, or whether it represents a thin magnetic structure under a light drift cover. In general, any routine method must be modified in certain portions of an area, and the generalization given above indicates maximum rather than minimum spacings.

### *Magnetic Instruments*

Three types of instruments are used for the detection of magnetic variations. One of these, the sun-dial compass, can be used to measure changes in the direction of the horizontal component of the earth's field. Formerly such readings were used a great deal to trace magnetic "lines," but at present they are taken mainly to permit the running of traverses with an ordinary compass in certain areas on cloudy days when the sun dial cannot be used. The other two instruments are the ordinary dip needle, or dip, and the Superdip.

The ordinary dip needle contains a magnetic needle centered on a pivot which has two pointed ends supported by cup jewels. The south end of the needle is counterweighted. When read, the instrument is held so that the needle is free to swing in the vertical plane of the magnetic meridian. The reading is in degrees, with the zero degree marking corresponding to a horizontal position of the needle. The readings are called plus when the north end of the needle is down. The instrument is equipped with one leveling bubble, which is used to bring the zero degree marking into a horizontal position. The dip is held by hand when the reading is taken, which introduces personal technique as a considerable factor.

The Superdip also has a magnetic needle centered on a pivot. This, however, rolls on quartz wedges which are horizontal when the instrument is leveled. The counterweight is fastened to a separate arm centered on the same pivot. The angle between the counterweight arm and the magnetic needle can be varied, and is described by giving the sigma<sup>2</sup> of the instrument. The sigma is 0° if the counterweight arm is horizontal when the needle is at right angles to the magnetic lines of force. In a magnetic field of which the inclination is 75° (about normal for this district), the angle between the arm and the needle is thus 15° when the sigma is 0°. In the same field, if the arm is parallel to the needle, the sigma is 15°, which is therefore the normal sigma of an ordinary dip of

---

<sup>2</sup> N. H. Stearn: Second reference of footnote 1.



perfect construction. The readings again are taken in degrees, with, however, the zero degree marking corresponding to a vertical position of the needle. When read, the Superdip is mounted on a tripod with a transit type head, so that it can be accurately leveled. Also, the plane in which the needle swings can be made to coincide almost exactly with the vertical plane of the magnetic meridian.

### Ordinary Dip Needle

*Adjustments.*—Moving the counterweight on the needle is the only adjustment made. This changes the position of the needle in the mag-

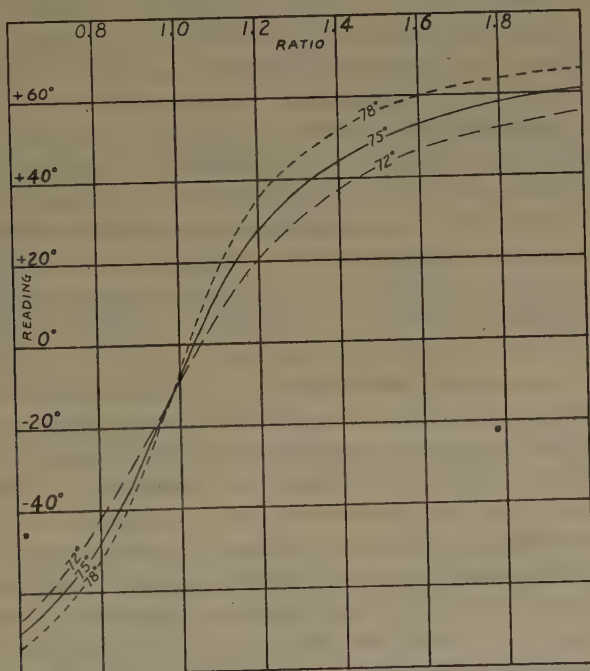


FIG. 1.—READINGS OF AN ORDINARY DIP NEEDLE CORRESPONDING TO CERTAIN INCLINATIONS OF THE EARTH'S FIELD AND TO CERTAIN RATIOS BETWEEN MAGNETIC AND GRAVITATIVE MOMENTS.

netic field when the reading is taken, which in turn modifies the sensitivity of the instrument to changes in the intensity and inclination of the magnetic field. The maximum sensitivity to changes in intensity is found when the needle is at right angles to the lines of force; that is, when the reading is about minus 15°. Ordinarily, sensitivity to changes in intensity is more desirable than sensitivity to changes in inclination. For this reason, the instrument should be adjusted to read between about plus 30° and minus 60°. However, because strongly minus readings introduce different effects, and because of factors involved in the operating technique, small plus readings are usually preferred.

Fig. 1 shows graphically some of the relations outlined above. Moving the counterweight changes the gravitative moment acting on the needle, and a change in the intensity of the field alters the magnetic moment. The ratio between these two moments is one factor that affects the readings, and it is the only factor subject to control by adjustment of the instrument. The horizontal dimension of the figure shows a certain range in this ratio. The inclination of the field also affects the reading. The effect of this factor is shown by joining the readings corresponding to certain inclinations. The figure may be interpreted as follows. If the field has an inclination of  $75^\circ$ , an increase in ratio from 1.0 to 1.2 increases the reading from minus  $7^\circ$  to plus  $28^\circ$ . This would be the effect of a 20 per cent increase in intensity, the inclination remaining constant. The same increase in intensity might also increase the ratio from 1.5 to 1.8 if the counterweight were moved, and it would then increase the reading from plus  $49^\circ$  to plus  $58^\circ$ . Such an adjustment of the counterweight would therefore decrease the sensitivity to changes in intensity. Clearly the dip needle is most sensitive to changes in intensity for ratios or readings corresponding to the steepest parts of the curves on the figure, and this sensitivity begins to drop off sharply when the readings exceed about plus  $30^\circ$ . Again, a change of inclination from  $75^\circ$  to  $78^\circ$  increases the reading from minus  $7^\circ$  to minus  $6^\circ$  if the ratio is 1.0; from plus  $45^\circ$  to plus  $52^\circ$  if the ratio is 1.4; and, obviously, from  $75^\circ$  to  $78^\circ$  if the ratio is infinitely large, as the needle would then lie parallel to the lines of force. Thus, if the counterweight is adjusted so that the readings range from plus  $30^\circ$  to plus  $60^\circ$ , changes in inclination become relatively important, which is not desirable. Further, it may be noted that when the instrument has strong negative readings an increase of inclination opposes an increase of intensity in its effects on the needle, which again is not desirable as a general condition.

*Corrections to Readings.*—Usually several instruments are used in the course of a survey. These are adjusted to read about the same, but exact adjustment in this respect is impractical. Therefore all the dips are read at some convenient point where the magnetic field is about normal. This normal reading is subtracted from the readings taken along the traverses when they are recorded on the map.

Dip needles may also vary considerably in sensitivity even when they read about the same. The main cause of this is imperfect centering of the needle on the pivot, which may be introduced by resharpening the pivot points. The result is that the sigma is not normal, and therefore the sensitivity is not normal. To correct for these variations in sensitivity, the instruments are read at several convenient stations that give a good range of readings. The data so obtained can be used to make up a correction chart or table for each instrument, one dip needle being regarded as standard.

*The Superdip*

The ratio of the Superdip may be changed in the same way as that of the ordinary dip needle, with the same results.

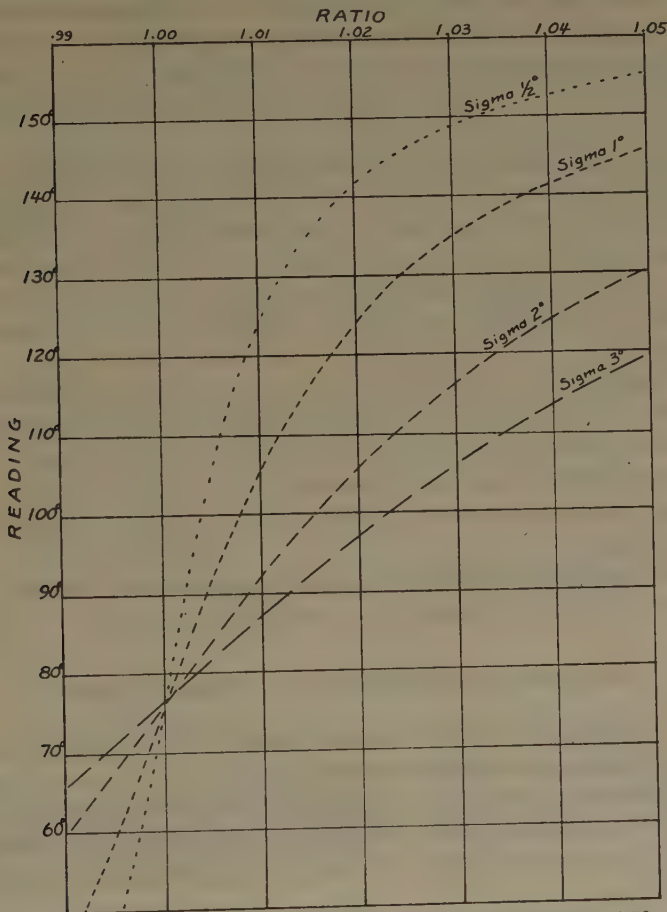


FIG. 2.—READINGS THAT WOULD BE OBTAINED IN A MAGNETIC FIELD OF  $75^\circ$  INCLINATION WITH INSTRUMENTS HAVING THE SIGMAS AND RATIOS INDICATED.

When the needle is horizontal, the Superdip reads  $90^\circ$ . An instrument having a  $1^\circ$  sigma and a ratio of 1.01 would give a reading of  $105^\circ$ . If the intensity of the field were to increase 1 per cent, the ratio would become approximately 1.02, and the reading would be  $124^\circ$ . Thus the slope of the curve shows the sensitivity to changes in intensity. If the inclination of the earth's magnetic field increased  $0.5^\circ$  the sigma would become  $0.5^\circ$ , and the reading would be  $141^\circ$ . Thus, the distance between curves shows the sensitivity to changes in inclination. For instruments reading below  $75^\circ$ , an increase in the inclination tends to lower the reading. The figure shows that instruments reading about  $75^\circ$  are most sensitive to changes in intensity, and are only slightly affected by changes in inclination. In this position, the needle is about perpendicular to the earth's field.

Changing the sigma is, of course, the added adjustment on the Superdip. A reduction of the sigma from  $15^\circ$  to  $3^\circ$  has the same mechan-

ical effect as an increase in the inclination of the earth's field from 75° to 87°. Fig. 1 shows that the sensitivity to changes in intensity and inclination increases as the inclination of the earth's field increases. With the Superdip, one may move from one curve to another at will, and thus, as far as the theoretical sensitivity of the instrument is concerned, one is independent of both the intensity and inclination of the earth's field. Fig. 2 shows readings that would be obtained with a Superdip in certain fields. From it one may draw the same conclusions regarding sensitivity as were made from Fig. 1.

*Corrections to Readings.*—Superdip readings are corrected for daily variations in the earth's magnetic field, for the effects of temperature changes on the instrument, and, where more than one instrument is employed, for variations in sensitivity and normal reading. The temperature correction is the first one made. Charts supplied with the instrument, or constructed from data secured in the field, are used for this purpose.

The effects of daily variations in the earth's magnetic field are determined by checking back periodically on previous stations during the course of a day's work. This information is then used to correct each reading for such changes. Day to day variations are determined by checking back on stations where readings were taken on previous days.

Where several instruments are used, the readings are standardized by the same method as that used for the ordinary dip needle.

### *Compilation and Interpretation of Magnetic Data*

The readings are recorded in figures on a map. This may be supplemented by joining the highest readings of adjacent traverses to indicate so-called magnetic "lines," or by profiling the readings along the traverses, or by contouring them. Where the magnetic field is irregular, as is usual, contouring is the best method of obtaining a picture of the variations.

After the magnetic data and all the direct information concerning the geologic structures have been plotted, the problem of interpretation is usually merely a matter of correlating the two types of information. If magnetic lines are found, these can be traced to places where the bed-rock structure is determinable from outcrops or explorations. The lines then serve to trace the magnetic formation where it is buried, and the bends or breaks in the line indicate concealed folds or faults. A line of subnormal attraction can be used similarly, or broad magnetic areas may be related to certain formations of uniform permeability. Other inferences from the magnetic data, which are rarely necessary or conclusive in this region, are discussed in the next section of the paper.



## COMMENTS ON THE PRACTICE

This section gives the writer's experience in dealing with certain problems involved in the general practice outlined in the preceding section.

*Choice of Magnetic Instrument*

The ordinary dip needle is more convenient and faster than the Superdip. Under ideal conditions for traversing, one may run a mile, taking 40 readings, in about  $1\frac{1}{2}$  hr. with the Superdip, and in about half the time with an ordinary dip. Where the going is very bad, so that the progress of the party is very slow anyway, the difference in speed is

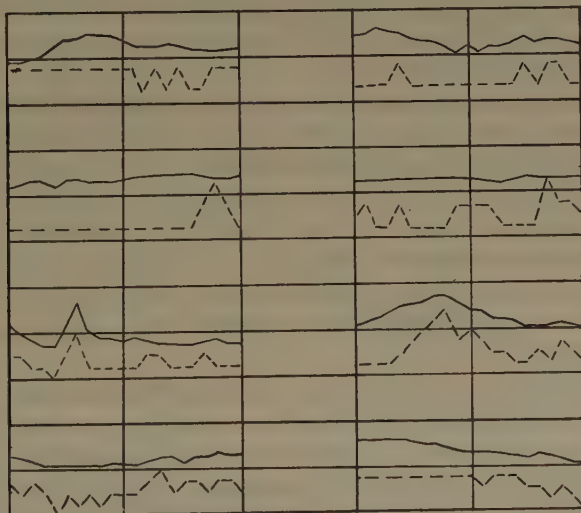


FIG. 3.—PROFILES FROM READINGS OF DIP NEEDLE AND SUPERDIP.

Dotted lines show profiles constructed from readings taken with a common dip needle; the full line immediately above each dotted one is the profile of Superdip readings taken over the same traverse. The vertical scale is such that one division equals  $2^\circ$  on the common dip needle, or  $10^\circ$  on the Superdip, which has a sigma of  $3^\circ$ .

not as great, but the inconvenience of carrying the Superdip with its tripod and transit head is much greater.

Accordingly the ordinary dip needle is preferred wherever the magnetic variations can be satisfactorily determined with it. The choice then depends on one's judgment of what constitutes a satisfactory difference in dip readings. This judgment must consider the probable error in traverse readings\* and the nature of the magnetic variations. Data on the first factor are given in the following paragraphs. The second factor may be said to introduce a variable factor of safety. For example, where the variation is sharp and regular, a difference in readings slightly greater than the probable error would be satisfactory. Also,

in this case the probable error would be smaller, because one could take more precautions. Usually, however, the variations are irregular, and often they occur gradually. As a rule, therefore, the maximum variation must be capable of producing a difference in readings that is several times the probable error in readings, if one is to obtain more than merely an indication of magnetic variations.

Estimates of the probable error in reading the ordinary dip needle vary considerably. Some believe that a dip can be depended on to the nearest  $0.5^\circ$ . This is true in the sense that a greater error in readings taken at a check station shows that the instrument is in need of reconditioning. However,  $0.5^\circ$  cannot be considered as therefore the maximum error in ordinary traverse readings, because of many apparently insignificant but actually important factors that influence traverse readings but not those at check stations. The following data give the actual errors found on certain traverses.

Fig. 3 shows profiles constructed from readings taken with an ordinary dip needle, and corresponding profiles made from Superdip readings taken over the same lines. The Superdip profiles, on the scale of the figure, are practically without error. The four upper profiles show errors in the dip readings up to  $2^\circ$ , and the four lower ones, errors up to  $1^\circ$ . The lower profiles were constructed from more recent data collected by N. H. Stearn and the writer, using methods subsequently described by him,<sup>3</sup> and may be considered typical of modern work with dip needles in good condition.

The profiles are also instructive with regard to the factor of safety required. The four lower profiles show variations up to  $2.5^\circ$ , with a maximum error of about  $1^\circ$ . Yet these variations are not sufficiently large to obtain a clear picture of the magnetic field, owing to irregularities in the attraction. The Superdip readings, however, are conclusive in this regard. In general, the writer believes that at least a  $5^\circ$  variation in dip readings should be found if the ordinary dip needle is to prove a satisfactory instrument where the attractions are broad or irregular.

#### *Adjustments of the Ordinary Dip Needle*

The first principle is that of having the instrument read not over plus  $30^\circ$  or  $40^\circ$ . Some workers, knowing that the dip needle is most sensitive when reading about  $0^\circ$ , adjust it to read about  $0^\circ$  in a normally magnetic locality, arguing that the instrument should be adjusted to pick up the weak attractions, since the strong ones will be found anyway. This is a mistake, however. A weakly magnetic formation near a strongly magnetic one is bound to be obscured, and the domination by the strongly magnetic structure is only increased if the dip needle is greatly influenced by changes of inclination. Further, there is the

<sup>3</sup> N. H. Stearn: *Trans. A. I. M. E.* (1929) **81**, 363.

fallacy of clouding the inferences from a good magnetic attraction in the hope of discovering weak ones. Of course, in large areas, it may be advisable to use dip needles with different adjustments. Fig. 4 illustrates some of the disadvantages resulting from an unsuitable ratio.

In a dip needle of perfect construction, the sigma cannot be changed without modifying the instrument. However, the grinding of new points

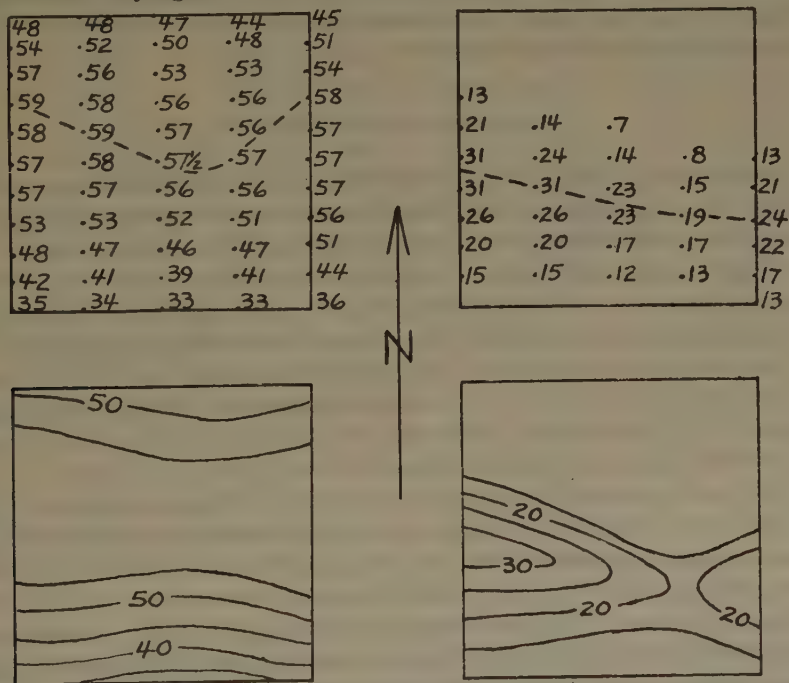


FIG. 4.—READINGS OF COMMON DIP NEEDLE. EACH OF THE FOUR SQUARES SHOWS THE SAME AREA,  $\frac{1}{2}$  MILE SQUARE.

The readings at the upper left were taken with a common dip needle having a high ratio for this area. It was, in fact, adjusted to read  $0^\circ$  in a region of normal attraction. As the formation dips north, the magnetic line joining the highest of these readings was thought to indicate a local synclinal trough. When the same readings are contoured, as shown in the lower left square, the magnetic line emphasizes a minor feature of this attraction. The readings at the upper right were taken with a common dip needle having a more suitable ratio for this area. The magnetic line joining the highest of these readings is practically straight. When these readings are contoured, as in the lower right square, marked longitudinal variations are shown. Work in adjacent areas associates the high spots with drag folds in the magnetic formation. The illustration also shows that a suitable ratio effects a large saving in the number of readings necessary to detail a magnetic line.

on the pivot often introduces a slight eccentric effect, the presence of which may be discovered by rotating the pivot in the needle and observing any change in reading so caused. A change in the reading shows that the needle is slightly unbalanced. By observing the rates at which the needle swings for different positions of the pivot, the most sensitive setting can be determined because the needle swings most slowly when most sensitive. The sensitivity of some instruments can be greatly

modified by this method. For example, one dip needle showed a difference in readings between two stations that ranged from  $3^{\circ}$  to  $12^{\circ}$ .

The writer's experience with highly sensitive dip needles has been generally unsatisfactory. Their slow action makes them difficult to read, and they are apt to need frequent reconditioning. As a rule, dip needles are adjusted to have a moderately fast action, and those satisfactory for field use rarely show more than a 50 per cent difference in sensitivity, indicating sigmas between  $12^{\circ}$  and  $18^{\circ}$ .

### *Adjustments of the Superdip*

Regarding the ratio, the same remarks apply to the Superdip. Occasionally the importance of the ratio is forgotten, with results that are even more unsatisfactory than with the ordinary dip needle.

Regarding the best sigma to use, opinions vary a good deal. Some workers believe that the sigma should be  $0.5^{\circ}$  to  $1^{\circ}$ . The writer, however, advocates sigmas of  $2^{\circ}$  to  $4^{\circ}$  in this region, for reasons given below.

One could enumerate many factors of importance in the choice of the proper sigma. However, the real limiting factor is the relationship between the instrumental error and the traverse error, which is an integration of several other factors.

The instrumental error is that found in checking a reading. The end point of a swing of the needle can be determined to the nearest half degree, giving a probable error of  $0.25^{\circ}$ . The rate at which the pivot is dropped on to the quartz wedges has considerable effect on the limit of the first swing. For this reason, the writer has made a practice of reading the end points of the first three swings (down, up and down again), from which the mean reading is calculated. The probable error is thus reduced to something less than  $0.125^{\circ}$ . For convenience, the writer records readings in tenths of a degree, and two readings at a check station almost invariably check within this amount. However, some leeway should be allowed for the instrumental error in an ordinary unchecked traverse reading. Accordingly this error is estimated at  $0.25^{\circ}$ , which seems a safe maximum.

The traverse error is one that may occur at an ordinary traverse station. It is composed of the instrumental error plus errors due to several other causes, of which some of the more important are given below. One factor is imperfect correction for daily variations in the magnetic field. Again, temperature corrections are also apt to be imperfect because the instrument may not be uniformly heated or cooled. Probably the most important factor, however, is the presence of local interference, or magnetic bodies near the instrument, which have no relation to bedrock structure. One soon learns to avoid obvious causes of local interference, such as steel culverts, rails, and wire fences, but it is impossible to avoid



such things as buried magnetic boulders in the drift, and it is impractical to check every slight variation in the readings by making other set-ups around it. In other words, the ordinary traverse reading is assumed to represent the average of all readings that might be taken halfway in all directions to adjacent stations, and this assumption is apt to introduce slight errors.

Fig. 5 gives some data on traverse errors. Errors up to about  $0.5^\circ$  are indicated, and other data show the same general results.

As the traverse error is more than twice the instrumental error, reducing the sigma would not give more reliable magnetic data, because the traverse error would be increased roughly in proportion to the increase in the difference in readings. In other words, a  $5^\circ$  variation in readings accurate to  $0.5^\circ$  is just as satisfactory as a  $20^\circ$  variation in readings accurate to  $2^\circ$ . However, a  $5^\circ$  variation in readings accurate to  $0.5^\circ$  is better than a  $1^\circ$  variation in readings accurate to  $0.1^\circ$ , as far as local interference is concerned, but only readable within  $0.25^\circ$ . Therefore the sigma can be reduced with advantage to the point where the traverse error definitely exceeds the instrumental error. This point corresponds to a sigma of  $2^\circ$  to  $4^\circ$  for normal conditions in this region. Any further reduction only limits the range of the instrument; that is, the lower the sigma, the greater the chance of encountering a change of inclination sufficient to reduce the sigma to  $0^\circ$  or to reverse its sign, or of finding a change of intensity sufficient to make the readings too high for satisfactory results. On the other hand, using a Superdip with a sigma of more than  $4^\circ$  is rarely advisable, as a magnetic variation beyond the range of such an instrument could be traced with an ordinary dip needle.

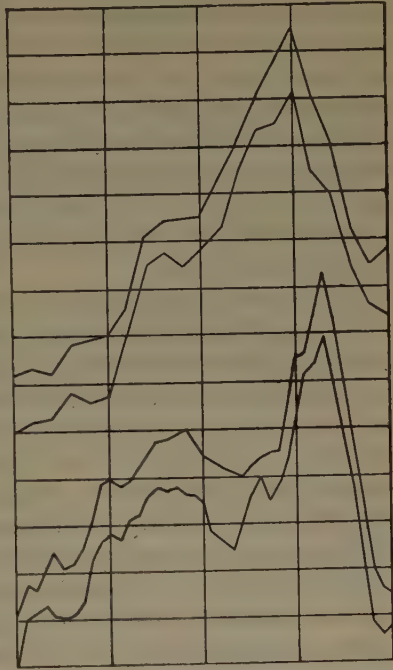


FIG. 5.—COMPARISON OF READINGS TAKEN WITH TWO SUPERDIPS HAVING THE SAME SIGMA OF  $3^\circ$ , AND APPROXIMATELY THE SAME RATIO.

Horizontal lines are spaced with a  $1^\circ$  interval in readings, and vertical ones connect corresponding readings for each pair of profiles. Readings were taken at ordinary traverse points, and thus give a measure of the traverse error. Profiles constructed from the observations with one instrument are separated from those with the other by an average of  $1^\circ$ . If each profile were superimposed upon its mate as closely as possible, there would be an average difference of  $0.2^\circ$ , and a maximum of  $0.6^\circ$ . The same average and maximum errors are indicated by comparing the difference between adjacent readings on one profile with the difference between corresponding readings on the other.

*Interpretation of Magnetic Data*

The interpretation of dip-needle data depends largely upon the use of empirical relations established separately for each area, as briefly outlined in the preceding section. Probably the opinion of many geophysicists will be that this type of interpretation neglects valuable physical principles that could be usefully employed. The following paragraphs attempt an explanation of this seeming neglect by showing that certain features of the magnetic data and geologic structures in the region make empirical methods generally adequate from a practical geologic viewpoint. Of course, physical theory is used to a certain degree, and the discussion below also indicates the limits determined by experience in this district.

In general, the character of a magnetic variation depends on the position, shape, size, attitude and permeability of the structure causing it. Also, the dip-needle readings produced by this variation are dependent on the adjustment of the instrument. Of the large number of possible magnetic variations, and pictures of these variations obtained from dip readings, relatively few are found in actual practice. To give the reader some perspective on conditions in this region, a few figures are included in the following discussion. The figures are based upon a list of the prominent magnetic variations that the writer has encountered. The total number is 43. The number of magnetic lines would be much larger, as, for example, where the flows of an area yield attractions, this is listed as one magnetic variation, even though there are several magnetic lines following various flows.

First, it must be emphasized that dip-needle readings do not give separate data on the inclination and intensity of the magnetic field, which limits the theoretical inferences possible. As far as possible, the instrument is adjusted to make intensity the dominant factor, but inclination always enters to some extent, particularly near strong attractions. For this reason, the crests of dip-needle profiles usually lie north of the buried outcrop of the magnetic structure, the distance varying with the adjustment of the dip needle, the depth of the drift cover, and the dip of the structure. The amount of this interval is generally determined by a comparison of the magnetic and geologic data. Rarely, there may be two sets of readings with dip needles adjusted differently, from which the intensity and inclination can be calculated, allowing an interpretation such as that illustrated in the last example given in the next section. Again, one may roughly estimate the intensity and inclination because the swing of the needle is slowest where the inclination is highest, and fastest where the intensity is greatest. This relation allows one to judge somewhat the position of the buried outcrop. Also, when taking readings in the field, one may be warned of a near-by attraction, especially when using a superdip, and can space the readings more efficiently.

The position of the magnetic body with respect to the observer depends mostly upon the depth of the drift cover. The factor of position can be largely eliminated, however, by ignoring readings on outcrop areas for purposes of structural interpretation. No loss is caused by doing this, as the local structure in outcrop areas is best determined from the exposures themselves. In the field, sharply irregular readings are a sign of shallow drift cover or local interference.

The shape of the magnetic body can be estimated from the shape of the area of magnetic variation, and the geologic probabilities. Of the variations encountered by the writer, 40 out of 43 represent tabular structures. The most valuable service of the magnetic data is that of showing folds or faults in a buried tabular structure by means of bends or breaks in the line of attraction.

The size of the magnetic body is also clearly related to the size of the area of magnetic attraction. In this region, uniformly magnetic structures with large outcrop areas are rare. In other words, the boundary between two series is followed magnetically by the presence of a line of attraction in one of them, rather than by a step-up in the level of the readings from one to the other.

The attitude, or strike and dip, of a magnetic body is reflected by the direction of the magnetic lines and the symmetry of the magnetic profiles. The relation between symmetry and dip is that a profile has a gentler slope on the side toward which the structure dips. However, this rule is not without exceptions. The magnetic structures usually dip steeply and are irregularly magnetic, which makes the profile roughly symmetrical with either side locally steeper. Also the adjustment of the instrument is a factor in the symmetry of profiles constructed from dip-needle readings. For these reasons, the dip is usually estimated from geologic data.

Generalizations relating permeability to type of rock are of little use in this region, as the following paragraphs will show. Of the 43 magnetic variations encountered by the writer, 17 are due to iron formations, 13 to other sedimentary rocks, 7 to volcanic series, and 6 to intrusives.

Iron formations are a prolific source of magnetic variations. The unoxidized type, or cherty carbonate, may contain magnetite either uniformly distributed, yielding fairly regular attractions, or spotty, causing a series of small local variations. Ferruginous cherts, which are dominantly hematite, limonite and chert, may or may not yield appreciable effects. In three localities the writer has observed slightly subnormal readings over this type of rock. Specular iron formations are generally magnetic, as specular hematite always has some magnetite with it. The magnetite-grunerite type of iron formation is highly magnetic. This is one case where the permeability is distinctive, as no other type of rock is quite as magnetic.



Other sedimentary rocks are also frequent sources of attractions. Often, the crests and troughs of the steeply pitching folds are more magnetic than the limbs, giving the magnetic contours the aspect of a series of crescentic hills. Most of the important attractions are positive. In two localities, however, the writer has found zones of subnormal attraction which marked sedimentary beds.

Flows rank next in importance. Probably the commonest cause is the presence of secondary magnetite in the upper part of the flows. Thin beds of tuff, slate, or iron formation cause magnetic attractions in some areas where the bedrock is dominantly volcanic, and such examples are included in the seven cases listed under this origin. The Keweenaw series produces many magnetic lines due to primary magnetite segregated in the flows or concentrated in certain so-called doleritic or pegmatitic streaks.

The writer has met only one strongly magnetic intrusive, a small body of gabbro. In two places the contacts of sills yield small positive attractions. This does not include, however, cases where beds become more magnetic near intrusives, as, in such cases, the general attraction follows the bed rather than the contact. In three localities, basic dikes and sills are marked by subnormal attractions.

Finally, it may be noted that fault zones, in addition to causing offsets in magnetic lines, often yield subnormal readings. Occasionally, however, there is an unusually high attraction along a fault.

#### EXAMPLES OF THE PRACTICE

##### *Example A*

Fig. 6 gives the magnetic and geologic data for a small area. The figures represent readings taken with an ordinary dip needle. Only two outcrops were found. They are situated west of the center of the area, and consist of ferruginous slate. In this area, strikes and dips shown by small outcrops are not very useful, however, as the beds have been crumpled in the very irregular fashion characteristic of a thick incompetent series.

The small arrows show the direction in which the traverse lines were run, illustrating a method that has proved useful where the attractions are irregular. After crossing the attraction, one offsets a distance equal to about one-third the distance between the main traverse lines, and runs back across the attraction. Then one offsets to the other side and runs across the attraction a third time, ending opposite the joint where the main traverse line was first left. One is then ready to continue the main traverse with a minimum of pacing error and a large number of readings along the attraction.

A zero contour is shown surrounding the high readings. Other contours could be drawn, but are hardly needed. This attraction is



rather exceptional in its sharpness and continuity. The sudden changes in the readings indicate a shallow drift cover, which actually is about 30 ft. thick. The subnormal readings near the high ones and the strong attractions at bends in the magnetic line are typical features.

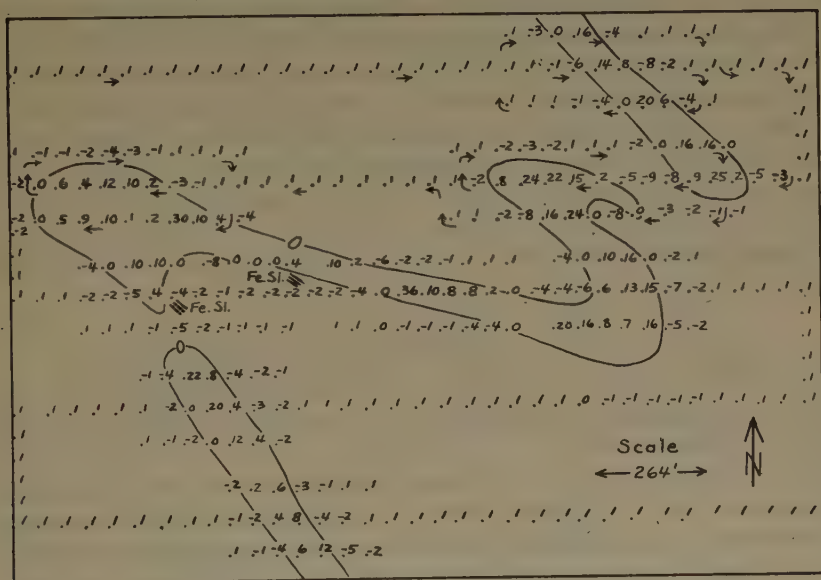


FIG. 6.—READINGS TAKEN WITH AN ORDINARY DIP NEEDLE.

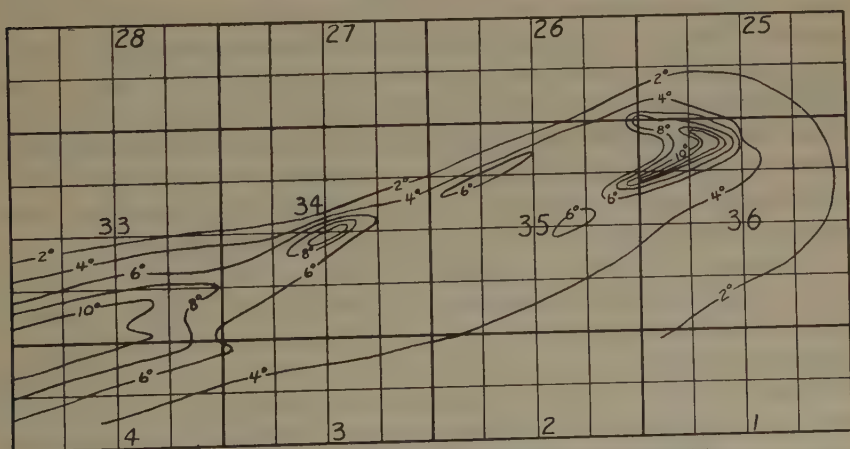


FIG. 7.—SUPERDIP READINGS. EACH SMALL SQUARE REPRESENTS  $\frac{1}{40}$ , OR AN AREA  $\frac{1}{4}$  MILE SQUARE. THE TOP OF THE FIGURE IS NORTH.

From the general geology of the district it is known that the formations consist of greywacke and slate overlying iron formation with a north-south strike and westward dip, and that magnetic lines are fairly common in the hanging-wall slate. Therefore the magnetic line in this figure is assumed to follow a bed in the hanging slate. The bends in the

line then show two drag folds pitching northwest. There is no marked asymmetry in the magnetic profile, so we may, as a first approximation, assume that the axial planes of the drag folds are vertical and that the pitch is steep, say  $45^{\circ}$  to  $60^{\circ}$ . In this connection, little help is obtained from structures known in adjacent areas, as a drag fold to the north is shown by mining operations to pitch about  $45^{\circ}$  northwest, and a drilling exploration to the south shows a flat roll in the iron formation. From the above, one might predict that a section from east to west across the iron formation would show a small syncline and anticline succeeded by a larger and deeper syncline before the formation finally turned downward to the west. The position of the crests and troughs and an estimate of the apparent dips could also be made. This was done, and the results accord fairly closely with information from a line of drill holes subsequently put down.

### *Example B*

Fig. 7 shows an area of about 8 square miles. The readings were taken with a Superdip having a sigma of  $3^{\circ}$ , and are referred to a normal of  $65^{\circ}$  on this instrument.

No outcrops were found. However, it is known from regional geologic information that a volcanic series with a general anticlinal structure underlies the area. The magnetic contours therefore suggest the presence of a magnetic member of the series in the form of an anticline, which pitches gently westward in the western part of the area, where it is buried deeply enough to yield a single broad crest, and pitches rather steeply eastward in the eastern part, where its uppermost portion has been eroded to yield a magnetic line in the form of a discontinuous loop. (The discontinuity is assumed to be due to local irregularities in the distribution of the magnetite, which may not be present to the west, or may have their effects merged by depth of burial). In general, the contours are more closely spaced on the north than on the south side of the attraction, which suggests that the axial plane of the anticline is inclined southward.

Geologic information to check definitely this inferred structure is not available. However, what is known of adjacent areas is in general accord with the inferred structure. About 3 miles to the south, explorations and mines show an iron formation in the form of a fold of which the axial plane strikes east-west and is inclined southward. To the northwest, several outcrops of a volcanic member in the overlying slate and greywacke series lie in a line parallel to the zone of attraction. In this case, the usefulness of the magnetic data is that of indicating a structural pattern for the correlation of scattered bits of geologic data.

Incidentally, it may be noted that the magnetic variation is not large enough to be determined satisfactorily with the ordinary dip needle, because many of the significant changes cause differences of only  $0.5$  to  $1^{\circ}$  in readings taken with the ordinary dip needle.

*Example C*

Fig. 8 gives the magnetic data over an area of 7 square miles on the south limb of the Marquette range. The full contour lines show the readings of an ordinary dip needle adjusted to read  $5^\circ$  in a normally magnetic area. The dashed contour lines show readings of a dip needle adjusted to read  $-32.5^\circ$  in a normally magnetic area.

Fig. 9 shows the outcrops found in the same area, and the formation boundaries decided on after an analysis of the geologic and magnetic data.

In general, the magnetic data show two lines of attraction. The northern one follows the center lines of sections 13, 14 and 15, and then

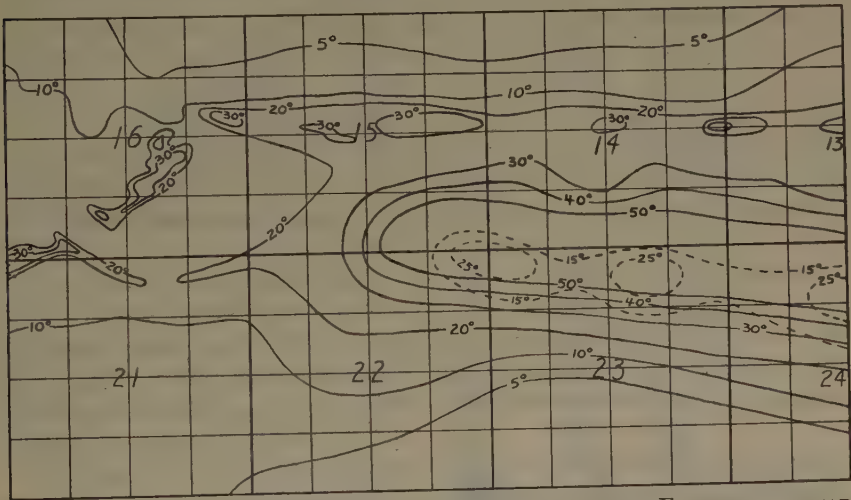


FIG. 8.—READINGS TAKEN WITH AN ORDINARY DIP NEEDLE. EACH SMALL SQUARE REPRESENTS  $\frac{1}{40}$ , BOUNDED BY NORTH-SOUTH AND EAST-WEST LINES, THE LATTER RUNNING ACROSS THE DIAGRAM.

swings sharply southwestward through section 16. Along this line, outcrops are found in section 16, and some test pits expose the bedrock in section 14. The rock is an impure sandy and slaty iron formation, called the Greenwood member. The southern line of attraction occurs along the north side of sections 24 and 23, and ends in section 22. It follows the Negaunee iron formation, which here is a magnetite-grunerite rock, as shown by drilling in section 23, and outcrops east of this area. As this attraction is very strong, it was also traced with a dip needle more heavily counterweighted than usual, giving the readings shown by the dashed contour lines.

Geologic knowledge of the Marquette range as a whole yields the following pertinent facts. This area is on the south limb of the Marquette syncline. The sedimentary succession consists of Goodrich quartzite and Michigamme slate of upper Huronian age, resting unconformably upon

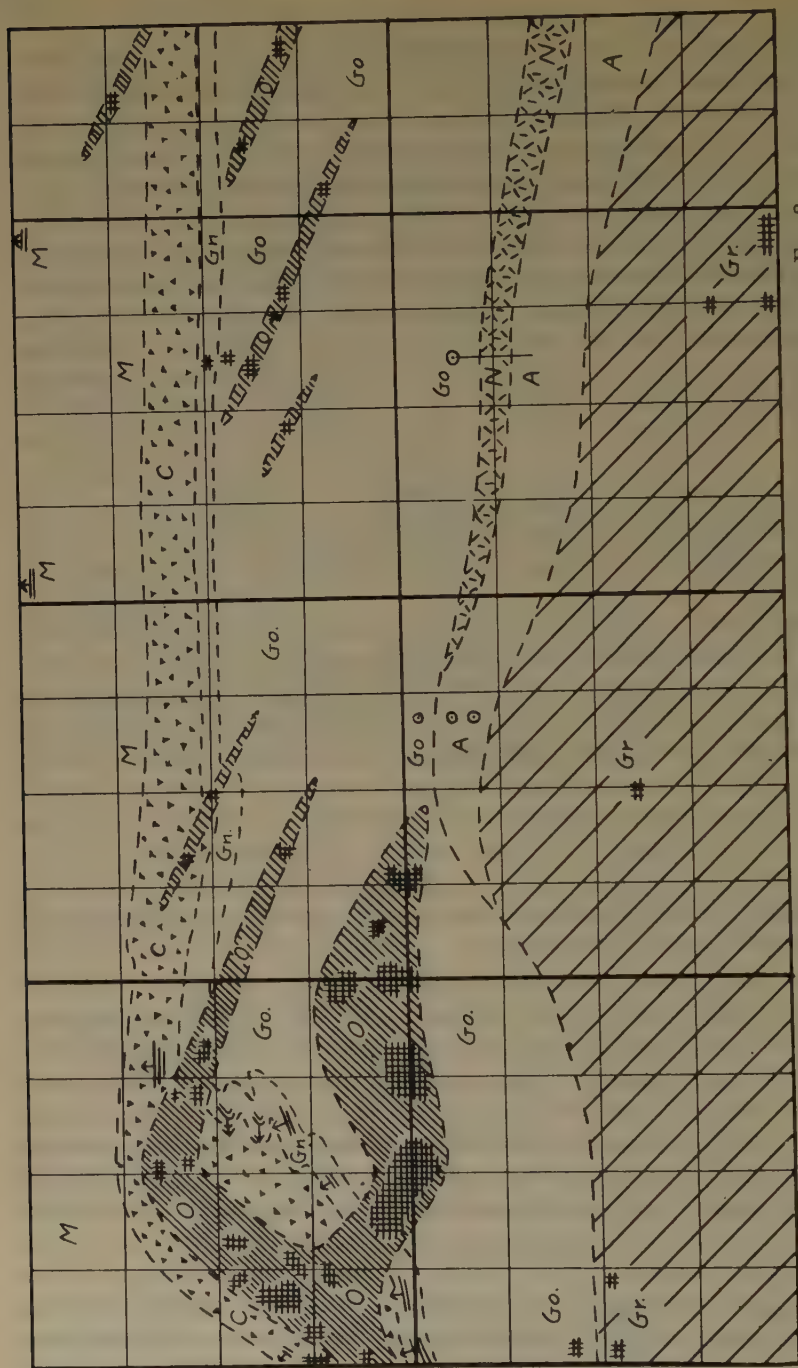


Fig. 9.—OUTCROPS AND GEOLOGIC BOUNDARIES OVER THE SAME AREA AS THAT COVERED BY FIG. 8.

Outcrops are shown by cross-hatching, or by strike and dip symbols. The different formations are lettered as follows: M, Michigan gamme slate and greywacke. C, Clarksburg tuff and agglomerate. Go, Goodrich slate, quartzite and conglomerate. N, Negaunee iron formation. Gr, granite and gneiss. O, ophite, diabase and porphyrite. A, Ajbik quartzite and slate.



the Negaunee iron formation and Ajibik slate and quartzite of middle Huronian age. Beneath the Huronian, in a purely geometric sense, is granite, which is partly stratigraphically below, forming an older basement, and is partly intrusive into the Huronian. Basic intrusives cutting the Huronian series are common.

The regional geologic information, the local outcrops, and the magnetic data enable one to place the boundaries of the sedimentary formations by the simple process of drawing the contacts so that they are parallel to the magnetic lines, one in the upper Huronian and one in the middle Huronian, and so that equivalent outcrops lie in the same member. Thus the upper Huronian is locally divided into the Goodrich, Greenwood, Clarksburg and Michigamme members, and the middle Huronian into the Negaunee iron formation and the Ajibik slate and quartzite.

Regarding the intrusive contacts, it is apparent that little help is obtained from the dip-needle readings in this area.

The boundary of the southern granite mass can be determined from outcrops in the western part of the area, but in the eastern part this basis allows too much latitude. As the granite on the Marquette range generally occupies the position one would expect of a basement granite, this generalization is used in the eastern part of the area. That is, the contact is drawn parallel to the boundaries of adjacent sedimentary formations.

The boundaries of the ophite in the western part of the area are defined pretty closely by outcrops. It may be noted that a weak line of attraction follows the southern contact of the mass of ophite along the north side of section 21.

Outcrops of ophite in the eastern part are scattered. The contacts shown are more or less speculative, and based on the following relations. In section 16, the attraction along the Greenwood member is frequently highest near outcrops of ophite. Also, high readings occur where the beds are sharply folded. Drag folds are common on the limbs of the Marquette syncline, and, on the south limb of a syncline pitching westward, as is the case here, the drag folds should pitch north of west. Dikes frequently follow the axial planes of drag folds, or small faults associated with them, in this district. The ophite outcrops can be joined along lines trending west-northwest, and also lines parallel to these can be drawn to join high spots on the Greenwood attraction with high spots on the Negaunee attraction. All these relations make it reasonable to show the ophite in the eastern part of the area as dikes striking west-northwest.

In this area, two sets of dip-needle readings are available along the southern magnetic line, which permits a calculation of the inclination and intensity of the earth's field. This allows certain further deductions to be made, as follows:

One dip needle, whose readings are shown by the full contours, may be called dip I, and the other, dip II. Let  $M$  be the maximum gravitative moment of dip I. For any reading,  $R^\circ$ , the gravitative moment is then  $M \cos R^\circ$ . Let  $F$  be the maximum magnetic moment, which is effective

when the needle reads  $(90^\circ - I^\circ)$ , where  $I^\circ$  is the inclination of the earth's field.  $F$  is, of course, proportional to the intensity of the earth's field for a given needle. For any reading,  $R^\circ$ , the magnetic moment is then  $F \cos (90^\circ - I^\circ + R^\circ)$ . Now, dip I reads plus  $5^\circ$  in a normal field, whose inclination in this region is  $75^\circ$ . Therefore,  $M \cos 5^\circ = F \cos 20^\circ$ ; whence,  $F = 1.06 M$ . Dip II reads minus  $32.5^\circ$  in the same field. Let  $X$  be the maximum gravitative moment of dip II. Then,  $X \cos 32.5^\circ = 1.06 M \cos 17.5^\circ$ ; whence,  $X = 1.20 M$ .

Suppose two readings are taken near a magnetic body, where the inclination and intensity are unknown. Let the reading on dip I be plus  $60^\circ$ , and that on dip II, plus  $14^\circ$ . Then we may write:

$$M \cos 60^\circ = F \cos (90^\circ - I^\circ + 60^\circ),$$

$$\text{and, } 1.2 M \cos 14^\circ =$$

$$F \cos (90^\circ - I^\circ + 14^\circ).$$

From these two equations I can be calculated in degrees and  $F$  in terms of  $M$ . Table 1 and Fig. 10 show the results obtained for stations A to F.

Station A is 200 paces ( $\frac{1}{10}$  mile) north and 700 paces west of the northeast corner of section 23, and station F is 1000 paces south of station A.

The declination along this line ranged from  $3^\circ$  to  $7^\circ$  east, which permits plotting the results directly on a north-south plane. The magnetic anomalies at the stations are shown in Table 2 and Fig. 10.

On Fig. 10, the lines showing the local anomalies at stations B, C, D and E converge nearly at one point, marked with a circle. The proportional strengths of the anomalies also agree fairly well with those calculated for this center of attraction. The anomalies at stations A and

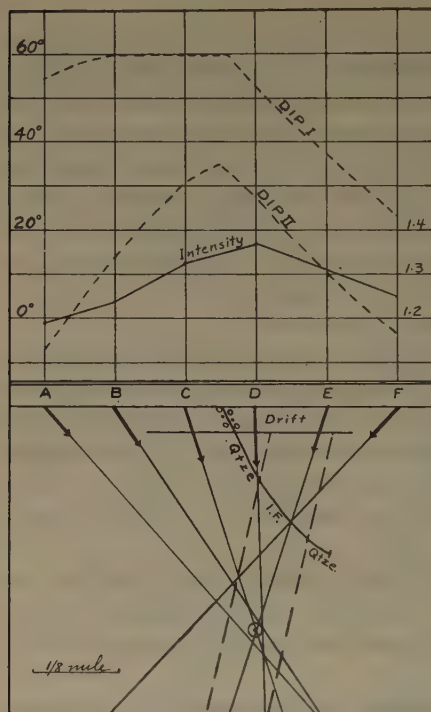


FIG. 10.—UPPER PART GIVES TWO SETS OF DIP-NEEDLE READINGS ALONG LINE FROM A TO F; ALSO INTENSITIES CALCULATED FROM THESE READINGS. LOWER PART IS VERTICAL SECTION.

Each heavy line ending with an arrow-head represents the magnetic anomaly at a station. The drill hole gives depth of glacial drift and position of Negaunee iron formation, which lies between Goodrich and Ajibik quartzites.

TABLE 1.—*Readings for Stations A to F*

Station	Readings, Deg.		Calculated	
	Dip I	Dip II	Inclination	Intensity (F)
A	53	— 7	83 15	1.19 M
B	60	14	83 45	1.24 M
C	60	31	82 10	1.33 M
D	52	28	78 50	1.37 M
E	37	11	74 30	1.31 M
F	23	— 3	70 30	1.25 M

TABLE 2.—*Magnetic Anomalies*

	Components		Anomalies	
	North-south	Vertical	North-south	Vertical
Normal field.....	0.274 north	1.024	0	0
Station A.....	0.134 north	1.182	0.140 south	0.158
Station B.....	0.135 north	1.233	0.139 south	0.209
Station C.....	0.181 north	1.318	0.093 south	0.294
Station D.....	0.265 north	1.344	0.009 south	0.320
Station E.....	0.350 north	1.262	0.076 north	0.238
Station F.....	0.417 north	1.178	0.143 north	0.154

F, however, indicate a center of attraction that is to the north and not as deep.

It may be assumed that the center of attraction lies in the Negaunee iron formation. By estimating the dip from geologic data, one could determine the position of the buried outcrop. In this case, however, a drill hole shows the position of the iron formation near the surface, which permits a determination of the dip. Also the depth of the drift cover gives the body the effect of being uniformly magnetic, and it can be considered as a series of bar magnets lying side by side and extending down the dip. As the poles of a bar magnet are usually about one-tenth of the length of the bar from either end, and as one pole is here  $\frac{1}{4}$  mile below the outcrop, one may infer that the iron formation continues with the same character about  $2\frac{1}{2}$  miles down the dip. In geologic terms, the inference is that the Goodrich unconformity, which truncates the iron formation about  $\frac{3}{4}$  mile to the west along the strike, does not do so for at least 2 miles down the dip, nor does the iron formation become nonmagnetic within this distance. Parenthetically, it may be noted that the iron formation outcrops on the north limb of the Marquette syncline about 3 miles away, where it dips steeply southward, is composed of ferruginous chert, and causes little or no magnetic variation.

## DISCUSSION

(*Sherwin F. Kelly presiding*)

S. ROYCE, \* Crystal Falls, Mich.—We have done a certain amount of this same work in scattered areas. We found that the 2° to 4° sigma on the Superdip would not display the type of things that we had to trace in order to map buried folded iron formations that had weak bands of magnetic attraction, especially in the oxidized areas. We used a sigma minimum of 0.5° and averaged 1°, and with that we were able to trace formations that were far too weak in magnetic attraction to see anything with a 2° to 4° sigma.

For instance, the formation mapped as a drag fold in Mr. Swanson's paper is a strong but discontinuous zone of magnetic attraction on the hanging side of the iron formation, and is very satisfactorily traced, where present, with 4° sigma if depth of cover is not over 150 ft. With a sigma of 0.5° to 1° it has been found possible to trace the details of an anticlinal structure in oxidized iron formation with up to 200 ft. of cover; to determine and trace around the anticline the most highly oxidized (least magnetic) horizon; and by locating drill holes on this to develop an orebody. The strong hanging-wall magnetic, which could be followed by a 4° sigma, was present only in discontinuous occurrences insufficient to trace the structure. A sigma of more than 1° failed satisfactorily to trace the weak magnetics present or to give any clue to the most highly oxidized portions of the iron formation, which are of course the best chances for exploration.

Where there are strong and consistent magnetic bands clearly related to the formation sought, the larger sigma is of course most satisfactory. But where this is not the case the finer sensitivity obtained by a smaller sigma makes possible the tracing of weak magnetics, which in iron formation are often more persistent than the stronger ones. Also, with a small sigma the character of the magnetic profile shows much as to the condition and type of the iron formation, which facilitates selection of favorable horizons or areas, and higher sensitivities more readily reflect changes of rock other than iron formation, such as clay slates, carbonate slates, limestones, granites, igneous intrusions, etc.

The chief objection to high sensitivity is the magnification of "accidental" local attractions such as boulders, culverts, fences, wires, pipes, etc. Except in settled areas such as villages, mine locations, towns, etc., where we have found magnetic work of little value, these "accidentals" are nearly all avoidable except boulders. The latter make comparatively little trouble in most areas we have surveyed, and where present are usually readily eliminated because of their sporadic and irregular occurrence. In one instance a buried boulder train caused a little difficulty for a short distance, but finally was diagnosed correctly by detail work which traced it to its outcrop.

J. FISHER, † Houghton, Mich.—We use occasionally a 1° to 1.5° sigma, but the various local attractions found are of very little importance as far as we are concerned. The small sigma, of course, gives the higher sensitivity and, therefore, picks up all the local attractions.

---

\* Pickands, Mather & Co.

† Head, Department of Mathematics and Physics, Michigan College of Mining and Technology.



# Magnetic Measurements on Auriferous Veins in Brazil\*

BY MARK C. MALAMPHY,† RIO DE JANEIRO, BRAZIL

(New York Meeting, February, 1934)

DURING colonial times, Brazil was famous for the richness of her alluvial gold deposits. Paul Ferrand has estimated that the gold produced during the period from 1700 to 1820 was the equivalent of some 64 million pounds sterling. Since that time, most of the more prolific alluvial deposits have been exhausted. A few gold mines are still functioning, notably the Morro Velho mine, which is one of the deepest mines in the world.

Today, the gold production of Brazil is insignificant when compared with world figures, but there are still many gold-bearing regions and it is probable that in at least some of them profitable returns would result from an exploitation program taking advantage of all the most modern innovations in gold mining and ore treatment on a large scale.

In order to demonstrate the value of some of these abandoned prospects and stir up interest in increasing the national gold production, the government has stimulated research. Experimental plants have been and are being established in various places, and tests on large quantities of ores are being carried out on a semicommercial basis. The Geological Survey of the State of Minas Geraes is very active in this line and the Federal Institution is also showing an increased interest in the matter.

One of the lesser known gold-bearing regions of Brazil is in the vicinity of Lavras, in the State of Rio Grande do Sul. Gold was first reported from this region in the early part of the nineteenth century. In 1811, D. João VI sent an experienced prospector from Minas Geraes to investigate the validity of the reports. According to the reports of Baron Eschwege, he succeeded in extracting some 30,000 *Oitavos* (about 105 kg.) during the first few years, but the production costs exceeded the value of the gold obtained.

---

Manuscript received at the office of the Institute Dec. 14, 1933.

\* This paper is a résumé of a part of a more complete report on geophysical prospecting in Rio Grande do Sul, which is to be published as a Bulletin of the Departamento de Produção Mineral.

Published by permission of the Director, Departamento de Produção Mineral of Brazil.

† Consulting Geophysicist, Diretoria de Minas, Departamento de Produção Mineral, Ministerio de Agricultura.

Eugene Hussak, in an unpublished manuscript, reports that in 1854-55 the gold produced in this region amounted to some 40,000 oitavos, or approximately 140 kg. This production apparently was due mainly to the activities of the English company operating under the name of Rio Grande do Sul Gold Mining Co. A few years later this company abandoned its work and today we find only a few old shafts and galleries to mark the site of its activities. Some years later a Belgian company

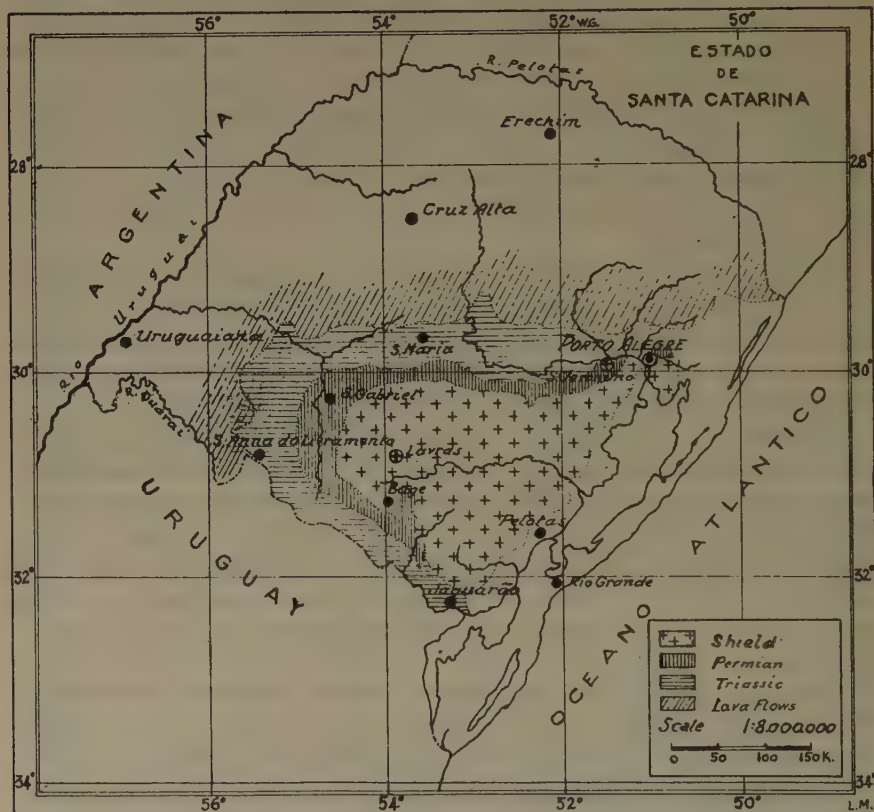


FIG. 1.—SKETCH MAP OF STATE OF RIO GRANDE DO SUL, SHOWING REGIONAL GEOLOGY AND LOCATION OF LAVRAS AND SÃO JERÔNIMO AREAS.

The "shield area" is composed of granites, gneiss and old metamorphic schists, sometimes covered with thin sediments in isolated patches.

attempted to exploit the region but also failed. Today, a few abandoned buildings and rusty obsolete machinery are left to bear mute testimony to the hopes that failed to materialize.

A few years ago the engineers of the Brazilian Geological Survey made a rapid study of the region and treated some few tons of selected ores with rather encouraging results. On the basis of their findings, the Companhia Estrada de Ferro e Minas São Jerônimo was induced to make a more detailed study of the area, and this work is now in progress.

In May, 1932, the writer was requested to study the possibility of applying the geophysical methods to this problem with the hope of reducing the exploration costs. In this paper we will give a few details on the work done there and the results obtained. The problem is difficult, undoubtedly, and our results were not particularly brilliant. However, it is believed that our data represent another advance in the application of the magnetic method of prospecting. In presenting these data, we wish to give others the opportunity to profit by the experience we have gained, and perhaps stimulate the trial of geophysics, even though conditions appear to be unfavorable to its successful application.

### GEOGRAPHY AND GENERAL GEOLOGY

The Lavras area is in the central part of the State of Rio Grande do Sul (Figs. 1 and 2). The approximate geographical coordinates of the town are: latitude  $30^{\circ} 48.5'$  S., longitude  $53^{\circ} 54.4'$  W. of Greenwich. It is reached by rail from Porto Alegre via Santa Maria, and from the city of Rio Grande do Sul via Bagé. The railroad does not actually pass through the town of Lavras, the nearest station being at a distance of some 40 kilometers.

Lavras is within the granitic area that Paulino F. de Carvalho describes as the *Escudo riograndense* or Rio Grande shield area. It is a typically granitic region with low rounded hills and V-shaped valleys. The humid climate and large seasonal temperature variation are conducive to relatively rapid decomposition and the decomposed zone of the rocks frequently extends to depths of 10 meters or more.

The auriferous formations are pegmatite veins or dikes with a considerable percentage of quartz, either in veins or in small masses. These veins or filões usually outcrop along the crests of the hills, sometimes along the flanks, and occasionally in the beds of the streams in the valleys. They vary in width from a few centimeters to sometimes more than a meter. Not only is there considerable variation between similar veins, but any given vein may also vary in thickness, composition and direction within a short distance.

Although the individual veins, or dikes, may branch out, converge, wind in a sinuous form, sometimes wide and sometimes narrow, and disappear only to appear again at some distance, when taken as a group they are fairly regular.

We find two systems of veins, one oriented approximately N.  $60^{\circ}$  W. and the other N.  $50^{\circ}$  E. These directions correspond with the lines of major fracturing in the granitic mass and the first system is more important than the latter in that generally it produces longer and wider veins.

Although the region is predominantly granitic, we also find indications of eruptive rocks such as andesites, trachy-andesites, and melaphyres with some volcanic breccia and tuffs. These rocks are sometimes metamorphosed and mineralized, generally with copper.

A short distance to the east of Lavras there is a zone in which the andesitic rocks predominate. Gold-bearing veins also occur in this region. They are principally quartz and are very small and irregular, although somewhat richer than the pegmatite veins of the granitic area.

The granite of the Lavras region is somewhat variable. It is porphyroidal with a considerable percentage of hornblende and a relatively low percentage of magnetite and ilmenite. Its grain size varies from medium to coarse and its color from pinkish gray to grayish pink.

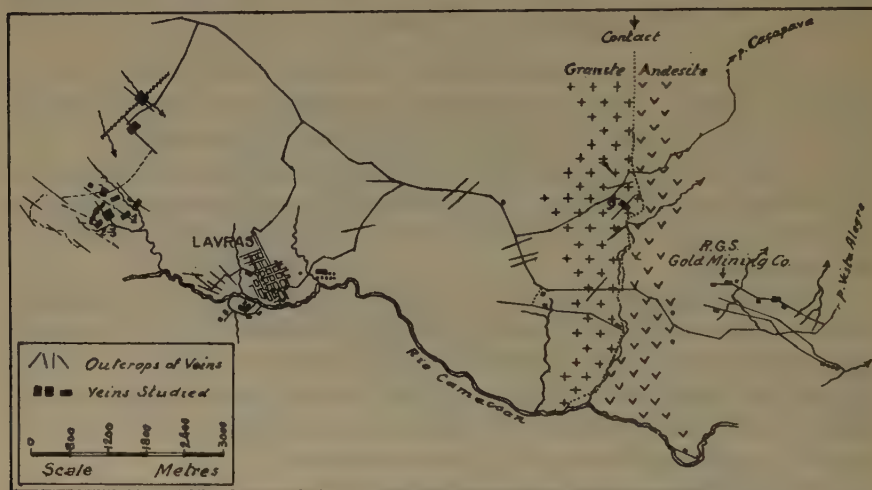


FIG. 2.—SKETCH OF LAVRAS AREA, SHOWING OUTCROPPING VEINS AND VEINS UNDER STUDY.

Small numbers indicate veins for which magnetic curves are given. The granite-andesite contact is shown and the roads along which magnetic profiles were made.

The pegmatite dikes or veins are very irregular, not only in composition and form but also in the amount of mineralization. The mineralization consists chiefly of pyrites deposited along the contacts between the pegmatite, the quartz, and the granite. Chalcopyrites and galena are also found but less commonly. The feldspar of the pegmatite frequently is altered to Pinguite and free gold is found usually in the decomposed parts of the veins in the form of tiny flakes.

Treatment of some tens of tons of selected ore by the engineers of the Geological Survey showed values ranging from 8 to 22 grams of free amalgamable gold per ton. Analysis of hand samples showed values equivalent to from 2 to 140 grams per ton. The average value of the vein rock is much less than that indicated by these figures. It is a low-grade ore, and profitable exploitation would depend on large-scale operations with low operating costs and maximum extracting efficiency.



A plant for such work would require the outlay of considerable capital, which would be justified only if the existence were known of sufficient ore to give a profitable return proportional to the risks.

The São Jeronymo company has begun a study of the area by means of galleries and trenches, which will enable them to take representative samples from a large number of the veins and the analysis of this material will give data for the calculation of the average value of the ore in sight.

The geophysical work that will be discussed here was intended to show whether the continuation of veins not visible on the surface could be traced without the necessity of trenching and tunneling.

#### APPLICATION OF GEOPHYSICAL METHODS

The physical differences between the country rock and the vein material were not sufficient to enable any geophysical method to give unquestionable results. The mineral content of the veins was too low and too disseminated for the application of electrical methods, and the low magnetite content of the granite was against the use of the magnetic method. However, since the application of the latter method represented only a small expenditure, it was decided to give it a trial.

The instruments used were the familiar Schmidt-Lloyd vertical magnetic field balance manufactured by Askania Werke of Berlin. The instrument was adjusted for a sensitivity of slightly less than 30 gammas per scale division and to read in the center of the scale for the normal vertical intensity of the area,  $-11,000\gamma$  approx. Careful tests at a base station showed that the zero reading did not change appreciably during the entire three months of field work, and repeated calibrations by means of a Helmholtz coil showed that the sensitivity remained constant during the entire period.

Stations were taken along straight lines perpendicular to the veins, at intervals of from 2.5 to 10 meters. A secondary base was established on every line and readings were repeated at this station every 15 to 25 min. After correction for temperature, the readings at this base station were plotted as a function of time and the resulting graph was used for the diurnal variation and base corrections. In general, two to three observations were taken between repetitions of the base, and since the instrument was never returned to the case during the day's work, the temperature gradient was more or less constant. Any important errors in the temperature correction were automatically eliminated in the base-station curve. Repetitions of various stations indicated that the results in general were accurate within experimental error; i. e., within 3 to 5 gammas.

Veins were selected on which excavational work was in progress and the first line always crossed a known portion of the vein. Later lines were run parallel in areas where there were no visible outcrops. The data

were interpreted and the results of subsequent excavations served for checking the interpretations.

An attempt was also made to use the method for the detection of unknown veins, but the complexity of the vein system and the variations in the granite made the interpretation of these data very doubtful.

### RESULTS OF INVESTIGATIONS

It is impossible to give here the results of all the observations made in this extended period, therefore we will restrict the description to a few

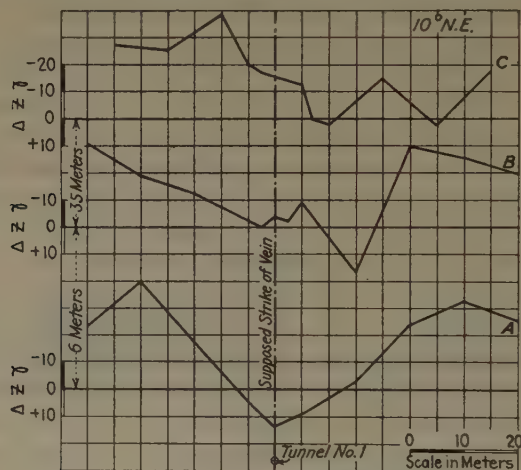


FIG. 3.—MAGNETIC PROFILES OVER VEIN 1.

Note effects of increased thickness of cover and division of main vein.

of the more characteristic veins. In general, the pegmatite veins gave negative anomalies; i. e., decrease in normal negative vertical intensity. Sometimes these anomalies were of moderate magnitudes but generally they were so small that they could be detected only by the most careful measurements.

#### *Vein No. 1*

Fig. 3 shows the magnetic profiles obtained over the vein designated as No. 1 by the São Jeronymo company. Line A was taken near the outcrop of the vein, which is moderately wide and shows a definite anomaly of some 50 gammas. The center of the anomaly is directly over the vein. Passing to line B, some distance away from the outcrop, we find that the anomaly is less regular and the minimum shifts slightly to the right. Passing to line C, at a still greater distance, we find that the minimum has now definitely divided into two and perhaps three minima, and the shift to the right of one of them is still more

pronounced. Subsequent excavations actually indicated that the vein curves to the right and later divides into two moderate sized veins, with possibly a third smaller one following the direction of the outcrop. This fact is entirely in accord with the magnetic data.

### Veins 2 and 3

Fig. 4 shows the results obtained over two approximately parallel veins. There is a small negative anomaly directly over vein 2, and a larger indefinite anomaly over No. 3. As we pass to line *B*, we find that the anomaly over No. 3 has shifted considerably to the left while that at No. 2 has apparently divided into two anomalies. In analyzing these data we suggested that other veins that did not outcrop might exist, and that vein 3 had been dislocated to the left. The large negative anomaly shown in dotted lines in *A* was purely local, as it disappeared in a repeated station at about 2 m. distance, slightly out of the line. Examination of the area and subsequent excavational work showed that vein 2 was really two veins close together while vein 3 was lost in the tunnel. By fol-

lowing a small stringer, it was found once more at a distance of some 8 to 10 m. to the left. The occurrence of a similar dislocation of vein 2 was also found, outside the point at which the gallery entered into the vein proper. Thus, although the data here are not so clear as in the other case, there is still a marked concordance between the magnetic data and actual subsurface conditions.

### Vein No. 6

In this locality there exists a thick pegmatite dike mineralized along its contacts. Several outcrops are found but they are quite irregular. Some ten magnetic profiles were determined in this area, of which the intensity curves are shown in Fig. 5. The curves are quite irregular and the writer was somewhat skeptical about their interpretation. However, the various anomalies were finally connected in the manner shown and were supposed to indicate a family of veins. In order to test the validity of this interpretation, an extension of the trenches was requested, with the

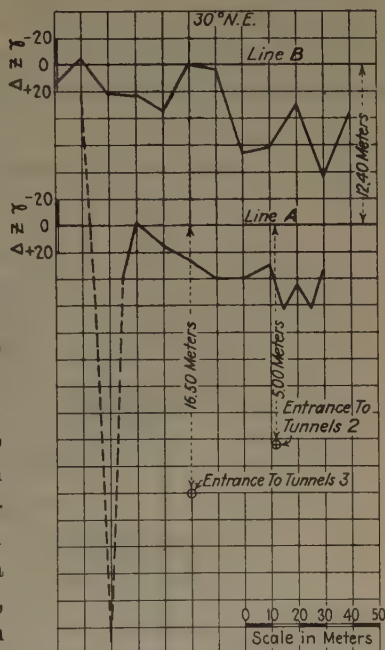


FIG. 4.—MAGNETIC PROFILES OVER VEINS 2 AND 3.

Note displacement of anomaly due to vein 3 on curve *B*.

results shown in Fig. 6. At least five decomposed remains of veins were found a short distance below the surface of the alluvium, and in the approximate positions that had been indicated by the magnetic data. The writer does not presume that these veins actually follow the lines indicated on the sketch, and it is quite probable that some of these anomalies represent merely changes in the composition of the granite or the thickness of the alluvium. The area also contains moderate amounts

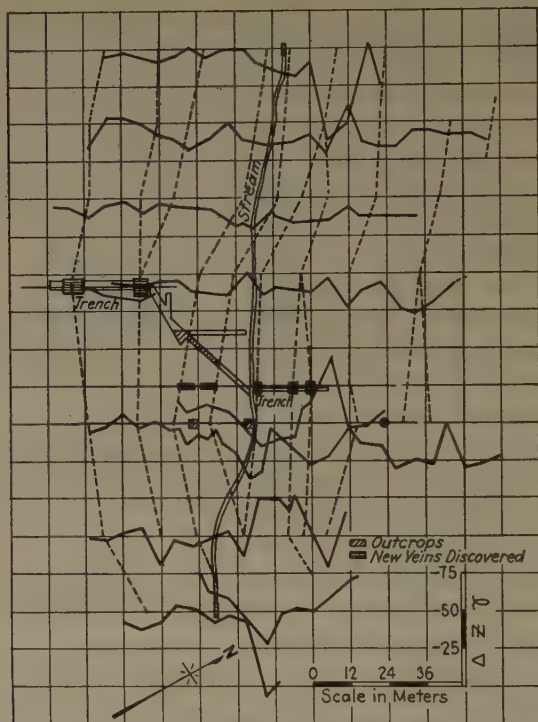


FIG. 5.—MAGNETIC PROFILES OVER VEIN 6.

Dotted lines represent correlation of anomalies. Hatched areas represent outcrops of veins and veins discovered by posterior excavations.

of placer gold and similar deposits of magnetic sands might influence the distribution of the magnetic intensity. However, the fact that several new veins were discovered on the basis of the magnetometric investigations indicates that the interpretation is not entirely in error.

### *The Dourado Extra*

This region is interesting because of the complex network of quartz veins rather than because of its gold-bearing quality. It is almost on the border of the andesite region but still within granite rocks. Several parallel profiles were observed, with the results shown in Fig. 7. The anomalies here are very irregular and small in magnitude. An attempt



was made to connect the trend of the anomalies as had been done in the last example, but it was unsuccessful. Apparently there is no relation

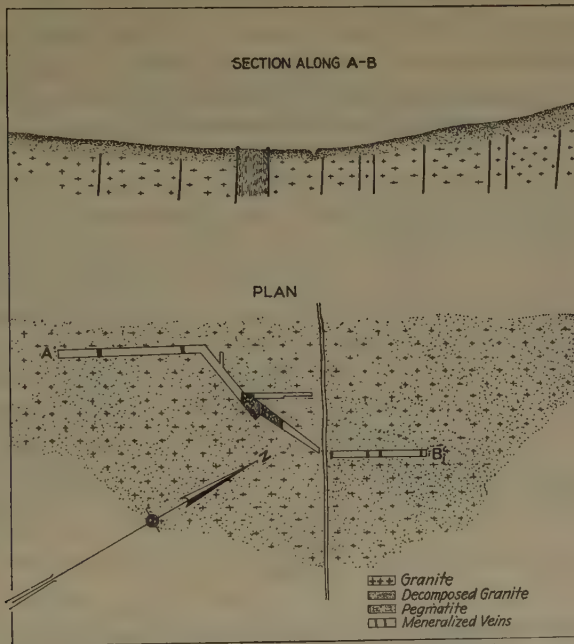


FIG. 6.—PLAN AND SECTION OF VEIN 6.

Veins discovered in trenching subsequent to magnetic survey are indicated.

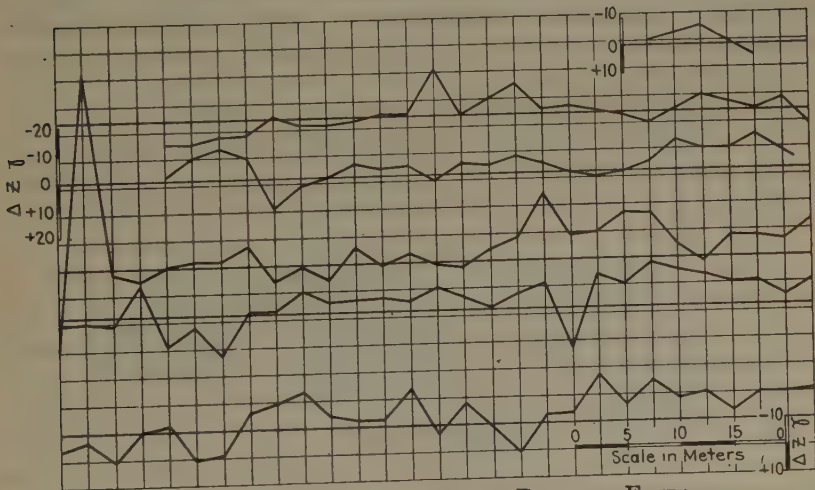


FIG. 7.—MAGNETIC PROFILE OVER DOURADO EXTRA.

between the anomalies and the quartz veins, nor should any be expected. It is more probable that these anomalies represent changes in the character of the granite and possibly lines of fractures.

*The Granite-andesite Contact*

It was not considered worth while to attempt to study the veins in the andesite region. Their great number and very small size made the method entirely inadequate, even had they possessed appreciable differences in their magnetic properties. However, an attempt was made to outline the contact between the andesite and granite rocks. Two lines

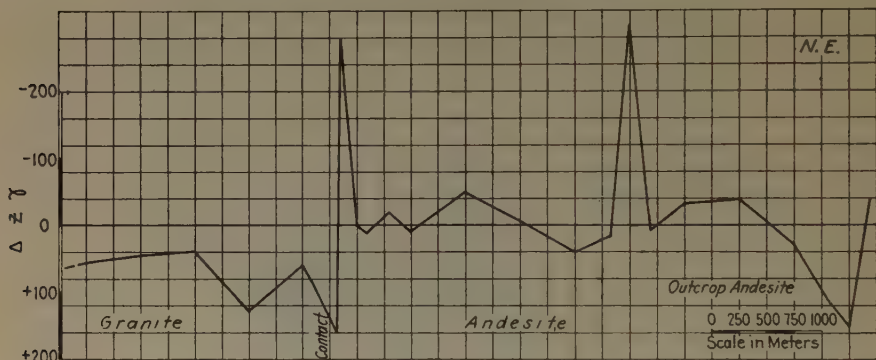


FIG. 8.—MAGNETIC PROFILE ALONG LAVRAS-ÇAÇAPAVA ROAD OVER GRANITE-ANDESITE CONTACT.

were run across the supposed position of the contact. Although certain samples of the andesite were pronouncedly magnetic, the anomalies obtained were not as large as was expected. On the road to Çaçapava, several large anomalies were obtained over outcrops of andesite, and the general level of the curve was somewhat higher in the andesite region.

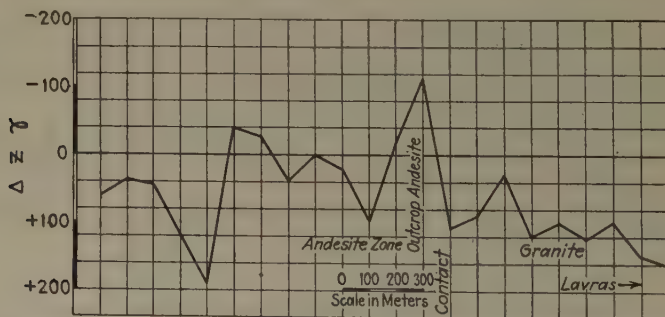


FIG. 9.—MAGNETIC PROFILE ALONG LAVRAS-VISTA ALEGRE ROAD OVER GRANITE-ANDESITE CONTACT.

On the other line along the road to Vista Alegre, similar although less pronounced differences were obtained. From these data we might presume that the andesite is fragmental and not a massive intrusion. The magnetic curves for these two lines are shown in Figs. 8 and 9.

## VALUE OF MAGNETIC METHOD

From the results obtained in this experimental investigation, we may draw the following conclusions:

1. The magnetic method cannot be used for reconnaissance work in the discovery of auriferous veins of this type.
2. When used as a detailed method for the study of the continuation of veins that disappear under alluvial covering, fair results may be expected.
3. The data obtained in such detailed work would be of exceptional value in directing the excavational work of prospecting, in that it would eliminate many useless trenches and galleries and indicate the more favorable locations for such excavations.
4. Although the method was not applicable for the quartz veins, nor in the andesite region, it can be used in the determination of the extent of such regions by tracing approximately the line of contact.
5. In similar regions in other parts of the world, it might give either better or worse results, but its trial is recommended.

## APPENDIX.—MAGNETIC OBSERVATIONS IN THE SÃO JERONYMO COAL MINE

Although the data to be presented in this appendix have nothing in common with the major part of this paper, we present them here because they may be of some interest, although hardly worthy of separate publication.

The São Jeronymo coal mine is some tens of kilometers to the west of the city of Porto Alegre. Although a small mine, it is of considerable importance and produces about 1200 metric tons of coal per day. The coal is of Permo-Carboniferous age and the coal measures lie at a depth of approximately 100 meters, with the granite crystalline basement at slightly greater depth. The beds have suffered intrusions of diabase, sometimes in the form of dikes but frequently in the form of larger masses, and the heat generated has altered the coal in some places to produce a valueless coke.

These intrusions are prejudicial to the operation of the mine. In the case of the dikes, there is added expense and loss in time in the extension of the galleries to the productive areas on the other side, while in the case of the larger intrusions, the coal has been completely destroyed and the galleries must be abandoned. This problem reached serious proportions a few years ago when shaft No. 3 had to be abandoned, being completely enclosed by diabasic rocks or burned out coke.

At the request of the officials of the company, the writer made a few measurements with the magnetometer in this area to determine whether the magnetic method was capable of predicting the presence of such intrusives and their probable extent. It is obvious that such data would

be very useful when it becomes necessary to extend the area under exploitation by the opening of new shafts and galleries.

The field procedure followed in these measurements was identical with that described for the Lavras areas, the only difference being that

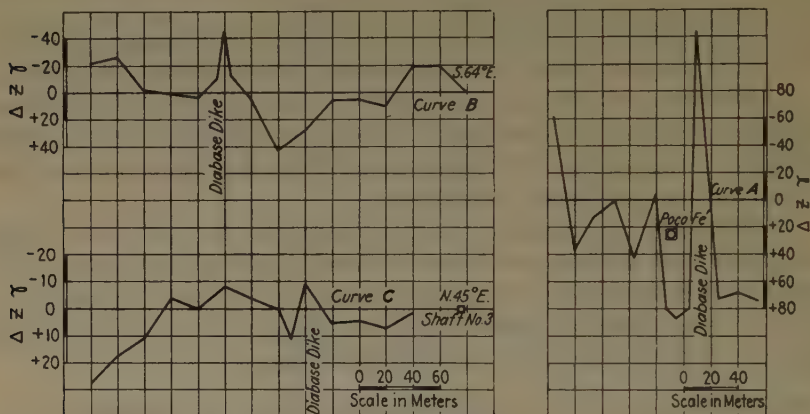


FIG. 10.—MAGNETIC PROFILES OVER DIABASE DIKES IN THE SÃO JERONYMO MINES.

here, the anomalies being somewhat larger, slightly greater station intervals were used. Magnetic profiles were taken over zones where diabase was known to exist as the result of underground workings or drilled tests and over areas where coke had been found to have replaced the coal. The results of these studies are represented by the characteristic graphs of Figs. 8 to 10.

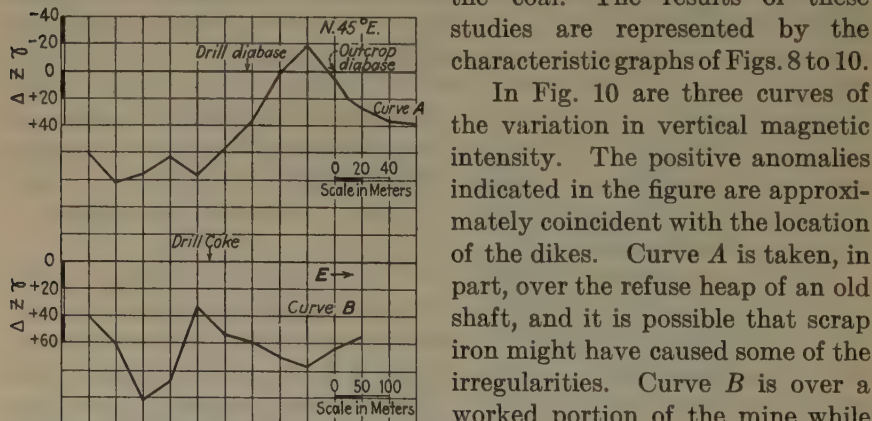


FIG. 11.—MAGNETIC ANOMALIES OVER BASIC INTRUSIONS IN THE SÃO JERONYMO MINES.

other intrusions exist to the left of the dike indicated.

In Fig. 11 are two profiles over the territory to the north of the abandoned mine No. 3. An outcrop of diabase occurs as indicated on curve A and a test drilled slightly to the left also entered diabase. In curve B



several drilled tests showed either diabase or coke, indicating the near presence of intrusive rocks.

Fig. 12 is an isogamic chart of an area bordering the abandoned mine of the east. The anomaly here indicates that the intrusion is massive; not a dike. It is probably of lacolithic form and the source of some of the dikes that completely enclosed mine 3 on this side. Work underground did not reach this intrusion, the mine having been abandoned in coke.

Results indicate that fairly definite anomalies are found, which may be correlated with the known igneous intrusions. We may suppose then that a careful detailed magnetic survey of the entire area of the mine would locate at least the more important of other igneous intrusions that might exist. If the magnetic data were carefully analyzed and placed on the map, it would greatly facilitate the location of new shafts so that a minimum of intrusive rocks would be found, and would aid in the orientation of galleries so that they might either avoid the intrusions or pass them at the most advantageous points.

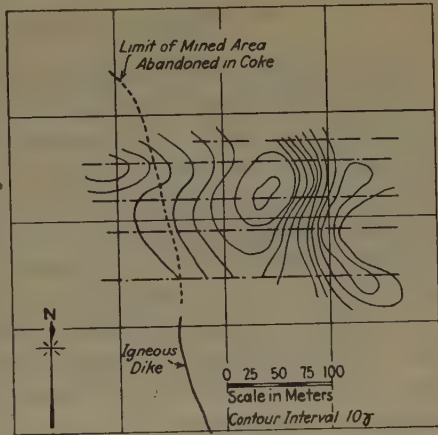


FIG. 12.—ISOGAMIC MAP OVER ONE BASIC INTRUSION, WHICH RESULTED IN PRODUCTION OF COKE IN EASTERN PART OF SHAFT MINE No. 3.

#### ACKNOWLEDGMENTS

The writer wishes to express his appreciation to Dr. Fleury da Rocha, Director of the Departamento de Produção Mineral, and to Dr. Djalma Guimarães, Director of the Diretoria de Minas, for their kind permission for the publication of these data. He wishes also to express his thanks to the Director of the Instituto Geologico e Mineralogico do Brasil, Dr. Euzebio P. de Oliveira, and the geologists of the same institution, Dr. Paulino F. de Carvalho and Dr. Nero Passos, for their kind cooperation. He is also indebted to the officials of the Companhia Estrada de Ferro e Minas São Jeronymo for many favors and for information relative to the progress of the excavational work and the characteristics of the rocks encountered.

During the field work, and the preparation of the original report, the author had the able assistance of Dr. Henrique A. Capper de Souza, Dr. Irnack C. de Amaral and Dr. Decio S. Oddone, all engineers of the Diretoria de Minas. These men actually made most of the observations and calculations and studied the detailed geology of the area and the petrographic character of the rocks.

# An Accurate Simplified Magnetometer Field Method

BY HUBERT O. DE BECK,\* BURNSVILLE, N. C.

THE following descriptions and explanations apply specifically to the use of the Hotchkiss Superdip, but there are no apparent reasons why they should not apply to any magnetometer. This paper is a product of work in the practical field for several years with the Hotchkiss magnetometer, mostly on mineral deposits in the southeastern United States. The paper describes the result of an attempt to develop a practical and economical field method that approaches, as nearly as possible, the utmost accuracy of which the magnetometer is capable.

As there are many published descriptions of various magnetometers and magnetic methods, it would be superfluous to describe such instruments here, but a limited bibliography on the Hotchkiss and Askania magnetometers is appended. The Hotchkiss and the vertical Askania magnetometers have, respectively, maximum sensitivities of approximately 5 and 30 gamma per instrument scale division.

## PURPOSE OF NEW METHOD

The purpose of the method described in the following paragraphs is to eliminate, as far as possible, all corrections of field data that cause complexities and inaccuracies in the results of magnetometer surveys. Magnetometer field observations must be corrected for periodic variations in the intensity of the earth's magnetic field, as well as for temperature variations, both of which take place during the course of a day. These variations do not seriously handicap magnetometer work on highly magnetic deposits, but it is impossible to obtain accurate results, by the conventional methods in use today, over weakly magnetic or diamagnetic deposits. This is due to the physical inability to obtain by such methods sufficiently accurate data in the field to make dependable corrections.

The magnitude of the necessary corrections of field observations frequently exceeds the magnitude of local magnetic anomalies obtained over various types of mineral deposits. Therefore if these corrections are neglected or made on the basis of inaccurate data, the entire magnetic picture of the area concerned is at least distorted, and perhaps destroyed altogether.

---

Manuscript received at the office of the Institute April 12, 1934.

\* Consulting Geological Engineer.

From a study of some of the work of others, as well as of previous work of my own, I believe that much of the magnetometer work to date has been somewhat inaccurate, owing to the fact that few operators seem to have realized the importance and magnitude of these factors. To estimate the amounts that such errors have cost various organizations would be a most difficult task.

#### BASIC PRINCIPLE OF METHOD

If two similar magnetometers, adjusted exactly alike, are properly set up within a short distance of each other (10 to 100 ft.) on terrain devoid of local magnetic anomalies, the readings will be, under normal conditions, identical and equal, when the instruments are read simultaneously. This is true because the terrestrial magnetic intensity and atmospheric temperature will not vary appreciably in such a short space interval at any given time; and so, at the same instant, will be of equal magnitude at the two instruments. Of course, the magnetometers should always be properly shaded. If the location is devoid of local anomalies, there are no other factors that might influence the action of the magnetometers.

If this operation of simultaneous reading is repeated after an elapsed time interval of 10 min. (or any other time interval), the readings will again be equal, but they may not be equal to the first set of observations, for both temperature and terrestrial intensity may vary with time. The amount of inequality between the two sets of readings is proportional, in some ratio, to the combined change in temperature and intensity, though, individually, these changes may be additive to or subtractive from each other.

If the space interval (at 25 ft. for illustrative purposes) between the two instruments is maintained, and the pair is advanced into a zone of local magnetic anomalies, again properly set up, and the operation of simultaneous reading repeated, a difference will be noted between the readings of the two instruments. This *difference* represents, in terms of scale divisions of the magnetometers, the difference in magnetic intensity between the two points of observation. This is true because the instruments are read simultaneously, and therefore the effects of atmospheric temperature and periodic terrestrial magnetic intensity variations are identical at the two points at the time of reading. Thus, these variables are reduced to corrective constants that are applicable to both readings, though the magnitude of these constants is unknown. However, if they are equal and apply to both readings, they may be neglected, regardless of what their magnitude may be.

Therefore, corrections for atmospheric temperature and periodic terrestrial magnetic intensity variations are entirely eliminated merely by using in unison two instruments of similar type and identical adjustment.



## FIELD METHOD

In attacking any field problem by this method, the first step is to decide upon a particular sensitivity and to adjust both instruments to it. Care must be taken to obtain identical settings on the magnetometers. (A description of proper setting up and adjustment of the Hotchkiss will be found in the third publication listed in the bibliography at the end of this paper.) The instruments are then properly set up a short distance from each other on normal terrain (devoid of local anomalies), and counter-weight variations are made until there are obtained at least three simultaneous readings that exactly check. This completes the preparation of the instruments for field observations.

The second step is to move both magnetometers to the first station or point of observation. They are set up here and readings again checked to insure proper adjustments. The average of the triplicate readings of one instrument subtracted from that of the other should equal zero. This, with the station location, is the first entry in the field notebook.

The third step is to move *one* magnetometer to the next station and set it up. Simultaneous readings of the instruments are again made in triplicate and entered in convenient manner in a suitable notebook. (See illustration of notebook sheet herewith.) The triplicate readings for each magnetometer are averaged, and that of the front instrument is subtracted from the average reading of the rear one, or vice versa, but the same relationship must be maintained. The difference, whether plus or minus in character, represents, in terms of instrument scale divisions at the particular sensitivity value used, the difference in magnetic intensity between the two points concerned.

The fourth step is to move the rear instrument ahead to the third station, where the above operation is repeated. The difference in readings thus obtained, whether plus or minus, is algebraically added to the last difference, and the total is carried along with station designations in the field notes. Thus the method of keeping notes is somewhat similar to that used in a precise level survey.

This system is then repeated, the rear instrument being moved ahead and the relationship of the two being reversed at each succeeding observation. At the end of each day's field work, the *total differences* are plotted against distance on suitable graph paper, and the points thus determined are connected to form a graphic magnetic picture of the area covered.

If the notes are completed in the field after each observation, the party chief is always in possession of up-to-date data and in complete control of the work. Thus, errors are discoverable at time of commitment and may be corrected immediately. Station intervals may be varied, without loss of time, when necessary to obtain complete data.



## NOTE BOOK SHEET

Date: June 1, 1933.Project: John Doe's Tract.Location: Rutherford County.Line No: 30 Sheet No: 32Hotchkiss Inst. Nos.: X and Y.Sigma: 1° 00'. Theta: 67° 15'Tau: 21° 45' Adjust. by: JCSRecorder: JCS

Station (feet)	Front Inst. (plus)	Rear Inst. (minus)	Difference (+) or (-)	Total Difference	Remarks (time)
+ 0	157 158 158 Tot. 3)473 Ave. 158	158 159 158 Tot. 3)475 Ave. 158	0	0	Clear Weather. Normal.  9:01 A.M.
+10	162 163 161 Tot. 3)486 Ave. 162	159 158 160 Tot. 3)477 Ave. 159	+ 3	+ 3	Normal ground. No clouds.  9:06 A.M.
+15	178 178 180 Tot. 3)536 Ave. 179	164 163 164 Tot. 3)491 Ave. 164	+15	+18	Hanging wall of quartz vein.  9:10 A.M.
+20	156 159 160 Tot. 3)475 Ave. 158	180 182 184 Tot. 3)546 Ave. 182	-24	- 6	Approx. foot wall of quartz.  9:18 A.M.
+25	167 166 165 Tot. 3)498 Ave. 166	162 160 160 Tot. 3)482 Ave. 161	+ 5	- 1	Normal ground. Clear.  9:24 A.M.
+30	172 173 174 Tot. 3)519 Ave. 173	171 172 173 Tot. 3)516 Ave. 172	+ 1	0	Normal ground. Clear.  9:31 A.M.
+40	176 177 178 Tot. 3)531 Ave. 177	175 176 176 Tot. 3)527 Ave. 176	+ 1	+ 1	No clouds in sight.  9:38 A.M.

Sigma is sensitivity angle used. Theta is the normal average inclination of the earth's magnetic lines of force. Tau is the angle between the counterweight arm and the magnetic bar of the instrument.

Note: The anomaly over the quartz vein caused a total variation of 24 Hotchkiss scale divisions. The combination of temperature and terrestrial intensity variations (other than that due to the quartz vein) caused a total difference of 18 Hotchkiss scale divisions in a time interval of 37 minutes. In single-instrument methods the latter difference would appreciably dampen the effect of the anomaly over the quartz vein and thus cause difficulties in interpreting the results.

## STATION AND STATION-LINE INTERVALS

The station interval used depends on the nature of the problem concerned. The stations are generally located by transit and chain methods along lines run at right angles to the average strike of the geologic feature

to be determined. The interval between station lines also depends on the nature of the project.

In the Ducktown copper district of Tennessee, station and station-line intervals of 25 and 200 ft., respectively, were used satisfactorily in the determination of large deposits of copper and iron sulfide. Station and station-line intervals of 10 and 50 ft., respectively, were successfully used in Rutherford County, North Carolina, in the location of small auriferous quartz veins averaging 12 in. in thickness. In the latter case, the intervals were reduced frequently in order to obtain complete data.

### FIELD PARTY

In this method of geomagnetic surveying, the field party is composed of one recorder-party chief, two instrument operators and two umbrella carriers. Of course it is essential to have a transit and chain party in addition to the magnetometer party, though the two are frequently combined so that the same personnel executes the duties of both parties.

The recorder-party chief times the readings and keeps the notebook up to date; the operators set up and read the instruments; the umbrella carriers keep the instruments properly shaded and assist in moving them from point to point.

The recorder-party chief should be a geologist who is familiar with the geology of the area concerned. The qualifications necessary for an operator are similar to the combination of those necessary for the operation of an analytical balance and for a precise level.

With a station interval of 25 ft. or less, a well trained field party of this kind can make, on average terrain, well over a hundred observations per eight hours. Such a party is capable of making as many observations as may be obtained in a given time by a one-instrument party over similar terrain, or more complete observations than the one-instrument party. The method described herein will cost no more than the single-instrument method, since one-third to one-half of the time of the single-instrument party is spent in obtaining data for terrestrial periodic variation determinations, and in making the necessary calculations to correct the notes obtained in the field; furthermore, a great amount of time is consumed in adjusting the instrument to each new location, which is unnecessary with the method just described. Regardless of what the difference in cost might be, it is actually a choice between an accurate reliable method and one that is always doubtful.

### MAGNITUDE OF TERRESTRIAL INTENSITY VARIATIONS

What is the nature and magnitude of terrestrial magnetic variations which so seriously handicap single-instrument methods of magnetometer surveying? For such information concerning specified locations, refer to publications of the United States Coast and Geodetic Survey on the

subject of terrestrial magnetic intensity variations. Results of continuous observations are published periodically by this bureau.

A study of any group of this bureau's daily charts on terrestrial magnetic intensity variations will show that the earth's magnetic field at any given location generally reaches a minimum intensity at or near 2 o'clock, a.m. When near this minimum, the magnitude of the intensity varies very nearly in accordance with some definite increment. Around 2 o'clock, p.m., this magnetic field usually reaches a maximum in magnitude of irregular variations, and in intensity.

If these periodic variations followed any particular increment for a time interval of even one hour, they would present little difficulty, but such a phenomenon seldom, if ever, happens. It is not unusual for variations of a magnitude of 0.1 to 2.0 per cent of the normal average intensity of the earth's magnetic field to take place in a time interval of 5 to 10 min., and I have frequently observed variations as high as 5.0 per cent in 10 min. to take place on a perfectly clear and apparently normal day.

The average sensitivity adjustment in the use of the Hotchkiss gives a value of approximately 0.04 per cent of the earth's normal average intensity per instrument scale division. Thus, a periodic intensity variation of 2.0 per cent would produce an instrument reading of 50 scale divisions above or below the normal reading. The magnitude of such an *apparent* anomaly is comparable to the magnitude of the *true* anomaly that characterized a chalcopyrite orebody in Swain County, North Carolina. The ambiguous results that may be obtained with single-instrument methods are, therefore, quite obvious.

#### ADVANTAGES AND CONCLUSIONS

The advantage of greatest importance in the use of this method is that it permits a much higher degree of accuracy and reliability than is obtainable by any other magnetometer method. It also permits the determination of anomalies of smaller magnitude than may be accomplished by any other means.

It is probable that no geophysical method will attain its maximum effectiveness and usefulness until it is reduced to a state that permits economical operation and is *completely controllable* by the average geologist. The very low cost of operation of this method hardly permits comparison with any other. Because of its extreme simplicity, the total absence of mathematical calculations and other complexities, any geologist who is capable of using a transit and analytical balance (or similar instruments) can efficiently accomplish geomagnetic surveys by this means. At most, he would not require a great deal of instruction or demonstration.

The versatility of any geophysical method is largely dependent upon its degree of control, which is the accuracy with which irrelevant factors can be determined and corrections made for them. The method described herein permits almost absolute control, and is adaptable, therefore, to the solution of any geophysical problem that may be solved by geomagnetic methods. Thus, this method greatly broadens the scope of magnetometer surveying.

### SUMMARY

In this paper, there has been described a method of geomagnetic surveying which involves the simultaneous use of two magnetometers, instead of the usual one. This is done to eliminate correction factors that are difficult to ascertain, and thereby to obtain more reliable results.

The basic principle of the method is: If two like magnetometers are adjusted identically and set up reasonably near each other, they will be subject to the same atmospheric temperature and periodic terrestrial magnetic intensity variations at any given time. If the instruments are read simultaneously, corrections for these variations are eliminated. Therefore, any difference between the two readings represents the difference in magnetic intensity between the two points, in terms of instrument scale divisions at the particular sensitivity adjustment used.

This method not only broadens the use of the magnetometer, but may also increase the number of users. It permits accurate determinations of weakly magnetic as well as strongly magnetic mineral deposits and of other geological features. Also, owing to the complete elimination of mathematics and other complexities, it permits the average geologist to execute accurate surveys of this character.

This method was created and developed in the field with the Hotchkiss Superdip, therefore special emphasis has been placed on the field methods of the Hotchkiss. Though the practical field was the only laboratory used, I believe the method will endure any theoretical tests to which it may be submitted. The satisfactory results obtained are a matter of record, which no amount of theory can displace.

### ACKNOWLEDGMENTS

I am greatly indebted to the Ducktown Chemical and Iron Co., Isabella, Tenn., for affording an opportunity for the study of geomagnetic methods during the years 1930 and 1931. I wish to thank Mr. T. A. Cox, Jr., and Mr. B. B. Bible, former fellow staff members of that company, for their cooperation and able assistance while we were all connected with the company, as well as for that of recent date. Mr. Cox and Mr. Bible, who are civil engineers, are now engaged in engineering work for the United States Forestry Service and the Tennessee Valley Authority, respectively.



## SELECTED BIBLIOGRAPHY

- N. H. Stearn: A Background for the Application of Geomagnetism to Exploration. *Trans. A.I.M.E.* (1929) **81**, 315.
- N. H. Stearn: The Hotchkiss Superdip: A New Magnetometer. *Bull. Amer. Petr. Geol.* (1929) **13**, No. 6.
- N. H. Stearn: Practical Geomagnetic Exploration with the Hotchkiss Superdip. *Trans. A.I.M.E.* (1932) **97**, 169.
- C. A. Heiland: Construction, Theory, and Application of Magnetic Field Balances. *Bull. Amer. Assn. Petr. Geol.* (1926).
- L. Spraragen: Use of Magnetometer in Oil Fields. (Instrument described and information given regarding manner of taking and making corrections.) *Oil & Gas Jnl.* (Sept. 27, 1928) **27**, No. 9, 38.
- C. A. Heiland: Theory of Adolf Schmidt's Horizontal Field Balance. *Trans. A.I.M.E.* (1929) **81**, 261.

# Theory and Experiments Concerning a New Compensated Magnetometer System

BY C. A. HEILAND,\* GOLDEN, COLO. AND W. E. PUGH,† DENVER, COLO.

(New York Meeting, February, 1932)

## A. INTRODUCTION

(C. A. HEILAND)

### I. PRINCIPLES OF TEMPERATURE COMPENSATION IN MAGNETIC INSTRUMENTS

The principle underlying the majority of magnetic intensity variometers is a comparison of the force to be measured with another force of known magnitude. The known force may be (*a*) of a magnetic nature, such as magnetic fields produced by magnets or coils, or (*b*) of a mechanical nature, such as (1) the elastic forces of wires, or (2) the force of gravity, such as employed in bifilar magnetometers and magnetic balances.

In instruments of such type, usually a magnetic system is employed, free to move about either a horizontal or vertical axis, on some sort of a suspension. If the earth's magnetic field alone were present, such a system would adjust itself into the direction of the field or that of its components. Owing to the simultaneous action of the comparison force, however, the magnetic needle assumes a position that differs from the direction of the magnetic force; for all such instruments, the angle of deflection  $\varphi$  is given by  $\tan \varphi = F/X$ , where  $F$  is the known and  $X$  the unknown earth magnetic force component. In other words, the magnetic system merely serves as an "indicator" for the position of balance of the two forces.

Considering the matter from this point of view, it is not immediately obvious why the temperature of such a magnetic system should modify the results.

In magnetic instruments, we may distinguish two different effects of temperature: (1) a magnetic effect and (2) a mechanical effect. The first is due to the fact that the magnetic moment of a magnet drops with an increase in temperature. This drop is characterized by the temperature coefficient of the magnetic moment  $\mu$  (see equation 1). The second effect is due to the change in the torsion of suspension wires with temperature or to the expansion of lever arms of masses acting on magnetic balances.

---

\*Professor of Geophysics, Colorado School of Mines.

†Geophysicist, Plains Exploration Co.

As said before, it is not evident at first sight why a magnetic system that merely serves as an indicator of the balance between two magnetic forces (types under group *a*) should be influenced by temperature. For, if the temperature coefficient of its magnetic moment is  $\mu$  the apparent change of the one force with temperature  $\theta$  would be  $\frac{dF}{d\theta} = -F\mu$ , and the change of the other force would be  $\frac{dX}{d\theta} = -X\mu$ . Therefore,  $\mu$  would cancel in the result.

The only reason there is a temperature effect on such type of magnetometer is that the known force  $F$  frequently depends on the temperature. If this force  $F$  is, for instance, produced by a magnet of known strength, the temperature coefficient of it enters into the results. However, this can largely be eliminated by using coils instead of magnets. Then the only temperature effect left in such instruments is that due to the suspension, if a wire is used, and this effect can be made so small that it is negligible.

Therefore, we find that in the type of intensity magnetometers that are based on a comparison of two magnetic forces, the conditions are most favorable for an *elimination* of temperature effects.

Matters are totally different for magnetometers which are based on a comparison of magnetic with mechanical forces. It is readily seen why the temperature influences such magnetometers considerably. For,  $\mu$  affects only the unknown earth magnetic force, but not the mechanical comparison force; therefore, the temperature coefficient of the "indicator" does not cancel out. In addition, the "mechanical" effect of the temperature now enters, affecting the mechanical comparison force. It is obvious that in such type (*b*) magnetometers it is difficult to *eliminate* the temperature effect. Only by making the "mechanical" temperature effects opposite in sign as compared with the magnetic effects is it possible to *compensate* the magnetic system for temperature.

This paper will deal only with methods for compensating, not for avoiding, the temperature effects.

### 1. Principles of Temperature Compensation in Magnetometers in General

As stated before, a temperature compensation may be accomplished by balancing the mechanical effects of the temperature against the magnetic effects.

Frequently, however, the mechanical effects are not great enough to balance the magnetic effects. One way to overcome this handicap is to reduce the magnetic effect, by making  $\mu$  as small as possible. This is done by using magnets of comparatively great magnetic moment (as  $\mu$  is inversely proportional to the magnetic moment of a magnet), and by employing steels that have small  $\mu$ 's. Another way to reduce the

magnetic effects of temperature would be to employ a coil instead of a magnet.<sup>1</sup> However, this would amount to an elimination of the temperature rather than compensation, and the object of this paper is not to deal with such methods.

Even though magnets of good grade of steel and great magnetic moments may be selected, the reduction of the magnetic temperature effect by such means is usually not sufficient. Then an additional compensation is required.

This compensation may be accomplished (1) magnetically or (2) mechanically. That is to say, either the magnetic temperature coefficient is decreased by another opposing magnetic temperature effect, or the existing mechanical temperature coefficient is increased by an additional mechanical effect. There follows a list of magnetic and mechanical temperature compensations which have been suggested and applied.

*a. Magnetic Temperature Compensation.*—A stationary auxiliary magnet is so placed near the moving magnetic system that its north pole faces the north pole of the system (corresponding to an apparent decrease in intensity). With an increase in temperature of the deflector, the repulsion is lessened, resulting in an apparent increase in intensity, which may be balanced against the apparent drop in intensity due to the drop of the moment of the needle.<sup>2</sup>

*b. Mechanical Temperature Compensation.*

1. On wire suspensions.

(a) The temperature changes the torsion of twisted wire.

(b) The temperature acts on a U-shaped frame to which the suspension is fastened.

2. On the optical system.

A bracket holding the scale expands so with temperature as to offset the decrease of the reading.

3. On a liquid in which the magnetic system floats.

An increase in temperature so changes the center of buoyancy as to offset the magnetic temperature effect.<sup>3</sup>

4. On the center of gravity of a magnetic balance.<sup>4</sup>

<sup>1</sup> R. Bock: Theorie einer neuen galvanischen Waage. *Ztsch. Geophysik* (1930) 6, (4/7), 251-253.

<sup>2</sup> H. E. McComb and A. K. Ludy: Temperature Compensation and Adjustment of Magnetic Variometers. *Terr. Mag.* (March, 1930) 32.

G. Hartnell: An Intensity-variometer Corrected for Temperature. *Terr. Mag.* (Sept., 1925) 117-124.

<sup>3</sup> H. Andreessen: Dissertation, Kiel, 1905.

<sup>4</sup> C. A. Heiland und P. Duckert: Beschreibung, Theorie und Anwendung einer Neukonstruktion von Ad. Schmidt's Feldwage. *Ztsch. angew. Geophysik* (1924) I, (10), 289-315, 321-329.

C. A. Heiland: Theory of Ad. Schmidt's Horizontal Field Balance. *Trans. A. I. M. E.* (1929) 81, 290.



The metals are so arranged in the system that those with the greater expansion coefficient are on the north side, so as to displace the center of gravity toward that side as the temperature rises. This is done either by moving the steel blades to the south side of the system, or by providing spindles of suitable metals on the sides of the system.

## 2. Temperature Compensation in Vertical Intensity Magnetometers

In vertical intensity magnetometers, most of the compensation methods described before have been used at one time or another. The author has used the magnetic compensation occasionally on stationary instruments (see Fig. 1*a*). The temperature compensation on the suspension has been used by Angenheister<sup>5</sup> in his tungsten wire balance. Andreesen (see above) applied torsion and liquid compensation to his recording vertical balance. The methods most extensively used (see Fig. 1, *b* and *c*) are the shifting of the blades and, in the new Askania system, the attachment of suitable expansion spindles. The method applied by Haalck<sup>6</sup> in his universal balance, to fasten the steel blades on only one side of the magnetic system, is, in its effect, identical with the methods described above.

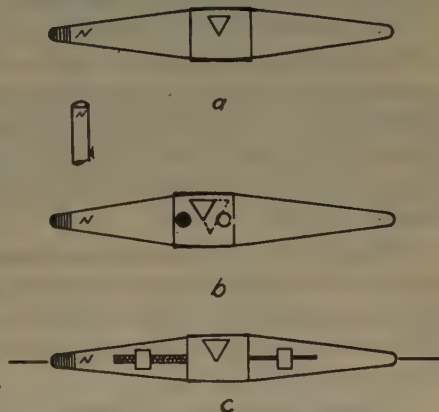


FIG. 1.—TEMPERATURE COMPENSATION IN VERTICAL MAGNETOMETERS.

*a*, Magnetic compensation; *b*, mechanical compensation by shifting blades; *c*, mechanical compensation by spindles.

## II. HISTORICAL REVIEW OF TEMPERATURE COMPENSATION IN VERTICAL INTENSITY BALANCES

Probably the first to apply a mechanical temperature compensation to vertical balances was H. Wild,<sup>7</sup> who used an arrangement very similar to that in the new magnetic system. Fig. 2 gives an approximate idea of his magnetic system, which was tubular in form.

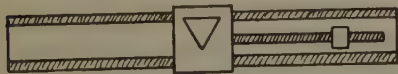


FIG. 2.—WILD'S MAGNETIC SYSTEM (DRAWN FROM MEMORY).

Up to about 1920, most of the vertical intensity balances in use were observatory instruments. The recording rooms were kept at a fairly constant temperature; hence

<sup>5</sup> G. Angenheister: *Magnetische Wage mit Fadenaufhängung. Ztsch. Geophysik* (1926) II, (1), 43-44.

<sup>6</sup> H. Haalck: *Die magnetischen Verfahren der angewandten Geophysik*, 72. Berlin, 1927. Gebr. Borntraeger.

<sup>7</sup> H. Wild: *Repertorium fuer Metereologie* (1883) 8. No. 7. (St. Petersburg.)

the need for an accurate compensation was not great. Instruments of the spindle type had been made by the Schultze and Toepfer companies of Potsdam, but the chief purpose of the spindle was latitude adjustment and not temperature compensation.

### 1. *Compensation of Magnetic Systems in Old Type Schmidt Balances*

The development of the Schmidt balance had been started by Toepfer, and was continued, largely with his assistance, by the Askania-Werke. While in charge of the latter's geophysical work, the writer has made extensive studies of various methods of temperature compensation.

Spindles of various materials (zinc, rubber, etc.) were tried. The results proved conclusively that an adequate compensation could be obtained by the use of such spindles,<sup>8</sup> but the method of shifting the steel blades continued in favor because it was considered undesirable to add any masses to the system which might be displaced during transportation and also because the compensation by shifting the blades seemed to give satisfactory results.

To get a more complete mechanical compensation and at the same time counteract the change in latitude adjustment caused by shifting the blades to the south, often a hole was drilled in the south side of the aluminum cube and a corresponding hole on the north side was filled with German silver (Fig. 1b).

During the period of extensive field operation of the magnetometers, from 1926 to 1930, occasional complaints were received about abrupt changes in temperature coefficients. It was concluded that such changes were due to differential tensions set up between the aluminum cube and the magnets, screwed tightly to it. Therefore it was decided to replace the aluminum cube by the same material of which the magnets are made.

### 2. *Compensation in New Magnetic System*

The aluminum cube has been replaced by a light steel frame, as the older experiments had shown that the system was somewhat too heavy in comparison with the masses used on the spindles. The tungsten steel magnets have been replaced by cobalt steel of greater magnetic moment and smaller temperature reaction, resulting in a decrease of  $\mu$  (see above).

To overcome objections from the standpoint of stability of readings in transportation, the spindles are screwed tightly to the steel frame and held firmly in position by set screws. In addition, the bronze nuts on the spindles are slotted, and screwed together by two small set screws each.

---

<sup>8</sup> The following figures may serve to illustrate variation of temperature coefficients (horizontal field balance) with spindle material: Normal magnetic system, +8.8; zinc spindle added, with small brass nut, +7.8; zinc spindle, with large brass nut, +5.7; rubber spindle, with medium weight, +4.2; rubber spindle, with larger weight, +2.2  $\gamma$ .

Fig. 3 shows the new magnetic system. A diagrammatic sketch of it is shown in Fig. 6. Hardly anything more need be added to the description given above except that the "temperature spindle" in the north is made of aluminum and the "latitude spindle" in the south is of invar steel.

This new magnetic system was developed during 1930 by the Askania-Werke in Berlin. The first tests made with the system showed that, in its temperature behavior, it was much superior to the old type system (Fig. 4).



FIG. 3.—NEW ASKANIA VERTICAL MAGNETOMETER SYSTEM.

In the summer of 1931, the Askania-Werke asked the writer to give this magnetic system a thorough test. Several months were devoted to this work, and the results obtained thus far are given herewith. The magnetic laboratory of the Colorado School of Mines was used for the

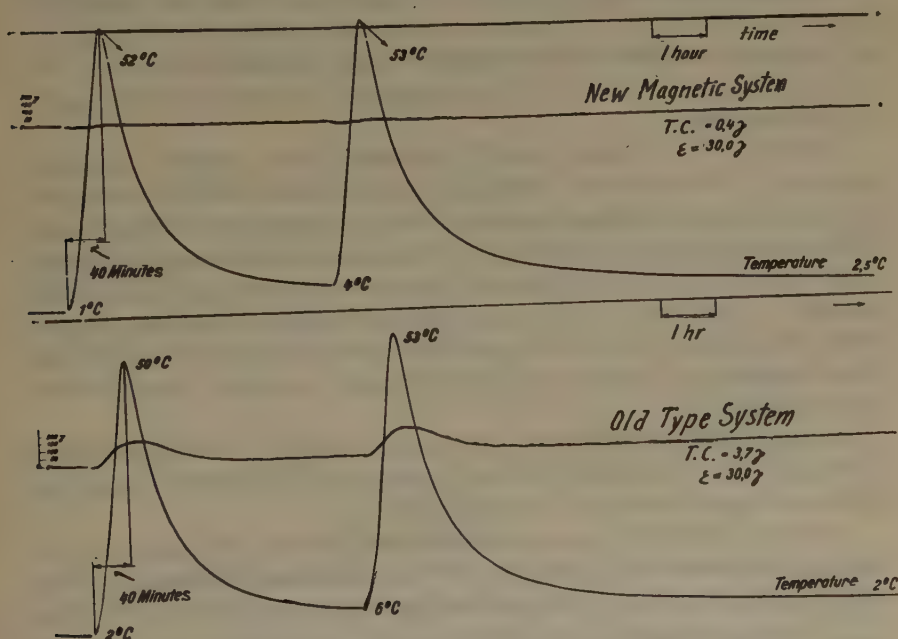


FIG. 4.—COMPARISON OF RECORDS OBTAINED WITH OLD AND NEW TYPES OF MAGNETIC SYSTEM. (Courtesy Askania-Werke.)

temperature registrations, which are described in the latter part of this paper.

The experimental results naturally gave rise to a thorough revision and perfection of the theory of similarly compensated magnetic systems. It may be mentioned that the theory and experimental results are in much

better agreement than was expected. *The deviations from the mean of observed and theoretical values were seldom greater than  $\pm 0.3$  gammas, which may be considered at least within the average error of temperature coefficient determinations.*

In concluding this introductory chapter, the writer wishes to express his thanks to the American Askania Corporation for placing the magnetic system at his disposal and for making this interesting investigation possible.

## B. THEORY OF TEMPERATURE COMPENSATION IN THE NEW MAGNETIC SYSTEM

(C. A. HEILAND)

An effort has been made to derive this theory in the most simple and usable, yet accurate form. The very close agreement between theory and experiment shows that, despite the extremely simple final equations no essential factors have been neglected.

The fundamental equations for the temperature effect are, naturally, composed of two parts. The first expresses the influence of the drop of the magnetic moment of the system as the temperature rises. The second expresses the effect of the expansion of the metals in the system upon the reading.

Therefore, it seems advisable to discuss the magnetic influence separately. That is to say, the equations will be given first for a magnetic system of which the temperature coefficient is due solely to the influence of the temperature upon its magnetic moment, and in which the metals are so disposed or are of such nature that their expansion is of no material influence. After that (in II), the combined magnetic and mechanical effects of the temperature will be considered, with special reference to such an arrangement of metals as to produce zero or nearly zero temperature coefficients.

In the next three chapters of this theory (in III, IV and V) the effect of changes of (1) latitude, (2) scale value and (3) deflection upon the temperature coefficient will be considered.

It should be noted that all equations refer to the temperature *coefficient* (abbreviation, T.C.), and not to the temperature *correction*. The temperature correction is the *negative* temperature coefficient.

## I. MAGNETIC EFFECT OF TEMPERATURE

This influence will be considered separately for scale value and reading, as these two effects are of totally different magnitude.

The magnetic effect of temperature is due to the fact that the magnetic moment of the system decreases with an increase in temperature as expressed by the equation

$$M_{\theta} = M_{20}(1 - \mu\theta) \quad [1]$$



$M_\theta$  is the magnetic moment at the temperature  $\theta = t - 20^\circ \text{C.}$ ,  $M_{20}$  the moment at  $20^\circ \text{C.}$ ;  $\theta$  is the temperature in centigrades above  $20^\circ \text{C.}$  and  $\mu$  is the temperature coefficient of the magnetic moment.  $\mu$  is positive if the equation is written as above.

$\mu$  varies considerably for various types of steel. It is smaller for cobalt than for tungsten steel.  $\mu$  varies, in addition, with the magnetic moment. It is smaller for a stronger, greater for a weaker magnet.  $\mu$  is essentially a constant for varying temperatures.

For the old type of magnetic system,  $\mu$  varied between 30 and  $50 \times 10^{-5}$ . For the new system, it was determined experimentally (see section C-I-6) and found to be  $13.8 \times 10^{-5}$ .

In the theory given below, the symbol  $\gamma$  will be used always for the  $10^{-5}$  unit even if this mode of designation may not be quite correct from the physical standpoint (*e. g.*, the expansion coefficient of aluminum will be stated as  $2.3\gamma$ ).

$M_{20}$  of the magnetic system was determined by means of a deflection experiment on a magnetometer. It was found to be 1225 C.G.S.

### 1. Magnetic Temperature Effect on Scale Value

At normal temperature, the scale value is

$$\epsilon_{20} = \frac{mgd}{2fM_{20}} \quad [2]$$

where  $m$  is the mass of the magnetic system,  $g$  the gravity,  $d$  the vertical distance of the center of gravity from the axis of revolution,  $f$  the focal length of the objective lens (in scale divisions,  $2f = 1333$ ).<sup>9</sup>

Then the scale value at the temperature  $\theta$

$$\epsilon_\theta = \frac{mgd}{2fM(1 - \mu\theta)}$$

and therefore  $\epsilon_\theta = \frac{\epsilon_{20}}{1 - \mu\theta}$  or, the temperature coefficient of the scale value,

$$\frac{\epsilon_\theta - \epsilon_{20}}{\theta} = \mu\epsilon_{20} \quad [3]$$

The temperature coefficient of the scale value, for a noncompensated system, is positive (increase of scale value, or loss of sensitivity, with an increase in temperature). The temperature coefficient is proportional to the scale value.

The T.C. of the scale value is small; for  $\epsilon = 30\gamma$ , it is only  $0.004\gamma$ . From this it is obvious that a compensation for the magnetic effect of temperature on the scale value, *i. e.*, in the vertical direction, is not required.

<sup>9</sup> See Theory of Vertical Balance in second reference of footnote 4.

## 2. Magnetic Effect of Temperature on the Reading

This effect is much larger than that on the scale value. For the reading at normal temperature  $S_{20}$  ( $S_{20}$  equals the actual reading or  $S'$  minus 20, the center reading)

$$S_{20} = \frac{2f(M_{20}Z - mga)}{mgd} \quad [4]$$

where  $Z$  is the vertical intensity corresponding to the reading  $S'$ , and  $a$  is the horizontal distance of the center of gravity from the axis of revolution.

Then the reading at a temperature  $\theta$ , provided the magnetic effect only of the temperature is considered, would be

$$S_{\theta} = \frac{2f\{M_{20}Z(1 - \mu\theta) - mga\}}{mgd} \quad [5]$$

After subtracting 4 from 5, and substituting the value for  $\epsilon$  from equation 2, the temperature coefficient (T.C.) of the reading, expressed in gammas, is

$$\text{T.C.} = \frac{\epsilon(S_{\theta} - S_{20})}{\theta} = -\mu Z \quad [6]$$

This is an important equation, which states:

1. That for an uncompensated system, the temperature coefficient is negative (which is in accordance with observations); in other words, that a reading at higher temperature is smaller than a reading at lower temperature;

2. That the temperature coefficient changes with the magnetic vertical intensity (with magnetic latitude);

3. That the T.C. for an uncompensated system is very large; from equation 6, with the value given for  $\mu$  before, we have for Golden latitude ( $Z = 0.531_{1931}$ ) T.C. =  $-7.3\gamma$ .

This last value may seem small in view of much larger coefficients frequently encountered by magnetometer observers. It must be borne in mind, however, that it is computed for the new system, which has a large magnetic moment and a small  $\mu$ . For an old type system, the magnetic moment of which is about three-fourths that of the new, and which on account of tungsten steel being more frequently used than cobalt steel, has a  $\mu$  of nearly  $50\gamma$ , the T.C. for the uncompensated system would be: T.C. (old type, uncomp.) =  $-25\gamma$ .

## II. COMBINED MECHANICAL AND MAGNETIC EFFECT OF TEMPERATURE

In extending the theory for the combined effect, the expansion of the metals in the magnetic system with rise in temperature must be considered.

In writing the equation for the mass displacements with temperature, advantage is taken of the fact that the displacement of any number of masses in any direction may be represented by the resultant displacement of the resultant center of gravity lever.

From Fig. 5 it is readily seen that, if two masses  $m_1$  and  $m_2$  are attached by a lever of the same expansion coefficient to the frame of a magnetic system, they move in opposite directions when the metals expand; however, this may be represented by the simple relation  $a_g = a_{20}(1 + \gamma\theta)$  if  $\gamma$  is the expansion coefficient of the metal under consideration.

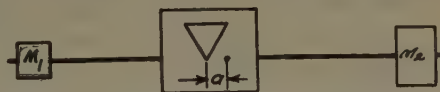


FIG. 5.—ARRANGEMENT OF MASSES IN A MAGNETIC SYSTEM.

If the masses are attached to lever arms made of metals with different expansion coefficients, another coefficient must be substituted in the terms just given, which is a more or less complex function of the masses, lever arms and expansion coefficients involved.

Designating such coefficients by  $p$  for the horizontal expansion and by  $q$  for the vertical expansion, we may write

$$\begin{aligned} a_g &= a_{20}(1 + p\theta) \text{ and} \\ d_g &= d_{20}(1 + q\theta) \end{aligned} \quad [7]$$

In the equations which follow, the influence of fixed masses has been considered separately from the influence of masses that may be moved by the observer (scale-value screw, latitude screw, temperature screw, latitude and temperature spindles).

### 1. Combined Mechanical and Magnetic Effect of Temperature on the Scale Value

If  $m_d$  is the mass of the magnetic system minus the mass of the scale value adjustment screw,  $m_v$ ;  $y_v$  is the distance of the center of gravity of this screw from the axis of rotation and  $y_d$  is the vertical distance of the center of gravity of the system from the axis of rotation after the scale value adjustment screw is taken out, we can write

$$d = \frac{m_d \cdot y_d + m_v \cdot y_v}{m_d + m_v} \quad [8]$$

where  $d = \frac{2fM}{mg} \cdot \epsilon$  and follows from equation 2 for any scale value. Only  $y_d$  is unknown and is obtained directly from equation 8, as all other quantities are given.

The influence of the temperature on the scale value may then be written

$$\epsilon_{20} = \frac{g(m_d \cdot y_d + m_v \cdot y_v)}{2fM} \quad [9a]$$

$$\epsilon_{\theta} = \frac{g \cdot m_d \cdot y_d(1 + \gamma\theta) + gm_o \cdot y_o(1 + \gamma\theta)}{2fM(1 - \mu\theta)} \quad [9b]$$

where  $\gamma$  is the expansion coefficient of steel. Subtracting 9a from 9b, and neglecting, in the denominator,  $\mu$  as compared with  $1/\theta$ , we have for the temperature coefficient of the scale value,

$$\frac{\epsilon_{\theta} - \epsilon_{20}}{\theta} = (\gamma + \mu)\epsilon_{20} \quad [10]$$

In other words, the temperature coefficient of the scale value, considering the expansion of the metals, is greater than the purely magnetic temperature coefficient of the same. However, as  $\gamma$  is only about one-tenth of  $\mu$ , it follows that what was said before about the temperature coefficient of the scale value still holds—the temperature coefficient of the scale value is negligible.

In reference to equation 9b it may be added that the numerator may be expressed by the equation 7, or

$$mgd_{\theta} = mgd_{20}(1 + q\theta) = mgd_{20}(1 + \gamma\theta),$$

from which it follows that  $q$  is equal to  $\gamma$ , the expansion coefficient of steel.

## 2. Combined Mechanical and Magnetic Effect of Temperature on the Reading

For the reading at standard temperature,

$$S_{20} = \frac{2f(M_{20}Z - mga_{20})}{mgd_{20}} \quad [11]$$

Substituting the values for  $a_{20}$  and  $d_{20}$  from equation 7, we have the reading at the temperature  $\theta$

$$S_{\theta} = \frac{2f\{MZ(1 - \mu\theta) - mga(1 + p\theta)\}}{mgd(1 + q\theta)} \quad [12]$$

Subtracting [11] from [12], dividing by  $\theta$  and neglecting  $q$  as compared with  $1/\theta$ ,

$$\frac{S_{\theta} - S_{20}}{\theta} = \frac{-2f}{mgd} \{MZ(\mu + q) - mga(q - p)\} \quad [13]$$

which may be written, since  $\frac{2fM}{mgd} = \frac{1}{\epsilon}$

$$\text{T.C.} = \frac{\epsilon(S_{\theta} - S_{20})}{\theta} = \frac{mga}{M}(q - p) - Z(\mu + q) \quad [14]$$

In words: if the temperature coefficient is expressed in gammas, it is independent of the scale value of the instrument.



This is true provided a change in scale value does not change the horizontal distance  $a$  of the center of gravity from the axis of rotation; i. e., provided the threaded hole for the scale-value screw is exactly at right angles to the magnetic axis of the system. This factor will be discussed in section B-IV.

Equation 14 immediately suggests two possibilities for constructing a magnetic system, which is compensated for temperature:

(1) To make  $\mu = -q$  and  $p = q$ ; that is to say, the arrangement of the metals in both the horizontal and vertical direction should be so made as to conform to these relations.

(2) To make  $q$  negligibly small and to compensate only in the horizontal direction, so that  $q = 0$ ,  $\mu = -p$ .

This last arrangement is made in the new Askania magnetic system, in which the central frame is made of steel of which the expansion coefficient is only about one-tenth of  $\mu$ . This is identical with the result obtained before, that the influence of the expansion upon the scale value is negligible.

The influence of disregarding the temperature coefficient of the scale value may readily be computed. For, if the compensation in the horizontal direction is perfect; that is, if  $\mu = -p$ ,

$$\frac{S_\theta - S_{20}}{\theta} = -\mu S_{20},$$

which even for the largest readings is so small that it may be neglected; besides, if it were larger, it could be eliminated by a slight overcompensation in the horizontal direction.

Finally, equation 14 shows that  $q$ , even if it were larger, would cancel out if the readings of the instrument were always taken near the center of the scale ( $S' = 20$ ); for, in that case, there is a balance between gravity and magnetic force; that is,  $\frac{mga}{M} = Z_0$ . Therefore,

$$\frac{mga}{M} \cdot q - Zq = 0.$$

There being ample reason to neglect  $q$ , it follows from equation 14 that

$$\text{T.C.} = \epsilon \frac{(S_\theta - S_{20})}{\theta} = -\frac{g}{M} \times \text{amp} - Z\mu \quad [15]$$

*This is the principal equation of this theory, which has been used throughout the following computations.*

It shows, in the first term on the right-hand side, the influence of compensation; in the second term, the uncompensated (magnetic) influence of the temperature.

It further shows that the system may be completely compensated, for readings around 20, by making  $p$  negative and equal to  $\mu$ , since near  $S' = 20$ :

$$\text{T.C.} = -Z_0(p + \mu) \quad [15a]$$

For readings differing from 20, a small correction is introduced, depending on how much  $Z$  deviates from  $mga/M$ . This influence is small and will be discussed in section B-V.

The next problem is to make  $p$  negative and equal to  $\mu$ . This is done in the new Askania system (Fig. 6), by two spindles on either side

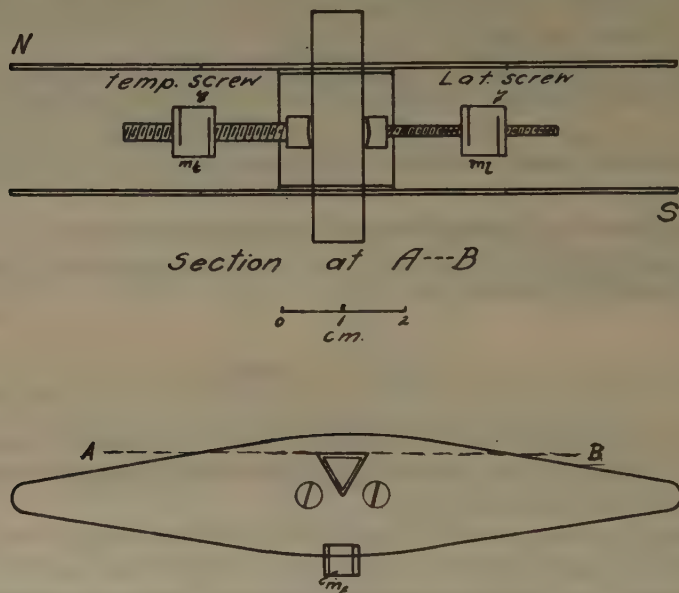


FIG. 6.—DIAGRAM OF NEW MAGNETIC SYSTEM.

of the central frame, bearing weights. The spindle on the north-pole side of the system is made of aluminum, the spindle on the south-pole side of invar steel. The latter carries the only screw that should be used in latitude adjustments, and invar is chosen so as to make the change in the position of the weight on this spindle as ineffective as possible.

When the temperature rises, the magnet loses its moment, or the vertical intensity apparently becomes smaller, resulting in an upward movement of the north pole. At the same time, however, the aluminum spindle expands, throwing the mass attached to it farther out from the knife edge and thus producing an opposite or downward moment.

At the latitude of Golden, the distances of the two weights on the spindles from the knife edge are almost equal. For this system, we may write

$$a = \frac{m_a x_a + m_l x_l - m_t x_t - m_{al} x_{al} + m_{st} x_{st}}{m_a + m_l + m_t + m_{al} + m_{st}} \quad [16]$$

where  $m_a$  = mass of system without horizontal spindles and masses,

$x_a$  = abscissa of center of gravity of system,

$m_l$  = mass of bronze nut on latitude spindle,

$x_l$  = distance of its center from the knife edge,

$m_t$  = mass of bronze nut on temperature spindle,

$x_t$  = distance of its center from knife edge,

$m_{al}$  = mass of aluminum (temperature) spindle,

$x_{al}$  = distance of its center from knife edge,

$m_{st}$  = mass of the steel (latitude) spindle,

$x_{st}$  = distance of its center from knife edge,

$m$  = total mass of system,

$m = m_a + m_l + m_t + m_{al} + m_{st}$ .

In equation 16, all quantities may be readily determined by callipers and scale, except  $a$  and  $x_a$ . From the position of equilibrium, i.e., the latitude adjustment,  $a$  follows as

$$a = \frac{MZ_0}{mg}$$

and

$$x_a = \frac{am - m_l x_l + m_t x_t + m_{al} x_{al} - m_{st} \times x_{st}}{m_a}$$

Then  $a$  at a temperature  $\theta$  is given by

$$\begin{aligned} am(1 + p\theta) = & m_a x_a(1 + \gamma\theta) + m_l x_l + m_l(x_l - c)\delta\theta - m_t x_t \\ & - m_t(x_t - c)\beta\theta - m_{al} x_{al} - m_{al}(x_{al} - c)\beta\theta \\ & + m_{st} x_{st} + m_{st}(x_{st} - c)\delta\theta \end{aligned} \quad [17]$$

where

$\beta = 2.3 \times 10^{-5}$  is the expansion coefficient of aluminum,

$\gamma = 1.15 \times 10^{-5}$  is the expansion coefficient of steel,

$\delta = 0.14 \times 10^{-5}$  is the expansion coefficient of invar steel,

$\mu = 13.8 \times 10^{-5}$  is the temperature coefficient of the magnetic moment, and

$c = 0.63$  cm., the distance of the point of attachment of both temperature and latitude spindles from the knife edge.

Subtracting [16] from [17] and dividing by  $\theta$

$$\begin{aligned} amp = & \gamma m_a x_a - \beta[m_t(x_t - c) + m_{al}(x_{al} - c)] + \\ & \delta[m_l(x_l - c) + m_{st}(x_{st} - c)] \end{aligned} \quad [18]$$

For the system as adjusted for Golden latitude, we obtained after substituting the numerical values into this equation

$$amp = -9.25\gamma$$

As  $-g/M$  is  $-0.80$  for Golden latitude, and as  $-Z_0\mu = -7.33\gamma$ , we have from equation 15

$$\text{T.C.} = +7.40\gamma - 7.33\gamma = +0.07\gamma$$

computed from the theory; the observed value was

$$\text{T.C.} = +0.03\gamma.$$

*These figures show that the observed and computed values agree much beyond the observational error of temperature coefficient determinations, which is, for average temperature gradients, about  $\pm 0.5$  gammas.*

### III. EFFECT OF CHANGES IN MAGNETIC LATITUDE

When a magnetometer that is adjusted for one magnetic latitude is taken to an area with a different vertical intensity, the magnetic system is readjusted by moving the bronze nut on the latitude spindle. As this spindle is made of invar, this does not affect the factor  $amp$  in equation 15 very much. However, the difference in vertical intensity enters with its full value in the factor  $-Z\mu$ . The change in gravity does not affect the reading or temperature coefficient to any noticeable degree.

In order to compute the influence of latitude changes upon the temperature coefficient, only four steps are necessary:

(1) Calculation of  $am$  from  $am = \frac{m}{g} \times Z_0 = 1.25 \times Z_0$ .

(2) Calculation of  $m_ix_i$  from

$$m_ix_i = am - m_ax_a + m_ix_i + m_{ai}x_{ai} - m_{ai}x_{ai} \text{ or} \\ m_ix_i = am + 4.81$$

(3) Calculation of  $\delta m_ix_i$ ,

(4) Calculation of  $amp$  from equation 18, in which everything remains as before except  $\delta m_ix_i$ .

The result of such computation is shown below for the same latitudes for which actual determinations of temperature coefficients were made (see section C-II-2).

The results prove that a magnetic system which is compensated for Golden vertical intensity would have a temperature coefficient of  $-2.7\gamma$  for vertical intensities greater than that at the pole, a coefficient of  $+1\gamma$  at Houston, a coefficient of  $+3.7\gamma$  in Central America and of  $+6.1\gamma$  in the northern part of South America.

This is evidence that the system, although compensated for Golden latitude only, may be used without recompensation throughout a large part of North America.

The variation of the temperature coefficient with latitude is shown by the graph, Fig. 7. The computed, not the observed, values are plotted.



The graph shows that there is a linear drop of temperature coefficient with an increase of latitude.

Table 1 shows the results of the computed temperature coefficients compared with the observed values; *the average of the middle errors of five values is only  $\pm 0.3 \gamma$ , i.e., less than the observational error.* However, four out of the five observations are larger than the computed values, so that there is a possibility that  $\mu$  is somewhat too great.

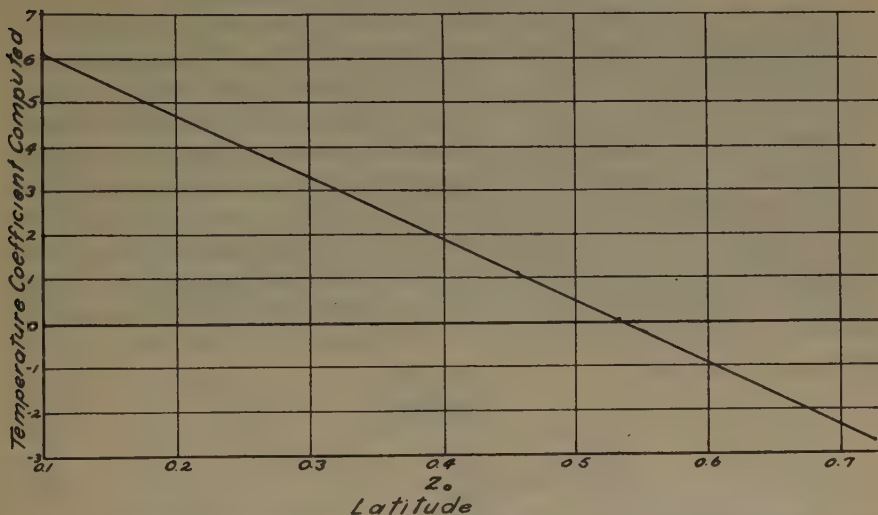


FIG. 7.—CHANGE OF TEMPERATURE COEFFICIENT WITH LATITUDE. (COMPARE WITH FIG. 12.)

TABLE 1.—Comparison of Calculated and Observed Temperature Coefficients for Various Latitudes

Approximate Locality	$Z_0$	Mechanical Coefficient, $-\frac{gamp}{M}$	Magnetic Coefficient $-Z\mu$	Temperature Coefficient	
				Computed	Observed
Value greater than at North Pole; Kursk-anomaly magnitude.....	0.7286	+7.37	-10.06	-2.7	-1.6
Golden, Colo.....	0.5310	+7.40	- 7.33	+0.1	0.0
Houston, Texas.....	0.4556	+7.41	- 6.29	+1.1	+1.6
Nicaragua.....	0.2744	+7.44	- 3.78	+3.7	+4.7
Amazon River.....	0.1007	+7.46	- 1.39	+6.1	+6.7
	Gauss	$\gamma$	$\gamma$	$\gamma$	$\gamma$

## IV. EFFECT OF CHANGES OF SCALE VALUE

As stated before, it does not follow from the equations previously given that there should be an effect of scale value changes on the temperature coefficient, if the latter is expressed in gammas.

However, if the threaded hole, in which the scale-value screw moves up and down, is not at right angles to the magnetic axis of the system, a change in  $a$  is produced when the scale value is changed.

How great this change is can be readily determined by experiment. If, for instance, the reading is 2 scale division (from center) and the scale value  $30\gamma$ , the field is  $60\gamma$ . If, then, the scale-value screw is moved up to a scale value of  $15\gamma$ , the reading should now be four scale divisions. However, if a horizontal displacement of the center of gravity took place as the screw was moved up (the threaded hole not being vertical), the reading probably will not be four scale divisions, but will be different from four, say five. In other words, for  $30\gamma$  scale value  $\epsilon_0 \times S_0 = 60\gamma$ ; and instead of being  $60\gamma$  for the  $15\gamma$  scale value,  $\epsilon S$  is now  $75\gamma$ . If we call the original  $\epsilon_0 S_0 = 60\gamma = \Delta Z$ , the displacement in the center of gravity  $\Delta a$  is proportional to the difference  $75\gamma - 60\gamma$  or  $\epsilon S - \Delta Z$ , since

$$\epsilon S = Z - \frac{mga}{M} \quad [19a]$$

$$\Delta a = \frac{M}{mg}(\epsilon S - \Delta Z) \quad [19b]$$

An experiment such as just described may readily be made, starting out with large scale values and small deflections, computing  $\epsilon_0 S_0 = \Delta Z$ , changing the scale value to smaller values and observing the corresponding readings  $S$ . Then for any scale value,  $\epsilon S$  should be constant and equal to  $\Delta Z$  if there is no lateral displacement of the center of gravity when the scale-value screw is moved. The values obtained by an experiment of such nature in Golden are shown in Table 2.

The resultant changes in temperature coefficients may be readily computed by substituting the  $\epsilon S - \Delta Z$  (or  $\epsilon S - Z$ , as  $\Delta Z = Z - Z_0$ ) values directly in equation 15, using equation 19a,

$$\text{or,} \quad \text{T.C.} = p(\epsilon S - Z) - Z\mu \quad [20]$$

This transforms readily into equation 15a when  $S = 0$  (reading 20), for then  $Z = Z_0$ .

Equation 20 shows that the temperature coefficient increases with scale value, if  $\epsilon S$ , instead of remaining constant, increases with a decrease in scale value (Fig. 8).

This has been observed for the investigated system. In other words, in this system the angle between the threaded hole and magnetic axis was

smaller than  $90^\circ$  on the *south* side of the system, or  $a$  was decreased when the scale-value screw was moved up.

For another magnetic system, the opposite is equally possible; for, when the angle between the *north* side of the needle and the threaded hole is smaller than  $90^\circ$  an increase of  $a$  would correspond to an increase of sensitivity; that is, the product  $\epsilon S$  would become smaller and smaller. In that case, a decrease of the temperature coefficient with increase in scale value, instead of an increase, will be found.

It is also seen from equation 20 that the change in temperature coefficient with scale value must be dependent upon the magnetic latitude. For a change in  $a$  brought about by a change in  $\epsilon$  is larger in proportion to  $a$  in low magnetic latitudes than in high latitudes. Consequently, the increase in temperature coefficient with scale value is much greater for low magnetic latitudes than for high latitudes.

Table 2 shows the results of a computation of temperature coefficients as a function of scale value, made for both high and low latitudes. The computations are based directly on the observed and adjusted values for  $\epsilon S$ ; that is, the change of reading when the scale value is changed, but the

TABLE 2.—*Temperature Coefficients as a Function of Both Scale Value and Latitude*

Values used:			GOLDEN		AMAZON RIVER	
			$p = -13.94$		$-74.07$	
			$\mu Z = -7.36$		$-1.41$	
Observed Values			$p(\epsilon S - Z), \gamma$		Temperature Coefficient, $\gamma$	
$S'$	$\epsilon, \gamma$	$\epsilon S, \gamma$	Golden	Amazon River	Golden	Amazon River
22.7	80.8	218	+7.40	+7.46	+0.04	+6.05
24.3	65.0	280	+7.39	+7.41	+0.04	+6.00
27.1	48.4	345	+7.38	+7.36	+0.03	+5.95
30.2	37.9	386	+7.38	+7.33	+0.02	+5.92
36.1	26.6	430	+7.37	+7.30	+0.02	+5.89
51.2	15.2	474	+7.37	+7.27	+0.01	+5.86
54.5	13.9	480	+7.36	+7.26	+0.01	+5.85

vertical intensity is left constant. In the middle columns, the "mechanical" coefficients in  $\gamma$  are shown for two latitudes and seven scale values; subtracting from this the  $Z\mu$  values from Table 1 or the "magnetic" coefficient for the two latitudes, the temperature coefficients shown in the last columns are obtained.

These temperature coefficients are represented graphically in Fig. 8. It is clearly seen that the change of the T.C. with scale value is greater for low than for high latitudes; also, that the changes are much below the observational error for high latitudes. For low latitudes, if accurate

determinations are made, the change in temperature coefficient with scale value is noticeable. However, the actual curves (Sec. C-II-3) do not show such a regular trend as the computed values. At any rate, the increase of the coefficient with scale value can be recognized in some of the curves (Fig. 14). The reason for some of the deviations probably is that the change of the T.C. with scale value is in most cases very close to the observational error. That there is a detectable change is, without a doubt, seen from the curves shown in Fig. 12; for if there were no increase of the T.C. with scale value, all the curves shown should coincide.

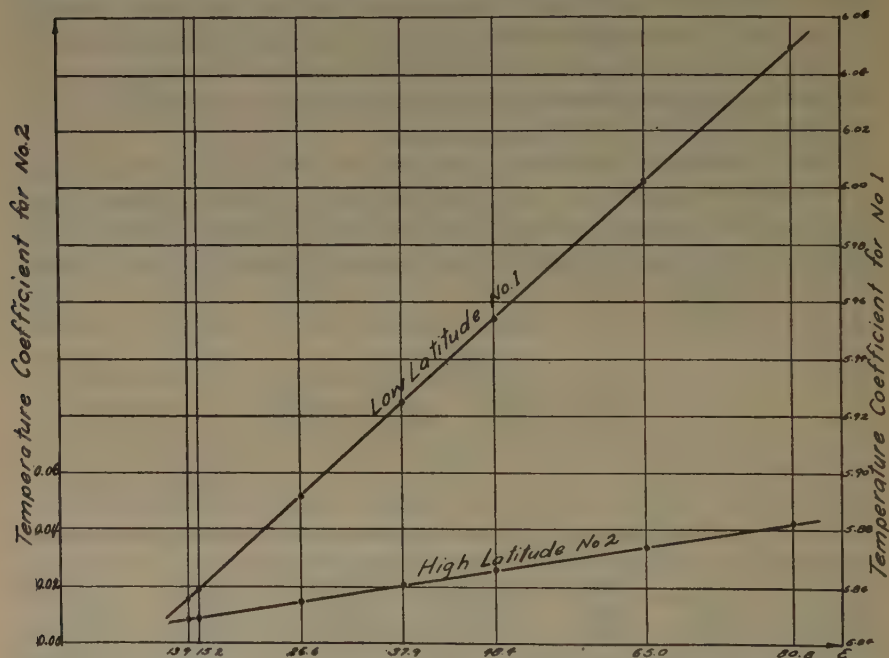


FIG. 8.—TEMPERATURE COEFFICIENTS AS FUNCTION OF SCALE VALUES AND LATITUDES.

## V. EFFECT OF CHANGES OF DEFLECTION OF THE SYSTEM

It has been stated repeatedly that in this theory the temperature coefficients were computed for the central part of the scale.

That is to say, for any latitude, the  $a$  has been computed from the relation  $a = \frac{MZ_0}{mg}$ . If the reading is different from 20,  $Z$  differs from  $Z_0$  by the amount  $\epsilon S$  and the change in temperature coefficient is simply  $-\epsilon S \mu$ , as the "mechanical" coefficient remains constant. Therefore, for readings greater than 20 a positive T.C. is smaller, a negative T.C. is greater than the T.C. for a reading 20. For readings smaller than 20, a positive T.C. is greater, a negative T.C. is smaller than the coefficient for the reading 20.



TABLE 3.—*Influence of Deflection of System on Temperature Coefficient for Three Scale Values, Four Readings and Five Latitudes*

Temperature Coefficient for																	
		$\epsilon = 10\gamma$				$\epsilon = 30\gamma$				$\epsilon = 90\gamma$							
		-20	0	40	60	-20	0	40	60	-20	0	40	60				
Z	T.C. for $S' = 20$	-2.68	-2.63	-2.65	-2.71	-2.74	-2.51	-2.60	-2.77	-2.85	-2.14	-2.43	-2.93	-3.23			
0.7286																	
0.5310																	
0.4556																	
0.2744																	
0.1007																	

A number of temperature coefficients are shown in Table 3, computed for three scale values, four readings and five latitudes. The latitude is shown in the first, and the corresponding T.C. for the reading 20 in the next column. Then follow the T.C.'s for three scale values and four readings. The influence is the same for all latitudes. The deviations are somewhat larger than the observational error if great precision is used, for the extreme readings  $-20$  and  $60$  for the scale value  $30\gamma$  and for all readings for the scale value  $90\gamma$ . It should be remembered, however, that scale values of  $90\gamma$  are seldom used; if so, they are used because the magnitude of the anomalies require it, and then any temperature correction, particularly if it is small, is neglected. In addition, for the customary scale value of  $30\gamma$ , the scale is usually not read on the extreme ends. Therefore, it may safely be stated that the influence of the scale reading upon the T.C. may be disregarded for practical purposes.

### C. EXPERIMENTAL RESULTS

(W. E. PUGH)

The primary object of this investigation was to test the temperature compensation of a new magnetic system for Schmidt magnetometers and to ascertain whether changes in latitude setting or scale value affected the compensation.

As the work progressed, numerous complications arose which necessitated a great deal of detail work, unforeseen at the time the investigations were started. That is, the original intention was to obtain all of the observational data mechanically (by photographic means) in order to maintain proper accuracy with a minimum amount of manipulative effort. The preliminary work proved to be of such a nature, however, that many observations were obtained visually to save both time and expense, hence a great amount of detail was necessary to secure a reasonable accuracy in the results.

That this detail was worth while is shown by the really remarkable agreement between theory and observations. Furthermore, the results brought about an elaboration of the general theory of Schmidt magnetometers and verified many theoretical considerations not previously tested.

### I. PRELIMINARY INVESTIGATIONS

#### 1. *General Arrangement of Apparatus*

Fig. 9 shows the set-up of the apparatus for photographic recording of temperature change and diurnal variation. *A* is the photographic recorder; *B*, magnetometer for registering change due to temperature and housing the new type magnetic system which was tested for temperature coefficient; *C*, magnetometer for registering diurnal variation; *D*, coil for scale-value determination; *E*, rheostat, switch and milliammeter

for scale-value coil; *F*, wires leading to heating coil; *G*, transformer and rheostat for adjustment of heating element; and *H*, auxiliary magnet for latitude control. The magnetometer tripods were placed on a thick concrete base to prevent vibration.

The photographic recorder was equipped with a straight filament, 6-volt, electric lamp to furnish the light rays to the mirrors in the recorder attachments of the magnetometers. The recorder was set for one revolution every two hours. Description and instructions for the operation of this type of recorder (Askania) are given by Heiland.<sup>10</sup>

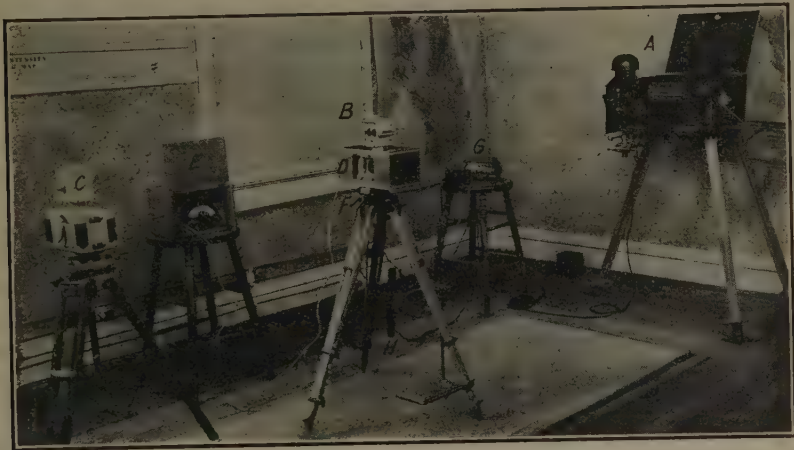


FIG. 9.—ARRANGEMENT OF APPARATUS FOR TEMPERATURE TESTS.

In order to maintain nearly constant temperature conditions with respect to the variation recording instrument, a fan of the blower type was installed in the laboratory.

Precautions were taken to keep the magnetic conditions as stable as possible. Even so, troublesome variations were encountered due to unavoidable surges in the current of the electric lighting system and to the proximity of an interurban trolley line.

*Heating Element.*—The heating element was built by Charles H. Hull, instrument maker at the Colorado School of Mines. It consists of a high-resistance coil of fine platinum wire enclosed in brass, and so arranged that its base fits into the tripod head while at the same time the magnetometer may be properly oriented and clamped in position. The plug in the base of the magnetometer is removed and the part containing the heating coil fits snugly into the hole. This type of heating device has been found to be decidedly superior to the old type of heating box in that a more constant temperature gradient can be secured. Also less time is

<sup>10</sup> C. A. Heiland: Directions for Use of Vertical Field Balance, 10-12. Askania-Werke, Geo. 72E-D, 1927.

required to raise the temperature the desired amount. Again, readings of temperature and of the magnetometer are much easier to take when making visual observations.

### *2. Arrangement for Recording Variation*

The magnetometer *C* used for recording magnetic variation contains an old type magnetic system. This instrument has seen considerable field service and under numerous tests has been found to have a constant scale value and a fairly low temperature coefficient ( $0.1 \pm$  scale divisions per degree Centigrade at a scale value of  $29\gamma$ ). Furthermore, nearly constant temperature conditions were maintained in the laboratory during experimental work (see above). The recorder attachment contains one  $45^\circ$  adjustable mirror which reflects the position of the balance system on the photographic film.

### *3. Arrangement for Recording Temperatures*

The mirror attachment on magnetometer *B* contains three mirrors; one adjustable  $45^\circ$  mirror which gives the position of the magnetic system, one attached to the case for a base-line record and one attached to a Bourdon tube thermometer for temperature recording. The last two may be moved either up and down or to the right and left for adjustment of the light rays.

The standardization of the Bourdon tube was accomplished simply by heating the instrument and recording visually the temperature given by the case thermometer while the temperature record of the tube was being photographed. Thus, a scale value in degrees per millimeter of displacement from the base line on the film was obtained. Care was taken during the various experimental tests to check this scale value, as the repeated heating and cooling of the instrument seemed to create tensions in the Bourdon tube, which caused some variation in the scale value.

*Determination of Time Lag.*—The case temperature readings were plotted on the photographic record and from a comparison of the curves the lag of the Bourdon tube behind the case temperature was computed to be approximately 14 min. It did not seem probable that the Bourdon tube represented the temperature of the magnetic system because of the difference in their thermic and elastic properties. At the time, the magnetic system tested was adjusted for Golden latitude and compensated for temperature change; hence the change in reading due to temperature change was so small that it was impossible to determine the lag of the system behind the case temperature. To get an idea of the magnitude of this lag a test was run with an old type system which had a large temperature coefficient. This lag was computed to be about 10 minutes.



Later, as tests on the new system were made at lower latitude settings, the temperature effect became large enough to compute its lag, which was found to be 6 min. *Herein, we have an added advantage of the new magnetic system.* The reduction in the lag of the magnetic system behind the case temperature is probably caused by the fact that the new system consists, in the greater part of its mass, of one material, and has, on account of the use of a frame instead of a cube for its central support, a greater radiating surface. In field operation the new system will give more accurate results because the lag behind existing temperature conditions has been reduced to nearly one-half of its former value.

Fig. 10 shows a diagrammatic representation of the temperature lag relation and some of the photographic records used in this determination.

*Since the magnitude of the time lag is dependent upon the temperature gradient, as is the temperature coefficient, an effort was made to maintain a constant gradient throughout all the experiments. For all practical purposes, this was accomplished. The gradient used was 1.7° C. per 5 minutes.*

#### 4. Method for Scale-value Determination

The scale-value determinations of the magnetic systems had to be recorded photographically in order to get the calibration in terms of gammas per millimeter of the film. The coil, shown in Fig. 9, was used in preference to auxiliary magnets, because of increased ease of operation and greater accuracy.

This coil, developed by Keiser, is based on the principle of the Helmholtz coil and produces a fairly homogeneous magnetic field at its center. Current supplied by a dry cell, controlled by a rheostat and measured by a milliammeter, is sent through the coil, and causes a certain deflection. By reversing the direction of the current, the field is reversed and an equal deflection occurs in the opposite direction.

Actually, there are two coils in the coil box, one of which produces a stronger field than the other and thus furnishes an additional check. The coil constants were 173.2 $\gamma$  per milliamperere for the small coil and 364.5 for the large coil.

The formula for the scale value is

$$\epsilon = \frac{2KI}{S_1 - S_2}$$

in which  $\epsilon$  is the scale value,  $K$  the coil constant;  $I$  the current in milliamperes, and  $S_1, S_2$ , the deflections of the magnetometer.

Fig. 11 shows a photographic record of scale-value calibration for the variation instrument and the test instrument.

*Effect of Misorientation on Scale Value.*—Here, an interesting complication arose. Because of the fact that the concrete base was not

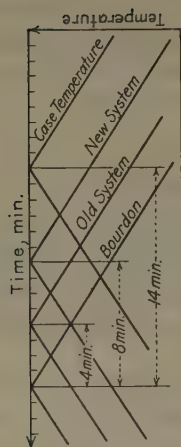


FIG. 10a.—TEMPERATURE LAG RELATION.

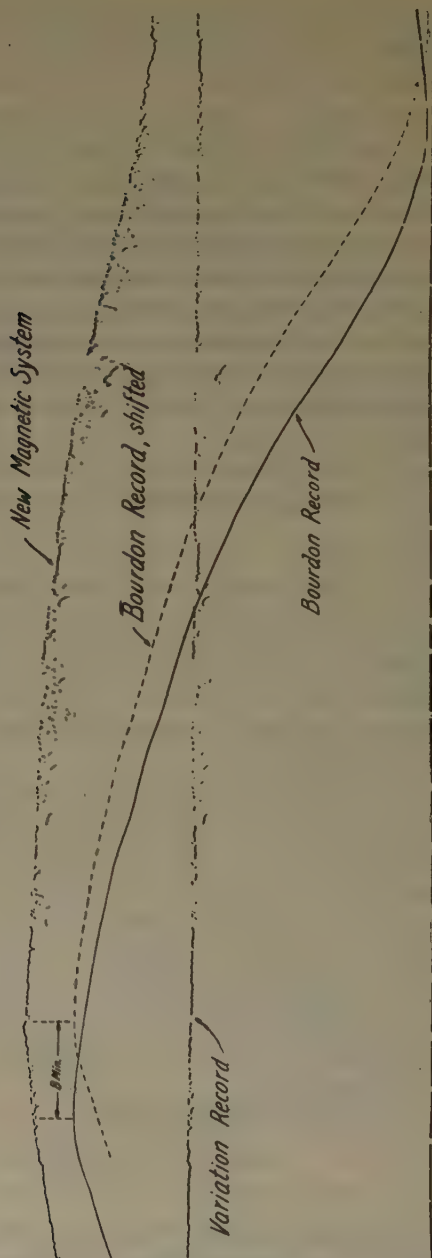
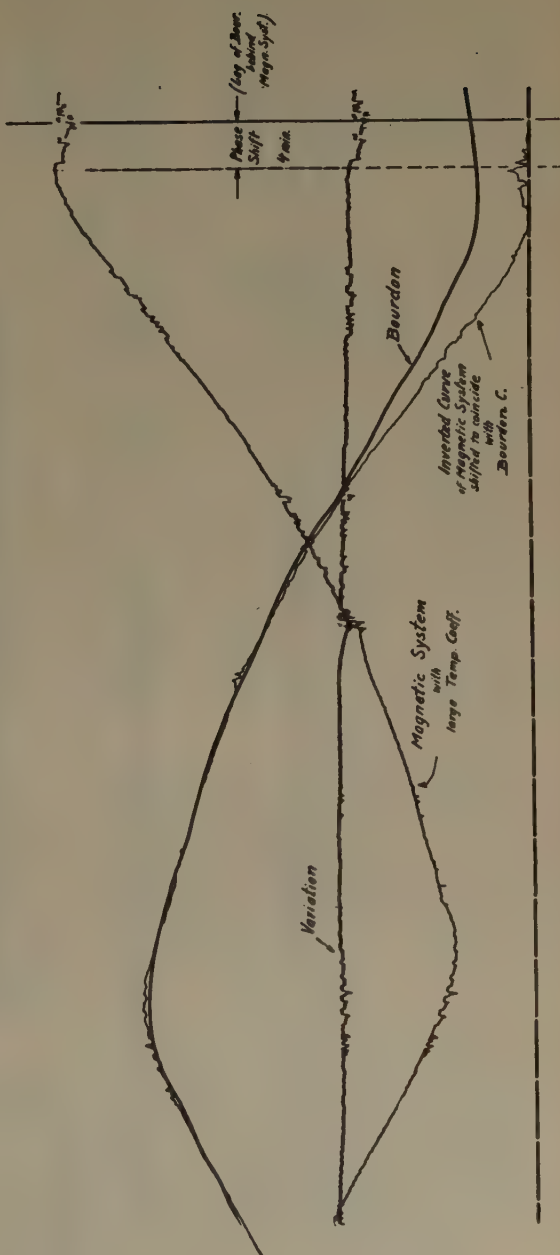
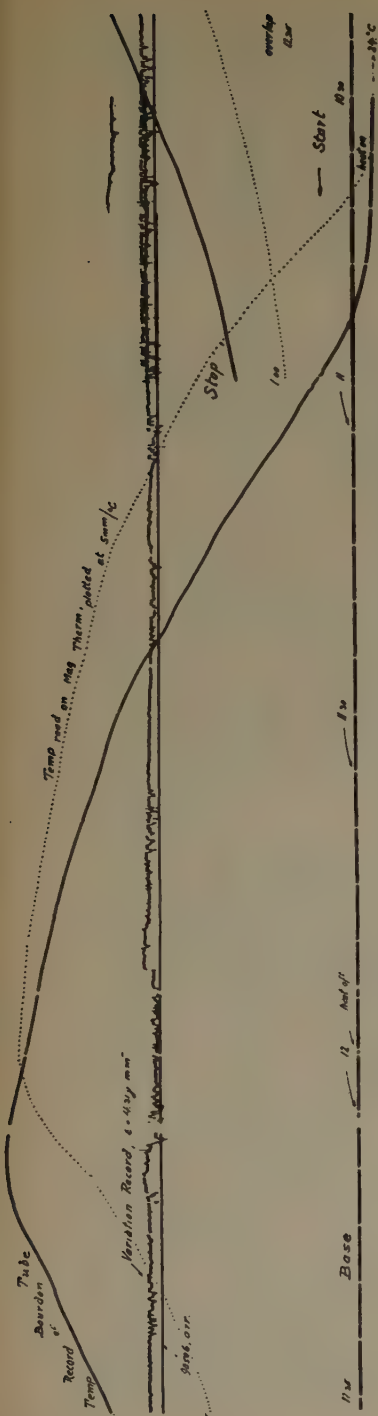


FIG. 10b.—LAG OF BOURDON RECORD BEHIND NEW SYSTEM.



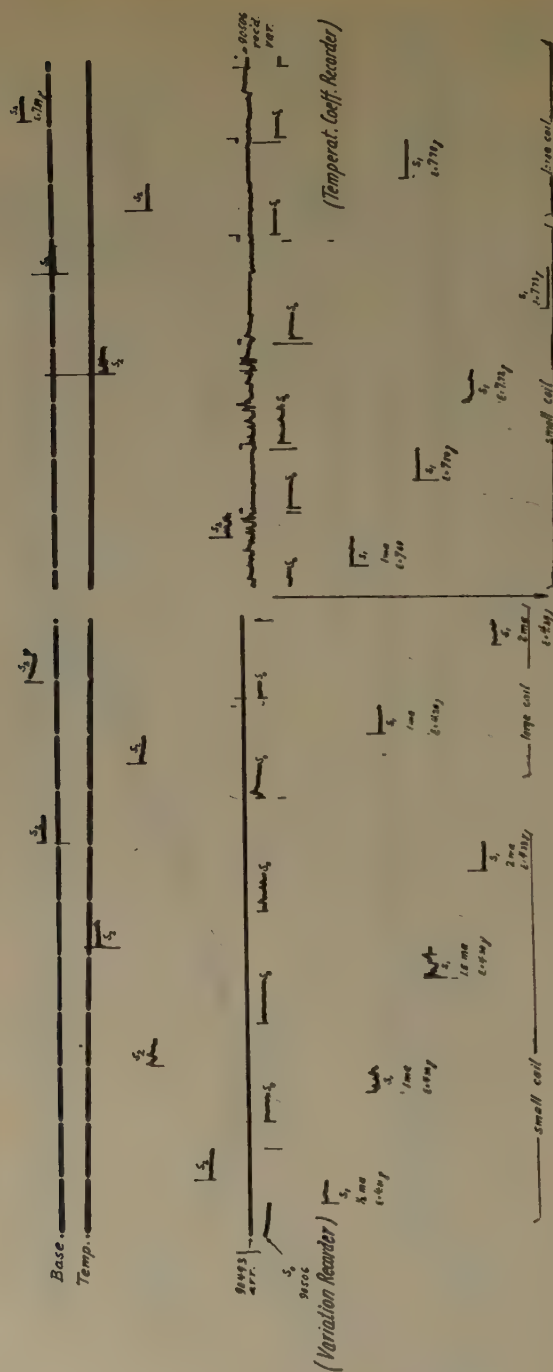


FIG. 11.—PHOTOGRAPHIC RECORD OF SCALE-VALUE CALIBRATION.



oriented in the north-south direction, it was necessary that the magnetometers be oriented at an angle to the customary east-west position in order to get their simultaneous records on the film.

Up to this time, it had not been shown that orientation affected scale value. Such proved to be the case and, in light of this knowledge, there was no difficulty in showing that this change in scale value is a function of the angle of misorientation, the horizontal intensity and the focal distance of the optical system. In other words,

$$\epsilon_s = \epsilon_{E-W} - \frac{H \sin \delta}{2f}$$

where  $\epsilon_{E-W}$  is the scale value when properly oriented,  $H$  the horizontal intensity,  $f$  the focal distance and  $\delta$  the angle of misorientation.

This formula was found to be correct by experimental tests.

### 5. Method for Changes of Latitude

In the new system the latitude adjustment is much more readily made than in the old system. The latitude screw is situated on the south-pole side of the magnetic system, as is the center of gravity (for instruments to be used in the northern hemisphere); hence, a movement of the screw towards the south pole compensates an increase in  $Z$ , and a movement towards the north pole compensates a decrease in  $Z$ .

To simulate changes in latitude ( $Z$  increasing positively from equator to pole) standardized auxiliary magnets were used in the first Gauss position.

To avoid any effect of temperature on the standard magnets, which had to be placed rather closely to the heating element, a bar magnet of large magnetic moment was used instead of the auxiliaries after the desired latitude adjustment had been made (Fig. 9).

In the temperature coefficient determinations, the following values, in gammas, of the vertical intensity were used: 72,860; 53,100; 45,560; 27,440 and 10,070. These values represent a change of  $Z$  within the usable range of the vertical magnetometer and are for localities defined earlier in the paper (p. 19).

*Determination of Effect of Latitude Change on Scale Value.*—Theoretically there should be no change in scale value with change in latitude; dependent, of course, upon an accurate horizontal placement of the latitude spindle. To verify this, tests were made of all scale values used in the experiments at the various latitude settings. For all determinations no appreciable change could be noted, thus checking the theory and complimenting as well the precision work of the manufacturers.

Table 4 of observed data demonstrates this fact very clearly, since the variation in scale value is certainly within the range of observational error.

TABLE 4.—*Observed Data*

Latitude Setting	Scale Value, $\gamma$ per Mm.	
72,860	14.2	3.9
53,100	14.3	3.9
45,560	14.2	3.9
27,440	14.2	3.9
10,070	14.1	3.8

### 6. *Method for Changes in Scale Value*

Scale value or sensitivity changes are accomplished by a vertical movement of the screw on the under side of the magnet system; raising the screw decreases the scale value or increases the sensitivity.

Experiments show that, for the new magnetic system, one complete revolution of the scale-value screw changes the telescope scale value by approximately 5  $\gamma$  per scale division throughout the entire range of scale values.

The scale values used in the temperature coefficient determinations were 4.1, 7.7, 14.6 and 18.3 expressed in gammas per millimeter of the photographic film. These values represent telescope scale values, if the instrument were oriented in the east-west position, of 16.0, 30.0, 56.9 and 71.3 respectively.

*Determination of Effect of Scale-value Change on Latitude.*—The next test necessary was to ascertain whether a movement of the vertical screw (change in scale value) produced any change in apparent latitude. A small effect was noted, which should be included in the base correction in field procedure.

A change in telescope scale value from 80.8  $\gamma$  to 13.9  $\gamma$  produced an apparent increase in  $Z$  of 262  $\gamma$ . (Refer to the theoretical discussion by Dr. Heiland on page 350.) This variation is due probably to the fact that the axis of the screw hole is not exactly vertical. Its value must be ascertained separately for each instrument.

### 7. *Determination of Magnetic Moment of System*

This determination was made very simply by placing the magnetic system in its wooden box vertically below the variation magnetometer and noting the change in deflection caused by reversing the poles. The tests were made at various distances to furnish checks on the results.

An average of a number of determinations gave the magnetic moment a value of 1225 C.G.S. with a middle error of  $\pm 0.1$  C.G.S.

*Determination of Temperature Coefficient of Magnetic Moment of System.*—In order to compute the theoretical values of the temperature coefficient of the magnetic system, it was necessary to determine experi-

mentally the magnetic effect of temperature change; that is, the temperature coefficient of the magnetic moment of the system.

To do this, the magnetic system was placed, in arrested condition, in a vertical magnetometer box and was used in first Gauss position with reference to a horizontal magnetometer; the deflection of the latter was noted while the former was being heated.

An auxiliary magnet was used to balance the magnetic system of the horizontal magnetometer in the zero or vertical position.

Extreme care was exercised in orienting the instruments along a line parallel to the magnetic meridian and also to make the line through the centers of the magnets horizontal. The magnetometers were placed as close together as possible, so as to cause a large deflection when heat was applied and thus reduce the effect of any observational error.

In such a determination the temperature coefficient of the magnetic moment is given by the formula

$$\mu = -\frac{\frac{dF}{d\theta}}{F}$$

in which  $\frac{dF}{d\theta}$  is the change in field strength produced by unit change in temperature and  $F$  is the total field before heat is applied. The value of  $\mu$  was determined to be  $+0.000138$ .

From the formula  $M_{\theta} = M_{20}(1 - \mu\theta)$  the moment at any temperature  $\theta$  may be found. It follows immediately from the formula that a rise in temperature produces a decrease in magnetic moment.

## II. TESTS OF TEMPERATURE COEFFICIENTS

With the completion of the discussion of preliminary investigations, we come to the temperature tests for which these experiments were originally begun.

The actual procedure under which these tests were made consisted in adjusting the scale value, making all temperature tests for the various latitude settings, then changing the scale value and repeating the tests for each latitude. There is no reason to believe that the results would have been different if a somewhat different procedure had been followed.

The discussion will take up (1) the determination of the temperature coefficient for normal conditions at Golden; (2) the effect of latitude change; and (3) the effect of scale-value change.

### 1. *Under Normal Conditions at Golden Latitude*

These tests prove conclusively that, under such conditions ( $\epsilon = 30.0$ ,  $Z = 53,100$ ), the temperature effect upon this new magnetic system has been almost completely compensated; we might say, as far as is humanly possible. To the field man, such an instrument would certainly

be an asset. Fig. 13b shows a typical photographic record of this determination.

## 2. Under Different Latitude Conditions

While the temperature tests were being made for latitude change with normal scale value, it was quite evident that the temperature coefficient was changing considerably; or, that  $T.C. = F(Z)$ . At first, this was rather difficult to explain, as statements to that effect are not contained in any of the previous publications on magnetometer theory. With the application of the theory to the new magnetic system, however, the reason

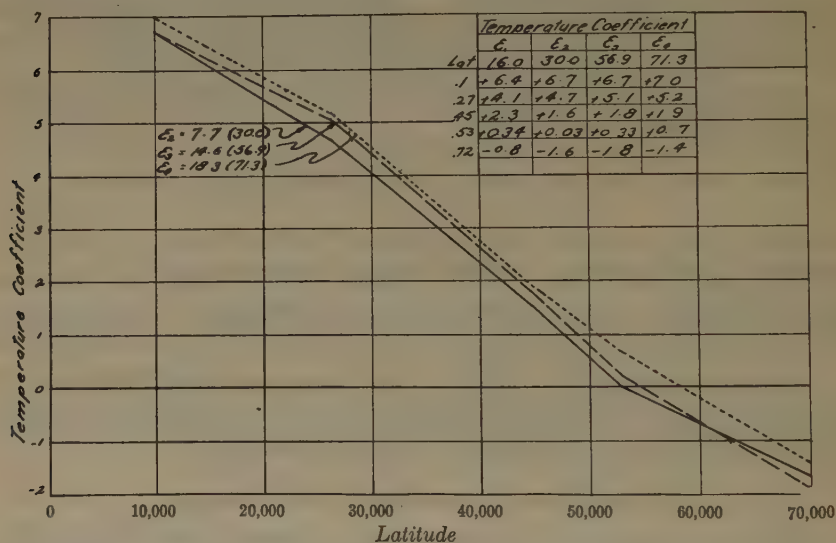


FIG. 12.—TEMPERATURE COEFFICIENT AS FUNCTION OF LATITUDE, FOR VARIOUS SCALE VALUES.

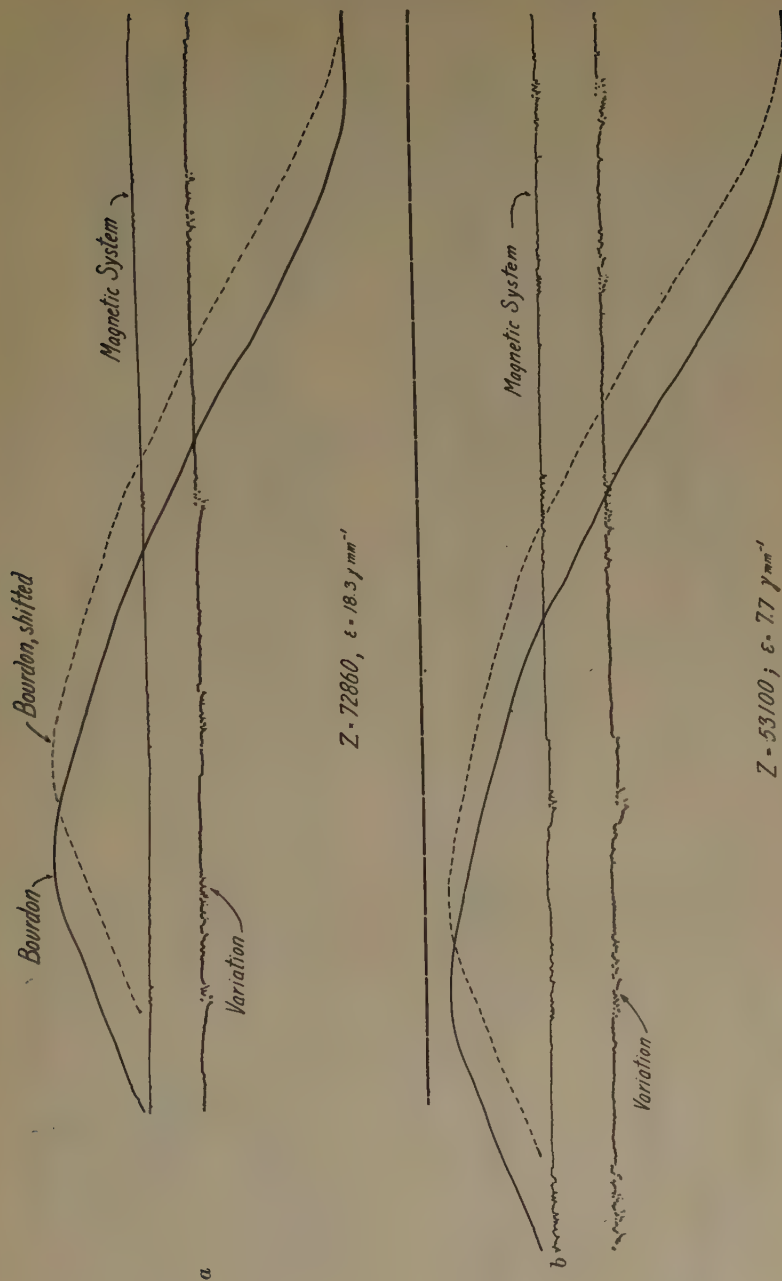
for such variation of temperature coefficient with latitude is apparent (see Sec. B).

Fig. 12 shows the observed temperature coefficient values plotted against latitude for three different scale values. The coefficients are also tabulated for four scale values.

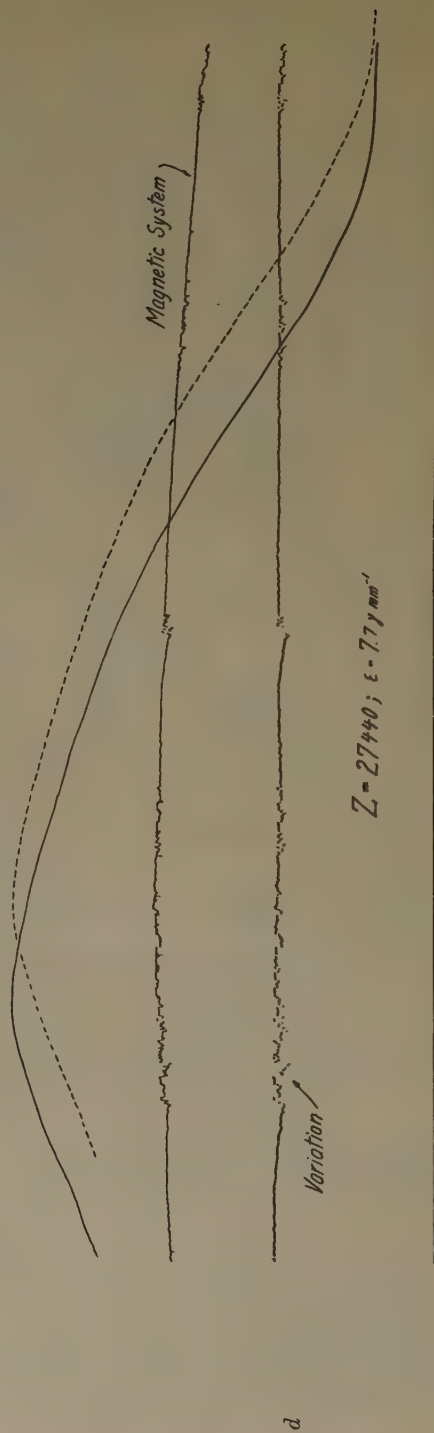
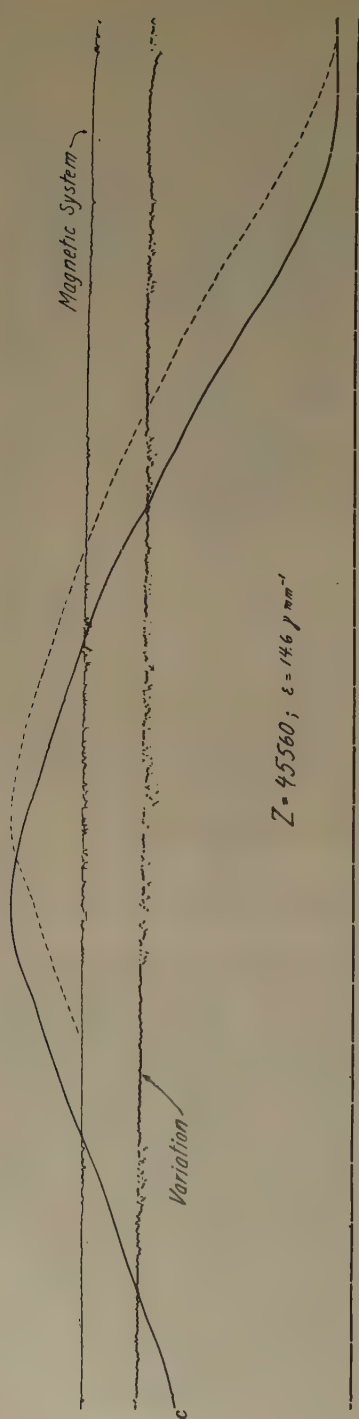
The results for high sensitivity ( $\epsilon = 16$ ) are not plotted in the graph because, although they conform in general trend to the other values, one or two of the points are somewhat out of line and their plotting would only serve to obscure the other curves.

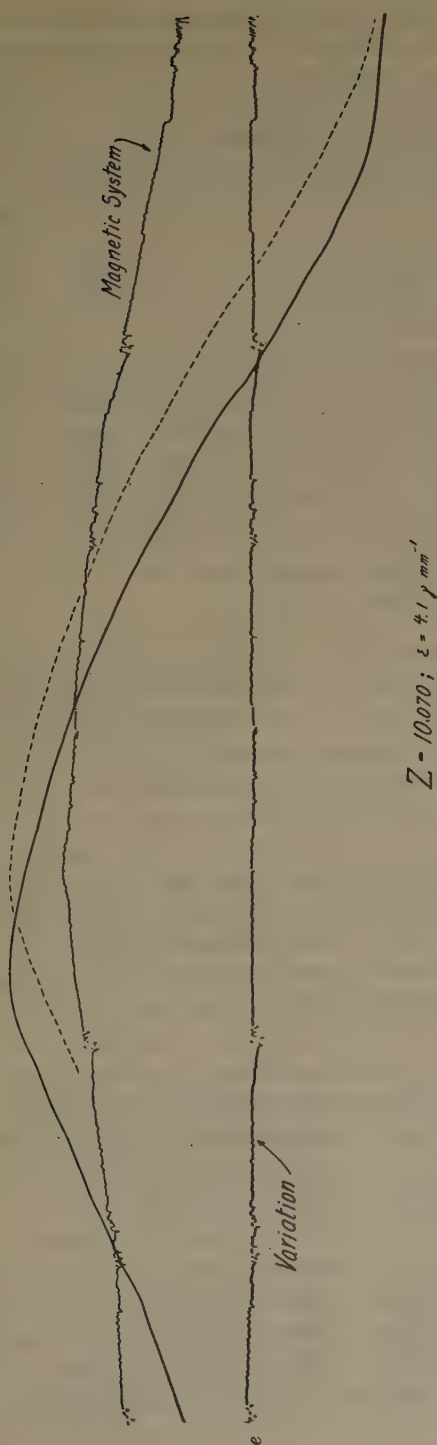
The graph shows that the magnetic system tested could be used with a vertical intensity range of about  $10,000\gamma$  without temperature correction. That is, a system adjusted for zero coefficient where  $Z = 50,000$  could be used within an area in which  $Z$  varies from  $45,000$  to  $55,000$ , since any temperature correction of less than  $\pm 1\gamma$  per degree may ordi-





FIGS. 13a AND b.—RECORDS OF TEMPERATURE COEFFICIENTS.





Figs. 13 c, d, e.—RECORDS OF TEMPERATURE COEFFICIENTS.

narily be neglected. The usable range may be extended considerably if the anomalies are of fairly large magnitude or if the instrument is used only for reconnaissance work.

TABLE 5.—*Evaluation of Curves*

	1	2	3	4	5	6	7	8	9	10
	Variation Instrument	Variation, Mm.	Variation, $\gamma$	Test Instrument	Change, Mm.	Change, $\gamma$	6-3	Temp., Mm.	Temp. Change, Deg. C.	Temp. Coefficient, $\gamma$ per Deg. C.

Tabulation for Figure 13a; Temperature Coefficient  $-1.4 \pm 0.05$ 

Base	74.0			93.5						
1	74.5	+0.5	+2.0	92.5	- 1.0	- 18	- 20	66.5	14.5	-1.4
2	74.0			92.0	- 1.5	- 27	- 27	83.0	18.0	-1.5
3	74.5	+0.5	+2.0	92.0	- 1.5	- 27	- 29	93.5	20.3	-1.4
4	74.0			92.0	- 1.5	- 27	- 27	101.5	22.1	-1.2
5	75.0	+1.0	+2.0	92.0	- 1.5	- 27	- 31	104.0	22.6	-1.4

Tabulation for Figure 13b; Temperature Coefficient  $+0.03 \pm 0.03$ 

Base	72.0			94.0						
1	72.0			94.0				89.5	19.5	0.0
2	71.5	-0.5	-2	94.0			+ 2	102.0	22.2	+0.09
3	69.5	-2.5	-11	93.0	- 1	- 8	+ 3	112.0	24.4	+0.12
4	72.0			94.0				118.0	25.7	+0.0
5	71.5	-0.5	-2	93.5	- 0.5	- 4	- 2	120.0	26.1	-0.08

Tabulation for Figure 13c; Temperature Coefficient  $+1.8 \pm 0.06$ 

Base	69.0			88.5						
1	70.0	+1.0	+4	91.0	2.5	+ 37	+ 33	81.0	17.6	+1.9
2	70.5	+1.5	+6	91.5	+ 3.0	+ 44	+ 38	92.5	20.1	+1.9
3	70.0	+1	+4	91.5	+ 3.0	+ 44	+ 40	99.5	21.6	+1.9
4	69.5	+0.5	+2	91.5	+ 3.0	+ 44	+ 42	108.0	23.5	+1.8
5	70.5	+1.5	+6	91.5	+ 3.0	+ 44	+ 38	109.5	23.8	+1.6

Tabulation for Figure 13d; Temperature Coefficient  $+4.7 \pm 0.05$ 

Base	52.0			78.0						
1	52.5	+0.5	+2	89.5	+11.5	+ 89	+ 87	82.0	17.8	+4.9
2	52.5	+0.5	+2	91.0	+13.0	+100	+ 98	96.0	20.9	+4.7
3	52.5	+0.5	+2	92.0	+14.0	+108	+106	105.5	22.9	+4.6
4	52.0			93.5	+15.5	+120	+120	117.5	25.5	+4.7
5	52.5	+0.5	+2	93.5	+15.5	+120	+118	119.0	25.9	+4.6

Tabulation for Figure 13e; Temperature Coefficient  $+6.4 \pm 0.13$ 

Base	74.0			93.5						
1	74.5	+0.5	+2	122.0	+28.5	+117	+115	90.5	19.6	+5.9
2	75.0	+1.0	+4	132.5	+39.0	+160	+156	108.0	23.5	+6.6
3	75.0	+1.0	+4	135.0	+41.5	+170	+166	116.0	25.2	+6.6
4	75.0	+1.0	+4	136.5	+43.0	+176	+172	124.0	27.0	+6.4
5	76.0	+2.0	+9	139.5	+46.0	+189	+180	130.0	28.3	+6.4



Also, the temperature coefficient of any one system of this type may be reduced towards zero from either a negative or positive value by a proper movement of the spindles or screws. Such work should be done only by men thoroughly acquainted with the theory and experienced in adjusting magnetic systems.

Photostats of some of the photographic records are given in Fig. 13 and the tabulated evaluation for these curves is shown in Table 5.

### 3. *Evaluation of Records*

In order not to make this paper unduly long, details as to the procedure followed in the evaluation of the records have been omitted.<sup>11</sup>

In Table 5, columns 1, 2, 4, 5 and 8 are in millimeters; 3, 6 and 7 are in gammas; 9 is in degrees Centigrade; and the last column gives the temperature coefficient in gammas per degree Centigrade. The temperature calibration was 4.6 mm. per degree for the records shown. The scale value of the diurnal variation instrument was  $4.3\gamma$  per millimeter.

### 4. *Under Different Scale Values*

After the evaluation of the curves was begun, it was noticed that the temperature coefficient seemed to vary with scale value. This change was discussed earlier in this paper (pp. 342 and 350). Unfortunately, in this instance, we do not get as accurate a check with the theory. This is due, no doubt, to the fact that the change, theoretically, is within the limits of observation error.

That there was a change, however, brought about the tests which explained it. Furthermore, the graphs (Fig. 14) of variation of temperature coefficient with scale value and Table 5 show clearly the general tendency of the temperature coefficient to increase positively with the scale value. This very evident relation does coincide with the theory.

As suggested in the last section, the results that furnish the poorest check with the theory are those connected with high sensitivity. Previous experience has shown that observations with magnetometers of this type set for high sensitivity are often unreliable, since the condition of instability of the magnetic system has been approached.

Finally, this variation of temperature coefficient with scale value is of little practical importance. The change is due to an apparent increase or decrease in  $Z$ , and if this is not greater than the value given in sec. B-IV the temperature effect may be neglected. The change in  $Z$ , however, must be taken care of in the base correction in field procedure.

---

<sup>11</sup> See W. E. Pugh: Temperature Compensation on a New Magnetic System for Schmidt Vertical Balances. Thesis, 1932, Colorado School of Mines.

### 5. Possible Sources of Error

Visual tests were made to ascertain whether or not the orientation of the magnetometer had any effect. Provided account was taken of the change in scale value, no appreciable change in the temperature coefficient could be found, regardless of the angle of orientation.

The experiment subject to the greatest error was probably that of determination of  $\mu$ , the temperature coefficient of the magnetic moment

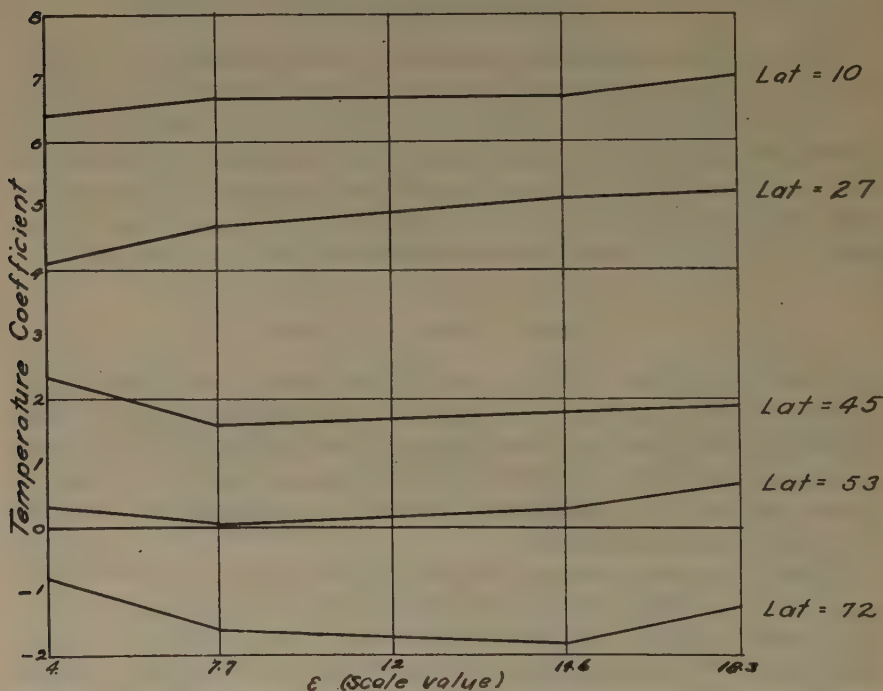


FIG. 14.—TEMPERATURE COEFFICIENT AS FUNCTION OF SCALE VALUE, FOR VARIOUS LATITUDES.

of the system, because of the difficulty in setting up the apparatus accurately. Hence most of the discrepancy between theoretical and observed coefficient may be charged to an error in the value of  $\mu$ . It seems probable, then, that the observed values in most cases are more nearly correct than the theoretical.

Other sources of error lie in the distribution and induction coefficients, which were neglected and may have had some effect.

It is believed that the results of the temperature tests are as accurate as could be obtained under the circumstances. The values of the coefficients certainly are within the usual observational error of such experiments.

## SUMMARY

(C. A. HEILAND)

The angle of deflection in magnetic intensity variometers indicates a balance between the magnetic force component to be measured and another known force, which is either (1) of a magnetic, or (2) of a mechanical nature (torsion of wires, gravity moment). Only in the first case can the influence of temperature be avoided, as the temperature coefficient of the needle cancels; in the second case, a compensation for temperature is possible, as its magnetic effect can be partly neutralized by an opposing "mechanical" effect. Although the magnetic effect is usually reduced as much as possible by using systems of great moment, as a rule it remains greater than the mechanical effect. Then additional compensation is required, which may be of a magnetic (auxiliary magnet) or of a mechanical nature (temperature affecting torsion of suspensions or the position of the center of gravity, etc.) In vertical magnetometers, the last type of compensation is used mostly. In the old type of Schmidt balance it was accomplished by shifting the blades; in the new system, by suitably arranged temperature and latitude spindles.

The theory of the temperature effect on a magnetic system is given in two parts. First, the magnetic temperature coefficient only is considered, in its effect on scale value and reading. The magnetic T.C. of the scale value is negligible ( $= \mu\epsilon$ ),  $\mu$  being the temperature coefficient of the magnetic moment. The magnetic T.C. of the reading is very large (T.C.  $= -\mu Z$ ), *proving that the T.C. depends on the latitude.*

Second, the combined "mechanical" and "magnetic" effects are discussed. For the T.C. of the scale value: T.C.  $= (\delta + \mu)\epsilon$ ,  $\delta$  being the expansion coefficient of steel, the T.C. of the scale value is again negligible. For the temperature coefficient of the reading, T.C.  $= -Z_0(p + \mu)$ ,  $Z_0$  being the vertical intensity for which the system is adjusted,  $p$  representing the "mechanical" temperature coefficient; it may be made negative and equal to  $\mu$  by a suitable arrangement of the masses in the system.

There is an influence of latitude upon a compensated system, as  $Zp$  remains practically constant, but  $-Z\mu$  changes. The temperature coefficient, therefore, increases with an approach of the equator. The change is not very great; a system compensated for Golden may be used without readjustment practically throughout the United States.

If the T.C. is expressed in gammas, changes in scale value should not affect it; however, there may be such an influence, if a change in the  $\epsilon$ -screw changes the lateral position of the center of gravity. In the magnetic system investigated, the T.C. increases with scale value; the increase is small for high, great for low magnetic latitudes; yet, in both cases close to the observational error. The theory shows also that, if

the T.C. is not determined near the reading 20, the deflection of the system enters, as it changes  $Z$ ; however, the influence is small.

Computations of T.C. based upon the theory as outlined have been checked by the experiments with an accuracy of  $\pm 0.3\gamma$  and less.

The proposed experimental work required a number of preliminary investigations, such as the determination of the magnetic moment of the system and of its temperature coefficient, investigations into the most suitable procedures for changing temperatures, scale values and latitudes. It was found that the simultaneous recording of the magnetic variations was required, which in turn necessitated a fairly constant temperature in the recording room. For the accurate determinations of temperature coefficients, arrangements had to be made to use always the same temperature gradient in order to obtain comparable values for different scale values and latitudes. The amount of lag of the reading behind the recorded temperature was accurately determined for the gradients employed.

Numerous temperature curves were recorded for normal conditions at Golden, for different latitudes varying between vertical intensities near the magnetic equator and intensities exceeding  $Z$  at the pole, and, finally, for different scale values.

The results are shown graphically, and are in close accord with the theoretical deductions. They show a decrease (Fig. 12) of the temperature coefficient with increase in latitude.

It is concluded that the new magnetic system gives reliable results for a great variety of latitude, scale value and temperature conditions. The derivation of the complete theory makes it possible to determine accurately the influence of any changes in these factors upon the T.C., and to calculate the change in T.C. for any changes in the distribution of the masses of a magnetic system.



## A Magnetic Gradiometer

BY IRWIN ROMAN\* AND THOMAS C. SERMON,† HOUGHTON, MICH.

(New York Meeting, February, 1934)

IT has been known for many years that when a wire is moved in a magnetic field, an electromotive force is developed which is proportional to the rate at which the wire is moved in a direction perpendicular to the magnetic intensity and to the magnetic intensity itself. If the ends of the wire are connected to a current indicator, the current behaves exactly as though the source of electromotive force were a galvanic cell. If a wire is wound circularly and rotated uniformly around a diameter not parallel to the intensity, the current flowing through the wire will be alternating of sinusoidal shape. If, instead of a single loop, there are several turns wound in a short helix, the electromotive force developed will be approximately proportional to the number of turns, the area of the helix and to the speed of rotation. The maximum electromotive force will be developed when the axis of rotation is perpendicular to the field; if this is not so, only the component of the intensity that is perpendicular to the axis of rotation is effective. This is the principle of the usual earth inductor. With a few turns of wire and comparatively slow rotation, it is possible to produce a considerable deflection of a galvanometer.

If two similar coils are rotated together at two different points for which the magnetic field intensities perpendicular to the axes of rotation are different, the electromotive forces developed will each depend on its corresponding intensity and be a measure of that intensity. If the intensities are sufficiently different so that the electromotive forces may be compared, the two intensities may be compared. This is the principle



FIG. 1.—MAGNETIC GRADIOMETER.

---

Manuscript received at the office of the Institute Nov. 27, 1933.

\* Assistant Professor of Mathematics and Physics, Michigan College of Mining and Technology.

† Instructor in Mathematics and Physics, Michigan College of Mining and Technology.

on which the magnetic gradiometer has been designed. So far as known, there has been no work done on such an instrument, all previous work having been done with a single instrument moved from one point to another. The present instrument has been constructed to test the possibilities of the method and not to investigate the refinements. The instrument, a photograph of which is shown in Fig. 1, was constructed during the summer of 1933. Use was made entirely of materials that were on hand and parts were designed during the course of construction with special reference to the machines and tools available in the shops of the Michigan College of Mining and Technology. As will be seen later, many individual items of design will require more careful consideration in order to bring the instrument to even an approximate state of refinement. Field tests indicate that in its present form the instrument is not only reliable but is more sensitive than the authors had expected. Personal equations have been reduced and observations have been repeated with close agreement, even after several weeks.

### CIRCUIT

In order to compare the electromotive forces generated in the two coils, it is necessary either to measure each electromotive force separately

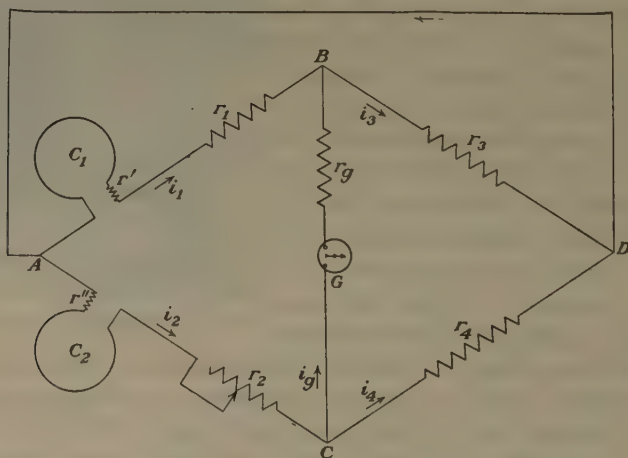


FIG. 2.—SIMPLIFIED CIRCUIT.

or to measure some quantity which is determined by and which determines the degree of inequality. Because of the small electromotive forces developed, and more especially because the electromotive forces depend on the speed of rotation, it did not seem feasible to attempt the measuring of the separate electromotive forces with a view to calculating the differences. Similarly, the algebraic sum and difference of the two electromotive forces would determine the

separate electromotive forces if the speeds could be maintained accurately constant, but this condition seemed too difficult of accomplishment within the necessary limits of tolerance. Accordingly, a circuit was devised which would measure the ratio of the two electromotive forces. This circuit is shown diagrammatically in its simplified form in Fig. 2. In the actual circuit, shown in Fig. 3, a reversing switch is used to help eliminate inaccuracies in the resistances used. In its simple form, the circuit consists of a Kirchhoff net with six elements. The two coils of which the electromotive forces are to be compared are connected by

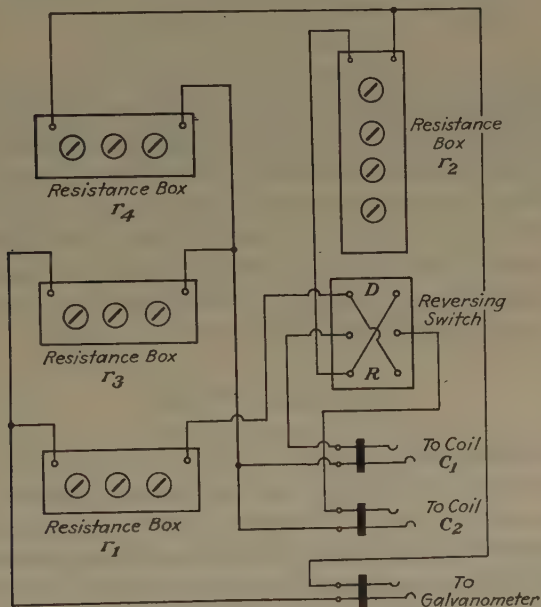


FIG. 3.—ACTUAL CIRCUIT.

the corresponding leads joined at the point *A*, with the other end of each coil connected to two resistances in series, the farther ends of these resistances being connected at *D*. The point *D* is connected to the point *A* by a wire of negligible resistance. The galvanometer or other current indicator is connected between the points *B* and *C*, separating the two resistances of each branch of the network.

#### *Equations of Balance*

Since *A* and *D* are at the same potential, the electromotive force developed by the coil *C*<sub>1</sub> (Fig. 2) is:

$$e_1 = i_1(r_1 + r_3 + r')$$

where *r'* is the resistance of the coil *C*<sub>1</sub> itself, *i*<sub>1</sub> is the current through that branch of the network when the circuit is balanced and no current

flows through the galvanometer  $G$ . Similarly, the electromotive force developed by the coil  $C_2$  is:

$$e_2 = i_2(r_2 + r_4 + r'')$$

Since  $B$  and  $C$  are at the same potential, it follows that:

$$i_1 r_3 = i_2 r_4$$

Hence the ratio of the two electromotive forces is:

$$\frac{e_2}{e_1} = \frac{(r_3)(r_2 + r_4 + r'')}{(r_4)(r_1 + r_3 + r')}$$

which depends only on the resistances in the circuit when no current flows through the galvanometer. If a galvanometer could be made to follow the fluctuations in the potential difference between  $B$  and  $C$ , as in the Rosa Curve Tracer, the balance would furnish the instantaneous ratio. Actually, the ratio is an integrated ratio and if  $C_1$  and  $C_2$  are not in the same phase, the galvanometer mirror or needle will fluctuate. The circuit itself is limited in sensitivity only by the accuracy with which the resistances are known, the sensitivity of the current detecting device and the method of contacting the coils.

#### *Sensitivity of Circuit*

If the circuit is not balanced, a current  $i_g$  will flow through the galvanometer. For definiteness, let the currents flowing through the various elements of the net be positive when in the direction indicated by the arrows in Fig. 2. Then, neglecting the resistances of all lead wires, connections and switches, the equations of the circuit are:

$$\begin{array}{ll} \text{At } B: & i_3 = i_1 + i_g \\ \text{At } C: & i_2 = i_4 + i_g \\ \text{Through } ABDA: & e_1 = i_1 r_1 + i_1 r' + i_3 r_3 \\ \text{Through } ACDA: & e_2 = i_2 r_2 + i_2 r'' + i_4 r_4 \\ \text{Through } CBDC: & i_4 r_4 = i_g r_g + i_3 r_3 \end{array}$$

Since  $e_1$ ,  $e_2$  and the resistances may be considered as known, there are thus five equations in the five currents. Eliminating all of the currents except  $i_g$ , this system of equations leads to the relation:

$$i_g = \frac{a_2 e_2 - a_1 e_1}{J}$$

where

$$\begin{aligned} a_1 &= \frac{r_3}{r_1 + r' + r_3} & a_2 &= \frac{r_4}{r_2 + r'' + r_4} \\ J &= r_g + a_1(r_1 + r') + a_2(r_2 + r'') \end{aligned}$$



Hence:

$$e_2 = \frac{a_1}{a_2}e_1 + \frac{J}{a_2}i_g$$

The first term is the value of  $e_2$  for a perfect balance, while the second term shows the increase in  $e_2$  necessary to cause a current  $i_g$  to flow through the galvanometer and is independent of the value of  $e_1$ . This second term is a measure of the tolerance in  $e_2$  when the circuit is balanced experimentally.

As a numerical example of the sensitivity, assume:

$$r' = r'' = 19, \quad r_3 = r_4 = 481, \quad -r_1 = 500, \\ r_g = 300 \text{ and write } r_2 = 500 + x$$

For definiteness we may assume all resistances to be measured in ohms, currents in amperes and electromotive forces in volts, but any self-consistent system of units may be used. For the case selected, we have:

$$a_1 = \frac{481}{1000} \quad a_2 = \frac{481}{1000 + x} \\ J = 300 + \frac{(481)(519)}{1000} + \frac{(481)(519 + x)}{1000 + x} \\ \frac{J}{a_2} = \frac{(300)(1000 + x)}{481} + \frac{(1000 + x)(519)}{1000} + (519 + x) \\ = 1661.7 + 2.1427x$$

For a given value of  $e_1$  the value for  $e_2$  for balance is

$$e_2 = \left(1 + \frac{x}{1000}\right)e_1$$

and the tolerance is  $(J/a_2)I$  where  $I$  is the least detectable current through the galvanometer. Thus the ratio of  $e_2$  to  $e_1$  may be determined with a tolerance of  $JI/(a_2e_1)$  which decreases as  $e_1$  increases. For small values of  $x$ , which means values of  $r_2$  near 500, and for  $I = 10^{-8}$ , the value of  $JI/a_2$  is about  $1.66 \times 10^{-8}$ . For  $e_1 = 0.01$ , the tolerance in the ratio  $e_2/e_1$  is  $1.66 \times 10^{-3}$ , or slightly less than two parts in a thousand. For values of  $r_2$  less than 500, the tolerance is smaller than this value and for values of  $r_2$  larger than 500, the tolerance is larger, but it remains less than two in a thousand unless  $r_2$  exceeds the value 658, corresponding to a value 1.158 for  $e_2/e_1$ . This conclusion is in agreement with the actual experimental observations. Actually, the galvanometer used will detect a current of about  $10^{-9}$  amp. under favorable circumstances, but the authors have preferred to be conservative in their interpretations, postponing the closer evaluations until a more refined instrument has been built and tested by actual field surveys.

It was supposed at first that the building of a phantom circuit would be a short and simple task, but this was not the case. The first circuit tried replaced the two coils by two dry cells, but it was impossible to

effect a balance with any consistency. This was analyzed as due to the fact that the dry cells were old and had deteriorated. Accordingly, new dry cells were selected from a shipment that had just arrived from the manufacturer. These eliminated the difficulty of effecting a balance, but the balance was found to be different at various times during the course of an afternoon, although the cells were on open circuit between readings, beyond a common junction at the point *A* (Fig. 2). While effecting a balance, a tapping key was used, so that only a very small amount of current was drained from the cells. Finally a phantom circuit was devised in which the coils were replaced by two one-ohm resistances in series, the potential drop across these two resistances, caused by a single dry cell, being used as the electromotive forces to be compared. The resistances in parallel with the one-ohm resistances were so large that it was safe to assume that the current drain from the circuit was negligible. With this phantom circuit, the balance was quickly effected and the ratio of the two electromotive forces remained constant over several days. The difficulties of building the phantom circuit illustrate the sensitivity and reliability of the circuit.

#### PRESENT INSTRUMENT

To test the theory qualitatively, the instrument shown in Fig. 1 was constructed with a view to an early completion rather than the best possible design. The materials were selected from those on hand and in many instances were manifestly not the best for the purpose. The dimensions were selected for strength rather than convenience and accordingly the present instrument is to be considered as experimental.

The frame is oak with a square cross-section  $1\frac{1}{2}$  in. on a side. The frame is about  $5\frac{1}{2}$  ft. long and about 18 in. wide, as may be seen by comparison with the man in Fig. 1. Near the center are two cross members and on each side of these cross members is a pair of diagonal bracings.

Across the center is the main driving shaft terminating on one side in a handle for turning the coils and on the other in the main driving gear. Mounted on the side of the frame opposite the handle are two transmission shafts, each carrying a gear at each end. The main driving gear meshes with one of the gears on each transmission shaft and the gear at the other end of the shaft meshes with a gear rigidly fastened to the shaft of one of the coils. In this way, turning the crank handle results in turning the two coils at the same rate and by proper adjustment of the various gears, the two coils are maintained in parallel planes.

The coils are mounted to rotate about axes accurately at right angles to the length of the frame and 4 ft. apart. The coils are of oak, the inner diameter being about 9 in., the outer about 12 in. and the groove about  $\frac{1}{2}$  in. deep and 1 in. wide. The two coils were made as nearly alike as possible and each was wound with 375 turns of No. 22 copper wire, cotton-

covered and paraffined; the entire coils were varnished to make them waterproof.

Each coil is connected to a commutator rigidly mounted on its shaft. The commutator is of the double type and arranged so that when the brushes are placed on the center sections it acts as a reversing commutator; when the brushes are placed on opposite outer sections, the commutator acts as a pair of slip rings. Thus, by properly arranging the brushes, either direct or alternating current may be taken from the coils. The brushes are of the usual carbon type and each is carried in a bakelite brush cup threaded through a brass brush block which may be set at any azimuth around the coil shaft.

The tripods are of the usual transit type and each mounting base is of oak bolted to a brass plate carrying a shoulder threaded to fit the tripod. One tripod is used to hold the frame and circuit box while the other holds the galvanometer and serves also as a field table for recording the observations.

The circuit box carries the four resistance boxes and the reversing switch. Each of the two coils is connected into the circuit by means of a telephone-type jack mounted in a bakelite panel on the top of the box; the galvanometer is similarly connected. The resistance  $r_2$  consists of a four-dial decade box with a least count of  $\frac{1}{10}$  ohm; this is mounted in the upper half of the circuit box with its switch dials accessible on top. The resistances  $r_1$ ,  $r_3$  and  $r_4$  consist of three-dial decade boxes with a least count of one ohm; these are mounted in the lower half of the circuit box with the switch dials down and accessible by holes drilled through the bottom of the box. A false bottom screwed to the box protects the bottom of the box and permits easy resetting of the dials if desired. A slip cover protects the top of the circuit box when not in use. The reversing switch is mounted on the side of the box so that its bakelite rocking arm is flush with the side of the box when the switch is in the neutral position.

The galvanometer is a Leeds & Northrup 2400A type, with a telescope and scale. The original suspension had been broken and the replacement suspension was such that the galvanometer had a sensitivity of about  $10^{-8}$  amp. per division; under favorable conditions, it has been possible to detect a current of the order  $10^{-9}$ . It was found convenient to remove the scale and to use a landmark for detecting a motion of the mirror, since the galvanometer was used as a null instrument.

## FIELD WORK

### *Procedure*

After a station has been selected, the gradiometer tripod is leveled and rotated so that the axis of the frame is in the magnetic meridian.



The brushes are set so that they are perpendicular to the direction of the magnetic field and in the center segment, the insulating segment of the commutator being in the plane of the coil. In this way, the current through the galvanometer is a rectified current while that through the coil is sinusoidal alternating. The binding posts, which are connected to the brushes by means of flexible leads, are connected into the circuit by means of telephone plugs inserted into the corresponding jacks of the circuit box, and the galvanometer is similarly connected. The circuit box is placed on top of the frame with the switch opposite the operator who turns the crank, thus placing the controls of the resistance  $r_2$  on the near side of the circuit-box top. The galvanometer tripod is leveled and connected to the circuit box by a twisted cable. When stations are to be taken within

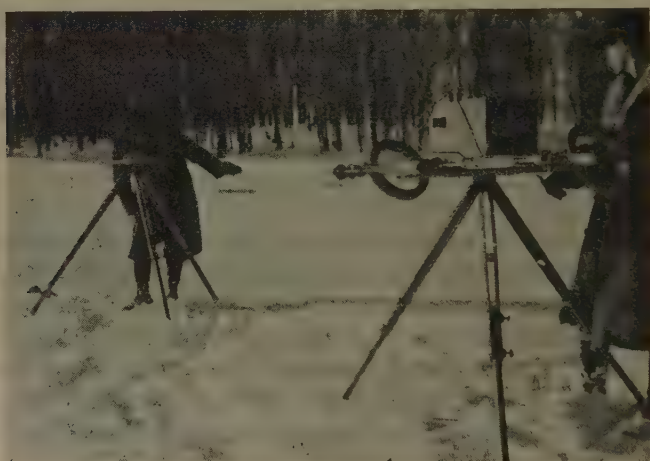


FIG. 4.—MAGNETIC GRADIOMETER IN THE FIELD.

200 ft. of each other, the galvanometer lead is made long enough so that one setting of the galvanometer is sufficient for all of the stations within that range; when stations are too far apart for this arrangement, the tripod for the galvanometer must be set up each time, and for these cases, the lead is made between 15 and 25 ft. long.

After the apparatus has been set up, including the checking or setting of all connections, switches and brushes, the observer at the galvanometer signals the operator by voice or arm position when the galvanometer has come to rest. The operator rotates the coils slowly in order to get an approximate balance. The observer indicates whether the setting of  $r_2$  is too large or too small and the operator makes the adjustment accordingly. In this manner, the resistance  $r_2$  is rapidly adjusted to a balance, after which the operator calls the reading to the observer, who records the value in the notes. This technique tends to eliminate observational prejudice. Next the reversing switch is thrown and a new balance



obtained, the purpose of this being to counteract errors in the resistances and to check the readings. After these two readings are taken, the gradiometer is rotated  $180^\circ$  on the tripod head and the brushes reset. The two balances are then made as before, the purpose of this reversal being to eliminate the effects of differences between the two coils and their brush contacts.

After making the four observations in the magnetic meridian, the brushes are set in the plane of the frame and the axis of the frame turned into the east-west plane. The four observations are then made in this plane perpendicular to the magnetic meridian. The eight observations constitute a complete set for the station. It is hoped that eventually the axis will be set in three mutually perpendicular directions, so as to obtain the vector gradient, but the present instrument is not adapted to such an arrangement. A photograph of the apparatus in operation is shown in Fig. 4.

### *Calculation of Gradient*

As was derived in the section on the equations of balance of the circuit, the ratio of the two electromotive forces is:

$$\frac{e_2}{e_1} = \frac{r_3(r_2 + r'' + r_4)}{r_4(r_1 + r' + r_3)}$$

If  $r_3 = r_4$  and  $r_1 + r' + r_3 = M$  while  $r_2 = r_1 + x$ , then the ratio simplifies to

$$\frac{e_2}{e_1} = 1 + \frac{x}{M}$$

In actual use, the values of  $r_1$ ,  $r_3$  and  $r_4$  have been made equal to 500, 481 and 481 ohms, respectively, while the measured resistance of each of the coils has been 19 ohms. For this case,  $M = 1000$  and the calculation of the ratio  $e_2/e_1$  has been simplified.

Let the axial plane be defined as the plane through the centers of coils of the gradiometers and perpendicular to the axes of rotation of the coils. Then only the components of the magnetic fields in this axial plane will be effective in inducing an electromotive force in the coils as they rotate. Let this component be  $U$  and let the center of symmetry be selected as the origin. If we expand the function  $U$  in a Maclaurin's series, we have, to the first order:

$$U = U_0 + x \left( \frac{dU}{dx} \right)_0$$

If the distance between the axes of rotation of the coils is taken as unity, the coils may be considered as having their centers at  $-\frac{1}{2}$  and  $+\frac{1}{2}$ , respectively. We shall assume that the field is sufficiently smooth

over the extent of the gradiometer so that its effective value over each coil is the same as its value at the center of that coil. Then, to the first order:

$$\frac{U_2}{U_1} = \frac{U_0 + \frac{1}{2}\left(\frac{dU}{dx}\right)_0}{U_0 - \frac{1}{2}\left(\frac{dU}{dx}\right)_0} = 1 + \frac{\left(\frac{dU}{dx}\right)_0}{U_0 - \frac{1}{2}\left(\frac{dU}{dx}\right)_0}$$

Neglecting the term  $-\frac{1}{2}\left(\frac{dU}{dx}\right)_0$  with respect to  $U_0$ , this becomes:

$$\frac{U_2}{U_1} = 1 + \frac{1}{U_0}\left(\frac{dU}{dx}\right)_0$$

The electromotive force developed is approximately equal to:

$$e = 2\pi r^2 U w N \times 10^{-8} \text{ volts}$$

where  $w$  is the number of revolutions per second,

$r$  is the effective radius of the coil, in centimeters,

$N$  is the number of turns of wire on the coil,

$U$  is the effective field for the coil, in Gauss.

Hence we may write:  $U = ke/w$  where  $k$  is a constant for a particular coil. Let the coils be identified by the symbols  $C_1$  and  $C_2$ , respectively. Let the coil position be direct when the coil  $C_1$  is in a position selected as principal and let the reversing switch be considered as direct when coil  $C_1$  is in series with the resistance  $r_1$ . As a matter of notation, we may use the symbols  $DD$ ,  $DR$ ,  $RD$  and  $RR$ , where the first letter refers to the coil position and the second to the switch position,  $D$  and  $R$  representing direct and reversed, respectively. We shall consider the principal position as at  $+\frac{1}{2}$  and always calculate the relative increase of the principal intensity over the secondary. Let  $e_i$  represent the electromotive force developed in the coil in series with the resistance  $r_i$ ; and  $V_i$  represent the electromotive force developed in the coil  $C_i$ , while  $P$  and  $S$  will be used to represent the electromotive force of the coil in the principal and secondary positions, respectively.

Then the four cases are:

$DD$	$\begin{cases} P = V_1 = e_1 \\ S = V_2 = e_2 \end{cases}$	$\frac{P}{S} = \frac{e_1}{e_2}$
$DR$	$\begin{cases} P = V_1 = e_2 \\ S = V_2 = e_1 \end{cases}$	$\frac{P}{S} = \frac{e_2}{e_1}$
$RD$	$\begin{cases} P = V_2 = e_2 \\ S = V_1 = e_1 \end{cases}$	$\frac{P}{S} = \frac{e_2}{e_1}$
$RR$	$\begin{cases} P = V_2 = e_1 \\ S = V_1 = e_2 \end{cases}$	$\frac{P}{S} = \frac{e_1}{e_2}$

As shown above, for the particular settings used,

$$\frac{e_2}{e_1} = 1 + \frac{x}{1000}$$

For a particular azimuth, a principal coil is selected, oriented with respect to the magnetic meridian, and the gradient is calculated with respect to this principal direction, not with respect to the circuit. Specifically, in the magnetic meridian the principal direction is selected as north and a positive gradient implies that the field component is increasing to the north; at right angles to the magnetic meridian, the principal direction is selected as east and a positive gradient implies that the vertical component of the magnetic field is increasing to the east. In the magnetic meridian, the effective component is that in the magnetic vertical plane through the center of the gradiometer, but for the short distances involved this is essentially the total intensity; in the east-west plane, the effective component is essentially the vertical component of the field.

If the two coils are exactly alike, the coil constants  $k_1$  and  $k_2$  will be exactly equal and the ratio of the field intensities will be the same as the ratio of the induced electromotive forces. If they are not alike, we may assume that they are so nearly alike that we may write  $k_2 = k_1(1 + y)$  where  $y$  is so small that powers beyond the first may be neglected. Then, for the cases  $DD$  and  $RR$  the ratio of the fields  $U_p$  and  $U_s$  is  $k_1e_1/k_2e_2$  where  $U_p$  and  $U_s$  are the effective intensity components at the principal and secondary coils, respectively. It should be noted that the angular speed disappears from this relation because the coils move together. The ratio  $U_p/U_s$  in the cases  $DR$  and  $RD$  is  $k_2e_2/k_1e_1$ . In the former cases, the ratio of the principal to the secondary intensity component is:

$$\frac{U_p}{U_s} = \frac{k_1e_1}{k_2e_2} = \left( \frac{1}{1+y} \right) \left( \frac{1000}{1000+x} \right) = 1 - y - \frac{x}{1000}$$

In the latter cases, this ratio is

$$\frac{U_p}{U_s} = \frac{k_2e_2}{k_1e_1} = (1+y) \left( 1 + \frac{x}{1000} \right) = 1 + y + \frac{x}{1000}$$

If we define the gradient as:

$$G = 1000 \left( \frac{U_p}{U_s} - 1 \right)$$

then we have:

$$\begin{aligned} G_{DD} &= -x_{DD} - 1000y \\ G_{DR} &= +x_{DR} + 1000y \\ G_{RD} &= +x_{RD} + 1000y \\ G_{RR} &= -x_{RR} - 1000y \end{aligned}$$

where the subscripts indicate the positions in which the observations were taken. Hence the arithmetical average of the four determinations of  $G$  is:

$$G_0 = \frac{1}{4}(x_{DR} + x_{RD} - x_{DD} - x_{RR})$$

independently of the coil constants, if we neglect the powers beyond the first. Thus, reversing the coils tends to eliminate the variations of the coils from each other.

### *Plotting Results*

After the gradients are calculated, it is convenient to plot the results on a survey map in order to represent them pictorially and to interpret them. If the magnetic inclination is  $V$ , the vertical component of the intensity is the actual total intensity multiplied by  $\sin V$ . Accordingly, the north gradient is multiplied by  $\sin V$  before plotting.

### TEST SURVEYS<sup>1</sup>

For the purpose of testing the present apparatus, the gradiometer was used in three areas; the first was one in which it was reasonable to assume that the magnetic intensity was uniform in a vector sense; the second was one in which high magnetic anomalies were known to exist; the third was one in which little was known geologically or geophysically.

*Pilgrim River Station.*—Because it has been used as a base station for magnetic work done by the College, this station was selected as lying in a region without magnetic anomalies. The work at this station gave a gradient that was practically negligible and the principal contribution of these results was to emphasize the importance of careful brush setting. Errors that cannot be eliminated have proved to be very troublesome when the brushes were not set at right angles to the magnetic component.

*Isle Royale Survey.*—This area is one of high magnetic anomalies. The ordinary dip needle shows noticeable variations over a few feet. After some preliminary work in this region, to eliminate difficulties in operation, two lines were laid out at right angles, but the early arrival of cold weather prevented the completion of the survey beyond six stations. The results for these six stations are shown in Table 1 and Fig. 5.<sup>2</sup> The

<sup>1</sup> In these tests settings were quite consistent and could be repeated with but little change after a lapse of several days. Also, interchanging observer and operator has resulted in no material variation in the settings and in several cases where the operator deliberately tried to mislead the observer the attempts were unsuccessful. The observer has been able in some cases to tell from the behavior of the galvanometer whether the resistances were connected in the proper manner and to detect poor brush contacts, faulty switch position and even lack of parallelism in the coils or brush settings. When functioning properly the galvanometer indicator is fairly steady.

<sup>2</sup> Because of the complexity of this region and the small number of stations completed no correlation has been attempted. It is hoped that a program already planned will make a correlation possible in the near future.



station numbers represent the distances in feet measured approximately  $13^\circ$  south of west from the initial station.

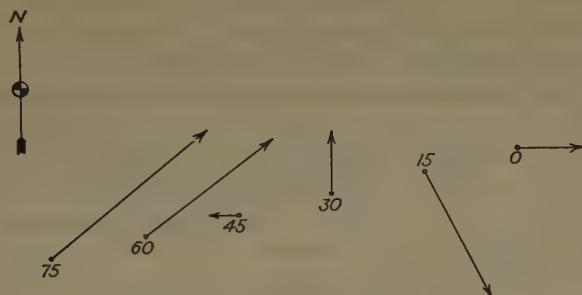


FIG. 5.—ISLE ROYALE SURVEY.

*Trout Creek Survey.*—This area was selected because of what appeared to be outcropping Keweenawan traps for which no definite structural correlation has been attempted. So far as known locally, there has been no systematic study made of this region and it was thought to be a desir-

TABLE 1.—Results at Isle Royale  
October 23, 1933

Sta- tion	Inclina- tion	Princi- pal Coil	Observer	Resistances				Gradients				Average Gradient
				DD	DR	RD	RR	DD	DR	RD	RR	
0	72°	N	S	510	490	510	488	-10	-10	10	10	2
	0	E	R	507	491	512	490	-7	-9	12	10	
15	72°	N	S	519	482	510	490	-19	-18	10	10	-4
	0	E	R	508	494	512	490	-8	-6	12	10	2
30	72°	N	S	508	493	511	489	-8	-7	11	11	2
	0	E	R	509	490	510	490	-9	-10	10	10	
45	72°	N	S	512	488	511	488	-12	-12	11	12	-1
	0	E	R	510	490	508	492	-10	-10	8	8	
60	72°	N	S	504	496	512	487	-4	-4	12	13	3
	0	E	R	508	493	515	485	-8	-7	15	15	4
75	72°	N	S	506	496	514	487	-6	-4	14	13	4
	0	E	R	507	495	517	484	-7	-5	17	16	5

able location in which to test the method without prejudice. The results of the survey are shown in Table 2 and Fig. 6, with the omission of some observations at the north end of the line, within the town of Trout Creek, and a few intermediate stations which add no information to the map.<sup>3</sup>

<sup>3</sup> The work done in this region has been of too small an extent to justify publishing any conclusions beyond the definiteness with which the gradiometer has recorded the magnetic effects.

*Projects.*—The work of testing the instrument has been less than might be desired. In both of the areas mentioned a definite program has been arranged and it is to be hoped that conditions will permit the completion of both projects at an early date. The program of testing also includes an area containing a known mineralized fissure, one in which the Hotchkiss Superdip shows a large anomaly and a line across the Keweenaw fault.

TABLE 2.—*Results at Trout Creek*  
November 15, 1933

Station	Inclination	Principal Coil	Observer	Resistances				Gradients				Average Gradient
				DD	DR	RD	RR	DD	DR	RD	RR	
0	75°	N	S	510	490	510	490	-10	-10	10	10	
	0	E	R	510	491	509	492	-10	-9	9	8	
2,500	75°	N	S	511	489	512	489	-11	-11	12	11	
	0	E	R	510	490	510	491	-10	-10	10	9	
5,000	75°	N	S	514	487	510	490	-14	-13	10	10	-2
	0	E	R	512	490	512	490	-12	-10	12	10	
7,500	75°	N	S	515	487	510	489	-15	-13	10	11	-2
	0	E	R	511	490	511	489	-11	-10	11	11	
10,000	75°	N	S	510	490	511	490	-10	-10	11	10	
	0	E	R	510	490	510	490	-10	-10	10	10	
12,500	75°	N	S	514	486	510	489	-14	-14	10	11	-2
	0	E	R	510	490	509	491	-10	-10	9	9	
15,000	75°	N	S	512	488	511	488	-12	-12	11	12	
	0	E	R	510	490	511	490	-10	-10	11	10	
17,500	75°	N	S	516	484	511	490	-16	-16	11	10	-3
	0	E	R	512	489	512	489	-12	-11	12	11	
20,000	75°	N	S	510	491	511	489	-10	-9	11	11	1
	0	E	R	511	490	510	488	-11	-10	10	12	

#### PROBLEMS OF DESIGN

In the course of the work with the present instrument numerous problems of design have been presented. Some of these may be mentioned without detailed discussion:

1. Metal might be substituted for wood in the instrument.
2. The bearings should be given careful consideration.
3. The design of the coils should be made with regard to mechanical strains and increased speeds of rotation.
4. The coils might possibly be wound in various planes properly connected to the commutator.
5. The best type and size of wire should be investigated and a larger resistance built into the coil itself.

6. The coils should be wound so as to be as nearly alike as possible.  
 7. The coils should be geared up with respect to the crank handle.  
 8. As many of the resistances as possible should be of the fixed-coil type.

9. A current detector to be used as a null instrument should be selected or built in accordance with the conditions of the circuit.

10. With the present instrument direct current has given better results than alternating, but it is conceivable that under favorable conditions alternating current can be used to advantage especially in connection with a vacuum tube amplifier.

11. If the gradiometer can be built light enough it could be mounted at right angles to the magnetic field instead of level. In addition to simplifying the field technique, this would have the advantage of measuring the gradient of the actual magnetic intensity.

### SUMMARY AND CONCLUSIONS

In this paper a magnetic gradiometer has been described for determining the space rate at which the earth's magnetic field is changing. This instrument consists of two similar coils rotating around parallel shafts in such a manner that the planes of the coils always remain parallel. Since the electromotive force induced in a coil is proportional to the field in which the coil rotates, the ratio of the fields at the two coils may be measured by the ratio of the two electromotive forces. This ratio is measured by a specially devised Kirchhoff net.

To test the method a preliminary instrument was built and proved by actual tests to check the theory beyond expectations. Examples of the field tests have been included as indicative of what may be done.

Some of the problems of design have been discussed with reference to the building of an improved gradiometer as soon as conditions permit.

### ACKNOWLEDGMENTS

The authors wish to express their thanks to Prof. James Fisher, head of the Department of Mathematics and Physics of the Michigan College of Mining and Technology, for his interest and coöperation in the development of this instrument and for permission to publish these results. They also wish to thank the members of the shops for the prompt assistance given during the construction of the apparatus.

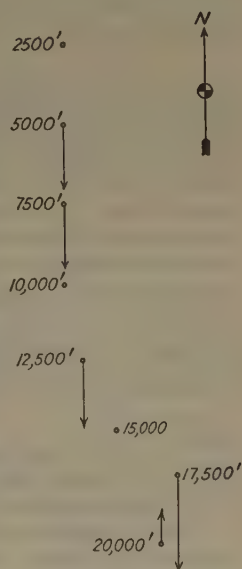


FIG. 6.—TROUT CREEK SURVEY.

## DISCUSSION

(E. DeGolyer *presiding*)

J. FISHER,\* Houghton, Mich.—I would like to emphasize one feature of this instrument. With it an attempt is made to obtain the horizontal magnetic gradient, in a way comparable to that in which the horizontal gravity gradient is obtained with the torsion balance.

E. DEGOLYER,† New York, N. Y.—Do you believe the method presents improvements over the ones in use at present?

F. L. PARTLO,‡ Houghton, Mich.—It measures the gradient directly, and gives results that are dependable and can be repeated.

E. DEGOLYER.—Yes, but will the data be superior to those obtained by existing methods and instruments?

F. L. PARTLO.—Yes, the gradiometer has a higher degree of accuracy than either the Superdip or the magnetic balances.

M. K. HUBBERT,§ New York, N. Y.—It may clarify the situation somewhat to point out certain analogies between the magnetic and gravitational techniques of observation. When studying the force of gravity, you can use a pendulum to measure its absolute strength, or you can use a torsion balance to measure the gradient, or the rate of variation of gravity in a given direction. Similarly, when observing the earth's magnetic field, you can use a magnetometer to measure the total magnetic force, or you can use such an instrument as this magnetic gradiometer to observe its variation in a given direction, or its gradient.

E. DEGOLYER.—I am glad you brought that out, because this point is particularly interesting in view of the present tendency in oil work to go over to the use of the pendulum in order to get absolute gravity. The use of the magnetic gradiometer would indicate an opposite tendency in mining work.

M. K. HUBBERT.—Another advantage that should be mentioned in this connection is that in measuring the gradient of the earth's magnetic field we are measuring a constant quantity. The absolute value of the magnetic field varies during the day, unlike the absolute value of gravity which remains constant in time. Therefore, in ordinary magnetic observations corrections must be made for diurnal variation. Fortunately, however, the gradient of the field remains constant in time, despite the changes in absolute value. Therefore, in working with the magnetic gradiometer there is the advantage of making observations on a quantity that requires no correction for temporal variations.

C. A. HEILAND, Golden, Colo. (written discussion).—The principle of the earth-inductor gradiometer was proposed first by H. Haalek<sup>4</sup> in 1925. The arrangement as given by Haalek is as follows: Two coils of equal (or nearly equal) area, turn

---

\* Head, Department of Mathematics and Physics, Michigan College of Mining and Technology.

† Petroleum Geologist.

‡ Assistant Professor of Mathematics and Physics, Michigan College of Mining and Technology.

§ Instructor in Geophysics, Columbia University.

<sup>4</sup>H. Haalek: *Ztsch. f. tech. Physik* (1925) [8] 6, 377–380.



number and orientation are rigidly connected to one another by a shaft. The coils are connected in series and opposition so that, when the shaft is rotated, no electromotive force is produced if the earth's magnetic field is equal at the points where the coils are located. Haalck has calculated that a field difference of the order of 10 gammas will produce a maximum current of about one-half microampere with the suggested coil dimensions, and a frequency of rotation of 30 cycles. A telephone is used as the indicator of balance, and the higher frequency necessary for its operation is obtained by using a multisegment commutator for taking off the differential electromotive force from the rotating shaft.

Haalck proposes to use this instrument qualitatively as a means for locating iron bodies, by determining the direction of the magnetic disturbance vector. For the indication will be zero if the axis of rotation of the two coils is at right angles to the vector. To determine its direction, the axis of rotation of the double coil system may either be tilted until a balance is obtained, or the whole arrangement may be moved from point to point, with horizontal axis of revolution, until a balance indicates that the disturbing object is below the center of the inductor. In other words, a principle similar to that applied in binaural hearing, or in binaural geophone work, is employed.

As far as I know, Haalck has never put his idea into practice, and it is therefore gratifying to note that the authors of this paper have established the practicability of the earth-inductor gradiometer with such good results.

The chief advantage of this instrument appears to lie in the fact that it can be used on moving support. In the experiments with magnetic measurements from airplanes, which I conducted a number of years ago, a similar arrangement was tried with fairly good success, in addition to the constant-speed principle discussed several years ago.<sup>5</sup>

I. ROMAN AND T. C. SERMON (written discussion).—It is still too early to be certain that the present gradiometer will furnish data of better quality and ease of interpretation than previous instruments, but the gradiometer introduces a distinct departure from them. In particular, the circuit is such that the ratio of the two induced electromotive forces is measured directly. The instrument is not a direction finder and is not intended to be a detector of temporal disturbances in a balanced field. It differs from the device suggested by Haalck in that the latter consists of opposed coils to be used as a binaural device. It differs from devices measuring the induced electromotive force in an inductor running at constant speed at different places and different times. The method does not attempt to measure the induced electromotive force or the earth's field. It measures a relative gradient, not the actual gradient, as ordinarily interpreted—as, for example, with the torsion balance for the gravity gradient. For prospecting purposes, the actual gradient is not necessary; the relative gradient and actual gradient are nearly proportional.

The gradiometer, including the balanced coils and the measuring circuit, has several advantages over the previous methods:

1. The coils need not be turned at a known, or even constant, speed. The ratio of the induced electromotive forces is independent of the speed. This eliminates the need for controlling or measuring the speed of rotation, a decided advantage in any arrangement, especially a portable instrument.
2. The gradiometer need not be oriented by trial and error. It is oriented in each of two arbitrary perpendicular horizontal directions and the vector relative gradient is thereby determined.
3. The ratio of the two induced electromotive forces is measured. This is simpler than the measurement of each separate electromotive force with the corresponding accuracy.

<sup>5</sup> C. A. Heiland: *Trans. A.I.M.E.* (1932) 97, 213.

4. The method is sensitive without being delicate. With the circuit, it has been possible to detect the ratio of two apparently equal resistance coils with consistent results. Field readings have been repeated with good agreement.

5. While both the gravimetric and magnetic intensities at a specified point vary with time, the temporal variations of the gradients of both intensities are much smaller than the variations measured in prospecting. A cloud passing in front of the sun will cause a measurable effect on the magnetic intensity at a point, but the effect of that same cloud on the ratio of the two intensities at the coils will be negligible. In the gradiometer the effect of the diurnal variation is negligible while with the magnetometer or Superdip a correction must be made for it.

6. The present arrangement involves an integrated balance, so that extraneous disturbances are not noticed unless they persist over a considerable number of rotations of the coils.

7. The instrument is conveniently portable and needs no outside equipment other than a truck for transportation. No elaborate calibrations or calculations are needed. If desired, the circuit can be calibrated directly.

# Reflection Methods in Seismic Prospecting

By H. M. RUTHERFORD,\* TULSA, OKLA.

(New York Meeting, February, 1932)

THE reflection method in seismic prospecting has aroused much interest in the past few years. The purpose of the present paper is to present the method of reflections in the mapping of geologic structure and also to give some indication of its limitations. The reflection method is well adapted to the mapping of geologic structure in the Mid-Continent fields, and has been found most useful there. The refraction method is ideally suited to the finding of structures, such as domes, where the amount of relief is very large. This explains the brilliant success of the refraction method in the Gulf Coastal region of Texas and Louisiana. The additional fact that salt has a much higher velocity than the surrounding sediments made their discovery much easier. By the use of the reflection method, differences of relief of 25 to 50 ft. to the mile may be detected at a depth of 5000 ft., and the depth points accurately plotted on a map. This is hardly possible by the use of the refraction method.

The reflection method has been in almost continuous use in the Mid-Continent area since 1926, but very little, if anything, has been published until recently<sup>(7)</sup>† regarding either the method or the results. The discovery of several oil fields is now attributed to the use of the reflection method.

Reflection methods have been used by the Germans to find the thickness of the ice of several glaciers.<sup>(2,8)</sup> The depths there considered were of the order of only a few hundred feet. For the method to be of any practical value in this country, it must be able to work to depths of several thousand feet. As was indicated above, this is now possible, though there are many problems connected with the reflection method yet to be solved.

The refraction method requires that the shooting be done over long ranges. It was necessary, for example, to take distances out to several miles in order to penetrate some five thousand feet. Naturally this uses a good deal of dynamite. In the reflection method the distances are much shorter and the amounts of dynamite are much smaller, within limits which will be noted below. The chief distinction between refraction and reflection methods is to be found in the analysis of the seismogram. Refraction shooting makes use of only the first arrival of energy

---

\* University of Tulsa.

† Superior figures in parentheses refer to bibliography at end of paper.

on the seismogram; that is, the minimum time path. In refractions, no use has as yet been made of the later phases, such as the transverse waves. In reflection methods, the seismogram is analyzed and an attempt is made to identify the arrival of energy which is reflected from some interface; for example, the interface between the Viola limestone and its overburden.

Because the first was the only phase on the seismogram that was used in the refraction method, naturally instruments were designed to give a large magnification for the first arrival without regard to the true motion of the ground. With the advent of the reflection method, more care was necessary in the design. When the shot length is small, the surface waves, as well as various refracted waves, arrive before and tend to obscure the reflection. The shot length can be made long enough so that the reflection arrives before the surface, or Rayleigh wave. Also, the period of the instrument can be made short enough so that there is no appreciable magnification of the surface wave. These surface waves have a frequency of about four per second; the reflected waves about fifteen or twenty. It is desirable to have instruments in which the period can be changed to fit the varying conditions to be found in any territory.

#### GENERAL CONSIDERATIONS

The problems connected with the reflection method may be summarized in part as:

1. General design of instruments.
2. Identification of the reflection on the seismogram.
3. The correlation of the reflection with the reflecting bed.
4. Methods of computation.

No complete discussion will be given of the design of instruments, since that is not the purpose of this paper. D. C. Barton<sup>(1)</sup> has given a discussion of the various types of instruments which are in use at the present time. In general, however, it is necessary to have a seismograph with a suitable period, or, better, capable of being varied to suit conditions; and a method whereby the motion may be magnified and recorded on a moving film. This may be accomplished either electrically or mechanically, though most of the seismographs in use at the present time are of the electrical type. Some method must be arranged whereby the instant of blast is recorded in order to get the time of travel of the waves. It is obvious that there must be a timing arrangement, and this is usually accomplished by means of a tuning fork. Most consulting companies assume that the only practical instrument for reflection shooting is the electrical seismograph, but this is not the case. Mechanical seismographs may be made, which will give good results. It is undeniable, however, that it is of great advantage to have all the traces on the same film.



## GENERAL THEORY

When an elastic wave, either longitudinal or transverse, traveling through a stratum of velocity  $V_1$  is incident upon another stratum, of velocity  $V_2$  greater than  $V_1$ , it is in general broken into four parts. If the incident waves are longitudinal, the only case in which we are interested here, the derived waves will consist of refracted and reflected longitudinal waves and refracted and reflected transverse waves. For angles of incidence lower than the critical angle, part of the energy is reflected and

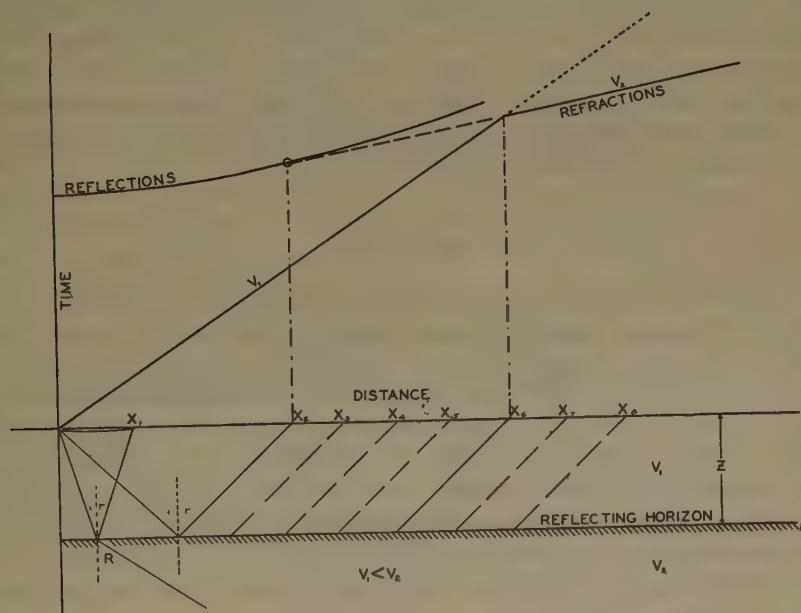


FIG. 1.—TIME-DISTANCE GRAPH AND RAY PATHS.

part refracted. For those angles greater than the critical angle all of the energy is reflected.

The relative amounts of energy which go into reflected and refracted waves can only be computed when the physical constants of the two media are known. In seismic prospecting it is hardly practicable to measure these constants. In general, however, the reflected longitudinal waves may be expected to carry only small amounts of energy, since most reflection work is done at angles much smaller than the critical angle.

## TRAVEL TIMES

In Fig. 1, consider waves which originate at  $O$  and are recorded at distances  $X_1$ ,  $X_2$ ,  $X_3$ , and so on. Each of the layers, of velocity  $V_1$  and  $V_2$ , respectively, is considered to be homogeneous and isotropic throughout its extent. Also, it is assumed that  $V_1$  is less than  $V_2$ . For any

distance less than  $X_2$  the minimum time path is through the upper stratum  $V_1$ . If distances, with their corresponding minimum times, be plotted for distances less than  $X_2$ , a line will be determined with reciprocal slope of  $V_1$ . For distances greater than  $X_2$  the minimum time path will be a wave which travels over the surface of  $V_2$  and thence back to the surface. If these distances are plotted with their corresponding times, the line thus determined will have the reciprocal slope  $V_2$ . This theory of refraction is assumed in dealing with all straight-line seismic calculations. It has been shown that the amount of energy propagated along the interface between two isotropic and homogeneous media is negligible. However, because the paths are curved, even though only slightly at times, a wave is returned to the surface. Thus, if computations are made on the theory that the wave is refracted from the interface, usable results may be obtained. Some mention will be made later regarding curved paths.

It is well known that

$$\frac{\sin i}{\sin R} = \frac{V_1}{V_2}$$

where  $i$  is the angle of incidence and  $R$  is the angle of refraction. The shortest distance at which a refracted wave can emerge is  $X_2$ , since for any distance shorter than that  $R$  is less than  $90^\circ$ . At distances equal to or greater than  $X_2$ ,  $R = 90^\circ$ , and the refracted wave returns to the surface. It is obvious, from geometrical considerations, that the first refracted wave is also a reflected wave. Thus at this point,  $X_2$  in Fig. 1, the reflected wave line is tangent to the refraction line  $V_2$ . As the distance increases, the depth becomes negligible with respect to the distance and the reflection curve is asymptotic to the line  $V_1$ . This gives a method for identifying the reflection with the horizon that is producing the reflection.

The usual procedure in the identification of reflections is somewhat different from that outlined above. This method is to shoot (or record) at various depths in a well and thus obtain an average velocity. Shots are then taken for reflections and by picking waves which have times that correspond to times found from horizons which are arbitrarily chosen as likely to reflect, the reflection is "identified." This method of shooting in a well is open to serious objections and is limited to regions in which wells have been drilled. Regarding it, Barton has the following to say:<sup>(1)</sup>

The impossibility of recognizing the reflecting bed is a serious disadvantage of the reflection method in comparison to the refraction method. In the latter method, the velocity,  $V_2$ , of the lower bed is determinable and in many places is a sufficient criterion for the identification of the lower, refracting bed. The velocity,  $V_2$ , of the reflecting bed is not determinable by the reflection method and it is therefore impossible to identify the reflecting bed from the results of the reflection shooting and beds may be jumped without suspicion of the fact.

Barton's objections are well founded. As long as there are enough wells, to check by the usual method might serve for obtaining reliable depths. Where beds occur close together, it complicates the identification of the reflecting bed.

However, as shown above, if the seismograms are analyzed by first shooting a refraction profile and plotting the various phases which occur, the reflections may be identified as coming from some certain horizon. If the beds are sloping, it would be necessary to shoot reversed profiles, not for the purpose of analyzing the seismograms, but for the purpose of identifying the bed by its velocity, which, in general, is unique. The point of tangency will always occur where the first refraction returns to the surface, regardless of whether the bed is sloping or not. The number of beds does not necessarily complicate the problem; the case of several beds will be discussed below.

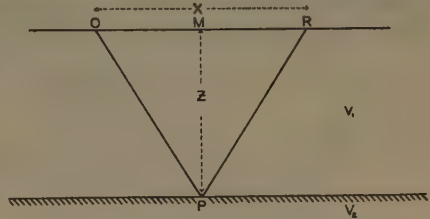


FIG. 2.—PATH OF A REFLECTION.

### REFLECTION FORMULAS

Consider the waves which originate at *O*, in Fig. 2, and suffer optical reflection at a point *P* at the interface between  $V_1$  and  $V_2$ . The time of travel of such a wave is designated by  $t_r$ , and the distance on the surface by  $X$ . If the depth is  $Z$ , the following equation may be written, providing the surface and the interface are parallel:

$$\frac{x^2}{4} + Z^2 = \frac{v^2 t_r^2}{4}$$

or

$$Z = \frac{1}{2} \sqrt{v^2 t_r^2 - x^2} \quad [1]$$

This is the formula most generally used in computing the depth of horizons by the reflection method. This is the equation of the hyperbola. Its graph is shown in Fig. 1.

### METHODS OF OBTAINING AVERAGE VELOCITY

In actual practice, this arrangement is made so that *MP* lies in a well. The geologic column is obtained. It is noted on the geologic column that *P* is a bed which should produce reflections. A geophone, or microphone, is put into the well until it rests at the point *P*. A shot is fired at *O* and the time of transit measured between *O* and *P*. This is divided by the distance *OP* and the average velocity is thus computed. This may be done for several horizons. After this, shots are placed on the surface and records obtained at several distances. The depth as taken from the

geologic column, and the average velocity as determined by shooting in a well, are substituted in formula 1. This gives the time of transit the reflected wave should take in going over the path  $OPR$ . Thus, by correlating this time with the phases on the seismograms, the reflected wave is identified. The reliability of this method depends upon: (1) knowing that the horizon picked will give a reflection; (2) assuming that the phase picked is the phase which correlates with this horizon.

A variation of this method is to take shots at  $O$  and record at  $R$ . From the geologic column, beds are picked which might give reflections. From the records, times for various phases are picked. By substituting

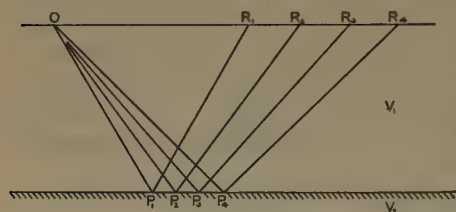


FIG. 3.—ARRANGEMENT OF RECORDING STATIONS FOR IDENTIFICATION OF REFLECTED PHASE.

these times and the depths as found from the geologic column, the average velocity to any bed may be determined. An average value is then taken if several values of  $t_r$  are used. In general, the methods described above have been found to be satisfactory within certain limits.

There is no reason to suppose that a reflected wave should be of much higher frequency than other waves, as is assumed by some investigators. It may be, as Rayleigh points out, that the overtones may be reflected and not the fundamental, but this cannot be taken as an established fact in seismic prospecting at the present time.

Additional information in regard to the identification of a reflected phase on the seismogram may be obtained by placing the shots as in Fig. 3. There is very little difference in path between  $OP_1R_1$ ,  $OP_2R_2$ , and so on, provided  $R_{i+1} - R_i$  is not too large. Hence, the reflected times will not change by any appreciable amount. Other types of waves, however, especially the surface waves, will show large changes in comparison with the reflection times.

It might appear that the best way to obtain an average velocity with the minimum of expense and time is to take such an arrangement as that pictured in Fig. 3 and observe the times of transit of the reflected phase on the seismograms. These could then be substituted in equation 1, thus forming a set of simultaneous equations which could be solved for the depth  $Z$  and the average velocity  $V$ . However, the times cannot be determined accurately enough for this. Consider, then, the following:

Formula 1 may be written  $V^2T^2 = X^2 + 4Z^2$  where  $T = t_r$ . In this formula, it is assumed that  $Z$  and  $V$  remain constant, though of course  $X$  and  $T$  vary with the shot. This equation may be written:

$$a_i w - \varphi = b_i$$

[2]



where

$$\begin{aligned} a_i &= T_i^2 & \varphi &= 4Z^2 \\ b_i &= X_i^2 & w &= V^2 \end{aligned}$$

If there are  $n$  shots, there result  $n$  equations containing the two variables  $Z$  and  $V$ . These may be solved by the method of least squares. The normal equations are as follows:

$$\begin{aligned} Aw - B\varphi &= D \\ Bw - n\varphi &= E \end{aligned}$$

where

$$\begin{aligned} A &= \sum a_i^2 & D &= \sum a_i b_i \\ B &= \sum a_i & E &= \sum b_i \end{aligned}$$

The solutions, in the form of determinants, are:

$$w = \frac{\Delta w}{\Delta} \qquad \varphi = \frac{\Delta \varphi}{\Delta}$$

where  $\Delta = \begin{vmatrix} AB \\ Bn \end{vmatrix}; \quad \Delta w = \begin{vmatrix} DB \\ En \end{vmatrix}; \quad \Delta \varphi = \begin{vmatrix} DA \\ EB \end{vmatrix}$

$$V = \sqrt{w} \text{ and } Z = \frac{1}{2}\sqrt{\varphi}$$

This cannot give very reliable results because the elements of the determinants  $A$ ,  $B$ ,  $D$  and  $E$  are much larger than the determinants

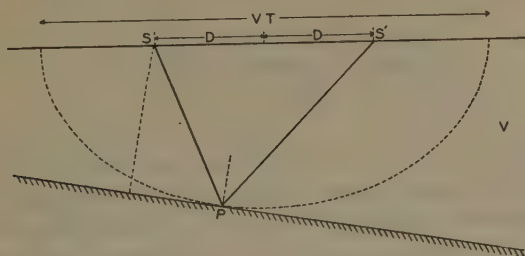


FIG. 4.—GRAPHIC METHOD FOR MAPPING STRUCTURE BY REFLECTIONS.

themselves. The writer has solved a great many of these systems for the average velocity and depth but has never found a profile where the times could be determined to the degree of accuracy necessary for reliable results.

#### GENERAL FORMULA FOR REFLECTIONS

Let  $S$  be the origin and  $S'$  the recording point for a reflected ray, as in Fig. 4.  $P$  is the point of reflection. The time for the reflected ray may be written

$$T = \frac{SP + S'P}{V} \quad [3]$$

where  $V$  is the average velocity of the material from the surface to the

buried layer. If  $SP + S'P$  is a minimum,  $T$  will be a minimum. This time will be a minimum if  $P$  is a point on an ellipse to which the bed is tangent at point  $P$  (Principle of Least Time).  $S$  and  $S'$  will be the foci of the ellipse. The origin of the ellipse may be considered to be at  $\frac{1}{2}SS'$ . From equation 3,

$$SP + S'P = \text{length of major axis} = VT$$

Then the length of the semimajor axis is  $\frac{1}{2}VT$ , and of the semiminor axis

$$\sqrt{\frac{V^2T^2}{4} - D^2} \text{ where } D = \frac{1}{2}SS'.$$

The equation for the ellipse is usually written

$$\frac{X^2}{A^2} + \frac{Z^2}{B^2} = 1$$

where  $A$  and  $B$  represent the semimajor and semiminor axes respectively. In this case,

$$A = \frac{1}{2}VT$$

and

$$B = \sqrt{\frac{V^2T^2}{4} - D^2}$$

or

$$\frac{X^2}{\left(\frac{V^2T^2}{4}\right)} + \frac{Z^2}{\left(\frac{V^2T^2}{4} - 4D^2\right)} = 1 \quad [4]$$

By taking several values of the distance and time, equation 4 may be used to obtain the various values involved and thus to map a horizon, but this becomes so involved algebraically that it will not be given here. The writer obtained a solution, but it was in a form that would not lend itself to ready computation without undue labor. The chief gain in using this formula comes from its use graphically. This may be done as follows:

Take a shot at point  $S_1$  and record at  $S_1'$ ; call this time  $T$ . With  $S_1$  and  $S_1'$  as foci, describe an ellipse with a major axis equal to  $VT$ , where  $V$  is the average velocity of the overburden and  $T$  is the time of travel for the reflected wave. Do this for other shot lengths and times. The tangent, if the bed has the same slope at every point, may be drawn in graphically. If this process is continued, the reflecting bed will be mapped, the accuracy depending on the spacing of the depth determinations. It is assumed that the plane in which the reflections are obtained lies in the plane of the dip. If this is not so, the plane of dip will have to be determined. This may be done by graphical methods which are in common use in geological work. Once the plane of dip is determined, the

true depth at any point may be determined. It is better to determine the dip and place the shot lines so that they lie in this plane.

Another method which results from the use of the same principle is as follows. This method makes use of the image point in the case of a reflection.  $O$  in Fig. 5 is the origin of rays which are reflected from points  $P_1, P_2, P_3$ , and so on, which lie on the interface between the beds of velocities  $V$  and  $V_2$  and are recorded at points  $R_1, R_2, R_3$  such that the distance  $OR_i = X_i$ . The velocity of the overburden is taken, as in the previous cases, to be  $V$  and of the high-speed reflecting bed,  $V_2$ , such that  $V$  is less than  $V_2$ .  $I$  is the image point of these reflected rays. In Fig. 6,  $OM$  is  $H$ , or the perpendicular distance from point  $O$  to the high-speed bed  $V_2$ . If  $I$  is the image point,  $OM = MI$  and  $OP_1 = IP_1$ . The slope of the high-speed bed is taken to be  $\omega$ .  $\theta$  is the angle between  $OX$  and

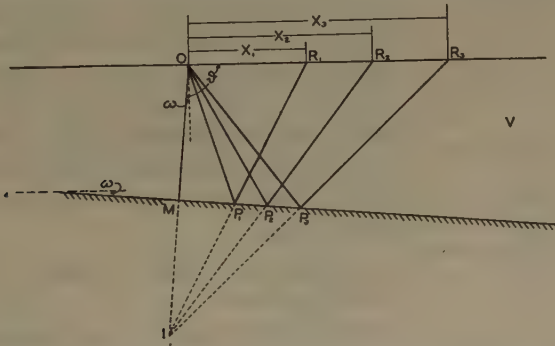


FIG. 5.—USE OF IMAGE POINT IN COMPUTING DEPTHS.

$OM$ . From the figure, it is seen that  $\omega = \theta - 90^\circ$ . For any ray reflected from a point  $P$

$$T = \frac{OP}{V} + \frac{PR}{V} = \frac{IP + PR}{V} = \frac{IR}{V}, \text{ or } IR = VT$$

The angle  $\theta$  can be written in terms of  $V$ ,  $T$ ,  $H$  and  $X$  by means of the law of cosines:

$$\cos \vartheta = \frac{X^2 + 4H^2 - V^2T^2}{4HX} \quad [5]$$

The depth is usually measured perpendicular to the surface of the ground, thus

$$Z = H / \cos \omega$$

If  $\omega = 0$ , equation 5 reduces to equation 1:

$$Z = H = \frac{1}{2} \sqrt{V^2T^2 - X^2}$$

Equation 5 contains three unknowns. It should be possible, by taking three shots, to solve for these. However, in actual practice, this is not the case. A method of reasoning, somewhat similar to that used

in the least square solution of equation 1, would show that the values obtained for  $H$  or  $Z$ ,  $\theta$  and  $V$  could not be very reliable. Formula 5 is more general than formula 1. In actual practice, formula 1 is the most used. This is due to the fact that  $T$  cannot be determined with sufficient accuracy to enable one to use formula 5 instead of formula 1. In addition to this fact,  $\omega$  is usually small and the difference it may cause can be neglected. However, it must be pointed out that if  $\omega$  were very large, formula 1 would give erroneous results.

### PATH OF REFLECTED RAY IN CASE OF SEVERAL BEDS

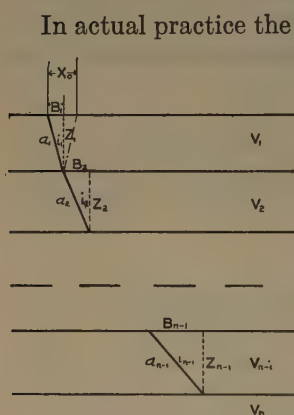


FIG. 6.—EFFECT OF SEVERAL BEDS.

$Z_1 \dots Z_n$ . It can be shown that a ray progresses through the layers according to the law

$$\frac{V_1}{\sin i_1} = \frac{V_2}{\sin i_2} = \dots = \frac{V_n}{\sin i_n}$$

For any particular path the ratio of the velocity to the sine of the angle of incidence is a constant. Call this constant value  $I$ , or,

$$I = \frac{V}{\sin i}$$

Thus  $I$  may be considered as a parameter which determines the particular path a wave would follow.

The expression for the time may be written from Fig. 6 as

$$\frac{T}{2} = \frac{a_1}{V_1} + \frac{a_2}{V_2} + \dots + \frac{a_{n-1}}{V_{n-1}} \quad [6a]$$

The distance is given by

$$\frac{X}{2} = B_1 + B_2 + \dots + B_{n-1} \quad [6b]$$

In actual practice the ideal conditions which have been assumed up to this point do not exist. The overburden may be, and usually is, made up of a series of layers or beds. Each of these beds may have a velocity greater or less than the velocity of the bed above. It is possible, and is sometimes done, to get a reflection from the base of a high-speed bed, but the thickness of the bed must be at least one-half a wave length.

Assume a series of parallel layers with the velocities  $V_1, V_2, \dots V_n$ . Consider each of these layers to be homogeneous and isotropic throughout its extent. The thicknesses corresponding to these velocities are



Fig. 6 shows that

$$a = \frac{Z}{\cos i}$$

But since  $\sin i = V/I$ ,

$$\cos i = \sqrt{1 - \frac{V^2}{I^2}} = \frac{1}{I} \sqrt{I^2 - V^2}$$

and

$$a = \frac{ZI}{\sqrt{I^2 - V^2}}$$

Substituting the value for  $a$  in equation 6a gives

$$\frac{T}{2} = \frac{Z_1 I}{V_1 \sqrt{I^2 - V_1^2}} + \frac{Z_2 I}{V_2 \sqrt{I^2 - V_2^2}} + \dots + \frac{Z_{n-1} I}{V_{n-1} \sqrt{I^2 - V_{n-1}^2}} \quad [7a]$$

Further, Fig. 6 shows that

$$\tan i = B/Z$$

Since the values for the sine and cosine are known,

$$\tan i = \frac{V}{\sqrt{I^2 - V^2}}$$

and

$$B = \frac{ZV}{\sqrt{I^2 - V^2}}$$

Substituting this value in equation 6b gives

$$\frac{X}{2} = \frac{Z_1 V_1}{\sqrt{I^2 - V_1^2}} + \dots + \frac{Z_{n-1} V_{n-1}}{\sqrt{I^2 - V_{n-1}^2}} \quad [7b]$$

For two layers, these formulas become

$$\frac{T}{2} = \frac{Z_1 I}{V_1 \sqrt{I^2 - V_1^2}}$$

$$\frac{X}{2} = \frac{Z_1 V_1}{\sqrt{I^2 - V_1^2}}$$

The expression in  $T$  and  $X$  may be written, solving the above equations for an expression in  $T$ ,  $X$  and  $Z$ , as

$$T = \frac{\sqrt{4Z_1^2 + X^2}}{V_1}$$

which is the usual formula for reflection time in two horizontal layers.

If  $I$  is  $V_n$ , that is, equal to the velocity of the bed from which the wave is reflected, the reflection is at the critical angle and the distance is the critical distance, or

$$\sin i_{n-1} = \frac{V_{n-1}}{V_n}$$

An example of the above may be easily shown by considering only the first two layers of Fig. 6, whose velocities are  $V_1$  and  $V_2$ , for the case

$$\sin i_1 = \frac{V_1}{V_2}, \quad \tan i_1 = \frac{V_1}{\sqrt{V_2^2 - V_1^2}}$$

The critical distance is then seen to be

$$X_0 = 2Z \tan i$$

or,

$$X_0 = 2Z \frac{V_1}{\sqrt{V_2^2 - V_1^2}}$$

The critical distance, according to the formula for  $2B$ , where  $I = V_2$  is given by

$$\frac{X_0}{2} = Z \frac{V_1}{\sqrt{V_2^2 - V_1^2}}$$

#### THE AVERAGE VELOCITY

It is much simpler to use an average velocity in figuring the depth to any marker. This is possible if the average velocity does not change too greatly with depth and distance from the shot point. For any constant distance, the average velocity may be written as

$$V_a = \frac{\sqrt{(Z_1 + Z_2 + \dots + Z_n)^2 + K^2}}{T}, \text{ where } K = X$$

It is desirable to know the change of average velocity with any change in thickness of the last layer. For three beds, with constants of  $V_1 = 7000$  ft. per sec.,  $V_2 = 9000$  ft. per sec.,  $V_3 = 11,000$  ft. per sec.,  $Z_1 = 2000$  ft.,  $Z_2 = 2000$  ft. and  $Z_3 = 1000$  ft., for a distance  $X = 6000$  ft. approximately, it can be shown by a rather cumbersome differentiation and substitution, which need not be reproduced here, that

$$\frac{\partial V_a}{\partial Z_3} = 0.538$$

This means that the amount of error in the average velocity can be determined for any change in depth or thickness of any layer. Thus, knowing how much error is made in the depth for any error in the average velocity, a better approximation to the true depth can be made.

#### THE SURFACE (OR "WEATHERING") CORRECTION

Practically everywhere there is a zone of surface material in which the velocity is very low as compared with the average velocity of beds below it. This zone is commonly called the "weathering" in the field, though it does not in general coincide with what geologists call the "zone of weathering." For the computation of reliable depths, it has been

found advisable to refer all calculations to the bottom of this surface correction zone.

Fig. 7 shows a diagram of the method of treating the surface correction zone.  $W_s$  is the thickness of the zone at the shot point, and  $W_r$  at the recording point.  $E_s$  is the elevation of the surface of the ground at the shot point, referred to mean sea level, and  $E_r$  at the recording point. The depth of the surface correction zone  $W$  is small in comparison with the depth  $Z$ , hence the path  $E_sO$  can be taken as equal to the path  $AO$ . Since  $T_w$  is small and the depth is small, an average value can be determined for the surface correction velocity in any one area. In reality,  $T_a$  is the time it takes for the sound ray to go through the surface correction zone and back, but the difference  $T_w - T_a$  is well within experimental error and either may be chosen. According to this, then, if a shot is put off at the surface and recorded at distances long enough to penetrate the surface correction zone (200 ft. or so), the depth of the surface correction zone can be computed according to the formula

$$W = \frac{1}{2} V_o T_w \quad [8]$$

The average velocity in any area is computed from the base of the surface correction zone. Hence in computing depths the amount of time the sound ray travels in the surface correction zone must be deducted from the total time of the reflection. This time, which is to be subtracted, is given by the formula

$$T_w = \frac{(W_s - H) + W_r}{V_o} \quad H < W_s \quad [9]$$

where  $H$  is the depth of the shot.

$$T_w = \frac{W_r}{V_o} \quad H > W_s \quad [10]$$

If the shot is placed below the surface correction zone, the depth is taken below this point and the base of the surface correction zone at the recorder.

#### REDUCTION TO MEAN DATUM

To reduce to mean datum, the elevation at the midpoint between shot and recorder is taken, minus the average value of the surface correction

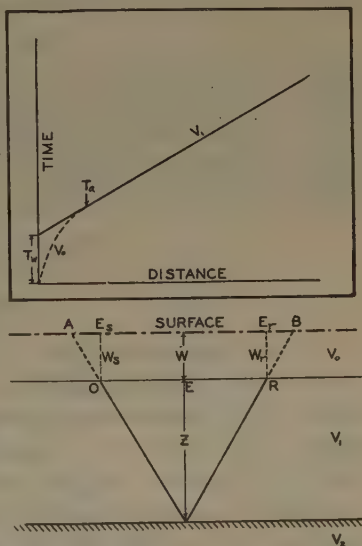


FIG. 7.—SURFACE (OR “WEATHERING”) CORRECTION.

zone between these two points. If the shot is below the weathering, the mean is taken between this depth and the surface correction at the recorder. Written as a formula, this gives

$$E = \frac{E_s + E_r}{2} - \frac{W_s + W_r}{2} \quad H < W_s \quad [11]$$

or

$$E = \frac{E_s + E_r}{2} - \frac{H + W_r}{2} \quad H > W_s \quad [12]$$

After the depth has been computed according to the formula

$$Z = \frac{1}{2} \sqrt{V^2 T^2 - X^2}$$

where  $V$  is the average velocity (from the base of the surface correction zone),  $T$  is the total time of reflection minus time required to traverse the surface correction zone and  $X$  is the distance between shot and recorder. Mean datum is then given by

$$D_m = E - Z \text{ at point } X/2 \quad [13]$$

#### CURVED PATHS

It has been found that rays do not always travel paths which are straight lines. Ewing and Leet<sup>(4,5)</sup> have given examples of data taken in the Gulf Coast area which definitely prove that the rays follow curved paths. The writer has computed depths by the same method as that used by Ewing and Leet and found close agreement with their work. The curvature in loose soil is very great whereas in granite, for example, the curvature is so small that if it is assumed that the rays travel straight lines no serious error is made. This slight curvature of path causes a ray to return to the surface. Since the curvature may be slight in the higher speed bed, and the ray travels just under the surface, depths may be computed on the basis of rectilinear refraction as defined by common usage in seismic prospecting.

By shooting refraction profiles in an area, the paths which rays follow may be computed and a curve of ray penetration versus depth may be plotted. From these data it is possible to derive a value for the average velocity at any distance. When reflection shots are taken, the appropriate average velocity for any distance is used. Where the distances, on the surface, for a series of shots do not vary much, the same average velocity may be used. This method is a very powerful one, and in certain areas is especially valuable, where there are no existing wells by which a velocity may be calibrated. The use of curved paths is of importance, also, in computing the surface correction zone, where the depth is great enough so that straight-line interpretation gives unreliable results.



It should be pointed out that in the use of formula 1 the assumption is made that the distances  $X$  do not vary over a wide range, if the same value of the average velocity  $V$  is used. Of course, if a calibration curve is drawn, as indicated above, the appropriate value of  $V$  may be chosen for any value of  $X$ . This introduces further proof that formula 1 could not be used to obtain  $V$  and  $Z$  by a least-square solution, for  $X$  would have to be chosen large in order to reduce the effect of errors in  $T$  and in doing this  $V$  would change. The fundamental assumption in the use of this method is that  $V$  remains constant over the complete profile.

### EXAMPLES OF REFLECTIONS

Fig. 8 shows the graph of a refraction profile and on it the reflections are also plotted. This profile was interpreted by means of straight lines. Thus, the velocities as drawn on the graph are  $V_1 = 9000$  ft. per sec.,  $V_2 = 10,050$  ft. per sec.,  $V_3 = 12,400$  ft. per sec.,  $V_4 = 17,800$  ft. per sec.  $V_4$  is a very hard limestone and is a definite marker in the territory where the profile was shot. If  $V_1$ ,  $V_2$ ,  $V_3$  and  $V_4$  are taken as definite

TABLE 1.—*Example of Reflection Formula for Several Beds*

$V_1 = 11,000$  ft. per sec.;  $V_2 = 13,000$  ft. per sec.;  $V_3 = 20,000$  ft. per sec.  
 $Z_1 = 1200$  ft.;  $Z_2 = 2970$  ft.

$$\frac{T_r}{2} = \frac{Z_1 I}{V_1 \sqrt{I^2 - V_1^2}} + \frac{Z_2 I}{V_2 \sqrt{I^2 - V_2^2}}; \frac{X}{2} = \frac{Z_1 V_1}{\sqrt{I^2 - V_1^2}} + \frac{Z_2 V_2}{\sqrt{I^2 - V_2^2}}$$

$I$	$T_r$	$X$	Average Velocity
14,000	1.580	17,958	12,532
15,000	1.234	12,942	
16,000	1.082	10,578	
17,000	0.994	9,108	
18,000	0.934	8,076	
19,000	0.892	7,296	
20,000	0.860	6,678	
21,000	0.836	6,174	
22,000	0.816	5,752	
23,000	0.800	5,390	
24,000	0.788	5,078	
25,000	0.776	4,804	
26,000	0.768	4,560	
27,000	0.760	4,344	
28,000	0.752	4,150	12,412
29,000	0.746	3,972	
30,000	0.740	3,812	
31,000	0.736	3,664	
32,000	0.732	3,528	
33,000	0.728	3,402	
34,000	0.724	3,286	
$\infty$	0.674	0,000	
			12,381
			12,373

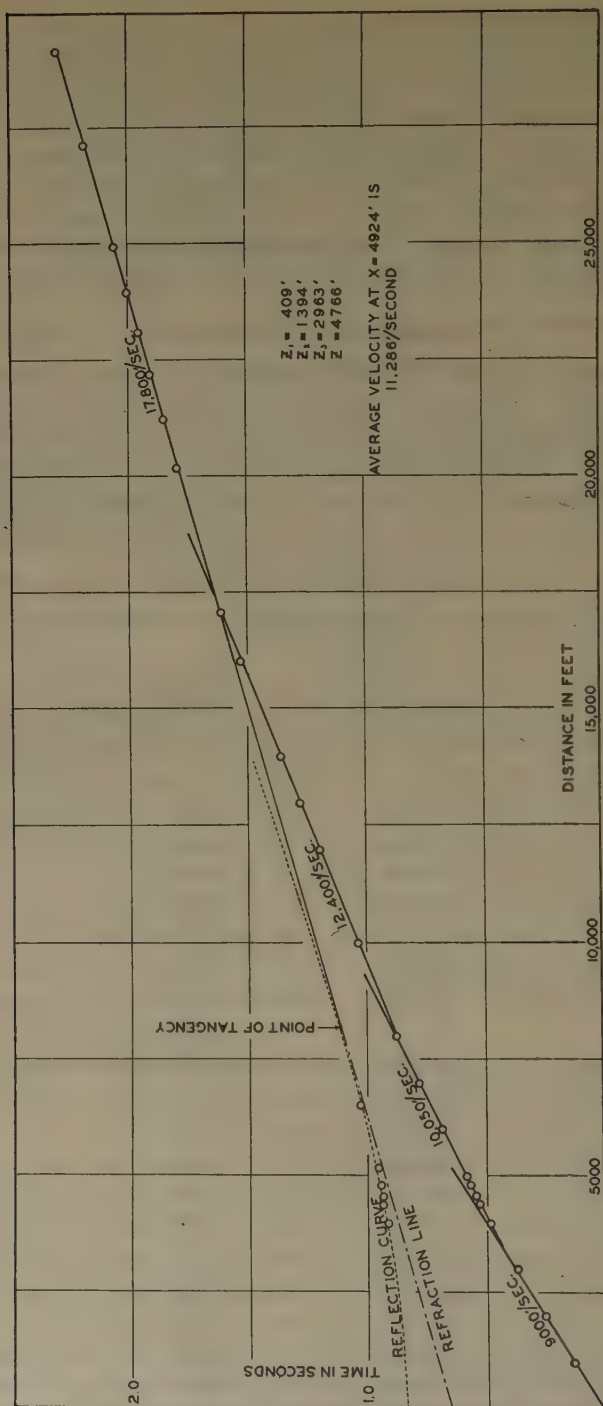


FIG. 8.—REFLECTIONS PLOTTED ON TIME-DISTANCE GRAPH OF REFRACTION PROFILE.

horizons, the thickness of each is  $Z_1$ ,  $Z_2$ ,  $Z_3$ , or the total of these three gives the depth from the surface to the top of the  $V_4$  horizon, which is the limestone, a total  $Z = 4766$  ft. Formulas for the computation of the depths of several beds have been worked out by numerous authors;

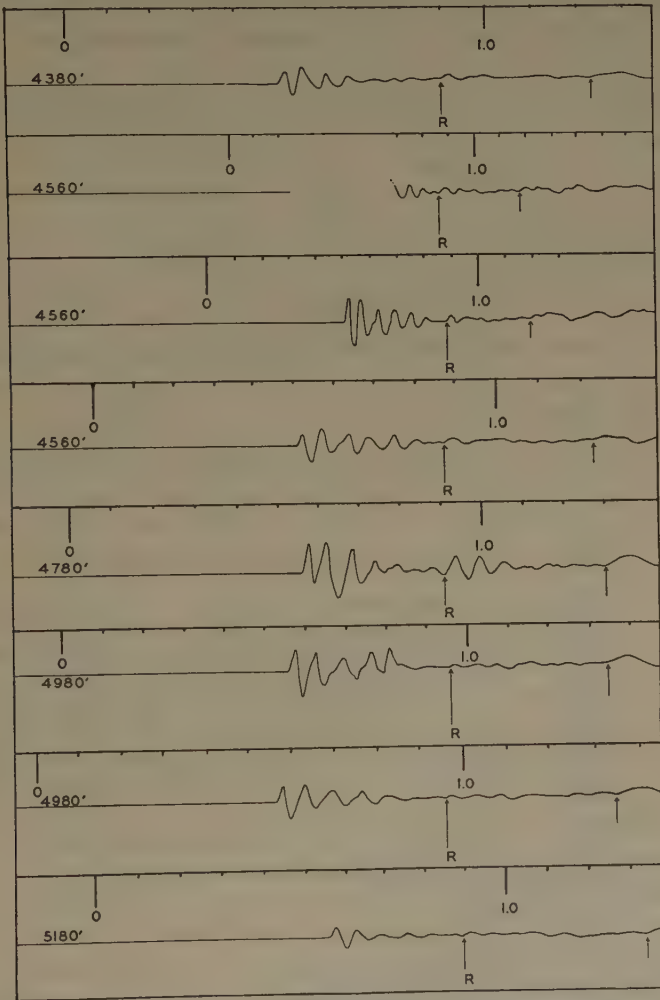


FIG. 9.—TRACINGS OF REFLECTION RECORDS OBTAINED WITH A MECHANICAL SEISMOGRAPH.

Phases marked  $R$  are reflections; those following  $R$  are surface waves.

Barton<sup>(1)</sup> gives some. By the use of formulas 7a and 7b the reflection curve was plotted. This reflection curve agrees, within experimental error, with those taken from the records. An example of the records is shown in Fig. 9. The reflections, as identified there, are definite arrivals of energy, and the time picked is that of the *beginning of the phase*. The average velocity at a distance  $X = 4900$  ft. is 11,290 ft. per sec., to

the nearest 10 ft. Table 1 gives some idea of how the velocity changes with distance from the origin. The depth, as determined from the reflections, agrees within experimental limits with the depth as taken from a well situated close to the profile. The amounts of dynamite used vary from charges of 2 to 10 lb. for the reflection shots. Table 2 shows a typical computation form for the reduction of reflection data.

TABLE 2.—*Computation Form for Reduction of Reflection Data<sup>a</sup>*

Shot position.....				Location.....							
Date.....	No. Shots.....				No. O. K. Records.....						
Mean Datum	-3538 ± 16 ft.		at		2500 ft.		From Shot Point.....				
Constants: $V_s = 2000$ ft. per sec.; $V = 10,930$ ft. per sec.											
Record No.....	C1	A1	B1	A3	D3	D4	C4	C3	D1	B3	
$X$ .....	5600	5000	5000	4600	5400	5200	5200	5400	5600	4600	
$T_g$ .....											
$T_{ws}$ .....	0.030										
$T_{wr}$ .....	0.040										
$H$ .....	24	21	21	21	24	24	24	24	24	21	
$T_w$ .....	0.023	0.025	0.025	0.025	0.023	0.023	0.023	0.023	0.023	0.025	
$E_s$ .....	930.5										
$E_r$ .....	994.7	977.9	977.9	997.5	980.6	981.3	981.3	980.6	994.7	997.5	
$E_m$ .....	963	954	954	964	956	956	956	956	963	964	
$W$ .....	35										
$E_m - W$ .....	928	919	919	929	921	921	921	921	928	929	
$Wt$ .....											
$T_r$ .....	0.994	0.960	0.963	0.940	0.981	0.967	0.967	0.975	0.992	0.948	
$T_w$ .....	0.023	0.025	0.025	0.025	0.023	0.023	0.023	0.023	0.023	0.025	
$T_r - T_w$ .....	0.971	0.935	0.938	0.915	0.958	0.944	0.944	0.952	0.969	0.923	
$V^2T^2$ .....	112.2	104.1	105.0	100.0	109.5	106.3	106.3	108.1	112.0	101.6	
$X^2$ .....	31.30	25	25	21.15	29.10	27	27	29.10	31.30	21.15	
$V^2T^2 - X^2$ .....	80.9	79.1	80.0	78.85	80.4	79.3	79.3	79.0	80.7	80.45	
$Z$ .....	4495	4445	4470	4440	4480	4450	4450	4445	4490	4480	
$D$ .....	-3567	-3526	-3551	-3511	-3559	-3529	-3529	-3524	-3562	-3551	
Diff.....	+29	-12	+13	-27	+21	-9	-9	-14	+24	+13	
$D_m$ .....	-3538										

<sup>a</sup> The various terms on the form, which are not self-explanatory, are as follows:

*V<sub>s</sub>*, average velocity in surface correction zone.

*V*, average velocity of overburden.

*X*, horizontal distance from shot to recorder.

*T<sub>g</sub>*, time of first impulse on record.

*T<sub>ws</sub>*, travel time of surface correction zone shot at shot point.

*T<sub>wr</sub>*, travel time of surface correction zone shot at recorder.

*H*, depth of charge below surface.

*T<sub>w</sub>*, average time to penetrate surface correction zone.

*E<sub>s</sub>*, elevation of shot above sea level.

*E<sub>r</sub>*, elevation of recorder above sea level.

*E<sub>m</sub>*, average elevation between shot and recorder.

*W*, average thickness of surface correction zone.

*Wt*, weight determined by quality of record.

*T<sub>r</sub>*, time for reflection.

*Z*, depth of horizon below surface correction zone.

*D*, datum, referred to mean sea level.

Diff., difference between average datum for profile and the value found in each column

*D<sub>m</sub>*, average datum for profile.



Fig. 10 is a graph of a reflection profile. Here the first arrivals, the reflections and the transverse waves have been identified. The first



FIG. 10.—TIME-DISTANCE GRAPH OF REFLECTION PROFILE.

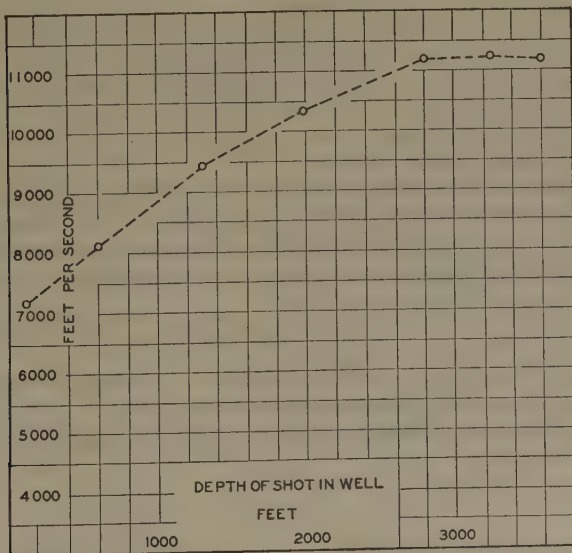


FIG. 11.—VELOCITY CALIBRATION BY SHOOTING IN A WELL.

arrivals are waves which have been refracted; the transverse waves are also refracted waves. The ratio  $V_T : V_L = 0.508$ .

Fig. 11 shows the velocities obtained by placing shots in a well and recording the time of transit from various depths on the surface near the well. This graph is self-explanatory.

### CONCLUSIONS

It is pertinent to point out that seismic methods of prospecting have not reached, and may never reach, a stage where the calculations are merely a matter of routine. Geological conditions are not the same all over the country. They vary considerably even in any one region. Methods that might give close approximations to true conditions in one territory may be found to give very great errors if used in another. In general, the results presented in this paper are the outgrowth of several years of experience in seismic prospecting. Much work remains to be done, both experimentally and in methods of interpretation of data.

### ACKNOWLEDGMENTS

The writer wishes to express his appreciation to Dr. Maurice Ewing and Dr. L. Don Leet, and to others, for valuable help in the preparation of this paper. The data presented are by the kind permission of the Continental Oil Company.

### BIBLIOGRAPHY

1. D. C. Barton: The Seismic Method of Mapping Geologic Structure. *Geophysical Prospecting*, 1929, A. I. M. E., 572-624.
2. B. Brockamp and H. Mothes: Seismische Untersuchungen auf dem Pasterzegletscher, I. *Ztsch. f. Geophysik* (1930), 6, 482-500.
3. A. B. B. Edge and T. H. Laby: Principles and Practice of Geophysical Prospecting; seismic method in Chap. 6. Cambridge Univ. Pr., 1931.
4. M. Ewing and L. D. Leet: Seismic Propagation Paths. *Trans. A. I. M. E., Geophysical Prospecting* (1932) 245-260.
5. M. Ewing and L. D. Leet: Comparison of Two Methods for Interpretation of Seismic Time-distance Graphs Which Are Smooth Curves. *Trans. A. I. M. E., Geophysical Prospecting* (1932) 263-270. (Formulas are developed by Ewing in the appendix of this paper which give the relation between the time-distance data and the velocity-depth function.)
6. C. G. Knott: Reflexion and Refraction of Elastic Waves with Seismological Applications. *Phil. Mag.* (July, 1899).
7. E. McDermott: Application of Seismography to Geological Problems. *Bull. Amer. Assn. Petr. Geol.* (1931) 15, 1311-1334.
8. H. Mothes: Seismische Dickenmessungen von Gletschereis. *Ztsch. f. Geophysik* (1927) 3, 121-123.
9. Hubert: *Ztsch. f. Geophysik* (1924-25).

---

[For some discussion of this paper, see pages 461 and 471.]

# Certain Instrument Problems in Reflection Seismology\*

By C. A. HEILAND,† GOLDEN, COLO.

(New York Meeting, February, 1933)

## CONTENTS

	PAGE
I. Description of reflection equipments. . . . .	412
A. Design features of present types. . . . .	412
B. Reflection equipment designed by writer . . . . .	418
II. Characteristics of reflection seismographs . . . . .	421
A. Types of coupling in electromagnetic seismographs. . . . .	421
B. Action of pickup, amplifier and galvanometer. . . . .	424
C. Combined action of pickups, amplifiers and oscillographs . . . . .	433
D. Static and dynamic constants . . . . .	434
E. Desirable values for static and dynamic constants . . . . .	435
III. Calibration of reflection apparatus . . . . .	442
A. Dynamic tests without shaking table. . . . .	442
B. Calibration methods . . . . .	445
C. Various other tests. . . . .	451

## INTRODUCTION

IN the past five years, the reflection method of seismic prospecting has been developed to a high degree of perfection. Its success in mapping oil structure is due to the unique and definite nature of the depth data obtained.

While articles on the principle and results of this method continue to appear in increasing number, there is virtually nothing published about the instruments used in this work. Several years ago, the writer started an experimental and theoretical investigation with the object of determining which characteristics would be best adapted to the problem at hand. As a result, an equipment was developed which has proved its usefulness in a great number of field tests.

W. E. Pugh, now with the Empire Oil and Refining Co., joined the writer, in 1931 and 1932, in the laboratory experiments and field tests. In 1933, a paper was written on Certain Instrument and Field Problems in Reflection Seismology, and submitted to the Institute. The part of that paper dealing with field tests was published as *Contribution 34* (reprinted in this volume, p. 455). Since then, considerably more labora-

---

\* Part I, Series of Publications No. 47, Department of Geophysics, Colorado School of Mines.

† Department of Geophysics, Colorado School of Mines.

tory and field experience has been accumulated, so that this part, on instrument problems, has been completely rewritten.

In this paper, instrument problems in reflection seismology are considered from two general viewpoints: (1) which physical characteristics are best suited to a good reproduction of the ground movement and practicability of field operation; (2) which methods are best adapted to the calibration and supervision of performance of the equipment in the laboratory. In order to afford the reader an insight into the problems involved, a description and classification of reflection equipments in present day use, as well as a description of the equipment developed by the writer, has been added. Frequent use has been made of the theory of coupled vibrations, and of free and forced oscillations of single systems with the fundamentals of which the reader is assumed to be familiar.

## I. REFLECTION EQUIPMENTS

### A. DESIGN FEATURES OF PRESENT TYPES

Although the design of the majority of reflection equipments now used by consultants and oil companies goes back to the original construction developed by Karcher and McDermott, there is a great variety in the construction of the constituent parts. Despite great latitude in the design of the units of a reflection equipment, generally good results can be obtained provided certain fundamental requirements are met.

Three primary and two secondary devices are the fundamental constituents of the majority of reflection equipments: (1) an electrical pickup device, (2) an amplifier, (3) indicating devices, and further, (4) apparatus for providing accurate time marks, and (5) a device for recording the instant of the shot on the record.

#### 1. *Pickup (Seismograph)*

Although mechanical seismographs were used at one time for the observation of reflections, the general practice now is to employ electrical seismographs. The function of the latter is to convert the mechanical ground vibrations into fluctuations of electric current. Without exception the vertical component of the ground movement is being recorded. A tabulation is given below of the types that are being used or have been used, classified with respect to construction principle, and arranged approximately in order of present importance: (See also Fig. 1.)

Electromagnetic types:

Induction (constant air-gap) type.

Reluctance (variable air-gap) type.

Capacitive types:

Tuned circuit type.

Grid coupled type.



**Pressure types:**

Carbon microphone type.

Contact accelerometer type.

Piezoelectric type.

*Electromagnetic Type.*—The characteristic feature of the electromagnetic type is that the relative movement of ground and instrument frame, with respect to the seismograph\* mass, produces induction currents which may be recorded with or without valve amplification by galvanometric instruments. In the induction types, the coils usually move with the seismograph mass, or levers attached to it, in a magnetic field. The principle of the reluctance types, on the other hand, is that ordinarily some sort of an armature is attached directly, or by means of a lever system, to the seismograph mass, and moves in the field of a permanent magnet to which coils are attached; by the change of flux, induction currents are produced in the coils.† Thus, both the induction and the reluctance type correspond to two types of loudspeakers, using them as generators instead of motors. The induction type represents the inversion of the dynamic speaker; the second, which represents the inversion of the magnetic speaker, is similar in construction either to the headphone receiver or the Baldwin type of loudspeaker.

The following are representative of the induction type: The original Karcher type, the Imperial Geophysical electromagnetic seismograph, the Askania electromagnetic seismograph, and the Cambridge electromagnetic seismograph. The first is named after the author of patent 1706066 (March 19, 1929). It is essentially a dynamic speaker, with ring-shaped electromagnet and a plunger coil attached to the seismograph mass. In the seismograph of the Imperial Geophysical Survey,<sup>(10)</sup> ‡ an electromagnet acting as the seismograph mass is suspended from a thin steel diaphragm. Attached to the base, and passing between the poles of the electromagnet, is a flat stationary coil. The Askania electromagnetic seismograph is similar to the Schweydar mechanical seismograph; except that at the end of the aluminum cone, attached to the seismograph mass, there is a plunger coil, which moves between the poles of a loudspeaker electromagnet. In the Cambridge electromagnetic seismograph,<sup>(9)</sup> a fine wire attached to the end of the aluminum cone rotates the armature of a permanent magnet generator constructed like a galvanometer. This description of induction seismographs refers to models to which there is reference in the literature, and while they were used mostly in refraction work in the earlier days of seismic prospecting, their construction principle, with modifications of dimensions necessitated by the

\* Frequently called the "stationary" or "steady" mass in the seismic literature.

† Both types are also used with coils or armatures stationary and with magnets as seismograph mass.

‡ Numerals in brackets refer to the bibliography at the end of the paper.

application to the detection of reflection frequencies, may be utilized for reflection receivers. The reflection seismographs used by the Geophysical Research Corporation, the McCollum Exploration Co., and by Rosaire and Kannenstine, are reported to be of the inductive type. In the seismograph designed by the writer, to be described later, the principle of coils moving in magnetic fields is also applied.

The reluctance, or variable air-gap type, appears to enjoy more preference at the present time than the induction type. Most of them, like the pickups reported to be used by the Geophysical Service Inc., by the Seismograph Service Inc., by the Texas Co., the Empire Oil Co. and the Humble Oil Co., are similar to the Baldwin receiver (or Dubois iron-plate oscillograph) in construction: A thin plate of soft iron is supported on a knife edge or a pin between the pole gap of a permanent magnet or magnets, with its plane at right angles to the magnetic field. It is held in this position by a spring on one and a lever connection to the seismograph mass on the other side. The movement of the mass changes the flux between the poles and induces currents to flow in a coil which surrounds the iron plate. In modifications of this construction the magnet assembly acts as the seismograph mass. Another type of reluctance seismograph, constructed like a headphone receiver, has recently been described by Benioff.<sup>(19)</sup>

In the capacitive type of seismograph, the mass is mounted close to a stationary plate whereby this arrangement may be made to act as a variable condenser. It may be used (1) to change the tuning of an oscillatory circuit, or (2) to change the grid voltage on the first stage of an amplifier. In the first arrangement, the frequency and thus the plate current are changed in the oscillatory circuit by the movement of the pickup mass; these fluctuations, in turn, may be transferred to a resonance circuit, or directly to an amplifier, or else the heterodyne principle may be employed, as in Whiddington's ultramicroscope. When used to change the grid voltage, the seismograph is used much the same way as a condenser microphone; in a modification of this construction a movable plate connected to the seismograph mass is used between two stationary condenser plates, thus acting in a push-pull circuit. As a whole this capacitive type seismograph is capable of a great deal of variation. Seismographs based on this principle have been suggested or constructed by a number of authors, such as Duckert, Gerdien, Thoma, Obata, Haeno<sup>(12)</sup> and others. It is used at present in the refraction and reflection seismographs of the Petty Geophysical Engineering Corporation. A schematic illustration of the inductive, capacitive and pressure types is given in Fig. 1.

Most of the pressure types were in favor in the days of refraction shooting, except the piezoelectric type. The carbon microphone type was not very satisfactory, because of the frying of the carbon granules.

The I.G.E.S. carried out some tests with the Western Electric mining detector, which is of the carbon type, and with a hot-wire microphone seismograph.<sup>(10)</sup> Neither has thus far found application in reflection work. The Ambronn seismograph<sup>(2,6,14)</sup> is representative of the contact-accelerometer type, which has been employed extensively in refraction work but has not, to the author's knowledge, been used for recording reflections. In the piezoelectric type of pressure seismographs, the

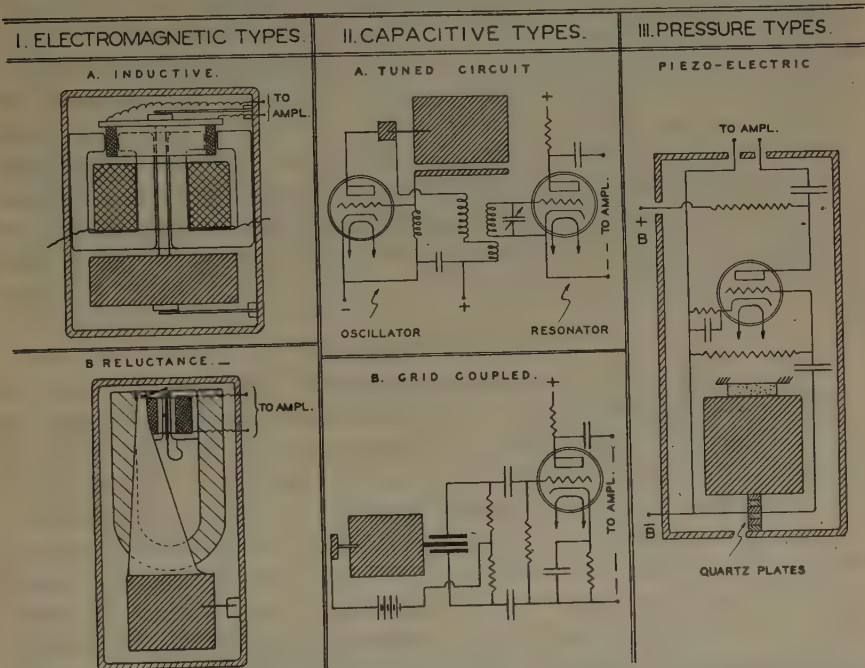


FIG. 1.—SCHEMATIC ILLUSTRATION OF INDUCTIVE, CAPACITIVE AND PRESSURE TYPES OF SEISMOGRAPHS.

seismograph mass bears down on the narrow sides of a battery of quartz plates cut parallel to their optical axes, thus producing cumulative charges of electricity on the larger sides as the pressure varies with the motion of the seismograph mass. This idea has been used in station seismology by Galitzin, Wood,<sup>(1)</sup> and Kato,<sup>(11)</sup> was used by Rieber<sup>(7)</sup> in refraction seismographs, and lately has been employed by Ambronn<sup>(32)</sup> in both refraction and reflection instruments.

## 2. Amplifiers

Virtually all reflection equipments now in use employ an amplifier between seismograph and indicating device. The variety of designs in use is exceedingly great, both in regard to number of stages and type of interstage coupling. At present preference seems to be for the resistance-



coupled type, although a number of companies are also employing impedance and transformer coupling. The number of stages varies greatly; generally their number is three; some companies, however, employ as many as six operated with reduced plate voltage. Despite these variations in design, a number of features are usually common to all amplifiers. To give preference to the reflection frequencies, and in order to reduce the response to undesired low and high frequencies, arrangements are generally made for selective action, either by a separate filter system in the input or by filters built into the stages. Another feature common to most amplifiers is an input and output transformer for matching the impedance of the pickup and of the indicating device. All amplifiers are battery operated and the tube filaments are lighted either from dry cells or storage batteries. Most amplifiers are provided with a plate current meter and controls for the filters and amplification, and filament and output switches. Some companies prefer not to have an amplification control and to balance the over-all sensitivity on the indicating device.

### 3. *Indicating Devices*

The purpose of the indicating devices is to record on rapidly moving photographic paper the output of the pickups which has been stepped up by the amplifier. Therefore the indicating devices are galvanometric instruments of various types; those most generally used at present are: (1) coil galvanometers, (2) oscillographs and (3) string galvanometers. The coil galvanometers are of the d'Arsonval type but with torsional wire or ribbon instead of jewel suspension. They are of much shorter natural period than the ordinary coil galvanometers, and therefore are really strongly damped vibration galvanometers. Usually they have high current sensitivity but do not possess the same dynamic sensitivity for higher frequency as oscillographs and string galvanometers, on account of their comparatively great moment of inertia. On the other hand, they have the advantage of the possibility of electrical damping and good optical reproduction, because large mirrors can be used. Oscillographs, are perhaps less frequently used than coil galvanometers; they have the advantage of high sensitivity and high natural frequency combined, but greater care has to be devoted to the design of a good optical system. String galvanometers share most of the advantages of the oscillograph, but have the drawback of shadow photography, which is somewhat tiring for office work on the records; furthermore, the possibility of attaining high sensitivity of the string under a microscope of fairly great magnification cannot be utilized if it is desired to use a harp of strings in the field of one microscope as is generally advantageous for field recorders. Some companies use string galvanometers without damping, tuned to reflected wave frequencies.



#### 4. *Time Marking*

The accuracy required for the timing of reflection impulses in the record is of the order of one thousandth of a second. Consequently it has become general practice to project time lines at one hundredth of a second interval on the paper and interpolate to the accuracy stated above. This may be accomplished in a number of ways. One method, which is in rather general use, is to have a 100-cycle tuning fork drive a synchronous motor to the shaft of which a wheel with 10 spokes is attached, one spoke being thicker to mark tenths of seconds on the record. This arrangement is used for shadow photography with string galvanometers. For black on white records the spoke wheel is replaced by a disk with the same number of slots and same arrangement of width in respect to one of the slots. Another arrangement is to provide the prongs of a 50-cycle tuning fork with slotted diaphragms and to project the slot opening every hundredth of a second directly upon the paper. This, however, involves a parallax of oscillograph and time record, which can be allowed for when evaluating the record. Still another method is to excite the primary of an induction coil with a 100-cycle fork and to connect a neon tube to the secondary; the image of the neon glow is projected on the paper. Finally, a vibrating reed with attached mirror may be used to project the time lines on the paper; the reed is tuned to 50 cycles and its vibration kept up by a vacuum tube oscillator or a tuning fork. The direct photography of the wave motion of a reed, or of an oscillograph driven from an electromagnetic tuning fork, is not used in regular field practice on account of the superiority of time lines for the full width of the paper in the timing of multiple records. The method is used, however, in laboratory calibration and for checking the accuracy of the time lines. The latter is generally accomplished with calibrated forks, or with radio time signals. (See p. 451.)

#### 5. *Shot-instant Transmission*

The instant of the shot is transferred to the recorder either by wire or by radio. Contrary to refraction shooting, only short base lengths are involved in most cases, and therefore wire transmission is generally preferred to radio transmission. The shot-instant line consists mostly of a double wire and is also used for telephone communication with the shot point. Current is supplied to the line by a dry-cell battery and the line is shot apart when the shot is fired. This may be done by winding it around the charge or around a series cap. The latter is preferable when the shooting is done in holes with casing that often will produce a re-shortening of the line when it is blown out of the hole. For the recording of the shot instant, a separate element may be provided in the recorder, being either of the reed type or a regular oscillograph. In most reflection

equipments, however, one of the oscillographs, galvanometers or string galvanometers used for the seismograph record is also employed for the shot-instant record. In that case, the shot-instant line is coupled to this oscillograph through a resistor or a transformer. Resistance coupling will produce an offset in the oscillograph record when the shot is fired, while transformer coupling produces an inductive kick. When using radio transmission for the shot instant, a transmitter is set up at the shot point and transmits a note or buzz. At the instant of the shot, the B-battery lead of the transmitter is broken and thus the transmitter cut off; by using a special contact device and a series cap, the transmitter



FIG. 2.—SIX REFLECTION PICKUPS.

may also be put on the air when the shot is fired. The receiver on the recording end may be provided with a telephone and mirror, or may be connected through a transformer to one of the regular oscillographs.

#### I-B. REFLECTION EQUIPMENT DESIGNED BY THE WRITER

The equipment consists of six pickups (Fig. 2), six amplifiers in two cases (Fig. 3) and the recorder with six oscillographs, camera, timing device, etc. (Fig. 4). Field procedure and recording car are shown in Fig. 5. In regard to physical characteristics, the equipment has been designed in accordance with the results of theoretical and practical considerations given further on in this paper.

The pickups are of the induction type; i.e., coils attached to the seismograph mass and moving in magnetic fields. Through a waterproof plug a double lead goes from each pickup to the amplifiers, which are mounted in the truck. A practical feature about these pickups is that they do not have to be arrested and released in field operation, and that the interior mechanism is readily accessible for laboratory tests. On

top of the pickups are a level vial and a dust cap; the direction of the shot point is indicated by an arrow as it has been found essential to orient the pickups always the same way for equality of reproduction.

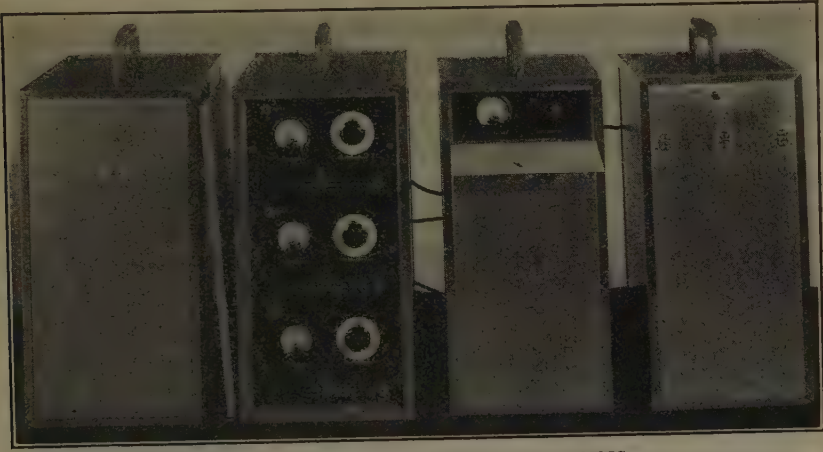


FIG. 3.—AMPLIFIERS AND BATTERY BOXES.

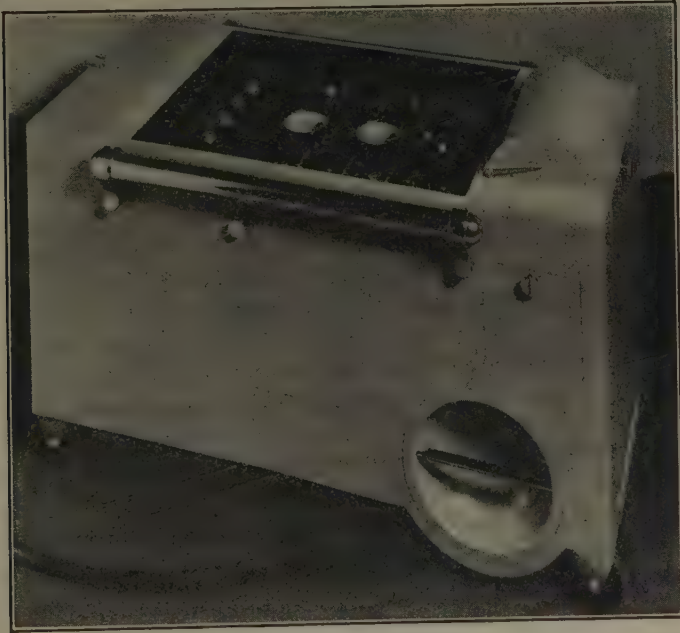


FIG. 4.—RECORDER.

The amplifiers are two-stage resistance coupled. An alternative design employs three resistance coupled stages with built-in filter, while in the design first mentioned the filters are separate units preceding the input stage. Plate current meter, volume control, filament and output



switch are on the panel. Three amplifiers are mounted in a case; the same holds for sets of three batteries shown in their boxes on the right of Fig. 3. A voltmeter is provided in each box to supervise the voltage of each battery set, which is particularly essential in resistance coupled amplifiers. The four boxes containing amplifiers and batteries are of same size and fit into the operator's rack in the recording truck.

The recorder box contains six oscillograph galvanometers with their lighting system, timer unit, camera with electromagnetic clutch, the control panel with sensitivity control for the oscillographs, testing arrangement for the latter, shot-instant input and switch, light switch and meter, and a combination switch to turn on the timer and paper clutch immediately before firing. Provision is made for visual observation while the photographic record is taken. The paper is driven at a speed of 10 to 15



FIG. 5.—RECORDING TRUCK IN OPERATION.

in. per second by a spring motor and may be changed readily in the same manner as an ordinary photographic camera. Each oscillograph is self-contained and may be replaced easily; the vertical and horizontal adjustment of the oscillographs is at the top of the recorder behind the control panel. The oscillograph galvanometers have a damping of 0.7 critical (see p. 441) and a sensitivity from 0.1 to 0.8 mm. scale deflection for one microampere. Their natural frequency is adjustable in small limits and around 200. Records may be taken in daylight but the paper must be removed when the truck is closed; however, the arrangement may be modified for daylight developing. The shot instant is transferred to the truck by a double line and coupled to one of the oscillographs; and provision is made for a separate shot indicator, which may be preferred under certain conditions, particularly when using radio transmission.

Fig. 5 shows the recording car (Ford V-8 panel delivery) in operation. A reel stand with six pickup lead reels is used, which is folded up for moving and placed in the truck. The reels may also be mounted individually on the outside of the car. In addition to the amplifier and battery boxes,



the truck carries the recorder, which may be adjusted to the operator's position on a movable rack, the telephone, developing trays, and two cabinets for radio parts, etc., and chemicals. The pickups are mounted behind the driver's and companion's seats. Originally provision was made on the recorder to fire the shot from the observer's station, but this practice has been abandoned in favor of firing by signals from the shot-master's location. This is more advantageous for field operation because it saves a double line from the truck to the firing point.

## II. CHARACTERISTICS OF REFLECTION SEISMOGRAPHS

In the following chapter a discussion is given on the characteristics of reflection equipment based upon the theory of interaction of pickup, amplifier, and galvanometer. The latter holds for electromagnetic seismographs only but it may readily be modified for the capacity and piezoelectric type of pickup, while the relations for amplifier and galvanometer remain the same, of course. The electromagnetic type of pickup has been selected for this discussion because it is the type most widely used at this time; furthermore, it includes the inductive and the reluctance type, the frequency characteristics of which are the same, and the sensitivity constants only slightly different. While for simplicity, therefore, the sensitivity constants are written for the inductive type of pickup in the following discussion, the respective constants for the reluctance pickup may be substituted in their place as derived, for instance, by Benioff.<sup>(19)</sup>

In order to determine the most desirable characteristics for reflection seismographs, it is necessary to inquire first into the nature of the mechanical and electrical quantities that constitute the important characteristics, and to this end the type of coupling or interaction existing between the various constituents of a reflection equipment must be investigated first (A). Then the relations can be stated which control the action of pickup, amplifier and galvanometer under the influence of such forces individually (B), and combined (C). These final relations will permit of stating which static and dynamic characteristics are essential for the over-all response (D), and how their values should be selected for the most advantageous results (E).

### A. TYPES OF COUPLING IN ELECTROMAGNETIC SEISMOGRAPHS

Considering the transfer of energy between the various constituents of a reflection seismic equipment, it will be found that combinations of essentially three types of coupling are involved. These are in ascending order of the time derivatives of the displacements: (1) force coupling; (2) viscosity and friction coupling, and (3) inertia coupling.

The differential equations for each system are given below for the three types of coupling. The single dots stand for the first, the double dots for the second derivatives of the displacements with respect to time. The subscripts refer to the systems 1 and 2. The equations hold for small displacements; i.e., small angular deflections  $\phi$ , thus avoiding elliptical functions resulting from  $\sin \phi$  terms. The equations are universal for all mechanical (seismograph, pendulum, magnetometer, spring suspension, galvanometer, oscillograph) and electrical circuit phenomena. Thus,  $m$  stands for the mass in linear, and for the moment of inertia in angular displacements, and for the inductance in electrical systems;  $c$  is the restoring force for unit displacement (the spring constant), or other elastic, or magnetic, or gravitational force in mechanical systems, or the reciprocal capacity in electrical circuits.  $\sqrt{\frac{c}{m}}$  is in all cases equal to the natural angular frequency  $\omega_0$  of the system.

$$\text{Force Coupling: } \begin{cases} m_1 \ddot{x}_1 + c_1 x_1 = c_1 k_1 x_2 \\ m_2 \ddot{x}_2 + c_2 x_2 = c_2 k_2 x_1 \end{cases} \quad [1]$$

in which  $k_1$  and  $k_2$  are coupling coefficients.

The force coupling applies to all reproducing instruments such as telephones, galvanometers, oscillographs and the like (and electromagnetic seismographs in calibration, see p. 444)

$$\text{Viscosity and Friction Coupling: } \begin{cases} m_1 \ddot{x}_1 + c_1 \dot{x}_1 = -p_1 (\dot{x}_1 - r_1 \dot{x}_2) \\ m_2 \ddot{x}_2 + c_2 \dot{x}_2 = -p_2 (\dot{x}_2 - r_2 \dot{x}_1) \end{cases} \quad [2]$$

in which  $p$  is the damping resistance (force on a mass moving with unit velocity), and  $r$  the frictional resistance.

Friction and viscosity coupling is involved in the transfer of the ground motion to the seismograph mass through mechanical friction and the damping fluid.

In these equations, two assumptions are made: (1) that the velocity of the currents set up by  $\dot{x}$  in the damping fluid is so small that a term considering damping proportional to the square of the velocity may be neglected; (2) that the frictional resistance is proportional to the velocity of the damped motion of the second system. This is for forced oscillations. For free oscillations Coulomb friction appears as a constant force. The frictional coefficients are the same in either case. For the static determination, see p. 446.

$$\text{Inertia (Acceleration) Coupling: } \begin{cases} m_1 \ddot{x}_1 + c_1 x_1 = G_1 \ddot{x}_2 \\ m_2 \ddot{x}_2 + c_2 x_2 = G_2 \ddot{x}_1 \end{cases} \quad [3]$$

in which  $G_1$  and  $G_2$  are the coefficients of acceleration coupling. The equations express conditions of energy transfer in undamped inertia systems, like the transfer of ground movement to an undamped seismograph.

These relations can be simplified for the present problem by assuming that the transfer of energy takes place in one direction only; i.e., that the secondary systems receive no energy from the primary systems. Thus, it is assumed that the ground receives no energy from the seismograph mass, that the amplifiers do not react back on the seismograph coil, and that the amplifier is not affected by the galvanometer movement. True enough, there is a reaction of amplifier upon seismograph through the primary of the input transformer if it is used, but this is taken care of in a term expressing electromagnetic damping. The galvanometer likewise is affected by the secondary of the output transformer of the amplifier, but there again this effect may be included in the damping. The use of an amplifier between seismograph and galvanometer prevents the coupling of galvanometer and seismograph through the rectifier action of the tubes. If such is not the case—if the galvanometer is connected directly to the seismograph, as in Galitzin seismographs—the mutual coupling leads to fourth order differential equations for which Wenner<sup>(4)</sup> has worked out the solution.

The restrictions given to the transfer of energy allow of applying the above equations to the coupling occurring in electrical seismograph systems; they occur there in combined form. Energy is transferred from the ground to the seismograph mass; first, by virtue of the inertia of the mass and second through the damping fluid. Therefore combination of both equations 3 and 2 applies. The mechanical energy of the seismograph mass is transferred into electrical energy in proportion to the first time derivative of the mass displacement. The coupling of the seismograph coils to the amplifier is involved and depends on the type of input, output, and interstage coupling used. As both inductive and capacitive coupling is involved, it may be assumed in first approximation that the electrical action of the amplifier is equivalent to a combined force and inertia coupling, combined with damping. The indicating device is connected to the amplifier by force coupling. Its action is expressed therefore by equation 1, and combined with damping.

The significance of the above equations goes, however, further than that. It will be shown later that an inertia system provided with an electrical output device may be converted into a force-coupled system if the generator action is reversed to motor action. This is a valuable help in the calibration of seismographs, for it reduces the dynamic determination of the output characteristics of an electrical seismograph on a shaking table to a much more convenient method with the seismograph stationary. By a simple combination of two such determinations for both seismograph and amplifier-oscillograph, and one calculation combining the two, the shaking table may even be dispensed with for determining the over-all characteristics of the entire equipment. Details on this method will be found in part III, on calibration.



## II-B. ACTION OF PICKUP, AMPLIFIER, AND GALVANOMETER

1. *Pickup*

*Mechanical Action.*—In view of what was said in the foregoing paragraph about the transfer of energy in coupled systems, the equations for the constituent parts of the apparatus may now be set up. For the inertia coupling of ground and seismograph, equations 3 are applied.

Dividing by  $m$ , substituting  $\sqrt{\frac{c}{m}} = \omega_0$  as natural undamped frequency, and with a coupling coefficient of  $\frac{G}{m} = -1$ ,

$$\ddot{x}_1 + \omega_0^2 \cdot x_1 = -\ddot{x}_2$$

In most electromagnetic seismographs the coil or armature is attached by a lever to the moving mass to magnify the movement. Introducing the ratio of coil displacement  $a$  to mass displacement  $x_1$ , and designating  $\frac{a}{x_1}$  by  $V$  (geometric or static magnification), as customary in seismology:

$$\ddot{a} + \omega_0^2 a = -V\ddot{x}_2 \quad [4]$$

Reflection records obtained by various investigators with equipments of widely varying construction indicate that the ground displacements occurring when a reflected wave impinges on the surface may be closely enough considered as a damped harmonic motion of the form

$$x = X \cdot e^{-\beta t} \cdot \sin \omega t \quad [5]$$

where  $X$  is its maximum amplitude,  $x$  its value at the time  $t$ ,  $\omega$  the ground frequency, and  $\beta$  a damping exponent.

For a preliminary consideration of the action of an undamped seismograph also the damping of the ground motion may be temporarily disregarded so that the solution of eq. 4 is:

$$a = Vx \frac{\omega^2}{\omega_0^2 - \omega^2}, \quad \text{or} \quad W = V \frac{\omega^2}{\omega_0^2 - \omega^2} \quad \text{or} \quad W = V\omega^2 f \quad [6]$$

with  $f = \frac{1}{\omega_0^2 - \omega^2}$  as the undamped frequency factor and  $W = \frac{a}{x}$  the dynamic undamped magnification. In case of resonance,  $\omega = \omega_0$ , and  $W$  is theoretically  $\infty$ ; if the ground frequency is much greater than the instrument frequency,  $W = -V$ ; i.e., the dynamic magnification is equal to the static magnification. If, finally, the instrument frequency is much greater than the ground frequency,  $W = \frac{V}{\omega_0^2} \cdot \omega^2$ , the seismograph responds to the square of the ground frequency; i.e., the ground acceleration, but with a much reduced magnification  $\frac{V}{\omega_0^2}$ .



The mechanism of an undamped seismograph has been considered merely as a means of preliminary orientation in the problem. In reflection seismographs, damping is an absolute necessity, to reduce the duration of natural free oscillation to a minimum, as well as to smooth out the dynamic response curve. To set up the equations for this case, the viscosity damping has to be added (eq. 2) to the inertia coupling so that with disregard of friction and regeneration, division by  $m$  as before and substitution of  $2\epsilon$  for  $\frac{p}{m}$ :

$$\ddot{x} + 2\epsilon\dot{x} + \omega_0^2 x = -V\ddot{x} \quad [7]$$

For the ground displacement, again a periodic damped motion is assumed, as given in eq. 4 and substituted in eq. 7. Then the solution

$$x = Ae^{-\epsilon t} \sin(\omega_d t + \psi) + VX\omega^2 e^{-\beta t} \frac{1}{\sqrt{(\omega_0^2 - \omega^2)^2 + 4\epsilon^2 \omega^2}} \sin(\omega t + \varphi) \quad [8]$$

This equation represents the superposition of two damped motions. The first particular solution is the damped free motion of the seismograph with the maximum amplitude  $A$  at the start,  $\omega_d$  the damped frequency, ( $\omega_d = \sqrt{\omega_0^2 - \epsilon^2}$ ), and  $\psi$  the phase angle at  $t = 0$ . The second particular solution is the dynamically magnified ground motion which is recorded with a phase shift  $\varphi = \arctan \frac{2\epsilon\omega}{\omega_0^2 - \omega^2}$ . Thus in the stationary state, after the first term has vanished,\* the dynamic magnification is given for corresponding phases by dividing the second term of eq. 8 by eq. 5. Then the dynamic damped magnification:

$$\left. \begin{aligned} W_d &= V\omega^2 \cdot \frac{1}{\sqrt{(\omega_0^2 - \omega^2)^2 + 4\epsilon^2 \omega^2}} \text{ or} \\ W_d &= V\omega^2 f_d, \text{ with } f_d = \frac{1}{\sqrt{(\omega_0^2 - \omega^2)^2 + 4\epsilon^2 \omega^2}} \end{aligned} \right\} \quad [9]$$

where  $f_d$  is the damped frequency factor. The geometric relation of the reciprocal damped and undamped frequency factors and phase shift is shown in Fig. 7; hence

$$f_d = f \cos \varphi \text{ and } W_d = W \cos \varphi \quad [10]$$

The damped dynamic magnification is thus less than the undamped dynamic magnification.

Fig. 6 shows the variation of phase shift with the "tuning factor"  $n$ ; i.e., the ratio of ground and instrument frequency. On the left of the resonance point, the recorded motion is in the same direction as the ground motion; on the right, in opposite direction. If damping were not present there would be a sudden change from one direction to the other in passing the resonance point. Damping, particularly near critical, provides

---

\* A discussion of onset conditions is found on page 441.

for a gradual transition. This may be enhanced by selecting the natural frequency low enough to place the phase change with ground frequency in the range of least change on the right (see p. 437). Fig. 8 shows the dynamic response of the seismograph for various degrees of damping as a function of the tuning factor. The damping degree  $\eta = \frac{\epsilon}{\omega_0}$  is the ratio of actual to critical damping. On the right of the resonance point the

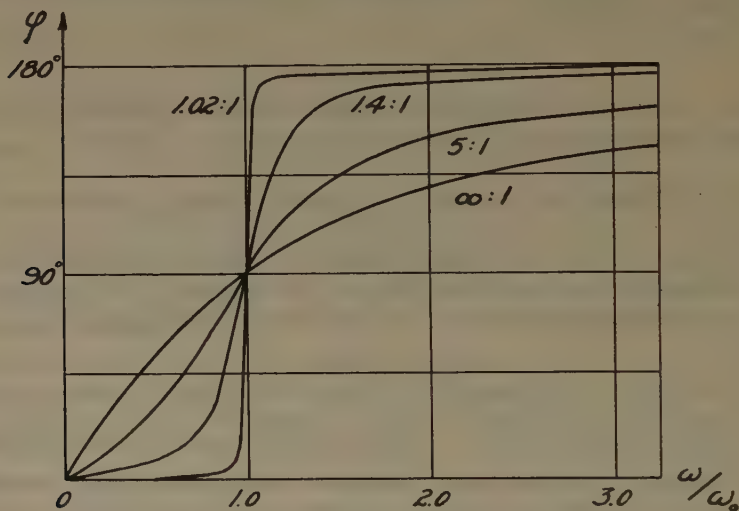


FIG. 6.—RELATION OF PHASE SHIFT AND TUNING FACTOR  $n = \omega/\omega_0$ .

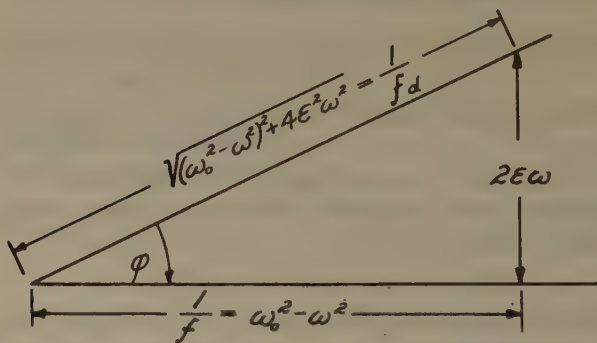


FIG. 7.—GEOMETRIC RELATION OF PHASE, AND DAMPED AND UNDAMPED FREQUENCY FACTORS.

abscissas are reciprocals of the tuning factor. For ground frequencies smaller than instrument frequency, the dynamic magnification increases approximately with the square of the ground frequency; on the right, if the instrument frequency is much lower than the ground frequency, the dynamic response is essentially equal to the static response regardless of damping. If a band of ground frequencies is well defined in frequency,

it is desirable to operate with a low instrument frequency and high static magnification level. Both requirements, fortunately, can be combined (see p. 437). If there is danger of frequencies trespassing in a region near the resonance point, additional damping must be provided for. The necessity of strong damping follows, besides, from the need of suppressing free oscillations.

The principal feature of the response curve for inertia coupling is that for strong damping the dynamic magnification *increases* steadily with extraneous frequency to the static magnification level. The oppo-

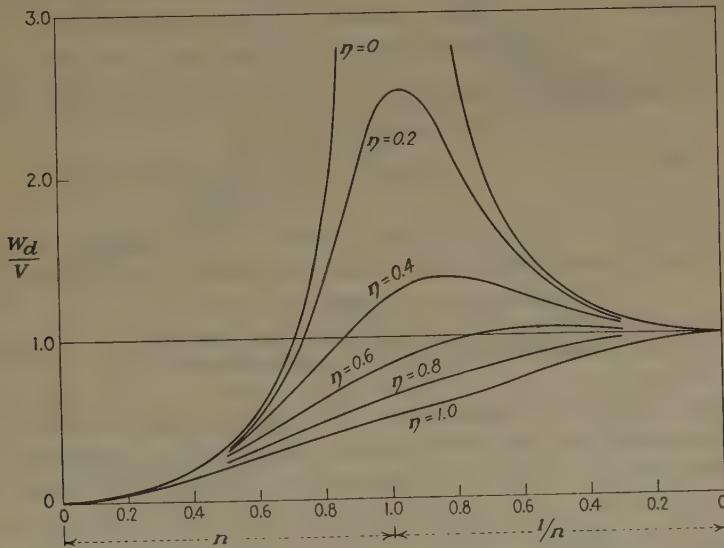


FIG. 8.—FREQUENCY RESPONSE OF INERTIA-COUPLED SEISMOGRAPH, MECHANICAL ACTION.

site holds for force coupling (Fig. 9) where the dynamic magnification *decreases* with frequency from the static magnification level.

The damped resonance frequency in an inertia-coupled system is greater than the undamped resonance frequency; in a force-coupled system it is less. The resonance frequency for a damped mechanical seismograph follows from a differentiation of the square of the reciprocal of  $\omega^2 f d$  (eq. 9) with respect to  $\omega^2$  to

$$\omega_r = \frac{\omega_0^2}{\sqrt{\omega_0^2 - 2\epsilon^2}} \quad [11]$$

which reduces to  $\omega_r = \omega_0$  for the undamped system. Fig. 10 shows the relation of undamped natural frequency, damped frequency, and resonance frequencies for inertia and force coupling.

Further data on the mechanical action of seismographs, particularly in regard to spring suspensions, will be found on page 438.

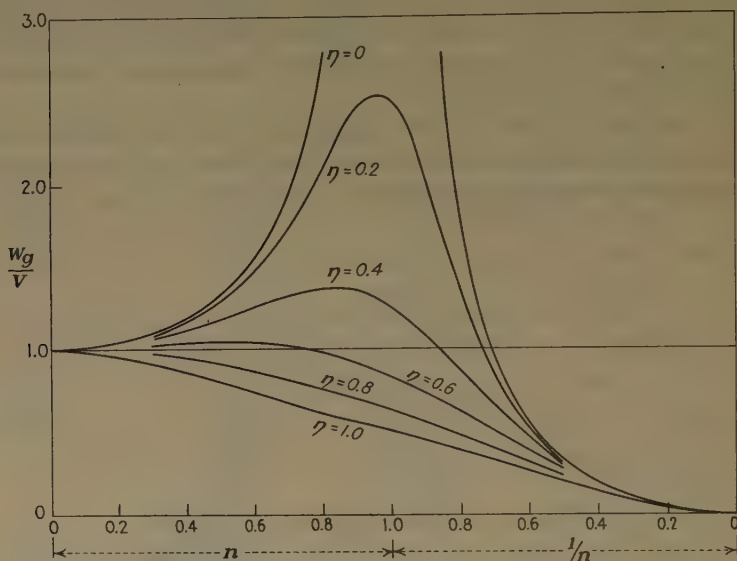


FIG. 9.—FREQUENCY RESPONSE OF FORCE-COUPLED SEISMOGRAPH, ELECTRICAL-MECHANICAL ACTION. (See also page 433.)

*Electrical Action of Seismographs.*—The equations given in the following section hold for the electromagnetic type only. Specifically, the derivations are given for the induction type. For the reluctance type,

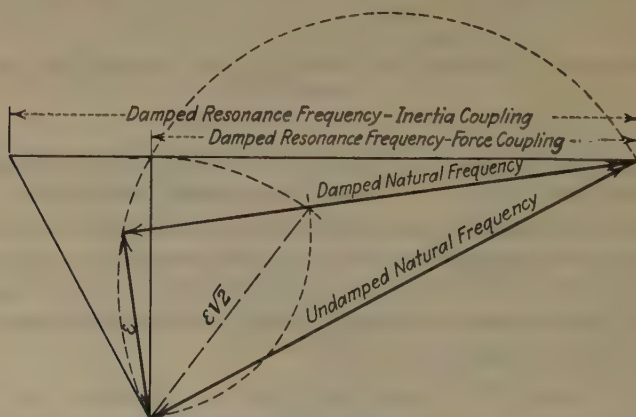


FIG. 10.—RELATION OF UNDAMPED AND DAMPED NATURAL FREQUENCIES, AND DAMPED RESONANCE FREQUENCIES.

the formulas have been derived by Benioff and need not be repeated here. The voltage output of both the induction and the reluctance types are proportional to the velocity of the moving mass.



For a simple type of induction pickup with a number of circular coils moving in radial magnetic fields with annular pole pieces (dynamic speaker type) the induced electromotive force is:

$$E = -H_s \cdot l \cdot \frac{da}{dt} \quad [12]$$

with  $H_s$  as average strength of the magnetic fields and  $l$  the total length of wire; for a circular coil,  $l = d\pi N$  where  $d$  is the mean diameter and  $N$  the number of turns.

Into the last equation, the value previously obtained for the coil amplitude  $a$  (eq. 8) is substituted. The electromotive force produced by the free oscillation of the damped mechanical system is proportional  $Ae^{-\epsilon t}(\omega_d \cos \omega_d t - \epsilon \sin \omega_d t)$  and may be disregarded for small values of  $\omega_d$ ; i.e., strong damping. The electromotive force due to the forced oscillation is:

$$E = -H_s l V X \omega^2 \frac{1}{\sqrt{(\omega_0^2 - \omega^2)^2 + 4\epsilon^2 \omega^2}} \cdot \omega \sin(\omega t \pm \frac{\pi}{2} + \varphi) \quad [13]$$

where for simplification the assumption of damping of the primary motion has been dropped. Using previous symbols, eq. 13 may be written:

$$E = T \omega V \omega^2 f_d X \sin(\omega t \pm 90^\circ + \varphi) \quad [14]$$

with  $T$  as transmission constant. The equation shows that the induced electromotive force increases with the frequency of the ground motion. This is verified by Reutlinger's experiments<sup>(5)</sup> (Fig. 11) which also show that the voltage output is hardly affected by the mechanical seismograph characteristics *provided* the natural frequency is low. The linear voltage characteristics are modified, however, by force-coupling the seismograph to the galvanometer (curve *b*). The peaking of this last curve will further be affected by the characteristics of the amplifier as shown below.

## 2. Amplifier

To set up an accurate equation for a seismograph amplifier would require individual consideration of all circuits and couplings involved. In view of the wide variety of circuits employed, it is doubtful whether a complicated system of equations would be of general value in revealing the general relations applying to any kind of amplifier. Only a most general and approximate solution is attempted here. For setting up the amplifier equations the relations given on page 422, with their electrical equivalents, may be used.

As far as the coupling of the amplifier to the seismograph is concerned, the assumption is made that the energy passes into the former without effect on the latter (except for the effect of the input transformer primary on the electromagnetic damping of the seismograph, which is incorporated in the damping). The coupling coefficient of amplifier to seismograph

if done inductively may be put  $= k_1 = \frac{L_{12}}{\sqrt{L_1 L_2}}$ ; in a similar manner, the output coupling to the galvanometer  $k_2 = \frac{L_{34}}{\sqrt{L_3 L_4}}$ . The interstage coupling coefficients  $k_3, k_4$ , etc. depend on the type of coupling used. The over-all voltage gain, consisting of tube and interstage, as well as input and output amplification, may be designated by  $V_a$ . The combined action of all inductances is assumed to be represented by  $L$ , that of the capacities by  $C$ , and of the resistances  $R$ . This permits of considering

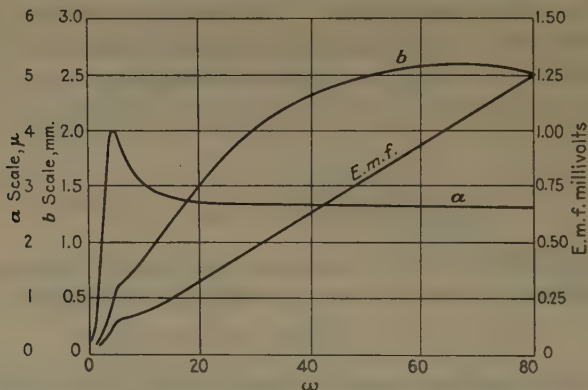


FIG. 11.—EXPERIMENTAL RESPONSE CURVES OF ELECTROMAGNETIC SEISMOGRAPH, AFTER REUTLINGER.

$a$ , dynamic mechanical response; e.m.f., induced voltage;  $b$ , galvanometer response.

the amplifier as a damped oscillatory system with the damping factor  $\epsilon_a = \frac{R}{2L}$ , the natural undamped frequency  $\omega_a = \frac{1}{\sqrt{LC}}$ , and the damped frequency  $\omega_{da} = \frac{1}{2L} \sqrt{\frac{4L}{C} - R^2}$ .\* It is assumed that all circuits in the amplifier are highly damped.

With a periodic voltage output  $E$  of the frequency  $\omega$  furnished by the seismograph the current output of the amplifier may be written

$$i = Be^{-\epsilon_a t} \sin(\omega_{da} t + \psi_a) + \frac{EV_a \omega}{L} \frac{1}{\sqrt{(\omega_a^2 - \omega^2)^2 + 4\epsilon_a^2 \omega^2}} \sin(\omega t + \varphi_a) \quad [15]$$

The first portion of the equation again represents free oscillations of the amplifier with an initial maximum amplitude  $B$  and phase angle  $\psi_a$  corresponding to the displacement at the time  $t = 0$ . This term may be disregarded provided the amplifier is strongly damped. The second term is a measure for the dynamic magnification of the output current for the impressed voltage and is thus

$$W_a = \frac{V_a \omega}{L} \cdot f_{da} \quad [16]$$

\* See page 448 for significance of these quantities

where  $f_{da}$  is the damped frequency factor of the amplifier or  

$$\frac{1}{\sqrt{(\omega_a^2 - \omega^2)^2 + 4\epsilon_a^2 \omega^2}} \cdot \varphi_a$$
 is the phase shift of current and voltage  
 nput;  $\varphi_a = \arctan \frac{2\epsilon_a \omega}{\omega_a^2 - \omega^2} = \arccos \frac{f_{da}}{f_a}$ .

The current output is proportional to the first time derivative of the voltage input. This is verified by laboratory experiments. The dynamic response curves of selective amplifiers such as now used in reflection work show, in laboratory tests, such close approximation to damped oscillatory systems in regard to their frequency response that the equation stated above may be assumed to be essentially correct. (See also p. 448.)

### 3. Oscillographs and Other Types of Recording Instruments

The types of recording instruments generally employed are (a) oscillographs; (b) coil galvanometers and (c) string galvanometers. The differential equations for these types will be given in the same order. They are force-coupled to the amplifiers; hence, eq. 1 applies, combined with 2, to take care of the damping.

In the oscillograph a loop is placed in the field of the air gap of a magnet of the length  $L$  and the field strength  $H$ . The distance of the loop wires or ribbons is  $2d$ . Its plane of rest is parallel with the lines of force. A current  $i$  produces the couple  $-2HiLD \cos \varphi$  where  $\varphi$  is the angle of deflection; thus, the couple is  $-HiS \cos \varphi$  with  $S = 2Ld$  as effective loop area. For static deflections this is equal to the elastic restituting force of an equivalent single wire with the torsional coefficient  $\tau$ , so that the elastic couple =  $\tau\varphi$ . Thus the equation of motion, with  $K$  = moment of inertia; and putting  $\cos \varphi = 1$  for small deflections:

$$K\ddot{\varphi} + \tau\varphi = HSi \quad [17]$$

To this, damping has to be added. It is composed of electromagnetic and/or liquid damping. The former is due to the electromotive force induced in the moving loop, which in turn generates a magnetic field acting as braking resistance to the movement. As the counter e.m.f.

is  $HS\dot{\varphi}$ , and its current  $\frac{HS}{z_0 + Z_0} \cdot \dot{\varphi}$  ( $z_0$  = oscillograph, and  $Z_0$  = shunt,

and transformer secondary impedance), the braking moment is  $\frac{H^2 S^2}{z_0 + Z_0} \cdot \dot{\varphi}$ .

Substituting for the factor of  $\dot{\varphi}$  an electromagnetic damping force  $d_e$  and adding to it the force of liquid damping  $d_m$ , if such is applied, eq. 17 becomes

$$K\ddot{\varphi} + \dot{\varphi}(d_e + d_m) + \tau\varphi = HSi \quad [17a]$$

After division by  $K$ , substitution of  $2\epsilon_g$  for  $\frac{d_e + d_m}{K}$ , of  $\omega_g^2$  for  $\frac{\tau}{K}$  and of  $\frac{b}{2f_0}$  ( $b$  = paper amplitude of light spot, if autocollimational recording is used, with  $f_0$  as focal length of lens before oscillograph mirror) for  $\varphi$ , the differential equation of motion of the oscillograph

$$\ddot{b} + 2\epsilon_g \dot{b} + \omega_g^2 b = \frac{2f_0 HS}{K} i \quad [18]$$

For a coil galvanometer suspended by a string with the torsional coefficient  $\tau$ , the moment of inertia  $K$ , and the number of turns  $N$ , the last equation is

$$\ddot{b} + 2\epsilon_g \dot{b} + \omega_g^2 b = \frac{2f_0 HSN}{K} i \quad [19]$$

In a string galvanometer, the lateral displacement of a wire or a harp of wires in a magnetic field is photographed through a microscope or a number of them. If  $L$  is the length of the string between the pole pieces,  $H$  again the field strength and  $i$  the current, the force exerted upon the string by the current is  $HiL$ . With  $m$  as the mass of the string,  $\lambda$  its total length,  $a$  its sectional area and  $\rho$  its density, and  $P$  the tension, the natural frequency of the first fundamental is  $\omega_g = \frac{\pi}{\lambda} \sqrt{\frac{P}{a\rho}}$ . Hence the equation of motion

$$m\ddot{b} + m\omega_g^2 b = HLi$$

which may be written for amplitudes  $b$  on the paper obtained through magnification of a microscope with power  $M$ , and with (combined air and electromagnetic) damping  $2\epsilon_g$ :

$$\ddot{b} + 2\epsilon_g \dot{b} + \omega_g^2 b = \frac{MHL}{m} \cdot i \quad [20]$$

Equations 18, 19 and 20 may be combined into one general equation for all types of recording galvanometers by introducing the ratio of direct current sensitivity  $V_g$  and moment of inertia  $K$ , or  $\frac{V_g}{K}$ , for  $\frac{2f_0 HS}{K}$ , or  $\frac{2f_0 DHSN}{K}$  or  $\frac{MHL}{m}$ . Then the general equation:

$$\ddot{b} + 2\epsilon_g \dot{b} + \omega_g^2 b = \frac{V_g}{K} i \quad [21]$$

the solution of which for a periodic current of the frequency  $\omega$  and the peak value  $I$

$$b = Ce^{-\epsilon_g t} \sin(\omega_d t + \psi_0) + \frac{IV_g}{K} \frac{1}{\sqrt{(\omega_g^2 - \omega^2)^2 + 4\epsilon_g^2 \omega^2}} \sin(\omega t + \varphi_0) \quad [22]$$



$\varphi_g$  is the phase shift of galvanometer movement and impressed current;  $\varphi_g = \arctan \frac{2\epsilon_g \omega}{\omega_g^2 - \omega^2} = \arccos \frac{f_{dg}}{f_g}$  (ratio of damped and undamped galvanometer frequency factor). The first term is the free damped movement of the galvanometer and may again be disregarded for the consideration of the damped dynamic magnification characteristics, and provided the damping is sufficiently strong; the second is the dynamically magnified current. Thus the dynamic galvanometer magnification may be written:

$$W_g = \frac{V_g}{K} \cdot f_{dg} \quad [23]$$

The dynamic response of recording galvanometers is shown in Fig. 9. The magnification falls off with increasing frequency below the static magnification (or d.c. sensitivity). This is opposite to the mechanical behavior of a seismograph, the dynamic magnification of which increases with an increase in frequency until it approaches the static magnification level. The former is a peculiarity of force coupling, the latter a peculiarity of inertia coupling. For an electromagnetic seismograph, they may be converted into one another, as discussed on page 444.

The damped resonance frequency of a force-coupled system is different from that of an inertia-coupled system. While in the latter it is greater than the undamped resonance frequency, it is smaller in the former and is given by

$$\omega_{rd} = \sqrt{\omega_0^2 - 2\epsilon^2} \quad (\text{see Fig. 10}) \quad [24]$$

## II-C. COMBINED ACTION OF PICKUPS, AMPLIFIERS AND OSCILLOGRAPHS

In order to find the combined action of the constituents of a reflection equipment, eq. 22 is used. For  $i$ , its value obtained in eq. 15 is substituted; the voltage input in eq. 15, in turn, is obtained from eq. 13. For the calculation of the combined dynamic response and with the assumption of strong damping all terms describing the free damped oscillations are disregarded.\* Thus with  $\varphi_r$  as the resultant phase shift:

$$b = \frac{TVV_aV_g\omega^4}{KL} f_d \cdot f_{ad} \cdot f_{gd} \cdot X \sin(\omega t + \varphi_r) \quad [25]$$

Thus the over-all dynamic magnification  $W_r$

$$W_r = W_d \cdot W_a \cdot W_g \cdot \omega T \quad [26]$$

where the constituent dynamic magnifications are given by equations 9, 16 and 23 and the term  $\omega T$  designates the transfer of mechanical into electrical energy in the pickup as given in eq. 14.

$f_d$ ,  $f_{ad}$  and  $f_{gd}$  are the damped frequency factors of seismograph, amplifier and galvanometer as used before, which for critical damping

\* For a discussion of onset conditions, see page 441.

$$f_d = \frac{1}{\omega_0^2 + \omega^2}; \quad f_{ad} = \frac{1}{\omega_a^2 + \omega^2}; \quad f_{gd} = \frac{1}{\omega_g^2 + \omega^2}$$

and for damping 0.7 critical  $\left(\eta = \frac{\epsilon}{\omega_0} = \sqrt{\frac{1}{2}}\right)$  (see p. 441).

$$f_d = \frac{1}{\sqrt{\omega_0^4 + \omega^4}}; \quad f_{ad} = \frac{1}{\sqrt{\omega_a^4 + \omega^4}}; \quad f_{gd} = \frac{1}{\sqrt{\omega_g^4 + \omega^4}} \quad [27]$$

By substitution of  $\frac{\tau}{K}$  for  $\omega_0^2$ ,  $\omega_a^2$  for  $\frac{1}{\sqrt{LC}}$ , and  $\omega = n\omega_0 = n_a\omega_a = n_g\omega_g$

( $n$  = tuning factor), and  $\eta = \frac{\epsilon}{\omega_0}$  (ratio of actual to critical damping)

$$b = \frac{TVV_aV_gC\omega^4}{\omega_0^2\tau} \frac{1}{\sqrt{(1-n^2)^2 + 4\eta^2n^2}} \cdot \frac{1}{\sqrt{(1-n_a^2)^2 + 4\eta_a^2n_a^2}} \cdot \frac{1}{\sqrt{(1-n_g^2)^2 + 4\eta_g^2n_g^2}} X \sin(\omega t + \varphi_r) \quad [28]$$

From this equation the dynamic response curve of the entire equipment may be calculated for any ratio of ground frequency to natural frequencies of the various constituents, and any ratio of actual damping to critical. However, when an equipment is available, it is much easier to determine the over-all dynamic characteristics by response tests of seismograph and amplifier with oscillograph, and to combine them as discussed in further detail in part III.

Among other things, the galvanometer deflection is inversely proportional to the natural frequency of the seismograph. This can also be proved by another line of reasoning offered in part II-E.

#### D. STATIC AND DYNAMIC CONSTANTS

The dynamic response of the entire reflection apparatus and its constituent parts is characterized by two types of instrument constants: (1) those that affect only the sensitivity, and (2) those that affect both sensitivity and frequency response. The former are not related to time and may be called static; the latter may be called dynamic constants. The static constants are: (1) the geometric magnification of the pickup; (2) the electrical sensitivity of the pickup; (3) the gain of the amplifier, inclusive of amplification due to input and output coupling, and (4) the d.c. sensitivity of the oscillograph.

The second type are frequency constants and comprise: (1) the natural frequencies of pickup, amplifier and oscillograph, and (2) the damping factors of pickup, amplifier and oscillograph.

With the exception of damped and resonance frequencies, all other quantities utilized before—dynamic magnification, phase shift, damped and undamped frequency factors—are of secondary nature and depend upon the extraneous frequency.

## II-E. DESIRABLE VALUES FOR STATIC AND DYNAMIC CONSTANTS

In a reflection apparatus consisting of three units (pickup, amplifier and oscillograph), which in themselves permit a wide variation in their mechanical and electrical design, there are, naturally, a number of ways in which units of different characteristics may be combined to give the same result. This holds for both sensitivity and frequency characteristics. While it is generally agreed that high sensitivity is desirable, the total sensitivity may be accomplished by making either the pickup, or the amplifier, or the oscillograph, or all of them, or any two of them, very sensitive. It is rather general practice to use a selective equipment; the selectivity may theoretically be obtained by either peaking the pickup, or the amplifier, or the oscillograph. On account of this situation it is naturally impossible to give specific values for the static and dynamic characteristics of each unit; however, certain conclusions can be drawn from the theory and practical field experience as to their general magnitude. As a matter of fact, design practices are widely at variance; yet it is surprising that good and apparently faithful reproduction can be obtained with most of them. The purpose of the following discussion is to set forth, on the basis of the theory derived above, certain principles of construction which the writer has found successful in practice.

### 1. *Static Characteristics*

As far as static characteristics are concerned, the over-all sensitivity should be as great as possible as is consistent with stable field operation. The geometric magnification of the pickup can be increased by providing lever attachments or transmission links on the mass to the coil or armature, but this is subject to decided limits due to the possibility of friction, secondary resonance peaks, too delicate construction and necessity of arresting and releasing. For field operation it is desirable to avoid the latter if possible. In the next paragraph it will be shown that a low natural frequency of the pickup is desirable and, fortunately, this is consistent with high geometric magnification. The electrical sensitivity is dependent chiefly on the strength of the magnetic field and the length of the wire. For this reason it is advisable to provide for such arrangements of the magnetic fields and coils that all or most of the wire is utilized for the production of current. Correct selection of materials for permanent magnets, electromagnets, pole-piece material and wire is important—not to forget good insulation. The gain of the amplifier should be as high as is consistent with stability of operation and freedom from extraneous disturbances. Impedances of input and output devices should be matched correctly to pickup and oscillograph for most efficient performance. The d.c. sensitivity of the oscillographs, coil galvanometers, or string galvanometers should be high. Unfortunately, this



cannot be combined with high natural frequency, as postulated in the next paragraph. However, by using strong magnetic fields and great optical magnification, this disadvantage can be largely overcome. In this respect the string galvanometer is inferior to the oscillograph because, if a harp of strings is to be kept in the field of one microscope, the magnification cannot exceed a limit for safe spacing of the strings. Coil galvanometers have the advantage of high sensitivity and good optical reproduction, but the disadvantage of high moment of inertia, therefore lower natural frequency and less high frequency response. For these reasons the writer believes that oscillographs with high frequency and high sensitivity are preferable.

Generally speaking, it appears preferable to work toward increased output of the source of power—the pickup. It is possible, of course, to overcome lack of sensitivity of the pickup by strong amplification and high indicator sensitivity; but unless the amplifier is carefully shielded against extraneous disturbances it is apt to be too sensitive to them, particularly with a sensitive indicating device. In some designs, therefore, the first amplifier stage is incorporated in the pickup in order to have sufficient signal strength before the impulses reach the amplifiers in the recording truck. The only drawback to that is the necessity of multiple leads from the truck to the pickup unless battery supply is provided for in or next to the pickup.

## 2. *Dynamic Characteristics*

As far as frequency response is concerned, design practices vary greatly. At least one fact seems rather agreed upon; namely, that a frequency selectivity of the over-all response is desirable: (1) for giving emphasis to the reflections, (2) to eliminate undesirable wave types, and (3) to eliminate extraneous disturbances. Undesirable frequencies, for instance, are in the lower wave band, the weathered layer waves which appear at the end of the record and for certain distances interfere with the deeper reflections. In the high-frequency band, there are wind, unrest, sound waves, tuning fork effect on amplifier, etc. Fortunately in most cases the frequency of the reflected waves varies between 35 and 70; that is, lies just between the undesirable high and low frequency bands.

Theoretically, there are three possibilities in reflection apparatus to increase the response to the desired frequencies; on pickup, on amplifier and on oscillograph. Their comparative efficiency and field practice ability will be discussed presently. The problem is first, however, whether peaking by relaxation of damping (resonance peaking) or bypass peaking (by nonresonant filters) is preferable. The former appears to be inferior to the latter because it increases the tendency to free oscillations, which for reflections of short-time sequence are apt to interfere with the proper interpretation of the first impulses. On the other hand,



the bypassing of undesirable frequencies from an essentially linear over-all frequency response will produce the desired peak response without the byproduct of free oscillations. Furthermore, as will be shown in the next paragraph, peaking of seismograph or of oscillograph at reflection frequencies is not desirable from the viewpoint of dynamic sensitivity, which leaves the amplifier as the most suitable place for a filter system.

*Natural Frequencies; Pickup.*—Obviously, there are three alternatives for the natural frequency of the pickup in reference to that of the reflected waves: (1) same frequency; (2) higher frequency; (3) lower frequency.

1. Peaking the pickup at reflection frequencies would have an effect upon the mechanical response only if the damping were small. That in

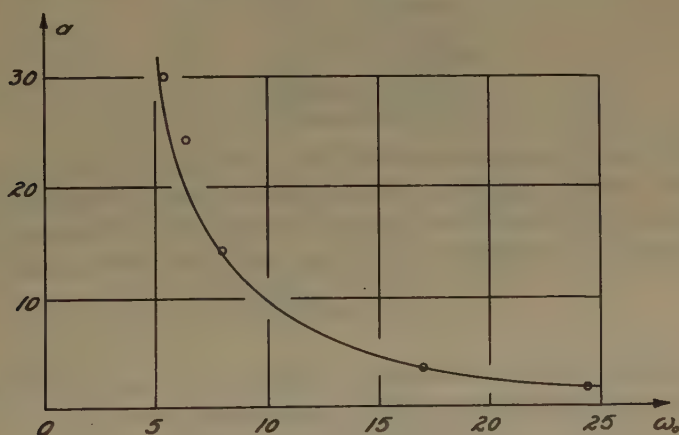


FIG. 12.—RELATION OF STATIC DEFLECTION AND NATURAL FREQUENCY.

turn is not desirable from the viewpoint of suppressing free oscillations. Furthermore, the electrical response is quite different from the mechanical response (Fig. 11); it is dominated entirely by the linear increase with ground frequency, to which the amplifier adds another frequency power. Therefore, other considerations have to determine the desirable pickup frequency, leaving the alternatives 2 and 3.

2. For small tuning factors, it is seen from eq. 6 that the mechanical response not only lacks uniformity of variation with ground frequency but also sensitivity, as the magnification is smaller on the left side of the response curve (Fig. 8) (accelerometer type) than on the right side (low-frequency type). Furthermore, eq. 28 states definitely that the galvanometer response decreases with the square of the natural frequency of the seismograph. It can be verified by laboratory experiment that the static deflection of a seismograph is inversely proportional to its natural frequency (Fig. 12). Summing up, natural frequencies higher than reflection frequencies for the pickup are undesirable.

3. This leaves natural frequencies lower than reflection frequencies as desirable; for them, the dynamic response is more uniform; the sensitivity is great, the electrical output is more uniform.

There are innumerable ways of constructing vertical seismographs, and of selecting spring and mass arrangements that will give the desired natural frequencies and amplitudes. The following is a tabulation of spring and mass arrangements generally used, and formulas for the calculation of the corresponding natural frequencies:

Spring suspensions.  
     Single springs.  
         Horizontal plate spring.  
         Vertical coil spring.  
     Springs in multiple.  
     Springs in series.  
     Diaphragms.  
     Levers and springs.  
     Two-mass systems.

The action of a single horizontal spring, loaded at its end with a mass is defined by the following relation between static deflection  $a$ , force  $F$  ( $= mg + f$ , where  $m$  is the attached mass + about 30 per cent of the spring mass, and  $f$  additional extraneous force), and spring constant  $c$ :

$$a = \frac{F}{c} = \frac{mg + f}{c}.$$

Thus,  $c = F$  if  $a = 1$ ; or the spring constant is the force producing unit elongation; it is related to its natural angular frequency  $\omega_0$ , by

$$\omega_0 = \sqrt{\frac{c}{m}} = \sqrt{\frac{F}{am}} \quad ; \quad \text{thus } a = \frac{g}{\omega_0^2} \quad [29]$$

As stated before, the displacement is inversely proportional to the square of the natural frequency (Fig. 12). With  $E$  = Young's modulus,  $l$  = length,  $b$  = breadth and  $h$  = thickness,

$$c = \frac{1}{4} \frac{Ebh^3}{l^3} \quad \text{and} \quad \omega_0 = \frac{1}{2} \sqrt{\frac{Eb}{m} \left( \frac{h}{l} \right)^3} \quad [30]$$

For a coil spring with  $\mu$  = modulus of rigidity,  $d$  = thickness of wire,  $N$  = number of turns,  $r$  = radius of same, again

$$\omega_0 = \sqrt{\frac{c}{m}}; \quad \text{as } c = \frac{d^4 \mu}{64Nr^3}, \quad \omega_0 = \frac{d^2}{8r^2} \sqrt{\frac{\mu}{Nrm}} \quad [31]$$

Springs in multiple (Fig. 13) act the same as capacities in multiple; thus, the natural frequency of a multiple-spring arrangement

$$\omega_{0r} = \sqrt{\frac{c_1 + c_2 + \dots}{m}} \quad [32]$$

The figure shows a number of multiple-spring arrangements which are customary in reflection seismographs.

Springs in series act as capacities in series, or

$$\omega_o = \sqrt{\frac{c_1 c_2 \cdots}{(c_1 + c_2 + \cdots)m}} \quad [33]$$

They are, however, seldom used in prospecting seismographs. Loaded diaphragms are employed in the geophone and condenser types of reflection seismographs, but are not used as frequently as spring suspensions, because of their high natural frequency. The natural frequency of a

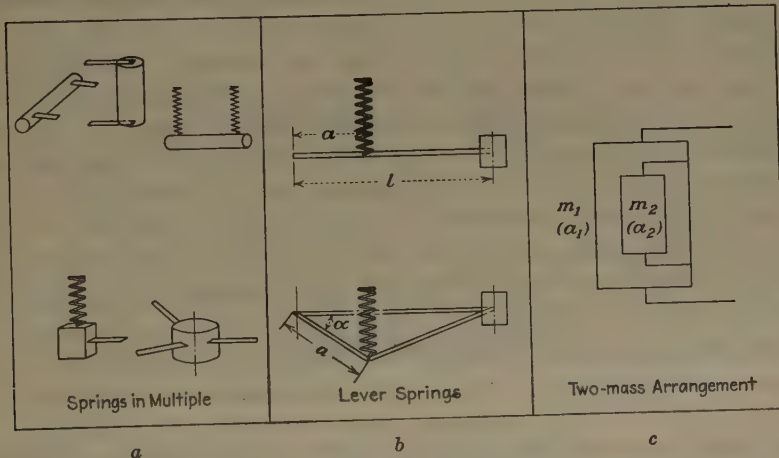


FIG. 13.—SPRING SUSPENSIONS.

diaphragm with the attached mass  $m$  and the total (diaphragm and attached) mass  $M$  is

$$\omega_o = 3 \frac{d}{r^2} \sqrt{\frac{E}{\rho(1-\sigma^2)}} \cdot \frac{1}{\sqrt{1 + \frac{5m}{M}}} \quad [34]$$

with  $d$  = thickness,  $r$  = radius,  $\rho$  density and  $\sigma$  Poisson's ratio.

A combination of a lever with spring such as shown in Fig. 13 is rather customary in electromagnetic seismographs because it gives the possibility of making the natural frequency of the seismograph less than that of the spring alone. The natural frequency of the assembly is  $\omega_o = \frac{a}{l} \sqrt{\frac{c}{m}}$  when the lever is used as shown in the upper part of Fig. 13b, and

$$\omega_o = \frac{a}{l} \sqrt{\frac{c}{m} \left[ \cos^2 \alpha - \frac{mgl}{ca^2} \tan \alpha \right]} \quad [35]$$

when the spring is attached below the lever axis.

A mass suspension as shown schematically in Fig. 12c gives the possibility of increasing the amplitude of the seismograph mass, as the displacements of the moving bodies so coupled are inversely proportional to their masses or

$$\frac{a_1}{a_2} = \frac{m_2}{m_1} \quad [36]$$

The equations for this type of seismograph may be set up by using both sets of equations stated on page 422 for coupled inertia systems.

*Frequency Characteristics of Amplifiers.*—The frequency characteristics of the amplifier are generally adjusted so that the over-all dynamic magnification of the entire apparatus is peaked at the desired reflection frequency. If the recording galvanometer is peaked as in some reflection equipments, the amplifier response may be essentially flat except for cutoffs at undesirable high and low frequencies. If the galvanometer is not peaked the amplifier should be so peaked that the maximum response is obtained at the desired reflection frequencies for both amplifier and oscillograph combined; the latter response may be determined in the laboratory, using each amplifier in combination with the correct galvanometer (see page 449). The desired amplifier response may be obtained either by separate filters or by providing filtering action in the appropriate amplifier circuits.

*Oscillographs.*—The dynamic magnification of an oscillograph for frequencies much greater than its natural frequency is given by  $\frac{-V_g}{\omega^2}$ , while in the opposite case it is  $\frac{V_g}{\omega_0^2} = \text{const.}$  This condition leaves two possibilities for the design of oscillographs for reflection work: (1) to make the natural frequency high so that the dynamic magnification is uniform in the reflection frequency range, and (2) to make the natural frequency low so that maximum sensitivity may be obtained. As stated before, conditions here are more unfavorable than they are at the pickup. However, at the oscillograph the decrease of sensitivity with natural frequency can be overcome by stronger magnetic fields and smaller torsional coefficients, so that uniform low frequency response may be combined with high sensitivity. Incidentally, the rapid decline of dynamic magnification with extraneous frequency of a damped low-frequency galvanometer brings about the sharp drop of the over-all characteristics in a Galitzin type seismograph. In defense of the coil galvanometer, it should be recalled that with proper selection of its natural frequency its high frequency cutoff may be utilized for the elimination of these frequencies, rather than to provide for it in the amplifier, or amplifier filter.

*Damping.*—In regard to damping, design practices vary greatly. For the recording instrument, for instance, some designs use no damping (string galvanometer) while others go to the other extreme and apply critical or overcritical damping. Damping has to serve two purposes:



(1) to suppress resonance unless the particular unit is peaked at that frequency; (2) to limit natural free oscillations to a reasonably short time.

If the response of pickup and oscillograph is to be made uniform and the peaking is done in the amplifier by filter circuits, the damping required for such pickup and oscillograph response may be readily calculated. The minimum damping ratio to be used is the one for which the resonance frequency vanishes. Thus, from formulas 11 and 24,  $\omega_r = 0$  if  $2\epsilon^2 = \omega_0^2$ ; i.e., the resonance frequency for inertia coupling becomes infinite, that of force coupling 0. Hence, the minimum damping ratio for both pickup and oscillograph:

$$\eta_{\min.} = \sqrt{1/2} = 0.707 \text{ critical} \quad [37]$$

This corresponds to a log decrement  $\Lambda = 2\pi$  and a ratio of damped amplitudes of 535:1.

As far as free oscillations are concerned, it is generally known that critical damping must be used if it is desired to stop them completely; it gives minimum time to a reduction of a given deflection to zero without overshoot. However, this time in which the new equilibrium condition is reached is made unduly long by the latter stipulation and may be reduced by about one-half if about 5 per cent overshoots are permitted. It can be shown that also from the standpoint of suppressing free oscillations a damping ratio of 0.7 critical will be satisfactory, as with it a given amplitude would be reduced to about  $2/1000$  of its original amount within the time of one period.

In accordance with the above, damping ratios in most reflection seismographs vary between 0.7 and critical.

*Dynamic Characteristics from Viewpoint of Onset Conditions.*—It must be borne in mind that the preceding discussion has been based upon the assumption of stationary conditions; i.e., the adjustment of an oscillating system or systems to extraneous periodic forces of indefinite duration after the natural free oscillations of the system had vanished.

For onset conditions—that is, for the beginning of the motion—this assumption no longer holds. There, the free motion of the affected system is superimposed upon the extraneous oscillation and can no longer be neglected. In such case the effect depends upon: (1) the tuning factor, (2) the damping ratio, and (3) the phase of the affected system and of the extraneous motion at the time 0.

Koch and Zeller<sup>(15, 21, 28)</sup> have made an exhaustive study of the relation of ground movement and seismograph record for such onset conditions in a mechanical seismograph (see also Wilson<sup>(21a)</sup>). They found that the record obtained by a seismograph of a period greater than that of the ground motion generally does not allow an extrapolation to the true ground movement in the first part of its oscillation, but only from the third or fourth maximum on, and concluded that for a more faithful representation of the ground motion at the onset an accelerometer of a period shorter than that of the ground motion would be more suitable.

This does not seem to be in accordance with the requirement for longer natural period deduced from the theory before; however, the reason for the discrepancy of views is obvious: Koch and Zeller deal with mechanical seismographs only. In electrical seismographs, and electromagnetic reflection equipments in particular, the electromagnetic pickup device performs a first, and the amplifier a second derivation of the displacement with respect to time. Thus the gradual change in the equilibrium position discussed by Koch and Zeller hardly becomes apparent, and their conclusion in regard to accelerometric representation of onset conditions is confirmed, only in a different manner, and without the detrimental effect that the high natural frequency of an accelerometer would exert on the static magnification of the seismograph. The derivations resulting from a consideration of onset conditions are beyond the scope of this paper; be it sufficient to state that for the consideration of the desirable instrument characteristics the simplifying assumption of stationary conditions is sufficient.

### III. CALIBRATION OF REFLECTION APPARATUS

Calibration of reflection apparatus and its constituent parts is necessary for two reasons: (1) to give the units the desired sensitivity and frequency response; (2) to make the units as much alike as possible. For the interpretation of reflection records, it is advisable to have the 4 or 6 units balanced in reference to amplitude; for the timing of the impulses the phase angle of the units should be closely the same. The latter in turn depends on the damping and the natural frequency. Owing to the nature of the work, it is not necessary that the various quantities shall be obtained accurately as far as their absolute values are concerned. The greatest possible similarity between units—accurate relative quantities—is what is aimed for.

The tests made concern static and dynamic characteristics and may, therefore, be divided into (A) static tests and (B) dynamic tests. The definition that will apply to these is as follows: static tests are such that the desired quantity is obtained from static deflections, or free oscillations resulting from such deflections. Dynamic tests involve forced oscillations, either with stationary or with moving pickup (Table 1). To this may be added (C) various other tests for timer rate, phase, parallax, etc. Before the various tests enumerated in Table 1 are described, a method will be discussed for obtaining the dynamic characteristics of the seismograph and of the entire apparatus without a shaking table.

#### III-A. DYNAMIC TESTS WITHOUT SHAKING TABLE

Shaking table experiments have been, and are being widely used for the determination of the characteristics of station and prospecting seismographs. A fairly complete reference list on shaking tables will be found

TABLE 1.—*Static and Dynamic Tests*

Units	Receiver				Amplifier				Oscillograph						
	Static		Dynamic		Static		Dynamic		Static		Dynamic				
Characteristics	V	H <sub>d</sub>	f	ω <sub>0</sub>	ε	W = f(ω)	V <sub>a</sub>	ω <sub>0</sub>	ε <sub>a</sub>	W <sub>a</sub> = f(ω <sub>a</sub> )	V <sub>o</sub>	f	ω <sub>0</sub>	ε <sub>o</sub>	W <sub>o</sub> = f(ω <sub>o</sub> )
Symbols of Characteristics <sup>a</sup>															
A. <i>Static tests.</i>															
I. Deflections.....															
Mechanical.....	×		×	×	×						×			×	
Electrical.....	×	×	×	×	×										
II. Free oscillations.....															
Photographic methods..			×	×	×							×	×	×	
Visual methods.....															
Stroboscopic, neon....				×	×										
Stroboscopic disk.....															
B. <i>Dynamic tests.</i>															
I. Unit stationary.....				×	from W	×	×	×	from W	×			×	from W	×
II. Shaking table.....				×	from W	×									→
C. <i>Various other tests.</i>															→
Timer.....															×
Phase.....															
Parallax.....															

<sup>a</sup> V, static; W, dynamic magnification; f, friction; H<sub>d</sub>, proportional to electrical sensitivity of pickup; ω<sub>0</sub>, natural frequency; ε, damping.

at the end of the bibliography.<sup>(34)</sup> They are used primarily to determine the mechanical frequency response of seismographs, and the over-all frequency characteristics of the entire equipment. It will be shown in the following that owing to the physical characteristics of the electromagnetic seismograph, its mechanical frequency response may be determined without a shaking table, and that, furthermore, the over-all characteristics of the equipment may be derived by simple calculation from dynamic seismograph, amplifier and oscillograph tests without shaking tables.

The solution of the problem is comparatively simple because an electromagnetic seismograph may be used with either inertia or force coupling; that is, either as a generator or as a motor. A second fact that makes this possible is that the response curve obtained for force coupling may be changed over to the response curve for inertia coupling by reflection on the ordinate. This can be proved as follows:

$$W = \frac{\omega^2}{\omega_0^2 - \omega^2} = \frac{n^2}{1 - n^2} \text{ for undamped inertia coupling}$$

and 
$$W = \frac{1}{\omega_0^2 - \omega^2} = \frac{1}{1 - n^2} \text{ for undamped force coupling} \quad [38]$$

Inertia and force coupling are thus reciprocal; that is, the inertia-coupled response for a given tuning factor  $n$  is equal to the force-coupled response to  $1/n$ , and vice versa. This is true for undamped as well as for damped response, as is seen from the relationship of the damped resonance frequencies for inertia and force coupling. From equations 11 and 24, the damped resonance frequencies are:

$$\frac{\omega_r}{\omega_0} = \frac{1}{\sqrt{1 - 2\eta^2}} \text{ for inertia coupling}$$

and 
$$\frac{\omega_r}{\omega_0} = \sqrt{1 - 2\eta^2} \text{ for force coupling} \quad [39]$$

Plotting the dynamic response as function of  $n$  (and  $1/n$  past the resonance point) (Figs. 8 and 9), the response curve for force coupling can be converted into the response curve for inertia coupling by the simple means of reflection on the ordinate.

Therefore, by determining the mechanical response of a seismograph to constant electrical input and reversing the curve, the mechanical dynamic magnification of the seismograph is obtained. Previously, the seismograph response to varying ground frequencies could be determined only on a shaking table. A simple device for performing this test will be described in the next section.

The procedure for determining the over-all characteristics of the entire equipment is as follows: After the mechanical dynamic response has been determined, the result is multiplied, for each test frequency, by



$H_s l \omega$  (where  $H_s l$  is proportional to the electrical sensitivity of the seismograph), and an electromotive force proportional to this last product [ $H_s l \omega a_{dyn.}$ ] is applied, at various test frequencies, to an amplifier combined with its regular oscillograph. Another alternative is to perform the usual test of amplifier with oscillograph on constant input, but varying frequency first and then multiplying the result by the factor [ $H_s l \omega a_{dyn.}$ ]. The factor  $H_s l$  is unessential for the shape of the curve and may therefore be omitted for relative determinations.

### III-B. CALIBRATION METHODS

Table 1 gives a brief description of the various tests that may be performed on seismic reflection equipment. Some of these are alternative tests and it is a matter of taste and laboratory equipment which of them are preferred. Various other tests are intermediate in nature and need only be made for design purposes; i.e., at the beginning of the construction of a series of units. The experienced seismologist will find no difficulty in separating important from less important tests, depending on the extent to which he can rely on the precision of construction and thus on the identity of physical characteristics.

There is no particular sequence in which these tests have to be performed except those that concern interdependent physical quantities. It is immaterial whether the order of pickup, amplifier, oscillograph is adhered to; nevertheless, the tests will be described below in that order. For each individual unit the tests are discussed in the order in which they are generally made.

#### 1. *Pickup*

After a pickup is completed, the item that is generally checked first is whether the mass or coil, armature, is free to move. This friction test can generally be combined with the determination of the natural frequency. The apparatus used for this purpose is shown schematically in Fig. 14. It consists of a ring that fits over the top of the pickup and carries a frequency standard as well as a mirror spindle, which is connected by means of a thread to the seismograph mass of which the movement is thus photographed on a recorder drum. An impulse is given to the mass mechanically or electrically. If the latter is used, the friction, natural period and electrical sensitivity can be determined with one record.

Friction manifests itself on the record by a displaced zero position at the end of the motion. The extreme displacements of the zero position are separated by the amount  $2f$  ( $f$  = friction; friction force =  $cf$ ). A small amount of friction will often not show as well in the zero displacement as in the type of amplitude decline. Although the friction tests are made without regular damping, there is always a small amount of

damping present in addition to friction. The latter may occur in the lever transmission from mass to coil or armature, or if such lever transmission is not used, in the spring suspensions and the wires from coils to frame (if movable coils are used). Needless to say that friction must be kept as low as possible, and for that reason must be identified and separated from damping in the record. This may be done roughly by connecting the peaks of the wave record; if this line is straight, friction is present; if it is an exponential curve, damping alone occurs. For closer analysis, a number of subsequent amplitudes may be measured and both their differences and ratios may be calculated. If the difference is constant, friction is present, while for damping the ratio of subsequent amplitudes is constant. Damping decreases the natural frequency;

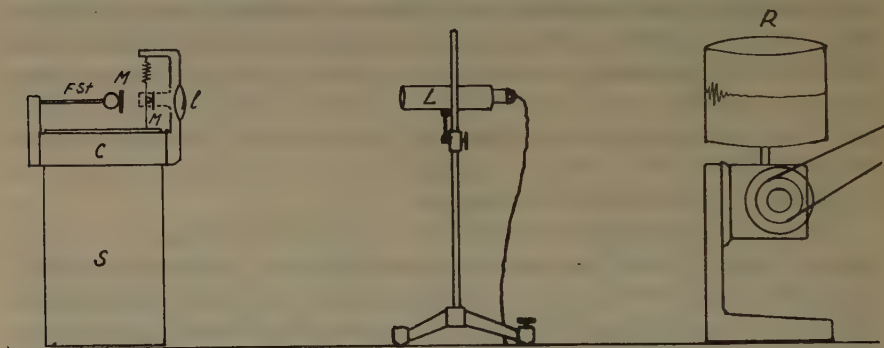


FIG. 14.—TESTING APPARATUS FOR SEISMOGRAPHS.

S, seismograph; M, mirrors; L, lens; L, lamp; R, recorder; c, clamp; F St, frequency standard.

friction does not. For the determination of the natural frequency, numerous methods are available:

1. An impulse may be given to the seismograph mass mechanically or electrically, and the free motion recorded photographically, together with a frequency standard which may be: (a) a calibrated spring, (b) a calibrated tuning fork, (c) an oscillographic record from a calibrated oscillator, or from 60-cycle current, or (d) time lines projected on the paper by any of the means used in reflection records (p. 417).

2. The frequency standard may be made of the same frequency as that to which the pickup is to be adjusted.

3. Visual methods of determining natural frequencies may be employed: (a) a neon-light stroboscope operated from an oscillator of variable frequency, or of fixed frequency to which the natural frequency of the pickup is adjusted; (b) a stroboscopic disk (Reutlinger<sup>(5)</sup>) operated from a synchronous motor; (c) comparison with a frequency standard by reflecting light from the standard to the seismograph mirror and adjustment of seismograph to standard for stationary image, or by using the same method on a mirror device (oscillograph, for instance), operated by

variable frequency until the seismograph frequency is determined by stationary image.

4. The natural frequency may be determined also by connecting the seismograph to an electrical oscillator and by locating the point of undamped resonance frequency by maximum amplitude.

5. The same test may be made on a shaking table.

6. Finally, the natural frequency may be determined indirectly from static deflections as they are inversely proportional to the square of the natural frequency. The deflections are produced electrically or mechanically by placing a weight on the seismograph mass.

The geometric magnification of a pickup with arm or lever attached to coil or armature may be determined by measuring with a microscope the comparative displacement of coil and mass.

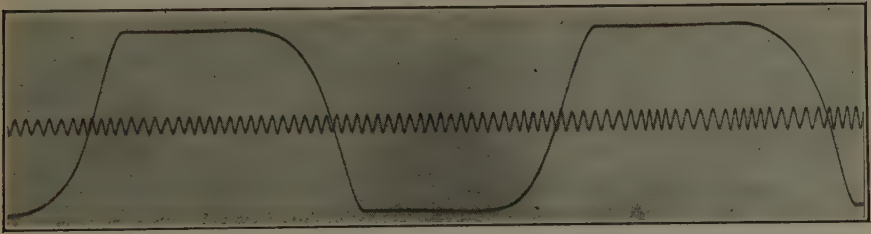


FIG. 15. — ELECTRICAL SENSITIVITY TEST OF A CRITICALLY DAMPED SEISMOGRAPH.

The term  $H.l$ , which is the transmission constant  $T$  for the transfer of a mechanical into electrical energy in the pickup, is determined by measuring the "electrical sensitivity" of the pickup; i.e., the displacement for unit current. This may be done visually or photographically. Fig. 15 is a record of an electrical sensitivity test of a critically damped seismograph.

A number of methods are available for determining damping: (1) from the time required for the seismograph mass to adjust itself to a new position, obtained from a record of the type shown in Fig. 15; (2) from the damped frequency, and ratio of subsequent amplitudes from a record obtained by giving the seismograph mass an instantaneous electrical or mechanical impulse (Fig. 16); (3) from a frequency-response curve obtained with stationary seismograph and force coupling (Fig. 9); (4) from shaking-table experiments—that is, from a determination of the damped mechanical response. For design purposes damping often is determined for varying conditions; that is, for various compositions of damping fluid, various heights of damping fluid in pickup case, for various temperatures, shunt values and distances of damping magnets, and so forth.

The total dynamic response of the pickup, finally, may be obtained from shaking-table experiments or, more simply, from electrical mechanical tests with constant input as described before in detail.



## 2. Amplifier

The number of tests that can be made on an amplifier is much smaller than can be made on the receiver. To start with, static tests are hardly possible; all measurements are made with inputs that vary with time. Before the dynamic tests are made, however, the amplifier is put on its galvanometer and a test is made to see whether the amplifier has a tendency to be unrestful or to oscillate. The next test is usually made for the relation of current output to voltage input, to study curve form and phase shift for short impulses. Theoretically the current output should be the first time derivative of the voltage input with a phase shift following from equation 15. The gain  $V_a$  of the amplifier may be determined for the straight part of the response curve; i.e., with filters cut out. Any essential variation from a uniform response such as introduced by unremovable input or output devices must be considered in the frequency factor of the dynamic response. Various methods are available for gain determination, one of the best known involving the use of a standard (low-voltage) signal generator and tube voltmeter. Natural frequency and damping cannot be determined except approximately from the dynamic response curve. It must be remembered that the natural frequency as defined before was introduced for the simplification of the mathematical treatment to obtain the equivalent of a frequency which a mechanical system with the same dynamic response curve would have if it were not damped. This does not mean that the amplifier would oscillate with that frequency if it were not damped. The same holds for the damping. The amplifier in its individual circuits may be critically damped; yet the dynamic response curve obtained by bypassing certain high and low frequencies leads to much less damping, which in turn is only the equivalent damping of a fictitious oscillatory system of the same response curve, introduced for the ease of theoretical treatment. At any rate, when taking the dynamic response curve as described below, the equivalent natural frequency and damping are

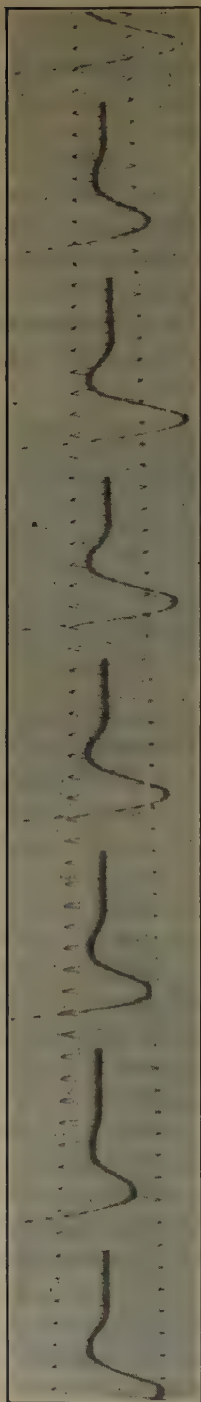


FIG. 16.—DAMPED FREE OSCILLATIONS OF A SEISMOGRAPH.



generally not calculated, but this curve is taken as a whole, as described before, and combined with the dynamic seismograph curve to the over-all response curve. The dynamic response of an amplifier is determined by using a low-frequency oscillator (range from 5 to 400 cycle sufficient), and the oscillograph with which the amplifier is to be used, or measuring its output. The voltage output of the oscillator should be constant, which should be checked before every

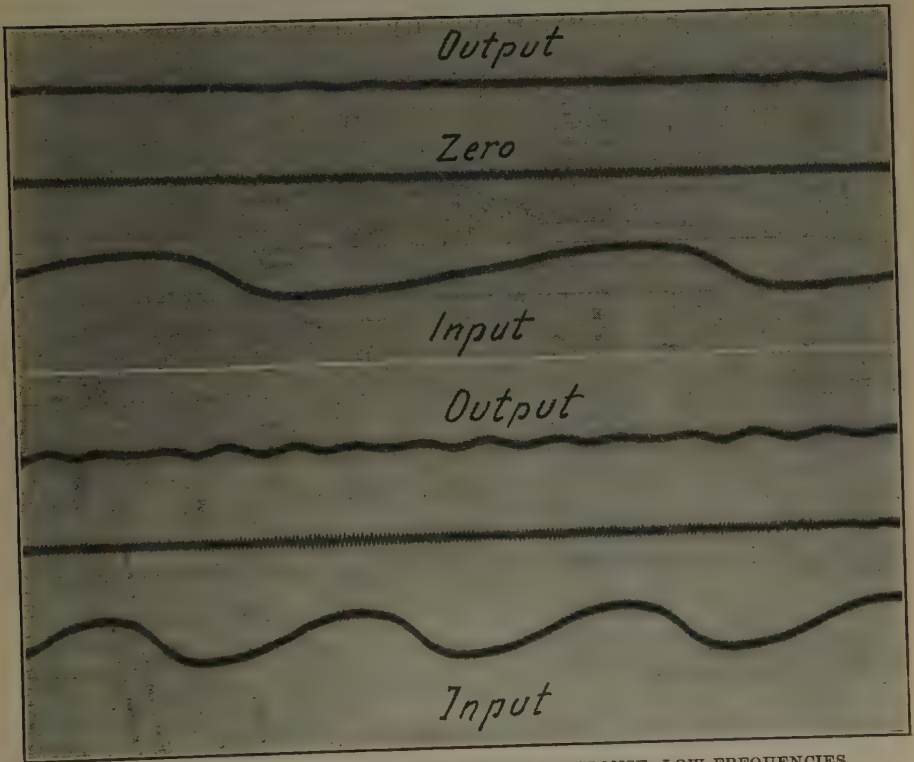


FIG. 17.—RECORDS OF AMPLIFIER FREQUENCY RESPONSE, LOW FREQUENCIES.

frequency test by the amplifier oscillograph. The ratio of current output to voltage input gives the dynamic magnification. If the division is not made, the oscillograph readings give directly the combined response of amplifier and oscillograph (indicated by arrow in Table 1), which is a quantity of greater interest than the amplifier response alone. The dynamic amplifier and oscillograph tests may also be made by taking simultaneous photographic records of the input with a voltage oscillograph and of the output with a current oscillograph (Figs. 17 to 19). If the amplifier is provided with filter control a number of such tests for various settings of the controls are made.

### 3. Oscillograph Galvanometers

Oscillograph tests are concerned with the determination of: (1) friction, (2) d.c. sensitivity, (3) natural frequency, (4) damping and (5) dynamic response. Friction is generally determined in connection with sensitivity tests, although theoretically it could again be obtained from the shape of the free oscillation curve. The d.c. sensitivity is obtained from a test

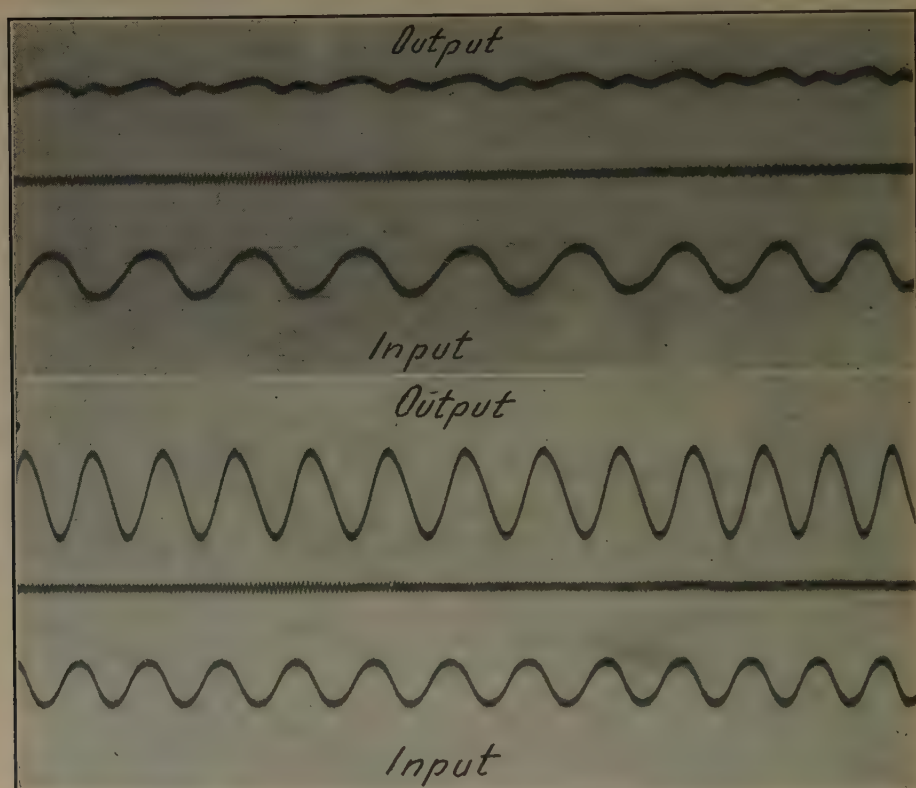


FIG. 18.—RECORDS OF AMPLIFIER FREQUENCY RESPONSE, INTERMEDIATE FREQUENCIES.

with a dry cell, resistance, milliammeter, and reversing switch, which for constant supervision of the galvanometer performance may most conveniently be installed on the recorder control panel. The natural frequency can be obtained from free oscillations, but may more conveniently be determined from a resonance test of the undamped galvanometer with a calibrated oscillator. For the same purpose, some of the visual tests described before for the determination of the natural frequency of the pickup may also find application. Damping may be calculated from: (a) the damped natural frequency, (b) the damped resonance frequency, or (c) the adjustment time in static deflections. For any determination of

damping, it is, of course, necessary to maintain connection to the secondary of the output transformer of the amplifier. The dynamic response is determined for constant input from an oscillator by observing the deflection as a function of the impressed frequency.

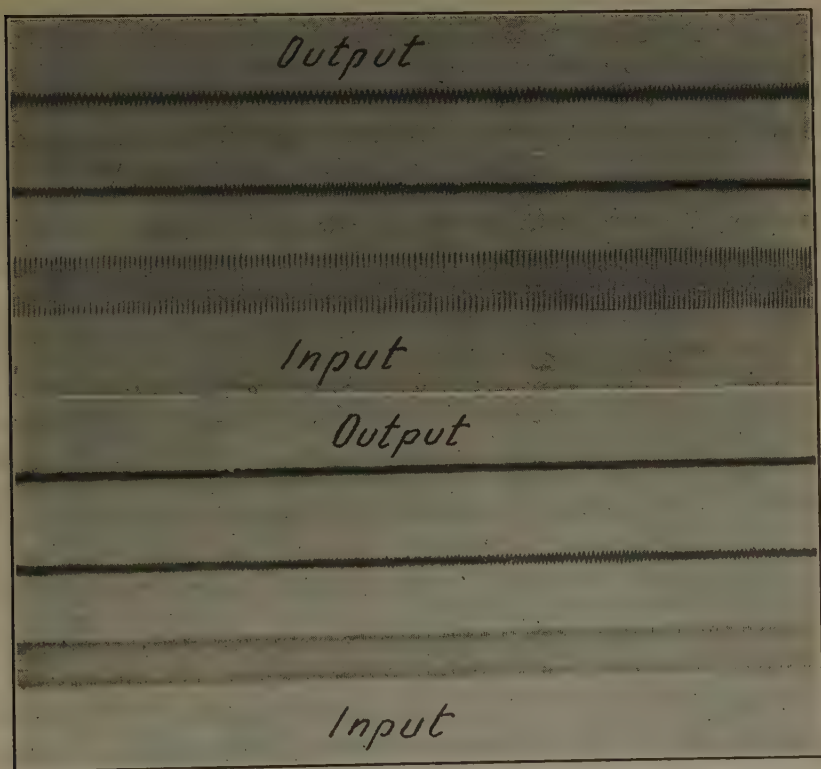


FIG. 19.—RECORDS OF AMPLIFIER FREQUENCY RESPONSE, HIGH FREQUENCIES.

### III-C. VARIOUS OTHER TESTS

A number of other tests must be made in addition to the static and dynamic tests discussed above.

#### 1. *Timer Tests*

The accuracy of the timing device must be carefully checked at regular intervals. Calibrated forks, preferably arranged for oscillographic recording, generally furnish the required accuracy. Absolute times are not required; relative time values are sufficient as long as they stay reasonably constant, that is, maintain an accuracy of  $\pm 1$  to 2 thousandths of a second at the end of one second. The variation of the timer rate with temperature, if any, must be determined. Tuning forks and other timing devices which are not calibrated may be checked against

radio time signals, gravity pendulums, or quartz oscillators in the laboratory.

## 2. Phase Tests

So-called phase shots are made in the field at intervals (or after changes in the equipment have been made) to make sure that for a given ground impulse the impulses in the record are in phase and approximately balanced. During the laboratory tests of the equipment, a number of checks may be made to see whether the electrical connections are correct with regard to phase or polarity, by observing, for instance, the direction of deflection of seismograph and oscillograph when testing their electrical sensitivity. Wiring of output and input transformer, of amplifiers, of pickup leads, reel connections, and of connections of amplifiers to oscillographs must be correct in regard to polarity, so that in case of emergency the constituent parts of the equipment may be interchanged without changing the phase.

Rapid checks of phase may be made in the field by taking a record, with all pickups close together, of ground taps at a point at right angles to the line in which the pickups are set up. Sometimes, particularly when strong lasting impulses are lacking, the peculiarities of pickup location become apparent, so that for the very last ground movement the recorded movements are not as well in phase as in the first part of the record. This is not serious so long as the motion is correctly in phase for the first seven to ten half cycles.

## 3. Parallax Observations

Owing to the phase shifts in the various constituent parts of the equipment, to the time difference between explosion and shot-instant wire break, and to the optical parallax between oscillograph light spots, there is generally a time parallax between the first seismic impulse and the shot-instant record. This may be determined by shooting a cap not farther away than one foot from the seismograph and recording both seismic impulse and shot instant, as described further by Mr. Pugh in the second part (p. 455, this volume).

## BIBLIOGRAPHY

1. H. O. Wood: On a Piezoelectrical Accelerograph. *Seis. Soc. Amer. Bull.* 11 (1921) 15-57.
2. J. G. Siñeriz: Los Métodos Geofísicos de Prospección. *Inst. Geol. Min. España Bol.* X (3) (1928) 275-305.
3. D. C. Barton: The Seismic Method of Mapping Geologic Structure. *Trans. A.I.M.E.* (1929) 81, 572-624.
4. F. Wenner: A New Seismometer Equipped for Electromagnetic Damping and Electromagnetic and Optical Magnification. *U. S. Bur. Stds. Research Paper* 66 (1929).



5. G. Reutlinger: Eine experimentelle Ueberpruefung der Theorie der Schwingungsmesser. *Gerland's Beiträge* (1929) **24** (2/3), 168-240.
6. R. Ambron: Modern Instruments for Seismic Prospecting. *Eng. & Min. Jnl.* (1929) **128**, 93-99.
7. R. Rieber: Adaptation of Elastic-wave Exploration to Unconsolidated Structures. *Trans. A.I.M.E.* (1929) **81**, 654-667.
8. H. Martin: Bodenseismik. Geophysik III. *Handbuch der Experimentalphysik* (1930) **15** (3), 251-302.
9. H. Shaw: A Field Test with a New Seismograph. *Min. Mag.* (1930) **42** (4), 201-212.
10. A. B. B. Edge and T. H. Laby: The Principles and Practice of Geophysical Prospecting, Chapters VI and X. Cambridge, 1931.
11. Y. Kato and S. T. Nakamura: On the Piezoelectric Accelerometer, etc. *Japan. Jnl. Astron. and Geophys.* (1931) **8** (3), Abstracts, 33.
12. S. Haeno: The Radio Seismograph. *Japan. Jnl. Astron. and Geophys.* (1931) **8** (2), 39-50.
13. E. McDermott: Application of Seismography to Geological Problems. *Amer. Assn. Petr. Geol. Bull.* **15** (1931) 1311-1334.
14. R. Maillet and T. Bazerque: La Prospection Seismique du Sous Sol. *Ann. des Mines* (1931) **22** (10), 287-341.
15. H. W. Koch and W. Zeller: Kritik der Aufzeichnung von Schwingungsmessern. *Ztsch. Ver. deut. Ing.* (1931) **75**, 1509.
16. F. S. Scrase: The Instrumental Phase Difference of Seismograph Records. *Proc. Phys. Soc. London* (1931) **43**, 259.
17. I. Roman: Least Squares in Practical Geophysics. *Trans. A.I.M.E.* (1932) **97**, 460-506.
18. E. McDermott: The Reflection Seismograph. *Physics* (1932) **3**, 39-52.
19. H. Benioff: A New Vertical Seismograph. *Seis. Soc. Amer. Bull.* **22** (1932) 155-169.
20. H. M. Rutherford: Reflection Methods in Seismic Prospecting. Page 391, this volume.
21. H. W. Koch und W. Zeller: Der Einschwingvorgang bei Seismographen und Beschleunigungsmessern. *Verkehrstechnik* (1932) **13** (15), 290-3.
- 21a. H. R. Wilson: Calculation of the Motion of the Ground from Seismograms. *Physics* (1932) **2** (3), 186-199.
22. B. Gutenberg, H. O. Wood and J. P. Buwalda: Experiments Testing Seismographic Methods for Determining Crustal Structure. *Seis. Soc. Amer. Bull.* **22** (1932) 185-246.
23. E. McDermott: Application of Reflection Seismograph. *Amer. Assn. Petr. Geol. Bull.* **16** (1932) 1204-1211.
24. O. C. Lester, Jr.: Seismic Weathered or Aerated Surface Layer. *Amer. Assn. Petr. Geol. Bull.* **16** (1932) 1230-34.
25. V. S. Thomander: Characteristics of the Oscillograph Galvanometer. *Jnl. Franklin Inst.* (1932) **213**, 41-55.
26. C. A. Heiland: Ueber die seismische Reflexionsmethode. *Erg. hefte angew. Geophysik* (1933) **3** (3), 282-336.
27. C. A. Heiland: Elements of Geophysical Prospecting. *World's Fair Bulletin and Colo. School of Mines Quarterly* (1933) **28** (4), 36-43.
28. H. W. Koch and W. Zeller: Zur Theorie der Schwingungsmesser. *Ztsch. Instrumentenkunde* (1933) **53** (2), 64-70.
29. H. W. Koch und W. Zeller: *Ztsch. tech. Phys.* (1933) No. 4.
30. H. Salvatori: Correlation of Reflection Seismic Records in California. *Amer. Assn. Petr. Geol. Bull.* **17** (1933) 257-267.

31. F. Goldstone: Mapping of Geologic Structure by the Reflection of Elastic Waves. *Proc. World's Petr. Congress* (1933) B-I, 155-164.
32. R. Ambrohn: Ein neuer Erschuetterungsmesser fuer seismische Bodenuntersuchungen. *Proc. World's Petr. Congress* (1933) B-I, 165-168.
33. E. E. Rosaire and J. L. Adler: Applications and Limitations of Dip Shooting. *Amer. Assn. Petr. Geol. Bull.* 18 (1934) 119-132.
34. *References on Shaking Tables:*
  - B. Mano: Pub. Earthquake Invest. Comm. (1900) 3, 85.
  - B. Galitzin: C. R. Comm. Seism. Perm. 1 (1902) 1, 162.
  - C. Mainka: Zentr. Internat. Seis. Assoc. *Veroeff.* [A] (1909) Strassburg.
  - B. Galitzin: Verh. 4. Internat. Konferenz, 188. Manchester, 1911.
  - B. Galitzin: Methodik der seism. Beobachtungen. Petersburg, 1913.
  - J. Geiger: *Ztsch. Maschinenbau* (1922) Nos. 5 and 6.
  - E. Rothé and J. Lacoste: Pub. Bur. Centr. Seism. Internat. [A], 60. Toulouse (1927) 1.
  - E. Rothé and A. Remy: Pub. Bur. Centr. Seism. Internat. [A], 98. Toulouse (1927) 4.
  - J. Lacoste: *Compt. rend.* (1927) 185, 469.
  - W. Hort and F. Huelsenkamp: Untersuchung von Spannungs und Schwingungsmessern. Berlin, 1928.
  - G. Reutlinger: Reference 5 of this bibliography.
  - L. S. Jacobsen: Seis. Soc. Amer. *Bull.* 19 (1929) 1.
  - L. S. Jacobsen and H. D. Dewell: Seis. Soc. Amer. *Bull.* 20 (1930) 196, 231.
  - F. Auerbach and W. Hort: *Handbuch der phys. u. tech. Mechanik* (1930) 4, 329.
  - M. F. Behár: Measurements of speed and acceleration. *Instruments* (1931).
  - F. Wenner: *Trans. Amer. Geophys. Union* (1931) 12, 72.
  - F. Wenner: Nat. Res. Council Pub. 71-72 (1931).
  - F. W. Lee and G. A. Irland: U. S. Bur. Mines *Tech. Paper* 518 (1932).
  - A. Ramspeck: *Ztsch. Geophysik* (1932) 8 ( $\frac{1}{2}$ ), 71-74.
  - R. Koehler: *Ztsch. Geophysik* (1932) 8 ( $\frac{1}{2}$ ), 74-84.
  - F. Gassmann: Schweiz. *Tech. Ztsch.* (1933) 3, 38-42.

## Certain Field Problems in Reflection Seismology\*

By W. E. PUGH,† DENVER, COLO.

(New York Meeting, February, 1933)

THE object of the following is to discuss a few of the problems encountered in the practical field application of reflection seismology. Very little has been published on this phase of the work and it is to be hoped that discussions will be presented by many seismologists who have met with these problems in the field. No attempt will be made to discuss the general principles of reflection prospecting, nor to outline the general field procedure. These phases have been presented more or less in detail in previous publications<sup>1</sup> while economy of space and time prevents their being repeated or amended here.

If, in the following pages, some criticism is offered of those who have already given their time and efforts to present valuable papers on reflection shooting, we trust that it will be accepted in the constructive light under which it is offered. We do not wish to give the impression that the following paragraphs represent ultimate achievement in field procedure; they are presented more to illustrate methods we have found satisfactory thus far. We believe that the following three subjects are inexorably linked with the continued future successes and more widespread use of the reflection method which, at the present time, is the most

---

\* Part II, Series of Publications No. 47, Department of Geophysics, Colorado School of Mines.

† Plains Exploration Co.

<sup>1</sup> E. McDermott: Application of Seismography to Geological Problems. Amer. Assn. Petr. Geol. *Bull.* 15 (1931) 1311-1334. With discussion by Weatherby, Weaver and Westby.

I. Roman: Least Squares in Practical Geophysics. *Trans. A. I. M. E.* (1932) **97**, 460-506.

E. McDermott: Application of the Reflection Seismograph. *Physics* (1932) **3**, 39-52.

H. M. Rutherford: Reflection Methods in Seismic Prospecting. See page 391, this volume.

B. Gutenberg, H. O. Wood and J. P. Buwalda: Experiments Testing Seismographic Methods for Determining Crustal Structure. *Seis. Soc. Amer. Bull.* 22 (1932) 185-246.

C. A. Heiland: Ueber die Seismische Reflektionsmethode. *Gerland's Beiträge* (1933) *Erg. H.* 3 (3).

E. McDermott: Application of Reflection Seismograph. Amer. Assn. Petr. Geol. *Bull.* 16 (1932) 1204-9.

powerful of all geophysical methods for accurately delineating and delimiting subsurface structures.

### SHOT SIGNAL TRANSMISSION

The great time accuracy required in reflection prospecting (0.001 sec.) has necessitated a profound study of all possible errors attendant on the available methods of transmitting and recording shot moment signals and their remedies. Many methods feasible in refraction shooting are not practicable in reflection work. In most cases the errors are of a variable nature and are difficult to evaluate; hence must be eliminated. Finally, the ultimate choice must answer practical and economical considerations.

#### *Time Parallax*

Nothing has been published previously concerning the determination of the transmission parallax. We do not refer to the optical parallax, such as is encountered when using a shot transmission oscillograph set up next to a Schweydar type of mechanical seismograph, which should be eliminated in the electrical recorders now in widespread use. The time parallax referred to represents the difference in the time of transfer of electricity in the shot signal transmission line as compared with the transfer of the seismic impulse from pickups through amplifiers to recorders.

This parallax may be of the order of thousandths of seconds and must be corrected for. Fortunately, ordinarily the error may be considered as constant and is not difficult to determine.

The more common method of determining the parallax consists of carrying out the regular procedure of shot recording. However, instead of dynamite, a blasting cap is used as the charge and is exploded very close to a seismometer. The shot signal and the elastic impulses are recorded in the accepted manner. Then the parallax, if any, may be evaluated from the shot record.

The cap may be either stuck in the ground or simply placed on the ground *within one foot* of the receiver. The latter distance is important because the velocity of the impulse in air or in the immediate surficial covering is of the order of 1000 ft. per second. Obviously, the travel time of the impulse must be less than 0.001 second.

The parallax determination should be repeated at frequent intervals, particularly if any changes are made in the apparatus or instrumental arrangement.

#### *Transmission of the Shot Moment*

Whereas in refraction shooting radio has been utilized because of the relatively large shot distances involved, in reflection shooting the explo-



sion time is usually transmitted by wire. The ordinary procedure has been to hook up one of the oscillograph vibrators, harp strings or a separate indicating device in such a manner that the explosion of the dynamite would either open or close an electrical circuit. The deflection thus effected is recorded on the photographic film and represents the actual shot moment.

The wire line to the recording device may be (1) wrapped around a blasting cap in series with the firing cap or (2) wrapped around the charge itself. Usually, only one wire has been used, completing the circuit through the ground. Also, the telephone line is ordinarily employed to avoid laying out an extra line.

Method 1 would seem to be the most economical and satisfactory. However, the small charges used in reflection work coupled with deep shot holes cause difficulties with the grounded circuit; that is, the wires are not blown out of the shot hole, so that the ground connection is quite often repeated through the broken end of the wire. This repetition is especially objectionable if the shot signal is recorded on one of the vibrators used in recording the seismic impulse.

The next recourse is to use method 2. Experience has shown, however, that in using caps in series, there is a time lag caused by a lack of simultaneity in their explosion. According to G. H. Westby (oral communication) the error thus introduced may be as much as 0.01 sec. The lag apparently is due to chemical differences in the caps, or may be due to insufficient current in the firing line. At any rate, the error is a variable one and can hardly be evaluated.

In the work with the Colorado School of Mines reflection outfit, we discovered the difficulties inherent in the two methods described above, and decided that the laying out of two wires, thus making a continuous circuit of the transmission line, would give us a dependable accuracy. Here, also, there is some possibility of the wires joining again momentarily after the explosion; in fact, this seemingly remote phenomenon has actually occurred and been recorded. For that reason, it is believed more satisfactory to use either a separate vibrator, other than those used to record the seismic impulses, or an electromagnetic device actuated as is the diaphragm of a telephone receiver.

Incidentally, if a separate device were used, it might obviate the necessity of a continuous two-wire circuit. This would depend on the characteristics of the recording unit. In some cases, the shot signal impulses are picked up inductively by the vibrating elements of the recorder.

There is some possibility of transmitting the shot signal directly through the break in the firing circuit. In this case, the circuit would have to be continuous, but if the firing is accomplished at the recording truck, the connecting leads would be very short. Considerable care

would have to be exercised in designing any such device; any continuous current passing through the circuit must necessarily be minute, so that any danger of premature explosion of the charge is eliminated.

Also, it is possible to connect inductively to the firing line. Here again, though, the time break may be given by the surge of current in the line so that any cap lag will produce a variable error.

### SURFACE CORRECTION ZONES

By the "surface correction zone" we mean the comparatively thin surficial layer in which the seismic velocities are considerably lower than in the layers immediately below.<sup>2</sup> Unless this zone is corrected for—i.e., if the average velocity to the reflecting horizon were applied from the surface—depth determinations would be quite unreliable. Depths to reflecting horizons and, indeed, the average velocities values used in calculating the depths are dependent upon accurate correction-zone determinations. In this connection, it is suggested that the choice of the first fast layer (from the top of which the average velocity value is applied) warrants considerable study.

Probably the greatest source of error in reflection prospecting devolves from the inaccuracies in these determinations. Yet, in the few articles discussing the surface zone, the subject has been treated rather casually. It is admitted that often the errors are not of great magnitude and may be unimportant. But there are cases in which such errors are serious, particularly where the subsurface structures are of low dip.

The usual procedure in delimiting the correction zone has involved the use of the refraction method on a miniature scale.

### *Interpretation*

From a consideration of the travel-time curve plotted from the records obtained as above, computations are made for the thickness of the zone and the velocities therein. Here we have our primary difficulty. Shall we use the straight path or the curved path? Shall we use the refracted ray or the so-called "vertical" ray?<sup>3</sup>

Experience has shown that the interpretation of some refraction surveys over known geologic sections was more correct provided the vertical-ray method was used.<sup>4</sup> In the computations of depths and thicknesses in the correction zone, we are dependent upon the velocities calculated

<sup>2</sup> See O. C. Lester, Jr.: Seismic Weathered or Aerated Surface Layer. Amer. Assn. Petr. Geol. *Bull.* 16 (1932) 1230-34. Mr. Lester's article appeared after this paper was written.

<sup>3</sup> The solution of this problem has meanwhile been advanced considerably by O. V. Schmidt [*Ztsch. Geophysik* (1932) 8, No. 8], who comes to the conclusion that the refraction path and not the vertical path is most likely the correct one to use in depth computations.

<sup>4</sup> See footnote 3.

from the travel-time curves. Anyone familiar with the methods of refraction interpretation and the formulas for depth in multilayer cases will realize the errors that may arise in this miniature application. Beds may be missed entirely while the velocities may be only apparent and not actual.

Another method commonly employed in commercial practice is the "intercept" method. That is, the velocity curves are extended until they intersect the time ordinate. Depths and thicknesses are then calculated from the velocity and time-intercept values. This is merely an approximation but is probably just as accurate as the refraction method and is less tedious in computation. It will usually give slightly smaller results for depths than the application of accurate refraction formulas.

It has been stated that the surface correction zone does not correspond in most cases to any recognizable geologic boundary, such as the zone of weathering, etc. This being true, we have no way of checking the mode of interpretation geologically, except by some other (e. g., electrical) geophysical method. However, the very fact that we may have been using an incorrect interpretative procedure may be the reason that the correction zone does not correspond to any geologic horizon in some areas, because it does not seem reasonable that such changes in physical constitution as correspond to increases in velocity sometimes as great as three to four times should not be noticeable geologically.

The subject presents a problem of interest and importance and considerably more research should be carried out in this direction.

### *Complex Correction Zones in Colorado*

In most of the literature thus far published, the correction zone seems to have been assumed to have a constant thickness and constant velocity. At least, an average value for both has been applied to both shot and receiving points for any one station.

In our work with the Colorado School of Mines reflection outfit in eastern Colorado, we found the zone to vary within wide limits in short distances. Also, we discovered that the zone could be divided into several sections on the basis of velocity. Usually there are two upper low-velocity layers. The lowest layer whose thickness was great enough to be placed in the average-velocity layer had a velocity of 7500 ft. per second. This layer evidenced itself on every

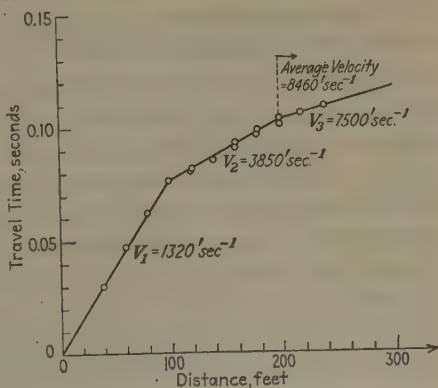


FIG. 1.—TRAVEL-TIME CURVE FOR SURFACE CORRECTION ZONE.



travel-time curve plotted from the correction zone shots. Thus every layer that exhibited a velocity less than 7500 was included in the correction zone.

In an area of about two square miles, the thickness of the zone varied between less than 50 to over 100 ft., while the various velocities ranged between 1110 and 5550 ft. per second. As a result, it was necessary to make determinations at all receiving and shot points. Our interpretation was based on the refracted ray method. Assuming this to be correct, the error introduced if an average value for the zone had been used would have been in some cases as much as 0.01 seconds.

While an approximation average may suffice in some areas, it certainly does not seem applicable in eastern Colorado. The application of an average value might result in a false location of the high point of a structure. In areas where the formations are dipping gently and the amount of closure is small, such an error may cause a structure to be missed entirely or may show a structure where none exists. However, if the survey is for reconnaissance purposes in an area where the dip is fairly steep, it may be possible to use average values for the correction zone without causing serious error. Fig. 1 shows a typical travel-time curve for a correction zone determination in eastern Colorado.

## AVERAGE VELOCITY DETERMINATIONS

### *General Procedure*

The correctness of the computation and interpretation of reflection records depends primarily upon the accuracy of the average velocity determinations.

The most satisfactory method of determining the average velocity to any reflecting horizon requires the availability of a logged well in which the depth to the bed in question is accurately known. Then by shooting in the well at the desired depth with the receivers on the surface or vice versa, an accurate value can be obtained for the average velocity to that depth. A series of shots, using the well as the midpoint between shot and receiver, may serve the same purpose. Another possible method would be to shoot refraction profiles in the area under survey. Then the average velocity may be calculated from a consideration of the velocity-depth curves. This method is open to serious objections, the most important of which is the usual error attendant on the refraction method, and the possibility of *missing layers thinner than the critical thickness in a given depth*.

If no wells are available in the area to be surveyed, and it is believed that a refraction profile will not divulge the desired information with the accuracy required in a successful application of the reflection method, we



must of necessity<sup>5</sup> have recourse to a method of *mathematical analysis of a series of reflection records obtained at one location*.

To elucidate, a number of shots are made at one shot point while the shot distance is varied for each receiver and each shot. Thus we obtain a different reflection time corresponding to each variation in shot distance. By assuming that the unknowns, depth and average velocity, remain constant, the resultant data from the series of shots may be solved by the method of least squares to obtain the most probable values of the two unknowns.

Rutherford<sup>6</sup> dwells at some length on this subject and arrives at the conclusion that the method is totally unsatisfactory. With this statement, the writers cannot agree. Rutherford blames the unreliability of his results partly on the error in reflection-time determinations. He had been using mechanical seismographs, which, to the best of our knowledge, do not have more than one-tenth of the time accuracy of the better and more recent types of electrical reflection units.

The really serious error made by Rutherford, however, is in the mathematics of the problem. In the first place, he uses the special case of the reflection equation that assumes the reflection bed to be horizontal. While this is not objectionable provided the records are taken in areas of gentle dips, unless the latter is true one source of error is apparent. Secondly, and more important, he considers the reflection equation as a linear function and proceeds accordingly. Such a procedure simplifies the solution and computation, but there lies his difficulty. The times and shot distances are measured in the first power, but his application of the method of least squares requires that these observed quantities be raised to the second and in some, cases, the fourth power.

### *Application of Method of Least Squares*

Thus we arrive at the primary purpose of this section. We feel that the reliability of the least squares solution and its practicability from the point of view of the field engineer can and should be proved. We had hoped to demonstrate this by application of the method to records obtained both at the surface and in wells, but were hindered by lack of finances from completing our plans. While we have satisfied ourselves

---

<sup>5</sup> In this connection it may be pointed out that the method of "slope shooting" may be applicable here, at least from a reconnaissance point of view. The use of this method requires that the profiles be made in the direction of dip. If shooting up dip, the reflection time interval between two successive receivers decreases with distance from the shot point, and conversely, if shooting down dip, the time interval increases. The applicability of this method involves a lateral homogeneity in the sediments for any given locality.

<sup>6</sup> Reference of footnote 1.

by the results of one field survey, we do not wish to say definitely that the method is practicable until we have more evidence in its favor.

The necessity of establishing the accuracy of the method will be evident from consideration of the large amount of undeveloped territory in which no wells have been drilled. If the reflection method is to be applied successfully, we must have an efficient and inexpensive way of determining the average velocity. Another advantage will be in the determination of the variation of the average velocity as a function of horizontal distance. Westby<sup>7</sup> points out that north of the Seminole area the average velocity increases, in a distance of 80 miles, 1000 ft. per second to a depth of 3500 ft. A few determinations by the method suggested above would establish whether or not the change is uniform or abrupt. We offer the following pertinent quotation from Birge.<sup>8</sup>

One may summarize the situation by saying that, except in especially favorable cases, least squares' results, and their computed probable errors, are not as reliable as indicated by theory. This fact seems unfortunately so well known that many persons have chosen to use other methods (or no method at all) for calculating their results. I use the word "unfortunately" because these alternative methods are, without exception, inferior to least squares . . . the fact that a certain system of computation is not as reliable as over-zealous advocates may claim is no excuse for using in its place a still less reliable system.

This is not intended to be a treatise on the method of least squares. Roman<sup>9</sup> has developed the application of the method to seismics very satisfactorily. The following will show merely the general method of attack and will give the complete development for the special case of a horizontal reflecting bed with average velocity and depth unknown. Roman has given the derivation of the formulas for the application of the method of least squares for the general case where dip, direction of dip, average velocity and depth are unknown. In addition, he has stated the observation and normal equations for the special case of a horizontal reflecting bed with average velocity and depth unknown, and has also given a tabulation showing the evaluation of the observed data in this case. On account of the practical importance of this special case, we will give below the complete derivation of the formulas for the application of the method of least squares for the determination of average velocity and depth. Before proceeding to this analysis, we will briefly discuss the general idea underlying the application of the method of least squares in reflection shooting.

The basic step in least squares procedure is the setting up of the observation equation; that is, an equation that expresses the relationship

---

<sup>7</sup> Reference of footnote 1.

<sup>8</sup> R. T. Birge: Calculation of Errors by the Method of Least Squares. *Phys. Rev.* (1932) **40**, 207-261.

<sup>9</sup> Reference of footnote 1.

between the observed and the unknown quantities. For the general case—the determination of the three coordinates of the “image” point of the shot—the equation is:

$$t_i = \frac{1}{v} \sqrt{(x - x_i)^2 + (y - y_i)^2 + (z - z_i)^2} \quad [1]$$

in which  $t_i$  is the reflection time;  $v$ , the average velocity to the reflecting horizon;  $x$ ,  $y$  and  $z$ , the coordinates of the image point of the shot;  $x_i$ ,  $y_i$  and  $z_i$ , the coordinates of the receiving point. The origin of the coordinates is the shot point.

Since in actual practice a correction has to be applied for the low-velocity surface zone, the data are reduced to a plane of reference. (See Fig. 3.) The seismic impulse is assumed to start and be received in this plane; hence  $z_i$  is equal to zero, and the imaginary shot point then becomes the origin of the coordinates.

The image point of the shot is on a line perpendicular to the reflecting plane, which is tangent to the reflecting horizon. Also, the image point is the same distance below the reflecting plane as the imaginary shot point is above it.

The observation equation given above assumes a straight-line path for the seismic wave. It is quite possible that the wave may travel a curved path. However, Ewing and Leet<sup>10</sup> have shown that if care is observed in choice of the shot distance, the error introduced in assuming a straight-line path is practically negligible.

The solution of the general equation gives the dip and strike of the reflecting horizon, as well as the depth and the average velocity. The mathematics of the solution are given in detail by Roman and will not be repeated here.

#### *Solution of Special Case; Horizontal Reflecting Bed*

The solution of the general case is somewhat involved and the computations are rather tedious. In making a reconnaissance in areas of low dip, it will usually be sufficient to use the more simple case that assumes the reflecting horizon to be horizontal. If one has a general idea of the direction of regional dip, accuracy will be aided if the line between shot and receivers is in the direction of the strike.

On account of its practical importance, we will give the derivation of the formulas for the application of a least-square solution to the special case where average velocity and depth are unknown. This will thus supplement the statement of the solution as given by Roman, and will

---

<sup>10</sup> M. Ewing and L. D. Leet: Seismic Propagation Paths. *Trans. A. I. M. E.* (1932) **97**, 245-62.

aid the field man in performing the calculations for this case. In order to tie this derivation in with the solution and tabulations published by Roman, his notation will be used.

In the case of the horizontal reflecting bed, we have to put  $x = 0$ ,  $y = 0$ ,  $y_i = 0$  and  $z_i = 0$  in the general observation equation given above (equation 1), so that:

$$t_i = \frac{1}{v} \sqrt{x_i^2 + z^2} \quad [2]$$

or

$$f_i(z, v) = \frac{1}{v} \sqrt{x_i^2 + z^2} - t_i = 0 \quad [3]$$

We may obtain an approximate solution in any desired manner such that  $(f_i)_0 = f_i(z_0, v_0)$  in which  $z_0$  and  $v_0$  are the approximate solutions. The usual method of arriving at these approximate values is to solve an exact case. That is, we take the observed values of the reflection time for corresponding shot distances and solve simultaneously for values of the average velocity and depth. The following formulas may be used for these determinations:

$$v = \sqrt{\frac{x_2^2 - x_1^2}{t_2^2 - t_1^2}} \text{ and } z = \sqrt{\frac{x_2^2 t_1^2 - x_1^2 t_2^2}{t_2^2 - t_1^2}} \quad [4]$$

Ordinarily, the two extremes for the shot distance and time are used in the above solution; however, this is purely arbitrary.

As mentioned above, our observation equation, which contains the observed quantities in the second power, *cannot* be considered *linear* because these quantities are linear. No least-square adjustment is valid unless the observation equation is linear, hence we must reduce the function to linear form by expanding in a series. This is accomplished by using Taylor's theorem. The general principle involved is the determination of the correction that must be applied to our approximate values to reduce them to more probable values that fit all of our observed values.

Neglecting products and higher powers of the corrections, we get, from Taylor's theorem:

$$f_i(z, v) = (f_i)_0 + (z - z_0) \left( \frac{\partial f_i}{\partial z} \right)_0 + (v - v_0) \left( \frac{\partial f_i}{\partial v} \right)_0 \quad [5]$$

Now 
$$f(z, v) = \frac{1}{v} \sqrt{x_i^2 + z^2} - t_i$$

and the derivatives are 
$$\frac{\partial f_i(z, v)}{\partial z} = \frac{z}{v \sqrt{x_i^2 + z^2}}$$



and

$$\frac{\partial f_i(z, v)}{\partial v} = \frac{-\sqrt{x_i^2 + z^2}}{v^2}$$

Further,

$$(f_i)_0 = \frac{1}{v_0} \sqrt{x_i^2 + z_0^2} - t_i$$

and

$$\frac{\partial (f_i)_0}{\partial z} = \frac{z_0}{v_0 \sqrt{x_i^2 + z_0^2}}$$

$$\frac{\partial (f_i)_0}{\partial v} = -\frac{\sqrt{x_i^2 + z_0^2}}{v_0^2}$$

To simplify the nomenclature, let

$$\gamma = z - z_0$$

$$r = v - v_0$$

$$\xi_i = x_i$$

$$\zeta_i = -z_0 \quad \text{and} \quad \rho_i = \sqrt{\xi_i^2 + \zeta_i^2}$$

Then

$$\left. \begin{aligned} (f_i)_0 &= \frac{\rho_i}{v_0} - t_i \\ \frac{\partial}{\partial z} (f_i)_0 &= \frac{\zeta_i}{v_0 \rho_i} \\ \frac{\partial}{\partial v} (f_i)_0 &= -\frac{\rho_i}{v_0^2} \end{aligned} \right\} [6]$$

Substituting these values in equation 5, we get

$$f_i(z, v) = \left( \frac{\rho_i}{v_0} - t_i \right) + \gamma \left( \frac{-\zeta_i}{v_0 \rho_i} \right) + r \left( \frac{-\rho_i}{v_0^2} \right)$$

Rearranging terms and equating to zero, we have the linear observation equation

$$\gamma \zeta_i + \frac{r \rho_i^2}{v_0} = v_0 \rho_i \left( \frac{\rho_i}{v_0} - t_i \right) \quad [7]$$

For further simplification, let

$$\omega = \gamma \zeta_i = -z_0 \gamma$$

$$\lambda = \frac{r}{v_0}$$

$$\epsilon_i = \frac{\rho_i}{v_0} - t_i$$

Substituting these values in equation 7, we have the observation equation in its *final form*:

$$\omega + \rho_i^2 \lambda = v_0 \rho_i \epsilon_i \quad [8]$$

According to the usual procedure in least squares, we may write the following *normal equation* for  $n$  observation equations:

$$\left. \begin{aligned} n\omega + \Sigma \rho_i^2 \lambda &= v_0 \Sigma \rho_i \epsilon_i = \Sigma v_0 \rho_i \epsilon_i \\ \Sigma \rho_i^2 \omega + \Sigma \rho_i^4 \lambda &= v_0 \Sigma \rho_i^3 \epsilon_i = \Sigma v_0 \rho_i^3 \epsilon_i \end{aligned} \right\} [9]$$

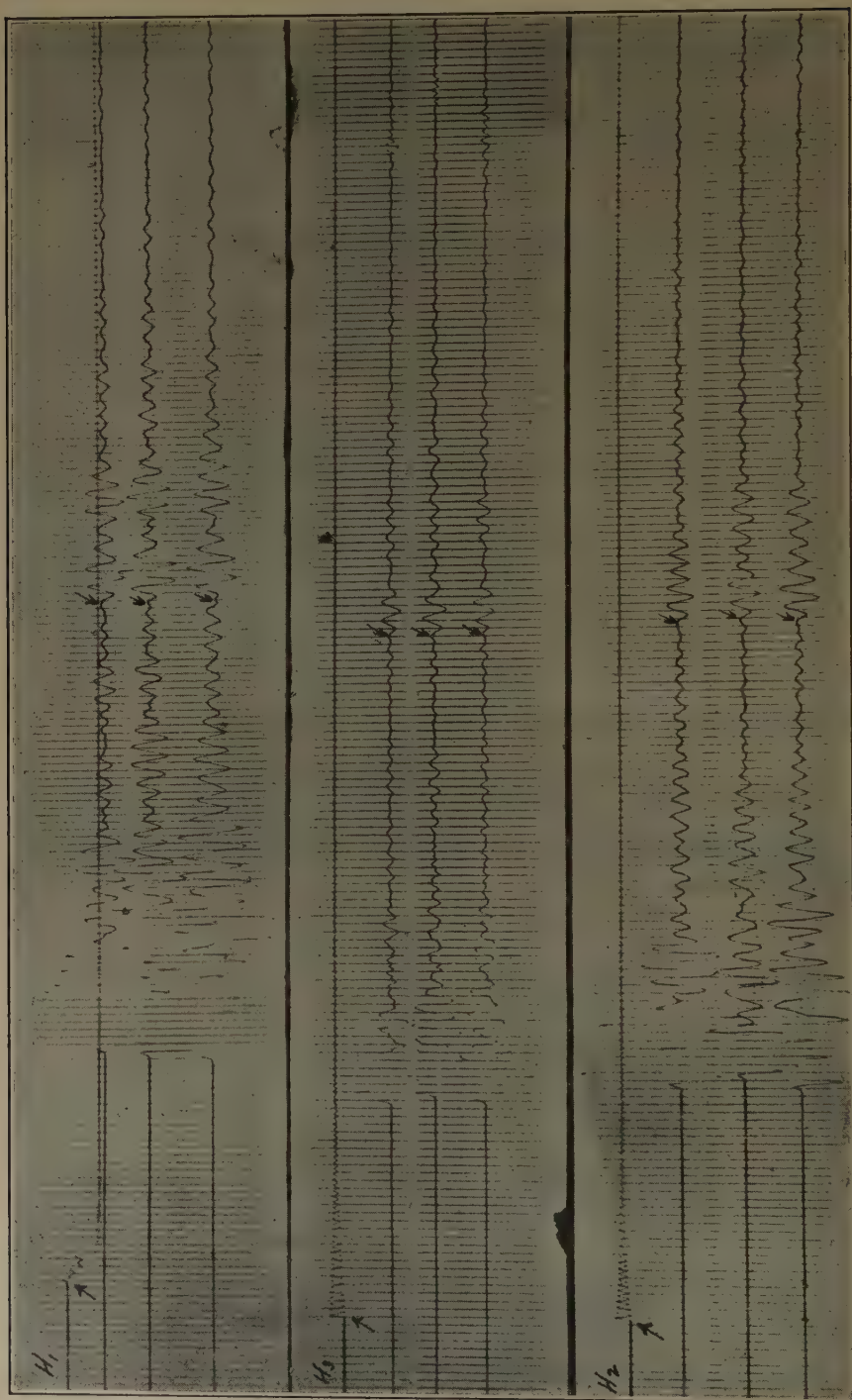


FIG. 2.—THREE REFLECTION RECORDS.

Equation 9 may be solved simultaneously for  $\lambda$  and  $\omega$ , where

$$\left. \begin{aligned} \omega &= \frac{\Sigma \rho_i^4 \Sigma v_0 \rho_i \epsilon_i - \Sigma \rho_i^2 \Sigma v_0 \rho_i^3 \epsilon_i}{n \Sigma \rho_i^4 - (\Sigma \rho_i^2)^2} \\ \lambda &= \frac{n \Sigma v_0 \rho_i^3 \epsilon_i - \Sigma v_0 \rho_i \epsilon_i \Sigma \rho_i^2}{n \Sigma \rho_i^4 - (\Sigma \rho_i^2)^2} \end{aligned} \right\} [10]$$

Then

$$\left\{ \begin{aligned} z &= z_0 - \frac{\omega}{z_0} \\ v &= v_0(\lambda + 1) \end{aligned} \right. [11]$$

If the values  $z$ ,  $v$ , as found by the above solution differ to a large extent from the approximate values,  $z_0$ ,  $v_0$ , the new solutions should be used as approximate solutions and the calculations repeated. As soon as any set of approximate and calculated solutions agree within the limits of error of the particular problem, the latter are taken as the final solution of the problem. The factors in equation 10 may be arranged in any convenient form of tabulation for ease in computation.

In his example 6 (ref. 1), Roman has demonstrated how the approximate values  $z_0$  and  $v_0$  are computed from reflection times recorded in two distances, and how the formulas derived above may be used to compute the corrected values of depth and average velocity from the least-square adjustment of an excessive number of observations. It may occur to the reader that if we were to use the least squares solution many of the variable errors previously mentioned might be disregarded on the basis of the law of probability. Unfortunately, this is not so, since they are practically all on one side of the probability curve (reducing the reflection time). Thus they have the nature and effects of constant errors, in that they will not be eliminated in the solution.

To insure accuracy of computation and to aid in retaining the correct number of significant figures, it is suggested that in denoting distances the decimal point be

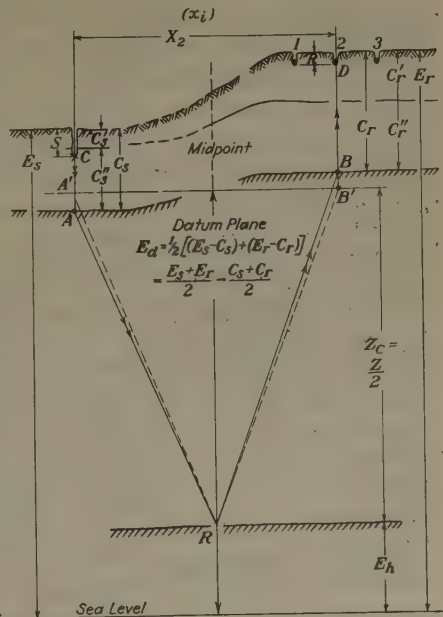


FIG. 3.—DATA USED IN COMPUTATION OF DEPTH FROM REFLECTION RECORDS.

moved so that the number representing thousands of feet shall be the first number to the right of the decimal point; i. e., a shot distance of

5020 ft. will be written 0.502. Reflection times are then of the same numerical order as shot distances.

### EXAMPLES OF DEPTH DETERMINATIONS IN THREE POINTS

The proper application of least squares requires an excess of observation equations. That is, we have just two unknowns but our solution is more nearly correct if we use a comparatively large number of reflection records obtained at one location. Our method, using three seismometers, was to make four shots while varying the

TABLE 1.—*Computation Form for Reflections*

$V_s = 8460$  ft. per sec.<sup>-1</sup>

Symbols and Their Meanings	Record Number								
	$H_1$			$H_2$			$H_3$		
	Seismometer Number								
	1	2	3	1	2	3	1	2	3
$x$ , shot distance.....	1730	1780	1840	1780	1860	1790	1640	1720	1640
$C_s$ , thickness of correction zone at shot point.....	58			53			58		
$C_r$ , thickness of correction zone at receiving point.....	87			100			74		
$S$ , shot depth.....	20			22			19		
$R$ , receiver depth.....	1			1			1		
$T_s$ , travel time of impulse in correction zone.....	0.049			0.043			0.041		
$E_s$ , elevation of shot point above sea level.....	4734			4702			4651		
$E_r$ , elevation of receiving point above sea level.....	4781	4781	4781	4718	4719	4719	4696	4697	4696
$(E_s - C_s)$ , elevation of average velocity layer at shot point.....	4676	4676	4676	4649	4649	4649	4593	4593	4593
$(E_r - C_r)$ , elevation of average velocity layer at receiving point.....	4694	4694	4694	4618	4619	4619	4621	4621	4621
$E_d$ , datum elevation; equals $\frac{(E_s - C_s) + (E_r - C_r)}{2}$ .....	4685	4685	4685	4634	4634	4634	4607	4607	4607
$T_r$ , total reflection time.....	0.921	0.920	0.922	0.870	0.872	0.870	0.841	0.843	0.841
$T_d$ , reflection time below datum; equals $T_r - T_s$ .....	0.872	0.871	0.873	0.827	0.829	0.827	0.800	0.802	0.800
$V_s^2 T_d^2 - x^2$ .....	51.43	51.12	51.15	45.78	45.72	45.75	43.11	43.07	43.11
$Z_s$ , depth to reflecting horizon below datum.....	3585	3575	3576	3383	3381	3382	3283	3280	3283
$E_h$ , elevation of reflecting horizon above sea level.....	1100	1110	1109	1251	1253	1252	1324	1327	1324

shot distance within wide limits. Thus, we obtain 12 observation equations, which under ordinary conditions should give excellent results in least squares computation. At the same time, we usually accomplish a determination of the most favorable shot distance for the desired reflected impulse.



In this manner, we determined the average velocity in the area under survey as  $v_a = 8460$  ft. per sec.<sup>-1</sup>. With this velocity, depths are computed from records obtained in this area. We have selected three records that will demonstrate the method of calculation. Photostats of these records, as obtained with the Colorado School of Mines outfit, are shown in Fig. 2 on a reduced scale.

The calculations of these records are given in Table 1, and the quantities used are represented further in Fig. 3.

In Table 1, note the excellent agreement of depth values obtained by three receivers, which is particularly good in points  $H_2$  and  $H_3$  and is undoubtedly due to the *good quality* of the *reflection records*. The results obtained at  $H_1$ ,  $H_2$  and  $H_3$  show that a dip of the formations is present in the direction from  $H_1$  to  $H_3$ . These are, of course, examples only and *not the only depth determinations* made on the structure.

### CONCLUSION

A more recent field practice utilizes the so-called "vertical shooting" method. That is, the seismometers are placed comparatively close to the shot point (within 200 to 600 ft.). This method has many advantages, some of which are: practically all of the preliminary impulses have completely passed before the reflected impulses arrive; in areas where the surface zones are not complex, the first impulses of the reflection records may be used to compute the low-velocity layers; interpretation may be considerably simplified since there is such a slight difference between the curved- and straight-path times. The success of this method in numerous areas is almost phenomenal, particularly in consideration of the fact that the shot distances are so much less than critical that it would not be expected that much of the energy would be reflected. The theory of "layer oscillation" advanced some time ago is recalled because it offers a plausible explanation of the large vertical energies.

In the usual field organization, the observer is in charge of the field work, while the party chief is responsible for the interpretation of the results. Such being the case and assuming an efficient instrumental set-up, the success of the field party depends to a great extent upon the ingenuity and resourcefulness of the observer, since the field technique will vary with the geology, topography and locality.

For interpretation, we are dependent upon the skill and knowledge of the party chief, whose ability to distinguish and correlate reflections, coupled with the virtue of consistency in marking phases, must be fortified by a sound knowledge of geological principles. Also, it is believed that while an observer should be an excellent instrument technician, he should have also the basic geologic knowledge necessary to the proper placing of shots, profile directions, etc.; furthermore, he should

be cognizant particularly of the many geologic factors affecting the desired reflected impulses.

Up to the present time, more stress has been applied to the physical side of reflection seismology mainly because most of the work has been carried out in areas of which the geology was fairly well known, and in which check wells have been available. Also, in many cases, the region had been surveyed previously by the refraction method, so that the seismic properties of the subsurface were known.

As we reduce our instrumental errors down to the personal limit, more time can and should be spent upon field experimentation than upon laboratory research.

We reiterate the necessity of sustained research on the several problems in the foregoing and on others probably equally as important. Many of these problems have apparently been considered as secret. If the seismic reflection method is to have continued success, many basic relationships must be discussed in constructive and informative detail.

## DISCUSSION

*(Paul Weaver presiding)*

I. ROMAN,\* Houghton, Mich. (written discussion).—For recording the time of explosion, it has been found necessary to use two wires from the charge to the recorder in refraction surveying at the Michigan College in Mining and Technology. Because of the short time intervals involved in determining the depths to shallow ledges of rock, the repeated grounding of a single wire during the shattering of the earth have frequently prevented the identification of the first refracted impulse. A double lead has caused false records on some occasions, but the probability that two thin wires will swing together or short across the same lump of earth is much more remote than is the probability that a single wire will make contact with the main body of the earth either directly or by way of contiguous lumps of earth. Even when the wire has been blown completely out of the hole, a single wire has caused multiple contacts. Since the experience of the Colorado School of Mines was not known at the time, it is both interesting and important that the remedy was identical at both institutions. While a separate recorder would remove the need of a double wire timing circuit, the extra equipment would introduce objections more serious than the use of a double wire.

With regard to firing from the recording truck, experience indicates that such a technique is not desirable. Some of the objections are:

1. The truck observer is often located so that the firing charge is invisible to him.
2. The truck observer has too many other operations to keep in mind.
3. The man who fires the charge should be the one nearest the charge and he should have no other duties during the period in which the firing circuit is connected.
4. By firing near the charge, less wire is needed, thus reducing the chances of a misfire due to broken wires or poor connections.
5. The firing lines should be entirely distinct from all other current lines, to prevent accidental discharge by shorting or incorrect connections.

---

\* Assistant Professor of Mathematics and Physics, Michigan College of Mining and Technology.

6. The firing circuit should be left completely disconnected until everything else is ready for the shot and should be connected by the man who is to do the firing. This man should have a clear view not only of the charge position but of the entire danger zone. Even on short shots, this precaution is desirable. Whether a blasting magneto or a dry cell is used, both wires to the charge should be disconnected and shorted with each other except while the charge is to be fired. Battery clips have proved convenient for this purpose. In this arrangement, accidental firing is impossible except during the short interval when the observer is waiting for the firing signal.

The fact that the weathering zone does not correspond to a geological layering is no objection to its use. The thickness and speed of such a layer may correspond to a uniform equivalent layer, while the actual formation may be very complex and may have speeds varying from point to point. Since the concept of weathering zone is a fiction to permit a correction to discordant observations, it is not necessary that it have any physical or geological reality. If the data were sufficiently accurate, it might be possible to select a law of speed variation that would make the geological layers lead to the observations, but it is doubtful whether there would be any gain from this formulation, at least for identifying deep structures.

As the author indicates, a system of applying the method of least squares to reflection data has been published in detail. Because of failure to understand the basis of the method, many engineers prefer individual, intuitive schemes for deciding the "best" value to accept from observed data. While the method does not pretend to determine a "true" value for the measured quantity, it does, on the basis of probability, lead to the best value that can be deduced from the measurements made, independent of the reliability of the data. The data are assumed to be impartially obtained, and free of all systematic and personal errors, in which case the value deduced will be reasonably close to the correct one. If this assumption is not valid, no method of interpretation is valid. In particular, if the reflection times are unreliable, as Rutherford contends,<sup>11</sup> the results cannot be reliable, whether obtained by the method of least squares or by any other method.

If the points of reflection are approximately on a plane surface, the method of least squares should give good results. The best speed may not correspond with the speed of any geological formation, since it averages numerous irregularities. It is not necessary that the speed be identified with the geology. The path need not even be rectilinear. The method replaces the actual path by an equivalent rectilinear path in a homogeneous medium. If the actual path is symmetrical with reference to the normal to the surface of reflection, the results will be correct as to depth, and that is all that we are seeking. The speed is simply an intermediate value.

The usual triangle law for reflections assumes horizontal layering, an assumption often overlooked. There is no way to justify this assumption except by the results or by knowing from the geology that the dip of the reflecting layer is small. The other objection raised by Heiland and Pugh is theoretically justified, but for practical purposes the method mentioned by Rutherford is satisfactory. The difference in the interpreted depths is not large, usually. As a specific example, consider the data given in example 6 of the paper to which the author has referred. If we use the method mentioned by Rutherford, the depth is calculated as 2010 ft., while if the correct method is used, the depth is 2006 ft. There may be cases in which the discrepancy is larger. For office interpretation, the correct method should be used, but for field calculations the simplification is justified.

Rutherford has made an error not mentioned by Mr. Pugh. He states that the coefficients in the normal equations are so large that the results are not reliable. I fail to see how this is possible, since the carrying of more significant figures

---

<sup>11</sup> See page 400.



will always make the forcing errors of calculation less important. Using more significant figures is usually not desirable or convenient, but this fact can hardly invalidate the method. A better method was known to Rutherford as early as 1927, but he failed to note it in his paper or to recall it in his calculations, apparently. In this method, the observations are reduced to certain average values, thus reducing the coefficients in the normal equation so that fewer significant figures need be carried in the calculations. Details of this method are being published elsewhere.<sup>12</sup>

The simplified method referred to by Rutherford also has another advantage. If the square of the distance from shot to receiver be plotted as ordinate against the square of the observed reflection time as abscissa, the graph will be a straight line, if the speed is approximately constant. The straightness of the graph is a criterion of the validity of the assumption. The least square method as used determines the best line to draw, not the best speed or depth. However, the two methods lead to values of the depth in as close agreement as two independent trials of taping the depth in a drill hole. The advantage referred to above is the following: If reflection profiles obtained at neighboring shot points are plotted as just described, each will have a line as a graph. If these lines are reasonably straight and parallel, we may assume that the only change in structure has been in the depth to the marker. If  $D$  is the vertical distance between the two graph lines and  $h$  is the approximate depth, the change in the depth between the two points of reflection is  $D/8h$ . The percentile error in  $D/8h$  is of the same order as that in  $D$  or in  $h$ , but the actual magnitude of the change is relatively small and hence the error in the change of depth is small. Thus, it is possible to outline a structure as to shape quite accurately without knowing the actual depth. Specifically, the change in depth may be found to within a few feet when the actual depth is known to within several hundred feet. If the graphs are parallel, but not straight, the same formula will give some indication of the change in depth, but the formulas have not been derived for the general case.

---

<sup>12</sup> See pages 522-524, this volume.



## Seismic Refraction Methods as Applied to Shallow Overburdens

By F. L. PARTLO\* AND JERRY H. SERVICE,\* HOUGHTON, MICH.

(New York Meeting, February, 1934)

THE following investigation was undertaken to develop a method for determining with reasonable accuracy the depth of overburdens of 100 ft. or less. Seismic methods seemed to offer good possibilities. The problem differed from that of the familiar salt-dome location in that the depth of overburden to be determined is much less than is encountered in oil prospecting. This means that a much shorter time interval must be measured with accuracy. Refraction methods seem at present to offer greater possibilities than reflection. The air sound persists for from 0.1 to 0.5 sec., because of echoes, and seismic reflections coming during this time are difficult to detect. A seismometer sensitive to vertical vibrations only offers possibilities and has been used here with some success. It is hoped that the application of this type of seismometer to reflection shooting in this region may be investigated still further.

The apparatus used consisted of a carbon-button seismometer followed by a three-stage, transformer-coupled, vacuum-tube amplifier and a General Radio string oscillograph. Time marks are provided by a 1000-cycle, 600-r.p.m., synchronous motor provided with five spokes which intercept the light to the camera at  $\frac{1}{50}$  sec. intervals. This motor is driven by a two-stage vacuum-tube amplifier of 3 watt output, actuated by a tuning fork. The power supply for the seismometer amplifier is one 2-volt storage and one 45-volt B battery. The motor amplifier is powered by a 6-volt storage battery and 6 to 225-volt, 15-watt motor generator. The temperature-frequency characteristics of the tuning fork have been determined and for ordinary working temperatures the error in time that would be introduced is less than  $\frac{1}{2}$  millisecond for time intervals up to 100 milliseconds.

The impact is produced by a sledge blow for surface distances less than 100 ft. and dynamite for greater distances. Two steel balls with wires attached form an electric circuit through a 1-ft. piece of railroad rail upon which they rest. When the rail is struck by the sledge the balls rebound, opening the circuit and indicating the time of impact by a break in the oscillograph record line as at A, Fig. 3. When dynamite

---

\* Assistant Professor of Mathematics and Physics, Michigan College of Mining and Technology.

is used a piece of enameled wire is wrapped around the blasting cap. The exploding cap breaks this wire and the opening circuit indicates in the same way as with the sledge. Fig. 3 is a record of a dynamite impact at a distance of 100 feet.



FIG. 1.

FIG. 2.

FIG. 1.—EQUIPMENT, SHOWING AMPLIFIERS AND OSCILLOGRAPH WITH CAMERA IN PLACE.

FIG. 2.—EQUIPMENT ON TRUCK. CAMERA REMOVED AND FOCUSING AND VIEWING SCREEN IN PLACE.

In the analysis of records the times of the impact and of the onset of the first arrival, *A* and *B* Fig. 3, are measured from an arbitrary zero time. Their differences give times of travel, which are plotted against their corresponding distances to locate tentative travel-time lines. Records are then examined for interferences, as at *C*, Fig. 3, which would

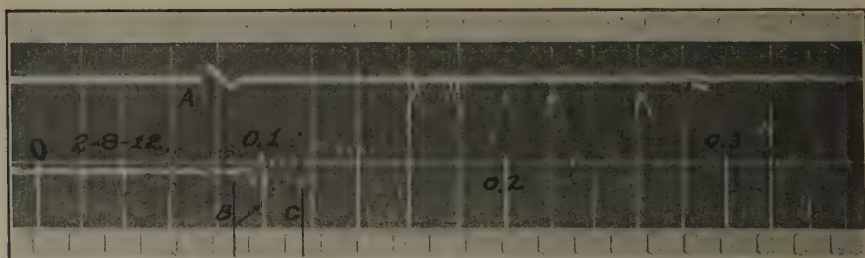


FIG. 3.—SAMPLE OF SEISMIC RECORD. IMPACT AT *A* AND ONSETS AT *B* AND *C*. NOTE AIR SOUND ARRIVING AT 0.158 SECONDS.

give additional points on or near the tentative travel-time lines. The lines are then redrawn and the apparent velocities determined. The calculations are made as outlined in the following theory and in Tables 1 and 2, which are abridgments of the calculation table.

It frequently happens that the travel-time line of the surface medium intercepts the time axis above the origin. This is always a small amount, 6 or 8 ms., and in the calculations the origin has been taken at this intersection. The effect would be that of neglecting a possible thin surface layer of slow-velocity material which, if included, would add slightly to the observed depth.

### THEORY

Suppose that the receiver is located at the surface, which is assumed plane, and that beneath the plane of the surface are one or more planes, which are the contacts between homogeneous, isotropic media. (See Fig. 4.) The receiver is at  $R$  and shots are fired successively at various

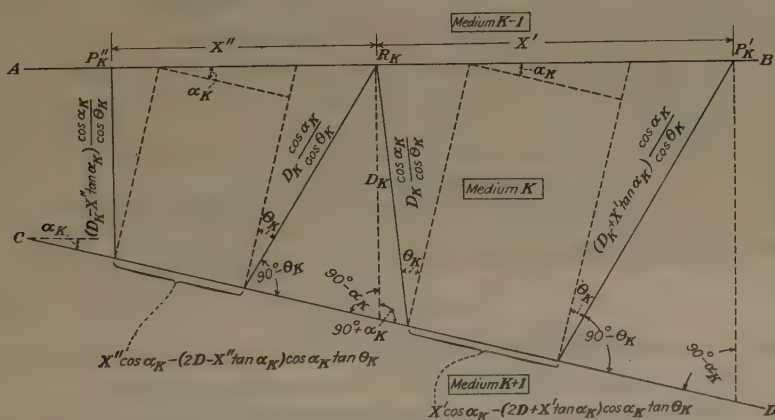


FIG. 4.—METHOD OF OBTAINING DEPTH TO PLANE OF CONTACT.

points  $P'$ ,  $P''$ , etc., which lie upon a straight line through  $R$ , in the surface. The plane of the figure is the plane containing the receiver and line of shots, that is perpendicular to the plane of contact of the  $K$  and  $K + 1$  media, here the first and second media.  $CD$  is the trace of this plane of contact. If the plane of the figure is not vertical, depth to plane of contact  $D$  must be divided by  $\cos Y$  (where  $Y$  is the angle between plane of the figure and the vertical) to obtain vertical depth to plane of contact at the receiver.

If several shots are fired successively at a series of distances comparatively small, waves arriving first at  $R$  will travel entirely in the upper layer and the travel time-distance curve will be a straight line such as 1, Fig. 5. As the distance is increased beyond a critical value, the first arrivals will travel by path 2, which passes into the second layer; the travel-time curve for these waves will be a straight line such as 2, Fig. 5. As the distance is still further increased beyond a second critical value, the first arrivals will travel the path 3, which passes into the third layer; the travel time for these waves will be another straight line, such as 3.

It is here assumed that the velocity in a layer becomes greater, the deeper the layer. The full-line portions of the travel-time curves are for the times of first arriving waves. The dotted portions correspond to waves that arrive later. For example, Fig. 5 shows that for distance  $d$  the first arrivals were by path 2, then came waves by path 3, and finally came the waves by path 1.

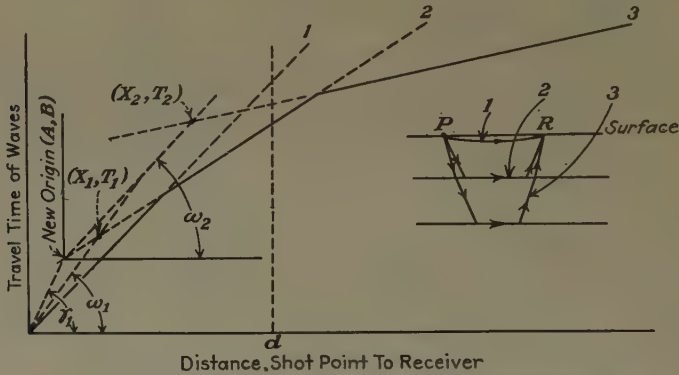


FIG. 5.—TRAVEL-TIME DISTANCE CURVE AS A STRAIGHT LINE.

The equation of line 1, Fig. 5, is

$$t = V_1 x \quad [1]$$

where  $V_1$  is the speed in the first layer.  $V_1$  is thus the reciprocal of the slope of line 1, and is so obtained from the travel-time graph.

The equation of line 2, Fig. 5, is derived by reference to Fig. 4.  $\theta_1$  is the critical angle between the first and second layers, so that

$$\begin{aligned} \sin \theta_1 &= \frac{V_1}{V_2}. \text{ For "down ledge" shooting from } P'' \text{ to } R, \\ t'' &= \frac{(2D_1 - x'' \tan \alpha_1) \cos \alpha_1 \cos \theta_1}{V_1} + \frac{x'' \cos \alpha_1 \sin \theta_1}{V_1} \\ \text{or } t'' &= \frac{\cos \alpha_1 \sin \theta_1 - \sin \alpha_1 \cos \theta_1}{V_1} x'' + \frac{2D_1 \cos \alpha_1 \cos \theta_1}{V_1} \\ \text{or } t'' &= \frac{\sin (\theta_1 - \alpha_1)}{V_1} x'' + \frac{2D_1 \cos \alpha_1 \cos \theta_1}{V_1} \end{aligned} \quad [2]$$

Similarly, for shooting "up ledge" from  $P'$  to  $R$ ,

$$t' = \frac{\sin (\theta_1 + \alpha_1)}{V_1} x' + \frac{2D_1 \cos \alpha_1 \cos \theta_1}{V_1} \quad [3]$$

Both of these equations are of the form  $y = mx + b$ , and we can readily obtain  $\alpha_1$ , also  $\theta_1$  and thence  $V_2$ , from the slopes of the travel-time curves 2, down ledge and up ledge, respectively. Calling these slopes  $m''_2$  and  $m'_2$ , respectively, we have



$$\theta_1 - \alpha_1 = \arcsin V_1 m''_2 \quad [4]$$

$$\theta_1 + \alpha_1 = \arcsin V_1 m'_2 \quad [5]$$

$$\theta_1 = \frac{\arcsin V_1 m'_2 + \arcsin V_1 m''_2}{2} \quad [6]$$

$$\alpha_1 = \frac{\arcsin V_1 m'_2 - \arcsin V_1 m''_2}{2} \quad [7]$$

$$V_2 = \frac{V_1}{\sin \theta_1} \quad [8]$$

$V_1$ ,  $\theta_1$  and  $\alpha_1$  being thus known,  $D_1$  might be found from the  $t$  intercepts of the travel-time curves 2, which are seen from equations 2 and 3 to be equal to  $\frac{2D_1 \cos \alpha_1 \cos \theta_1}{V_1}$ .

From other considerations, however, it seems preferable to find  $D_1$  by means of the coordinates of the points on the travel-time curves 2 that correspond to total reflection from  $CD$ ; that is, to travel along path 2, arriving at and leaving the second layer at angle  $\theta_1$  with the normal but with zero travel in the second layer. Let us call the coordinates of these points on the travel-time graph, for down ledge and up ledge, respectively,  $(X_1'', T_1'')$  and  $(X_1', T_1')$ .

Referring directly to Fig. 4, since there is no travel in the second layer, we have for the down-ledge case

$$T_1'' = \frac{(2D_1 - X_1'' \tan \alpha_1) \cos \alpha_1}{V_1 \cos \theta_1} \quad [9]$$

and for the up-ledge case

$$T_1' = \frac{(2D_1 + X_1' \tan \alpha_1) \cos \alpha_1}{V_1 \cos \theta_1} \quad [10]$$

Since  $(X_1'', T_1'')$  lies upon the down-ledge curve 2,  $X_1''$  and  $T_1''$  must satisfy equation 2, whence

$$\begin{aligned} \frac{2D_1 \cos \alpha_1}{V_1 \cos \theta_1} - \frac{\sin \alpha_1}{V_1 \cos \theta_1} X_1'' &= \frac{\sin (\theta_1 - \alpha_1)}{V_1} X_1'' + \frac{2D_1 \cos \alpha_1 \cos \theta_1}{V_1} \\ [\sin (\theta_1 - \alpha_1) \cos \theta_1 + \sin \alpha_1] X_1'' &= 2D_1 \cos \alpha_1 (1 - \cos^2 \theta_1) \\ X_1'' &= \frac{2D_1 \cos \alpha_1 \sin \theta_1}{\cos (\theta_1 - \alpha_1)} \end{aligned} \quad [11]$$

Substituting in eq. 9 gives:

$$T_1'' = \frac{2D_1 \cos^2 \alpha_1}{V_1 \cos^2 (\theta_1 - \alpha_1)} \quad [12]$$

$$\cot \omega_1'' = \frac{X_1''}{T_1''} = \frac{V_1 \sin \theta_1}{\cos \alpha_1} \quad [13]^1$$

<sup>1</sup>See Fig. 5.

In like manner, we find

$$X_1' = \frac{2D_1 \cos \alpha_1 \sin \theta_1}{\cos (\theta_1 + \alpha_1)} \quad [14]$$

$$T_1' = \frac{2D_1 \cos^2 \alpha_1}{V_1 \cos (\theta_1 + \alpha_1)} \quad [15]$$

$$\cot \omega_1' = \frac{V_1 \sin \theta_1}{\cos \alpha_1}, \text{ as before.}$$

$$\text{From eq. 11, } 2D_1 \cos \alpha_1 \sin \theta_1 = X_1'' \cos (\theta_1 - \alpha_1)$$

$$\text{From eq. 14, } 2D_1 \cos \alpha_1 \sin \theta_1 = X_1' \cos (\theta_1 + \alpha_1)$$

Thus  $X_1'' \cos (\theta_1 - \alpha_1)$  and  $X_1' \cos (\theta_1 + \alpha_1)$ , except for experimental errors and errors in the assumptions, will be equal. Both these quantities may be obtained from the travel-time graphs,  $X_1'$  and  $X_1''$  directly (Fig. 5) and the cosines by means of eqs. 4 and 5 and the graphs. Calling the mean of  $X_1' \cos (\theta_1 + \alpha_1)$  and  $X_1'' \cos (\theta_1 - \alpha_1)$ ,  $a_1$ , we have

$$2D_1 \cos \alpha_1 \sin \theta_1 = a_1 \quad [16]$$

$$\text{From eq. 12, } 2D_1 \cos^2 \alpha_1 = V_1 T_1'' \cos (\theta_1 - \alpha_1)$$

$$\text{From eq. 15, } 2D_1 \cos^2 \alpha_1 = V_1 T_1' \cos (\theta_1 + \alpha_1)$$

Proceeding as above, obtaining  $T_1'' \cos (\theta_1 - \alpha_1)$  and  $T_1' \cos (\theta_1 + \alpha_1)$  from the travel-time graphs, and calling the mean of these quantities  $b_1$ , we have

$$2D_1 \cos^2 \alpha_1 = V_1 b_1 \quad [17]$$

Squaring eq. 16, dividing it by eq. 17 and solving for  $D_1$ , we obtain

$$D_1 = \frac{a_1^2}{2V_1 b_1 \sin^2 \theta_1} \quad [18]$$

Our working equations are 4, 5, 6, 7, 8, 13, 18, which we now express in more general form. In the general case let the virtual receiver and shot positions be  $R$  and  $P$ . The general equations thus become

$$\theta_K - \alpha_K = \arcsin V_K m_{K+1}'' \quad [4a]$$

$$\theta_K + \alpha_K = \arcsin V_K m_{K+1}' \quad [5a]$$

$$\theta_K = \frac{\arcsin V_K m_{K+1}' + \arcsin V_K m_{K+1}''}{2} \quad [6a]$$

$$\alpha_K = \frac{\arcsin V_K m_{K+1}' - \arcsin V_K m_{K+1}''}{2} \quad [7a]$$

$$V_{K+1} = \frac{V_K}{\sin \theta_K} \quad [8a]$$

$$\cot \omega_K = \frac{V_K \sin \theta_K}{\cos \alpha_K} \quad [13a]$$

$$D_K = \frac{a_K^2}{2V_K b_K \sin^2 \theta_K} \quad [18a]$$

in which  $a_K$  and  $b_K$  are as explained preceding eqs. 16 and 17.

If the lower bounding plane of the  $K$  medium is parallel to the upper bounding plane of the  $K$  medium, so that  $\alpha_K$  equals zero, as shown by the fact that  $m_{K+1}' = m_{K+1}''$  on the travel-time graphs, these equations assume much simpler forms as follows:

$$V_{K+1} = \frac{1}{m_{K+1}} \quad [8b]$$

$$\cot \omega_K = V_K \sin \theta_K, \text{ where } \sin \theta_K = V_K m_{K+1}$$

$$\text{so that} \quad \cot \omega_K = \frac{V_K^2}{V_{K+1}} \quad [13b]$$

$$D_K = \frac{1}{2} \sqrt{V_K^2 T_K^2 - X_K^2} \quad [18b]$$

Since the actual velocity in the  $K+1$  medium is the reciprocal of  $m_{K+1}$  when  $\alpha_K$  equals zero, it is convenient to call the reciprocals of  $m_{K+1}'$  and  $m_{K+1}''$  the apparent velocities  $V_{K+1}'$  and  $V_{K+1}''$  up and down ledge, respectively. Then  $\theta_K'$  and  $\theta_K''$  are the corresponding apparent critical angles, and

$$\sin \theta_K' = \frac{V_K}{V_{K+1}'}, \text{ and } \sin \theta_K'' = \frac{V_K}{V_{K+1}''}$$

whence eqs. 4a, 5a, 6a and 7a may be written

$$\theta_K - \alpha_K = \theta_K'' \quad [4b]$$

$$\theta_K + \alpha_K = \theta_K' \quad [5b]$$

$$\theta_K = \frac{\theta_K' + \theta_K''}{2} \quad [6b]$$

$$\alpha_K = \frac{\theta_K' - \theta_K''}{2} \quad [7b]$$

It has been shown how two media can be investigated by refraction shooting on both sides of a fixed receiver position, the shots being fired along a straight line through the receiver. The theory applies to the cases where the media are approximately homogeneous and are bounded by surfaces approximately plane. From the travel-time curves can be obtained:

1. The speeds of the compressional waves in the two media, that in the second medium giving some information as to the nature of that medium.

2. The angle (in the plane through the shot line perpendicular to the lower bounding surface of the upper medium) between the upper and lower bounding surfaces of the first medium; and what is more important,

3. The vertical distance from receiver to lower bounding surface of first medium.

If there is a third medium, we can conceive our actual receiver and shot positions to be replaced by virtual receiver and shot positions as

indicated in Fig. 6, where  $R_K'$ ,  $P_K'$  and  $R_K''$ ,  $P_K''$  are the virtual receiver and shot positions, respectively, for up-ledge and down-ledge shooting, respectively, for investigation of the  $K$  and  $K + 1$  media. The figure is drawn on the assumption that the bounding surfaces of the  $K - 1$  medium are approximately parallel. By reducing the shot to receiver

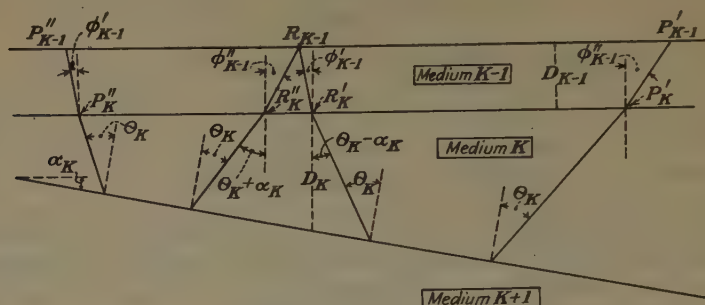


FIG. 6.—ACTUAL AND VIRTUAL RECEIVER AND SHOT POSITIONS WITH THREE MEDIA. distance by  $D_{K-1}(\tan \phi_{K-1}' + \tan \phi_{K-1}'')$  and the travel time of the wave over  $K + 1$  path by  $\frac{D_{K-1}}{V_{K-1}}(\sec \phi_{K-1}' + \sec \phi_{K-1}'')$ , that is by shifting to a new origin ( $A_{K-1}$ ,  $B_{K-1}$ ) on the time-travel graph, we can use all the equations already derived to carry our investigations one layer farther.  $A$  and  $B$  are given by the equations:

$$A_K = D_K(\tan \phi_K' + \tan \phi_K'') \quad [19]$$

$$B_K = \frac{D_K}{V_K}(\sec \phi_K' + \sec \phi_K'') \quad [20]$$

For example, it has already been shown how, by using curves 1 and 2, media 1 and 2 can be investigated by means of eqs. 4, 5, 6, 7, 8, 13 and 18. If a third layer is now to be investigated, we have only to use curves 2 and 3 instead of 1 and 2, shifting to a new origin ( $A$ ,  $B$ ) which lies on curve 2 as the original origin did on curve 1, and use the same equations with every subscript increased by one. Since the receiver and shot positions already used were the original ones at the top of the first medium  $K - 1$  was 1. Hence  $K$  will be 2 and should be so used in eqs. 19 and 20 for finding the coordinates of the new origin.

Since ( $A$ ,  $B$ ), the new origin, lies on curve 2, it will be found most conveniently on the travel-time graph by laying off the angle  $\gamma_1$  as shown in Fig. 5, where

$$\cot \gamma_1 = \frac{A_1}{B_1}$$

Substituting the values of  $A$  and  $B$  and solving, we have

$$\cot \gamma_K = \frac{V_K \sin (\phi_K' + \phi_K'')}{\cos \phi_K' + \cos \phi_K''} \quad [21]$$



$\phi_K''$  and  $\phi_K'$  are given by the equations

$$\frac{\sin \phi_K'}{\sin \theta_{K+1}'} = \frac{\sin \phi_K''}{\sin \theta_{K+1}''} = \frac{V_K}{V_{K+1}} \quad [22]$$

$\sin \theta_{K+1}'$  and  $\sin \theta_{K+1}''$  are given by eqs. 4b and 5b. This will give:

$$\sin \phi_K' = \sin \theta_K \sin \theta_{K+1}' \quad [23]$$

$$\sin \phi_K'' = \sin \theta_K \sin \theta_{K+1}'' \quad [24]$$

In case  $\alpha_K = 0$ , eq. 21 reduces to

$$\begin{aligned} \cot \gamma_K &= \frac{V_K \sin 2\phi_K}{2 \cos \phi_K} \\ &= V_K \sin \phi_K \\ &= \frac{V_K^2}{V_{K+2}} \end{aligned} \quad [25]$$

If the lower surface makes an angle  $\alpha_1$  with the upper surface the transfer becomes somewhat less simple. In that case the distances must be reduced by  $D_1 \tan \phi_1' + (D_1 + x \tan \alpha_1) \tan \phi_1''$ ; that is, by  $A_1 + x \tan \alpha_1 \tan \phi_1''$ , to a first approximation. To a first approximation, the travel times must be reduced by  $\frac{1}{V_1}[D_1 \sec \phi_1' + (D_1 + x \tan \alpha_1) \sec \phi_1'']$ , that is, by  $B_1 + \frac{x \tan \alpha_1 \sec \phi_1''}{V_1}$ . By transferring to the new origin  $(A_1, B_1)$ , then rotating the  $t$  axis through an angle  $\beta_1$  clockwise and the  $x$  axis through an angle  $\epsilon_1$  counterclockwise, all our purposes are accomplished,  $\beta_1$  and  $\epsilon_1$  being defined by the equations 26 and 27.

$$\tan \beta_1 = \tan \alpha_1 \tan \phi_1'' \quad [26]$$

$$\tan \epsilon_1 = \frac{\tan \alpha_1 \sec \phi_1''}{V_1} \quad [27]$$

or in general

$$\tan \beta_K = \tan \alpha_K \tan \phi_K'' \quad [26a]$$

$$\tan \epsilon_K = \frac{\tan \alpha_K \sec \phi_K''}{V_K} \quad [27a]$$

If the lower surface of the medium  $K$  does not make too large an angle  $\alpha_K$  with the upper surface of that layer, a first-order correction may also be made as follows. Assume media as indicated in Fig. 7. The ray that refracts critically into medium  $K + 2$  travels through a greater depth of medium  $K$  and a lesser depth of medium  $K + 1$  by the approximate amount  $x \sin \alpha_K$ . This will be seen to be in error by two small factors: (1)  $x$  is too large, and (2) if  $x$  were exactly right  $x \sin \alpha_K$  would be too small. So the errors are opposite in direction, and both small. Then the time of travel will be increased by the difference in times of

travel in the two media through the distance  $x \sin \alpha_K$ . Calling this time correction  $\Delta t$ ,

$$\begin{aligned}\Delta t &= \frac{x \sin \alpha_K}{V_K} - \frac{x \sin \alpha_K}{V_{K+1}} \\ &= \frac{V_{K+1} - V_K}{V_K V_{K+1}} x \sin \alpha_K\end{aligned}\quad [28]$$

Let this amount be subtracted from the times of each of the points on the line whose slope is  $m_{K+1}'$  and added to the times of the points on the  $m_{K+1}''$  line. This together with the proper translation of the axes as

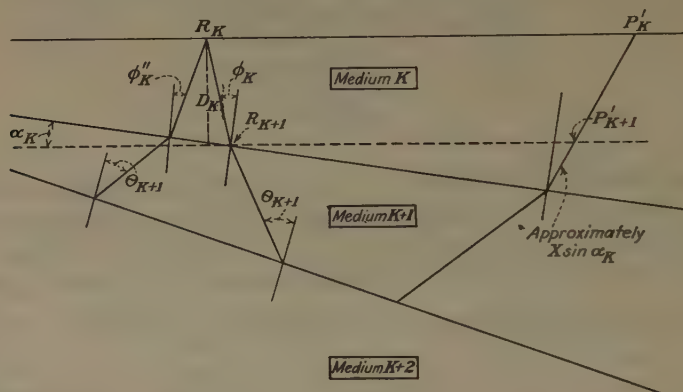


FIG. 7.—FIRST-ORDER CORRECTION.

heretofore considered, will, without sensible error, affect the removal of receiver and shots from  $R_K$  and  $P_K$  to the virtual positions  $R_{K+1}$  and  $P_{K+1}$ . Instead of plotting new points, an equivalent result may be obtained by rotating the  $m_{K+1}$  line about its intersection on the  $t$  axis through an angle  $\tan^{-1} \Delta t/x$ .

#### DEPTH OF OVERBURDEN BY REFRACTION SHOOTING

As pointed out and explained under Theory, if the surface is underlain by fairly homogeneous layers bounded by approximately plane faces, shots fired along a straight line through the receiver and extending in both directions from the receiver will enable the observer to compute: (1) the vertical distance below the receiver to each bounding surface; (2) the inclination of each bounding surface to the horizontal in the direction of the shot line; and (3) the velocity of the fastest waves in each medium. If a similar line of shots is fired making approximately a right angle with the first line, checks on vertical distances and velocities are obtained, and the inclination of each bounding surface to the horizontal in the other direction is determined.

As a test of the method, four locations were selected where the geology is rather well known. These four locations were investigated by

refraction shooting on 2-3 day, on 2-4 and 2-5 days, on 2-6 day, and on 2-7 and 2-8 days, respectively. On the location investigated on 2-4 and 2-5 days, two shot lines at right angles as above discussed were used. On each of the other three locations only one shot line was used, the line extending in both directions from the receiver position on each location. A travel-time graph was drawn for each shot line, by plotting travel times, as taken from the string oscillograph records, against distances from shot point to receiver. Fig. 8, for example, shows the travel-time graph for the location investigated on 2-7 and 2-8 days.

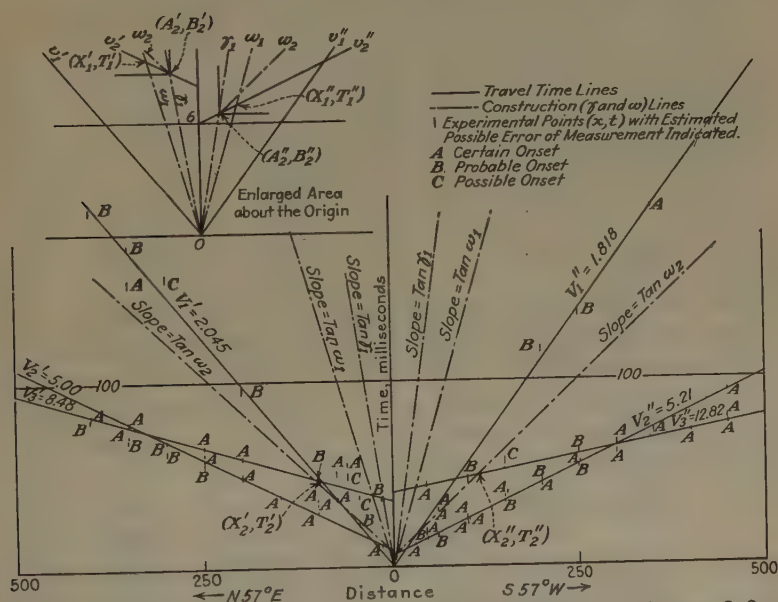


FIG. 8.—TRAVEL-TIME GRAPH FOR LOCATION INVESTIGATED ON 2-7 AND 2-8 DAYS.

The travel-time graph obtained from the location investigated on 2-3 day was analyzed by four different methods of computation. Tables 1 and 2 give in outline the computations for the first three of these methods, designating the three computations in the day columns as 2-3 I, 2-3 II, and 2-3 III. The receiver position was very close to a diamond-drill hole, so that the correct depth to ledge is known as given under Record. Method 2-3 I assumes horizontal interfaces, and treats the shot lines on the two sides of receiver position as separate lines to be computed separately by eqs. 4b, 5b, 6b, 7b, 8a, 13a, 18a and 25. These two separate lines yield values of depth to ledge which differ from each other by 6 per cent, while their average differs from the drill-hole value by only 3 per cent.

The second method, 2-3 II Table 1, assumed both upper and lower faces of the second layer to be inclined to the horizontal, and applied the

TABLE 1.—*Computations of Travel-time Graphs*

Day	K	$V_K'$	$V_{K''}'$	$\theta_K'$	$\theta_{K''}$	$\theta_K$	$\alpha_K$	$\gamma_K$	$\text{Cot } \omega_K$	$X_K'$	$T_{K''}$	$T_{K''}'$	$A_{K''}$	$B_{K''}$	$A_{K''}'$	$B_{K''}'$	$\text{Cot } \gamma_K$	$D_K$	Record
2-3 II <sup>a</sup> 1 <sup>d</sup>	1	1.27	1.24	13°35'	9°30'	11°32'	2°2'	1.25	0.250	9	38	13	52	0	0	0	0.0695	26.5	D.D.H. 93
	2	5.32	7.58	22°50'	9°32'	16°11'	6°39'	6.25	1.758	31	18	49	28	4	51	3	36.5	68.5	
	3	16.1	37.6					22.4									Depth = 95.0		
2-3 III <sup>b</sup> 2 <sup>c</sup>	1	1.27	1.24	13°35'	9°30'	11°32'	2°2'	1.25	0.250	9	38	13	52	0	0	0	0.0628	26.5	D.D.H. 93
	2	5.32	7.58	25°1'	7°53'	16°27'	8°34'	6.25	1.788	33	17	50	29	3	51	2	36.5	71.5	
	3	14.7	45.5					22.1									Depth = 98.0		
2-6 II <sup>c</sup>	1	2.31	2.32					2.31	1.102	32	30	31	27	0	5	0	0.476	28.9	
	2	4.85	4.80	37°30'	14°0'	25°45'	11°45'	4.83	2.145	69	37	74	31	12	30	11		73.7	
	3	7.94	20.00					11.10									Depth = 102.6		
2-7, 8 I	1	2.045	1.818					1.932	0.728	7	9.5	5	7	0	0	0	0.367	7.4	98'
	2	5.00	5.21	37°40'	23°30'	30°35'	7°5'	5.12	2.625	102	38.5	110	42.5	3	9	3	6.5	89.8	
	3	8.48	12.82					10.05									Depth = 97.2		
2-4, 5 I	1	2.12	2.20					2.16	1.053	9.0	8.4	3.5	3.4	0	6	0	0.246	5.6	D.D.H. 58'
	2	4.46	4.38	20°33'	18°51'	19°42'	0°51'	4.42	1.490	33.3	22.4	54.3	36.7	2	12.7	1	8.3	60.9	
	3	12.6	13.7					13.1									Depth = 66.5		
2-5 I	1	1.98	2.44	10°12'	5°10'	7°41'	2°31'	2.21	0.296	12	44	13	49.3	0	6.0	0		56.4	D.D.H. 58'
	2	12.5	24.6					16.5									Depth = 56.4		

<sup>a</sup> Treated as two sloping interfaces, travel-time line rotated.<sup>b</sup> Treated as two sloping interfaces,  $t$ -axis and  $x$ -axis rotation.<sup>c</sup> Treated as one horizontal and one sloping interface.<sup>d</sup>  $\Delta t/x = 0.0227$ .<sup>e</sup>  $\tan \beta_K = 0.00282$ ,  $\tan \epsilon_K = 0.0289$ .<sup>f</sup> Obtained by measurement on map of U.S. Geol. Survey *Prof. Paper* 144.<sup>g</sup> The DDH record here is 64', receiver location being 6' below the top of the casing.



TABLE 2.—*Computations of Travel-time Graphs*

Day	K	$V_K'$	$\text{Cot } \omega_K$	$X_K$	$T_K$	$A_K$	$B_K$	$\text{Cot } \gamma_K$	$D_K$	Record
2-3 I <sup>a</sup>	1	1.27	0.301	12	38.5	0	0	0.081	24.3	D.D.H.  93'
	2	5.32	1.415	41	29	3	36.5		74.3	
	3	20.00						Depth = 98.6		
	1	1.24	0.203	10	51.5	0	0	0.061	31.6	
	2	7.58	2.295	40	17	3	51		61.3	
	3	25.00						Depth = 92.9		
								Ave. = 95.7		
2-6 I <sup>a</sup>	1	2.31	1.100	32	30	0	5	0.670	30.7	
	2	4.85	2.95	126	43	17	31		83.4	
	3	7.94						Depth = 114.1		
	1	2.32	1.120	32	27	0	7	0.270	26.9	
	2	4.80	1.150	35	30	6	29		69.8	
	3	20.00						Depth = 96.7		
								Ave. = 105.4		

<sup>a</sup> Treated as two separate determinations of two horizontal interfaces.

theory covered by Fig. 7 and theory following eq. 27a. The depth to ledge thus computed differed from the drill-hole value by only 2 per cent.

The computation labeled 2-3 III in Table 1 involved the same assumptions as to inclined interfaces as 2-3 II, but used the method of calculation involving rotation of both new axes as explained in theory following eq. 25. The rotation required for the new time axis was found to be negligible. The depth to ledge so obtained is seen to have a discrepancy of 5 per cent from the drill-hole value.

Finally for this location the depth to ledge was computed by means of the intercepts on the time axis by means of the relation:<sup>2</sup>

$$\text{Intercept on } K + 1 \text{ curve} = \frac{2D_K \cos \alpha_K \cos \theta_K}{V_K}$$

Solving for  $D_K$ , we obtain:

$$D_K = \frac{\text{Intercept}_{K+1} \cdot V_K}{2 \cos \alpha_K \cos \theta_K} \quad [29]$$

The "intercept" was taken as the average of the two intercepts on the up and down-ledge halves of the travel-time graph. The result is tabulated in Table 3, being designated there as 2-3 IV, and is seen to be at variance with the drill-hole value by 6 per cent. The average of the apparent velocities  $V_3'$  and  $V_3''$  for this location is 22.5 kilofeet per second. Calculations 2-3 II and 2-3 III give 22.4 and 22.1, respectively. Thus we can state safely that the velocity in the third layer lies between 22.1 and 22.5 and probably is near 22.3 kilofeet per second.

<sup>2</sup> See theory following eq. 8.

Regarding the inclination of the interfaces, it will be noted that the method of 2-3 II determines  $\alpha_2$  relative to the surface, whereas 2-3 III gives  $\alpha_2$  relative to the next interface above. Hence in 2-3 III the inclination of the ledge relative to the surface will be  $\alpha_2$  minus  $\alpha_1$  (they are in opposite directions), or  $6^\circ 32'$ , which differs from  $\alpha_2$  of 2-3 II by only 2 per cent, which is well within what may reasonably be expected.

TABLE 3.—*Summary of Results*

Day	Calculation Method	Depth Obtained, Ft.	Depth Record, Ft.	Error, Per Cent
2-3 I	Horizontal interfaces	95.7		+ 3
2-3 II	Travel-time line rotation	95.0		+ 2
2-3 III	Axis rotation	98.0		+ 5
2-3 IV	<i>t</i> intercept	98.2	93	+ 6
2-4, 5 I	Inclined ledge	66.5		+15
2-5 I	Inclined ledge	56.4		- 3
		Ave. 61.4	58	+ 6
2-4, 5 II	<i>t</i> intercept	68.2		+18
2-5 II	<i>t</i> intercept	44.7		-24
		Ave. 56.5	58	- 3
2-6 I	Horizontal interfaces	105.4	160	"
2-6 II	Inclined ledge	102.6		
2-6 III	<i>t</i> intercept	100.1		
2-7, 8 I	Inclined interfaces	97.2		- 1
2-7, 8 II	<i>t</i> intercept	96.5	98	- 2

<sup>a</sup> See discussion of results.

The 2-6 day results were analyzed by three methods. In the first (2-6 I, Table 2) horizontal interfaces were assumed and the two halves of the travel-time graph computed separately; in the second method (2-6 II, Table 1) the upper and lower surfaces of the second layer were assumed horizontal and inclined, respectively, and the travel-time graph computed as a unit. The first two methods gave depth of overburden as 105.4 and 102.6 ft., respectively, thus differing from each other by some  $2\frac{1}{2}$  per cent. In the third method the depth of overburden was computed by the time intercept method, eq. 29, and was found to be 100.1 ft. (2-6 III, Table 3). It may be stated that this location was chosen as one of the few where there are drill holes over the sandstone. The shot line was known to be near the Keweenaw fault but was supposed to be definitely over the sandstone. When the travel-time graphs were drawn, however, it was at first suspected that one end of the line was over the sandstone and the other over the trap. Calculation 2-6 I was made because of this belief. Another possibility is the same ledge material all along the line but with a sloping ledge surface. Calculation

2-6 II was made upon this basis. The ledge velocity, 11.10 kilofeet per second, obtained in 2-6 II, is reasonable for sandstone, but the depth of overburden does not check with the diamond-drill hole value, which is 163 ft. However, when a shaft was sunk near by several years ago a layer of hardpan was encountered at about 100 ft., which was at first mistaken for ledge. It is the belief of the authors that it is this layer of hardpan that gives us a depth here of about 104 feet.

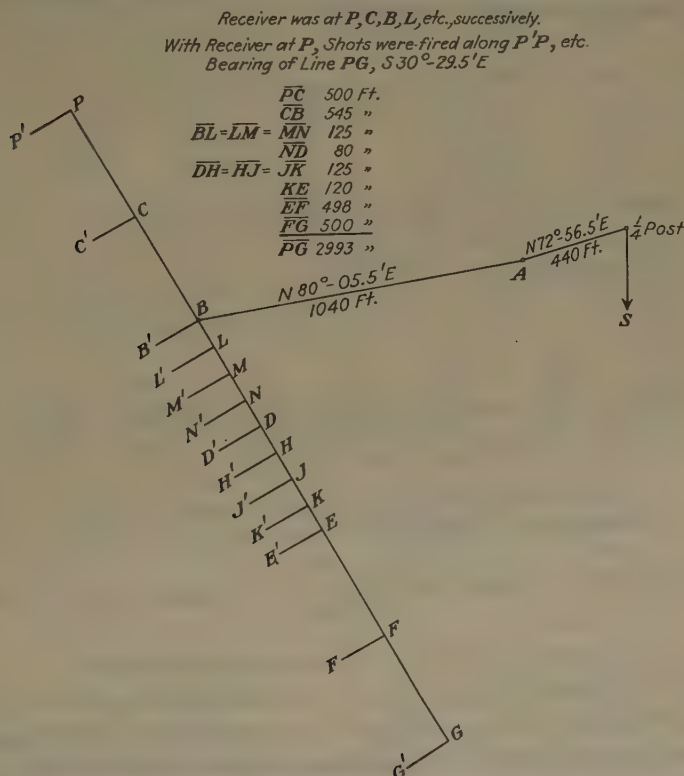


FIG. 9.—DETAILS OF SURVEY IN AREA CROSSED BY CONCEALED MAJOR FAULT BETWEEN SANDSTONE AND TRAP.

The travel-time graph for the work on 2-7 and 2-8 days is reproduced in Fig. 8. The data were computed by two methods. In the first method, which is outlined in Table 1, the assumption is that the upper and lower surfaces of the second layer were horizontal and inclined, respectively. The second method involved the use of time intercepts and eq. 29, and, as shown in Table 3, gave a depth of overburden of 96.5 ft. Just as this paper was to be submitted it was discovered that the drill-hole value for depth of overburden was 116 ft. from a level 12 ft. above the receiver position.

The two travel-time graphs for the location investigated on 2-4 and 2-5 days, besides having depth of overburden calculated by eq. 29 with

the results given on Table 3, 2-4, 5 II, and 2-5 II, were calculated as outlined in Table 1, the assumptions being made that the upper and lower surfaces of the second layer were horizontal and inclined, respectively. The two values of depth of overburden in Table 1 are seen to agree within 15 per cent, while their average agrees with the drill-hole value within 6 per cent. The average of the two values by the intercept method, Table 3, agrees within 3 per cent with the drill-hole value; the two values themselves, however, are badly discordant.

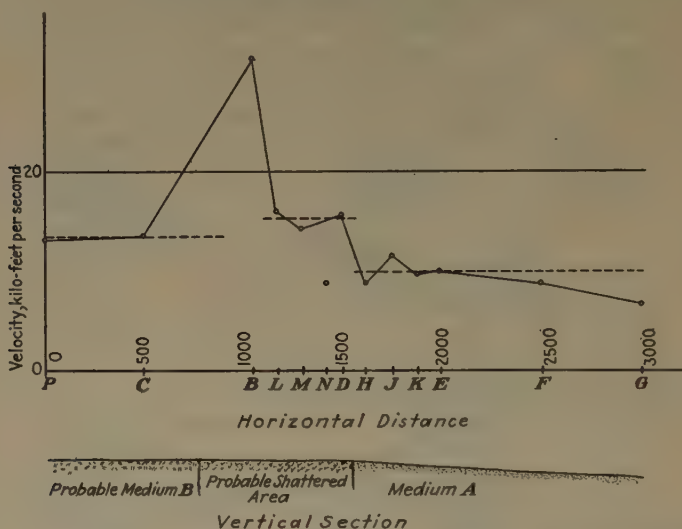


FIG. 10.—VELOCITY IN LEDGE WITH GEOLOGICAL VERTICAL SECTION INTERPRETED THEREFROM.

#### FAULT LOCATION BY REFRACTION SHOOTING

In an area known to be crossed by a concealed major fault between sandstone and trap, a line *PG* (Fig. 9) was selected and surveyed by an azimuth and stadia survey, taking departure and initial azimuth from a quarter section post and a section line, respectively. Fig. 9 shows the details of the survey.

The receiver (carbon-button microphone buried 1 ft. below surface) positions were successively at *P*, *C*, *B*, . . . *G* on line *PG*; the shot lines, usually 200 ft. long, are shown in Fig. 9. For brevity these shot lines will be designated by their respective receiver positions, as *P* line, *C* line, etc.

Table 4 gives the data obtained from the field work. The travel times were plotted against corresponding distances for each shot line; from the relations of the points so plotted each travel time was classified as representing a surface wave through the overburden, or a refracted wave through the second layer.

$V_1$  and  $V_2$  are in kilofeet per second. When the value of  $V_1$  is enclosed in parentheses it was estimated from the values measured on



TABLE 4.—*Data Obtained in Field on Location of Fault*  
(See Fig. 9)

B Line				M Line			
Distance, Ft. <sup>a</sup>	Time, Sec. <sup>b</sup>	Disturbance <sup>d</sup>	V <sub>1</sub> 6.45	Distance, Ft. <sup>a</sup>	Time, Sec. <sup>b</sup>	Disturbance <sup>d</sup>	V <sub>1</sub> 4.83
10	0.008	Sledge		10		Sledge	
20	0.0123	Sledge	V <sub>2</sub> 31.3	20	0.006	Sledge	V <sub>2</sub> 14.3
30	0.0140	Sledge		30	0.008	Sledge	
45	0.0157	Sledge	D 12	45	0.012	Sledge	D 3
60	0.0183	Sledge		60	0.0135	Sledge	
75				75		Sledge	
100	0.0173°	½ stick dyn.		100	0.010°	½ stick dyn.	
150	0.0193°	½ stick dyn.		145	0.0135°	½ stick dyn.	
200	0.0203°	1 stick dyn.		200	0.017°	1 stick dyn.	
H Line				K Line			
10	0.0057	Sledge	V <sub>1</sub> 2.73	10		Sledge	V <sub>1</sub> 5.70
20	0.0117	Sledge	V <sub>2</sub> 8.80	20	0.004	Sledge	V <sub>2</sub> 9.60
30	0.0153	Sledge		30	0.009	Sledge	
45	0.0217	Sledge	D 3	45	0.0117	Sledge	D 3
60		Sledge		60	0.0133	Sledge	
75	0.0323	Sledge		75		Sledge	
100	0.0113°	½ stick dyn.		100	0.0080°	½ stick dyn.	
150	0.0160°	½ stick dyn.		150	0.0157°	½ stick dyn.	
200	0.0233°	1 stick dyn.		200	0.0220°	1 stick dyn.	

<sup>a</sup> From point of disturbance to receiver along shot line.<sup>b</sup> Travel time of first arriving elastic wave from shot point to receiver.<sup>c</sup> Travel time definitely classified as belonging to refracted waves.<sup>d</sup> Disturbances marked "Sledge" were set up by setting a piece of railroad rail 1 ft. long on the ground and striking it a heavy blow with a sledge; those marked " $\frac{1}{2}$  stick dyn." were set up by one-half of a  $\frac{1}{2}$ -lb. stick of dynamite lowered into a 2-in. hole driven 2 ft. into the soil, well tamped with clay and fired electrically.

neighboring shot lines; when not so enclosed in parentheses, the value of  $V_1$  was measured on the line itself.

As a first approximation the upper surface of the second layer was assumed parallel to the upper surface of the overburden.  $V_2$  for each shot line was, therefore, taken as the reciprocal of the slope of the second line on the travel-time graph for that shot line, and  $D$  was calculated by means of eqs. 13b and 18b. As a matter of fact,  $D$  came out practically

TABLE 4.—(Continued)

(See Fig. 9)

E Line				G Line			
Distance Ft. <sup>a</sup>	Time, Sec. <sup>b</sup>	Disturbance <sup>d</sup>		Distance, Ft. <sup>a</sup>	Time, Sec. <sup>b</sup>	Disturbance <sup>d</sup>	
10		Sledge	V <sub>1</sub> 4.20	10		Sledge	V <sub>1</sub> 4.45
20	0.0043	Sledge	V <sub>2</sub> 9.95	20	0.0143	Sledge	V <sub>2</sub> 6.90
30		Sledge		30	0.0165	Sledge	
45	0.0097	Sledge	D 3	45	0.020	Sledge	D 3
60	0.0150	Sledge		60	0.0213	Sledge	
75	0.0180	Sledge		75	0.0265	Sledge	
100	0.0107°	½ stick dyn.		100	0.0180°	½ stick dyn.	
150	0.0160°	½ stick dyn.		150	0.0247°	½ stick dyn.	
200	0.0207°	1 stick dyn.		200	0.0303°	1 stick dyn.	
P Line				C Line (2-9 Day) See Data from 2-12 day			
			V <sub>1</sub> (6.00)				V <sub>1</sub> (6.00)
95	0.0170°	½ stick dyn.	V <sub>2</sub> 13.20	100	0.0183°	½ stick dyn.	V <sub>2</sub> 13.60
150	0.0225°	½ stick dyn.		150		½ stick dyn.	
200	0.0255°	1 stick dyn.	D 3	200	0.0253°	1 stick dyn.	D 3
D Line				J Line			
							V <sub>1</sub> (4.00)
100	0.0090°	½ stick dyn.	V <sub>2</sub> 11.80	100	0.0117°	½ stick dyn.	V <sub>2</sub> 11.50
150	0.0160°	½ stick dyn.		150	0.0187°	½ stick dyn.	
200	0.0213°	1 stick dyn.	D 3	200	0.0217°	1 stick dyn.	D 3

zero for every shot line except line *B*. This is consistent with the fact of numerous outcrops in the northern part of the area, and with the fact that the rod used for driving the shot holes encountered altered sandstone on practically all receiver positions in the southern part of the area. Where the calculations gave *D* equal practically to zero, it is recorded as 3 (feet), because the drive rod was driven down in the overburden from 2 to 3 ft. along every shot line. Attention should be called to the fact that the purpose here was *fault location*, and not measurement of depth of overburden.

The data of Table 4 are summarized graphically in Fig. 10. In the upper part of the figure, velocity in the second layer is plotted against distance of receiver from *P* along *PG*. The indications are: (1) that to

TABLE 4.—(Continued)

(See Fig. 9)

F Line				L Line			
Distance, Ft. <sup>a</sup>	Time, Sec. <sup>b</sup>	Disturbance <sup>d</sup>	V <sub>1</sub> (4.30)	Distance, Ft. <sup>a</sup>	Time, Sec. <sup>b</sup>	Disturbance <sup>d</sup>	
100	0.019°	½ stick dyn.	V <sub>1</sub> 8.80	91	0.0050°	½ stick dyn.	V <sub>2</sub> 15.90
150	0.0240°	½ stick dyn.		150	0.0070°	½ stick dyn.	
200	0.030°	1 stick dyn.	D 3	200	0.0130°	1 stick dyn.	D 3
N Line				C Line (2-12 Day) See Data from 2-9 Day			
75	0.008°	½ stick dyn.	V <sub>2</sub> 8.80	130	0.018°	½ stick dyn.	
125	0.012°	½ stick dyn.		170	0.022°	1 stick dyn.	
175	0.0205°	1 stick dyn.	D 3				

southward from line *H* (toward *G*) a fairly homogeneous medium *A* (probably sandstone) lies under the overburden; (2) that a probable shattered area (fault zone) begins between line *H* and line *D* and extends to somewhere between line *B* and line *C*; (3) that probably some other medium *B* lies to northward of the shattered area.

The records for line *N* were poor records, with explosions and onsets indistinct. The velocity plotted for that line is given little weight. The records for *P*, *B*, *M*, *E*, *F*, *G* lines were excellent and consistent, in spite of the apparently excessive velocity on *B* line. Records on line *H* were good; those on lines *C*, *L*, *D*, *J*, *K* were only fair.

#### CONCLUSION

From Table 3 we see that best agreement is obtained upon the assumption of sloping interfaces when  $V_{K'}$  and  $V_{K''}$  differ materially. However, very satisfactory agreement is obtained with the simple assumption of horizontal interfaces. The *t*-intercept method is somewhat simpler to calculate than the line method and also gives acceptable results.

The application of the refraction method to the location of a concealed fault is definitely satisfactory. In the test case the indication was more precise than the actual position of the fault is known. A greater depth of overburden would not have been a disadvantage and this depth would have been determined also.

#### ACKNOWLEDGMENTS

The authors wish to express their appreciation to Dr. Irwin Roman for his helpful suggestions and to Mr. C. M. Marquardt and Mr. C. G. Stipe for their assistance in obtaining the experimental data.

## DISCUSSION

(*E. DeGolyer presiding*)

E. DEGOLYER,\* New York, N. Y.—In this shallow work, do you deal with the problem which we have in oil work, that of the weathered layer?

F. L. PARTLO.—Yes. We treat it as a separate layer and determine its depth.

F. W. LEE,† Washington, D. C.—Do you use the first arrivals?

F. L. PARTLO.—We use principally the first arrivals in the interpretations. However, we utilize the later arrivals to aid in clarifying the situation.

F. W. LEE (written discussion).—This paper serves as a good illustration of how seismic methods may supplement electrical resistivity methods for the determination of bedrock and overburden where the contours are bedded planes. If possible two or more independent methods should be used to reduce this risk of geological interpretation. The combination of the seismic with the electrical resistivity are ideal in this respect, since each functions in an entirely different manner, using properties of the ground which are not related to each other.

---

\* Petroleum Geologist.

† U. S. Bureau of Mines.



## Analysis of Seismic Profiles

BY IRWIN ROMAN,\* HOUGHTON, MICH.

(New York Meeting, February, 1933)

NUMEROUS results and formulas have been published for analyzing seismic records, but most of them apply only to large-scale phenomena such as are encountered in studying earthquakes. In a few cases,<sup>1</sup> formulas have been published for some of the simpler structures. In the present paper, an attempt will be made to analyze several types of structures without using methods more advanced than those of a first course in calculus.

In tracing a disturbance through a medium, it is almost always possible to base the analysis on Fermat's Principle of Extreme Time, which states that waves of displacement travel between points in such a manner as to make the time of travel an extremum with respect to all neighboring paths. In the simpler cases, comprising most of those used in optics or geophysical prospecting, this time is a minimum and the principle is often referred to as the Principle of Least Time. Within a homogeneous medium, having a uniform speed of transmission of the disturbance in all directions and throughout the medium, the paths are straight and are refracted at the interfaces in accordance with the Snell law of refraction, which states that the ratio of the sine of the angle, made by the ray with the normal to the interface, to the speed of transmission is the same on both sides of the interface. Thus, in any medium composed of homogeneous sections, this same ratio has a constant value at all points. In particular, if all interfaces are horizontal, it is apparent that the angles of incidence are the angles made by the ray with the vertical direction. Furthermore, the incident ray, the refracted ray and the normal to the interface are all in the same plane at each refraction,

---

\* Contributing editor of Geophysical Abstracts, U. S. Bureau of Mines; Assistant Professor of Mathematics and Physics, Michigan College of Mining and Technology.

<sup>1</sup> The reader who wishes to pursue the subject further may consult one of the textbooks on the subject of geophysics, or the following references, in which a more complete bibliography may be found:

Geophysical Prospecting. *Trans. A.I.M.E.* (1929, 1932) **81, 97.**

Geophysical Abstracts, published monthly by the U. S. Bureau of Mines, Washington.

Annotated Bibliography for Economic Geology, published semiannually by Economic Geology Publishing Co., Urbana, Ill.

Engineering Index, Division of Geophysics; cards issued as printed.

so that if the interfaces are all horizontal, each ray must remain in the vertical plane in which it left the source.

For the purpose of simplifying the analysis, we shall assume that all interfaces are horizontal except for the edges of the intrusion, which we shall call a salt dome because of the fact that the first success of seismic prospecting was with that type of structure. It will be obvious that any other intrusion of simple form might be treated in the same manner. As for the edges of the salt dome, we shall assume them vertical. The edges will be perpendicular to the plane of the path for two of the faces and the dome will be assumed to extend infinitely in the directions perpendicular to the plane of the wave. In practice, no intrusion has such a simple shape, but as in many cases of application of theoretical results to practical problems, the idealization makes it possible to predict results that are as accurate as the data on which it is based. As the data become more accurate and the method is proved satisfactory, the assumptions are extended to more complicated conditions. The justification of the assumptions is based, usually, on the utility of the results.

The primary study in this paper will be that of a salt dome buried under the earth's surface, so that its exact position is to be determined by measurement of the times required for a disturbance to travel from a known shot point to a sufficient number of known receiving points, all of which lie near the surface of the earth. We shall calculate the times for various conditions and positions and then study the results of such theoretical deductions with a view to using the information in predicting the most probable structures from known observations of the times.

We shall also assume that the region has been explored so that the profile will lie directly across the dome, and on this assumption the paths will lie in a vertical plane perpendicular to the two finite edges of the dome. In actual practice, the waves will travel in such a plane if the profile is approximately across the dome, so that this assumption is not an important one.

We shall also assume that the speeds and thicknesses are known for each medium transmitting the disturbance, later discarding a part of this assumption in applying the results. We shall assume that the medium in which the upper part of the dome is embedded is so thick that the next lower layer does not enter the observations. For simplicity, we shall assume that the speeds increase downward in all cases. By the speed of a medium, we mean the speed with which the disturbance is transmitted in that medium. For the primary problem, we shall assume homogeneous layers, but in a later section we shall discard this assumption and replace it by the assumption of a single medium for which the speed varies linearly with the depth.

We shall also discuss reflections in a single medium and the determination of depths of several layers, in both cases, discarding the presence of the salt intrusion.

## NOTATION AND FORMULAS

*Depth of Burial ( $\zeta$ ).*—Let a salt dome  $M_s$  (Fig. 1) be embedded in a medium  $M_n$  at a depth  $\zeta$  below the interface marking the contact between the  $(n - 1)$ th and the  $n$ th media, counting  $M_1$  as the medium that forms the uppermost layer of the earth.

*Counters ( $k$ ).*—As a convenience in notation, let the counter  $k$  extend over the positive integers from one to  $(n - 1)$ . Where there will be no ambiguity, we shall use the simplified symbol  $\Sigma$  instead of the more

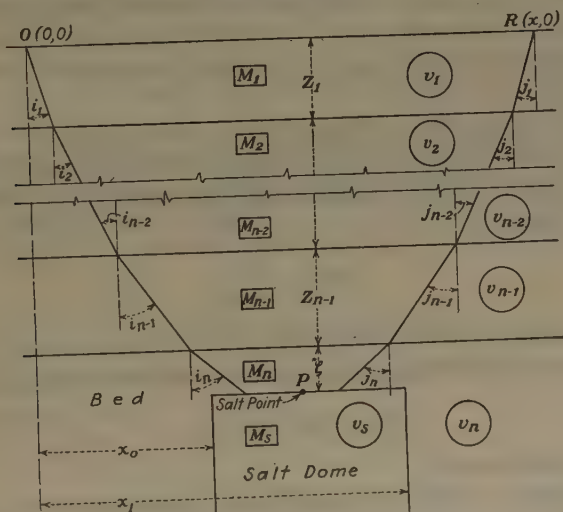


FIG. 1.—THE STRUCTURAL ARRANGEMENT.

usual complete form  $\sum_{k=1}^{n-1}$  to denote that the quantity affected by the symbol is to be formed for all values of the counter from unity to  $(n - 1)$  and the results added.

*Thicknesses ( $Z_k$ ).*—Let the thickness of the  $k$ th medium,  $M_k$ , be  $Z_k$  with the special agreement that  $Z_n$  shall equal  $\zeta$ , when such a convention shall be convenient.

*Speeds ( $v_k$ ;  $v_s$ ).*—Let the medium  $M_k$  transmit the seismic disturbance with a speed  $v_k$  and the salt  $M_s$ , transmit it with the speed  $v_s$ . In particular, let  $v_{k+1} > v_k$  and  $v_s > v_n$ .

*Shot Point (O).*—Let the source of the seismic disturbance be at the origin, which will be referred to as the shot point.

*Receiver (R; x).*—Let the receiver be placed on the surface of the earth at the point R, at a distance  $x$  to the right of the origin, the plane of transmission thus being the vertical plane through the shot point and the receiver.

*Extent* ( $x_0; x_1$ ).—Let the dome extend from  $x = x_0$  to  $x = x_1$ , where  $x_0 < x_1$ .

*Path*.—By the term “path,” we shall understand that path of travel from  $O$  to  $R$  for which the time of travel is an extremum with respect to all possible paths in the basic vertical plane. In particular, this extremum will be a minimum.

*Salt Path*.—The term “salt path” will indicate the path of travel from  $O$  to  $R$  for which the time of travel is a minimum with respect to all paths passing through or touching a point of the salt dome.

*Salt Point* ( $P; \xi$ ).—Let  $P$  be a point of the salt path, lying within, or on the surface of, the salt dome. Let its abscissa be  $\xi$ . It follows at once that  $P$  must be at the upper surface of the dome, in order to lie on the salt path.

*Normal Ray* ( $\theta_k$ ).—The “normal ray” is the path that is incident critically at the top of the bed  $M_n$ , when the salt is absent or ineffective. If the normal ray makes the angle  $\theta_k$  with the vertical in medium  $M_k$ , we have the relation:

$$\sin \theta_k = \frac{v_k}{v_n} \quad [1.1]$$

*Normal Point* ( $\xi_n$ ).—The “normal point” is the point of incidence of the normal ray with the top of the bed and has the abscissa:

$$\xi_n = \Sigma Z_k \tan \theta_k \quad [1.2]$$

which may be calculated.

*Normal Time* ( $\tau_n$ ).—The “normal time” is the time of travel from the shot point to the normal point along the normal ray, and has the value:

$$\tau_n = \sum \frac{Z_k \sec \theta_k}{v_k} \quad [1.3]$$

which may be calculated.

*Critical Ray* ( $\phi_k$ ).—The “critical ray” is the ray that is incident critically at the top of the salt. In particular, it may be absent in the group of possible rays. If the critical ray makes the angle  $\phi_k$  with the vertical in the medium  $M_k$ , we have the relation:

$$\sin \phi_k = \frac{v_k}{v_s} \quad [2.1]$$

*Critical Point* ( $\xi_c$ ).—The “critical point” is the point of incidence of the critical ray on the top of the salt and has the abscissa:

$$\xi_c = \Sigma Z_k \tan \phi_k + \zeta \tan \phi_n \quad [2.2]$$

which may be calculated. In particular,  $\zeta$  may vanish, but in all other cases it is positive.



*Critical Time ( $\tau_c$ ).*—The “critical time” is the time of travel from the shot to the critical point along the critical ray, and may be calculated from:

$$\tau_c = \sum \frac{Z_k \sec \phi_k}{v_k} + \frac{\zeta \sec \phi_n}{v_n} \quad [2.3]$$

*Direct Ray ( $i_k$ ).*—The “direct ray” from the shot to the salt point  $P$  satisfies the relations:

$$\sin i_k = \frac{v_k \sin i_n}{v_n} = \sin \theta_k \sin i_n \quad [3.1]$$

$$\xi = \sum Z_k \tan i_k + \zeta \tan i_n \quad [3.21]$$

where  $i_k$  is the angle made by the direct ray with the vertical in medium  $M_k$ .

*Corner Ray.*—The “corner ray” is the particular direct ray that has incidence on the top of the salt at the near corner of the dome. The salt path is cornered if  $\zeta = 0$  and  $\xi_c < x_0 < \xi_n$  or if  $\zeta > 0$  and  $\xi_c < x_0$ . The various vertical angles are determined by the relations:

$$\sin i_k = \sin \theta_k \sin i_n \quad [3.1]$$

$$x_0 = \sum Z_k \tan i_k + \zeta \tan i_n \quad [3.22]$$

In a specific case, these relations may be solved by successive approximation or by repeated trial.

*Corner Time.*—The “corner time” is given by:

$$\tau_r = \sum \frac{Z_k \sec i_k}{v_k} + \frac{\zeta \sec i_n}{v_n} \quad [3.3]$$

where the angles  $i_k$  have been determined from equations 3.1 and 3.22.

*Descent Paths and Times.*—There are several types of paths from the shot point to the salt dome, depending on the location of the left edge of the dome. If  $x_0 \leq \xi_c$  the dome extends to the left of the critical ray and the descent is critical. If  $\xi_c < x_0 < \xi_n$  the dome extends to the left of the normal ray, but does not extend as far to the left as the critical ray. In this case, the descent is cornered. If  $\zeta > 0$  the descent is always cornered when  $x_0 > \xi_c$ , so that we may interpret  $\xi_n$  as infinity. If  $x_n \leq x_0$  and  $\zeta = 0$ , the salt makes a complete break in the medium  $M_n$  and the descent path is normal. This case does not occur for positive values of  $\zeta$ . The time of descent from the origin to the salt point ( $\xi, \zeta$ ) for each type of descent is shown in Table 1, where  $\tau_r$  is the value obtained from equation 3.3 for the origin and the left corner of the dome and the other symbols have been explained.

*Ascent Paths and Times.*—Similarly, there are three types of ascent determined by the location of the right corner of the dome with respect to the receiver. The corresponding times and conditions are shown in

TABLE 1.—*Time of Descent*

Condition	Type	Time
$x_0 \leq \xi_0$	Critical	$T'_c = \tau_c + \frac{\xi - \xi_0}{v_s}$
$\xi_0 < x_0 < \xi_n$	Cornered	$T'_r = \tau_r' + \frac{\xi - x_0}{v_s}$
$\xi = 0$ and $\xi_n \leq x_0$	Normal	$T'_n = \tau_n + \frac{x_0 - \xi_n}{v_n} + \frac{\xi - x_0}{v_s}$

Table 2, where  $\tau_r''$  is determined by equation 3.3 for the receiver point and the right edge of the dome.

TABLE 2.—*Time of Ascent*

Condition	Type	Time
$x \leq x_1 + \xi_0$	Critical	$T''_c = \tau_c + \frac{x - \xi_0 - \xi}{v_s}$
$x_1 + \xi_0 < x < x_1 + \xi_n$	Cornered	$T''_r = \tau_r'' + \frac{x_1 - \xi}{v_s}$
$\xi = 0$ and $x_1 + \xi_n \leq x$	Normal	$T''_n = \tau_n + \frac{x - \xi_n - x_1}{v_n} + \frac{x_1 - \xi}{v_s}$

*Choice of Salt Point.*—The total time of travel is the sum of the descent time and the ascent time, using the same salt point for the two times. The specific salt point to be selected depends on the position of the dome. If  $x_0 \leq \xi_0$ , we may select  $\xi = \xi_0$  so that we have:

$$T'_c = \tau_c \quad [4.111]$$

$$T''_c = \tau_c + \frac{x - 2\xi_0}{v_s} \quad [4.112]$$

$$T''_r = \tau_r'' + \frac{x_1 - \xi_0}{v_s} \quad [4.12]$$

$$T''_n = \tau_n + \frac{x - \xi_n - x_1}{v_n} + \frac{x_1 - \xi_0}{v_s} \quad [4.13]$$

For  $x_0 > \xi_0$ , we may select  $\xi = x_0$ , so that we have:

$$T''_c = \tau_c + \frac{x - \xi_0 - x_0}{v_s} \quad [4.21]$$

$$T'_r = \tau_r' \quad [4.221]$$

$$T''_r = \tau_r'' + \frac{x_1 - x_0}{v_s} \quad [4.222]$$

$$T''_n = \tau_n + \frac{x - \xi_n - x_1}{v_n} + \frac{x_1 - x_0}{v_s} \quad [4.23]$$

*Reduced Time ( $t_c; t_n$ ).*—In the cases of the critical and normal rays, the fact that the rays are oblique to the vertical reduces the horizontal portion of the paths and the corresponding times. We shall find it convenient to introduce the term "reduced time" by the definitions:

$$t_c = \tau_c - \frac{\xi_c}{v_s} \quad [5.1]$$

$$t_n = \tau_n - \frac{\xi_n}{v_s} \quad [5.2]$$

*Increased Speed ( $v_r$ ).*—The presence of the salt of speed  $v_s$  in the horizontal portion of the bed path reduces the time of travel by an amount corresponding to an increased speed  $v_r$  defined by:

$$\frac{1}{v_r} = \frac{1}{v_n} - \frac{1}{v_s} \quad [5.3]$$

*Complete Path and Time.*—For the complete path, there are nine possible cases, as shown by the corresponding conditions and times in Table 3. The case of critical descent and critical ascent includes the case of an infinite layer. When  $\zeta$  is positive,  $\xi_n$  is infinite.

*Strata Lines.*—In the absence of an embedded salt dome, the path refracted critically at the top of medium  $M_u$  has the time:

$$T_u = \frac{x}{v_u} + 2 \sum_{k=1}^{u-1} \left\{ \frac{\sec \psi_{uk}}{v_k} - \frac{\tan \psi_{uk}}{v_u} \right\} Z_k \quad [6.1]$$

$$= \frac{x}{v_u} + 2 \sum_{k=1}^{u-1} \frac{Z_k \cos \psi_{uk}}{v_k} \quad [6.2]$$

$$= \frac{x}{v_u} + \frac{2}{v_u} \sum_{k=1}^{u-1} Z_k \cot \psi_{uk} \quad [6.3]$$

$$\text{where:} \quad \sin \psi_{uk} = \frac{v_k}{v_u} \quad [6.4]$$

*Corner-path Calculations.*—Theoretically, conditions of equations 3.1 and 3.22 determine the values of  $i_k$  uniquely. For two media only, these conditions become:

$$\sin i_1 = \sin \theta_1 \sin i_2 \quad [7.1]$$

$$x_0 = Z_1 \tan i_1 + \zeta \tan i_2 \quad [7.2]$$

$$\text{where:} \quad \sin \theta_1 = \frac{v_1}{v_2} \quad [7.3]$$

$$\text{Then} \quad x_0 = \frac{Z_1 \sin i_1}{\sqrt{1 - \sin^2 i_1}} + \frac{\zeta \sin i_2}{\sqrt{1 - \sin^2 i_2}} \quad [7.4]$$

TABLE 3.—Complete Time

<div>Ascent → Descent ↓</div>	Type	Critical	Cornered	Norma
Type	Condition→ ↓	$x \leq x_1 + \xi_c$	$x_1 + \xi_c < x < x_1 + \xi_n$	$\xi = 0$ and $x_1 + \xi_n < x$
Critical	$x_0 \leq \xi_c$	$T_{ec} = 2t_c + \frac{x}{v_n}$	$T_{cr} = t_c + \tau_r'' + \frac{x}{v_s}$	$T_{cn} = t_c + t_n - \frac{x_1}{v_r} + \frac{x}{v_n}$
Cornered	$\xi_c < x_0 < \xi_n$	$T_{rc} = \tau_r' + t_c + \frac{x - x_0}{v_s}$	$T_{rr} = \tau_r' + \tau_r'' + \frac{x_1 - x_0}{v_s}$	$T_{rn} = \tau_r' + t_n - \frac{x_1}{v_r} - \frac{x_0}{v_s} + \frac{x}{v_n}$
Normal	$\xi = 0$ and $\xi_n \leq x_0$	$T_{nc} = t_n + t_c + \frac{x_0}{v_r} + \frac{x}{v_s}$	$T_{nr} = t_n + \tau_r'' + \frac{x_0}{v_r} + \frac{x_1}{v_s}$	$T_{nn} = 2t_n - \frac{x_1 - x_0}{v_r} + \frac{x}{v_n}$



But,  $\sin i_2 = \frac{v_2 \sin i_1}{v_1}$  so that:

$$x_0 = \frac{Z_1 \sin i_1}{\sqrt{1 - \sin^2 i_1}} + \frac{\zeta v_2 \sin i_1}{\sqrt{v_1^2 - v_2^2 \sin^2 i_1}} \quad [7.5]$$

which may be solved for  $i_1$ .

For more than two media, the direct solution becomes too complicated and should be replaced by repeated trials or by successive approximations. In general, if Taylor's theorem is sufficiently reliable to retain only the first two terms, we have:

$$f(y) = f(y_0) + (y - y_0)f'(y_0) + \dots \quad [8.11]$$

$$\text{or} \quad \dot{y} = y_0 + \frac{f(y) - f(y_0)}{f'(y_0)} \quad [8.12]$$

Thus, if  $y_0$  is an approximate root of the equation  $f(y) = M$ , a better approximation is given by:

$$y = y_0 + \frac{M - f(y_0)}{f'(y_0)} \quad [8.13]$$

In the present case, if we write:

$$y = \sin i_1 \quad [8.21]$$

$$a_k = \frac{v_k}{v_1} \quad [8.22]$$

$$Z_n = \zeta \quad [8.23]$$

$$M = x_0 \quad [8.24]$$

the conditions become:

$$\sin i_k = a_k y \quad [8.31]$$

$$f(y) = \sum_{k=1}^n Z_k \tan i_k = \sum_{k=1}^n Z_k a_k \frac{y}{\sqrt{1 - a_k^2 y^2}} \quad [8.32]$$

$$f'(y) = \sum_{k=1}^n \frac{Z_k a_k}{(1 - a_k^2 y^2)^{3/2}} \quad [8.33]$$

For purposes of calculation, we may write:

$$R_k = \frac{Z_k a_k}{\sqrt{1 - a_k^2 y^2}} \quad [8.41]$$

so that:

$$f(y) = y \sum_{k=1}^n R_k \quad [8.421]$$

$$f'(y) = \sum_{k=1}^n \frac{R_k}{1 - a_k^2 y^2} \quad [8.422]$$

Often, a rapid preliminary calculation will determine  $y_0$  to a single decimal place, and occasionally a value estimated without calculation will be sufficiently accurate for the first approximation. After the value of  $i_1$  has been determined, to the desired degree of accuracy, the corner time is found, from equation 3.3, to be:

$$\tau_r = \sum_{k=1}^n \frac{Z_k}{v_k \sqrt{1 - a_k^2 y^2}} \quad [8.5]$$

*Corner Break* ( $\xi_c$ ;  $x_b$ ).—If the dome has  $\zeta = 0$  and  $x_0 > \xi_n$ , we may take a receiver position such that  $x < x_1 + \xi_c$  so that the ascent is critical. This is the case of a salt dome at the top of the bed, but not too near the shot point. For these conditions, the salt time is:

$$T_s = t_n + t_c + \frac{x_0}{v_r} + \frac{x}{v_s} \quad [9.11]$$

and the bed time is:

$$T_n = 2t_n + \frac{x}{v_n} \quad [9.12]$$

There is a value  $\xi_c$  such that if  $x = x_0 + \xi_c$  the two times  $T_s$  and  $T_n$  will be equal. If  $x$  exceeds  $x_0 + \xi_c$ , the salt time will be less than the bed time, while if  $x_0 + \xi_c$  exceeds  $x$ , the bed time will be the smaller. To determine the value of  $\xi_c$ , we have:

$$t_n + t_c + \frac{x_0}{v_r} + \frac{x_0 + \xi_c}{v_s} = 2t_n + \frac{x_0 + \xi_c}{v_n} \quad [9.21]$$

Hence

$$\xi_c = v_r(t_c - t_n) \quad [9.22]$$

The form given in equation 9.22 is convenient for determining the value of  $\xi_c$ , but another form shows its geometric significance more clearly. In terms of  $\phi_k$  and  $\theta_k$ , the increased speed is given, from equations 5.3, 1.1 and 2.1, by:

$$\frac{1}{v_r} = \frac{1}{v_n} - \frac{1}{v_s} = \frac{\sin \theta_k - \sin \phi_k}{v_k} \quad [9.31]$$

which has the same value for all values of  $k$ . The reduced critical time is given from equation 5.1 by:

$$\begin{aligned} t_c &= \tau_c - \frac{\xi_c}{v_s} = \sum \frac{Z_k \sec \phi_k}{v_k} - \frac{1}{v_s} \sum Z_k \tan \phi_k \\ &= \sum \frac{Z_k}{v_k} \left( \sec \phi_k - \frac{v_k}{v_s} \tan \phi_k \right) = \sum \frac{Z_k \cos \phi_k}{v_k} \end{aligned} \quad [9.32]$$

The reduced normal time is given, from equations 5.2 and 1, by:

$$\begin{aligned} t_n &= \tau_n - \frac{\xi_n}{v_n} = \sum \frac{Z_k \sec \theta_k}{v_k} - \sum \frac{Z_k \tan \theta_k}{v_n} \\ &= \sum \frac{Z_k}{v_k} \left( \sec \theta_k - \frac{v_k}{v_n} \tan \theta_k \right) = \sum \frac{Z_k \cos \theta_k}{v_k} \end{aligned} \quad [9.33]$$

Combining equations 9.22 and 9.3, we obtain:

$$\begin{aligned} \xi_e &= \frac{t_c - t_n}{\frac{1}{v_r}} = \sum \frac{\frac{Z_k \cos \phi_k}{v_k} - \frac{Z_k \cos \theta_k}{v_k}}{\frac{\sin \theta_k}{v_k} - \frac{\sin \phi_k}{v_k}} \\ &= \sum Z_k \frac{\cos \phi_k - \cos \theta_k}{\sin \theta_k - \sin \phi_k} = \sum Z_k \tan \frac{\phi_k + \theta_k}{2} \end{aligned} \quad [9.4]$$

This equation states that the dividing line between a salt lead and a salt lag is the line that has vertical angles midway between the corresponding critical and normal angles. This line is not refracted according to the Snell Law and hence does not represent a possible path.

The importance of this relation lies in its ability to locate the near edge of a salt dome that may be considered flat and near the top of the bed. The intersection of the salt profile with the bed profile is available from the time-distance curve. If we call its abscissa  $x_b$ , the edge of the dome is at  $x_b - \xi_e$ , where the value of  $\xi_e$  is known. If the salt break lies ahead of the bed break, the lines must be produced to meet.

Similarly, if the farther edge of the dome is beyond the point  $x = \xi_e$ , we have:

$$T_{cn} - T_{ce} = T_{rn} - T_{re} = T_{nn} - T_{ne} = t_n - t_e + \frac{x - x_1}{v_r} \quad [10]$$

which vanishes for  $x = x_1 + \xi_e$ . Hence, the intersection of the two straight lines that bracket the corner curve determines the farther edge of the dome in the same manner that the salt and bed lines determine the near edge. For  $\zeta = 0$ , there will be a salt lead if  $x_1 > \xi_e$  or  $x_0 < x - \xi_e$ .

*Profiles ( $x_m$ ).—*For  $\zeta = 0$ , the salt-profile curve consists of three portions:

1. From a point  $x = x_m$  to a point  $x = x_1 + \xi_e$ , the profile is a straight line with slope  $\frac{1}{v_e}$ .
2. From  $x = x_1 + \xi_e$  to  $x = x_1 + \xi_n$ , the profile is a transition or corner curve.
3. Beyond  $x = x_1 + \xi_n$ , the profile is a straight line with slope  $\frac{1}{v_n}$ .

For  $\zeta > 0$ , the salt profile consists of two sections:

1. The first section is the same as in the preceding case.
2. Beyond  $x = x_1 + \xi_c$ , the profile is a corner curve which rapidly approaches a line of slope  $\frac{1}{v_n}$ .

If  $x_0 \leq \xi_c$ , the first salt point has  $x_m = 2\xi_c$ , while for  $x_0 > \xi_c$ , the first salt point of the profile has  $x_m = x_0 + \xi_c$ .

*Effect on Time of Horizontal Position of Dome.*—For a dome of given horizontal extent and depth, the time of travel for a fixed receiver distance will be a minimum when as much as possible of the dome is included between the critical rays. The portions not included between the critical rays cannot affect the time of travel of the waves. Hence, if the left edge is to the left of the critical descent ray, the time can be reduced by moving the shot points to the left unless this causes the right edge to be to the right of the critical ascent ray. The corresponding analysis applies to the right edge. Thus, if the dome is sufficiently large horizontally, the time of travel will be a minimum when the dome extends over the entire distance between the critical rays. We may, therefore, restrict the analysis to small domes, such a dome being too small to span the entire distance between the critical rays. We may also assume that such a dome is entirely within the critical rays; i. e.,  $x_0 \geq \xi_c$  and  $x_1 \leq x - \xi_c$ . For  $\zeta = 0$ , the exact location of the dome within these limits is of no importance, the time of travel being the same for all such positions. For  $\zeta > 0$ , both the descent and ascent rays are cornered and we now proceed to show that the time is a minimum when the path is symmetrical, which is the case when the center of the dome is midway between the shot and the receiver.

For  $\zeta > 0$ , the salt time has been given by Table 3 as:

$$T_s = \frac{x_1 - x_0}{v_s} + \tau_r' + \tau_r'' \quad [10.1]$$

where:

$$x_0 = \sum Z_k \tan i_k + \zeta \tan i_n \quad [10.21]$$

$$x_1 = x - \sum Z_k \tan j_k - \zeta \tan j_n \quad [10.22]$$

$$\tau_r' = \sum \frac{Z_k \sec i_k}{v_k} + \frac{\zeta \sec i_n}{v_n} \quad [10.31]$$

$$\tau_r'' = \sum \frac{Z_k \sec j_k}{v_k} + \frac{\zeta \sec j_n}{v_n} \quad [10.32]$$

$$\sin i_k = \frac{v_k \sin i_n}{v_n} \quad [10.41]$$

$$\sin j_k = \frac{v_k \sin j_n}{v_n} \quad [10.42]$$

If the dome has a fixed extent  $l = x_1 - x_0$ , we may use, for the independent variable, the abscissa  $X$  of its center. Then equations 10.2 lead to:



$$x_0 = X - \frac{l}{2} = \Sigma Z_k \tan i_k + \zeta \tan i_n \quad [10.51]$$

$$x_1 = X + \frac{l}{2} = x - \Sigma Z_k \tan j_k - \zeta \tan j_n \quad [10.52]$$

and the salt time is, by equation 10.1:

$$T_s = \frac{l}{v_s} + \tau_r' + \tau_r'' \quad [10.6]$$

Differentiating equations 10.3, we obtain:

$$\frac{d\tau_r'}{dX} = \sum \frac{Z_k}{v_k} \sec i_k \tan i_k \frac{di_k}{dX} + \frac{\zeta}{v_n} \sec i_n \tan i_n \frac{di_n}{dX} \quad [11.11]$$

$$\frac{d\tau_r''}{dX} = \sum \frac{Z_k}{v_k} \sec j_k \tan j_k \frac{dj_k}{dX} + \frac{\zeta}{v_n} \sec j_n \tan j_n \frac{dj_n}{dX} \quad [11.12]$$

From equations 10.4, it follows that:

$$\frac{di_k}{dX} = \frac{v_k}{v_n} \sec i_k \cos i_n \frac{di_n}{dX} \quad [11.21]$$

$$\frac{dj_k}{dX} = \frac{v_k}{v_n} \sec j_k \cos j_n \frac{dj_n}{dX} \quad [11.22]$$

Inserting equations 11.2 in equations 11.1, the latter become:

$$\frac{d\tau_r'}{dX} = \sum \frac{Z_k}{v_n} \sec^2 i_k \tan i_k \cos i_n \frac{di_n}{dX} + \frac{\zeta}{v_n} \sec i_n \tan i_n \frac{di_n}{dX} \quad [11.31]$$

$$\frac{d\tau_r''}{dX} = \sum \frac{Z_k}{v_n} \sec^2 j_k \tan j_k \cos j_n \frac{dj_n}{dX} + \frac{\zeta}{v_n} \sec j_n \tan j_n \frac{dj_n}{dX} \quad [11.32]$$

Furthermore, by equations 10.4, we have:

$$\tan i_k = \sin i_k \sec i_k = \frac{\sin i_k}{v_k} v_k \sec i_k = \frac{\sin i_n}{v_n} v_k \sec i_k \quad [11.41]$$

$$\tan j_k = v_k \sec j_k \frac{\sin j_n}{v_n} \quad [11.42]$$

so that equations 11.3 may be written:

$$\frac{d\tau_r'}{dX} = \frac{\sin i_n \cos i_n}{v_n^2} \frac{di_n}{dX} (\Sigma Z_k v_k \sec^3 i_k + \zeta v_n \sec^3 i_n) \quad [11.51]$$

$$\frac{d\tau_r''}{dX} = \frac{\sin j_n \cos j_n}{v_n^2} \frac{dj_n}{dX} (\Sigma Z_k v_k \sec^3 j_k + \zeta v_n \sec^3 j_n) \quad [11.52]$$

By equations 10.5 we have:

$$1 = \Sigma Z_k \sec^2 i_k \frac{di_k}{dX} + \zeta \sec^2 i_n \frac{di_n}{dX} \quad [11.61]$$

$$1 = -\Sigma Z_k \sec^2 j_k \frac{dj_k}{dX} - \zeta \sec^2 j_n \frac{dj_n}{dX} \quad [11.62]$$

which become, by equations 11.2:

$$1 = \frac{\cos i_n}{v_n} \frac{di_n}{dX} (\Sigma Z_k v_k \sec^3 i_k + \zeta v_n \sec^3 i_n) \quad [11.71]$$

$$1 = -\frac{\cos j_n}{v_n} \frac{dj_n}{dX} (\Sigma Z_k v_k \sec^3 j_k + \zeta v_n \sec^3 j_n) \quad [11.72]$$

Dividing equations 11.5 by equations 11.7, we obtain:

$$\frac{d\tau_r'}{dX} = \frac{\sin i_n}{v_n} \quad [11.81]$$

$$\frac{d\tau_r''}{dX} = -\frac{\sin j_n}{v_n} \quad [11.82]$$

Differentiating equations (10.6) and inserting equations (11.8) we obtain:

$$\frac{dT_s}{dX} = \frac{\sin i_n - \sin j_n}{v_n} \quad [11.9]$$

whence, for an extreme value of  $T_s$ , for all possible values of  $X$ , we have:

$$i_n = j_n \quad [12.1]$$

and, by equations 10.4:

$$i_k = j_k \quad (k = 1, 2, 3, \dots, n) \quad [12.2]$$

Inspection of equation 11.9 shows that  $T_s$  is a minimum, not a maximum, since increasing  $X$  causes an increase in  $i_n$  and a decrease in  $j_n$ , whence  $\frac{dT_s}{dX}$  changes from negative to positive at  $i_n = j_n$ .

For  $i_k = j_k$ , the sum of equations 10.5 leads directly to:

$$X = \frac{x}{2} \quad [12.3]$$

which is the result we sought to prove.

*Symmetric Salt-dome Leads* ( $A$ ;  $B$ ;  $L$ ).—For a small salt dome symmetrically located, the salt time at a distance  $x$  is, for  $\zeta > 0$ :

$$T_s = \frac{x_1 - x_0}{v_n} + 2\tau_r \quad [13.11]$$

$$\text{where:} \quad \tau_r = \sum \frac{Z_k \sec i_k}{v_k} + \frac{\zeta \sec i_n}{v_n} \quad [13.12]$$

$$\sin i_k = \frac{v_k \sin i_n}{v_n} \quad [13.13]$$

$$x_0 = x - x_1 = \Sigma Z_k \tan i_k + \zeta \tan i_n \quad [13.14]$$

For a selected angle of departure  $i_1$ , the angles  $i_k$  and  $i_n$  are fixed by equation 13.13. The abscissa of the point at which this path cuts the top of the bed is:

$$\xi_i = \Sigma Z_k \tan i_k \quad [13.21]$$

and the time to bed is:

$$\tau_i = \sum \frac{Z_k \sec i_k}{v_k} \quad [13.22]$$

Then:

$$x_0 = x - x_1 = \xi_i + \zeta \tan i_n \quad [13.31]$$

$$\tau_r = \tau_i + \frac{\zeta \sec i_n}{v_n} \quad [13.32]$$

The salt time is:

$$T_s = \left[ \frac{x}{v_s} + 2 \left( \tau_i - \frac{\xi_i}{v_s} \right) \right] + 2\zeta \left[ \frac{\sec i_n}{v_n} - \frac{\tan i_n}{v_s} \right] \quad [13.41]$$

If  $T_x$  is the bed time for a receiver distance  $x$ , the salt lead is:

$$L = T_x - T_s = A - B\zeta \quad [13.42]$$

where:

$$A = \left( T_x - \frac{x}{v_s} \right) - 2 \left( \tau_i - \frac{\xi_i}{v_s} \right) \quad [13.43]$$

$$B = 2 \left( \frac{\sec i_n}{v_n} - \frac{\tan i_n}{v_s} \right) \quad [13.44]$$

Since:

$$B = \frac{2 \sec i_n}{v_n} \left( 1 - \frac{v_n}{v_s} \sin i_n \right) > 0 \quad [13.51]$$

the lead for a specific angle of departure is a linearly decreasing function of the depth of burial  $\zeta$ . The extent of the dome also decreases linearly in  $\zeta$ , since equation 13.31 leads to:

$$l = x_1 - x_0 = (x - 2\xi_i) + \zeta \tan i_n \quad [13.52]$$

Since, for small values of  $\zeta$ , the lead must be positive, it is apparent that  $A$  is positive.

In terms of the lead  $L$ , we have, for  $\zeta > 0$ :

$$x_0 = \xi_i + \zeta \tan i_n \quad [13.61]$$

$$\zeta = \frac{A - L}{B} \quad [13.62]$$

as the coordinates of the left edge of the dome. For  $\zeta = 0$ , two cases arise, according as  $x_0 < \xi_n$  or  $x_0 \geq \xi_n$ . In the former case, equation 13.62 shows that  $L = A$ , which determines the ray in terms of  $L$ , after which  $x_0 = \xi_i$ . If  $x_0 \geq \xi_n$ , the salt path is not cornered, but normal, and the lead is

$$L_n = \frac{x_1 - x_0}{v_r} \quad [13.63]$$

Reversely, if the lead exceeds the value  $\frac{x - 2\xi_n}{v_r}$ , the abscissa of the left edge is given by equation 13.61, while if the lead is less than this quantity,

the dome is not determined, except as to extent. Equation 13.42 also shows that there can be no salt lead if the depth of burial  $\zeta$  equals or exceeds the value:

$$\zeta_m = \frac{A}{B} \quad [13.7]$$

### A NUMERICAL ILLUSTRATION

As an illustrative example of the analysis, consider the special case shown in Fig. 2.

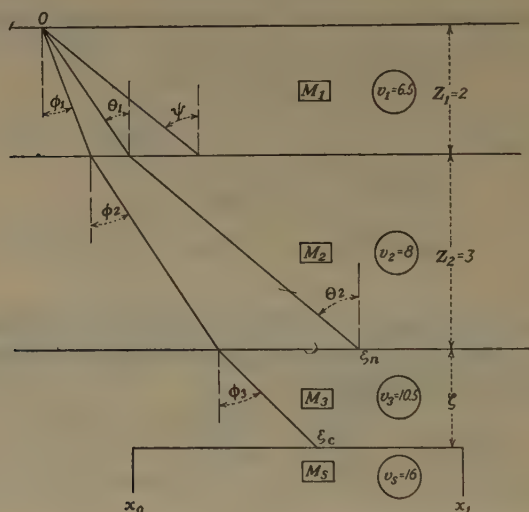


FIG. 2.—SECTION OF ILLUSTRATIVE EXAMPLE.

*Thicknesses and Speeds.*—Let the top layer have a thickness  $Z_1 = 2$  and a speed  $v_1 = 6.5$ . Let the second layer have a thickness  $Z_2 = 3$  and a speed  $v_2 = 8$ . Let the third layer, with a speed  $v_3 = 10.5$ , be the bed, extending indefinitely down, or at least far enough so that the next lower layer has no effect within the distance used for the observations. Let the salt have a speed  $v_s = 16$ .

*Units.*—While the units are arbitrary, we may, for convenience, take the unit of length as one kilofoot (1000 ft.) and the unit of time as one second.

*Angles.*—The critical angle between the top and second layers is  $\psi$  where:

$$\sin \psi = \frac{v_1}{v_2} = \frac{6.5}{8} \quad [14.11]$$

Hence: 
$$\psi = 54^\circ 20' \quad [14.12]$$



The normal angles are  $\theta_1$  and  $\theta_2$  where:

$$\sin \theta_1 = \frac{v_1}{v_3} = \frac{6.5}{10.5} \quad [14.211]$$

$$\sin \theta_2 = \frac{v_2}{v_3} = \frac{8}{10.5} \quad [14.212]$$

Hence:  $\theta_1 = 38^\circ 15'$  [14.221]

$$\theta_2 = 49^\circ 38' \quad [14.222]$$

The critical angles are  $\phi_1$ ,  $\phi_2$  and  $\phi_3$ , where:

$$\sin \phi_1 = \frac{v_1}{v_s} = \frac{6.5}{16} \quad [14.311]$$

$$\sin \phi_2 = \frac{v_2}{v_s} = \frac{8}{16} \quad [14.312]$$

$$\sin \phi_3 = \frac{v_3}{v_s} = \frac{10.5}{16} \quad [14.313]$$

Hence:  $\phi_1 = 23^\circ 58'$  [14.321]

$$\phi_2 = 30^\circ \quad [14.322]$$

$$\phi_3 = 41^\circ 1' \quad [14.323]$$

*Rays.*—The normal ray has incidence critically at the top of the bed at the normal point whose abscissa is:

$$\xi_n = Z_1 \tan \theta_1 + Z_2 \tan \theta_2 = 5.106 \quad [14.411]$$

The normal time to the bed is:

$$\tau_n = \frac{Z_1 \sec \theta_1}{v_1} + \frac{Z_2 \sec \theta_2}{v_2} = 0.971 \quad [14.412]$$

The reduced normal time is:

$$t_n = \tau_n - \frac{\xi_n}{v_3} = 0.485 \quad [14.413]$$

The critical ray is incident at the top of the salt at the critical point whose abscissa is:

$$\xi_c = Z_1 \tan \phi_1 + Z_2 \tan \phi_2 + \zeta \tan \phi_3 = 2.621 + 0.870\zeta \quad [14.421]$$

The critical time to the salt is:

$$\tau_c = \frac{Z_1 \sec \phi_1}{v_1} + \frac{Z_2 \sec \phi_2}{v_2} + \frac{\zeta \sec \phi_3}{v_3} = 0.770 + 0.126\zeta \quad [14.422]$$

The reduced critical time is:

$$t_c = \tau_c - \frac{\xi_c}{v_s} = 0.606 + 0.072\zeta \quad [14.423]$$

*Speeds.*—The increased speed is:

$$v_r = \frac{1}{\frac{1}{v_3} - \frac{1}{v_s}} = \frac{336}{11} = 30.545 \quad [14.51]$$

The reciprocals of the various speeds are:

$$\begin{aligned} \frac{1}{v_1} &= 0.154, & \frac{1}{v_2} &= 0.125, & \frac{1}{v_3} &= 0.095, \\ \frac{1}{v_r} &= 0.033, & \frac{1}{v_s} &= 0.063 \end{aligned} \quad [14.52]$$

*Strata Lines.*—For receiving points near the source, only the upper layer is effective. For this section, the time-distance profile has the equation:

$$T_1 = \frac{x}{v_1} = 0.154x \quad [14.61]$$

As the receiving point recedes from the shot, a point is reached for which the direct wave arrives at the same time as that along the path refracted critically at the top of the second layer. Beyond this point, the second-layer wave arrives before the direct ray. This section of the profile has the equation:

$$T_2 = \frac{2Z_1 \sec \psi}{v_1} + \frac{x - 2Z_1 \tan \psi}{v_2} = 0.359 + 0.125x \quad [14.62]$$

As the receiving point moves still farther away, the path refracted critically at the top of the bed has the fastest travel time. This section of the profile has the equation:

$$\begin{aligned} T_3 &= \frac{2Z_1 \sec \theta_1}{v_1} + \frac{2Z_2 \sec \theta_2}{v_2} + \frac{x - 2(Z_1 \tan \theta_1 + Z_2 \tan \theta_2)}{v_3} \\ &= 2t_n + \frac{x}{v_3} = 0.969 + 0.095x \end{aligned} \quad [14.63]$$

If the salt is absent, or very deep, the preceding section of the profile extends indefinitely. If the salt acts as an infinite layer, that is, if both  $x_0$  and  $x - x_1$  are less than:

$$\xi_0 = 2.621 + 0.870\xi \quad [14.421]$$

the profile has an additional section, whose equation is:

$$\begin{aligned} T_s &= \frac{2Z_1 \sec \phi_1}{v_1} + \frac{2Z_2 \sec \phi_2}{v_2} + \frac{2\xi \sec \phi_3}{v_3} + \\ &\quad \frac{x - 2(Z_1 \tan \phi_1 + Z_2 \tan \phi_2 + \xi \tan \phi_3)}{v_s} \\ &= 2t_o + \frac{x}{v_s} = 1.212 + 0.144\xi + 0.063x \end{aligned} \quad [14.64]$$

*Profile Breaks.*—The transition break from the first to the second section of the time-distance profile occurs at  $P_{12}$ , of which the coordinates are:

$$x_{12} = 12.437 \quad \text{and} \quad T_{12} = 1.913$$

The transition break from the second to the third section occurs at  $P_{23}$ , of which the coordinates are:

$$x_{23} = 20.506 \quad \text{and} \quad T_{23} = 2.922$$

If the salt appears on the intermediate line, the salt break is at  $P_{2s}$ , of which the coordinates are:

$$x_{2s} = 13.649 + 2.300\zeta \quad [14.711]$$

$$T_{2s} = 2.065 + 0.287\zeta \quad [14.712]$$

If the salt appears on the bed line, the salt break is at  $P_{3s}$ , of which the coordinates are:

$$x_{3s} = 7.416 + 4.390\zeta \quad [14.721]$$

$$T_{3s} = 1.675 + 0.418\zeta \quad [14.722]$$

*Corner Correction.*—The correction for passing from the profile breaks to the edges of the dome having  $\zeta = 0$  is:

$$\xi_o = v_r(t_c - t_n) = 3.708 \quad [14.8]$$

*Corner-path Calculations.*—To illustrate the method of calculating in the case of the direct ray to a corner, let us take  $\zeta = 5$  and two values of  $x_0$ , say  $x_0 = 8$  and  $x_0 = 19$ . To form an initial estimate as a basis for the successive approximations, we may note that the sine of the critical

TABLE 4.—*Corner-path Calculations*

$x_0$	8			19			
$y$	0.4200	0.4423	0.4411	0.6000	0.5902	0.5856	0.5850
$a_1y$	0.4200	0.4423	0.4411	0.6000	0.5902	0.5856	0.5850
$1 - a_1^2y^2$	0.8236	0.8044	0.8054	0.6400	0.6517	0.6571	0.6578
$\sqrt{1 - a_1^2y^2}$	0.9075	0.8969	0.8975	0.8000	0.8073	0.8106	0.8110
$R_1$	2.2039	2.2299	2.2285	2.5000	2.4774	2.4673	2.4661
$R_1/(1 - a_1^2y^2)$	2.6759	2.7721	2.7669	3.9062	3.8014	3.7548	3.7490
$a_2y$	0.5169	0.5444	0.5429	0.7385	0.7264	0.7208	0.7200
$1 - a_2^2y^2$	0.7328	0.7036	0.7053	0.4546	0.4723	0.4804	0.4816
$\sqrt{1 - a_2^2y^2}$	0.8560	0.8388	0.8398	0.6743	0.6873	0.6931	0.6940
$R_2$	4.3134	4.4019	4.3966	5.4758	5.3722	5.3272	5.3203
$R_2/(1 - a_2^2y^2)$	5.8862	6.2563	6.2337	12.045	11.375	11.089	11.047
$a_3y$	0.6785	0.7145	0.7126	0.9692	0.9534	0.9460	0.9450
$1 - a_3^2y^2$	0.5396	0.4895	0.4922	0.0607	0.0910	0.1051	0.1070
$\sqrt{1 - a_3^2y^2}$	0.7346	0.6996	0.7016	0.2463	0.3017	0.3242	0.3271
$R_3$	10.995	11.545	11.512	32.793	26.771	24.913	24.692
$R_3/(1 - a_3^2y^2)$	20.376	23.585	23.389	540.25	294.19	237.04	230.77
$f(y)$	7.3552	8.0396	8.0003	24.461	20.433	19.154	19.000
$f'(y)$	28.938	32.614	32.290	556.20	309.37	251.89	245.57
$y_1 - y$	+0.0223	-0.0012	0.0000	-0.0098	-0.0046	-0.0006	0.0000
$y_1$	0.4423	0.4411	0.4411	0.5902	0.5856	0.5850	0.5850
$Z_1/(v_1\sqrt{1 - a_1^2y^2})$			0.3428				0.3794
$Z_2/(v_2\sqrt{1 - a_2^2y^2})$			0.4465				0.5403
$Z_3/(v_3\sqrt{1 - a_3^2y^2})$			0.6787				1.4558
$\tau_r$			1.4680				2.3755

angle of departure is 0.4062 while the sine of the normal angle of departure is 0.6190; hence we must restrict the angle of departure for all direct rays between these two limits. The point of critical incidence has an abscissa  $\xi_c = 6.971$ , so that for  $x_0 = 8$  we may start with  $y = 0.42$ , which is slightly larger than the critical value. For  $x_0 = 19$ , we may start with  $y = 0.6$ , which is slightly less than the normal value. For both cases, we have:

$$\begin{array}{lll}
 Z_1 = 2 & Z_2 = 3 & Z_3 = 5 \\
 v_1 = 6.5 & v_2 = 8 & v_3 = 10.5 \\
 a_1 = 1 & a_2 = \frac{8}{6.5} = 1.2308 & a_3 = \frac{10.5}{6.5} = 1.6154 \\
 Z_1 a_1 = 2 & Z_2 a_2 = 3.6923 & Z_3 a_3 = 8.0769 \\
 \frac{Z_1}{v_1} = 0.3077 & \frac{Z_2}{v_2} = 0.375 & \frac{Z_3}{v_3} = 0.4762
 \end{array}$$

The calculations are shown in Table 4. The calculations are checked by the use of angles and their functions in Table 5. The calculations have

TABLE 5.—*Corner Angles and Times*

$\sin i_1$	0.4411	0.5850
$\sin i_2$	0.5429	0.7200
$\sin i_3$	0.7126	0.9450
$i_1$	26°10'	35°48'
$i_2$	32°53'	46°3'
$i_3$	45°27'	70°55'
$\tan i_1$	0.4913	0.7212
$\tan i_2$	0.6465	1.0373
$\tan i_3$	1.0158	2.8905
$\sec i_1$	1.1142	1.2329
$\sec i_2$	1.1908	1.4409
$\sec i_3$	1.4255	3.0586
$Z_1 \tan i_1$	0.9826	1.4424
$Z_2 \tan i_2$	1.9395	3.1119
$Z_3 \tan i_3$	5.0740	14.4525
$X_0$	7.9961	19.0068
$\frac{Z_1 \sec i_1}{v_1}$	0.3428	0.3794
$\frac{Z_2 \sec i_2}{v_2}$	0.4465	0.5403
$\frac{Z_3 \sec i_3}{v_3}$	0.6788	1.4565
$\tau_r$	1.4681	2.3762



been made to four places, but it is obvious that there is no theoretical limit to the degree of accuracy with which the calculations may be made.

*First Salt-profile Point.*—If  $x_0 \leq \xi_c$ , the first point of the salt profile will be at  $x = 2\xi_c$ ,  $T = 2\tau_c$ . Usually, this point is not obtainable directly. If  $x_0 > \xi_c$ , the first salt point of the profile is at  $x = x_0 + \xi_c$ .

*Appearance of Salt Profile.*—For small values of  $\zeta$ , the salt line appears on the intermediate line, the break being at  $P_{2s}$ . For large values of  $\zeta$ , the salt line appears on the bed line at  $P_{3s}$ . If  $P_{2s} = P_{3s}$ , we have  $\zeta_0 = 2.982$ . If  $\zeta \leq \zeta_0$ , the salt break is at  $P_{2s}$ , while if  $\zeta \geq \zeta_0$ , the salt break is at  $P_{3s}$ . The salt break is shown in Table 6 for certain values of  $\zeta$ .

TABLE 6.—*Salt-profile Data*

Depth $\zeta$	Effective Limits		First Salt Point $x_m$	Least Salt Time	Maximum Lead $L$
	$\xi_c$	$40 - \xi_c$			
0	2.621	37.379	13.649	3.712	1.067
1	3.491	36.509	15.949	3.856	0.923
2	4.361	35.639	18.248	3.999	0.779
3	5.230	34.770	20.585	4.143	0.636
4	6.100	33.900	24.975	4.287	0.492
5	6.970	33.030	29.365	4.430	0.348
6	7.840	32.160	33.755	4.574	0.205
7	8.709	31.291	38.145	4.718	0.061
8	9.579	30.421	42.535	4.862	none.

*Maximum Detectable Salt Depth.*—If, for the selected value of  $x$ ,  $T_s$  exceeds  $T_3$ , there can be no salt lead, for any depth. If we select  $x = 40$ , we have:

$$T_3 = 4.779 \quad \text{and} \quad T_s = 3.712 + 0.144\zeta \quad [15.11]$$

if the rays extend beyond both critical rays. Hence there can be no salt detection if  $\zeta$  exceeds 7.423, independently of the extent of the salt. (See Table 6.)

*Effective Extent of Salt and Maximum Lead.*—The portion of the dome to the left of  $x = \xi_c$  and the portion to the right of  $x - \xi_c$  do not affect the salt path at all. In Table 6 are shown the effective portions of the salt dome and the maximum possible leads for certain values of the depth  $\zeta$  when  $x = 40$ . These maximum leads occur when the salt extends over the entire interval between the critical rays. The table also shows the times for these same cases. When the entire effective extent is covered, the lead is:

$$L = 1.067 - 0.144\zeta \quad [15.12]$$

Furthermore, if  $x_1 < \xi_c = 3.708$ , there can be no salt lead for any depth.

Fig. 3 shows the various possible profiles when the entire effective extent is covered by the salt. This is equivalent to having a fourth layer of infinite extent. The three dashed lines show the times for the top, intermediate, and bottom media, respectively. The various full lines show the salt times for the depths indicated. The actual observable profile in a specific case is the group of lines representing the least time for each abscissa. In the absence of salt, this will be the top layer line from the origin to  $P_{12}$ , the intermediate layer line from  $P_{12}$  to  $P_{23}$ , and the bed line beyond  $P_{23}$ . The salt lead is obtained by noting the amount that the proper line lies below the normal profile for the selected value of  $x$ .

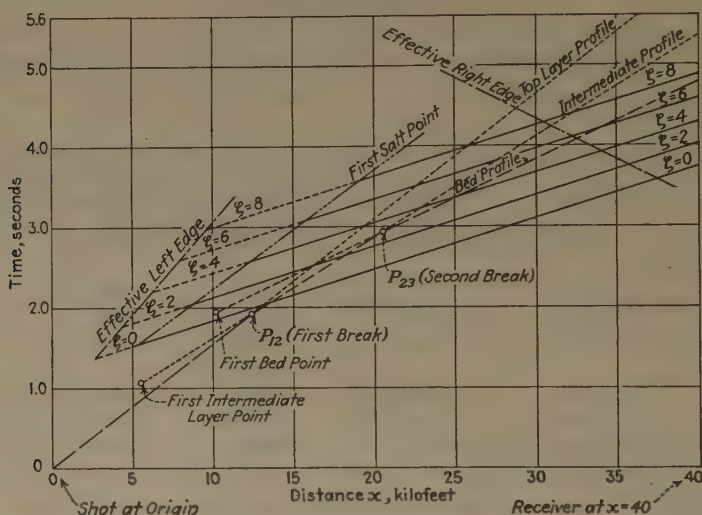


FIG. 3.—TIME-DISTANCE PROFILE LINES AND POINTS.

*False Depth.*—If the dome extends beyond the effective limits, and in some other cases, it is possible to make a false determination of the depth. For  $\zeta = 0$ , the salt line is:

$$T_s = 1.212 + 0.062x \quad [15.21]$$

which intersects the intermediate line at  $x_{2s} = 13.649$ , between  $x_{12}$  and  $x_{23}$ . While the intermediate line is not obliterated, it is obscured and may be missed in drawing the profile for actual observations. If so, the profile consists of the two lines:

$$T_1 = 0.154x \quad [15.22]$$

$$T_s = 1.212 + 0.144\zeta + 0.062x \quad [15.23]$$

The apparent depth is:

$$Z = 4.310 + 0.511\zeta \quad [15.24]$$

instead of  $5 + \zeta$ , so that the error is:

$$E = 0.690 + 0.489\zeta \quad [15.25]$$

For  $\zeta = 0$ , this error is 0.690, or 13.8 per cent, while for  $\zeta = 1$  the error is 1.179, or 19.6 per cent.

If the depth is such that the salt line obscures the bed line, but not the intermediate line, the profile consists of the three lines:

$$T_1 = 0.154x \quad [15.31]$$

$$T_2 = 0.359 + 0.125x \quad [15.32]$$

$$T_3 = 1.212 + 0.144\zeta + 0.062x \quad [15.33]$$

The apparent thicknesses are:

$$Z_1 = 2.000 \quad [15.41]$$

$$Z_2 = 3.000 + 0.664\zeta \quad [15.42]$$

The calculated depth is  $5.000 + 0.664\zeta$  so that the error is  $0.336\zeta$ . For  $\zeta = 0$ , the error is nil; for  $\zeta = 4$ , it is 1.345, or 15 per cent.

*Bounded Domes.*—If the dome does not extend beyond either effective limit, the salt line is not straight, but consists of two sections when  $\zeta$  is actually positive and three sections when  $\zeta$  is zero. The nine possible cases have times as follows:

$$T_{cc} = 1.212 + 0.144\zeta + 0.062x \quad [15.611]$$

$$T_{cr} = 0.606 + 0.072\zeta + 0.062x_1 + \tau_r'' \quad [15.612]$$

$$T_{cn} = 1.090 - 0.033x_1 + 0.095x \quad [15.613]$$

$$T_{rc} = 0.606 + 0.072\zeta - 0.062x_0 + 0.062x + \tau_r' \quad [15.621]$$

$$T_{rr} = 0.062x_1 - 0.062x_0 + \tau_r' + \tau_r'' \quad [15.622]$$

$$T_{rn} = 0.485 - 0.033x_1 - 0.062x_0 + 0.095x + \tau_r' \quad [15.623]$$

$$T_{nc} = 1.090 + 0.033x_0 + 0.062x \quad [15.631]$$

$$T_{nr} = 0.485 + 0.033x_0 + 0.062x_1 + \tau_r'' \quad [15.632]$$

$$T_{nn} = 0.969 + 0.033x_0 - 0.033x_1 + 0.095x \quad [15.633]$$

If  $x_0 \leq \xi_c < \xi_n \leq x_1$ , the salt line will be  $T_{cc}$  from  $x = 2\xi_c$  to  $x = x_1 + \xi_c$ . This is a straight line as for the infinite layer. For  $\zeta = 0$ , the curve will have two additional parts, but for  $\zeta > 0$ , the final part is missing. In both cases, there is a corner curve  $T_{cr}$  from  $x = x_1 + \xi_c$  to  $x = x_1 + \xi_n$ . From  $x = x_1 + \xi_n$  (when  $\zeta = 0$ ) to the right, the line  $T_{cn}$  is straight and is parallel to the bed line, with a lead:

$$L = 0.033x_1 - 0.121 \quad [15.7]$$

which is positive for all values of  $x_1 > \xi_c$ . The shape of the corner curve depends only on  $\zeta$  and  $(x - x_1)$ , not on  $x$ .

If  $\xi_c \leq x_0 \leq \xi_n$ , the three parts are:  $T_{rc}$  from  $x = x_0 + \xi_c$  to  $x = x_1 + \xi_c$ ,  $T_{rr}$  from  $x = x_1 + \xi_c$  to  $x = x_1 + \xi_n$ , and  $T_{rn}$  from  $x = x_1 + \xi_n$  to the right, the final section being absent for  $\zeta > 0$ .

If  $\xi_n \leq x_0$ , the three parts are  $T_{nc}$ ,  $T_{nr}$  and  $T_{nn}$ , the limits being at  $x = x_0 + \xi_c$ ,  $x_1 + \xi_c$ ,  $x_1 + \xi_n$  and infinity. The third section is missing for positive values of  $\zeta$ .

*Symmetric Domes.*—For a small dome, symmetrically placed, the salt lead over the normal bed time is given by equations 13.4. Each pair of values  $(L, i_1)$  determines a point whose coordinates are given by equations 13.6. For a selected value of  $L$ , these points lie on the locus of the left edge of all domes having that lead. The right edge is located symmetrically. For the particular case  $\zeta = 0$ , we determine  $x_0$  by:

$$x_0 = \frac{x - v_r L}{2} = 20 - \frac{168L}{11} \quad [15.8]$$

These results are tabulated in Table 7 for various values of the angle of departure  $i_1$  and are shown graphically in Fig. 4. The maximum possible lead is 1.067 corresponding to the effective extent. (See Table 6.)

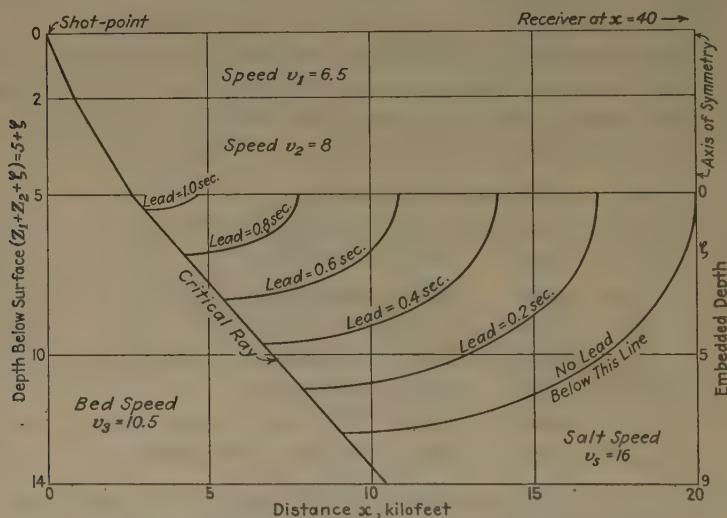


FIG. 4.—EDGE LOCUS FOR SYMMETRIC SALT DOME OF CONSTANT LEAD.

In Fig. 5 are shown the leads for various depths when the edges are kept in the same vertical planes. The leads are calculated from:

$$\text{For } \zeta = 0, \quad L = \frac{x_1 - x_0}{v_r} \quad [15.91]$$

$$\text{For } \zeta > 0, \quad L = A - B\zeta \quad [15.92]$$

$$\text{where:} \quad \zeta = \frac{x_0 - \xi_i}{\tan i_3} \quad [15.93]$$

*Corner Curves.*—The parametric equations of the corner, or transition, curve are:

$$x - x_1 = \xi_i + \zeta \tan i_3 \quad [16.1]$$

$$\tau_r = \tau_i + \frac{\zeta \sec i_3}{v_3} \quad [16.2]$$



For a selected value of  $\zeta$ , each value of  $i_1$  determines a point  $(x, \tau_r)$  of the curve. For  $\zeta = 0$ , the curve is a definite transition curve from the salt line at  $x - x_1 = \xi_c = 2.621$  to the bed line at  $x - x_1 = \xi_n = 5.106$ . For  $\zeta > 0$ , the curve extends indefinitely from  $x - x_1 = \xi_c = 2.621 + 0.870\zeta$  and rapidly approaches a straight line of slope  $\frac{1}{v_n} = 0.095$ .

### CONTINUOUSLY VARYING MEDIA

In a medium for which the speed of wave transmission is a continuous function of the depth, the methods of analysis just described lead to differential conditions instead of conditions of finite discontinuities. The methods are the same as those usually used in calculus. The medium is divided into uniform layers, each of which ultimately approaches the limit zero in thickness. In this way, equation 1.1 is replaced by:

$$\sin \theta = \frac{v}{u} \quad [17.1]$$

where  $\theta$  is the angle made by the curved ray and the vertical at the point, the ray becoming horizontal when the speed becomes equal to the constant  $u$ . The value  $u$  is a parameter, which determines the particular

TABLE 7.—*Symmetric Dome Coefficients*

$i_1$	$A$	$B$	$\zeta_{\max}$
24°	1.067	0.144	7.423
25	1.067	0.144	7.411
26	1.065	0.144	7.378
27	1.064	0.145	7.319
28	1.061	0.147	7.229
29	1.058	0.149	7.105
30	1.054	0.152	6.940
31	1.049	0.156	6.727
32	1.042	0.162	6.455
33	1.035	0.169	6.113
34	1.027	0.181	5.679
35	1.017	0.198	5.126
36	1.006	0.229	4.398
37	0.994	0.294	3.376
38	0.979	0.633	1.547

ray. The variables  $(\theta, v)$  belong to a specified point of the medium and

ray. Also, equation 1.2 is replaced by:

$$x = \int_0^Z \tan \theta dZ \quad [17.2]$$

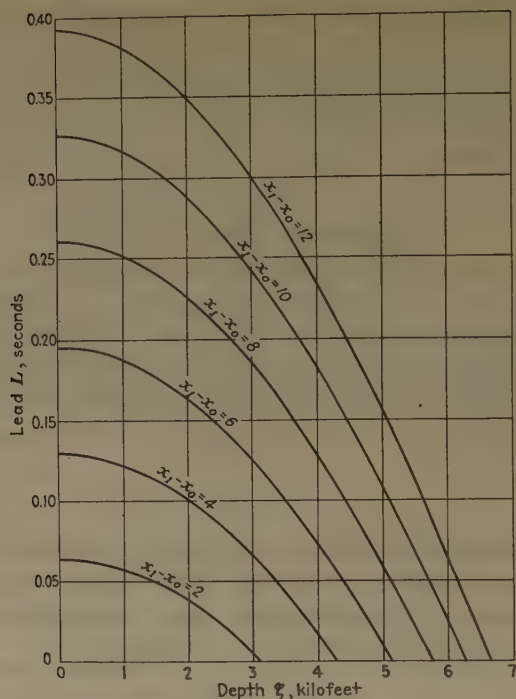


FIG. 5.—LEAD FOR VARIOUS EXTENTS OF SYMMETRIC DOME.

where  $x$  is the abscissa of that point of the ray whose depth is  $Z$ . Similarly, equation 1.3 is replaced by:

$$\tau = \int_0^Z \frac{\sec \theta}{v} dZ \quad [17.3]$$

In order to complete the indicated integrations, it is necessary that we know the law of variation of speed with the depth. As a special case,<sup>2</sup> suppose that the speed at the initial point is  $b$  and that the speed increases at the rate  $a$  per unit depth. It is not necessary that the initial point be at the surface of the medium, but we shall imagine the depths  $Z$  measured from a horizontal plane through the initial point. In this notation, the surface of the earth may have a negative depth, but no inconsistencies need arise from this convention. Thus, we may write:

$$v = aZ + b \quad [18.1]$$

For the descent path, we have:

$$\tan \theta = \frac{\sin \theta}{\sqrt{1 - \sin^2 \theta}} = \frac{v}{\sqrt{u^2 - v^2}} \quad [18.21]$$

<sup>2</sup> This is the case discussed by Ewing and Leet: *Seismic Propagation Paths*. *Trans. A.I.M.E.* (1932) 97.

$$\sec \theta = \frac{1}{\sqrt{1 - \sin^2 \theta}} = \frac{u}{\sqrt{u^2 - v^2}} \quad [18.22]$$

Thus,

$$x = \frac{1}{a} \int_b^v \frac{v dv}{\sqrt{u^2 - v^2}} = \frac{\sqrt{u^2 - b^2}}{a} - \frac{\sqrt{u^2 - v^2}}{a} \quad [18.31]$$

This may be written:

$$\left(x - \frac{\sqrt{u^2 - b^2}}{a}\right)^2 + \left(Z + \frac{b}{a}\right)^2 = \frac{u^2}{a^2} \quad [18.32]$$

and represents a circle with center at  $\left(\frac{\sqrt{u^2 - b^2}}{a}, -\frac{b}{a}\right)$  and radius  $\frac{u}{a}$ , so that the depth of penetration (since  $a$  and  $b$  are both positive) is:

$$Z_{\max} = \frac{u - b}{a} \quad [18.33]$$

Symmetry shows that the descent and ascent are similar, so that the entire path is a circle and the ray rises to the reference plane again at the distance:

$$x = \frac{2\sqrt{u^2 - b^2}}{a} \quad [18.34]$$

To find the time, we have, by equations 17.3 and 18.22:

$$\tau = \frac{u}{a} \int_b^u \frac{dv}{v\sqrt{u^2 - v^2}} = \frac{1}{a} \log \frac{b(u - \sqrt{u^2 - v^2})}{v(u - \sqrt{u^2 - b^2})} \quad [18.41]$$

The time from the initial point to the lowest point of the path is:

$$\tau_0 = \frac{1}{a} \log \frac{b}{u - \sqrt{u^2 - b^2}} = \frac{1}{a} \log \frac{u + \sqrt{u^2 - b^2}}{b} \quad [18.42]$$

and the time required for the wave to rise to the initial plane again is:

$$T = \frac{2}{a} \log \frac{u + \sqrt{u^2 - b^2}}{b} \quad [18.43]$$

Since the distance at which the ray rises to the initial plane is:

$$x = \frac{2\sqrt{u^2 - b^2}}{a} \quad [18.34]$$

it follows that:

$$u = \sqrt{b^2 + \left(\frac{ax}{2}\right)^2} \quad [18.51]$$

so that equation 18.43 becomes:

$$T = \frac{2}{a} \log \frac{\sqrt{b^2 + \left(\frac{ax}{2}\right)^2} + \left(\frac{ax}{2}\right)}{b} \quad [18.52]$$

$$= \frac{2}{a} \log \left( \sqrt{1 + \left(\frac{ax}{2b}\right)^2} + \frac{ax}{2b} \right) \quad [18.53]$$

If we write  $k$  for  $\frac{a}{2b}$ , this becomes:

$$T = \frac{2}{a} \log (\sqrt{1 + k^2 x^2} + kx) \quad [18.54]$$

If we take two observations with the shot and receivers at the same level, distinguishing the two sets by subscripts, we have:

$$\frac{T_2}{T_1} = \frac{\log (\sqrt{1 + k^2 x_2^2} + kx_2)}{\log (\sqrt{1 + k^2 x_1^2} + kx_1)} \quad [18.55]$$

For two selected values of  $x$  and observed times  $T$ , equation 18.55 becomes a relation with the single unknown  $k$ . After the value of  $k$  has been found, equation 18.54 determines the value of  $a$  for each of the two observations, the results being the same, except for errors in observation and calculation. After  $k$  and  $a$  are known, the value of  $b$  is found without difficulty. Finally, the maximum speed and the depth of travel for the ray are computed from equations 18.51 and 18.33, respectively. Equation 18.55 may also be written:

$$\frac{T_2}{T_1} = \frac{\log (\sqrt{1 + k^2 x_2^2} - kx_2)}{\log (\sqrt{1 + k^2 x_1^2} - kx_1)} \quad [18.56]$$

The solution of equation 18.55 or of equation 18.56 for  $k$  may be made by repeated trials or by successive approximations. If the latter method is used, it may be expeditious to first expand the right member as a power series in  $k$  or  $1/k$ , but this is not recommended unless several such equations are to be solved.

The relations of equation 18.31 and equation 18.41 are general for a medium in which the speed increases linearly with the depth. If discontinuities are present, but in each layer, the speed varies linearly, the path must be considered in sections, each of which may be treated as above. For known speed laws, the determination of the path is direct. If the law is to be determined from observations, the method is indirect, an attempt being made to find that law which will fit the observations most closely. This is, as usually, much more complicated, even if possible.



As a specific case of the use of these relations in a medium of linearly varying speed containing a discontinuity, suppose that at a depth  $h$  there is a high-speed layer which causes the waves to be reflected. For simplicity, assume the shot and receiver to be located at the surface of the earth. Let the contact occur at a depth corresponding to the speed  $v_h$  in the upper medium. The ray reflected at the receiver distance  $x$  after a time  $T$  satisfies the equations:

$$x = \frac{2(\sqrt{u^2 - b^2} - \sqrt{u^2 - v_h^2})}{a} \quad [19.1]$$

$$v_h = ah + b \quad [19.2]$$

$$T = \frac{2}{a} \log \frac{b(u - \sqrt{u^2 - v_h^2})}{v_h(u - \sqrt{u^2 - b^2})} \quad [19.3]$$

Equation 19.2 determines  $v_h$  in terms of  $a$ ,  $h$  and  $b$ . Each observation measures a pair of values  $x_i$  and  $T_i$ , but introduces a parameter  $u_i$ . Thus, if there are  $n$  observations, there are  $2n$  equations in  $(n + 3)$  variables and a unique solution requires at least three observations. Theoretically, three observations will make a solution possible. In practice, the variables  $a$  and  $b$  may be determined for the short shots, and the rest of the unknowns may then be determined for the longer shots.

### REFLECTION PATHS

If the receiver is placed close to the shot point, the only rays reaching the surface from the lower beds are those reflected from these beds. Consider a homogeneous bed of uniform thickness. Suppose that the speeds have been determined for the upper layer and the bed, as by refraction surveying. Let the upper layer have a speed  $v_1$  and the bed have a speed  $v_2$ . Let the upper layer have a thickness  $h$ . The critical angle of descent is  $\theta$  where  $\sin \theta = v_1/v_2$ . If  $x \leq 2h \tan \theta$ , the wave reaching the receiver from the bed must be reflected. It will have the time:

$$T = \frac{2\sqrt{h^2 + \left(\frac{x}{2}\right)^2}}{v_1} = \frac{\sqrt{x^2 + 4h^2}}{v_1} \quad [20.1]$$

If the values of  $T$  are plotted against the values of  $x$ , the resulting curve will be a hyperbola:

$$x^2 - v_1^2 T^2 = -4h^2 \quad [20.21]$$

which will be concave to the time axis. A refraction curve is usually concave to the distance axis.

The first point on a refraction profile and the last point on a reflection profile must each be due to the point for which the incidence is critical. For this case, we have:

$$x = 2h \tan \theta \quad [20.31]$$

$$v_1 T = 2h \sec \theta \quad [20.32]$$

If  $\phi$  is the angle (scales considered) between the time axis and the line joining the origin to the point corresponding to critical incidence, equations 20.3 show that:

$$\tan \phi = \frac{v_1 \tan \theta}{\sec \theta} = v_1 \sin \theta = \frac{v_1^2}{v_2} \quad [20.4]$$

Usually, this point is not observable on the graph, but since the speeds are known, the critical line may be constructed. If the refraction profile is produced back to the critical line, the intersection will furnish the point at which the profile changes from reflection to refraction. In this manner, a refraction profile may be used to calculate depths more accurately by using the reflection formula. The method is fairly reliable even when the beds are slightly tilted.

If, in equation 20.21, we plot  $b = x^2$  as ordinate against  $a = t^2$  as abscissa, we have the straight line:

$$\omega a_i - b_i = \zeta \quad [20.41]$$

where  $\omega = v_1^2$  and  $\zeta = 4h^2$ , the subscript denoting the specific observation. Each observation determines a value of the depth and of the speed, provided that the line is approximately straight, as indicated by equation 20.41. The slope of the line is  $\omega$  and the corresponding speed is  $v_1 = \sqrt{\omega}$ . The  $b$  intercept is  $-\zeta$ , from which the depth is  $h = \frac{1}{2}\sqrt{\zeta}$ . For a selected region,  $v_1$  is constant, so that the slope  $\omega$  is constant. If the bed is horizontal, the line will be straight. It is not necessary that the points be plotted with the origin on the graph, since similar triangles will furnish the necessary information.

If the speed to be used for a specified region is determined by reflections from a bed of known depth, we have only to solve equation 20.1 for  $v_1$  and then to use that value as valid for near-by points. However, the graphic method makes such an assumption unnecessary. In fact, such an assumption may lead to appreciable errors.

If the graph is approximately straight, we may assume that  $h$  and  $v_1$  are constant for the observations, so that we may write equation 20.41 in the form:

$$a_i \omega - \zeta = b_i \quad [20.42]$$

and obtain one such equation for each observation. If there are more than two observations, the values of  $\omega$  and  $\zeta$  may be determined by the method of least squares. However, before proceeding to the solution, it is usually desirable to refer times and distances to certain respective average values, in order to reduce errors of calculation. Let:

$$a_0 = \frac{1}{n} \sum_{i=1}^n a_i \quad [20.4311]$$

$$b_0 = \frac{1}{n} \sum_{i=1}^n b_i \quad [20.4312]$$

where there are  $n$  observations. Thus,  $a_0$  and  $b_0$  are direct arithmetic averages, while the times and distances are averaged by way of their squares. Also, write:

$$a_i = a_0 + \alpha_i \quad [20.4321]$$

$$b_i = b_0 + \beta_i \quad [20.4322]$$

Then, equation 20.42 becomes:

$$(a_0 + \alpha_i)\omega - \zeta = b_0 + \beta_i \quad [20.44]$$

The *normal equations* for the least square solution are:

$$A\omega - B\zeta = D \quad [20.511]$$

$$B\omega - C\zeta = E \quad [20.512]$$

where:

$$A = \Sigma(a_0 + \alpha_i)^2 = na_0^2 + 2a_0\Sigma\alpha_i + \Sigma\alpha_i^2 \quad [20.521]$$

$$B = \Sigma(a_0 + \alpha_i) = na_0 + \Sigma\alpha_i \quad [20.522]$$

$$C = n \quad [20.523]$$

$$D = \Sigma(a_0 + \alpha_i)(b_0 + \beta_i) = na_0b_0 + b_0\Sigma\alpha_i + a_0\Sigma\beta_i + \Sigma\alpha_i\beta_i \quad [20.524]$$

$$E = \Sigma(b_0 + \beta_i) = nb_0 + \Sigma\beta_i \quad [20.525]$$

By equation 20.43,

$$\Sigma\alpha_i = \Sigma a_i - na_0 = 0 \quad [20.531]$$

$$\Sigma\beta_i = \Sigma b_i - nb_0 = 0 \quad [20.532]$$

Thus, we may write equations 20.52 as:

$$A = na_0^2 + \Sigma\alpha_i^2 \quad [20.541]$$

$$B = na_0 \quad [20.542]$$

$$C = n \quad [20.543]$$

$$D = na_0b_0 + \Sigma\alpha_i\beta_i \quad [20.544]$$

$$E = nb_0 \quad [20.545]$$

The solutions of equations 20.51 are:

$$\omega = \frac{\Delta_\omega}{\Delta} \quad [20.611]$$

$$\zeta = \frac{\Delta_\zeta}{\Delta} \quad [20.612]$$

$$\text{where:} \quad \Delta_{\omega} = BE - CD = -n \Sigma \alpha_i \beta_i \quad [20.621]$$

$$\Delta_{\tau} = AE - BD = nb_0 \Sigma \alpha_i^2 - na_0 \Sigma \alpha_i \beta_i \quad [20.622]$$

$$\Delta = B^2 - AC = -n \Sigma \alpha_i^2 \quad [20.623]$$

$$\text{Thus,} \quad \omega = \frac{\Sigma \alpha_i \beta_i}{\Sigma \alpha_i^2} \quad [20.711]$$

$$\zeta = \frac{a_0 \Sigma \alpha_i \beta_i - b_0 \Sigma \alpha_i^2}{\Sigma \alpha_i^2} = a_0 \omega - b_0 \quad [20.712]$$

$$v_1 = \sqrt{\omega} \quad [20.721]$$

$$h = \frac{1}{2} \sqrt{\zeta} \quad [20.722]$$

If two groups of reflections result in parallel lines, we have two lines:

$$\omega a' - b' = \zeta' \quad [20.811]$$

$$\omega a'' - b'' = \zeta'' \quad [20.812]$$

where the superscripts refer to the two sets of observations. The vertical distance between the two lines is:

$$\Delta = \zeta' - \zeta'' = 4h'^2 - 4h''^2 = 4(h' - h'')(h' + h'') \quad [20.821]$$

If the change in  $h$  is small compared with either depth, we may write:

$$\Delta = 8h\delta \quad [20.822]$$

$$\text{where:} \quad \delta = h' - h'' \quad [20.823]$$

is the change in depth and  $h$  is the depth at either station. Finally, the change in depth is:

$$\delta = \frac{\Delta}{8h} \quad [20.824]$$

so that the change in depth is determinable in terms of the depth at either station and the vertical displacement caused in the "square" graph line. The percentile error in determining the changes in depth is about the same as the percentile error made in determining the depth directly. Thus, if the depth is known accurately at one point, as by drilling, the depth at a new point may be determined satisfactorily, if the new line is parallel to the old, on the graph.

#### MULTIPLE DEPTH DETERMINATION

The strata lines of equations 6 may be used to determine the depths to the various layers in refraction profiles with several straight line sections. In the preceding part, equation 20.4, we made use of the critical point of the profile for a single bed. In general, we have the time for the ray refracted at the top of medium  $M_u$  given by:

$$T_u = \frac{x}{v_u} + \frac{2}{v_u} \sum_{k=1}^{u-1} Z_k \cot \psi_{uk} \quad [6.3]$$

where

$$\sin \psi_{uk} = \frac{v_k}{v_u} \quad [6.4]$$



If all other impulses could be filtered out of the record, the first point of this profile would have the coordinates:

$$x_u = \sum_{k=1}^{u-1} 2Z_k \tan \psi_{uk} \quad [21.11]$$

$$T_u = \sum_{k=1}^{u-1} \frac{2Z_k \sec \psi_{uk}}{v_k} \quad [21.12]$$

Hence, for this point, we have:

$$(v_{u-1} \sin \psi_{u,u-1}) T_u - x_u = \sum_{k=1}^{u-2} \frac{2Z_k}{v_k} (v_{u-1} \sin \psi_{u,u-1} \sec \psi_{uk} - v_k \tan \psi_{uk}) \quad [21.2]$$

This represents a line whose  $x$  intercept is:

$$x_{u0} = \sum_{k=1}^{u-2} \frac{2Z_k}{v_k} (v_k \tan \psi_{uk} - v_{u-1} \sin \psi_{u,u-1} \sec \psi_{uk}) \quad [21.31]$$

and whose inclination to the  $T$  axis is  $\phi_u$  where

$$\tan \phi_u = v_{u-1} \sin \psi_{u,u-1} = \frac{v_{u-1}^2}{v_u} \quad [21.32]$$

Both  $x_{u0}$  and  $\phi_u$  are independent of  $Z_{u-1}$ , so that if the speeds are known for the layers above the  $u$ th, and if the thicknesses are known for the layers above the  $(u-1)$ th, the critical line may be plotted. Its intersection with the line of equation 6.3, representing the paths refracted at the top of the  $u$ th medium, furnishes  $x_u$  and  $T_u$ , after which equations 21.1 furnish:

$$2Z_{u-1} \tan \psi_{u,u-1} = x_u - \sum_{k=1}^{u-2} 2Z_k \tan \psi_{uk} \quad [21.41]$$

$$2Z_{u-1} \sec \psi_{u,u-1} = v_{u-1} T_u - \sum_{k=1}^{u-2} \frac{2Z_k v_{u-1} \sec \psi_{uk}}{v_k} \quad [21.42]$$

Equations 21.4 lead to:

$$Z_{u-1} = \frac{1}{2} \sqrt{\left( v_{u-1} T_u - \sum_{k=1}^{u-2} \frac{2Z_k v_{u-1} \sec \psi_{uk}}{v_k} \right)^2 - \left( x_u - \sum_{k=1}^{u-2} 2Z_k \tan \psi_{uk} \right)^2} \quad [21.5]$$

This is the analogue of the "triangle formula" used when  $u = 2$ , for which case it leads to equation 20.23, after a simple change of notation. Finally, if  $E$  is the elevation of the surface, the level of the top of the  $u$ th layer, referred to the same datum, is:

$$Z_u = E - \sum_{k=1}^{u-1} Z_k \quad [21.6]$$

For purposes of calculation, we may introduce the notation:

$$S_{uk} = \frac{2v_{u-1} \sec \psi_{uk}}{v_k} \quad [21.71]$$

$$N_{uk} = 2 \tan \psi_{uk} \quad [21.72]$$

$$B_{uk} = N_{uk} - S_{uk} \sin \psi_{u,u-1} \quad [21.73]$$

$$F_u = v_{u-1} T_u - \sum_{k=1}^{u-2} Z_k S_{uk} \quad [21.74]$$

$$G_u = x_u - \sum_{k=1}^{u-2} Z_k N_{uk} \quad [21.75]$$

In this notation, equations 21.3 and 21.5 become:

$$\tan \phi_u = \frac{v_{u-1}^2}{v_u} \quad [21.81]$$

$$x_{u0} = \sum_{k=1}^{u-2} Z_k B_{uk} \quad [21.82]$$

$$Z_{u-1} = \frac{1}{2} \sqrt{F_u^2 - G_u^2} \quad [21.83]$$

Thus, if the profile is sufficiently reliable, each thickness may be determined after the preceding ones have been. For a reflection after several refractions, the formulation is less satisfactory, at present.

### SUMMARY

In this paper, some general formulas for seismic prospecting have been developed and applied in the cases of horizontal layering, including rectangular intrusions such as salt domes. The results may be extended to other structures, such as faults and tilted layers.

The primary problem has been that of a prism of salt embedded in the lowest layer of a group of homogeneous horizontal beds. While the principal attempt has been to make the analysis of the various possible cases, a few more general conclusions may be drawn. Some of them are:

1. In many cases of refraction prospecting, the customary methods of analysis may lead to false determinations of depth, the calculated depth being too small.

2. For a dome whose top is fairly near the top of the embedding layer, the edges may be determined, at least approximately.

3. The results shown in the numerical example refer only to the selected system, as to magnitudes, but are typical of what may be expected in other cases.

4. The effective limits and the maximum depth at which a salt dome may be detected may be determined for assumed conditions.

5. If the medium has a speed varying linearly with the depth, the path of the wave is a circle, while the path is a straight line if the medium is homogeneous.

6. For determining the thickness of a single layer, a graphic or a least-square method is convenient in interpreting reflection data.

7. If the refraction time-distance profile consists of several straight line sections, it is possible to determine the depth of the contact causing each section.

## Recent Geothermal Measurements in the Michigan Copper District

BY JAMES FISHER,\* HOUGHTON, MICH., L. R. INGERSOLL,† MADISON, WIS. AND  
HARRY VIVIAN,‡ CALUMET, MICH.

(New York Meeting, February, 1932)

THE copper mines of the Keweenaw Peninsula in northern Michigan have long been of interest in connection with deep earth-temperature measurements. The extraordinary low geothermal gradient of 1° F. in 223.7 ft. announced by Agassiz<sup>1</sup> as a result of measurements dating from 1886, although later<sup>2</sup> stated as in error, served to focus attention on this region as one offering, because of the great depth of the mines, unusual opportunity along this line. Lane,<sup>3</sup> Van Orstrand<sup>4</sup> and others have made valuable contributions to this study.

Fresh opportunities afforded by the constant deepening of the mines, improvements in the accuracy and reliability of temperature-measuring instruments together with increasing knowledge of the heat conductivities and specific heats of the rocks, led the Michigan College of Mining and Technology in cooperation with some of the mining companies to renew work on this problem. It is planned eventually to complete a survey which will make use of the favorable opportunities for deep rock-temperature measurements presented in these mines. This survey should include the determination of a depth-temperature gradient in both conglomerate and amygdaloid mines, and also the variations in temperature at the same depth in different geological formations. The first problem has a direct bearing on the question of providing equipment for necessary ventilation with increased depth. The second may show that a relation exists between the natural rock temperature and the mineral content of the formation.

The measurements in all cases are to be guided by heat conduction considerations, to the end that they may represent as closely as possible

\* Professor of Mathematics and Physics, Michigan College of Mining and Technology.

† Professor of Physics, University of Wisconsin.

‡ Chief Engineer, Calumet and Hecla Consolidated Copper Co.

<sup>1</sup> A. Agassiz: *Amer. Jnl. Sci.* [3] (1895) 50, 503.

<sup>2</sup> Brit. Assn. Adv. Sci. Rept. of 71st meeting, 65 (1901).

<sup>3</sup> A. C. Lane: *Bull. Geol. Soc. Amer.* (1923) 34, 703.

<sup>4</sup> C. E. Van Orstrand: *Amer. Jnl. Sci.* (1928) 15, 495. See also N. H. Darton: U. S. Geol. Survey *Bull.* 701, 50.



the actual virgin temperature at the spot, unaffected by the mining operations. Due consideration is given, therefore, to the heat effects produced by the drilling and blasting operations and the ventilation of the mine openings.

## TEMPERATURE MEASUREMENTS

### *Temperature Stations*

The measurements so far have been confined to diamond-drill holes, and to the Calumet and Hecla mine in which most of the Agassiz measurements were also made. In the Agassiz work thermometers were sealed for weeks at the bottom of drill holes about 10 ft. deep in shafts or other passages which had themselves, in some cases, been exposed to ventilation for many months. A little calculation on the basis of heat conduction theory will serve to show that the results under such conditions would be largely influenced by the ventilation, and only in the most favorable cases could be depended on to give virgin rock temperatures unaffected by mining operations. The recent diamond-drill hole temperatures were taken by Dr. C. E. Van Orstrand of the U. S. Geological Survey, using his very complete equipment for this purpose with the clinical type of mercury in glass thermometers.

In the present mine work a radically different procedure was adopted from that formerly used. All the measurements were carried out in new workings; i. e., drifts or other cuttings which were advancing steadily a number of feet a week and which were well removed from other parts of the mine. At such a "temperature station" a "temperature hole" would be drilled only a few feet back from the breast, and in rock of which the face had been exposed only a few days. This hole was  $1\frac{3}{4}$  in. dia. ( $1\frac{1}{8}$  in. at the bottom) and 7 ft. or more deep, slanted up about  $3^\circ$  for drainage of water used in drilling. Temperatures were taken with one or more thermometers located at the inner end of this hole.

### *Thermometers*

After due consideration of the advantages and disadvantages of electrical temperature-measuring instruments, mercury in glass thermometers were finally chosen for this work, mainly because of their simplicity and reliability. Fifteen were especially made by Henry J. Green, measuring about 12 in. long, reading  $0^\circ$  to  $40^\circ$  C., in  $0.1^\circ$  C. The one tested by the U. S. Bureau of Standards showed a maximum error less than  $0.03^\circ$ , and frequent comparisons, as well as zero checks, indicated in no case a correction as much as  $0.1^\circ$ . To obviate the tendency for the mercury thread to separate, in transporting, an inert gas at a pressure of about one atmosphere is included above the mercury.

The mounting of these thermometers was a matter to which a great deal of attention was given. As they were intended primarily for taking the temperatures at the end of the drill hole it was vital that there be no change in the mercury column while the thermometer was being pulled from the hole and read. At the same time it was very desirable that the thermometer should not be too slow in taking the temperature of its surroundings, for in many cases it might be inconvenient to leave it in the hole for more than an hour.

After much experimentation, excellent results were secured by mounting the thermometer in a bakelite tube, 1 in. dia. and 14 in. long, slotted over the scale and with a special connecting device at each end for connecting the thermometers in tandem. The thermometer bulb fitted

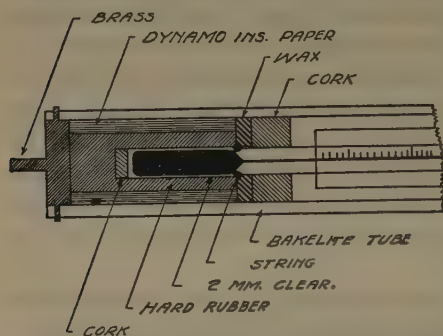


FIG. 1.—THERMOMETER IN ITS MOUNTING.

loosely into a small vulcanite tube, which was itself wrapped in special paper to fit the bakelite tube, the whole being waterproofed with wax and lacquer (Fig. 1). When placed in a drill hole or other region of constant temperature, a thermometer so mounted gave a series of constant readings in about one-half hour, but on removal a full minute would elapse before the mercury would show any change, even if the surroundings were at quite a different temperature. This allowed ample time for reading.

### *Temperature Readings*

As the holes were drilled in the usual manner with air-operated machines using a flow of water through the drill steel, there was almost no heating effect due to drilling. Temperature readings taken immediately after the hole was completed were sometimes a degree high, but after a few hours all evidence of drilling heat disappeared. To be on the safe side, however, little reliance was placed on readings made less than 24 hr. after drilling.

When readings were to be made, thermometers in tandem groups of three (sometimes two) were run into the hole with a stout wire. The thermometer nearest the mouth carried a rubber washer which fitted the hole, and the mouth of the hole was stopped with a wooden plug. After an hour or two the set was pulled out, read and replaced, to be read again about every 2 hr. until three or four sets of readings had been taken. The procedure was repeated the next day or the day after, and sometimes continued at intervals for weeks or even months. In addition, air, rock

face, psychrometer, and drill-water temperatures were occasionally taken in the drift to furnish general information as to thermal conditions at the station.

Because of the ventilation from the drills, etc., the air temperature in the drift usually averaged a degree or two lower than that at the far end of the hole. Also, the thermometer farthest in, whose reading was chiefly depended on, usually read a few hundredths of a degree higher than either of the other two, although occasionally this was reversed. When the temperatures at the end of the hole—i. e., 7 ft. into the rock—were plotted against time, the points were found to lie, as a rule, within about  $0.1^{\circ}$  C. of a straight line, sloping slightly downwards and indicating a cooling of the order of a degree per month. After the temperatures in the

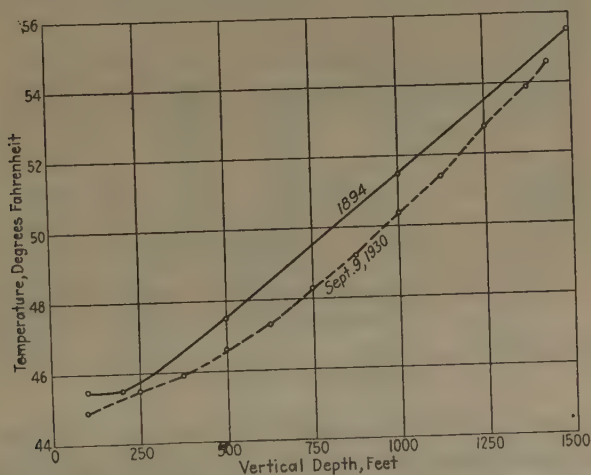


FIG. 2.—TEMPERATURE GRADIENT, DEEP WELL No. 2, CALUMET AND HECLA CONSOLIDATED COPPER CO.

first three holes had been studied for several months, the procedure for the remaining holes was shortened so that all observations could be completed within two or three days after drilling.

The procedure described above violates two traditions associated with measurements of this sort. These are to the effect that reliable measurements cannot be made in a temperature hole until some days or weeks after it is drilled; also, that all measurements should be far removed from blasting operations. Neither theory nor experiment could be found to support in any way the first tradition, which is doubtless a relic of times when holes were drilled dry, developing a great deal of heat, most of which was conducted into the rock. The second objection was not so easily disposed of. It is true that considerable heat is developed in blasting but it is hard to estimate just how much finds its way into the rock. Tests made immediately after a blast—which proved too dangerous to warrant

repetition—showed a slight warming of the rock surface, but not of the order of magnitude necessary to exert any effect on the temperature as measured in the hole.

To settle both these objections, however, the following experiment was tried: hole No. 3 was drilled about 200 ft. from No. 1, not, however, in the wall of the drift itself but in a little crosscut 16 ft. long. This hole was run in 14 ft. beyond the end of the crosscut, so that the end was 30 ft. from the wall of the drift. To keep ventilation from the crosscut, a

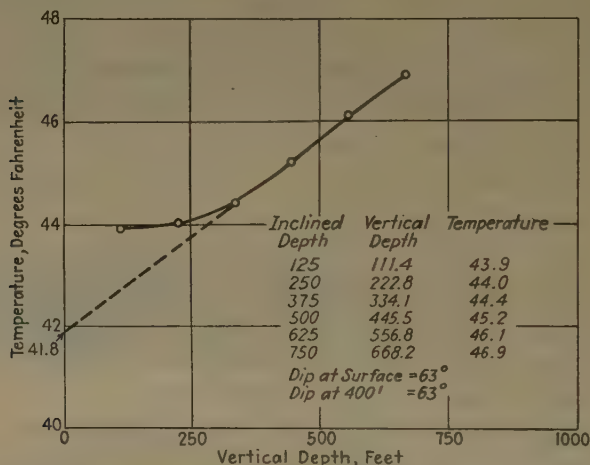


FIG. 3.—TEMPERATURE GRADIENT, DIAMOND-DRILL HOLE No. 72, COPPER RANGE CONSOLIDATED COPPER CO.

brattice was put up where it opened into the drift. In this hole the cooling was inappreciable during the first month after drilling. The mean of the temperatures taken one day after drilling was practically identical with that three days later and also three weeks later, and was within  $0.05^{\circ}$  C. of that of hole No. 1, in spite of the fact that hole No. 3 was much farther from the blasting operations.

## RESULTS

The results are shown in Figs. 2 to 4. These curves are from temperatures measured by Dr. Van Orstrand in drill holes starting from surface, excepting No. 16 (Fig. 4), where the drilled hole started on the 4700-ft. level of the Baltic mine. This drill hole starts about 4550 ft. from surface, is inclined  $64^{\circ}$  to the horizontal and is bottomed at approximately 6250 ft. from surface. Drill hole No. 2 (Fig. 2) is a vertical hole in the Eastern sandstone. The others are inclined holes in the Keweenaw flows overlain by glacial drift up to 250 ft. in thickness. All holes contain water to within a few feet of the top. The average temperature gradient for the vertical depth from 500 to 1500 ft. from surface in the trap rocks is 129 ft.



per degree. In the Eastern sandstone the average is 125 ft. per degree Fahrenheit. The average temperature distance graphs produced cut the surface line at  $41.8^{\circ}\text{F}$ . The mean annual air temperature for a period of 30 years as reported by the U. S. Weather Bureau at Houghton is  $40.5^{\circ}\text{F}$ . As the ground is covered with snow for several months during the year, and does not freeze, the mean annual ground temperature at surface is above the air-temperature average.

In the temperatures measured underground, "surface" is the collar of the Whiting shaft of the Calumet and Hecla Consolidated Copper Co.

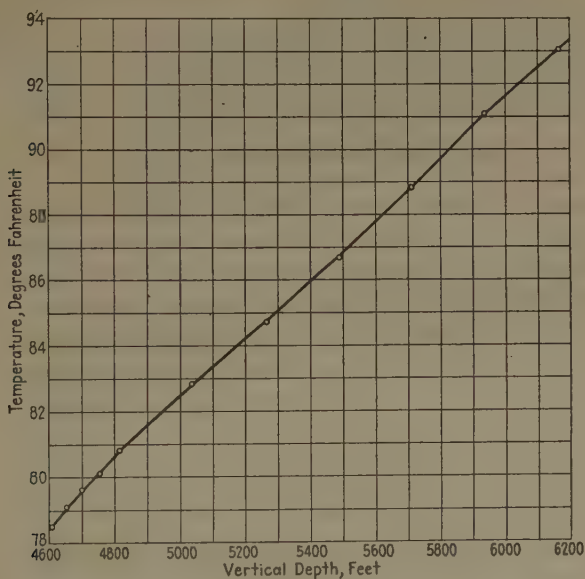


FIG. 4.—TEMPERATURE GRADIENT, DIAMOND-DRILL HOLE BALTIC No. 16, COPPER RANGE CONSOLIDATED COPPER CO.

The surface level above the mine does not vary much from this. The probable error (about  $0.1^{\circ}\text{C}$ .) listed with each is the estimated departure of the result from the virgin rock temperature at that point.

The points as plotted on the curve lie very nearly on a straight line which cuts the surface level at about  $40^{\circ}\text{F}$ . or some three degrees below the value taken by Lane<sup>5</sup> as the average surface temperature at Calumet. The average air temperature at Calumet for the years 1888 to 1930 inclusive is  $39.32^{\circ}\text{F}$ . Lane's value is arrived at in several different ways, all of which give nearly the same result, and is believed to be a very good average. It will be noted also that the shallow Agassiz points—with one extraordinary exception—would about strike this value. So far, in the

<sup>5</sup> Reference of footnote 3, 703-705.

present work, no opportunity has presented itself for making reliable measurements in the upper mine levels.

The results give as an average temperature gradient, from the surface down to 5500 ft. below,  $0.00922^{\circ}$  F. per foot, or  $1^{\circ}$  F. in 108.5 ft., and for the gradient 3500 to 5500 ft.,  $0.00970^{\circ}$  F. per foot or  $1^{\circ}$  F. in 103.1 ft. On the basis of these results, while the gradient for the deeper levels is somewhat steeper than for the surface, the difference is a matter of only a few per cent, a smaller difference than has formerly been thought to be the case. Lane<sup>6</sup> gives as an average gradient  $1^{\circ}$  F. in 105 ft., which is in good agreement with the present determination, but for the deeper levels his available data gave  $1^{\circ}$  in 90 feet.

The gradient of  $1^{\circ}$  F. in 108.5 ft. is equivalent to  $1^{\circ}$  C. in 59.5 m., which is less than one-half the value taken by Kelvin;  $1^{\circ}$  C. in 27.76 m.—as the average for the whole earth in his calculations on the age of the earth.<sup>7</sup>

### *Theoretical Interpretation of Results*

Any change of temperature at the earth's surface is propagated downwards as a wave. The diurnal changes are damped out in a few inches and even the annual variations disappear within a few feet in depth, but the slow climatic changes accompanying glacial periods may leave their impress for many thousands of feet. Theoretically, given a sufficiently complete knowledge of the geothermal gradient and character of the rock, one could reconstruct the previous thermal history of the region. Certain assumptions must be made, of course, and the matter is far from simple, but it may be possible in this way to supplement to some extent existing geological knowledge in this field. Lane<sup>8</sup> has already made an interesting start in this connection.

Two of the most important assumptions in this connection are (1) that the rock has the same thermal diffusivity at the depth of a mile as near the surface, and (2) that there are no heat sources giving local disturbances in the gradient. Both these assumptions must await further investigation for their proof, but from the knowledge at hand they appear to be justified for this region. In particular, it may be noted that there is very little evidence of reactions, either exothermal or endothermal, in the rock.<sup>9</sup> A further point of evidence for this is that the temperature points all lie well on the curve, in spite of the fact that some of the stations are separated horizontally by a distance of some two miles.

In handling the matter theoretically, it is first necessary to know the thermal diffusivity (thermal conductivity divided by the product of the

---

<sup>6</sup> Reference of footnote 3, 703.

<sup>7</sup> See Ingersoll and Zobel: *Mathematical Theory of Heat Conduction*, 88. New York, 1913. Ginn & Co.

<sup>8</sup> Reference of footnote 3, 711.

<sup>9</sup> Reference of footnote 3, 704.

specific heat and density) of the rock. B. O. Pierce<sup>10</sup> gives as the conductivity of two specimens of trap rock from the Calumet and Hecla mine the values 0.0031 and 0.0036 C.G.S. units which give, using 2.8 as the density and 0.19 as the specific heat, the average value of 0.0063 as the diffusivity. One of the authors (L. R. Ingersoll) recently determined the diffusivity of a specimen of trap from this mine by a new method. The specimen, in the form of a slab, was protected so that heat could flow only normal to the large faces. From readings of a thermocouple located in the center, when the slab was plunged in ice water, measurements were obtained from which the diffusivity is readily calculated.<sup>11</sup> This gave a diffusivity of 0.0077, which is provisionally accepted for the present calculations.

Using this value of the diffusivity, calculations were made of the temperature-depth curves corresponding to 24 different hypothetical "thermal histories" of the region. The simplest assumption would be that the surface temperature had been about as at present for 10,000 years and that before that the surface was covered with ice. Other assumptions involved a higher surface temperature after the last glacial epoch, while more complicated ones took account of no less than five glacial periods.

The equation<sup>12</sup> for calculating the points for this curve is

$$\theta = \frac{x}{2h\sqrt{\pi}} \int_0^t F(\lambda) e^{\frac{-x^2}{4h^2(t-\lambda)}} \times (t-\lambda)^{-3/2} d\lambda$$

where  $x$  is the distance below the surface at which the temperature is to be calculated,  $h^2$  the diffusivity and  $F(\lambda)$  the surface temperature function, which was given 24 different forms as indicated above. The curves were then all superposed on a uniform gradient, which caused them to pass through the two points 5.9° C. (Lane's value) at the surface and 34.3° C. at 1676 m. depth, which is the average of the three values at 5501 ft. They were then all plotted to the same scale on the same type of section paper.

A duplicate of the curve of observed points was then plotted on translucent section paper of just this size and placed over these 24 curves, one at a time, in the endeavor to see which gave the best "fit"; i. e., which of the assumed thermal histories gave the curve that most nearly fitted the facts as we now see them. The comparison seems to indicate clearly one point—that our data agree best with assumptions tending to push the time of the last glacial epoch back further than usually assumed, perhaps to 30,000 years ago.

<sup>10</sup> B. O. Pierce: *Proc. Amer. Acad. Arts and Sci.* (1903) **38**, 652.

<sup>11</sup> For a brief account of this method, see L. R. Ingersoll and O. A. Koepp: *Phys. Rev.* (1924) **24**, 92.

<sup>12</sup> See Byerly: *Fourier's Series and Spherical Harmonics*. New York, Ginn & Co.

## CONCLUSIONS

Temperature measurements in eight special drill holes in the Calumet and Hecla mine, together with one in an old hole which has suffered no appreciable temperature change in 10 years, all fall very nearly on a straight line. The temperatures range from  $74.75^{\circ}$  F. at 3562 ft. below the surface to  $95.31^{\circ}$  at 5679 ft. When taken in connection with Lane's value of  $43^{\circ}$  for the mean surface temperature, these give an average temperature gradient of  $1^{\circ}$  F. in 108.5 ft., or  $1^{\circ}$  C. in 59.5 m., which is only about one-half the Kelvin average for the whole earth ( $1^{\circ}$  in 27.76 m.). The gradient at an average depth of 4500 ft. is  $1^{\circ}$  F. in 103.1 ft.

The data are not sufficient as yet to allow any positive conclusions as to the time and extent of the glacial epochs, but point strongly to a value at least as large as 30,000 years as the time which has elapsed since the last epoch.

## ACKNOWLEDGMENTS

The authors wish to express their indebtedness to Mr. James McNaughton, President of the Calumet and Hecla Company, for his kindness in placing the facilities of the mine and the services of the engineering staff at their disposal. They wish particularly to thank Messrs. H. E. Jefferson, Robert Wilson and Harry Donald for their care in making the actual measurements as well as for many valuable suggestions.

## DISCUSSION

(Allen H. Rogers presiding)

A. C. LANE,\* Tufts College, Mass. (written discussion).—Ingersoll and Van Orstrand were kind enough to send me reprints of their papers in the New Orleans geophysical symposium.<sup>13</sup> These valuable and suggestive papers were followed by the longer A.I.M.E. publication by Fisher, Ingersoll, and Vivian, which appears in this volume. Another paper, by G. E. McElroy, gave further data.<sup>14</sup> A notice of Ingersoll's work in the *Bulletin* of the American Association of Petroleum Geologists (Sept., 1929, p. 949) singled out one of his least certain conclusions.

Then I learned that R. H. Cleland had prepared a paper on the Canadian mine temperatures.<sup>15</sup> Van Orstrand has also published other papers<sup>16</sup> and finally Ingersoll and Hotchkiss read another paper at the A.A.A.S. symposium in Chicago in June,

---

\* Professor of Geology and Mineralogy, Tufts College.

<sup>13</sup> *Physics* (1932) **2**, 154–158 and 139–153.

<sup>14</sup> G. E. McElroy: Natural Ventilation of Michigan Copper Mines. U. S. Bur. Mines *Tech. Paper* 516.

<sup>15</sup> R. H. Cleland: Rock Temperature in Mines. Canadian Min. and Met. *Bull.* (1933) No. 256, 379–409.

<sup>16</sup> C. E. Van Orstrand: *Jnl. Wash. Acad. Sci.* (1932) **22**, 529–539; *Ergaenzungshefte f. ange. Physik* (1933) **3**, 261–281 (Fig. 7 is corrected in the reprint and the next number).



1933, on the Michigan work,<sup>17</sup> and Prof. S. J. Truscott's lecture on Problems of Mining at Great Depths,<sup>18</sup> in discussing the same problem I treated in *Mineral Industry*,<sup>19</sup> also discusses the rate of increase of heat, which affects ventilation and working capacity, and the rigidity of rock.

To mining men the primary interest in these investigations is the effect of the rise in temperature on ventilation, the cost of keeping the temperature down to working conditions and the limit thereby set to mining. This is particularly true of the papers of Cleland and McElroy, and the present situation is well summarized in Professor Truscott's lecture.

A second economic interest has been brought out by Thom, and by Van Orstrand in the papers above cited, which led to studies under the auspices of the American Petroleum Institute, listed by him and summarized by K. D. Heald.<sup>20</sup> Still other problems in which the rate of increase downward of the earth's heat is an important datum are those stated in Holmes' lecture on the geothermal history of the earth,<sup>21</sup> in Daly's recent work,<sup>22</sup> and in DeLury's paper,<sup>23</sup> and in problems of underground water circulation.

The comments made here are not to be taken as hostile criticisms of any of these papers, but rather as supplementary. It is suggested, however, that *the rate of increase to be expected below the bottom of a mine will be best estimated by leaving out the first few hundred feet and taking the rate of increase shown in the bottom thousand feet or so.*

#### SURFACE TEMPERATURE EFFECTS

The flow of heat from the interior of the earth is like the flow of a river into a tidal sea or a lake, whose level is affected by waves of different periods from the ground swell to the daily tides. The effect of these waves is felt upstream with lessened amplitude. Even so, any wave of surface temperature has its amplitude flattened and the time of its arrival delayed by a factor that is proportional to the distance down and inversely proportional to the diffusivity and the duration of the wave. If, for instance, 50° daily wave of summer heat is flattened down to 0.5° at a depth of 2 ft., the annual wave of heat will, with the soil of the same diffusivity, be reduced to 1 per cent of its amplitude in  $2\sqrt{365}$ ; i.e., 38 feet.

As Ingersoll and Fisher and Van Orstrand point out, and as appears from Cleland's work, the mean soil temperature, the zero from which the geotherms start, is not the mean air temperature. It is affected by the radiant heat and the color of the soil and by evaporation and by the snow blanket. As Van Orstrand points out (p. 150) for the Long Beach, California, hill, the mean for the south side of a hill may be 73° while on the north side it is 71.4°. This may not all be due to difference of exposure to radiation.

Generally, as Van Orstrand says (p. 271), the mean air temperature is lower than the mean soil temperature, and this, in Calumet and Canada, is due mainly, I think,

<sup>17</sup> J. R. Ingersoll and W. O. Hotchkiss: *Jnl. of Geol.* (1934) **42**, 113-124.

<sup>18</sup> S. J. Truscott: *Nature* (1933) **132**, 229.

<sup>19</sup> A. C. Lane: How Deep Can We Mine? *Min. Ind.* (1895) 775.

<sup>20</sup> Tenth annual meeting of the Petroleum Institute and *Prod. Bull.* (1930) No. 205. See also papers by V. E. Barnes, McCutchin, Hawtof, Carlson, etc. *Bull. Amer. Assn. Petr. Geol.* (1932) **16**, 444.

<sup>21</sup> *Jnl. Wash. Acad. Sci.* (1933) **23**, 160.

<sup>22</sup> Daly: *Igneous Rocks and the Depths of the Earth*, especially Chap. 10. New York, 1933. McGraw-Hill Book Co.

<sup>23</sup> De Lury: *Thermal History of the Crust. Trans. Royal Soc. of Canada* (1932) sec. 4, 279.

to the blanketing effect of snow in winter. This has been worked out in detail by Callendar and McLeod for Montreal,<sup>24</sup> I showed it for Calumet,<sup>25</sup> and it appears also from Cleland's work. For instance, for Sudbury, Cleland (p. 380) gives the monthly mean temperatures as: J 7, F 8, M 20, Ap. 38, M 51, June 62, July 66, Au 62, S 56, O 44, N 30, D 16; year average, 38° F. If in getting the yearly average we replace the temperature for months where the average is below 32° by 32° (a temperature reached a couple of feet below the surface if the ground is snow covered), we should increase the average by 6.6° to 44.6°. The surface temperature indicated by the underground temperatures Cleland assumes to be (p. 404) 45.7° or, from his Fig. 14, somewhat lower. Similar calculations can be made from the mine data on page 402 and the Cochrane air temperature on page 380. From the yearly air average of 32.8°, an increase of 9.5° would give 42.3° for a surface rock temperature as against 38.5° and 40.5° which Cleland (p. 386) assumes. An excellent recent summary of the annual seasonal effects of surface temperatures has been given by Frank Reeves,<sup>26</sup> from which it appears that a mean annual range of temperature of 110° in North Dakota drops to 10° at 10 ft. depth, and to 1 per cent of the variation at a depth in feet equal to

$$6.78\sqrt{(\text{diffusivity in feet} \times \text{duration of wave in same time units as used for diffusivity})}$$

If we take the units in feet and years, the diffusivities will vary from about 85 to 400 as used by Kelvin, and the diffusivity found by Ingersoll for the Keweenaw rocks (0.0075 in c.g.s. units) becomes 254 in foot-year units. At this rate fluctuations of climate even as long as the 1400-year cycles suggested by Brooks and by Clough<sup>27</sup> will be reduced to 1 per cent of their surface value in 1550 ft. At that depth also, as has been noted, there is, if any, very little water circulation from the surface and a lessened ventilation effect. Thus the gradient from 1500 ft. down is more reliable and, if not affected by continuous ventilation, should be trustworthy.

One of the important things that appear from the group of papers under discussion is the comparative ease with which the rock temperature can be obtained within a degree or so in new or unventilated (dead end) workings. Whether a thermometer is left 30 min. or 18 hr. (Cleland, p. 383) or whether it is in a hole 5 ft. deep or 20 (pp. 383, 391) is not likely to make a difference of 0.5°. The ditch water will be at the same temperature or slightly higher, and the dry-bulb air temperature in advancing headings and dead ends will not differ from the rock temperature by more than 4° F., usually about 2° F., though temperature readings in advancing headings should wait until 3 hr. after drilling and/or blasting. On the other hand, continuous ventilation currents, which both in Michigan and Canada are generally upcast near the shafts, have a cumulative effect (which may be very important)<sup>28</sup> up to several degrees. The rather rough work done by the writer with a small pocket thermometer has therefore a real value as compared with later work that is more refined but more likely to be affected by continuous ventilation through years.

Suppose that a town is started and a boilerhouse is put over a mine, and that that raises the mean soil temperature 8°. In 25 years the 8° will have an 0.08° influence at the square root of 25 or  $5 \times 38$  ft. down; that is, 190 feet.

<sup>24</sup> H. L. Callendar: *Trans. Royal Soc. of Canada* (1895) [2] 1, sec. 3, Fig. 6. Also H. L. Callendar and C. H. McLeod: *Idem*, [2] 2, sec. 3, 109 and 3, sec. 3, 31.

<sup>25</sup> *Bull. Geol. Soc. Amer.* (1923) 34, 709.

<sup>26</sup> F. Reeves: *Virginia Geol. Survey Bull.* 36, 9-15.

<sup>27</sup> *Monthly Weather Rev.* (April, 1933) 107.

<sup>28</sup> For instance, in August, 1931, Ingersoll found in a diamond-drill hole in the Kearsarge lode, 81 level, 4792 ft. below surface, 86.77° F., which in 1921 gave 86.2° This may be due to heating up from below as the mine deepened.

Some such effect seems to be visible in some of the mines in Canada. In 1931 I found that in the Porcupine district the lowest temperatures were at something like 300 to 400 ft. down, whereas the temperatures in the levels above were from  $44^{\circ}$  to  $46^{\circ}$ . This may, of course, be due to the mine ventilation. But the possibility must not be overlooked that forest fires and settling up the locations, say 25 years ago, had started a heat wave now 5  $\times$  38 ft. down. Clayton also suggests that the climate has become milder, perhaps temporarily. This may account for the fact that the surface temperatures which Cleland computed from the mine temperatures below are less than those I computed above, with due regard to snow blanketing, and that (p. 402) for the "lowest geothermal gradients" as he computed them there is "the greatest temperature difference between indicated ground surface temperature and mean normal atmospheric. This appears in Fig. 4 of Cleland's paper, and also in some data kindly furnished me by E. Henderson of the Noranda mine (Fig. 5).

In the same way, if there was a sudden rise in temperature when the ice of the ice sheet retired, and that was something like 10,000 years ago, its effects would be reduced to 1 per cent of their range at something like 3800 ft. I had pointed out some such effect and the authors have revised my figures. That there is usually a flattening of the gradient in the upper parts of the well may be due to this as well as to convection by water.

The reviewer in the *Bulletin* of the Association of Petroleum Geologists called attention to the fact that Ingersoll thinks that his figures indicate a post-glacial wave for a period, say 30,000 years, since the last glacial overflow for this region. This is two or three times longer than I had assumed in my paper for the *Bulletin* of the Geological Society of America. But Ingersoll suggested it only tentatively and did not give the exact method of computation and at Chicago in his later paper<sup>29</sup> rather lessened the time. On the other hand, Ingersoll has added a new value for the diffusivity of the Keweenaw rocks (0.0075 c.g.s.) that is distinctly better than mine, which was indirectly computed. Naturally computations of time will be altered somewhat to match.

On the other hand if one takes Fig. 2 in Ingersoll's last paper, and notices that he assumes as an "initial curve" one starting from freezing at the surface and running to  $93^{\circ}$  F. at 5500 ft., four or five degrees less than the present temperatures at the bottom of the mine, and notices also that between 2800 and 3500 ft. there are three

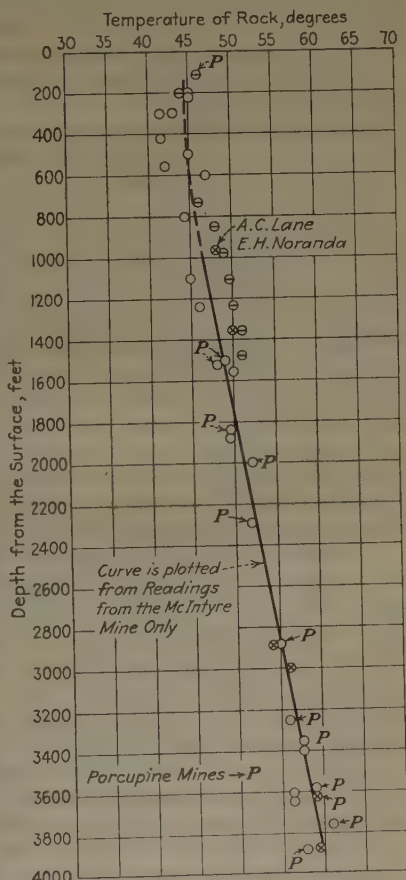


FIG. 5.—RELATION BETWEEN TEMPERATURE AND DEPTH IN CERTAIN CANADIAN MINES.

<sup>29</sup> *Jnl. of Geol.* (1934) 42, 119, 120, curve DE.



observations of present temperatures that fall below that line, it seems pretty clear that (neglecting my previous observations entirely) it would be possible on their observations to draw a curve of initial and present temperatures that would nearly touch at two-thirds of the depth, and indicate a post-glacial time four-ninths as long, something like the time recently found by Schlundt in the Yellowstone National Park. I mention this to call attention to the fact that what is needed in the Copper Country is not so much more observations at greater depth as more in newly opened entries and crosscuts between 2000 and 4000 ft. down.

The Canadian observations, being adjusted to a different surface temperature and diffusivity, cannot be used.

Of course if we could have equally accurate observations in the 10,000-ft. oil wells now going down (I understand it is impossible) climate changes a hundred thousand years back could be traced.

The Canadian mines show no clear sign of a postglacial heat wave, and a much lower gradient, conceivably due to a thicker and more radioactive crust.

I am by no means wedded to the precise figures of postglacial time which I give and I am delighted that others are taking up the method, and doubtless they will get better results. But the strength of the chain is the strength of its weakest link, and while Ingersoll's measurements are more accurate than mine, and their careful work showing the effect of ventilation, drilling, and blasting is of value anywhere that such measurements are taken, yet there are certain considerations that must be duly considered in their final conclusions.

In the first place, the effective depth cannot be measured from the collar of the shaft. As will be seen by considering Van Orstrand's papers, especially that "On the Correlation of Isogeothermal Surfaces with the Rock Strata," the topography of the country above must be considered.

Roughly speaking, the average elevation of the surface in a circle whose radius is the depth might be considered as the effective surface, and that would vary with the depth were it not for another consideration that comes in. The surface covering of glacial deposits suggests the question as to whether there were large boulders and stagnant masses of ice which remained embedded in these deposits and slowly melted so that the effective surface at 0° C. was not the present surface but the bedrock surface, especially for the deeper stations where the cooling gradient is adjusted to the temperature shortly after the ice retired. This is the same kind of effect with which Van Orstrand has to struggle when considering the recent domes over the oil deposits, where it is indicated there that the rate of erosion has, in some cases at least, been more rapid than the readjustment of the isogeotherms to the surface.

Now it so happens that over the Calumet mine there is a great deal of kettle-hole topography and of filled old lakes which may have been occupied with stagnant ice sometime after the disappearance of the main ice sheet. It may then be a fair question whether the surface of the ground or the surface of the bedrock should be taken as zero. Again, in a mine on the incline the depth is the depth for an area directly over the station where the observation is taken and not that of the collar of the shaft. However, over the Calumet mine, as also over the Laurentian Shield where the mines are that were studied by Cleland, the topography is relatively flat, so that this last factor will not be so important as it was in the discussion between Knopf and Johnson.<sup>30</sup> The question as to whether the present surface or the bedrock surface should be taken as the zero point of depth is, however, somewhat more important and probably makes extreme accuracy in computation without considering it impossible. It may make an uncertainty of up to 100 ft. in locating the zero point from which depths should be measured.

<sup>30</sup> Knopf and Johnson: Geothermal Gradient of the Mother Lode, California. *Jnl. Wash. Acad. Sci.* (1932) 22, 389.



I would call attention also to one source of inaccuracy in my earlier work. I combined records of temperatures for various mines, and this, as Professor Knopf has pointed out,<sup>31</sup> is not a safe thing to do. Nevertheless, the temperatures in so many of the mines were nearly the same in the upper 200 ft. and the rocks below so similar that I thought it was relatively safe. There was this advantage, that we did not have to allow so much for ventilation.

The effects of continued ventilation as studied by McElroy and Cleland are well worth considering in an old and deep mine. The evaporation in the mine abstracts heat if the air is dry going in and wet going out and the increase of humidity, on which they give figures, measures this. It varies with the seasons and, if compressed air is used, even with shorter changes in weather. As the Michigan and Canadian mine shafts are practically all up-cast and the air coming out laden with moisture, the air percolating down, as its temperature rises, picks up more moisture and reduces the temperature. When the air goes up the shaft it warms the rock around and as the hot vapor is condensed it warms the rock still more. The effects were seen in the early Agassiz measurements. Air circulating freely downward heats by the compression of the greater weight of the atmosphere above about 1° F. for 182 feet.

On the other hand, as I saw in the Victoria mine, compressed air cools when it is allowed to expand at the bottom of the mine. An interesting point in the Copper Country which might not occur elsewhere (which McElroy emphasizes on p. 21) is the dryness of the air in the No. 12 Hecla due to the calcium chloride in the mine water, which tends to act as a drying agent and prevents the air from containing as much moisture as otherwise it would. The hydration of calcium chloride is a strongly endomorphic reaction, which may explain a continuous tendency to lower temperatures, which Ingersoll noticed. The formation of chlorite may also be of the same nature.

Thus it is to be hoped that in further study of the question, the factors I have mentioned will be considered and also the curve of secular surface temperatures, which is to be used as most satisfactory to explain the temperatures going down, carefully studied.

The best judgment of those studying postglacial history by pollen and forests is that immediately postglacial time was warmer than at present; that it took more heat to melt off the ice than to keep it off when melted. This seems reasonable and, as Hotchkiss and Ingersoll point out, curves *D* and *E* (p. 120) agree. It will probably be well to get, from such studies as those presented by E. Antevs at the International Geological Congress in July, 1933, a curve of climates and convert it into a set of sine curves, which will be flatter and later as the depth grows greater. A variation in diffusivity (and Ingersoll has a better one than I had) would change the depth in proportion if the time is unchanged. On the other hand, if the time and the period of the surface-temperature fluctuations are changed in the same ratios and the distance changed in the square of that ratio, the ratio of the temperature to depth would be the same. It would thus be possible to make a small-scale model and vary its surface temperature and study the effects.

It would be interesting if Van Orstrand would prepare a map of the United States from his data, showing the difference between the present soil temperature and that which would be inferred from the temperature at the bottom of the wells and the rate of decrease toward the surface for the first few hundred feet. Obviously, moreover, the depth to which postglacial change of surface temperature will have appreciably penetrated will decrease as we approach the centers of glaciation, and the amount of this postglacial change may not be as great. It is hardly apparent in Cleland's figures. But there does seem, as above mentioned (Fig. 5), to be a minimum

<sup>31</sup> Reference of footnote 30.

rock temperature some 300 or 400 ft. down which suggests that Canada quite recently has become warmer, as H. H. Clayton tells me is the case.

This factor of temperature should be eliminated before we can carefully study the effect of other factors, for this is by no means the only factor. There is the effect of compaction and the diffusivity of the rock, for which we must allow as well as others mentioned in the *Bulletin* of the American Association of Petroleum Geologists by recent writers.<sup>32</sup> Yet long time changes of surface temperature are not necessarily due to the ice age. If, for instance, the land was covered with water recently and if wells were bored in the bottom of former extensions of the Great Salt Lake, or the Great Lakes, an effect should be observed.

The effect of compaction just mentioned will on the whole be the reverse of the effect of a surface rise of temperature. Like radioactivity, it will tend to produce a lower rate of increase with depth and a larger number of feet per degree rise, as shown in the depth-temperature curve in the Dubbeldevler bore hole.<sup>33</sup> Consider what the effect of varying diffusivity is. If we have a constant temperature in both sides of a sheet and different layers of differing diffusivity, the gradient will be least in the

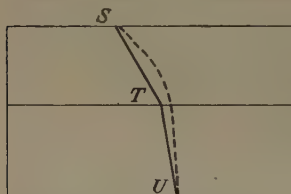


FIG. 6.—ILLUSTRATES GEOTHERMAL GRADIENT IN A "CONSTANT STATE" OF HEAT FLOW, AT  $S$  AND  $U$  THE TEMPERATURES NOT CHANGING, EITHER WITH A LESS DIFFUSIVE LAYER ( $ST$ ) OVER A MORE DIFFUSIVE ( $TU$ ), THE FULL LINE; OR WITH THE LAYER  $ST$  GENERATING RADIOACTIVE HEAT SO THAT THERE IS PRACTICALLY NO FLOW FROM A CONVECTIVE (?) LAYER BELOW (BROKEN LINE).

most diffusive material and greatest in the least diffusive material. That is, if we have (Fig. 6) a blanket of wool of low  $ST$  diffusivity on top of a sheet of iron  $TU$  of high diffusivity, the two sides of the iron will be more nearly at the same temperature than the two sides of the blanket. This is common sense.

On the whole, it seems likely that if there is no convective circulation of water, the upper strata will be less diffusive than the more solid compacted lower beds. That would tend to make the rate of increase of temperature more rapid in them than in the lower beds, especially if the pores of the beds are filled with air, which is notoriously a very good nonconductor. If they are full of water, so long as the pores are fine enough to check effective circulation, water has a high specific heat, and that again retards the diffusion. The fact, therefore, that we do not commonly find a greater increase of temperature near the surface but the reverse points to a change of temperature at the surface as being an important factor, though convection by circulating air (ventilation) or water will have the same effect.

#### RADIOACTIVITY

We now know that all rocks are more or less radioactive; in particular, granite, deep-seated oceanic sediments and black shales are relatively radioactive. Suppose that in an infinite sheet (Fig. 6) while the temperatures at  $S$  and  $U$  are fixed the bed  $ST$  is itself generating heat. Obviously the fall will not be so great and the temperature difference between  $U$  and  $T$  not so low and the temperature of  $T$  greater if it is not fixed. In other words, the effect on geotherms of generation of radioactivity is to a first approximation equivalent to making the beds  $STU$  more diffusive at the bottom and less so at the top.<sup>34</sup> The result will be that we may have slow increase of heat; i.e., low geothermal gradients in granites. But if we assume that there is a

<sup>32</sup> For compaction see D. H. Barton: *Bull. Amer. Assn. Petr. Geol.* (1933) 1052.

<sup>33</sup> *Trans. Geol. Soc. South Africa* (1923) 54, Fig. 1.

<sup>34</sup> This is shown in Van Orstrand's papers.

constant temperature at the top and bottom of a section, the lower part of which is granite, the greater the amount of granite and the nearer the surface, the more rapid the increase of temperature above it. If we have a thick sheet of iron with a thin blanket above it and a thin sheet of iron with several blankets above it, the two upper temperatures being the same and the bottom temperature at the boiling point, the thicker the iron, the slower will be the rate of increase in it and the greater the rate of increase in the beds above. This is what Van Orstrand (p. 280) pointed out and seems to be found over the domes and ridges of granite.

In granite and in places from which the heat has been exhausted from below, and where there has been a depression of beds and no igneous injections for a long time, as perhaps in the Keweenaw rocks of Michigan and the Laurentian sheets of Canada, we have low gradients. Holmes has suggested that there is a certain amount of convective current in the layer below the isostatic layer. If there are as reported by seismologists sharp breaks in the composition of the earth which can reflect earthquake waves, there can be no convection except between breaks. Then there may be a factor affecting geothermal gradients in a varying thickness down to a layer of which the temperature is practically constant, owing either to crystallization or to convective circulation. This is the factor to which Cleland appeals.

This may be one way of distinguishing between the Airy and the Pratt theories of isostasy. If granite upbulges are balanced by granite downward depressions, the resultant gradient must be very low unless the material making the bulge is heated by an extra amount of radioactivity, which is likely in granites, or in the process of bulging by intrusions of magma or magmatic waters or mashing which increases with depth.

Recent work by Paneth and Urry has given us a very fair idea of the radioactivity of the rocks of the Calumet-Hecla mine. Preliminary reports are in the mimeographed report to the Division of Geology and Geography of the National Research Council for 1931-32,<sup>35</sup> but the work is not finished. That will give us a good opportunity to allow for the radioactivity contribution to the geothermal gradient in the Copper Country, and for the first time have the necessary data in the same district.

Looking at Van Orstrand's figures,<sup>36</sup> we see that after a million years the temperature gradients do not vary much, i.e., there is nearly a steady flow of heat. Therefore, inasmuch as the Michigan and Canadian mines in question, so far as we know, have not been disturbed since Paleozoic time, no great error is involved in assuming stable conditions and steady flow. This is confirmed by Urry's observations. In that case the problem of the effect of radioactivity, which has been discussed by Van Orstrand<sup>37</sup> and Ingersoll and Zobel<sup>38</sup> can be handled rather simply (Fig. 6).

Let  $u$  be the temperature,  $y$  the distance from the surface, and  $t$  the time. The change in temperature in time  $+\frac{du}{dt}$  becomes 0, but this (compare Ingersoll and Zobel, eq. 65) is equal to

$$K \frac{d^2u}{(dy)^2} + Rdy = +\frac{du}{dt} = 0 \quad [1]$$

where  $R$  is the quantity of heat (in calories) generated per cubic centimeter of the rock

<sup>35</sup> Also in *Proc. Amer. Acad. Arts and Sci.* (1933) **68**, 139.

<sup>36</sup> Figs. 1 and 2, *Jnl. Wash. Acad. Sci.* (1932) **22**, 534, 535.

<sup>37</sup> Reference of footnote 16.

<sup>38</sup> An Introduction to the Mathematical Theory of Heat Conduction, 92-93. New York, 1913. Ginn & Co.



(not per gram) and  $K$  the diffusivity.<sup>39</sup>  $\frac{d^2u}{(dy)^2}$  is the change in temperature gradient.

Integrating from  $y = 0$  at the surface to  $y = d$ , which we may take to be the thickness of the formation for which the generation of radioactivity and the diffusivity is constant, if  $R$  is constant, we have:

$$\begin{array}{llll} y = d & y = d & & \\ K \frac{du}{dy} = Ry & = Rd & = \text{total radioactive heat generated per square centi-} & [2] \\ y = 0 & y = 0 & \text{meter for thickness of formation} & \end{array}$$

and in general 
$$K \left( \frac{du}{dy} - \left( \frac{du}{dy} \right)_0 \right) = -Ry$$

If, when  $y = d$ ,  $\frac{du}{dy} = 0$ , as might be if the radioactive heat were enough, there would be no flow from within. In that case

$$K \left( \frac{du}{dy} \right)_0 = Rd \quad [3]$$

(Compare Ingersoll and Zobel eq. 67.) That is, in a steady condition, the total generation of radioactive heat would be given from the diffusivity multiplied by the gradient at the surface.

If there is a generation of heat between  $S$  and  $T$  (Fig. 6),  $T$  would be hotter than it would be otherwise, and (as Van Orstrand's figures illustrate) for a limited time the generation of heat might be so great that at  $T$  when  $y = d$  the gradient  $\frac{du}{dy}$  might be negative and heat flow down. But this would not be a steady state.

Integrating equation 1 twice from  $y = 0$  to  $y = y$ , we have:

$$Ku = \frac{R(y)^2}{2} + Ky \left( \frac{du}{dy} \right)_0 + \text{Constant} \quad [4]$$

where  $\left( \frac{du}{dy} \right)_0$  is the geothermal gradient near the surface. The constant when  $y = 0$  is  $Ku$ , and is therefore  $= (Ku)_0$ .

Equation 4 is of a parabola such that if we take the vertical axis so that  $u = 0$  if  $y = 0$ , the parabola will cut that axis twice, once at  $(0, 0)$  and the second time at  $\frac{2}{R} K \left( \frac{du}{dy} \right)_0$ , which becomes, if equation 2 holds,  $2d$ , but which is generally greater.

The parabola is symmetrical to a horizontal axis through  $y \frac{K}{R} \left( \frac{du}{dy} \right)_0$ .

We may write equation 4 as follows (after finding the value of the constant by letting  $y = 0$ ):

$$(u - u_0) = y \left( \frac{du}{dy} \right)_0 - \frac{R}{2K} y^2 \quad [5]$$

We see that if there is no  $R$ , no radioactivity, the equation 5 reduces to the linear form—that the increase of temperature is proportional to the rate of increase and the depth. Also, the more the contribution of heat by radioactivity, the lower will be

<sup>39</sup> Ingersoll and Zobel call it  $h^2$ , Van Orstrand  $a^2$ , and I use  $y$  instead of  $x$  to emphasize that it is an up and down coordinate.



the bottom temperature that goes with a given surface gradient. If there is no contribution from the bottom as in Fig. 6,  $y = d$  and in equation 2

$$\left(\frac{du}{dy}\right)_d = 0 \quad [6]$$

In that case, of course, in steady flow, as appears from equation 2,

$$K\left(\frac{du}{dy}\right)_0 = Rd \quad [7]$$

which is the total amount of heat generated by radioactivity in the layer per unit of time.

We see from equation 5 that if we know the gradient at the surface, the surface temperature (having eliminated the effect of short-time temperature fluctuations), the diffusivity, and the rate of radioactive production of heat (quantities that at Calumet are respectively:  $1.89(10)^{-4}$ , 6 C.;  $7.5(10)^{-3}$ ; and  $2.07(10)^{-7}$ ), we may from the equation 5 have a formula to connect the thickness and the temperature at the bottom of the layer which has steady flow, and not variable diffusivity and generation of radioactivity.

At no depth, with the Calumet data, would there be no flow from the interior.

P. WEAVER,\* Houston, Tex.—I am interested in what Professor Lane said about the blanketing effect of snow. I had occasion to notice that phenomenon in Siberia, where we discovered that the rock temperature at comparatively shallow depths, about 4 meters, sometimes did not get down as low as freezing. So, it would seem that this blanketing effect may require us to start our calculations of the geothermal gradient above the mean air temperature.

L. GILCHRIST,† Toronto, Ont.—I am interested in rock temperatures above freezing, because I have found them myself in northern latitudes where the mean air temperature was well below freezing.

---

\* Geologist, Gulf Production Co.

† Professor of Physics, University of Toronto.

# Geophysics in the Nonmetallic Field

By C. A. HEILAND,\* GOLDEN, COLO.

(New York Meeting, February, 1934)

THE following summary is written for the benefit of the practical operator in the nonmetallic field who wishes to know what geophysics has done and may be expected to do in his line of work. His problem is quite different from that of the geophysicist who has operated with various or all methods and has followed the literature, and who is assumed to be familiar with the geologic possibilities and limitations of each method. This article is not written for the latter, although he may be interested in the four or five hitherto unpublished surveys described.

To the operator, on the other hand, geophysics is only secondary. His problem is to determine which geophysical method is best suited to his special needs. If he wanted to know, however, which method could be used to locate a certain material of given physical properties, building stone, for instance, he would have to wade through a tremendous amount of geophysical literature, bibliographies and articles, before he could find what he wanted.

Therefore, the purpose of this summary is to present the geological problems first and then to discuss the comparative merits of the geophysical methods that can be, or have been, applied.

## CHOICE OF GEOPHYSICAL METHODS IN OIL, CIVIL AND MINING ENGINEERING

In the first two of these fields, the geological problems are not nearly so complex as in the metal and nonmetallic mining fields. The selection of the correct geophysical method in these fields is not nearly so difficult for the operator. For oil prospecting, his problems have been discussed exhaustively by E. DeGolyer.<sup>(1)†</sup> In civil engineering (foundation and ground-water work), the usefulness of electrical methods has been so well established that there is hardly any choice of other methods at present. The situation may be changed in the future with the perfection of the seismic reflection method for shallow depths.

In the mining field the operator and often the geophysicist himself finds difficulty in determining which method is best suited for a given

---

\* Numerals in brackets refer to the bibliography at the end of the paper.

† Department of Geophysics, Colorado School of Mines.

mineral or a given geologic situation. The great variety of minerals and the complexity of their geologic occurrence makes it difficult to lay down any hard and fast rules. Nevertheless, there are a number of outstanding publications discussing the results obtained with all available methods for certain types of mineral deposits; for instance, the book by Edge and Laby,<sup>(3)</sup> and the two memoirs by Siñeriz.<sup>(4,5)</sup>

#### FACTORS AFFECTING CHOICE OF GEOPHYSICAL METHODS IN PROSPECTING FOR NONMETALLIC DEPOSITS

Before going into details regarding the application of geophysics to the location of various nonmetallic products, the general factors affecting their choice from the operator's point of view must be considered. These factors are tabulated below, and are essentially the same as in other fields of application of geophysics,<sup>(1)</sup> except, perhaps, that in view of the special conditions existing in the nonmetallic field their order of importance is somewhat different, as follows:

1. Type of mineral, rock and geology involved.
2. Reliability of results, on the basis of:
  - a. Inherent accuracy of method.
  - b. Surface or subsurface interferences.
  - c. Detail of survey.
3. Cost in relation to competitive (including geological and drilling) methods.
4. Time in relation to competitive activities.
5. Other incidental factors.

1. The type of mineral, rock and geology involved determines the difference in physical properties, dimensions and depths of the sought deposits and governs, therefore, in first consideration, the type of method to be selected. For instance, if a gravel deposit is to be located, which is known to differ materially from the surrounding strata in density, electric conductivity and elastic-wave speed, the gravitational, electric and seismic methods must be given first consideration, and the magnetic method would, in the absence of magnetic minerals in the deposits, be ruled out.

2. The reliability of the data obtained depends on both the accuracy of instruments and methods, and the possibilities of interpretation methods. In particular, the inherent accuracy of a method is important in the choice; that is, the accuracy and ease with which a method can furnish the quantity most useful in practice; namely, the depth. Therefore, it may be said, as a general rule for the application of geophysics in the nonmetallic field, that the geophysical methods that make possible control of the depth of penetration—that is, the electrical and the seismic methods—are generally to be preferred over others that do not possess this advantage, such as the gravitational, magnetic, and radioactive

methods. If, in spite of the process of elimination given above, the choice of methods is still doubtful, the surface and subsurface conditions must be seriously considered. Surface conditions are here interpreted in the broadest sense; they include not only the physical constitution of the surface, such as firmness for instrument set-up, accessibility and ease of transportation, but also the interference produced by topography and surface soil conditions upon geophysical methods. Certain electrical methods are seriously affected by topography and the conductivity of the surface soil; in seismic work, the transmission characteristics of the surface beds determine the ease with which records may be obtained. Last but not least, the subsurface section must be considered and an inquiry must be made if formations are present that may overshadow the effects sought. The choice of methods depends on whether a reconnaissance or a detailed survey is desired. Frequently it is advisable to select a cheaper and more rapid method first for general reconnaissance—for the approximate delineation of the deposit—and to follow this up with a slower and more expensive method to give details regarding depth and dimensions. The selection depends, moreover, on the geologic information already available. Where nothing is known about the geology, a reconnaissance method may give valuable information and save time for concentrating a subsequent detail survey on the important points. Where the geology is well known, a reconnaissance survey may be of no value whatever.

3. The consideration of the cost of the survey is an important item in the nonmetallic field. In many instances, the deposits sought occur close to the surface and the operator must decide whether it is cheaper to obtain the information by geological mapping or drilling or by a geophysical survey. This is an important consideration, especially in search for road material.

4. The time element is generally much more important in geophysical oil and ore prospecting than it is expected to be in the nonmetallic field. However, conditions may arise where a less accurate and faster reconnaissance method may be selected to establish leasehold in competition with other operators.

5. Other incidental factors, which may influence the choice of the method, are: whether apparatus or consulting services for a particular method are available; whether permission to enter properties may be obtained; whether the damages would be excessive, whether dynamite can be used.

#### DIRECT AND INDIRECT USE OF GEOPHYSICAL METHODS

Fortunately, geophysical methods often have a much greater range of application than would be suspected on the basis of the physical properties of the deposits to be located. This is due to the fact that the latter often are associated with minerals, formations, or geologic structures that



give much more distinct indications than the deposit itself. The first possibility, where a deposit affects the physical data by virtue of the physical properties of the sought mineral, may be called a *direct* application of geophysics. Where, however, the location of a deposit is based on the physical properties of a mineral associated with the sought mineral, or the general geologic conditions that characterize the occurrence of the deposit, the application is called *indirect*. Although this situation opens up a much greater field for geophysics, its drawbacks for the interpretation of the results should not be overlooked, as illustrated by two examples from the application of geophysics in metal mining. If the magnetic method is applied in the location of a magnetite deposit, it is rather certain that this mineral exists where pronounced magnetic anomalies are found. However, if a placer gold deposit contains magnetite, and magnetic anomalies have been found to correspond to the gold-bearing channels, the magnetic method may be used only with certain caution for the location of gold on virgin ground. In the same placer, magnetic anomalies may or may not correspond to gold concentrations; on another river bed the magnetic anomalies may mean magnetite only; not gold. Therefore, the usefulness of an indirect application of geophysics is very much a matter of the geologic conditions involved in each particular case.

#### DIVISION OF NONMETALLIC FIELD

For the purpose of discussing the applications of geophysics in the nonmetallic field, the latter will have to be divided in a manner somewhat different from the classification usually made from the point of view of economic geology. First, the branches of petroleum, natural gas, asphalt and related bitumina will be excluded, because the applications of geophysics in this field are well known and amply covered in the literature. The remainder will be classed under nine headings as follows: (1) coal, (2) sulfur, (3) salt, (4) nitrates, phosphates, potash, (5) building and road materials, (6) ground water, (7) abrasives, (8) materials of various industrial uses, (9) gems and precious stones.

Under each of these headings, direct and indirect uses of geophysics will be discussed; examples known from the literature will be described as briefly as possible, and recommendations regarding the most advantageous method will be added.

##### COAL—ANTHRACITE, BITUMINOUS, LIGNITE (BROWN COAL)

The application of geophysics in locating anthracite will be discussed first, as it offers the possibility of direct application, while virtually all other types of coal (with the possible exception of lignite) have been found to be amenable only to indirect prospecting.

The direct effect of anthracite, upon both self-potential measurements and potential or other methods, was discussed to some extent at the

Institute meeting in 1929.<sup>(6)</sup> Lundberg stated that some anthracitic coals are conductive while some are oxidizing; on the other hand, according to Leonardon,<sup>(7)</sup> the Schlumbergers have observed, in their potential studies, varieties of coal that acted as insulators.<sup>(11a)</sup> Kelly,<sup>(8)</sup> in his measurements at Wilkes-Barre, found that anthracite seams produce an effect on the self-potential method, but Koenigsberger<sup>(9)</sup> observed an unusually high resistivity of the coals in the Waldenburg district in Lower Silesia due to their high carbon dioxide content, which is assumed to have forced the electrolytic water out of the pores. It is not improbable, therefore, that the variation of occluded gases explain the great variations in the resistivity of coal that are observed. As a whole, therefore, direct prospecting for anthracite, and other types of coal, cannot be recommended; this is well expressed by Lundberg,<sup>(6)</sup> who states that thus far most electrical work in coal has failed.

Only indirect applications of geophysical prospecting have been put to some use in coal work; i.e., stratigraphic and structural investigations. In the order of practicability, the various methods that are applicable for detail work in coal districts may be ranked as follows: (1) electrical (potential or resistivity); (2) seismic; (3) torsion balance. For general reconnaissance, the magnetic method may be applicable, provided the uplift or general occurrence of carboniferous strata is related to the structure of (uniformly magnetized) basement rocks. Occasionally, pendulum observations have been applied in reconnaissance surveying for Paleozoic beds, such as were conducted a number of years ago in northern Germany under the auspices of the Stinnes concern.<sup>(10)</sup> The results obtained by electrical, seismic, torsion balance and magnetic surveys will be discussed briefly.

The most extensive experience in structural and stratigraphic coal studies has probably been accumulated by the Schlumberger company, which has published part of its results.<sup>(11)</sup> The method used in this type of work usually is the resistivity method, vertical electrical drilling at a number of points, and resistivity mapping with constant depth of penetration. A good example of this type of work has been published by Siñeriz<sup>(4)</sup> who directed not only electrical but also torsion balance, magnetic and seismic prospecting work in the Carboniferous syncline of Villanueva de Minas and Villanueva del Rio, on the Guadalquivir River in Spain. The equiresistivity map published by Siñeriz shows a rise of the Carboniferous trough to the north, and is in good agreement with the information derived from torsion balance and seismic investigations. The Carboniferous sediments and Cambrian rocks below them were found to have a higher resistivity than the sediments of the Miocene cover. Considerable work was done, also by the Schlumberger company, in the Saar coal basin.<sup>(7)</sup>

Next to the electrical method, the seismic method can render valuable service in the determination of the structure of carboniferous areas. Thus far, only refraction shooting has been applied, but there is no reason why reflection shooting could not obtain the same results with greater ease and economy of operation, provided the structural conditions are not too complicated. Siñeriz<sup>(4)</sup> has used refraction work in Spain extensively and published travel-time curves and depth determinations. He obtained velocities for the Tertiary, Carboniferous and Cambrian which are almost identical with those observed for the same formations by Barsch and Reich<sup>(12)</sup> at Dobrilugk in the Silesia coal basin. The same authors<sup>(13)</sup> then investigated other areas in the North German plain, where favorable indications for the occurrence of carboniferous strata are obtained by pendulum and torsion balance observations, in an effort to establish definitely the existence of carboniferous strata by seismic velocity correlations.

The Seismic Company, under the direction of L. Mintrop, conducted a number of surveys for the purpose of determining the structure of carboniferous areas. The majority of the results have not been published. Only Neville<sup>(14)</sup> gives an example of the location of faults in Carboniferous limestones, covered by Tertiary strata, together with the corresponding travel-time curves. An article by Shaw<sup>(15)</sup> deals with a similar problem, the location of a fault in Carboniferous limestone, flanked by clays and sandstones on the downthrow side.

Where conditions were favorable, structural conditions in carboniferous areas have been investigated frequently by means of the torsion balance. This involves chiefly the location of faults, a problem that has been discussed in its general aspects, with reference to the Westphalian Carboniferous, by Quiring.<sup>(16)</sup> A number of other authors have applied the torsion balance to the location of faults and structure in carboniferous areas, such as Matsuyama in the Fushun Colliery,<sup>(17)</sup> Schumann and Petraschek in Austria,<sup>(18)</sup> Numerov in the Donetz coal basin, Siñeriz<sup>(4)</sup> at Villanueva de Minas in Spain, and Barsch<sup>(19)</sup> in the coal-mining district near Dorsten in Westphalia. Actually, the number of surveys made in coal-bearing areas with the torsion balance by consulting geophysical companies is probably much greater than would seem to be the case from the few articles published.

The value of magnetic measurements for the location of coal-bearing structures is still a matter of controversy. It is an example of how much confusion can be created when the results obtained in one locality are generalized and followed by others as a dogma. Reich,<sup>(20)</sup> who made the first magnetic measurements in the Aachen and Erkelenz carboniferous district and extended his discussion to the magnetic conditions in Belgium, found that in these areas the carboniferous regions are characterized by magnetic minima. His disciples, for instance, A. Kaiser<sup>(21)</sup> and



W. Wolff,<sup>(22)</sup> who made magnetic measurements in carboniferous districts in Westphalia and near the Hartz, and failed to establish the rule of Carboniferous negative anomalies in many instances, did not recognize the probable significance of Reich's original observation that magnetic minima were observed in depressions of the magnetic basement rocks and could not possibly be expected in regions where the Carboniferous, and with it the magnetic basement, were uplifted. Instead, they attempted to explain their findings by an excessively magnetic basement, which was supposed to overshadow the negative effect of the Carboniferous sediments. Although we advocate the simpler interpretation given above, it does not mean that this interpretation holds for all magnetic anomalies in Carboniferous areas, as the composition of the basement rocks is apt to vary from one locality to another. This seems to be evidenced by Siñeriz'<sup>(4)</sup> observation at Villanueva de Minas and Villanueva del Rio of a magnetic picture quite different from the comparative simple structure given by the resistivity and torsion balance measurements. In spite of being deposited in a syncline, the carboniferous sediments appeared to show, at a number of localities, maxima instead of minima, which conflicts with the idea of diamagnetic carboniferous and depressed magnetic basement rocks. The general picture is not such as to make it probable that the carboniferous sediments were paramagnetic; on the contrary, taking into account the existence of intrusions in the vicinity of the area investigated, it seems likely that the magnetic highs above the carboniferous syncline may be due to similar intrusions into the basement rocks. Taken as a whole, much caution is necessary in using magnetic measurements, even as a reconnaissance method, for structural work in carboniferous areas.

A good deal of geophysical work has been done, with various methods, on lignite deposits. From the published accounts of such work, it appears that it is impossible to lay down a general rule as to whether or not lignite can be found directly. In the order of practicability, electrical resistivity methods, seismic and torsion balance observations are applicable. As far as the electrical method is concerned, the results seem to depend largely on the local stratigraphy and the water content of the lignite. W. Stern<sup>(23)</sup> has investigated this problem thoroughly and has encountered both types of response. In the first area at Ville in Germany, characteristic resistivity-depth curves were obtained, with the apparent resistivity increasing to the top of the lignite deposit and thence declining gradually. In this area, the peak of the curve corresponded (fortunately?) in every case to the top of the lignite; the type curve is similar to the three-layer curve and suggests an involvement of the ground water. This appears to be confirmed by the fact that in the second area (Niederlausitz) investigated by Stern, a relation of apparent resistivity and depth of the lignite could hardly be obtained, which, as the author states, is due to the fact



that the covering beds (gravel and sands) were abundant in water. Gilchrist<sup>(24)</sup> and Hawkins<sup>(25)</sup> have studied lignite deposits in Ontario, and the latter reports<sup>(26)</sup> that the results have generally been rather unsatisfactory; this, in the opinion of Lundberg,<sup>(26)</sup> might have been remedied by an application of different methods. Theoretically, it would seem possible to use the seismic method for the direct location of lignite deposits; however, to the knowledge of the writer, such observations have not been published. There are two references in the literature describing torsion balance observations on lignite deposits. However, conditions are not favorable for this type of geophysical work, as the balance does not react to horizontal boundaries and can detect only the place where the deposit is cut off. In the Halle brown coal area, in Germany, the situation is somewhat more favorable because the pressure of the glaciers has warped and twisted the lignite deposits; Schweydar<sup>(27)</sup> gives a number of examples of the results obtained in the area. Edge and Laby<sup>(3)</sup> investigated a brown coal deposit at Gelliondale in Victoria with the torsion balance and claim to have been able to pick up the lignite; however, the end of the deposit is cut off near a point where the older sediments rise, and it would seem doubtful whether the lignite would have been recognized in the measurements if nothing about its existence had been known beforehand.

Generally speaking, therefore, conditions would seem more favorable for the application of geophysics to the location of lignite if it can be done on a structural or stratigraphic basis. In this respect, electrical measurements would probably rank first, then seismic, and next torsion balance surveys. As far as electrical measurements are concerned, the survey made by Schlumberger<sup>(11,28)</sup> on the lignite deposits in the department of Landes, France, has probably been the most successful. In this area, the lignite occurs interbedded between conductive clays on top and more resistant sands below; thus, resistivity mapping reveals the areas where lignite existed, and where it was washed out, together with the covering clays, and was replaced by sand. Seismic structural investigations in search for lignite deposits have probably been made by some of the commercial geophysical companies, but nothing has been published about the results. Torsion balance surveys in search of faults delimiting lignite deposits have been described; for instance, by Schumann<sup>(29)</sup> in Austria and Seblatnigg<sup>(30)</sup> in Germany. The survey near Gelliondale, made by Edge and Laby and referred to above, may also be classed under this heading. Incidentally, magnetic measurements were also made on this locality, but the report is somewhat conflicting in regard to the interpretation of the results obtained. In some areas, lignite is found in the vicinity of basalt, and in that case magnetic measurements may be of assistance if caution is exercised in the interpretation of the results.<sup>(31)</sup>

In this connection, it may be mentioned that geophysical measurements have also been used on peat deposits<sup>(32)</sup> and that what has been said above about lignite applies to this also; namely, that the amount of water and its electrolytic character determines very largely the nature and reliability of the results obtained.

### SULFUR

In some texts and statistics on nonmetallic deposits, pyrite is classed as a nonmetallic because it is a sulfur mineral. However, the geophysical location of pyrite is a problem so different from those involved in the location of nonmetallics proper that it will not be considered here.

Geophysics has been applied on a fairly large scale to the indirect location of one type of sulfur deposit; that is, the sulfur found in the cap rocks of salt domes on the Gulf Coast. All methods that have been used for the location of salt domes are applicable to this problem, especially torsion balance and seismograph.<sup>(33,34)</sup> More than 100 salt domes have been found geophysically on the Gulf Coast, but of those drilled only two have thus far produced sulfur in commercial quantities. The first is the Long Point dome in Fort Bend County, Texas, which was discovered by the torsion balance in 1924 and upon which sulfur production was started by the Texas Gulf Sulphur Co. The second is the Grande Ecaille salt dome in Plaquemines Parish, Louisiana, on which a torsion balance survey was made in conjunction with prospect drilling, by the Freeport Sulphur Co. Although this record is modest enough, it must be assumed that the sulfur industry has gained considerably from the application of geophysics in the detailing of the cap rocks of known salt domes. The seismic methods suggested by McCollum and La Rue<sup>(35)</sup> for the utilization of wells for detailing cap rock and overhang of salt domes have proved particularly suitable for this work. Eby<sup>(36)</sup> has tabulated the sulfur valuation of salt domes, for the period from 1920 to 1931, against costs of geophysical work.

### SALT

Salt is obtained commercially from two sources: from salt brines and from salt beds or salt domes. Geologically and, therefore, geophysically, these possibilities represent three different geophysical problems, although the latter two involve similar requirements. Much literature dealing with the location of salt domes involved their commercial significance as source bed for potash, which is treated separately in this discussion.

The literature on the location of salt brines by geophysical methods is exceedingly meager and deals virtually with the location of brines in salt mines alone, such as the early publications by Ambronn<sup>(37)</sup> and Koenigsberger.<sup>(38)</sup> The only methods that would seem applicable to the

direct location of brines are electrical resistivity or inductive methods. It is reported that such work is going on for this purpose at the present time.

As far as salt beds and salt domes are concerned, the choice of geophysical methods is somewhat different. Ample experience has been obtained with geophysical methods in the location of salt domes in the Gulf Coast, Mexico, Rumania, Germany and Russia, which establishes fairly well that the order of choice is about as follows: Seismic and torsion balance with about equal merit, then electrical resistivity and electrical inductive, and pendulum and magnetic at the end of the list. For depth determinations on salt beds, however, the torsion balance loses first place in favor of seismic or resistivity work.

Although a tremendous amount of information was accumulated by commercial companies in the heyday of the seismic refraction method on the Gulf Coast, the literature contains only a very small fraction of it. Travel-time curves obtained with the seismic method on salt domes have been published by Barton,<sup>(34)</sup> Ambronn,<sup>(39)</sup> Rankine,<sup>(40)</sup> and Rosaire.<sup>(41)</sup> A good correlation of seismic, torsion balance, and pendulum results has been given by Schmidt<sup>(42)</sup> for the salt domes near Celle, Germany. Siñeriz<sup>(5)</sup> has published a monumental work in the last year, giving detailed travel-time curves and corresponding geologic sections for several potash-bearing salt-bed regions in Spain. Sokolov<sup>(43)</sup> has investigated the salt plugs at Kazakstan, in Russia, and gives a number of travel-time curves.

The literature on torsion balance results obtained on salt domes and salt beds is somewhat more abundant, yet none too much, considering the amount of commercial data that has been accumulated. Seblatnigg<sup>(44)</sup> and Schuh have published a complete map of the torsion balance data obtained for the salt dome of Luebtheen in Mecklenburg, Germany, and correlated these data with the magnetic and seismic data obtained on the same dome. Torsion balance results obtained on a number of other domes in Germany are contained in the prospectus of the "Exploration" Company. Barton<sup>(33)</sup> gives the torsion balance data obtained on the Nash and Hoskins mound and Esperson salt domes,<sup>(45)</sup> Logan<sup>(46)</sup> those for the Blue Ridge salt dome. Numerov<sup>(47)</sup> has investigated the salt and potash deposits at Solikamsk in the North Ural districts and claims to have been able to predict the depth to the salt beds within 10 per cent.

Electrical methods have frequently been used for the location of salt beds and salt domes. Two methods are available for this purpose. The first is more of an indirect nature, determining the depth of salt-water beds around the dome; thus, the dome shows up as a "hole" in the electrical indication. Zuschlag<sup>(48)</sup> gives an example. The second is the electrical resistivity method, which has been used primarily by the Schlumberger company in their salt-dome investigations. Probably



the best known examples of their work are the resistivity depth data and resistivity maps, obtained on salt domes in Alsace.<sup>(49)</sup> The latter offered rather favorable conditions on account of the conductive marls covering the salt. Details of this work are available, in particular for the Hetten-schlag salt dome; Poldini<sup>(50)</sup> gives resistivity depth curves, Geoffroy<sup>(51,52)</sup> torsion balance and magnetic data. In addition to these salt domes, the Schlumbergers have tested domes on the Gulf Coast, in Rumania and Jugoslavia. Recently, Kelly<sup>(53)</sup> has applied a new development in electrical prospecting, the Zuschlag Ground Comparator, in work for the Solvay company near Syracuse, where salt beds in a depth between 700 and 800 ft. were traced.

The magnetic method has been used in Germany and Alsace on salt domes, but as far as reliability is concerned is much inferior to the seismic, torsion balance and resistivity methods.

#### NITRATES, PHOSPHATES, POTASH

To the writer's knowledge, there is nothing in the geophysical literature concerning prospecting for either nitrates or phosphates. It is doubtful whether any commercial work has been done. This is largely due to the oversupply of these two products; Chile has a nitrate supply adequate to supply the world's needs for generations, and the phosphate deposits in the western United States are so extensive that they can supply the world's demand for centuries. Geologic conditions being suitable, it would seem that either electrical or seismic methods would be best adapted for prospecting for these minerals.

In regard to potash, the situation is somewhat different, as the commercially important potassium minerals occur with the salts; therefore the seismic, torsion balance and electrical methods, mentioned before for the location of salt, have found frequent application in the indirect location of potash deposits. In this connection, attention may again be directed to the extensive work done by Siñeriz<sup>(4)</sup> on the potash deposits of Callus, Suria, Sallent, Bellmunt and Navarra, in Spain.

Recently, investigations have been made which seem to offer the possibility of locating potash salts directly underground. About three years ago, it was discovered<sup>(54)</sup> that potassium gives forth a penetrating gamma radiation, which induced Kohlhoerster<sup>(55)</sup> to carry on extensive experiments underground in the potash mines of Stassfurt, in Germany. He found that the older and younger salt group were distinctly different in their reactions, the older group giving the stronger radiation, being richer in potassium. Kohlhoerster investigated also a number of potassium salts, ranging from 9 to 50 per cent metallic potassium, and found their activity in each case proportional to the amount of potassium contained. This discovery may point a way, in the future, to scientific soil investigation by radioactive methods, in order to determine the



fertility of various types of soils, as the penetrating radiation should be proportional to the potassium content of the soil.

## BUILDING AND ROAD MATERIALS

In this branch of the nonmetallic field, geophysical methods promise to play a very important part in the location of road and ceramic building materials and the investigation of civil engineering problems. A distinct classification of these subjects being difficult to give, the cement materials will be discussed first followed by gravel, sand and clay, building and road stone; and, finally, the use of geophysics in excavation and foundation work.

### *Cement Materials*

Although there are no descriptions as yet in the literature of geophysical methods having been applied for the specific purpose of locating cement material, many data are available, which were incidental to results obtained for different purposes and which point the way to the possibilities in this respect. For instance, it is evident from a number of geophysical data that gypsum possesses outstanding physical characteristics, such as high speed of elastic waves and great resistivity, which would recommend the electrical and seismic methods as probably the most advantageous for the location of this material. The high speed of elastic waves in gypsum (and anhydrite) has been established by various authors in seismic observations; for instance, by Schweydar and Reich<sup>(56)</sup> on the salt dome of Sperenberg, Germany, by R. Ambronn,<sup>(57)</sup> by Sokolov,<sup>(43)</sup> and by the numerous, unpublished results of seismic prospecting for salt domes. Practically the same is assumed to hold for electrical methods, although the literature contains but few specific examples. Anhydrite excels by its specific gravity, as evidenced by its effect, combined with that of limestone, in the caps of salt domes upon the torsion balance,<sup>(58)</sup> but it is doubtful whether torsion balance measurements will prove of practical value in the location of cement material. Gypsum and anhydrite occasionally may produce pronounced negative magnetic anomalies, particularly if they are near the surface and contrasted by formations of greater magnetic susceptibility,<sup>(59)</sup> but it is doubtful whether this would make magnetic measurements practicable for this purpose, in view of the greater reliability offered by seismic and electric measurements.

The physical properties of lime materials depend so much on their petrographic constitution and geologic occurrence that the choice of a geophysical method for their location is very much a matter of the individual case. However, as a general rule it may be said that probably electrical and seismic methods will prove to be more practical than others. As far as limestone in particular is concerned, experience with seismic and

electrical methods proves beyond doubt that it may be readily located, and its depth under cover determined with accuracy. As examples, reference may be made to the results published by Ambronn,<sup>(60)</sup> by Hanneman,<sup>(61)</sup> and Shaw,<sup>(62)</sup> by Schweydar and Reich,<sup>(56)</sup> and by Rankine<sup>(40)</sup> in regard to the effect of limestone on seismic travel time. The stratigraphic and structural investigations made by Schlumberger with resistivity methods, particularly those published for the May, Soumont, Toulouse and Sees syncline,<sup>(11)</sup> contain ample material for the electrical effect of limestones as contrasted with sands, clays, marls, etc. Likewise, Hubbert<sup>(63)</sup> found Devonian limestone of high resistivity under less resistant Mississippian shales, and Poldini<sup>(50)</sup> highly resistant Mississippian limestone under less resistant Pennsylvanian shales.

Often cement material is obtained from Cretaceous chalk deposits; if the problem arises to determine their extension under cover, or to locate new deposits in the vicinity, the electrical resistivity methods should prove to be the most practical for such purpose. Next in order of practicability would probably be the seismic method. Deposits of this type have also occasionally produced negative magnetic effects, particularly with overburden material of greater magnetic susceptibility.<sup>(64)</sup> Thus, by a magnetic reconnaissance, the location of thinnest overburden could be determined, but it is doubtful whether the information obtained with the magnetic method would compare with that furnished by the resistivity method.

In some cements, tuffs and bauxite are used. No information seems to be available in the literature regarding the electrical effect of tuffs, but it would appear on the face of it that electrical measurements would be the most suitable. The application of geophysics to the location of bauxite is treated elsewhere in this paper.

### *Gravel, Sand and Clay*

The recent geophysical literature contains a number of good examples for the location of these materials. The conductivity contrast of sand (or gravel) and clay makes the electrical resistivity methods particularly suitable; sand and gravel generally have a high electrical resistivity and clays have a low one. Second in the order of preference would probably be seismic methods, although they would be costlier and perhaps slower in the field application than electrical methods. Gravel deposits occurring as channel fills could be located by the torsion balance, but this method is too slow and costly; sometimes magnetic methods are applicable to the same problem (Figs. 4 and 5), if the bedrock is more magnetic than the channel material, and if the channel does not contain extensive concentrations of magnetite that would make the response curves too irregular.

Highway departments and geological surveys of various states in the Union have begun to recognize the value of geophysical surveys for the

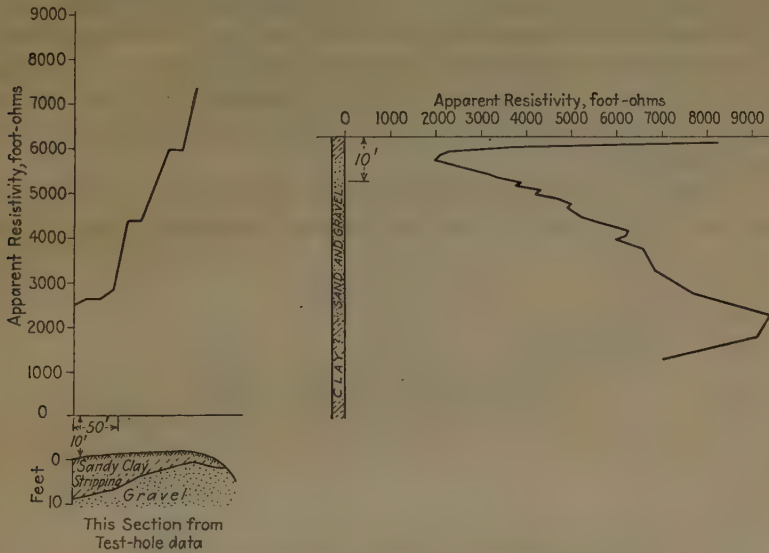


FIG. 1.—HORIZONTAL AND VERTICAL RESISTIVITY PROFILES ON A GRAVEL PROSPECT IN MINNESOTA. (Courtesy of Mr. Stanley W. Wilcox.)

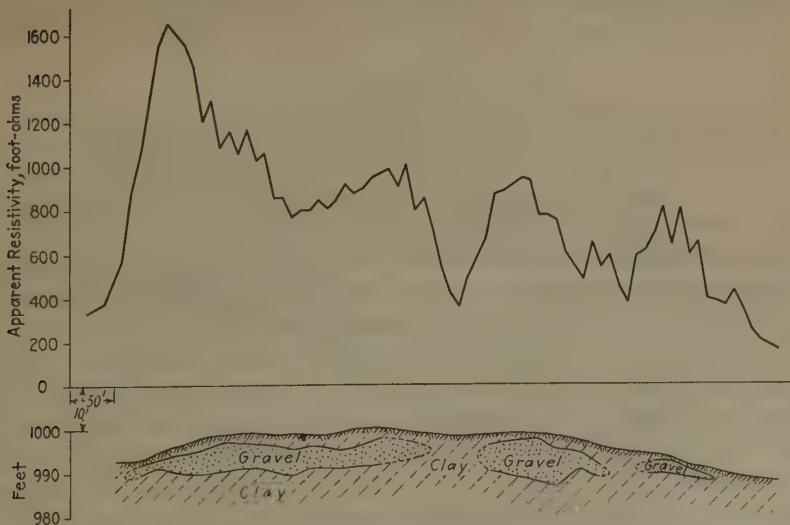


FIG. 2.—RESISTIVITY PROFILE AND SUBSURFACE SECTION ON A GRAVEL PROSPECT IN MINNESOTA. (Courtesy of Mr. Stanley W. Wilcox.)

Subsurface section below earth-resistivity step traverse is taken from an independent survey reconstructed from test-hole data.

location of deposits of road material and bedrock depth determinations, in order to determine the amount of excavation or filling required for

highways, railroads, bridges, tunnels and irrigation projects. The Conservation branch of the United States Geological Survey, the United States Bureau of Reclamation, the Geological Survey of Missouri, the State Highway Department of Minnesota, the Illinois Geological Survey, the Metropolitan Water District of Southern California, and the Department of Railways and Canals of Canada are among those that have been using or are using electrical resistivity methods as a part of their regular survey program.

Through the courtesy of Mr. Stanley W. Wilcox, of the State Highway Department of Minnesota, it has been possible to reproduce here a number

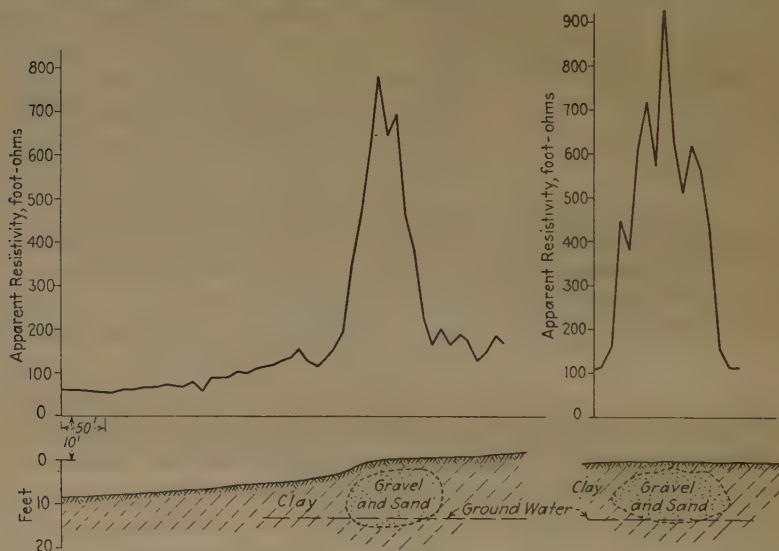


FIG. 3.—TWO RESISTIVITY PROFILES, AT RIGHT ANGLES TO ONE ANOTHER, ABOVE A GRAVEL POCKET IN MINNESOTA. (Courtesy of Mr. Stanley W. Wilcox.)

of examples (Figs. 1 to 3) of resistivity surveys for gravel, demonstrating without further explanation the value of electrical geophysical surveys for the location of road materials. The surveys shown in Figs. 4 and 5 were not made to locate road material but to locate auriferous gravel channels in California, and are reproduced through the courtesy of Mr. Ellsworth of the Pacific Section of McBride, Inc. However, they demonstrate the possibilities of magnetic measurements in the location of gravel deposits.

As stated above, the recent geophysical literature contains more examples of application of electrical methods to the location of sands, gravel and clays. The report of the Missouri Geological Survey<sup>(65)</sup> deals with electrical determinations of depth of overburden, and determination of thickness of clay beds with resistivity methods. The Illinois Geological Survey has published<sup>(63)</sup> a number of results that clearly demonstrate the possibility of locating gravel deposits by resistivity peaks in glacial till. A recent circular of information of the Bureau of



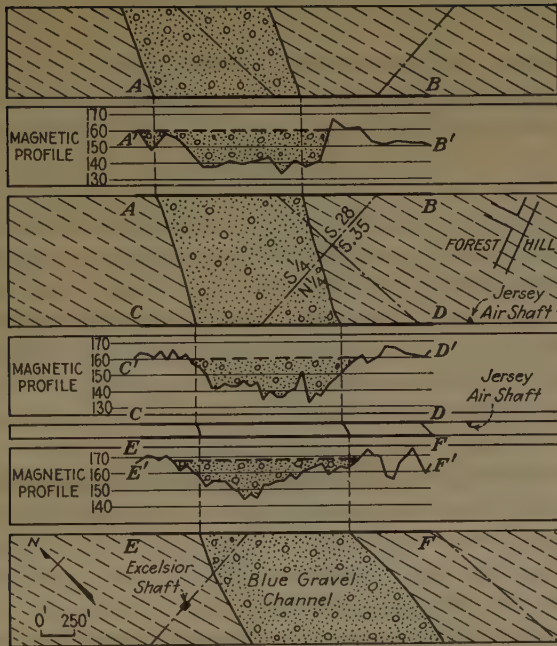


FIG. 4.—THREE MAGNETIC PROFILES AND MAP OF BURIED, AURIFEROUS, "BLUE GRAVEL" CHANNEL IN THE FOREST HILL DIVIDE, PLACER CO., CALIF.

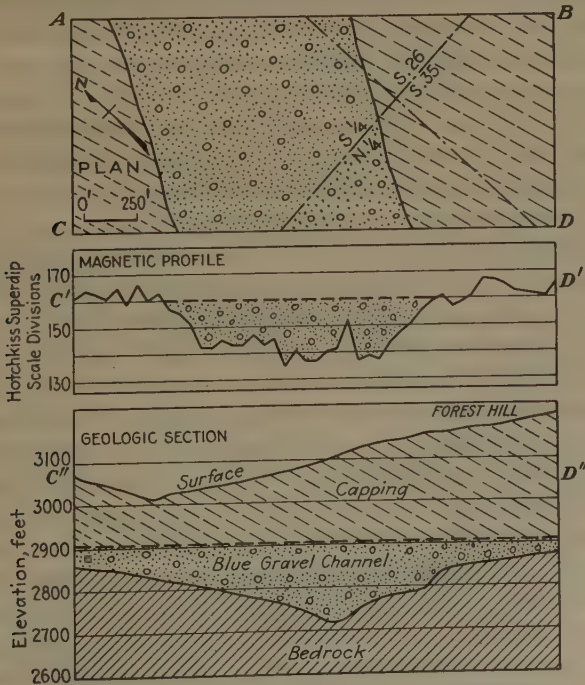


FIG. 5.—FOURTH MAGNETIC PROFILE, MAP AND GEOLOGIC SECTION OF SAME LOCALITY.  
(Figs. 4 and 5 courtesy of Mr. E. W. Ellsworth.)

Mines,<sup>(67)</sup> deals likewise with the subject of geophysical prospecting for gravel deposits.

The location of gravel channels by other geophysical methods, such as seismic and torsion balance, will be discussed later on under the heading of civil engineering applications.

### *Building and Road Stone*

There are but few articles in the geophysical literature in which the results of surveys for the location of building or road material is described; however, the problem is of such nature that its possibilities may be readily derived from the results of surveys that were conducted for different purposes. As far as the order of choice of methods is concerned, electrical resistivity methods would probably rank first, with magnetic second and seismic third, or possibly second, depending on the physical properties of the stone.

With an increasing amount of experience in the application and interpretation of resistivity measurements, it has been possible for the Schlumberger company, according to Kelly's report,<sup>(68)</sup> to correlate resistivity values with the degree of alteration of the material and absorption of moisture. The same company has recently carried out<sup>(53)</sup> resistivity measurements in Algeria in search for plugs of opelite to be used for road material. The greater the electrical resistivity of a building material, the smaller is generally its degree of alteration and its moisture content. Clastic rocks also generally have a smaller resistivity than crystalline materials, making it possible to differentiate, for instance, between sandstones and limestones by resistivity measurements. In this manner, the thickness of the sandstone cover above the limestone of the Mammoth Cave in Kentucky was determined.<sup>(69)</sup> Generally speaking, any change from one rock type to another, and any change in the composition of any given type of rock, may be detected under favorable circumstances by the resistivity method, particularly if the deposits occur close to the surface; especially, by a method that reacts to very small differences of conductivity, the Racom or potential-drop-ratio method.<sup>(70)</sup>

Next to the electrical method, magnetic methods of prospecting will be the second choice in exploration for road stone in most cases, because rocks that are preferable from the standpoint of road materials are usually magnetic. Igneous rocks are generally preferred to sedimentary rocks. In regard to toughness, the order is about as follows: basic plutonic and volcanic rocks, rhyolites and quartz porphyries, gabbros, granites and syenites. As to abrasive resistance, the order is: diabase and basalt, diorite and basic plutonic rocks, then acidic rocks. As is evident from the order of basic as compared with acidic rocks in respect to practically all three characteristics, the basic rocks are preferable. Field experience and laboratory tests of susceptibilities of igneous rocks have shown,

furthermore, that basic igneous rocks are generally more magnetic than the acidic, because of the greater abundance of magnetite. Therefore, magnetic methods seem to be well suited for reconnaissance prospecting for road material and have also often been applied for detail work. Schroeder and Reich<sup>(71)</sup> investigated a basalt quarry and found that the desired and unaltered portions of the material corresponded to positive magnetic anomalies while shattered zones and clay seams appeared to produce negative anomalies. Kelly<sup>(68)</sup> reports that Mason, Slichter and Gauld recently used the magnetic method extensively in prospecting for trap rock and for determining the thickness of the dike and the thickness of cover. Ahrens<sup>(72)</sup> conducted magnetic surveys in the volcanic area of the Eiffel in Germany, partly for the quarry industry there.

The literature on magnetic results above igneous rocks is much more extensive than these few references to measurements made for the specific purpose of locating road materials would seem to indicate. Brief reference may be made to some of the more important publications. Haalck<sup>(73)</sup> has given a summary of most of the magnetic surveys that have been made on igneous rocks; G. Meyer, on basalts in the Kaiserstuhl area, H. G. Wolff on serpentine and basalt in the Zobten Mountains, Brunhes and David on basalts of the Puys de Dome, E. Schaper on the basaltic Ottilien Mountain in Thuringia, Nippoldt and Schering on basalts of the Vogelsberg in Hessen, Goellnitz on basalts in the Lausitz, Krahmann on basalts in the Habichtswald, Keraenen on basic extrusives in northern Finland, Ljungdahl on the same types of rocks in southern Sweden. Other measurements on basalt and other basic igneous rocks, not mentioned by Haalck, include those made in Italy by Folgeraiter and Palazzo, by Broderick on gabbros in Duluth, by Locke, Hotchkiss, Aldrich, Stearns and Smyth in the Lake Superior region,<sup>(74)</sup> by Kegel<sup>(75)</sup> on the Lahn Dill district diabases, by Roessiger and Puzicha<sup>(76)</sup> on diabase dikes in the Harz mountains, by Gilchrist<sup>(77)</sup> on quart diabase at the Abana mine, by Schulze<sup>(78)</sup> on basic tertiary dikes in the Elbe-Sandstone area, by Meyer<sup>(79)</sup> who determined the location of brown iron ore in pockets of basalt, by Stoecke,<sup>(80)</sup> who surveyed the serpentine of the Frankenstein in Silesia, by Wilson<sup>(81)</sup> on the basaltic Valmont dike, by Hallimond<sup>(82)</sup> on the Swinnerton dike (also surveyed with the torsion balance), and by Levings,<sup>(83)</sup> who surveyed the basaltic Ralston dike near Golden, Colo. The citation of all this literature is made in order to acquaint the operator not only with the possibilities but also with the limitations of magnetic work on basic rocks as well. For the distribution of the magnetic anomalies is in many cases not only controlled by the presence or absence of the igneous material and its degree of weathering, but also by the distribution of magnetite streaks, as the carefully correlated magnetic and petrographic investigations of Roessiger and Puzicha have shown,<sup>(76)</sup> and by abnormal magnetization, such as is produced by



lightning and by magnetostrictive effects. Therefore, it seems advisable to use the magnetic method with care and primarily as a reconnaissance method in the quarry industry, and follow up the findings with detail resistivity work.

The extensive magnetic work that has been done in prospecting for oil has yielded much valuable information regarding the magnetic effects of basic igneous rocks, only a small fraction of which has been published; for instance, the work of Wilson on basalt dikes in Mexico,<sup>(84)</sup> and the data obtained by Rieber<sup>(85)</sup> and Lynton<sup>(86)</sup> on basalt and gabbro dikes in California.

Thus far, only the magnetic work on basic igneous rocks has been discussed. The literature available on magnetic effects of acidic igneous rocks is much scarcer, probably because their effects are not nearly so noticeable as those of basic igneous rocks. Haalek<sup>(73)</sup> mentions the following studies of granitic rocks: by Paulsen in Bornholm, by Wolff in the Zobten area, by Goellnitz in Saxony, and by Nippoldt in the Harz mountains, the Odenwald and the Spessart. Recently, Buehler<sup>(66)</sup> directed considerable magnetic work in Missouri, by which porphyritic bedrock was traced.

Much information has been accumulated in magnetic oil prospecting, in connection with the magnetic effects of granite ridges, only a small fraction of which has, however, been published. As examples, the magnetic surveys of the Amarillo granite ridge<sup>(88)</sup> and of the Nocona field in Oklahoma<sup>(89)</sup> may be mentioned.

As third choice of geophysical methods for the location of road materials, the seismic method was mentioned above. If the magnetic method is used for reconnaissance, the seismic method would occupy second place for detail work. It seems to have great possibilities for the location of road materials, not only in determining the depth of cover but also the composition, alteration, and general nature of the material. Contrary to the magnetic method, it is well adapted to both igneous and sedimentary rocks. Comparatively little systematic work has been done along this line, but what has been done seems to indicate that the method has good possibilities. Leet and Ewing have conducted<sup>(90,91)</sup> a number of careful studies of the velocities of propagation of seismic waves in nepheline-syenite, granite, limestones and norite, and have correlated the dynamic constants of these rocks, determined by wave-speed observations, with static determinations of their elastic properties in the laboratory. This work, done by Harvard University, promises to yield important data in relation to the mechanical properties of building and road materials and the possibility of their determination. The experience actually obtained in regard to speed of propagation of seismic waves in various igneous and sedimentary rocks has been much greater because the refraction method has been used extensively in prospecting



for oil. Practically nothing has been published regarding data so obtained on igneous rocks; only Rieber<sup>(85)</sup> gives an example of the location of basalt plug by seismic methods and later conformation by the drill.

Information that may be useful in this connection, on the location of hard road and building material by seismic methods, may also be obtained from the literature dealing with the application of the seismic method in coal mining and placer mining. As this has been, or will be discussed, it will not be necessary to elaborate upon it at this time.

As a matter of completeness it may be mentioned that torsion balance observations<sup>(92)</sup> have been applied in studies of dikes of igneous rocks, but this method is too slow and costly in comparison with magnetic, electrical and seismic work in prospecting for road or building stone, so that it is not recommended for this purpose.

### *Geophysics in Civil Engineering*

The application of geophysical methods in various phases of civil engineering, such as the planning and construction of highways, railroads, bridges, tunnels and dams, with their concomitant excavation, filling and material problems, is closely related to the problem of location of road and building material. A brief reference to this work will be sufficient because a number of comprehensive studies are readily available in the literature.<sup>(93-97)</sup>

As stated on page 560, geological surveys and highway departments of various states in the Union and in Canada are beginning to avail themselves of geophysical methods, the resistivity and potential-drop-ratio methods in particular, in highway, railroad, tunnel and dam foundation work. The Bureau of Reclamation has just completed its resistivity studies at a dam site on the Columbia River at Grand Coulee, and has been working on various other projects in the West with which the writer has been in indirect contact. A number of private enterprises, such as power and railroad companies, have applied geophysics to their civil engineering problems in the past years; for instance, the New England Power Association, the Electric Railway Company of British Columbia, the Metropolitan Water District of Southern California, the James MacLaren Company, and others.

There is hardly much doubt about the order of choice of methods in this work. First, the resistivity and potential-drop-ratio methods; second, the seismic method, and last, either the magnetic or the torsion balance method. The last two named cannot compare in practicability with the electrical and seismic methods; the magnetic on account of uncertainty of interpretation, the torsion balance on account of slowness and difficulty with topography.

Most of the outstanding examples of the possibilities of electrical prospecting in foundation work are contained in the publications referred

to above.<sup>(93-97)</sup> In addition, Hubbert<sup>(63)</sup> reports on some interesting studies performed for the Illinois Geological Survey, and Buehler<sup>(65)</sup> on some work in Missouri. Again, the number of practical applications made is probably greater than the number of studies published.

The application of the electrical resistivity methods rests upon the fact that in most foundation problems the covering materials, such as glacial till, clay, sands and gravels, have generally a lower resistivity than the harder bedrock below, which, in most cases thus far investigated, consisted of igneous or metamorphic rocks, limestones, quartzites, or materials of similar properties suitable for foundation work.

Likewise, the cover and bedrock materials usually show a marked contrast of elastic-wave speed which makes the application of seismic refraction methods suitable for this purpose. Edge and Laby<sup>(3)</sup> report about such depth determinations of slate and granite under alluvium, Ambronn<sup>(98)</sup> on studies of gneiss under alluvium; the prospectus of the Geophysical Company, Ltd.<sup>(99)</sup> shows the results obtained by seismic methods in locating a river channel in limestone, as correlated with torsion balance results.

As a last choice, the torsion balance is applicable to the location of gravel channels in more dense rock, for which there are a number of examples in the geophysical literature. The writer has published the results obtained by a torsion balance traverse on a gravel channel in the Rhine valley,<sup>(100)</sup> McIntock and Phemister<sup>(101)</sup> on a survey made with the torsion balance on the buried Kelvin Valley near Drumry, and Weinzierl has discussed<sup>(102)</sup> the difficulties encountered in oil prospecting with the torsion balance by such hidden river channels.

Under favorable circumstances, the magnetic method may be used for reconnaissance in the location of channels, if the bedrock is more magnetic than the channel material (Figs. 4 and 5), or if the channel, owing to magnetite concentrations, is accompanied by magnetic anomalies of such regular distributions that it may be readily traced.

#### LOCATION OF GROUND WATER

The possibility of applying geophysical methods to the location of ground water follows logically from their use in civil engineering work, which rests primarily on the effect of pore water on the electrical resistivity of rocks, and suggests that electrical resistivity or potential-drop-ratio methods would be the first choice for such work. As a second choice, the seismic methods may be applicable in limited cases.<sup>(97)</sup>

The location of ground water by geophysical methods is still in its infancy. In the present state of development, the electrical prospecting for ground water can hardly be called a direct method; for the water does not occur underground as an independent medium, as a pyrite lens may occur in the mother rock, but it occurs in the pore spaces in various types of

rocks, the resistivity of which then is determined by the relative pore volume, and the electrical conductivity of the liquid. These factors have been discussed in detail by Sundberg.<sup>(104)</sup> Therefore, depending on the salinity of the water, water-bearing formations may act electrically very differently in different areas. At the present time, electrical search for water, with a few exceptions, is classed as a structural problem rather than as one of a direct location. The complexity of the situation, and the possibility of various electrical and other methods, is well illustrated in Koenigsberger's recent article on geophysical location of water.<sup>(103)</sup>

The first published account of the possibilities of the location of water-bearing formations was given by Hotchkiss, Rooney and Fisher.<sup>(105)</sup> Edge and Laby<sup>(3)</sup> made a number of water studies in Australia and found that saline waters could be fairly well located, but that the indications obtained from fresh waters were indefinite. Loehnberg and Stern<sup>(106,107)</sup> investigated the water problem in the Karst area and obtained rather significant curves, which appeared to indicate that a drop in apparent resistivity coincided generally with the water-bearing cavities. The problem then was taken up on a larger scale by C. M. Tattam,<sup>(108)</sup> who obtained, in most instances, curves that showed the opposite trend from those observed by Stern; namely, curves corresponding to the three-layer case in the theory of apparent resistivity on horizontal beds. Similar curves have also been obtained<sup>(109)</sup> in a number of other areas, and with all due regard to the variations possible by the changing geologic conditions from one area to another, it cannot be denied that this type of curve has been observed more frequently than others, corresponding to the fact that certain general conditions are responsible for the occurrence of ground water more frequently than others. For determining the depth to water-bearing strata, the potential-drop-ratio method seems to give more definite reactions than the resistivity method, for which an example has been given by Lundberg and Zuschlag.<sup>(70)</sup> Kelly<sup>(53)</sup> reports that electrical methods have been recently applied by the Schlumberger company in Tunis for the purpose of outlining an artesian water supply. This study probably has been conducted as a structural problem. Another example of the possibilities of structural geophysical studies in the indirect location of ground water has been described by Buehler.<sup>(66)</sup> In Missouri, the trend of the porphyritic basement could be followed by magnetic methods under a cover of dolomite sediments from 200 to 300 ft. thick, and it was found that these sediments, owing to more intense fracturing, carried more water on the flanks of the porphyry highs.

Greater water content of formations increases generally their elastic-wave speed, and one case has become known<sup>(97)</sup> where it has been possible to determine the depth of the ground water by seismic refraction work. The possibilities of seismic work in structural search for ground water have not been exhausted. It appears probable that the reflection method



will be perfected some day to such an extent as to be applicable to the determination of the depth of shallow discontinuities, and then the seismic method should be a valuable adjunct to electrical work in civil engineering and search for ground water. Some time ago the Michigan College of Mines experimented with geophones for the location of the water table but the results have not been published. It is possible that continuous waves and interference methods may have to be used to determine shallow depth by acoustic or seismic reflections.

In this connection a few words may be said about the use of geophysical methods for the investigation of mineral springs. Radioactive methods have found an extensive application in the testing of the activity of spring waters for medicinal purposes. Ambronn<sup>(74)</sup> and Beyer<sup>(110)</sup> have compiled the references on this subject.

#### ABRASIVES

Diatomaceous earth, tripoli, pumice, quartz, sand and sandstone, grindstones, millstones, oil and rotten stones, garnet, emery, and corundum are generally classed under abrasives, in addition to the artificial materials, which are not under discussion here. So far, the writer knows of no geophysical work that has been done for the location of such materials. The statements made before about road and building materials apply to sand, sandstone and millstone material, and the electrical method would probably be best in such cases. The same would hold for work on deposits of diatomaceous earth.

#### MATERIALS OF VARIOUS INDUSTRIAL USES

*Fuller's Earth.*—So far as the writer knows, no geophysical work has been done on such deposits. What has been said before about the electrical effect of clay materials should apply.

*Fluorspar.*—It is reported that a good deal of research work has been done in order to determine the applicability of geophysical methods to the location of fluorspar deposits, and M. K. Hubbert has done some field work with resistivity methods on the deposits near Rosiclare, Ill. (See p. 40, this volume.) Although fluorspar is often associated with small amounts of galena, probably this will not affect the conductivity appreciably. However, as fluorspar is frequently found on fissure and fracture zones, indirect structural prospecting for these zones may apply. If these fracture zones are filled with mineral waters, various electrical methods will be found suitable to trace them.

*Talc and Soapstone.*—The Elbof electromagnetic method was applied on the graphite and talcum deposits near Affenz, Austria,<sup>(111)</sup> and it was found that the talc reacted as a poor conductor, the contrast being enhanced by adjacent graphite deposits. Therefore, it appears that the more quantitative methods for detecting differences in conductivity—



the resistivity and potential-drop-ratio methods—should be applicable to similar problems.

*Lithographic Stone.*—Nothing has been published about applications of geophysics to the location of lithographic stone; however, the statements made above in regard to the location of road and building materials should apply, the first choice being electrical methods.

*Sand.*—The use of sand for paving, building and abrasion purposes was discussed before, and methods suggested for its location. The same applies for the other industrial uses of sands; namely, for the manufacture of glass, for molding, filtering, and furnace use.

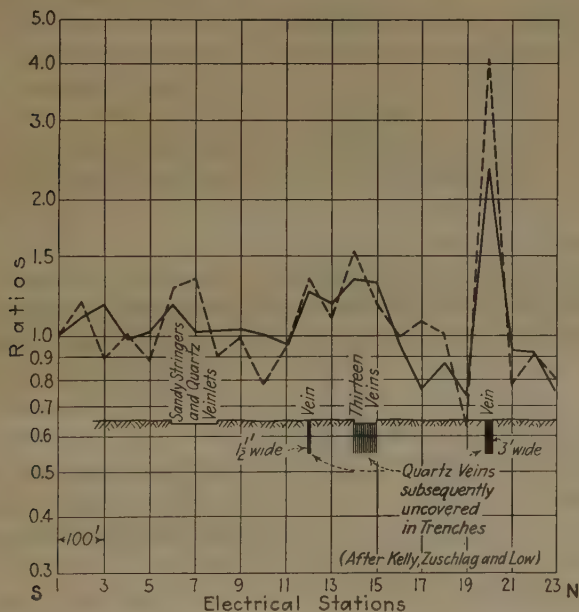


FIG. 6.—POTENTIAL DROP RATIO SURVEY OF QUARTZ VEINS IN MCDUFFIE CO., GEORGIA.

*Monacite Sands.*—Nothing has been published about application of geophysics to the location of monacite, and neither is it known whether or not radioactive methods would, on account of the thorium in these sands, help to locate concentrations. However, geophysics would be applicable in an indirect way to locate the course of the channels, by using the method discussed before under the heading of civil engineering applications.

*Serpentine.*—The most pronounced physical property of serpentine in regard to adaptability to geophysical work is its fairly high magnetic susceptibility. A number of magnetic surveys for the location of serpentine have been discussed before.<sup>(11,80,112,113)</sup> However, the magnetic susceptibility of serpentine is subject to a great deal of local variation, so

that the magnetic method probably would be useful only for reconnaissance, to be supplemented by electrical or possibly seismic measurements.

*Barite.*—The high density of barite should make the torsion balance particularly suitable for the location of barite dikes, provided the topography is suitable. Work of this type is reported to have been done but the writer has been unable to find anything concerning such measurements in the literature. Nothing seems to have been published concerning the electrical conductivity of barite; it should be a poor conductor and might be located in more conductive rocks in a manner similar to the location of quartz dikes by the potential-drop-ratio method, as demonstrated by Hedstrom<sup>(115)</sup> and by Kelly<sup>(124)</sup> (Fig. 6). On the other hand, if barite occurs together with conductive minerals such as pyrite, it may be located indirectly by any electrical method, as done by Mueller.<sup>(114)</sup>

*Graphite.*—Graphite often is an unwelcome conductor, which has made interpretation of electrical measurements difficult in a good many surveys. A number of writers have commented upon this fact. If it occurs in commercial deposits, the logical method to apply is the electrical method. The measurements of the Elbof<sup>(111)</sup> on the graphite deposits near Aflenz, Austria, have already been discussed. At Port Lincoln, South Australia, Edge and Laby<sup>(3)</sup> have investigated a graphite deposit in pre-Cambrian rocks. The equipotential line method was found not to give any definite reactions; however, when the potential-drop-ratio method was applied, the boundaries of the deposit could be recognized, both in the phase and the potential anomalies. Eve and Keys<sup>(116)</sup> have demonstrated the effect of graphitic slate upon the resistivity data, which would suggest that the resistivity method should be suitable for location of graphite deposits. Slichter<sup>(117)</sup> calls attention to the fact that graphite also produces strong self-potentials, which usually are observed in the form of positive reactions.

*Magnesite, Feldspar, Asbestos, Mica.*—Nothing has been published regarding experience obtained with geophysical methods on these mineral deposits. Their mode of geologic occurrence would suggest that any application of geophysical methods (probably magnetic or electrical) would have to be of an indirect nature.

*Bauxite, Beryl, Chromite.*—These minerals are classed together because sometimes they have been classified as nonmetallic minerals. The more common usage today, however, is to class them as metallic minerals. Some information regarding the use of geophysics is available on bauxite and chromite.

Bauxite usually is derived from basic igneous rock, therefore all methods applicable to the location of igneous rocks may be used as a means of indirectly locating such deposits. In central Arkansas, bauxite is found as a product of weathering of nepheline-syenite plugs, which

have been surveyed by Stearn<sup>(118)</sup> with the magnetic method. Leet<sup>(119)</sup> states that seismic work has been done on them.

Owing to the great present commercial importance of beryllium, it would be a good fortune if some geophysical method could be used to locate beryllium deposits. Nothing has been published regarding it, and the chances are not great on account of the small quantities involved. However, indirect methods may be devised for certain areas, for indirect structural applications. Recently, a penetrating gamma radiation for beryllium<sup>(120)</sup> has been discovered; whether this will make possible the direct radioactive location of the mineral appears to be doubtful.

Geophysical location of chromite has actually been attempted. Lundberg<sup>(123)</sup> states that it is a very poor conductor, but that it has been possible to locate it near the surface in Sotu, Rumania, by electrical measurements.

### PRECIOUS STONES

Under this heading, usually diamonds, emerald, opal, pearl, ruby and sapphire are classed as precious stones and agate, beryl, coral, garnet, jade and others as semiprecious. The direct location of gems by geophysical methods appears to be out of the question. To what extent an indirect location of the formation in which they occur would be useful depends on each case.

Information regarding indirect geophysical prospecting for gems is available only for diamonds. In Pike County, Arkansas, diamonds are found in peridotite plugs. Stearn<sup>(121)</sup> has carried out magnetic measurements in this area and shown that it is possible to locate these plugs fairly accurately under 3000 ft. of cover. Whether a similar method would be applicable in South Africa for the location of blueground appears to be very doubtful, according to Reich,<sup>(122)</sup> on account of the small susceptibility of this type of rock.

A small portion of diamond production is obtained from sands and gravels in stream and beach deposits, and, if it is at all a question of locating or tracing the extension of such gravel channels, the methods discussed before under the heading of civil engineering uses of geophysics should be applicable.

### CONCLUSION

In the foregoing summary, not all minerals of the nonmetallic field have been covered, but a good many of minor commercial or minor geophysical importance have been left out. After all, it must be realized that the main factor that determines the necessity for the application of a geophysical method is the demand for new deposits; a great many minerals and deposits are present, either at any given locality or in any given country, in such abundance or in such extent that a geophysical survey

would not be necessary, not even at the smallest cost, no matter how favorable the geological or physical conditions may be.

On the other hand, where mineral deposits are concerned for which there is a demand and on which geophysical measurements have been made, the chances are that much more commercial work has been done than is published in the literature, or has become known indirectly. In order to make this summary of value to the practical operator engaged in any branch of the nonmetallic industry, the writer will welcome any discussion or criticism intended to make the material more complete.

### BIBLIOGRAPHY

1. E. De Golyer: Choice of Geophysical Methods in Prospecting for Oil Deposits. *Trans. A.I.M.E.* (1932) **97**, 9-23.
2. C. A. Heiland: Elements of Geophysical Prospecting. Colo. School of Mines *Quarterly* (1933) **28** (4).
3. A. B. B. Edge and T. H. Laby: Principles and Practice of Geophysical Prospecting. Imperial Geophys. Survey Rept. Cambridge, 1931.
4. J. G. Siñeriz: Los metodos geofisicos de prospeccion. *Inst. Geol. y Minero Espana* (1928) **X** (3).
5. J. G. Siñeriz: La interpretacion geologica de las mediciones geofisicas applicadas a la prospeccion. *Inst. Geol. y Minero Espana Mem.* (1933).
6. H. Lundberg: Discussion. *Trans. A.I.M.E.* (1929) **81**, 39.
7. E. G. Leonardon: Discussion. *Trans. A.I.M.E.* (1929) **81**, 40.
8. S. F. Kelly: Experiments in Electrical Prospecting. *Eng. & Min. Jnl.* (1922) **114**, 623.
9. J. Koenigsberger: Field Observations of Electrical Resistivity. *Trans. A.I.M.E.* (1929) **81**, 236.
10. F. Kossmat: Schwerkraftsanomalien und geologische Untergrundsstruktur in der norddeutschen Tiefebene. *Preuss. Geodaet. Inst. Veroeff.* (1931) **106** (5), 89-100.
11. C. and M. Schlumberger: The Method of the Ground Resistivity Map and its Practical Applications. *Can. Min. Met. Bull.* 226 (1931) 271-294.
- 11a. C. and M. Schlumberger: Electrical Coring. 2d Int. Drilling Congress, Paris, Sept., 1929.
12. O. Barsch and H. Reich: Seismische Arbeiten in Norddeutschland. *Beitr. phys. Erf. Erdrinde, Pr. Geol. L-A*, Berlin (1930) **3**.
13. O. Barsch and H. Reich: Ergebnisse seismischer Untersuchungen ueber den Schichtenaufbau von Norddeutschland. *Erg. Hefte angew. Geophysik* (1930) **1** (2), 165-189.
14. E. H. Neville: Communication Regarding the Application of the Mintrop Seismic Method to Coal Measures and Mineral Deposits. *Int. Congress Mines, Met. Appl. Geol.* (June, 1930) 309-311.
15. H. Shaw: Application of Geophysics to Mining with Special Reference to the Location of Faults. *Trans. Inst. Min. Engrs.* (1930) **79**, 130-145.
16. H. Quiring: Koennen Schweremessungen zur Vorbereitung und Ergaenzung von Schuerf und Aufschlussbohrungen im rheinisch-westfaelischen Steinkohlenbecken dienen? *Glueckauf* (1924) **37**, 807-811.
17. M. Matuyama: On the Gravitational Field at the Fushun Colliery, Manchuria. *Japan. Jnl. Astron. Geophys.* (1924) **2** (2), 91-106.



18. W. Petraschek: Verein Bohrtechn. *Ztsch.* (1923) 209.
19. O. Barsch: Ergebnisse von Schweremessungen bei Dorsten in Westphalen. *Erg. Hefte angew. Geophysik* (1932) 2 (1), 14-21.
20. H. Reich: Magnetische Messungen im Aachener und Erkelenzer Steinkohlenggebiet und ein Versuch ihrer geologischen Deutung. *Jahrbuch Pr. Geol. L-A.* (1926) 47 (1) 84-115.
21. A. Kaiser: Magnetische Messungen in Nordwestdeutschland. *Beitr. phys. Erforsch. Erdrinde* 2, Pr. Geol. L-A. (1930).
22. W. Wolff: Magnetische Messungen im Osthaz und seiner weiteren Umgebung. *Beitr. phys. Erforsch. Erdrinde* 5, Pr. Geol. L-A. (1931).
23. W. Stern: *Braunkohle* (1931).
24. L. Gilchrist: Study of Geophysical Methods, 1930. Can. Dept. Mines, Geol. Survey *Mem.* 170 (1932).
25. R. H. Hawkins: Application of Resistivity Methods to Northern Ontario Lignite Deposits. See page 76, this volume.
26. H. Lundberg: Discussion of reference 25, page 120, this volume.
27. W. Schweydar: Aufschlussmethoden im Bergbau mit der Drehwage. *Jahrbuch. Hall. Verb.* (1924) 4 (2).
28. E. G. Leonardon and S. F. Kelly: Applications of Potential Methods to Structural Studies. *Trans. A.I.M.E.* (1929) 81, 192.
29. R. Schumann: Ueber die Leistungen der Eötvös'schen Schwerewagen. *Bergbau und Huette* (1920) 1: *Oesterr. Monatsschr. Oeff. Baudienst* (1920) 5 and 6; (1922) 198.
30. H. Seblatnigg: Zur Aufsuchung von Verwerfungen mittels der Drehwage. *Braunkohle* (1929) No. 23.
31. H. Krahmann: Magnetische Untersuchung im Habichtswald bei Kassel als Ergaenzung der geologischen Kartierung. *Ztsch. prakt. Geol.* (1926) 34 (1), 11-14.
32. I. Kell: Electrometry Applied to the Experiments of Technical Soil Amelioration. *Inst. Pract. Geophys. Bull.* 14 (1928).
33. D. C. Barton: Eötvös Torsion Balance Method of Mapping Geologic Structure. *Trans. A.I.M.E.* (1929) 81, 416.
34. D. C. Barton: The Seismic Method of Mapping Geologic Structure. *Trans. A.I.M.E.* 81, 572-622.
35. B. McCollum and W. W. LaRue: Use of Existing Wells as an Adjunct to Seismograph. *Oil Weekly* (June 19, 1931) 62, 29-34.
36. T. B. Eby: Relation of Geophysics to Geology. *Econ. Geol.* (1932) 27, 245.
37. R. Ambronn: Die Anwendung der Geophysik im Talsperren und Wasserbau. *Jahrbuch. Hall. Verb.* (1921) 3 (2), 27-46.
38. J. Koenigsberger: Ueber den Nachweis wasserfuehrender Stoerungen unter Tage mittels geophysikalischer Methoden. *Kali* (1926) 353.
39. R. Ambronn: Geophysical Prospecting in Mining. English prospectus of Prospektion, Goettingen, 1929.
40. A. O. Rankine: Physics in Relation to Oil Finding. *Nature* (May 4 and 11, 1929).
41. E. E. Rosaire and O. C. Lester: Seismological Discovery and Partial Detail of Vermilion Bay Salt Dome, Louisiana. *Amer. Assn. Petr. Geol. Bull.* 16 (1932) 1221-29.
42. C. Schmidt: The Salt-dome Area West of Celle, Germany. *Jnl. Inst. Petr. Tech.* (1931) 17, 372-375.
43. P. Sokolov: Experiment of Applying Artificially Generated Elastic Waves to Problems of Geological Prospecting. United Geol. and Prosp. Service U.S.S.R. *Fasc.* 214 (1932).

44. H. Seblatnigg: Gravimetrische Untersuchungen in Mecklenburg. *Geol. Landesanst. Mecklenburg* (1930) **39** (5), 47-58.
45. D. C. Barton: Torsion Balance Survey of Esperson Salt Dome Liberty Co., Texas. *Amer. Assn. Petr. Geol. Bull.* 14 (1930) 29-43.
46. J. Logan: Comparison of Torsion Balance and Geological Interpretation of Outline of Blue Ridge Salt Dome. *Oil Weekly* (Oct. 11, 1929) 37-41.
47. B. Numerov: General Characteristics of the Gravitational Method of Prospecting According to the Field Work Done by the Former Geological Committee in 1925-1928. *United Geol. and Prosp. Service U.S.S.R. Trans.* (1931) No. 36.
48. T. Zuschlag: Mapping Oil Structures by the Sundberg Method. *Trans. A.I.M.E.* (1932) **97**, 151.
49. G. Carrette and S. F. Kelly: Discovery of Salt Domes in Alsace by Electrical Exploration. *Trans. A.I.M.E.* (1929) **81**, 211.
50. E. M. Poldini: Les Sondages Electriques. *Bull. Tech, Suisse Romande Lausanne* (1932).
51. P. Geoffroy and P. Charrin: Etude Géologique par les Méthodes Géophysiques. *Cart. Geol. Alger. Bull.* (1932) **1** (4), 193.
52. P. Geoffroy and others: Results of Magnetic Measurements Made upon the Rock Salt Mass of Hettenschlag, Upper Rhine. *Of. Nat. Combust. Liq.* (Nov. Dec. 1929) **4** (6), 1015-1021.
53. S. F. Kelly: Geophysics in the Metallic and Nonmetallic fields. *Min. & Met.* (Jan., 1934) 37-38.
54. H. Behounek: Gamma Rays of Potassium. *Nature* (1930) **126**, 243.
55. W. Kohlhoerster: Gamma Strahlen an Kaliumsalzen. *Ztsch. Geophysik* (1930) **6** (½), 341-357.
56. W. Schweydar and H. Reich: Kuenstliche elastische Bodenwellen als Hilfsmittel geologischer Forschung. *Gerland's Beiträge* (1927) **17** (1), 121.
57. R. Ambronn: Fig. 19, English prospectus of the Prospektion.
58. A. Birnbaum: Drehwagenmessungen im Salzbergbau ueber und unter Tage. *Kali* (June 15, 1924) **18**, 144-148.
59. C. A. Heiland: Instruments and Methods for the Discovery of Useful Mineral Deposits. *Eng. & Min. Jnl.* (1926) **121**, 47-58.
60. R. Ambronn: Figs. 19, 21, 27 of English prospectus of Prospektion.
61. M. Hannemann: Ueber die seismischen Aufschlussmethoden und ihre Anwendung in der Praxis. *Ztsch. prak. Geol.* (1927) **35**, 168-173.
62. H. Shaw: A Field Test with a New Seismograph. *Min. Mag.* (April, 1930) 201-214.
63. M. K. Hubbert: See page 9, this volume.
64. R. Krahmann: *Abh. prakt. Geol.* (1926) **3**.
65. H. A. Buehler: Biennial Report of Missouri Bureau of Geology and Mines (1931) 15-16, and App. III.
66. H. A. Buehler: Biennial Report etc. (1933) App. IV.
67. J. R. Thoenen: Prospecting and Exploration for Sand and Gravel. *U.S. Bur. Mines Inf. Circ.* 6668.
68. S. F. Kelly: Geophysics in the Mining and Geological Fields. *Min. and Met.* (Jan., 1933) 30-31.
69. A. S. Eve and others: Geophysical Investigation of Mammoth Cave, Kentucky and Sudbury Basin, Ontario. *Can. Geol. Survey Mem.* 165 (1931).
70. H. Lundberg and T. Zuschlag: A New Development in Electrical Prospecting. *Trans. A.I.M.E.* (1932) **97**, 47-62.
71. R. Schroeder and H. Reich: Magnetische Untersuchung eines Basaltsteinbruchgelaendes. *Erg. Hefte angew. Geophysik* (1931) **1** (4), 432-436.

72. W. Ahrens: Ergebnisse magnetischer Untersuchungen im Vulkangebiet des Laacher Sees in der Eifel. *Erg. Hefte angew. Geophys.* (1932) **2** (4), 320–336.
73. H. Haalck: Zur Frage der Erklarung der Kursker magnetischen und gravimetrischen Anomalie. *Gerland's Beiträge* (1929) **22** (34), 214–255, 385–399.
74. R. Ambronn: Elements of Geophysics. New York, 1928.
75. W. Kegel: Erdmagnetische Messungen im Lahn-Dill Gebiet. *Pr. Geol. L.-A. Sitz. Ber.* (1929) 459–65.
76. M. Roessiger and K. Puzicha: Magnetische Messungen am Oberharzer Diabaszuge. *Erg. Hefte angew. Geophysik* (1932) **3** (1), 45–108.
77. L. Gilchrist: Magnetic Survey of Abana Property. *Can. Geol. Survey Mem.* 165, 48.
78. E. G. Schulze: Magnetische Vermessung einiger tertiarer Eruptivgaenge und Stoecke im saechsischen Elbsandsteingebirge. *Ztsch. Geophysik* (1930) **6**, (3), 141–156.
79. G. Meyer: Magnetische Messungen ueber Basalteisensteinlagern in Oberhessen. *Erg. Hefte angew. Geophysik* (1931) **1** (4), 420–431.
80. K. Stoecke: Magnetische Z-Variometermessung am Serpentin von Frankenstein in Schlesien. *Erg. Hefte angew. Geophysik* (1931) **1** (4), 457–468.
81. J. H. Wilson: Brunton Compass Attachment for Measurement of Horizontal Magnetic Intensity. *Amer. Assn. Petr. Geol. Bull.* 15 (1931) 1391–1397.
82. H. F. Hallimond: Magnetic Observations on the Swynerton Dike. *Min. Mag.* (July, 1929) 16–22.
83. W. S. Levings: A Magnetic Survey of the Ralston Dike, Jefferson County, Colorado. *Colo. School of Mines Quarterly* (1932) **27** (3), 30–34.
84. C. A. Heiland: Geophysical Prospecting, Principles and Recent Successes, 61.
85. F. Rieber: Choice of Geophysical Methods. *Min. and Met.* (June, 1930) 301–305.
86. E. D. Lynton: Some Results of Magnetic Surveys in California. *Amer. Assn. Petr. Geol. Bull.* 15 (1931) 1351–1370.
87. D. C. Barton: Belle Isle Torsion Balance Survey, St. Mary's Parish, La. *Amer. Assn. Petr. Geol. Bull.* 15 (1931) 1335–1350.
88. C. A. Heiland: Geophysical Methods of Prospecting. *Colo. School Mines Quarterly* (March, 1929) **24** (1).
89. C. A. Heiland: A Demonstration of the Geological Possibilities of Resistivity and Magnetic Prospecting Methods. *Terr. Mag.* (1932) **37** (3), 343–350.
90. E. D. Leet and M. Ewing: Velocity of Elastic Waves in Granite. *Physics* (1932) **2** (3) 160–173.
91. E. D. Leet and M. Ewing: Velocity of Explosion Generated Longitudinal Waves in Nepheline Syenite. *Trans. Amer. Geophys. Union* (1931) **12**, 61–65.
92. W. F. P. McIntock and J. Phemister: A Gravitational Survey over the Swynerton Dyke, Yarnfield, Staffordshire. *Min. Mag.* (Dec., 1927) 363–366.
93. S. F. Kelly: Engineering Uses of Geophysics. *Civil Eng.* (1932) **2** (10) 628–632.
94. I. B. Crosby and E. G. Leonardon: Electrical Prospecting Applied to Foundation Problems. *Trans. A.I.M.E.* (1929) **81**, 199.
95. E. G. Leonardon: Electrical Exploration Applied to Geological Problems in Civil Engineering. *Trans. A.I.M.E.* (1932) **97**, 99.
96. S. F. Kelly: Applying the Megger Ground Tester in Electrical Exploration. *Trans. A.I.M.E.* (1932) **97**, 114.
97. C. A. Heiland: Einige neuere Anwendungen der Geophysik bei Talsperren und Grundwasserproblemen. *Geol. Rundschau* (March, 1933) **23a**, 279.
98. R. Ambronn: Fig. 24, English prospectus of Prospektion, Goettingen.
99. Prospectus of Geophysical Co. Ltd., 20.



100. C. A. Heiland: Instruments and Methods for the Discovery of Useful Mineral Deposits. *Eng. and Min. Jnl.* (Jan. 9, 1926).
101. W. F. P. McIntock and J. Phemister: A Gravitational Survey over the Pentland Fault, near Portebello Midlothian, Scotland. *Great Brit. Geol. Survey Summ. Prog.* (1928) **2**, 10-28.
102. J. F. Weinzierl: One of the Many Problems Found in Torsion Balance Work. *Oil Weekly* (Oct. 29, 1926).
103. J. Koenigsberger: Aufsuchung von Wasser mit geophysikalischen Methoden. *Erg. Hefte angew. Geophysik* (1933) **3** (4), 463-525.
104. K. Sundberg: Effect of Impregnating Waters on Electrical Conductivity of Soils and Rocks. *Trans. A.I.M.E.* (1932) **97**, 367.
105. W. O. Hotchkiss and others: Earth-resistivity Measurements in the Lake Superior Copper Country. *Trans. A.I.M.E.* (1929) **81**, 51-68.
106. A. Loehnberg and W. Stern: Ein neuer Wg der karsthydrologischen Forschung durch Anwendung geoelektrischer Methoden. *Ztsch. Geophysik* (1932) **8** (¼), 283.
107. W. Stern: Das Widerstandsverfahren zur Untersuchung von Tektonik und Hydrologie des Unergrundes. *Erg. Hefte angew. Geophysik* (1933) **3** (4), 408.
108. C. M. Tattam: Application of the Electrical Resistivity Method of Geophysical Prospecting to Problems of Underground Water. Doctor's Thesis, Colo. School of Mines, 1932.
109. C. A. Heiland: *Terr. Mag.* (1932) **37** (3), 350.
110. F. Breyer: Radioaktive Untersuchungen am Salzdom von Spereberg. *Erg. Hefte angew. Geophysik* (1931) **1** (4), 416.
111. R. Krahmann: *Abh. prat. Geol.* (1926) **3**.
112. D. M. Collingwood: Magnetism and Geology of Yoast Field, Bastrop Co., Texas. *Amer. Assn. Petr. Geol. Bull.* 14 (1930) 1191-1197.
113. R. v. Eötvös: Verh. Allg. Conf. Internat. Erdmess. (1910) 16(A) 319-350.
114. M. Mueller: Geophysikalische Feldmessung mit niederfrequenten Wechselstromen. *Ztsch. Geophysik* (1929) **5** (¾), 256-259.
115. H. Hedstrom: Electrical Prospecting for Auriferous Quartz Veins and Reefs. *Min. Mag.* (1932) **46** (4), 201-219.
116. A. S. Eve and D. A. Keys: *Can. Survey Mem.* 165 (1928).
117. L. B. Slichter: Discussion. *Trans. A.I.M.E.* (1932) **97**, 35.
118. N. H. Stearn: Geomagnetic Surveying with the Hotchkiss Superdip. *Arkansas Geol. Survey Bull.* 5 and *Trans. A.I.M.E.* (1932) **97**, 194.
119. E. D. Leet: Seismic Prospecting. *Military Engr.* (July, Aug. 1931) **23**, 326.
120. H. Becker and others: *Naturwissenschaften* (May, 1932).
121. N. H. Stearn: Geomagnetic Exploration with the Hotchkiss Superdip. *Trans. A.I.M.E.* (1932) **97**, 195.
122. H. Reich: *Erzbergbau* (1930) **27**, 287.
123. H. Lundberg: *Min. and Met.* (Jan., 1931) 25.
124. S. F. Kelly, T. Zuschlag and B. Low: Discovering Gold-quartz Veins Electrically. *Min. and Met.* (June, 1934) 251.

## DISCUSSION

(Sherwin F. Kelly presiding)

W. M. WEIGEL,\* St. Louis, Mo.—A statement was made as to the higher resistivity of gravel. Suppose the gravel beds are water-saturated?

S. F. KELLY,† New York, N. Y.—They were water-saturated.

---

\* Mineral Technologist, Missouri Pacific R. R. Co.

† Geologist and Geophysicist, Combined Geophysical Methods, Inc.



W. M. WEIGEL.—Do they have a higher resistance than the underlying bedrock?

S. F. KELLY.—Yes. Apparently the higher resistance of the water in those gravel beds is due to the fact that the water is usually purer than the water contained in clays and such materials, with finer pore spaces and, consequently, it has a higher resistance. Pure water, as you know, has a tremendously high resistance. That may be part of the explanation.

K. S. KURTENACKER,\* Madison, Wis.—I would say that whether or not the gravels have a higher resistance than the underlying bedrock depends pretty much on what the bedrock is. If the bedrock is shale, the gravels would no doubt be higher; if sandstone, perhaps the gravels would have a lower resistance, especially if they were somewhat weathered.

E. DEGOLYER,† New York, N. Y.—The Grande Ecaille field was found by the seismic method and afterwards proved to be a salt dome by drilling, and was detailed by the gravity method.

One other point that I would like to make is that in all geophysics, as far as I know anything about it, the physicist or the field observer determines certain physical data. The interpretation of those data is the geologic problem of finding what particular set of conditions is most likely to occur which most nearly provides a solution for the data. That is an exceedingly important point in all geophysics and one that is quite often overlooked.

I do not think there has been any type of geophysics more definite and exact than the refraction surveys by which salt domes were found in the Gulf Coastal Plain of the United States. Yet the solution there is simply a solution that fits that country. In the normal country rock, the rate of speed transmission is something like 6000 to 7000 ft. per second. The rate of transmission through the rock salt is something like 16,000 to 18,000 ft. per second. Therefore, when a lead or a shortening of the time was recorded, anyone could tell that the solution was unique, that a rock-salt mass was there. On the other hand, if you wandered far afield with that same set of conditions and tried to apply the same solution, you would be lost. It would not be a difficult thing to go into New York, Pennsylvania, or any one of a number of other places and under certain conditions get 6000-ft. speeds and under other conditions get 16,000 to 18,000-ft. speeds. These differences would be the same as in the salt-dome region but the solution would be quite different.

---

\* Junior Geologist, Wisconsin Highway Commission.

† Petroleum Geologist.



# INDEX

(Note: In this index the names of authors of papers and discussions and of men referred to are printed in SMALL CAPITALS, and the titles of papers in *italics*.)

## A

- Africa: French equatorial, electrical exploration, 123
- Algiers, electrical exploration for bedrock in harbor, 128
- American Institute of Mining and Metallurgical Engineers: officers and directors, 7
- Committees: Geophysical Methods, personnel, 7

## B

- Barite: geophysical prospecting, 570
- Bauxite: geophysical prospecting, 570
- Brazil: auriferous veins, magnetic measurements, 313
- gold production, Rio Grande do Sul, 313
- magnetic observations in São Jeronymo coal mine, 323

## C

- Calumet and Hecla mine: geothermal measurements, diamond-drill holes, 528
- Canada: Ontario, electrical survey: for gold at Shillington, 70
- lignite deposits, Moose River Basin, 76
- Caspian Sea, near Bibi Eibat, electrical exploration, 126
- Cement materials: geophysical prospecting, possibilities, 557
- Chromite: geophysical prospecting, 570
- Civil engineering: geophysical prospecting, uses, 565
- Clay deposits: geophysical prospecting, 558
- Coal mines: magnetic observations in São Jeronymo mine, Brazil, 323
- Coal seams: geophysical prospecting, 549
- location by electrical measurements, 285
- Compass, sun-dial. *See* Magnetic Surveying.
- Copper mines: geothermal measurements, Calumet and Hecla, diamond-drill holes, 528
- Corrosion: pipe lines, location and study by surface electrical measurements, 60
- CREAGMILE, W. B.: *Discussion on Earth-resistivity Surveying in Illinois*, 31

## D

- DE BECK, H. O.: *An Accurate Simplified Magnetometer Field Method*, 326

- DE GOLYER, E.: *Discussions: on Earth-resistivity Surveying in Illinois*, 32, 33
- on Electrical Exploration of Water-covered Areas*, 134
- on Geophysics in the Nonmetallic Field*, 577
- on A Magnetic Gradiometer*, 388
- on Seismic Refraction Methods as Applied to Shallow Overburdens*, 492

- Diamonds: geophysical prospecting, indirect, 571
- Dip needle. *See* Magnetic Surveying.
- DOLBEAR, S. H.: *Discussion on Location of Faults by the Earth-resistivity Method*, 48
- Drill holes: crooked, electromagnetic survey, 268
- electrical measurements, 273
- temperature: determination with thermometer, 528
- electrical determination, 265
- Drilling, core. *See* Electrical Surveying.

## E

- Earth resistivity. *See* Electrical Surveying.
- Electrical surveying: anisotropic media, 159
- anticline: anisotropic, resistivity measurements across, 175
- buried, survey for, 23
- coal seams, locating through drill holes, 285
- combined with seismic for determination of bedrock and overburden where contours are bedded planes, 492
- coring to obtain bottom-hole data, 237
- coring, measurements, 273
- corrosion of pipe lines: location and study, 60
- soil corrosiveness, autogalvanic corrosion, electrolytic corrosion, 60
- depth to bedrock, 24, 31, 33, 38
- Tagg method, of interpretation, 24, 31, 33, 135
- drill-hole temperature determination, 265
- drill-hole measurements, 273
- earth-resistivity: interpretation of measurements, 135, 183
- earth-resistivity measurements: interpretation of three-layer curves, 148, 218
- interpretation of four-layer curves, 218
- interpretation, curve matching vs. empirical rules, 201, 233
- three-layer curves, interpretation, 148
- earth-resistivity survey: fault location, Hardin County, Illinois, 40
- fluorspar area in Illinois, 9
- gravel deposits of glacial drift, Illinois, 9

- Electrical surveying: earth-resistivity survey:  
     lead and zinc area in Illinois, 9  
     oil structures in Illinois, 9  
     water supply and gravel deposits in Illinois, 9  
     effect of small inhomogeneities near surface, 30  
     electrofiltration, 274, 288  
     Gish and Rooney method applied in Illinois, 9, 34  
     gold prospecting: features amenable, 62  
         Racom surveys, 66  
     gold-quartz veins, discovering with Ground Comparator, 75  
         highway problems, application and limitations, 49  
     horizontal exploration, 32, 122  
     Illinois, earth-resistivity survey on fluorspar, oil, lead and zinc, water supply and gravel deposits, 9  
     interpretation of earth-resistivity data, 24, 34, 135, 145, 183  
         curve matching vs. empirical rules, 201, 233  
         measurements in anisotropic media, 159  
         readings over faults and anticlines, 32  
     lignite deposits, Megger Ground Tester survey, 76  
     location of septic tank, 38  
     Megger Ground Tester. *See* Megger.  
     metal sheet in tank of water, resistivity, 14, 29, 35, 37, 38  
     placer and water-supply problems, 121  
     resistivitimeter, 266  
     resistivity. *See* earth resistivity (above).  
     syncline, anisotropic, resistivity measurements across, 175  
     Tagg's method of interpretation, 24, 135, 145, 183  
     vertical exploration, 32, 122  
     water-covered areas, 122  
     water-flow location in oil wells, 267  
     water-supply and placer problems, 121  
     Wenner method applied in Illinois, 9  
 Electromagnetic teleclinometer: Schlumberger, 269  
     survey of crooked holes, 268
- F
- Faults: electrical location, Hardin County, Illinois, 40  
 FISHER, J.: *Discussions: on Interpretation of Resistivity Measurements*, 147  
     *on A Magnetic Gradiometer*, 388  
     *on Some Interpretations of Earth-resistivity Data*, 197, 198  
     *on Use of Magnetic Data in Michigan Iron Ranges*, 312  
 FISHER, J., INGERSOLL, L. R. AND VIVIAN, H.: *Recent Geothermal Measurements in the Michigan Copper District*, 528  
 Fluorspar: earth-resistivity survey in Illinois, 9  
     geophysical prospecting, 568
- G
- Geophysical prospecting (See also Electrical, Magnetic, Seismic, Geothermal):  
     barite, 570  
     Geophysical prospecting: bauxite, 570  
         bedded planes, combined electrical and seismic methods for determining bed-rock and overburden, 492  
         building and road stone, 562  
         cement materials, 557  
         coal deposits, 285, 549  
         chromite, 570  
         in civil engineering, 565  
         clay deposits, 558  
         data apply only to region in which obtained, 577  
         fluorspar, 9, 568  
         functions of geophysicist and geologist, 33  
         graphite, 570  
         gravel deposits, 558, 577  
         ground water location, 566  
         interpretation of data must relate to geology of region, 577  
         mining fields, 5  
         nitrates, 556  
         nonmetallic field, 546  
         nonmetallic minerals, bibliography, 572  
         oil fields. *See* Oil.  
         phosphates, 556  
         potash, 556  
         salt deposits, 554  
         sand, 558  
         serpentine, 569  
         status in 1934, 5  
         sulfur deposits, 554  
         talc and soapstone, 568  
     Georgia: electrical surveying for gold-quartz veins, 75  
     Geothermal measurements: interpretation, theoretical, 534  
         Michigan copper district: Calumet and Hecla mine, diamond-drill holes, 528  
         radioactivity of rocks, 542  
         rock temperature in new or unventilated (dead end) workings, 528, 538  
         snow blanket effect, 537, 545  
         surface temperature effects, 537  
         thermometers, mercury in glass, 529  
     GILCHRIST, L.: *Discussions: on Application of Resistivity Methods to Northern Ontario Lignite*, 120  
         *on Interpretation of Resistivity Measurements*, 232  
         *on Recent Geothermal Measurements in the Michigan Copper District*, 545  
     Gish-Rooney geophysical apparatus, fault location, Hardin County, Illinois, 40  
     Gold: electrical surveying for, 62, 75  
     Gold mining: Brazil, extent, 313  
     Gold-quartz veins: electrical surveying for, 75  
         magnetic measurements in Brazil, 313  
     Gradiometer. *See* Magnetic Surveying.  
     Graphite: geophysical prospecting, 570  
     Gravel deposits: geophysical prospecting, 9, 558, 577  
     Gravity surveying: technique of observation, analogy with magnetic method, 388  
     Ground Comparator, electrical discovery of gold-quartz veins, 75  
     Ground water: location by geophysical prospecting, 566



## H

- HAWKINS, R. H.: *Application of Resistivity Methods to Northern Ontario Lignite Deposits*, 76; *Discussion*, 119, 120
- HEILAND, C. A.: *Certain Instrument Problems in Reflection Seismology*, 411  
*Geophysics in the Nonmetallic Field*, 546  
*Discussion on A Magnetic Gradiometer*, 388
- Highway problems: earth-resistivity surveys, application and limitations, 49
- Hotchkiss Superdip. See Magnetic Surveying.
- HOWELL, L. G.: *Discussion on Earth-resistivity Surveying in Illinois*, 34
- HEILAND, C. A. AND PUGH, W. E.: *Theory and Experiments Concerning a New Compensated Magnetometer System*, 334
- HUBBERT, M. K.: *Results of Earth-resistivity Survey on Various Geologic Structures in Illinois*, 9; *Discussion*, 29 et seq.  
*Discussions: on Electrical Methods in Prospecting for Gold*, 74  
*on Interpretation of Resistivity Measurements*, 147, 235  
*on Location of Faults by the Earth-resistivity Method*, 48  
*on A Magnetic Gradiometer*, 388
- HUBBERT, M. K. AND WELLES, J. M.: *Location of Faults in Hardin County, Illinois, by the Earth-resistivity Method*, 40

## I

- Illinois: geophysical prospecting: See Electrical Surveying.
- Hardin County, geology, 41
- INGERSOLL, L. R., FISHER, J. AND VIVIAN, H.: *Recent Geothermal Measurements in the Michigan Copper District*, 528
- Iron regions: magnetic surveying in Michigan, 290

## J

- JAKOSEY, J. J. AND WILSON, C. H.: *Geophysical Studies in Placer and Water-supply Problems* (Abstract), 121
- JOHNSON, H. N.: *Discussion on Earth-resistivity Surveying in Illinois*, 30, 33

## K

- KELLY, S. F.: *Discussions: on Earth-resistivity Surveying in Illinois*, 38  
*on Electrical Measurements in Drill Holes*, 289  
*on Geophysics in the Nonmetallic Field*, 576  
*on Location of Faults by the Earth-resistivity Method*, 48
- KELLY, S. F., ZUSCHLAG, T. AND LOW, B.: *Discovering Gold-quartz Veins Electrically* (Abstract), 75
- KIHLSTEDT, F. H.: *Electrical Methods in Prospecting for Gold*, 62; *Discussion*, 74  
*Discussions: on Electrical Exploration of Water-covered Areas*, 134  
*on Some Interpretations of Earth-resistivity Data*, 198

- KURTENACKER, K. S.: *Some Practical Applications of Resistivity Measurements to Highway Problems*, 49  
*Discussion on Geophysics in the Nonmetallic Field*, 577

## L

- LANE, A. C.: *Discussion on Recent Geothermal Measurements in the Michigan Copper District*, 536
- LEE, F. W.: *Discussions: on Earth-resistivity Surveying in Illinois*, 32  
*on Electrical Exploration of Water-covered Areas*, 134  
*on Electrical Measurements in Anisotropic Media*, 182  
*on Seismic Refraction Methods as Applied to Shallow Overburdens*, 492  
*on Some Interpretations of Earth-resistivity Data*, 197, 198
- Lee's partitioning method of geophysical prospecting, brief outline, 80
- LEONARDON, E. G.: *Discussions: on Application of Resistivity Methods to Northern Ontario Lignite*, 120  
*on Earth-resistivity Surveying in Illinois*, 30, 32, 33  
*on Electrical Measurements in Anisotropic Media*, 182  
*on Electrical Measurements in Drill Holes*, 288, 289  
*on Interpretation of Resistivity Measurements*, 147
- LEONARDON, E. G. AND SCHLUMBERGER, C. AND M.: *Electrical Coring; a Method of Determining Bottom-hole Data by Electrical Measurements*, 237  
*Electrical Exploration of Water-covered Areas*, 122  
*Location and Study of Pipe-line Corrosion by Surface Electrical Measurements* (Abstract), 60  
*A New Contribution to Subsurface Studies by Means of Electrical Measurements in Drill Holes*, 273  
*Some Observations Concerning Electrical Measurements in Anisotropic Media, and Their Interpretation*, 159
- Lignite deposits: Moose River Basin, electrical survey, 76  
geology, 76
- Limestone quarries. See Quarries.
- LOW, B., KELLY, S. F. AND ZUSCHLAG, T.: *Discovering Gold-quartz Veins Electrically* (Abstract), 75
- LUNDBERG, H.: *Discussions: on Application of Resistivity Methods to Northern Ontario Lignite*, 120  
*on Electrical Measurements in Drill Holes*, 288, 289

## M

- Magnetic surveying: auriferous veins in Brazil, 313

- Magnetic surveying: coal mine, Brazil, 323  
 compensated magnetometer system (Heiland and Pugh), 334  
 De Beck simplified field method, 326  
 dip needle, 292  
 gradiometer: construction, 373, 386, 388  
   favorable features, 388  
   field use, 379  
   test surveys, 384  
 instruments: effect of magnetic latitude, 348  
   effect of temperature, 334  
   Heiland system: arrangement and use of apparatus, 354  
     test of temperature coefficients, 363  
   temperature compensation: principles, 334  
     theory in Heiland system, 340  
     vertical intensity balances, historical review, 337  
     those used, 292  
 interpretation of data, 302  
 iron ranges, Michigan, 290  
 new compensated magnetometer system (Heiland), 334  
 sun-dial compass, 292  
 Superdip, 292  
 Superdip, simplified field method, 326  
 technique of observation, analogy with gravitational method, 388
- MALAMPHY, M. C.: *Magnetic Measurements on Auriferous Veins in Brazil*, 313
- Maps: Shillington area, Ontario, 70  
 State of Rio Grande do Sul, Brazil, regional geology, 315
- Megger Ground Tester: arrangement and field technique, 11, 26  
 earth-resistivity survey in Illinois, 9  
 lignite deposits, survey, 76  
 location of faults in Hardin County, Illinois, 40  
 location of septic tank, 38
- Michigan: electrical surveying, upper Peninsula, by Michigan College staff, 183  
 geothermal measurements, Calumet and Hecla mine, 528  
 iron ranges, magnetic surveying, 290
- N
- Nitrates: geophysical prospecting, 556
- Nonmetallic mineral deposits: geophysical prospecting, 546
- O
- Oil fields: crooked holes, electromagnetic survey, 268  
 electrical measurements in drill holes, 273  
 geophysical methods used, 5  
 water flows, electrical location, 267
- Oil structures: earth-resistivity survey in Illinois, 9  
 electrical coring, 245  
 water-covered, electrical exploration, 121
- Oklahoma: oil fields, electrical coring, 247, 254
- P
- PARTLO, F. L.: *Discussions: on A Magnetic Gradiometer*, 388
- PARTLO, F. L.: *Discussions: on Seismic Refraction Methods as Applied to Shallow Overburdens*, 492
- PARTLO, F. L. AND SERVICE, J. H.: *Seismic Refraction Methods as Applied to Shallow Overburdens*, 473
- PEARSON, J. M.: *Discussion on Earth-resistivity Surveying in Illinois*, 34
- Pechelbronn oil field, electrical coring, 245, 260, 262
- Petroleum. *See* Oil.
- Phosphates: geophysical prospecting, 556
- PIRSON, S. J.: *Interpretation of Three-layer Resistivity Curves*, 148
- Placer mining: electrical exploration, 121
- Potash: geophysical prospecting, 556
- Potentiometer, deflection: lignite deposits, survey, 76
- Precious stones: geophysical prospecting, direct location improbable, 571
- PUGH, W. E.: *Certain Field Problems in Reflection Seismology*, 455
- PUGH, W. E. AND HEILAND, C. A.: *Theory and Experiments Concerning a New Compensated Magnetometer System*, 334
- Q
- Quarries, limestone, electrical surveys, advantages, 50
- R
- Racom: gold prospecting, 66
- Reciprocity theorem, 235
- Rock temperatures. *See* Geothermal.
- ROGERS, A. H.: *Discussion on Electrical Methods in Prospecting for Gold*, 74
- ROMAN, I.: *Analysis of Seismic Profiles*, 493  
*Some Interpretations of Earth-resistivity Data*, 183  
*Discussion on Certain Field Problems in Reflection Seismology*, 470
- ROMAN, I. AND SERMON, T. C.: *A Magnetic Gradiometer*, 373; *Discussion*, 389
- ROYCE, S.: *Discussion on Use of Magnetic Data in Michigan Iron Ranges*, 312
- Rumania: oil fields, electrical coring, 247, 254
- Russia: Bibi Eibat oil field, electrical exploration in Caspian Sea, 126  
 electrical measurements in drill holes, Bibi Eibat, Grozny and Surakhany, 275
- RUTHERFORD, H. M.: *Reflection Methods in Seismic Prospecting*, 391
- S
- Salt deposits: geophysical prospecting, 554
- Sand: geophysical prospecting, 558
- Schlumberger electromagnetic teleclinometer, 269
- SCHLUMBERGER, C. AND M. AND LEONARDON, E. G.: *Electrical Coring; a Method of Determining Bottom-hole Data by Electrical Measurements*, 237  
*Electrical Exploration of Water-covered Areas*, 122  
*Location and Study of Pipe-line Corrosion by Surface Electrical Measurements (Abstract)*, 60

- SCHLUMBERGER, C. AND M. AND LEONARDON, E. G.: *A New Contribution to Subsurface Studies by Means of Electrical Measurements in Drill Holes*, 273  
*Some Observations Concerning Electrical Measurements in Anisotropic Media, and Their Interpretation*, 159
- Seismic prospecting: analysis of profiles, 493  
 bibliography, 410  
 combined with electrical surveying for determination of bedrock and overburden where contours are bedded planes, 492  
 horizontal beds, homogeneous, with prism of salt embedded in lowest layer, analysis of profiles, 493  
 horizontal layering, including rectangular intrusions, formulas, 493  
 least squares solution, reliability, 461  
 profiles, analysis, 493  
 recording time of explosion, two wires an advantage, 456, 470  
 reflection method: bibliography, 410, 452  
 field problems, 455  
 firing from recording truck, objections, 470  
 formulas, 395  
 instruments: calibration, 442  
 characteristics, 411  
 design, 411  
 Heiland equipment, 411  
 limitations, 391  
 shot signal transmission, 456  
 surface correction zones, 458  
 theory, 391, 393  
 velocity determinations, 460  
 vertical shooting, 469  
 refraction method: determining depth of shallow overburdens, theory and practice, 473  
 fault location, 488  
 shaking tables, bibliography, 454  
 slope shooting, 461
- SERMON, T. C. AND ROMAN, I.: *A Magnetic Gradiometer*, 373
- Serpentine: geophysical prospecting, 569
- SERVICE, J. H. AND PARTLO, F. L.: *Seismic Refraction Methods as Applied to Shallow Overburdens*, 473
- Shaking tables, bibliography, 454
- SLICHTER, L. B.: *Discussions: on Electrical Measurements in Anisotropic Media*, 181  
*on Electrical Measurements in Drill Holes*, 289  
*on Interpretation of Resistivity Measurements*, 234  
*on Some Interpretations of Earth-resistivity Data*, 197
- Soapstone: geophysical prospecting, 568
- Stone, building and road: location by geophysical prospecting, 562
- Sulfur deposits: geophysical prospecting, 554
- Sumatra, oil wells, electrical coring, 245
- SUNDBERG, K.: *Discussions: on Earth-resistivity Surveying in Illinois*, 31  
*on Interpretation of Resistivity Measurements*, 145
- Superdip. *See* Magnetic Surveying.
- Swamps: electrical surveys to find bottom, 56
- SWANSON, C. O.: *Use of Magnetic Data on Michigan Iron Ranges*, 290
- SWARTZ, J. H.: *Discussions: on Earth-resistivity Surveying in Illinois*, 29, 30  
*on Interpretation of Resistivity Measurements*, 233
- T
- TAGG, G. F.: *Interpretation of Resistivity Measurements*, 135; *Discussion*, 147  
*Discussion on Earth-resistivity Surveying in Illinois*, 33
- Talc and soapstone: geophysical prospecting, 568
- Teleclinometer. *See* Electromagnetic.
- Temperatures, underground. *See* Geothermal.
- Thermometers for geothermal measurements. *See* Geothermal.
- U
- U. S. S. R. (*See also* Russia): oil fields, electrical coring, 249, 254, 260
- V
- Venezuela: oil fields, electrical coring, 249, 254, 260
- VIVIAN, H., FISHER, J. AND INGERSOLL, L. R.: *Recent Geothermal Measurements in the Michigan Copper District*, 528
- W
- Water-covered areas: electrical exploration, 122
- Water supply: and gravel deposits: earth-resistivity survey in Illinois, 9  
 electrical exploration, 121
- WATSON, R. J.: *A Contribution to the Theory of the Interpretation of Resistivity Measurements Obtained from Surface Potential Observations*, 201; *Discussion*, 235
- WEAVER, P.: *Discussions: on Electrical Measurements in Anisotropic Media*, 181  
*on Recent Geothermal Measurements in the Michigan Copper District*, 545
- WEIGEL, W. M.: *Discussions: on Geophysics in the Nonmetallic Field*, 576  
*on Location of Faults by the Earth-resistivity Method*, 48
- WELLER, J. M. AND HUBBERT, M. K.: *Location of Faults in Hardin County, Illinois, by the Earth-resistivity Method*, 40
- Wenner method of geophysical prospecting, brief outline, 80
- WILSON, C. H. AND JAKOSKY, J. J.: *Geophysical Studies in Placer and Water-supply Problems (Abstract)*, 121
- Wisconsin: overburden and bedrock, list, 53  
 resistivity measurements in highway problems, 49
- Z
- ZUSCHLAG, T.: *Discussions: on Earth-resistivity Surveying in Illinois*, 30  
*on Interpretation of Resistivity Measurements*, 145
- Zuschlag Ground Comparator. *See* Electrical Surveying.
- ZUSCHLAG, T., KELLY, S. F. AND LOW, B.: *Discovering Gold-quartz Veins Electrically (Abstract)*, 75









Date